AD A085817

AD-E 300 788

DNA 2432H

TREE SIMULATION FACILITIES

Second Edition

General Electric Company-TEMPO
DASIAC, 816 State Street
Santa Barbara, California 93102

1 January 1979

Handbook

LEVEL III

CONTRACT No. DNA 001-79-C-0081

APPROVED FOR PUBLIC RELEASE;
DISTRIBUTION UNLIMITED.

DTIC
ELECTE
JUN 1 8 1980
D
C

THIS WORK SPONSORED BY THE DEFENSE NUCLEAR AGENCY
UNDER RDT&E RMSS CODE B337079464 P99QAXDC00809 H2590D.

Prepared for
Director
DEFENSE NUCLEAR AGENCY
Washington, D. C. 20305

DDC FILE COPY

80 4 17 007

Destroy this report when it is no longer needed. Do not return to sender.

PLEASE NOTIFY THE DEFENSE NUCLEAR AGENCY, ATTN: STTI, WASHINGTON, D.C. 20305, IF YOUR ADDRESS IS INCORRECT, IF YOU WISH TO BE DELETED FROM THE DISTRIBUTION LIST, OR IF THE ADDRESSEE IS NO LONGER EMPLOYED BY YOUR ORGANIZATION.

UNCLASSIFIED

SECURITY CLASSIFICATION OF THIS PAGE (When Data Entered)

REPORT DOCUMENTATION PAGE		READ INSTRUCTIONS BEFORE COMPLETING FORM
1. REPORT NUMBER DNA 2432H	2. GOVT ACCESSION NO. AD-A085817	3. RECIPIENT'S CATALOG NUMBER
4. TITLE (and Subtitle) TREE SIMULATION FACILITIES, Second Edition		5. TYPE OF REPORT & PERIOD COVERED Handbook 6. PERFORMING ORG. REPORT NUMBER
7. AUTHOR(s) Dr. Judy V. Rosenfeld		8. CONTRACT OR GRANT NUMBER(s) DNA 001-79-C-0081
9. PERFORMING ORGANIZATION NAME AND ADDRESS General Electric Company—TEMPO DASIAC, 816 State Street Santa Barbara, California 93102		10. PROGRAM ELEMENT, PROJECT, TASK AREA & WORK UNIT NUMBERS Subtask P99QAXDC008-09
11. CONTROLLING OFFICE NAME AND ADDRESS Director Defense Nuclear Agency Washington, D.C. 20305		12. REPORT DATE 1 January 1979 13. NUMBER OF PAGES 600
14. MONITORING AGENCY NAME & ADDRESS(if different from Controlling Office)		15. SECURITY CLASS (of this report) UNCLASSIFIED 15a. DECLASSIFICATION DOWNGRADING SCHEDULE

16. DISTRIBUTION STATEMENT (of this Report)

Approved for public release; distribution unlimited.

17. DISTRIBUTION STATEMENT (of the abstract entered in Block 20, if different from Report)

18. SUPPLEMENTARY NOTES

This work sponsored by the Defense Nuclear Agency under RDT&E RMSS Code B337079464 P99QAXDC00809 H2590D.

19. KEY WORDS (Continue on reverse side if necessary and identify by block number)

Transient Radiation	Steady-State Reactors	Linear Accelerators
Nuclear Weapon	Pulsed Reactors	LINAC
Environment	Gamma-Ray Sources	TRIGA Reactors
Simulation	Flash X-rays	

20. ABSTRACT (Continue on reverse side if necessary and identify by block number)

It is the purpose of this document to provide persons working in this area of transient radiation effects on electronics (TREE) with a reference document which characterizes on a technical basis TREE Simulation Facilities. Pulse reactors, flash X-rays, and LINACs are each characterized on an individual basis. The material is arranged to provide the TREE experimenter with the facility information he would need to know in order to run an experiment at one of the facilities.

DD FORM 1 JAN 73 1473 EDITION OF 1 NOV 65 IS OBSOLETE

UNCLASSIFIED

SECURITY CLASSIFICATION OF THIS PAGE (When Data Entered)

346420

JOB

PREFACE

All the contributions are gratefully acknowledged. The efforts of Mr. T.R. Smith and Mr. L. Choate of Sandia Laboratories, Dr. J. Rauch of Maxwell Laboratories, Dr. A. Kazi of Aberdeen Proving Grounds, Dr. P. Caldwell of Harry Diamond Laboratories, and Mr. L.L. Flores of White Sands Missile Range were so great, and their help was so generously given, that special mention seems appropriate. Thanks are also due to Major Mike Kemp, the DNA Project Officer, whose guidance and assistance made possible the preparation of this edition of the handbook.

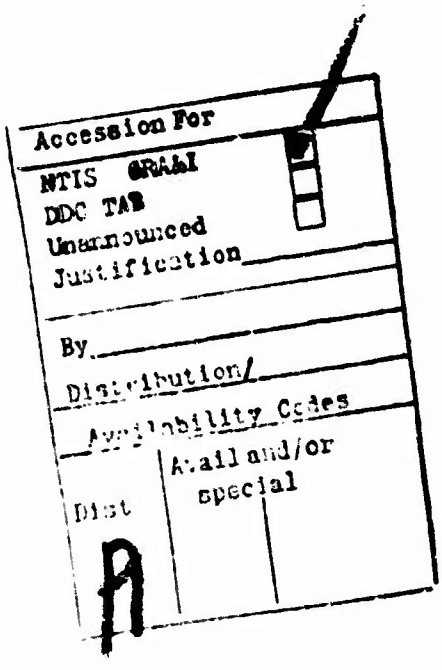

TABLE OF CONTENTS

Section			Page
1	INTRODUCTION		1-1
2	PULSE REACTORS		2-1
	2.1	Introduction	2-1
	2.2	Sandia Pulse Reactor (SPR-III)	2-6
		2.2.1 Physical Characteristics	2-6
		2.2.2 Operating Characteristics	2-6
		2.2.3 Environment	2-9
		2.2.4 Support Capabilities	2-15
		2.2.5 Applicability and Availability	2-17
		2.2.6 Security Clearance	2-17
	2.3	U.S. Army Material Testing Directorate, Army Pulse Radiation Facility (APRF)	2-19
		2.3.1 Characteristics	2-19
		2.3.2 Test Parameters	2-19
		2.3.3 Environment	2-23
		2.3.3.1 Fluence and Dose Maps	2-23
		2.3.4 Support Capabilities	2-37
		2.3.5 Procedural Information	2-40
		2.3.6 Applicability and Availability	2-41
		2.3.7 References	2-41
	2.4	Army Fast Burst Reactor Facility	2-43
		2.4.1 Operating Characteristics	2-43
		2.4.2 Environment	2-45
		2.4.2.1 Fluence and Dose Maps	2-45
		2.4.3 Support Capabilities	2-72
		2.4.4 Procedural Information	2-82
		2.4.5 Applicability and Availability	2-85
		2.4.6 References	2-85
	2.5	White Sands Missile Range Steady-State Neutron Generator	2-86
		2.5.1 Characteristics	2-86
		2.5.2 Operating Characteristics	2-86
		2.5.3 Environment	2-86
		2.5.4 Support Capabilities	2-86
	2.6	Sandia Pulse Reactor (SPR-II)	2-89
		2.6.1 General Characteristics	2-89
		2.6.2 Operating Characteristics	2-89
		2.6.3 Environment	2-92
		2.6.4 Support Capabilities	2-103
		2.6.5 Procedural Information	2-104
		2.6.6 Applicability and Availability	2-105
		2.6.7 Security Clearance	2-105
	2.7	Lawrence Livermore Laboratory Super Kukla Prompt Burst Reactor	2-107
		2.7.1 General Characteristics	2-107
		2.7.2 Operating Characteristics	2-107

TABLE OF CONTENTS (Continued)

Section			Page
	2.7.3	Environment	2-109
	2.7.4	Support Capabilities	2-109
	2.7.5	Procedural Information	2-116
	2.7.6	Applicability and Availability	2-117
	2.7.7	References	2-117
2.8	Northrop Reactor Facility		2-118
	2.8.1	General Characteristics	2-118
	2.8.2	Operating Characteristics	2-118
	2.8.3	Environment	2-122
	2.8.4	Support Capabilities	2-131
	2.8.5	Dosimetry	2-131
	2.8.6	Procedural Information	2-133
	2.8.7	Reference	2-133
2.9	Pennsylvania State University Breazeale Nuclear Reactor		2-134
	2.9.1	General Characteristics	2-134
		2.9.1.1 Horizontal Beam Tubes	2-134
		2.9.1.2 Central Thimble	2-134
		2.9.1.3 Pneumatic Tubes	2-134
		2.9.1.4 Pool Irradiations	2-135
	2.9.2	Additional Irradiation Facilities and Services	2-135
		2.9.2.1 The Cobalt-60 Gamma-Ray Facility	2-135
		2.9.2.2 The Cockcroft-Walton Neutron Generator	2-135
		2.9.2.3 Subcritical Reactor	2-135
		2.9.2.4 Hot Cells	2-135
	2.9.3	Operating Characteristics	2-136
	2.9.4	Support Capabilities	2-136
	2.9.5	Procedural Information	2-143
	2.9.6	Reference	2-143
2.10	General Atomic Company TRIGA Reactor Facility		2-144
	2.10.1	General Characteristics -- TRIGA Mark I	2-144
	2.10.2	TRIGA Mark I Operating Characteristics	2-144
	2.10.3	Environment	2-145
	2.10.4	Characteristics of ATPR	2-145
	2.10.5	ATPR Test Parameters	2-150
	2.10.6	Environment	2-153
	2.10.7	Support Capabilities	2-153
	2.10.8	Procedural Information	2-158
	2.10.9	References	2-158
2.11	Sandia Laboratories Annular Core Pulse Reactor (ACPR)		2-159
	2.11.1	General Characteristics	2-159
	2.11.2	Operating Characteristics	2-162
	2.11.3	Power Level and Energy Release	2-162
	2.11.4	Energy Release	2-162
	2.11.5	Pulse-Repetition Rate and Pulse Predictability	2-164
	2.11.6	Multiple Pulse Mode	2-164
	2.11.7	Transient Rod Runout Mode	2-164
	2.11.8	Tolerable Reactivity Worth of Experimental Sample	2-164

TABLE OF CONTENTS (Continued)

Section			Page
	2.11.9	Environment	2-164
		2.11.9.1 Neutron Fluence	2-164
		2.11.9.2 Neutron Energy Spectra	2-176
		2.11.9.3 Gamma Fluence	2-176
		2.11.9.4 Background Radiation Doses	2-176
	2.11.10	Special Capabilities	2-176
		2.11.10.1 Radiography Facility	2-176
		2.11.10.2 Flexo-Rabbit System	2-180
	2.11.11	Support Capabilities	2-182
		2.11.11.1 Staff	2-182
		2.11.11.2 Electronics	2-182
		2.11.11.3 Timing Signals	2-182
		2.11.11.4 Dosimetry	2-183
		2.11.11.5 Computational Facilities	2-183
		2.11.11.6 Shop Facilities	2-183
		2.11.11.7 Experiment Preparation Laboratories	2-183
		2.11.11.8 Photographic Equipment and Materials	2-183
	2.11.12	Procedural Information	2-183
		2.11.12.1 Scheduling	2-184
		2.11.12.2 Cost Information	2-184
		2.11.12.3 Shipping Address	2-184
	2.11.13	Applicability and Availability	2-184
	2.11.14	Security Clearance	2-184
2.12	State University of New York at Buffalo Reactor		2-187
	2.12.1	Characteristics	2-187
		2.12.1.1 Beam Tubes	2-187
		2.12.1.2 Thermal Column	2-187
		2.12.1.3 Pneumatic Conveyor	2-188
		2.12.1.4 Fission Plate	2-189
		2.12.1.5 Reactor Pulse Characteristics	2-189
	2.12.2	Applicability and Availability	2-189
2.13	AFRRI Reactor Facility		2-192
	2.13.1	Characteristics	2-192
	2.13.2	Test Parameters	2-192
	2.13.3	Support Capabilities	2-192
	2.13.4	Procedural Information	2-192
2.14	University of Wisconsin TRIGA Nuclear Reactor Facility		2-193
	2.14.1	Characteristics	2-193
	2.14.2	Test Parameters	2-193
	2.14.3	Support Capabilities	2-193
2.15	U.C. Irvine Department of Chemistry TRIGA Reactor		2-195
	2.15.1	General Characteristics	2-195
	2.15.2	Operating Characteristics	2-195
	2.15.3	Support Capabilities	2-195
	2.15.4	Procedural Information	2-195
2.16	Washington State University Reactor		2-196
	2.16.1	Characteristics	2-196

TABLE OF CONTENTS (Continued)

Section			Page
	2.16.2	Support Capabilities	2-198
	2.16.3	Procedural Information	2-198
2.17	Berkeley TRIGA Mark III		2-199
	2.17.1	Characteristics	2-199
	2.17.2	Test Parameters	2-199
	2.17.3	Environment	2-199
	2.17.4	Support Capabilities	2-200
	2.17.5	Procedural Information	2-201
2.18	Kansas State University (KSU) TRIGA Mark II		2-202
	2.18.1	General Characteristics	2-202
	2.18.2	Operating Characteristics	2-202
	2.18.3	Environment	2-202
	2.18.4	Support Capabilities	2-202
	2.18.5	Procedural Information	2-202
2.19	University of Texas at Austin TRIGA Mark I		2-203
	2.19.1	Characteristics	2-203
	2.19.2	Support Capabilities	2-203
	2.19.3	Procedural Information	2-203
3	FLASH X-RAY MACHINES		3-1
3.1	Introduction		3-1
3.2	FEBETRON 705 Electron-Beam System		3-4
	3.2.1	Characteristics	3-4
	3.2.2	Test Parameters	3-4
	3.2.3	Environment for Electron-Beam Mode	3-7
	3.2.4	Environment for X-Ray Mode	3-7
3.3	FEBETRON 706 Electron-Beam System		3-24
	3.3.1	Characteristics	3-24
	3.3.2	Test Parameters	3-24
	3.3.3	Northrop Research and Technology Center FXR Facilities	3-31
		3.3.3.1 Environment for Electron-Beam Mode	3-31
		3.3.3.2 Environment for X-Ray Mode	3-31
		3.3.3.3 Support Capabilities	3-31
		3.3.3.4 Procedural Information	3-37
		3.3.3.5 Reference	3-37
	3.3.4	Kaman Sciences Corporation FXR Facilities	3-37
		3.3.4.1 Test Parameters	3-37
		3.3.4.2 Environment for Electron-Beam Mode	3-39
		3.3.4.3 Environment for X-Ray Mode	3-42
		3.3.4.4 Support Capabilities	3-42
		3.3.4.5 Procedural Information	3-42
	3.3.5	Lockheed Palo Alto Research Laboratory FXR Facilities	3-45
		3.3.5.1 Electron-Beam Mode Environment	3-45
		3.3.5.2 X-Ray Mode Environment	3-46

TABLE OF CONTENTS (Continued)

Section			Page
		3.3.5.3 Support Capabilities	3-47
		3.3.5.4 References	3-48
	3.3.6	EG&G FXR Facilities	3-49
	3.3.7	Research Triangle Institute FXR Facility	3-49
	3.3.8	Westinghouse Electric Corporation FXR Facilities	3-49
3.4		Ion Physics Corporation FX-35 Electron-Beam Generator	3-50
	3.4.1	Characteristics	3-50
	3.4.2	Test Parameters	3-50
	3.4.3	Electron-Beam Mode Environment	3-54
	3.4.4	X-Ray Mode Environment	3-59
	3.4.5	Support Capabilities	3-59
	3.4.6	Procedural Information	3-61
	3.4.7	References	3-62
3.5		Boeing FX-75 Electron-Beam Generator	3-63
	3.5.1	Test Parameters	3-63
		3.5.1.1 Electrical Noise	3-66
		3.5.1.2 Diagnostic Techniques	3-66
	3.5.2	Support Capabilities	3-79
	3.5.3	Procedural Information	3-80
3.6		Harry Diamond Laboratories (HDL) FX-45 Electron-Beam Generator	3-81
	3.6.1	Test Parameters	3-81
		3.6.1.1 Electron-Beam Environment (High-Impedance Mode)	3-83
		3.6.1.2 Electron-Beam Environment (Low-Impedance Mode)	3-85
		3.6.1.3 X-Ray Mode Environment	3-94
	3.6.2	Support Capabilities	3-94
	3.6.3	References	3-99
3.7		Physics International Pulserads 225W, 738, 1150, OWL II, and PITHON II	3-101
	3.7.1	Characteristics	3-101
	3.7.2	Generator Diagnostics	3-105
	3.7.3	Electron-Beam Diagnostics	3-105
	3.7.4	X-Ray Diagnostics	3-106
	3.7.5	Noise Levels	3-107
	3.7.6	OWL II Data	3-107
		3.7.6.1 Electron-Beam Environments	3-107
	3.7.7	Model 1150 Pulserad Output Data	3-113
		3.7.7.1 Electron-Beam Environments	3-113
		3.7.7.2 X-Ray Environments	3-113
		3.7.7.3 Long-Pulse Environments	3-118
	3.7.8	PITHON II Data	3-119
		3.7.8.1 X-Ray Environments	3-119
		3.7.8.2 Imploding Plasma X-Ray Mode	3-119
	3.7.9	Pulserad 225W Output Data	3-121
		3.7.9.1 Electron-Beam Environment	3-121

TABLE OF CONTENTS (Continued)

Section			Page
		3.7.9.2 X-Ray Environment	3-122
	3.7.10	Pulserad 738 Output Data	3-122
	3.7.11	Available Support Services	3-123
	3.7.12	Procedural Information	3-124
	3.7.13	References	3-124
3.8	Maxwell BLACKJACK 3 and BLACKJACK 3 Prime		3-126
	3.8.1	Test Parameters	3-126
		3.8.1.1 Diagnostic Techniques	3-127
		3.8.1.2 Electron-Beam Mode Environment	3-128
		3.8.1.3 Environment Measurement Errors	3-130
		3.8.1.4 X-Ray Mode Environment	3-132
		3.8.1.5 Environment Measurement Errors	3-137
	3.8.2	Support Capabilities	3-137
		3.8.2.1 Optional Time and Material (T&M) Support	3-139
	3.8.3	References	3-140
3.9	TRW VULCAN and FEBETRON 705 X-Ray Facility		3-141
	3.9.1	FEBETRON 705	3-141
		3.9.1.1 Machine Specifications	3-141
	3.9.2	VULCAN	3-142
		3.9.2.1 Performance Characteristics	3-144
	3.9.3	Support Capabilities	3-152
3.10	HERMES II and REBA/REHYD Electron-Beam Generators		3-154
	3.10.1	HERMES II	3-154
		3.10.1.1 Repetition Rate and Pulse Reproducibility	3-155
		3.10.1.2 Electron-Beam Mode Environment	3-156
		3.10.1.3 Total Beam Energy	3-156
		3.10.1.4 Beam Geometry	3-160
		3.10.1.5 Energy-Deposition Drift Chamber	3-160
		3.10.1.6 Atmospheric Focusing Cone	3-160
		3.10.1.7 Energy Deposition with Focusing Cone	3-162
		3.10.1.8 Environment Measurement Errors	3-165
		3.10.1.9 X-Ray Mode Environment	3-165
	3.10.2	REBA	3-173
		3.10.2.1 Performance Characteristics	3-174
		3.10.2.2 Current Waveform and Distribution	3-174
		3.10.2.3 Repetition Rate and Pulse Reproducibility	3-175
		3.10.2.4 Electrical Noise	3-178
		3.10.2.5 Diagnostic Techniques	3-178
		3.10.2.6 Electron-Beam Mode Environment	3-178
		3.10.2.7 X-Ray Mode Environment	3-185
	3.10.3	REHYD	3-197
		3.10.3.1 Performance Characteristics	3-197
		3.10.3.2 Electron-Beam Mode Environment	3-199
		3.10.3.3 X-Ray Mode Environment	3-199

TABLE OF CONTENTS (Continued)

Section			Page
	3.10.4	Experimental Facilities	3-202
		3.10.4.1 Location	3-202
		3.10.4.2 HERMES II Test Area	3-202
		3.10.4.3 HERMES II Test Cell	3-202
		3.10.4.4 REBA Test Area	3-207
		3.10.4.5 REBA Test Cell	3-207
		3.10.4.6 REHYD Test Area	3-210
		3.10.4.7 REHYD Test Cell Area	3-210
	3.10.5	Instrumentation and Instrument Vans	3-210
		3.10.5.1 Screen Rooms and Electronics	3-210
		3.10.5.2 Instrumentation Vans	3-211
		3.10.5.3 User-Provided Instrument Vans	3-214
	3.10.6	Timing and Sequencing	3-214
		3.10.6.1 On-Line Computer Data Collection and Processing	3-215
	3.10.7	Support Staff	3-215
	3.10.8	Computational Facilities	3-216
	3.10.9	Experiment Preparation and Office Spaces	3-216
	3.10.10	Dosimetry	3-216
	3.10.11	Photographic Services	3-216
	3.10.12	Shop Facilities	3-217
	3.10.13	Scheduling and Contract Procedure	3-217
	3.10.14	Cost Information	3-218
	3.10.15	Security and Visitor Control	3-218
	3.10.16	Shipping Information	3-218
3.11	North Carolina State University Pulserad Model 940 Electron-Beam Generator		3-219
	3.11.1	Test Parameters	3-219
		3.11.1.1 Electron-Beam Mode Environment	3-219
		3.11.1.2 X-Ray Mode Environment	3-220
	3.11.2	Procedural Information	3-220
3.12	Harry Diamond Laboratories AURORA Facility		3-228
	3.12.1	General Characteristics	3-228
	3.12.2	Physical Characteristics	3-229
	3.12.3	Test Cell and Data Room	3-229
	3.12.4	Data Room Layout	3-231
	3.12.5	Operating Characteristics	3-232
	3.12.6	Dose Maps	3-235
	3.12.7	X-Ray Mode	3-235
	3.12.8	X-Ray Spectrum	3-235
	3.12.9	Electron Mode	3-238
	3.12.10	Support Capabilities	3-239
		3.12.10.1 Oscilloscopes	3-239
		3.12.10.2 Tape Recorders	3-239
		3.12.10.3 Oscillographs	3-240
		3.12.10.4 Data Scanner	3-240
		3.12.10.5 Timing Instrumentation	3-240

TABLE OF CONTENTS (Continued)

Section			Page
		3.12.10.6 Dosimetry	3-240
		3.12.10.7 Security Provisions	3-241
	3.12.11	Procedural Information	3-241
3.13	Honeywell FX-25 Electron-Beam Generator		3-242
	3.13.1	Test Parameters	3-242
	3.13.2	Diagnostic Techniques	3-243
		3.13.2.1 Electron-Beam Mode Environment	3-244
		3.13.2.2 X-Ray Mode Environment	3-247
	3.13.3	Support Capabilities	3-247
3.14	Raytheon Radiation Facility, Equipment Development Laboratory		3-256
	3.14.1	Operating Characteristics	3-257
		3.14.1.1 Field Emission Corporation Model 730/2650	3-257
		3.14.1.2 Ion Physics FX-25	3-257
		3.14.1.3 Electrical Noise	3-258
	3.14.2	Electron-Beam Mode	3-258
	3.14.3	X-Ray Mode	3-258
	3.14.4	Support Capabilities	3-261
	3.14.5	Dosimetry	3-262
	3.14.6	Computational Facilities	3-263
	3.14.7	Procedural Information	3-264
	3.14.8	Applicability and Availability	3-264
3.15	General Electric FX-25 Electron-Beam Generator		3-266
	3.15.1	Operating Characteristics	3-266
	3.15.2	Electron-Beam Mode	3-267
	3.15.3	X-Ray Mode	3-271
	3.15.4	Support Capabilities	3-271
	3.15.5	Procedural Information	3-271
3.16	Rome Air Development Center FXR Facility		3-274
	3.16.1	Electron-Beam Mode	3-274
	3.16.2	X-Ray Mode	3-274
	3.16.3	Support Capabilities	3-274
	3.16.4	Procedural Information	3-274
3.17	CASINO		3-275
	3.17.1	Operating Characteristics	3-275
	3.17.2	Supporting Facilities	3-276
		3.17.2.1 Exposure Cell	3-276
		3.17.2.2 User Data (Instrumentation) Room	3-278
		3.17.2.3 Trailer Area	3-278
		3.17.2.4 Miscellaneous Facilities	3-278
	3.17.3	Procedural Information	3-278
	3.17.4	Reference	3-279
3.18	Gamble		3-280
	3.18.1	Operating Characteristics	3-280
	3.18.2	Procedural Information	3-280

TABLE OF CONTENTS (Continued)

Section			Page
4	LINEAR ACCELERATORS		4-1
	4.1	Introduction	4-1
	4.2	IRT Corporation LINAC	4-4
		4.2.1 Characteristics	4-4
		4.2.2 Test Parameters	4-4
		4.2.3 Support Capabilities	4-5
		4.2.4 Procedural Information	4-9
		4.2.5 Applicability and Availability	4-9
		4.2.6 Reference	4-10
	4.3	NRL LINAC	4-11
		4.3.1 Characteristics	4-11
		4.3.2 Test Parameters	4-11
		4.3.3 Electron-Beam Geometry and Energy Spread	4-13
		4.3.4 Support Capabilities	4-14
		4.3.5 Procedural Information	4-15
		4.3.6 Applicability and Availability	4-17
		4.3.7 References	4-17
	4.4	BREL LINAC	4-18
		4.4.1 Characteristics	4-18
		4.4.2 Test Parameters	4-18
		4.4.3 Electron-Beam Geometry and Energy Spread	4-18
		4.4.4 Support Capabilities	4-28
		4.4.5 Procedural Information	4-28
		4.4.6 Reference	4-29
	4.5	NWEB LINAC	4-30
		4.5.1 Characteristics	4-30
		4.5.2 Test Parameters	4-30
		4.5.3 Support Capabilities	4-35
		4.5.4 Procedural Information	4-37
		4.5.5 Applicability and Availability	4-38
		4.5.6 References	4-38
	4.6	EG&G LINAC	4-39
		4.6.1 Characteristics	4-39
		4.6.2 Test Parameters	4-39
		4.6.3 Support Capabilities	4-40
		4.6.4 Procedural Information	4-47
		4.6.5 Applicability and Availability	4-47
	4.7	AFRRI LINAC Facility	4-48
		4.7.1 Characteristics	4-48
		4.7.2 Support Capabilities	4-48
		4.7.3 Test Parameters	4-48
		4.7.4 Procedural Information	4-48
	4.8	Rome Air Development Center LINAC	4-50
		4.8.1 Test Parameters	4-50
		4.8.2 Support Capabilities	4-51
		4.8.3 Procedural Information	4-51

TABLE OF CONTENTS (Continued)

Section			Page
4.9	Ogden Air Logistics Command LINAC		4-52
	4.9.1	Characteristics	4-52
	4.9.2	Test Parameters	4-52
	4.9.3	Support Equipment	4-55
	4.9.4	Support Capabilities	4-55
	4.9.5	Procedural Information	4-58
	4.9.6	Applicability and Availability	4-58
	4.9.7	References	4-59
4.10	LASL PHERMEX		4-60
	4.10.1	Characteristics	4-60
	4.10.2	Test Parameters	4-60
	4.10.3	Reference	4-60
4.11	Rensselear Polytechnic Institute (RPI) LINAC		4-61
	4.11.1	Characteristics	4-61
	4.11.2	Test Parameters	4-61
	4.11.3	Procedural Information	4-61
APPENDIX A	LIST OF ABBREVIATIONS		A-1

LIST OF ILLUSTRATIONS

Figure		Page
2-1	SPR-III width at half-maximum power versus temperature rise (pulse yield) free field.	2-7
2-2	SPR-III typical pulse shape for 300°C ΔT yield.	2-8
2-3	SPR-III profiles for 3-MeV leakage fluence free field.	2-10
2-4	SPR-III center line data.	2-11
2-5	SPR-III γ profile at core midplane for pulse conditions.	2-12
2-6	SPR-III glory hole center line and γ dose (rad (water)/°C ΔT).	2-13
2-7	SPR-III unperturbed glory hole spectra.	2-14
2-8	SPR-III unperturbed leakage spectra.	2-14
2-9	Sandia pulse reactor facility experiment plan.	2-18
2-10	Army pulse radiation facility.	2-21
2-11	Pulse trace.	2-22
2-12	Peak γ dose rate versus PWHM for APRF n/γ converters.	2-24
2-13	Peak γ dose rate versus total neutron fluence for APRF n/γ converters.	2-25
2-14	Radial fluence traverse.	2-26
2-15	Vertical neutron fluence distribution across APRF reactor decoupling shield.	2-26
2-16	APRF 106-mm-dia. glory hole neutron fluence distributions.	2-27
2-17	Normalized neutron fluence locations.	2-27
2-18	Normalized neutron fluence.	2-28
2-19	Normalized neutron fluence.	2-28
2-20	Normalized neutron fluence.	2-29
2-21	Total γ and neutron doses versus converter thickness (rad tissue at 1.3 x 10^{17}F)(66.3 kW-min).	2-30
2-22	Total γ and neutron doses versus converter thickness (rad Si at 1.3 x 10^{17}F)(66.3 kW-min).	2-31
2-23	APRF neutron spectra.	2-32
2-24	γ/n dose (tissue) ratio versus converter shield thickness.	2-37
2-25	Elevation section of FBR control building and reactor cell.	2-44
2-26	Total fast fluence for a given burst size and a given distance at the FBR.	2-46
2-27	Total fast fluence for a given burst size and a given distance at the FBR.	2-47

LIST OF ILLUSTRATIONS (Continued)

Figure		Page
2-28	Total fast fluence for a given burst size and a given distance at the FBR.	2-48
2-29	Average neutron fluence > 3.0 MeV on 6-in. horizontal circle.	2-60
2-30	Average neutron fluence > 3.0 MeV on 1-m horizontal circle.	2-61
2-31	Average neutron fluence > 3.0 MeV vertical traverse at 1 m from reactor axis.	2-62
2-32	Average neutron fluence > 3.0 MeV as a function of radial distance from core center, indoor.	2-63
2-33	Average neutron fluence > 3.0 MeV as a function of radial distance from core center, outdoor.	2-63
2-34	Average neutron fluence above various threshold energies on 1-m horizontal circle, indoor.	2-64
2-35	Average neutron fluence above various threshold energies on 1-m horizontal circle, outdoor.	2-65
2-36	Average neutron fluence above various threshold energies on a vertical traverse 1 m from reactor axis, indoor.	2-66
2-37	Average neutron fluence above various threshold energies on a vertical traverse 1 m from reactor axis, outdoor.	2-67
2-38	Average neutron fluence above various threshold energies as a function of radial distance from core center, indoor.	2-68
2-39	Average neutron fluence above various threshold energies as a function of radial distance from core center, indoor.	2-69
2-40	Average neutron fluence above various threshold energies as a function of radial distance from core center, outdoor.	2-70
2-41	Average neutron fluence above various threshold energies as a function of radial distance from core center, outdoor.	2-71
2-42	γ dose on 6-in. horizontal circle.	2-79
2-43	γ dose on 1-m horizontal circle.	2-80
2-44	γ dose vertical traverse at 1 m from reactor axis.	2-81
2-45	γ dose as a function of radial distance from core center, indoor.	2-81
2-46	γ dose as a function of radial distance from core center, outdoor.	2-82
2-47	WSMR neutron generator.	2-88
2-48	Burst width versus burst yield (yield is measured temperature rise).	2-91

LIST OF ILLUSTRATIONS (Continued)

Figure		Page
2-49	SPR-II burst time profiles for various-size bursts, as determined with a photodiode.	2-91
2-50	Free-field integral neutron fluence as a function of distance from the reactor vertical center line at 57.7 in. above the floor for a 200°C burst.	2-93
2-51	Integral neutron fluence ($E_n \geq 3.0$ MeV) on the outside shroud surface normalized to core temperature change as a function of distance from the top edge of the shroud.	2-94
2-52	Integral neutron fluence ($E_n \geq 3.0$ MeV) normalized to core temperature change for the glory hole center line versus vertical distance from the top of the glory hole flange.	2-95
2-53	Glory hole fluence at the nuclear center of the glory hole versus SPR-II.	2-96
2-54	Thermal neutron fluence ($E_n \geq 0.4$ eV) as a function of distance from the reactor vertical center line at 57.5 in. above the floor for a 200°C burst.	2-97
2-55	Horizontal placement of dosimeters.	2-98
2-56	Vertical placement of dosimeters.	2-98
2-57	Normalized γ dose as a function of distance from the reactor vertical center line at 57.5 in. above floor.	2-99
2-58	γ dose as a function of distance from the reactor vertical center line at 57.5 in. above the floor for a 1°C temperature rise.	2-99
2-59	γ dose on the glory hole center line as a function of vertical distance from the top edge of the glory hole for a 200°C burst.	2-100
2-60	Comparison of the glory hole and 2.5-cm spectra, proton recoil measurements.	2-100
2-61	n/γ ratios as a function of operation.	2-102
2-62	Sandia pulse reactor facility experiment plan.	2-106
2-63	Super Kukla pulse shape as a function of burst fission yields.	2-108
2-64	Vertical flux profile for Super Kukla.	2-110
2-65	Normalized neutron flux versus location from axis of reactor.	2-111
2-66	Neutron energy spectrum for the Super Kukla.	2-114
2-67	Neutron energy spectrum for the Super Kukla.	2-115
2-68	Plan view of Northrop reactor facility.	2-119
2-69	Peak power versus pulse worth.	2-121

LIST OF ILLUSTRATIONS (Continued)

Figure		Page
2-70	Pulse width versus pulse worth.	2-121
2-71	Integrated power versus pulse worth.	2-122
2-72	Neutron flux versus distance from exposure room window.	2-123
2-73	Neutron fluence for in-core vertical traverse.	2-124
2-74	Thermal neutrons for in-core vertical traverse.	2-124
2-75	Neutron and γ dose versus distance from exposure room window.	2-125
2-76	Neutron and γ dose versus distance from exposure room window.	2-126
2-77	Neutron and γ dose versus distance from exposure room window.	2-127
2-78	Neutron and γ dose versus distance from exposure room window.	2-128
2-79	Neutron and γ dose versus distance from exposure room window.	2-129
2-80	Neutron spectrum in exposure room at center of window normalized to reactor power of 1 W.	2-130
2-81	Flux intensity with energy greater than E as a function of E.	2-138
2-82	Flux intensity with energy greater than E as a function of E.	2-139
2-83	Flux intensity with energy greater than E as a function of E.	2-140
2-84	Flux intensity with energy greater than E as a function of E.	2-141
2-85	Neutron spectra in the TRIGA central thimble with spurious structure eliminated. (The spectra were measured from 2.65 to 23.65 in. above the core center line in 3-in. increments.)	2-142
2-86	Mark I pulsing characteristics.	2-146
2-87	Vertical section of ATPR facility.	2-149
2-88	Floor plan of ATPR facility.	2-149
2-89	J-tube position relative to the reactor core, ATPR.	2-151
2-90	ATPR pulsing characteristics.	2-152
2-91	Vertical neutron flux distribution.	2-155
2-92	γ dose in the water radial from ATPR core.	2-157
2-93	Floor plan of Building 6588.	2-160
2-94	Peak power as a function of reactivity insertion.	2-163
2-95	Core energy release as a function of reactivity insertion (upper energy release value is calculated for rods held out for 20 s after pulse initiation).	2-163
2-96	Peak power occurring in pulse versus energy release (rods held out for 20 s).	2-165
2-97	Initial power level in pulse tail versus core energy release (rods held out for 20 s).	2-165

LIST OF ILLUSTRATIONS (Continued)

Figure		Page
2-98	Fraction of energy in pulse tail versus total core energy release.	2-166
2-99	Effect of the magnitude of reactivity reinserted in 1.0 s at a delay time of 1.5 s ($2.50 pulse) versus fraction of energy yield in tail.	2-166
2-100	Maximum fuel temperature occurring in pulse versus core energy release (rods held out or rods reinserted).	2-167
2-101	Steady-state fuel and clad temperatures.	2-168
2-102	ACPR upgrade triple pulse ($1.1/$0.68/$0.82 α_2, PK1D).	2-169
2-103	Reactor yield versus time for ACPR upgrade triple pulse.	2-170
2-104	Reactor power history for transient rod runout ($3/7 s, BeO-2, PK1D).	2-171
2-105	Reactor yield versus time for transient rod runout operation.	2-172
2-106	Total pulse fluence versus energy release (normalized to S_δ - TWϕTRAN).	2-173
2-107	Flux at axial midplane in ACPR upgrade (group 1, 14.9 → 1.35 MeV; group 9, 0.005 → 0.06 eV).	2-174
2-108	Axial flux in cavity of ACPR upgrade.	2-175
2-109	Integral neutron spectrum in ACPR cavity.	2-177
2-110	Cavity flux spectrum in ACPR upgrade (TWϕTRAN - S_4, P_1, 18 group).	2-178
2-111	Differential energy flux for ACPR upgrade.	2-178
2-112	Cavity γ dose versus pulse energy release.	2-179
2-113	Experiment request plan.	2-185
2-114	Thermal flux and γ intensity in the dry fast rabbit facility.	2-190
2-115	Normalized neutron flux versus radial distance.	2-199
2-116	Normalized neutron flux versus axial distance.	2-200
2-117	Floor plan of University of Texas reactor laboratory complex.	2-204
3-1	Outline of data requested from FXR facilities.	3-2
3-2	Total output beam energy, E, versus charging V (V_{dc}) for the FEBETRON 705/tube 545C.	3-5
3-3	Beam energy, E, and energy density (fluence), W_o, at the tube face versus focusing field, H, at 8 kV for the FEBETRON 705/tube 545A.	3-6
3-4	Pulse-to-pulse repeatability test for the FEBETRON 705/ tube 545C.	3-7

LIST OF ILLUSTRATIONS (Continued)

Figure		Page
3-5	Electron-beam intensity profile in plane 0.5 in. from tube face for the FEBETRON 705/tube 545C.	3-8
3-6	Beam energy density profiles for various operating conditions for the FEBETRON 705.	3-8
3-7	Diameter of "useful beam" (energy density at edges equal to 80% of maximum energy density at center) versus beam energy density on axis for the FEBETRON 705.	3-9
3-8	Beam energy fluence, W_0, versus distance, r, from tube face.	3-9
3-9	Energy fluence, W_0, versus distance, r, from window for FEBETRON 705/tube 545D.	3-10
3-10	Electron-beam energy fluence map for the FEBETRON 705/ tube 545C.	3-11
3-11	Applied tube V, $V_a(t)$, and output beam I, $I_0(t)$, at 35-kV charging V for the FEBETRON 705/tube 545C.	3-12
3-12	Output beam power waveform, $P_0(t)$, at 35-kV charging V for the FEBETRON 705/tube 545C.	3-13
3-13	Energy spectrum determination for the FEBETRON 705/tube 545C.	3-14
3-14	Time-resolved electron energy spectrum for the FEBETRON 705/ tube 545C.	3-14
3-15	Integral electron energy spectrum Q(V)/Q for the FEBETRON 705/ tube 545C.	3-15
3-16	Dose versus depth in Al at 4 in. from tube face, versus charging V for the FEBETRON 705/tube 545C.	3-15
3-17	Dose deposition in several materials for FEBETRON 705 incident beam.	3-16
3-18	Dose deposition in several materials for FEBETRON 705 incident beam.	3-17
3-19	X-ray exposure map (in R) for FEBETRON 705/tube 545C, 30- and 35-kV incident beams.	3-18
3-20	X-ray exposure per pulse versus distance from x-ray target for the FEBETRON 705.	3-19
3-21	Angular distribution of x-ray exposure at large distances from the target for the FEBETRON 705.	3-20
3-22	Diameter of circular area which can be irradiated with uniformity versus exposure at center of area for a FEBETRON 705/tube 545C.	3-21
3-23	X-ray dose rate waveform for the FEBETRON 705/tube 545C.	3-22

LIST OF ILLUSTRATIONS (Continued)

Figure		Page
3-24	Estimated x-ray energy spectrum for the FEBETRON 705.	3-23
3-25	Waveform of transmitted electron I.	3-24
3-26	Measured electron dose versus depth in thick Al absorber 0.5 in. from the tube face.	3-26
3-27	Energy density profiles across the beam.	3-26
3-28	Beam energy density near the axis as a function of distance from tube face.	3-27
3-29	Map of electron beam in region near the tube window.	3-27
3-30	Electron dose versus depth in Al at 0.5 in. from 5515 tube face.	3-28
3-31	Energy-density profiles of 2 tubes in a plane 0.125 in. from the tube face.	3-28
3-32	Beam-energy density versus distance from tube face in air and in a vacuum.	3-29
3-33	X-ray penetration of Model 5515 tube.	3-30
3-34	X-ray dose versus distance for Model 5515 tube.	3-30
3-35	Plan view of Northrop reactor facility.	3-32
3-36	Northrop Research and Technology Center 2.3-MV FXR facility.	3-33
3-37	Typical electron-beam response of the Northrop FEBETRON 705.	3-34
3-38	TLD fixture positions for Northrop FEBETRON 705/tube 545C x-ray beam map.	3-35
3-39	Typical x-ray response of the Northrop FEBETRON 705/tube 545C.	3-36
3-40	Extracted beam energy of Kaman Sciences FEBETRON 705, electron-beam mode.	3-38
3-41	Normalized typical beam energy density contour (measured at 1 cm from anode) of Kaman Sciences FEBETRON 705, electron-beam mode.	3-39
3-42	Center-line beam energy density (typical) for Kaman Sciences FEBETRON 705/tube 545A, electron-beam mode.	3-40
3-43	Instantaneous beam power for Kaman Sciences FEBETRON 705/tube 545A, electron-beam mode.	3-40
3-44	Electron energy spectrum N(E) for Kaman Sciences FEBETRON 705/ tube 545A.	3-41
3-45	Normalized deposition in metals for Kaman Sciences FEBETRON 705/tube 545A, electron-beam mode.	3-41
3-46	Dose per pulse for Kaman Sciences FEBETRON 705/tube 545A, FXR mode.	3-43

LIST OF ILLUSTRATIONS (Continued)

Figure		Page
3-47	Dose contours, rad(Si), for Kaman Sciences FEBETRON 705/tube 545A, FXR mode.	3-43
3-48	Nominal dose rate for Kaman Sciences FEBETRON 705/tube 545A, FXR mode.	3-44
3-49	Photon spectrum for Kaman Sciences FEBETRON 705/tube 545A, FXR mode.	3-44
3-50	Lockheed FEBETRON 705 V waveforms.	3-46
3-51	Lockheed FEBETRON 705 bremsstrahlung waveform.	3-46
3-52	FXR pulse from FEBETRON 706. (#3060 detector at 50-cm distance on tube axis. Scales: 5 V/div, 2 ns/div.)	3-47
3-53	FX-35 beam mapping.	3-51
3-54	Pressure dependence of electron-beam energy monitored calorimetrically 20 cm from entrance window.	3-52
3-55	FX-35 bremsstrahlung traces.	3-52
3-56	FX-35 electronic-trigger performance.	3-53
3-57	FX-35 beam map.	3-54
3-58	FX-35 V and I pulses.	3-55
3-59	FX-35 electron-beam energy spectrum.	3-56
3-60	FX-35 electron-beam energy spectrum.	3-56
3-61	FX-35 electron-beam spectrum.	3-57
3-62	FX-35 electron-beam spectrum.	3-57
3-63	Time-resolved spectral measurements on FX-35.	3-58
3-64	2.0-MeV electron-beam energy deposition profile in Al for FX-35.	3-58
3-65	FX-35 exposure map.	3-59
3-66	FX-35 bremsstrahlung spectrum.	3-60
3-67	BREL FXR facility.	3-64
3-68	Typical fluence distribution curve.	3-65
3-69	Oscilloscope traces of 10 consecutive bremsstrahlung output pulses.	3-67
3-70	Composite magnetic field level in the BREL x-ray room (non-shielded room).	3-68
3-71	Composite electric field level in the BREL x-ray room (non-shielded room).	3-68

LIST OF ILLUSTRATIONS (Continued)

Figure		Page
3-72	Oscilloscope traces of electron-beam V and I.	3-70
3-73	Electron-beam spectra for 2 typical operating configurations.	3-71
3-74	Energy deposition profiles for FX-75 electron beam.	3-71
3-75	X-ray exposure map at 6.5-MV charging V (far field).	3-72
3-76	X-ray exposure rate map at 6.5-MV charging V (far field).	3-72
3-77	X-ray exposure map at 6.5-MV charging V (near field).	3-73
3-78	X-ray exposure rate map at 6.5-MV charging V (near field).	3-73
3-79	X-ray exposure map at 5.0-MV charging V (far field).	3-74
3-80	X-ray exposure rate map at 5.0-MV charging V (far field).	3-74
3-81	X-ray faceplate field map.	3-75
3-82	X-ray dose versus distance from tube face for the BREL FX-75.	3-76
3-83	Oscilloscope traces of bremsstrahlung pulse output.	3-77
3-84	Bremsstrahlung pulse output.	3-77
3-85	X-ray deposition for the BREL FX-75.	3-78
3-86	HIFX facility layout.	3-82
3-87	Detailed layout of HIFX exposure area, instrument room, and control room.	3-82
3-88	Electron-beam energy density versus position (total absorbing Cu calorimeter).	3-84
3-89	V, I, and R traces for high-impedance electron mode (Y scale as labelled; X scale: 20 ns/div).	3-85
3-90	HDL FX-45 electron-beam energy spectrum.	3-86
3-91	Electron energy spectra for high-impedance mode based on V and I monitor traces.	3-87
3-92	HFIX depth-dose profiles.	3-88
3-93	Low-impedance mode fluence versus axial position.	3-89
3-94	High-resolution fluence distribution maps for low-impedance mode electron beams.	3-90
3-95	V and I monitor traces for low-impedance mode.	3-91
3-96	V and I monitor traces for low-impedance mode.	3-92
3-97	Electron energy spectra for low-impedance mode based on V and I monitor traces.	3-93
3-98	X-ray angular distribution in the vertical plane.	3-95

LIST OF ILLUSTRATIONS (Continued)

Figure		Page
3-99	Oscilloscope traces of HDL FX-45 x-ray waveforms (photodiode scintillator measurements; time scale is 10 ns/cm).	3-96
3-100	X-ray waveform from Compton diode.	3-97
3-101	Calculated bremsstrahlung spectrum.	3-98
3-102	Application for use of HDL-HIFX facility.	3-100
3-103	Schematic shape of time-integrated electron energy spectra.	3-103
3-104	Electron deposition depth and peak energy deposition versus mean electron energy.	3-103
3-105	Characteristic shape of flash-bremsstrahlung spectra produced by pulsed electron accelerators.	3-104
3-106	Approximate bremsstrahlung yield from conventional Ta converters.	3-104
3-107	Total diode energy versus tube V and mean electron energy, OWL II.	3-108
3-108	Typical electron energy deposition profiles for OWL II.	3-109
3-109	Electron environment characterization of the OWL II small-area beam system, for 50-kJ diode energy.	3-110
3-110	OWL II small-area beam system fluence uniformity statistics. (Calorimetry data from 6 pulses are represented. Each "case" is 1 calorimeter block's fluence reading on 1 pulse, relative to that pulse's mean fluence value. A total of 125 cases are included.)	3-110
3-111	Fluence uniformity on OWL II large-area beam system.	3-111
3-112	Normalized fluence versus distance from cathode, OWL II large-area beam system.	3-112
3-113	Fluence versus target position, 1150 Pulserad. (Peak diode V, 5 MV; chamber pressure, 0.70 torr N_2; 7.6-cm-dia. C cathode. Each circle represents mean fluence in 9-cm^2 area at beam center, an average of nine 1-cm x 1-cm calorimeter block readings.)	3-114
3-114	Energy deposition profiles from 1150 Pulserad.	3-115
3-115	On-axis dose as a function of distance from target, 1150 Pulserad.	3-115
3-116	Dose profile across tube face, 1150 Pulserad.	3-116
3-117	Angular distribution of x-ray intensity at 0.5 m, 1150 Pulserad.	3-116
3-118	Dose profile showing lines of equal dose, 1150 Pulserad.	3-117

LIST OF ILLUSTRATIONS (Continued)

Figure		Page
3-119	Faceplate dose contours for torus cathode.	3-117
3-120	BSPEC calculation of thick-target γ-spectrum, including self-absorption in Ta converter, 1150 Pulserad at 5-MeV peak electron energy.	3-118
3-121	γ-spectrum of Figure 3-120 computationally transmitted through 0.5-in. Al.	3-118
3-122	Typical V and Faraday-cup waveforms for a low-V shot, 1150/LPG Pulserad.	3-119
3-123	Typical Al spectrum at 3.5 TW on PITHON.	3-120
3-124	V and I traces, 225W Pulserad.	3-121
3-125	BLACKJACK 3 magnetic field profile used for materials testing.	3-129
3-126	Electron beam potential and I waveforms for shot 1632 (the inductive V drop has been subtracted from the diode envelope potential).	3-130
3-127	Representative electron beam spectrum.	3-131
3-128	Measured depth dose in C for Shot 1629.	3-131
3-129	Electron beam potential I and power for BLACKJACK 3 shot #1534.	3-133
3-130	Electron energy spectrum for BLACKJACK 3 shot #1534.	3-134
3-131	PIN diode signal measured on Shot #1536.	3-135
3-132	Comparison between the calculated bremsstrahlung spectra for BLACKJACK 3 shots 1530, 1534, and 1543.	3-136
3-133	VULCAN facility floor plan.	3-143
3-134	VULCAN dose map, 90-kV charge.	3-145
3-135	VULCAN dose map, 80-kV charge.	3-146
3-136	VULCAN dose map, toroidal cathode.	3-146
3-137	VULCAN pulse shape.	3-147
3-138	VULCAN equilibrium thickness study.	3-147
3-139	High-impedance diode x-ray pulse shape.	3-155
3-140	High-impedance diode electron energy spectrum.	3-157
3-141	High-impedance diode electron beam transport to 88.9-cm drift chamber position.	3-158
3-142	High-impedance diode electron-beam energy transport at 400-torr drift tube pressure.	3-159
3-143	High-impedance diode electron-beam profiles at 400-torr drift tube pressure.	3-161

LIST OF ILLUSTRATIONS (Continued)

Figure		Page
3-144	Dose depth profiles in Be.	3-162
3-145	Center line fluence versus axial distance from the focusing cone.	3-163
3-146	Fluence versus radial position.	3-164
3-147	HERMES II high-impedance diode electron-beam depth-dose curves measured in the atmospheric focusing cone and calculated (incident fluence is approximately 80 cal/cm^2).	3-164
3-148	High-impedance diode x-ray dose per pulse as a function of distance from tube surface.	3-166
3-149	Transverse high-impedance diode bremsstrahlung dose profiles.	3-167
3-150	HERMES II high-impedance diode isodose curves.	3-168
3-151	HERMES II high-impedance diode photon spectrum.	3-170
3-152	Pinched-beam mode x-ray dose per pulse as a function of distance from tube surface.	3-171
3-153	Transverse pinched beam bremsstrahlung dose profiles.	3-172
3-154	Enhanced bremsstrahlung mode isodose contours.	3-173
3-155	Beam power output waveform.	3-175
3-156	Contour map of REBA beam at 22.5-torr pressure.	3-176
3-157	Beam profiles at experiment location.	3-177
3-158	Total beam energy versus rear-cone pressure.	3-180
3-159	Average fluence near beam center line versus rear-cone pressure.	3-180
3-160	REBA electron energy spectrum.	3-181
3-161	REBA energy deposition profile in Fe.	3-182
3-162	REBA energy deposition profile in Mo.	3-182
3-163	Low-impedance diode power output waveform.	3-184
3-164	Low-impedance diode electron energy spectrum (with B_θ sensor).	3-184
3-165	High-impedance diode dose/pulse as a function of distance from the tube surface.	3-186
3-166	Photon beam profiles normal to diode axial center line.	3-187
3-167	Photon beam large-scale profiles normal to the diode axial center line.	3-188
3-168	Photon dose rate versus time.	3-189

LIST OF ILLUSTRATIONS (Continued)

Figure		Page
3-169	REBA high-impedance x-ray mode photon spectrum.	3-190
3-170	Long-pulse-diode V and I waveforms.	3-191
3-171	Long-pulse beam power waveform.	3-191
3-172	Long-pulse photon dose rate versus time.	3-193
3-173	REBA photon output versus time (Compton diode monitor output normalized to unity peak).	3-195
3-174	Internal pinched-beam x-ray mode photon energy spectrum (forward 30 degrees). (Anode-cathode gap spacing is 7.62 cm and the anode is a 0.051-Ta converter (0.051-cm Ta, 0.823-cm C, and 0.051-cm Al).)	3-196
3-175	REHYD PIN diode pulse shape.	3-198
3-176	Electron-beam energy spectrum.	3-200
3-177	Total-beam energy.	3-200
3-178	Calculated REHYD photon energy spectrum for Shot No. 282.	3-201
3-179	REHYD x-ray spectra along forward-directed normal to converter for energies less than 0.2 MeV (normalized to 1.0 keV/sr-electron).	3-203
3-180	REHYD x-ray spectra along forward-directed normal to converter for energies greater than 0.1 MeV (normalized to 1.0 keV/sr-electron).	3-203
3-181	Map of Sandia Laboratories Technical Area V.	3-204
3-182	HERMES II facility area in Building 6596.	3-205
3-183	Detail plan view of HERMES II test cell and inset showing an elevation view.	3-206
3-184	REBA facility area in Building 6596.	3-208
3-185	Detailed plan view of REBA test cell.	3-209
3-186	Layout of REHYD and north radiation cell.	3-211
3-187	Faceplate dose distribution.	3-221
3-188	Dose levels on axis.	3-222
3-189	Isodose curves for 60-kV charging V.	3-223
3-190	Isodose curves for 80-kV charging V.	3-224
3-191	Isodose curves for 95-kV charging V.	3-225
3-192	X-ray pulse shapes.	3-226
3-193	Measured energy deposition profile in Al.	3-227

LIST OF ILLUSTRATIONS (Continued)

Figure		Page
3-194	AURORA facility floor plan.	3-230
3-195	Test cell and data room.	3-231
3-196	Isodose contours in the test cell.	3-236
3-197	Detailed isodose contours in 0- and 45-degree R-Z planes.	3-237
3-198	Detailed isodose contours in Z = 0- and 25-cm planes.	3-237
3-199	AURORA bremsstrahlung spectrum.	3-238
3-200	FXR facility layout.	3-242
3-201	Oscilloscope traces of electron-beam output waveform, V and I.	3-244
3-202	Electron beam spectrum with 3/8-in. cathode at 3.3 MV charging V.	3-245
3-203	Electron beam spectrum with 2-in. cathode at 3.3 MV charging V.	3-246
3-204	Depth dose with 3/8-in. cathode at 3.3 MV for stack of Al foils.	3-248
3-205	Depth dose with 2-in. cathode at 3.3 MV for stack of Fe foils.	3-249
3-206	Total dose versus distance along centerline.	3-250
3-207	Radial dose distribution at 40 cm distance (collimated) (dimensions in cm).	3-251
3-208	Dose distribution, horizontal plane.	3-252
3-209	Bremsstrahlung output pulses.	3-252
3-210	Honeywell FX-25 computed spectrum.	3-253
3-211	Raytheon Radiation Laboratory.	3-256
3-212	Pulsed electron-beam energy spectrum (normal mode).	3-259
3-213	Pulsed electron-beam energy spectrum (low-Z mode).	3-259
3-214	Dose spatial distribution for FX-25.	3-260
3-215	Radiation pulse profile, FX-25 (T = 10 ns/div).	3-261
3-216	GE FX-25 laboratory layout.	3-266
3-217	FX-25 electron-beam map (longitudinal).	3-268
3-218	Typical beam profile.	3-268
3-219	Pulse shape, electron-beam mode.	3-269
3-220	Electron energy spectrum of GE FX-25 unit.	3-269
3-221	Measured depth-dose data.	3-270
3-222	FX-25 x-ray dose map.	3-272

LIST OF ILLUSTRATIONS (Continued)

Figure		Page
3-223	Pulse shape, x-ray mode.	3-272
3-224	FX-25 bremsstrahlung spectrum.	3-273
3-225	Outline of CASINO simulator.	3-275
3-226	Typical CASINO photodiode output time history.	3-276
3-227	CASINO facility.	3-277
4-1	Data requested from organizations with LINAC facilities.	4-2
4-2	Beam mapping with 1/4-in. Al scatterer and 30-MeV electrons.	4-7
4-3	Beam mapping with 1/8-in. Al scatterer and 30-MeV electrons.	4-7
4-4	Beam mapping using 1/8-in. Al scatterer and 21-MeV electrons.	4-3
4-5	Beam mapping using 1/8-in. Al scatterer and 13-MeV electrons.	4-8
4-6	Beam loading characteristics.	4-12
4-7	LINAC laboratory floor plan.	4-16
4-8	BREL LINAC beam loading characteristics.	4-20
4-9	BREL LINAC electron-beam pulse shapes.	4-20
4-10	Theoretical electron and bremsstrahlung exposure rates as a function of distance from beam port.	4-22
4-11	Thick target bremsstrahlung energy-angle distribution.	4-23
4-12	Fast neutron (E > 3 MeV) flux density in permanent-damage test fixture.	4-24
4-13	Differential neutron spectrum.	4-25
4-14	Energy range for reactions used to obtain neutron spectrum (only 5% of the foil's total response lies above, and 5% below the energy indicated).	4-26
4-15	BREL LINAC bremsstrahlung.	4-27
4-16	NWEB LINAC pulse shape.	4-31
4-17	NWEB LINAC pulse shape.	4-31
4-18	Beam loading characteristics.	4-32
4-19	Exposure rate for electrons.	4-33
4-20	Exposure rate for x-rays.	4-33
4-21	Electron energy spectrum (21.7-MeV peak, values good to ±3% of peak value).	4-34
4-22	Electron energy spectrum (17.5-MeV peak, values good to ±3% of peak value).	4-34

LIST OF ILLUSTRATIONS (Continued)

Figure		Page
4-23	Maximum accelerated beam I.	4-40
4-24	Effect of electron energy on beam divergence, standard window, 100 cm, zero port.	4-41
4-25	Axial bremsstrahlung intensity from 0.15 radiation length Au-W target filtered by 1.125 in. of Al.	4-42
4-26	Bremsstrahlung angular distribution for 0.15 radiation length Au-W target with 1.125-in. Al filter.	4-43
4-27	Calculated bremsstrahlung spectra for LINAC target.	4-44
4-28	Neutron energy spectra produced by 20.5-MeV bremsstrahlung incident on D_2O target.	4-45
4-29	LINAC facility floor plan.	4-46
4-30	Beam loading characteristics.	4-53
4-31	Radiation pulse waveform.	4-54
4-32	Radiation pulse waveform (short pulse).	4-54
4-33	Radiation pulse waveform (10 pulses).	4-54
4-34	Intensity versus distance from target.	4-63

LIST OF TABLES

Table		Page
2-1	Reactivity worth of experimental assemblies and reflectors.	2-2
2-2	Outline of data requested from pulse reactor facilities.	2-4
2-3	SPR-III free-field pulse performance characteristics (dose and dose rates in the glory hole).	2-7
2-4	Measured SPR-III neutron spectrum (central cavity, horizontal and vertical center line, free-field).	2-15
2-5	Key APRF performance data.	2-20
2-6	APRF reactor leakage neutron spectrum.	2-33
2-7	APRF reactor leakage photon spectrum.	2-34
2-8	APRF 90-group leakage neutron spectrum.	2-35
2-9	Neutron threshold detectors.	2-49
2-10	Neutron fluence > 3.0 MeV per 1.0 x 10^{16} fissions (24.3°C ΔT) on 6-in. horizontal circle.	2-50
2-11	Neutron fluence > 3.0 MeV per 1.0 x 10^{16} fissions (24.3°C ΔT) on 1-m horizontal circle.	2-51
2-12	Vertical traverse of neutron fluence > 3.0 MeV per 1.0 x 10^{16} fissions (24.3°C ΔT) at 1 m from reactor center.	2-52
2-13	Neutron fluence > 3.0 MeV per 1.0 x 10^{16} fissions (24.3°C ΔT) as a function of radial distance from core center, indoor.	2-53
2-14	Neutron fluence > 3.0 MeV per 1.0 x 10^{16} fissions (24.3°C ΔT) as a function of radial distance from core center, outdoor.	2-54
2-15	Neutron fluence above various threshold energies per 1.0 x 10^{16} fissions (24.3°C ΔT) on four vertical traverses 1 m from core center, indoor.	2-55
2-16	Neutron fluence above various threshold energies per 1.0 x 10^{16} fissions (24.3°C ΔT) on four vertical traverses 1 m from core center, outdoor.	2-56
2-17	Neutron fluence above various threshold energies per 1.0 x 10^{16} fissions (24.3°C ΔT) as a function of radial distance from core center, indoor.	2-57
2-18	Neutron fluence above various threshold energies per 1.0 x 10^{16} fissions (24.3°C ΔT) as a function of radial distance from core center, outdoor.	2-58
2-19	Neutron energy spectrum as a function of radial distance from reactor center expressed in percent of neutrons above threshold energy and normalized to 100% above 10 keV.	2-59

LIST OF TABLES (Continued)

Table		Page
2-20	γ dose per 1.0 x 10^{16} fissions (24.3°C ΔT) on 6-in. horizontal circle.	2-73
2-21	γ dose per 1.0 x 10^{16} fissions (24.3°C ΔT) on 1-m horizontal circle, indoor.	2-74
2-22	γ dose per 1.0 x 10^{16} fissions (24.3°C ΔT) on 1-m horizontal circle, outdoor.	2-75
2-23	γ dose per 1.0 x 10^{16} fissions (24.3°C ΔT) vertical traverse at 1 m from reactor axis.	2-76
2-24	γ dose per 1.0 x 10^{16} fissions (24.3°C ΔT) as a function of radial distance from core center, indoor.	2-77
2-25	γ dose per 1.0 x 10^{16} fissions (24.3°C ΔT) as a function of radial distance from core center, outdoor.	2-78
2-26	Utilities available at the reactor cell.	2-83
2-27	Dosimetry equipment and instrumentation for the FBR.	2-84
2-28	Neutron fluences.	2-90
2-29	γ dose, rad (H_2O).	2-90
2-30	Relative fluence profile 15 in. from reactor center line.	2-97
2-31	Neutron spectrum at external position 1 in. above shroud on vertical center line.	2-101
2-32	Glory hole neutron spectrum.	2-101
2-33	n/γ ratios (10^9 n/cm^2-γ rad (H_2O)).	2-101
2-34	Preliminary Monte Carlo calculations of the Super Kukla neutron spectrum made by LLL utilizing the Sors-Alpha code (date: September 1967).	2-112
2-35	Experimental neutron spectrum and γ dose measurements.	2-113
2-36	Threshold detector results.	2-114
2-37	Northrop reactor performance data.	2-120
2-38	n/γ ratio for various irradiation positions.	2-132
2-39	Description of environment.	2-137
2-40	Dosimetry values for the TRIGA Mark I reactor (70 fuel elements, $3.00 reactivity insertion).	2-147
2-41	Dosimetry values for the TRIGA Mark I reactor at core center line in air-filled tube at outside edge of graphite reflector ($\bar{E}_n$ = 1.22 MeV) (70 fuel elements; $3.00 reactivity insertion).	2-147

LIST OF TABLES (Continued)

Table		Page
2-42	TRIGA Mark I reactor performance for 250-kW steady-state and 1,000-MW pulsing operation (experimental dosimetry values for a typical core loading of 70 fuel elements).	2-148
2-43	Air-filled J-tube dosimetry data ($\bar{E}_n$ = 0.79 MeV).	2-153
2-44	In-core dosimetry values for the ATPR ($4.00 reactivity insertion and 100 fuel elements).	2-154
2-45	Advanced TRIGA prototype reactor performance for 1.5-MW steady-state and 6,400-MW pulsing operation (experimental dosimetry values for a typical core loading of 94 fuel elements).	2-156
2-46	ACPR radiography facility specifications.	2-180
2-47	Thermal column fluxes.	2-188
2-48	Thermal neutron and γ fluxes in the fast rabbit tubes.	2-191
3-1	706 system electron-beam output specifications.	3-25
3-2	706 system x-ray output specifications.	3-25
3-3	Northrop FEBETRON 705/tube 545C x-ray beam map.	3-35
3-4	Operating characteristics of FX-35.	3-50
3-5	Performance characteristics of FX-35 in electron-beam mode.	3-55
3-6	Calculated values of the beam energy as a function of charging V for HDL FX-45.	3-83
3-7	Beam geometry for HDL FX-45.	3-83
3-8	Summary of pulsed electron-beam generator characteristics.	3-102
3-9	Typical electron beams, OWL II generator.	3-108
3-10	Sample electron beams from the 1150 Pulserad.	3-114
3-11	Pulserad 225W total diode energy versus mean electron energy (assuming matched load).	3-122
3-12	Representative Pulserad 225W electron environment parameters.	3-122
3-13	Radial dose variation from BLACKJACK 3.	3-133
3-14	Conduit routing.	3-149
3-15	Committed instruments, instrumentation screen room.	3-150
3-16	Pinched-beam x-ray mode data synopsis.	3-194
3-17	REHYD performance characteristics with MOD II diode configuration and advanced converter assembly.	3-201
4-1	Environment output characteristics.	4-6

LIST OF TABLES (Continued)

Table		Page
4-2	Types of dosimetry used.	4-15
4-3	BREL LINAC operating characteristics.	4-19
4-4	BREL LINAC environment characteristics.	4-21
4-5	AFFRI LINAC specifications.	4-49
4-6	Electronic equipment.	4-56
4-7	Instrument cabling.	4-57
4-8	Dosimetry available at LMTA.	4-57
4-9	RPI LINAC typical operating conditions.	4-62

SECTION 1

INTRODUCTION

This document is one of a series of Defense Nuclear Agency (DNA) publications on Transient Radiation Effects on Electronics (TREE). Its purpose is to bring together, in one volume, quantitative data which characterize simulation facilities suitable for TREE experimental studies.

This is the second revision of TREE Simulation Facilities. This revision consists of updating of facility descriptions, adding new facilities, expanding the descriptions where more data are available, and deleting the descriptions of facilities which have become inactive.

Data were obtained by corresponding with personnel at the individual facilities. Requests were made for information that would quantitatively characterize the simulation environment generated. The degrees of effort and concern of the personnel at the facilities to generate and document quantitative characterizing data varied. In the acceptance and interpretation of data, it should be kept in mind that uncertainties exist in measurement techniques even though they are not pointed out or explicitly acknowledged. Every effort has been made to faithfully and accurately present the characterizing data as submitted.

Facilities characterized in this volume utilize pulsed reactors, flash x-ray (FXR) machines, and electron linear accelerators (LINACs). Overall characteristics of each of the 3 types of simulation machines, along with outlines of the data requested from the facilities, are given in the introductions to the individual sections that follow.

There are four basic considerations to act upon when planning an experiment at a TREE Simulation Facility: (1) determine what needs to be measured and how to measure it, (2) plan the experiment in detail, (3) select the simulation facility or facilities and review the experiment with the facility staff, and (4) try to find any flaws in the experiment.

The TREE Handbook and TREE Preferred Procedures, published by DNA, are recommended references. The TREE Handbook is intended to provide information useful in designing and evaluating electronic equipment that is expected to be exposed to the radiation environment produced by a nuclear-weapon burst. This Handbook is directed toward individuals responsible for hardening electronic equipment to withstand the transient-radiation environment. It is not intended to satisfy all the needs of the experimentalist, vulnerability analyst, manager, or planner.

The information in the TREE Handbook can be categorized as follows:

1. Supporting information
2. Environmental information

3. Information on the effects of radiation on electronic materials and devices

4. Circuit considerations

5. System considerations.

Supporting information includes sections that explain the terms used in the Handbook, compare the simulated and nuclear-weapon-burst environments, explain the interaction of γ-rays, x-rays, and neutrons with matter, and list references containing additional information on transient radiation effects.

The TREE Preferred Procedures provides persons conducting TREE experiments with recommended procedures that experience has shown are efficient for determining transient radiation effects on electronic parts. The recommendations in this document are a consensus of current good practice arrived at after careful review by a limited group of individuals outstanding in the field of transient radiation effects. The object has been to formulate and recommend procedures by which radiation-test data on electronic components and radiation environments may be obtained and reported. This document contains sections on testing diodes, transistors, capacitors, microcircuits, and medium-scale integration/large-scale integration (MSI/LSI). In addition, valuable discussions on experimental design, radiation facilities, and dosimetry and environmental correlation are included.

The TREE Handbook and TREE Preferred Procedures were prepared as an integral part of a series of documents sponsored by DNA to assist and guide the TREE community. Other documents in this series include the DNA EMP Handbook, Nuclear Environment Descriptions, and a Management Guide to TREE. Initial distribution of these documents is to a DNA distribution list. Supplemental distribution is via the Defense Documentation Center, Cameron Station, Alexandria, VA 22314. Most Department of Defense (DoD) contractors working in the TREE area have one or more copies of these documents. Copies are usually held by a company's technical library or by senior staff members working in the TREE area (e.g., see the distribution list at the end of this document).

The experimental plan or design is to specify what must be done, why it must be done, and how it must be done to obtain information of the required accuracy and precision. This is probably the most important function since the running of the experiment frequently can be performed by a competent technician once an experiment is properly designed. The design is a dynamic document which will change as the experiment evolves to its optimum form. The design must be done in detail and should consider all significant variables and their effect on the results. This document also provides an effective means to communicate requirements to the simulation facility operators, an opportunity to critique the experiment, and it forces the experimenter to think through his experiment in detail and take into consideration all possible contingencies.

Assistance in selecting a simulation facility is the primary reason for the existence of this Handbook. Selecting the facility to be used must be done early in the planning stage of the experiment since this will affect the experimental design.

A portion of Section 4.0 of the TREE Preferred Procedures, "Radiation Facilities," is reproduced here:

General Considerations

The need for simulation of a given radiation environment to produce a predetermined effect requires careful source selection. The obvious parameters to be considered are, of course, cost, radiation type (generally photons, neutrons, or electrons for TREE work), energy spectrum, and time dependence. Other considerations, possibly less obvious at first glance but requiring attention from a practical standpoint, are listed below under Operational Considerations, though not necessarily in order of importance.

Within the scope of this Preferred Procedures document, there are basically two types of device responses of interest: transient response (typically, photocurrents generated in the bulk material) and permanent response (damage either in the bulk or surface of the devices). The basic test-environment requirements for these responses are given below.

Transient-Response Considerations

Transient responses typically result from photocurrents introduced through ionization phenomena due primarily to photon irradiation. However, neutron ionization can also cause photocurrents of interest. Therefore, a pulsed source of ionizing radiation in most cases is desirable having (1) rise and fall times short compared to diffusion times and long enough and with controllable pulse-length capabilities to achieve equilibrium photocurrent in the device under test; (2) sufficient intensity to produce the required range of dose rates in the device (i.e., to obtain data both where I_{pp} is linear with dose rate and at the high rates where nonlinearities appear); (3) sufficiently energetic photons or electrons to penetrate the case of the device and produce a uniform dose throughout the active volume; (4) an energy spectrum sufficiently well-known so that the dose rate in the active volume can be accurately determined by standard methods; and (5) spurious RF noise low enough to avoid confusion of effects. These are ideal characteristics and are not to be found in any one pulsed source.

Many LINAC's and flash x-ray machines closely approximate these criteria if proper precautions are taken. The LINAC has the advantages of variable and long pulse width and better-controlled beam diameter, position, intensity, and shot-to-shot performance. The flash x-ray facility has the advantage of larger irradiation-volume capability for tests on several devices simultaneously.

There are two other transient responses of devices which can be of concern with some systems and which therefore need to be briefly mentioned. The first response results from short-term annealing of bipolar transistor gain. Because transistor-gain degradation is primarily caused by neutrons, a pulsed source of neutrons with sufficient fluence ($>10^{12}$ n/cm^2) and short duration (depending on response times of interest) is needed. The appropriate pulse width for characterizing this effect will depend upon the system specification to be applied to the part being characterized.

Second, a transient response attributable to surface effects has been observed in some devices. Sources of ionizing radiation with pulse widths that are short with respect to the response times of interest should be used to evaluate the influence of this effect on device response.

Permanent-Response Considerations

Permanent responses of devices are attributed to physical-property changes which can persist for long periods of time as compared to the measurement circuit response time. For this document, permanent responses can be grouped into two categories: bulk and surface effects. The bulk effects are due to lattice displacements in the bulk of the material induced by high-energy radiation, primarily neutrons. Surface effects are primarily due to ionizing radiation causing changes in the surface conditions of the bulk material. Therefore, for permanent bulk-damage type of experiments, a neutron source is desirable having (1) sufficient fluence of energetic particles at the experiment position to produce, in reasonable experiment times, the desired bulk damage; (2) a spectrum sufficiently well-known to allow characterization of the spectrum in standard terms by standard methods; and (3) a known n/γ ratio that is high enough so that any effects due to the γ radiation are negligible in comparison with neutron-induced effects.

Pulsed reactors, some steady-state reactors, and some accelerator-generated neutron sources meet these criteria. Accelerator-generated neutrons may have the energy distribution of a fission spectrum if they are generated in the photofission process, or they may be nearly monoenergetic if a fusion reaction such as the $H^3(d,n)He^4$ reaction is used. There are also sources utilizing a plasma of deuterium and tritium gases which generate 14-MeV neutrons.

For permanent-surface-effect types of experiments, a source of ionizing radiation that produces a minimal amount

of bulk damage is necessary. For electrons in silicon, energies less than about 150 keV meet this requirement. However, if the total dose is less than about 10^6 rad(Si), bulk damage is negligible and higher energy radiations may be utilized. Isotope sources, ion accelerators, LINACs, and flash x-ray machines all can meet these criteria.

Once the test engineer has decided upon the type of radiation facility that he should use, the selection must be made of the particular facility which will permit him to attain his experimental objective with the resources at his command. The determining factors in this decision are the operational considerations. Operational considerations are those factors which can only be determined by the test engineer, usually after he has partially completed his experimental design. They depend upon such factors as the funds he has available, his own expertise as an experimenter in TREE effects, the physical dimensions of his experiment, and the accuracy and precision required to obtain his experimental objectives. At this time, a careful review of Section 2.5 of the TREE Preferred Procedures, "Experimental Hardware Considerations/ Techniques," may be helpful.

One obvious consideration is the cost of using the facility, including rental fees and transportation of personnel and equipment to the facility. This may be related to the support capabilities available at the radiation facility. Costs for using a facility can be obtained by contacting the facility and discussing your requirements with them. This is best left until after the preliminary experimental design is completed. For a small low-budget experiment, investigate the possibility of piggy-backing it on another larger experiment. This is possible when the experimental conditions of the larger experiment and the experimenter are agreeable to such an arrangement.

Other things to consider are:

1. If an experiment requires less than a whole day to complete, will the experimenter be charged for a whole day's use of the facility?
2. How flexible is the facility's staff if the experiment requires work during other than routine business hours?
3. Does the facility have a staff experienced in TREE testing available for consultation?
4. How much assistance will the staff of the facility be able to provide to the experimenter?
5. Will adequate (quality or quantity) test equipment be available at the facility or will the experimenter have to provide it himself?
6. What dosimetry services can the facility provide?

7. Can an outside vendor be used to provide supplemental dosimetry services for redundancy?

8. The problems of remote operation (including long-cable effects, the possible need for precision test-sample positioning, or frequent setup change) must be considered.

9. The size of the experiment with respect to the exposure area available must be considered. How uniform is the dose and/or dose rate at the location where the experiment will be performed, both across the front surface and from the front to the back of the experimental package? For experiments close to a point source it is usually necessary to prepare a jig to hold the device and dosimeters to assure that they receive the same dose. Trial calculations using the maximum positioning error of the experiment, assuming a $1/R^2$ dose dependence, will show the accuracy required in positioning the components of the experiment.

10. Are the energy spectrum and/or yield component ratio (n/γ ratio in a reactor, etc.) satisfactory?

11. Can the radiation source be pulsed by a signal from the experimenter (i.e., synchronization of the radiation pulse with an experimental equipment signal) or must the experimenter depend on a signal from the facility's operator?

12. What will be the uncertainty in knowing exactly when the pulse will occur?

13. What precautions will be necessary to protect the experiment from unwanted noise at the facility under consideration?

14. Will spurious signals, including charge scattering from the test fixtures and electromagnetic RF noise due to the radiation generator or the radiation itself, be more of a problem at one facility than at another?

15. Is a screen room available for the experimenter's use? Is it large enough for the planned experiment?

Most government-owned simulation facilities require justification as to why that facility must be used before permission to use it is granted. They also may require that the experiment be related to work on a government contract. When such authorizations involve more than one governmental agency, several weeks or even months of lead time may be necesary. If the material in an experiment becomes radioactive during irradiation, a license must be obtained to receive the specific radioisotopes that were generated. A lead time of from a few days to a few months is usually necessary when scheduling a test at a nongovernment-owned facility.

At many facilities, an experiment test plan must be submitted and approved before a firm scheduling commitment will be given. This should specify the limitations (accuracy) of what they can supply. It is the experimenter's responsibility to take these limitations into consideration in the experimental design.

SECTION 2

PULSE REACTORS

2.1 INTRODUCTION

Two types of pulse reactors are discussed in this section: the bare, all-metal, unmoderated fast type; and the water-moderated thermal TRIGA. The two types yield approximately the same total power and neutron fluence but differ in spectra, pulse width, and some other ways. Both types of reactors can be operated in either the pulse or steady-state mode.

The neutron spectrum of the bare reactors is a slightly moderated fission spectrum. Neutron lifetimes are short, resulting in a burst pulse width in the μs range. An exception is the Super Kukla (subsection 2.7). The large core size of this reactor results in a much longer prompt neutron lifetime than occurs in the smaller reactors, producing a considerably longer pulse width. The heat generated in bare reactors during a pulse limits the permissible power operating levels and the burst repetition rate which typically is of the order of 1 pulse/hr. Steady-state operation of bare reactors generally is discouraged because of the associated fission product buildup within the fuel material. Samples to be irradiated are placed near the reactor, next to the fuel material, or within the "glory hole," which is a hole running through the center of the fuel material.

TRIGA types have the reactor core suspended in a water-filled tank about 20 ft below the surface of the water. The core is a lattice of cylindrical fuel elements arranged in a right-circular cylindrical pattern. The individual elements are spaced to permit water flow throughout the core. The water serves as both a coolant for the fuel elements and as a neutron moderator. The neutron spectrum is a moderated fission spectrum with a significant thermal component. The neutron lifetimes are relatively long, producing pulse widths in the ms range. The heat generated during a burst places limits on the power which can be attained. The flow of water through the core permits fast cooling, allowing a repetition rate of many bursts per hour. TRIGA reactors can be operated in either the pulse mode or the steady-state mode at a reasonably high power level. The core is designed to accommodate the associated fission product buildup. Samples are irradiated at any of several locations in and around the core. Maximum fluence levels are near the center of the core, and samples are accommodated by removing a fuel element(s) and substituting the sample. Samples also can be placed in the pool around the outside of the reactor core. A dry environment is retained by using either a watertight tank placed in the pool or a cell-type room adjacent to the pool wall.

Samples placed in or around a reactor core exert a perturbing influence on the neutron flux, affecting the reactivity or nuclear characteristics of the reactor. For this reason, the reactivity "worth" of a particular sample placed in proximity to the core must be known. The reactivity worth of a sample is

related directly to its neutron absorption properties and, therefore, to its material composition and exposure position in the reactor. The units of measure used in describing reactivity are "dollars" ($). Where the data are available, tolerable levels of sample reactivity worth have been given in this Handbook. The worth of an experimental assembly must not exceed the tolerable level.

Sample reactivity worth must be calculated for each individual case. The data in Table 2-1 are representative of calculations made for samples placed in proximity of an enriched U 10 w/o Mo-alloy fast-burst reactor. The data are meant to be illustrative only and are not definitive.

Following Table 2-1 is the outline (Table 2-2) that was used for requesting data from the individual pulse reactor facilities. The data as reported are for specific core configurations normally used and considered typical for irradiation experiments. Because experimental samples change the spectrum and flux distribution, these data, although quantitative, are to be used only as a guide. It is recommended that, when precise environmental data are required by an experimenter, measurements be made while the experiment is performed.

As with all radiation field data, inherent uncertainties associated with radiation measurement techniques should be kept in mind.

Table 2-1. Reactivity worth of experimental assemblies and reflectors.

Description	Reactivity ($)
Missile guidance package, 35 cm in diameter at 6 cm from safety shield	0.20
Four lucite boxes (10 x 10 x 5 cm) containing Si oil and printed circuit boards arranged symmetrically around the core at 1 cm from safety shield; assorted detectors at 2.5 cm from safety shield	1.02
Two metal boxes containing semiconductors, electronic components, one B ball, and S pellets, at surface of safety shield	0.22
Three transistorized printed circuit boards arranged symmetrically around the core at 2.5 cm from safety shield	0.20
Two transistorized circuit boards, one B ball, and a dry-charge battery (25 x 20 x 5 cm) arranged symmetrically around the core at 2.5 cm from safety shield	1.09
About 50 transistors mounted on Styrofoam board having a radius of 12.7 cm. Components at about 1 cm from safety shield and surrounding 180 degrees of reactor	0.32

(continued)

Table 2-1 (continued)

Description	Reactivity ($)
One small transmitter and tower structure, one small power supply, one modulator and commutator, one battery pack, one sensor mount (thermistor and photodiode); all components at 0.5 cm from safety shield and surrounding 180 degrees of reactor.	0.85
Five transistorized printed circuit boards, 10 transistors on Styrofoam board arranged symmetrically around the core at 2 cm from safety shield; one B ball at 15.2 cm from safety shield	0.35
Boral box, inside dimensions 30.5 x 30.5 x 47.5 cm high, bottom open, top covered, box material 0.635 cm thick, contains 0.366 gm/cm^2 of B_4C, 5 cm from fuel to near surfaces of box	0.92
Four Al plates, each 20.3 x 20.3 x 1.9 cm, at 5.7 cm from fuel to near surfaces of plates	1.15
Four stainless-steel plates, each 20.3 x 20.3 x 2.54 cm, at 5 cm from fuel to near surfaces of plates	2.38
Four plywood plates, each 20.3 x 20.3 x 2.54 cm, at 5 cm from fuel to near surfaces of plates	0.71
Four lucite plates, each 20 x 20 x 1.9 cm, at 5.5 cm from fuel to near surfaces of plates	1.48
Lucite box, inside dimensions 41.3 x 41.3 cm x 61 cm high, ends open, wall thickness 1.9 cm, at 10.5 cm from fuel to near surfaces of box	1.74
Four paraffin plates, each 20 x 20 x 1.9 cm, at 5 cm from fuel to near surfaces of plates	2.25
Four water "plates" held in polyethylene bags placed in wire baskets having dimensions 20.3 x 20.3 x 2.5 cm at 8.5 cm from fuel to near surfaces of "plates"	0.95
Water "plates" identical to above and boral box, boral box placed between water and reactor fuel	1.83

Table 2-2. Outline of data requested from pulse reactor facilities.

I. Reactor Type (fast or thermal)
   A. Fast reactor
      1. Fuel
      2. Basic construction
      3. Immediate test environment
   B. Thermal epithermal reactor
      1. Fuel
      2. Reactor type/moderator
      3. Immediate test environment

II. Test Parameters
   A. Operating characteristics
      1. Power level(s) (total fission output per burst)
      2. Temperature-time profile and characteristics
      3. Available reactivity
      4. Reactivity insertion rate; pulse period
      5. Repetition rate and pulse reproducibility/predictability
   B. Environment (where appropriate, neutron data expressed as 1-MeV equivalent damage in Si)
      1. Fluence maps; neutron and γ (elevation and plan views; data to be presented as isoflux contours)
      2. Flux maps; neutron and γ (elevation and plan views; data to be presented as isoflux contours)
      3. Degree to which n/γ ratio can be varied
      4. Spectrum as function of time and position
      5. Pulse width; scope traces
      6. Background radiation levels (γ, RF, etc.)
      7. Diagnostic techniques used in the environment measurements (reactions analyzed in foil measurements of spectra)
      8. Discussion of errors in the environment measurements
      9. Electrical noise mapping (experimental-configuration dependent)

(continuued)

Table 2-2 (continued)

III. Support Capabilities

- A. Professional and/or nonprofessional technical support staff available
- B. Screen room
- C. General electronics available; power, cabling, and minimum cabling requirements
- D. Timing signals
- E. Dosimetry available (active and/or passive)
- F. Calculational capabilities available
- G. Shop facilities
- H. Experiment preparation laboratories
- I. Photographic equipment and materials

IV. Procedural Information

- A. Contact (technical and administrative)
- B. Scheduling (lead time)
- C. Cost information if available and/or releasable
- D. Shipping address

2.2 SANDIA PULSE REACTOR (SPR-III)

2.2.1 Physical Characteristics

SPR-III is an all-metal, unreflected, and unmoderated critical assembly in the form of a right-circular cylinder, 10.7 in. in dia. and 14.4 in. high. The assembly contains a total mass of 258 kg of fully enriched U (93.2% U-235), alloyed with 10 w/o Mo. A 7-in. dia. "glory hole" extends vertically through the center of the core, thereby facilitating internal as well as external irradiation of test samples. It is at the midplane of the glory hole that the principal performance criterion, 6×10^{14} n/cm^2 (E > 10 keV) for a maximum yield burst, is defined.

A thin-walled Al shroud approximately 22 in. O.D. and 32 in. high covers the fuel assembly. The shroud, coated with B, serves a dual purpose: first, it confines the cooling gas over the fuel system, thereby achieving relatively efficient cooling; and second, it diminishes the reactivity contribution of moderating test samples placed external to the reactor. Cooling reduces the maximum delay time between bursts to 2 hr.

The reactor is capable of operating in either the pulse mode or at a steady-state power of up to 15 kW for several hours. Steady-state operation is minimized, however, because it produces large fission-product inventories in the core.

Characterizing data presented herein are taken from detailed quantitative data obtained by Sandia Laboratories.

2.2.2 Operating Characteristics

The burst energy release is characterized by the temperature rise in the fuel. A standard SPR-III burst produces about a 350°C to 400°C temperature rise (maximum). Measured characteristics for a 300°C burst are given in Table 2-3. The peak power level is approximately 118,000 MW. Pulse width varies inversely with burst size; the larger the temperature excursion, the narrower the pulse. Figure 2-1 shows the relationship between pulse width and pulse yield. Figure 2-2 depicts a typical burst profile, as measured with a photodiode.

Cooling time (forced N) is approximately 1 hr.

Measured data regarding the tolerable reactivity worth of experimental samples indicate the following:

1. The protective shroud around the fuel material isolates the reactor from experiments placed external to the core. Hence, there are no limitations on experiments outside the reactor.
2. Samples placed within the glory hole are very strongly coupled to the reactor. Measurements have been made regarding the reactivity worth of various sample materials in this position. Experiment worths can be several $ in magnitude.

Table 2-3. SPR-III free-field pulse performance characteristics (dose and dose rates in the glory hole).

T (°C)	FWHM (μs)	n/cm^2/Pulse (E > 10 keV)	Peak $n/cm^2/s$ (E > 10 keV)	Rad (H_2O) Per pulse	Peak Rad (H_2O) Per s
100	237	1.51×10^{14}	6.37×10^{17}	4.28×10^{4}	1.81×10^{8}
150	150	2.47×10^{14}	1.65×10^{18}	6.33×10^{4}	4.22×10^{8}
200	116	3.08×10^{14}	2.66×10^{18}	8.38×10^{4}	7.22×10^{8}
250	98	4.12×10^{14}	4.20×10^{18}	1.06×10^{5}	1.08×10^{9}
300	90	4.57×10^{14}	5.08×10^{18}	1.31×10^{5}	1.46×10^{9}
350	82	5.33×10^{14}	6.50×10^{18}	1.48×10^{5}	1.80×10^{9}
400	76	6.10×10^{14}	8.03×10^{18}	1.69×10^{5}	2.22×10^{9}

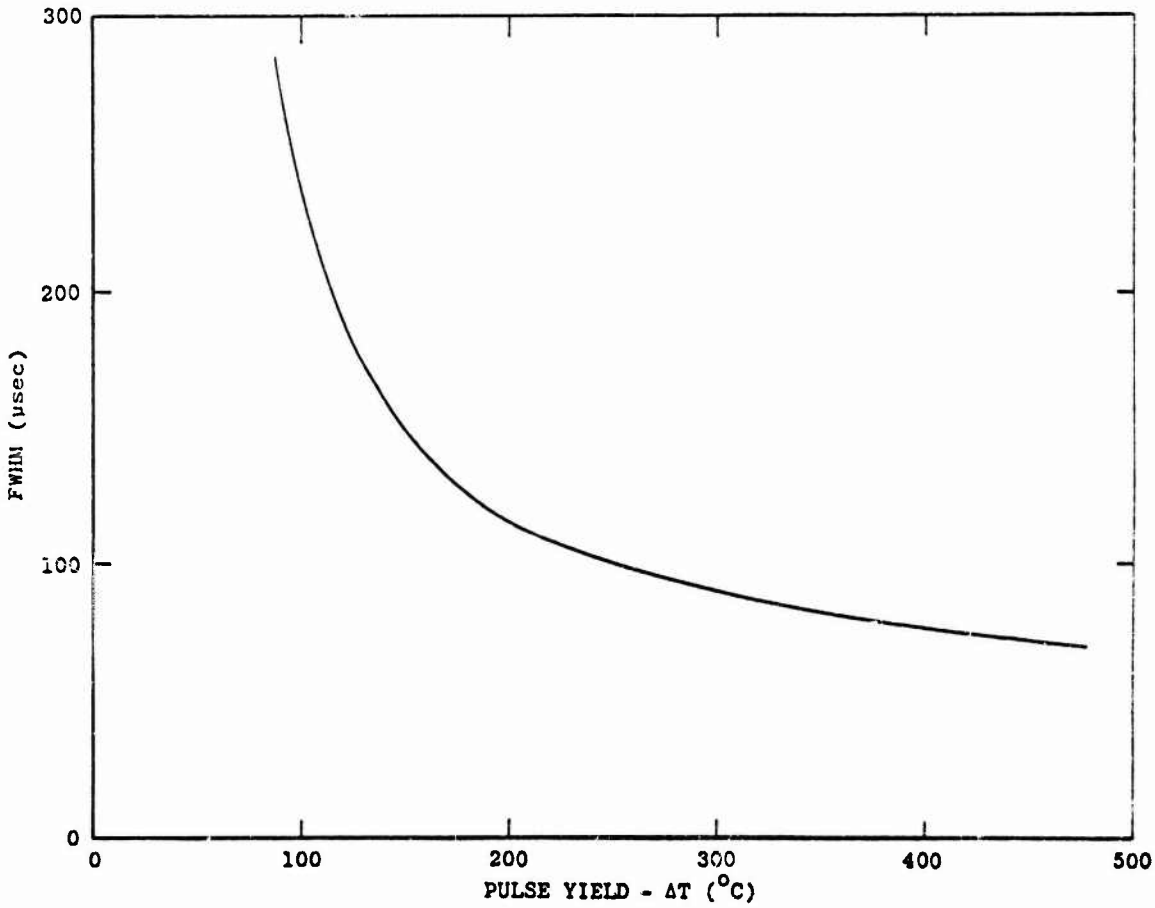

Figure 2-1. SPR-III width at half-maximum power versus temperature rise (pulse yield) free field.

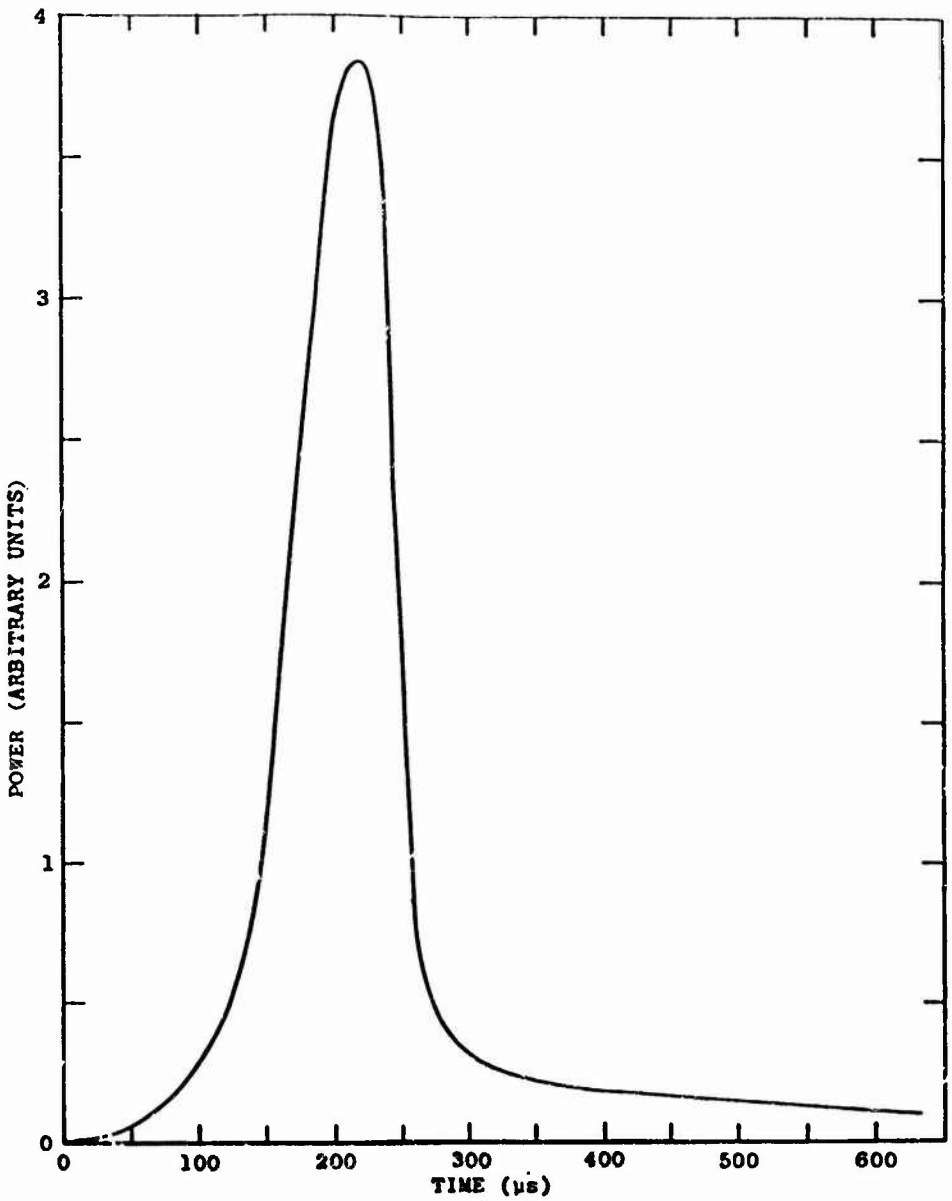

Figure 2-2. SPR-III typical pulse shape for 300°C ΔT yield.

An assessment of sample reactivity worth will be made by the reactor staff for each experiment conducted.

Reactivity insertion rate is approximately $10/s.

Burst frequency is approximately 2 hr, depending upon burst size.

2.2.3 Environment

Measurements of the neutron and γ environment in the glory hole and around the outside of the reactor and characterizing data taken from these results are presented here.

Neutron measurements were made utilizing threshold foils. The results are shown in Figures 2-3 and 2-4 and Table 2-3. The measurements were made essentially in a free-field condition; i.e., there were no spectrum-perturbing experiments near the reactor during the measurements. Therefore, the values given should be representative of any free-field location in the reactor room.

Absorbed γ dose measurements were made with TLD-400 (CaF_2) dosimetry. The results characterizing the SPR-III γ environment are presented in Figures 2-5 and 2-6.

Measurements imply that fluence and dose levels are approximately linear with fuel temperature rise.

Neutron spectra measurements were made with S foils and fission foils in B balls in the glory hole and at various distances outside the core. The results of these measurements are shown in Figures 2-7 and 2-8 and Table 2-4. Quantitative data regarding time-dependent spectra are not available.

Measurements show the variation of the n/γ ratio with position and types of reactor operation. Measurements were made using S foils to determine n/cm^2 ($E > 3$ keV) from which total dose can be inferred using the appropriate conversion factors which can be obtained from the spectra plots, and TLD-400 γ dosimetry to measure the absorbed dose. Figures 2-3 and 2-5 can be used for leakage ratios and Figures 2-4 and 2-6 for the glory hole.

Sources of error include positioning error of successive dosimetry packages, shadowing effects, counting statistics, and reactor repeatability.

At any given location in or around the reactor, the n/γ ratio is higher on a burst operation than on a power run of equivalent neutron fluence because of the delayed γ dose associated with the extended exposure time on a power run. A long power run at low power results in fewer n/γ than a short power run at high power (with the total number of kW-min equal in both cases) because a smaller fraction of delayed γ is emitted during the exposure time of the short power run.

As examples, the n/γ ratio in the glory hole is about 3.6×10^9 $n/cm^2/\gamma$ rad for pulse and about 2.8×10^9 $n/cm^2/\gamma$ rad for steady-state conditions.

Quantitative data on background radiation are not available. The experience of the facility operators indicates that RF background noise poses no serious problem.

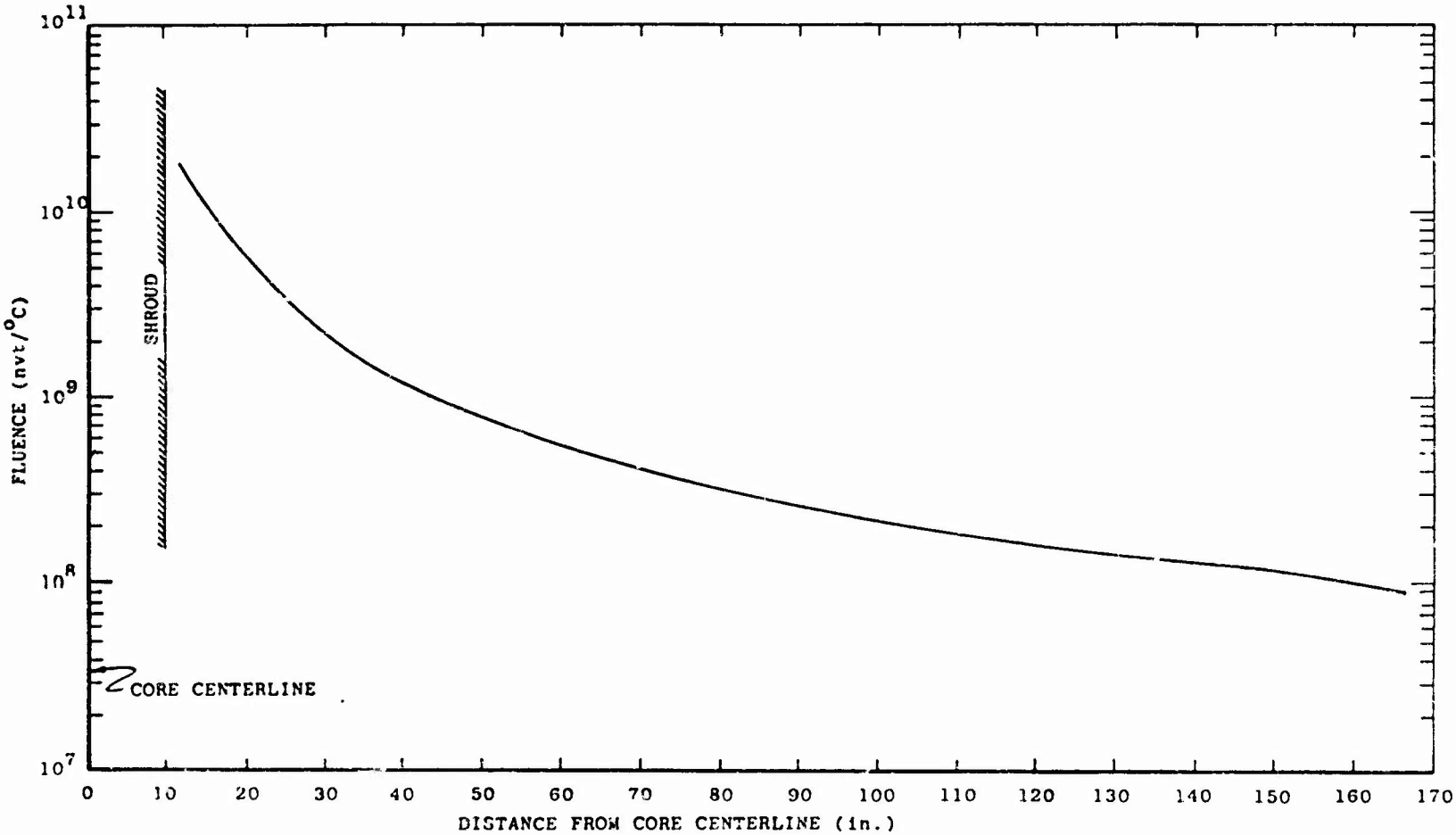

Figure 2-3. SPR-III profiles for 3-MeV leakage fluence free field.

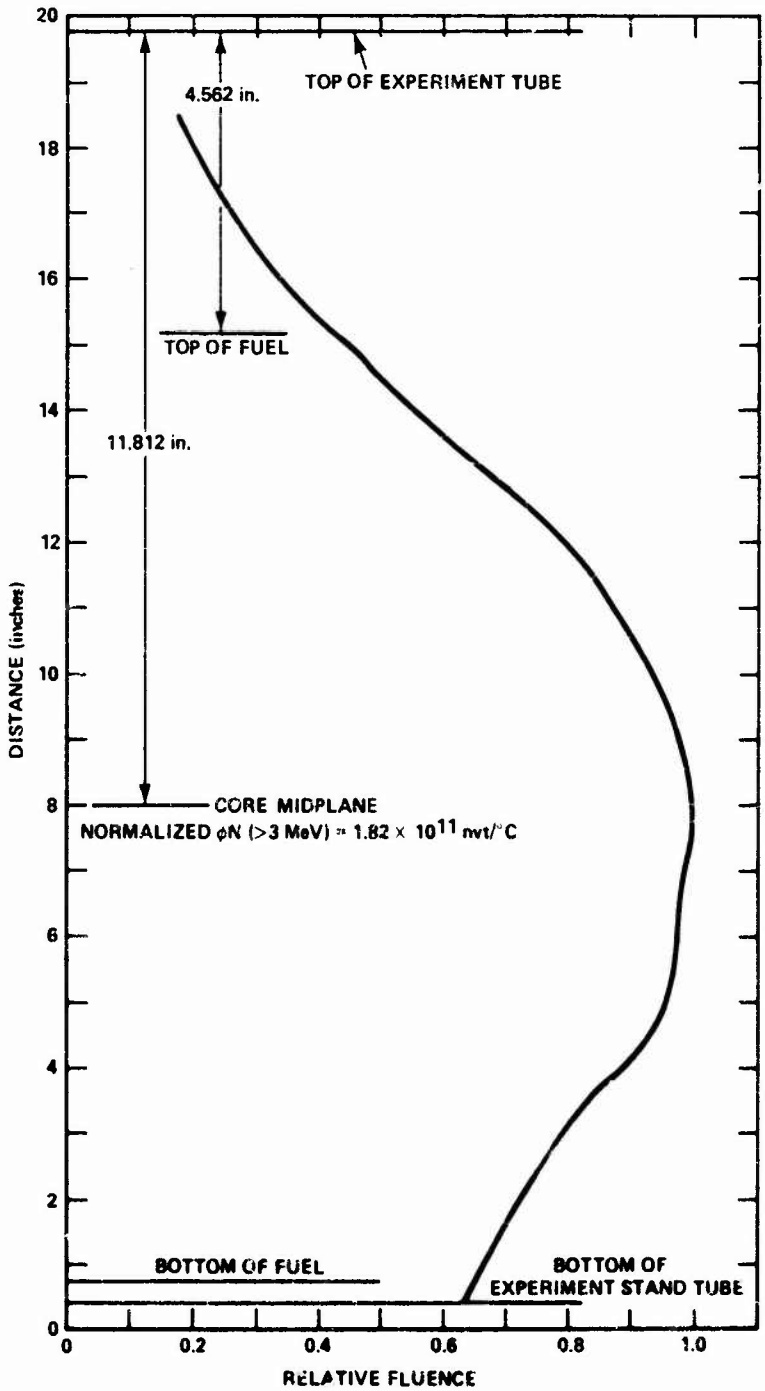

Figure 2-4. SPR-III center line data.

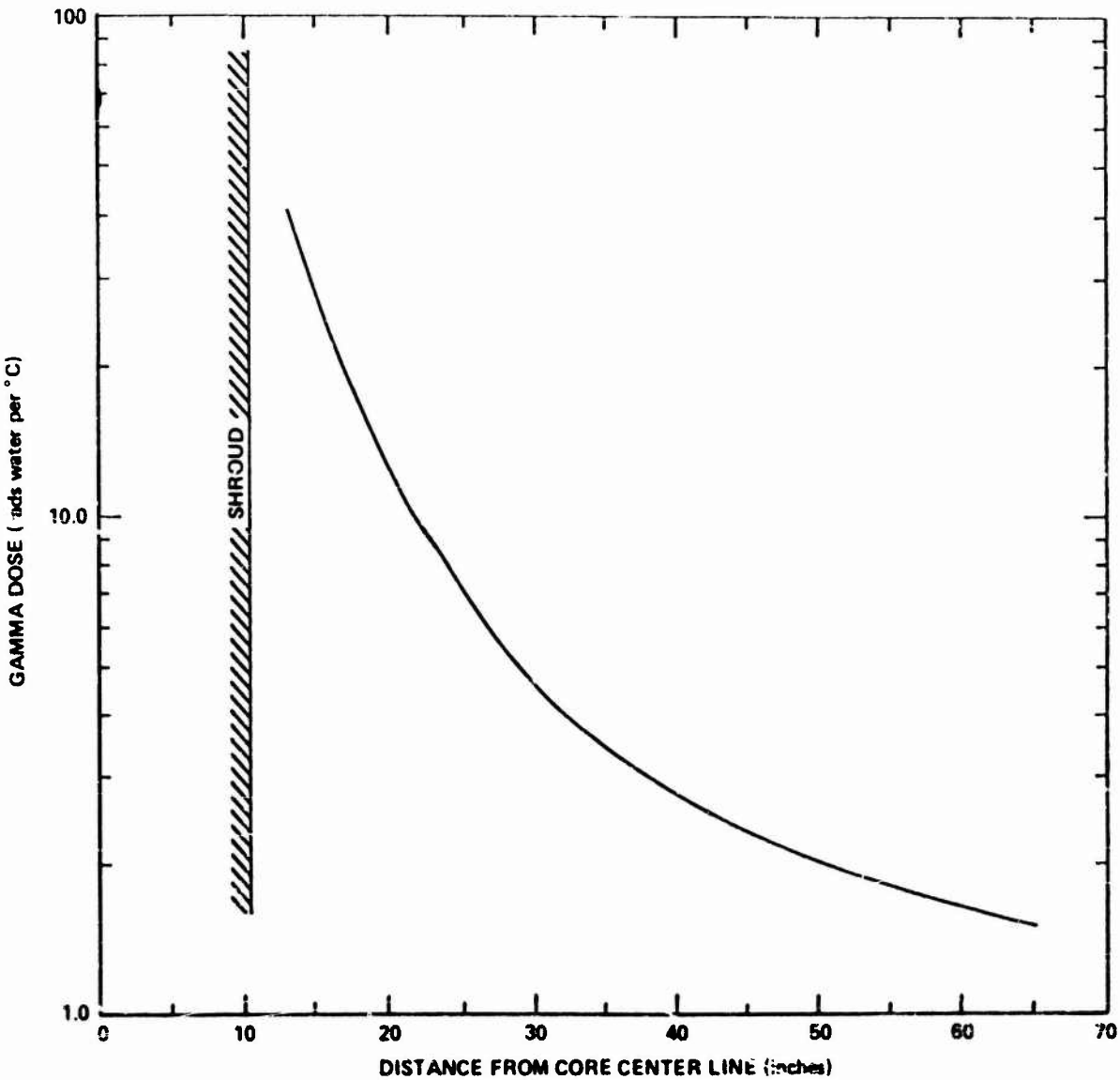

Figure 2-5. SPR-III γ profile at core midplane for pulse conditions.

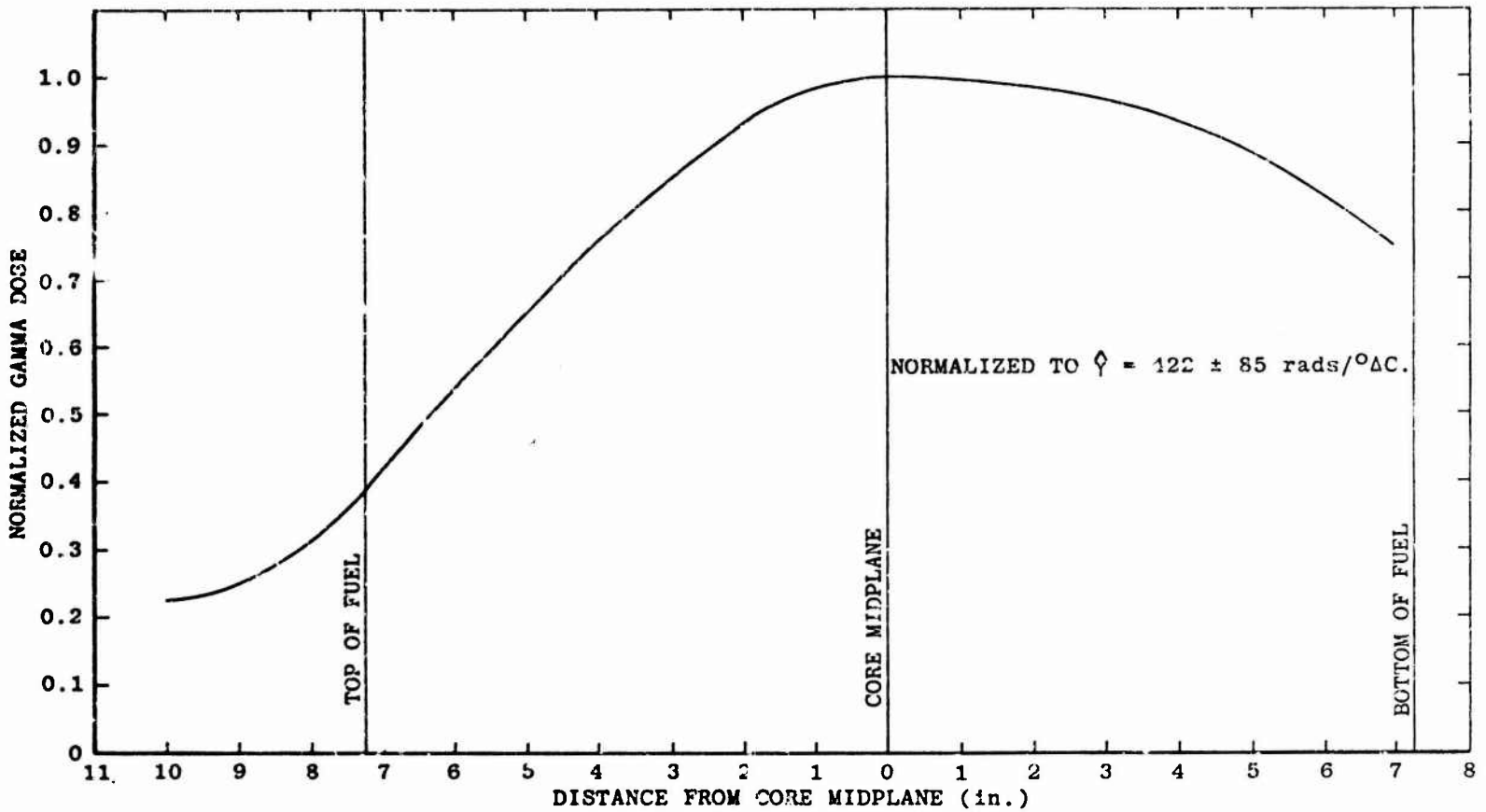

Figure 2-6. SPR-III glory hole center line γ dose (rad (water)/°C ΔT).

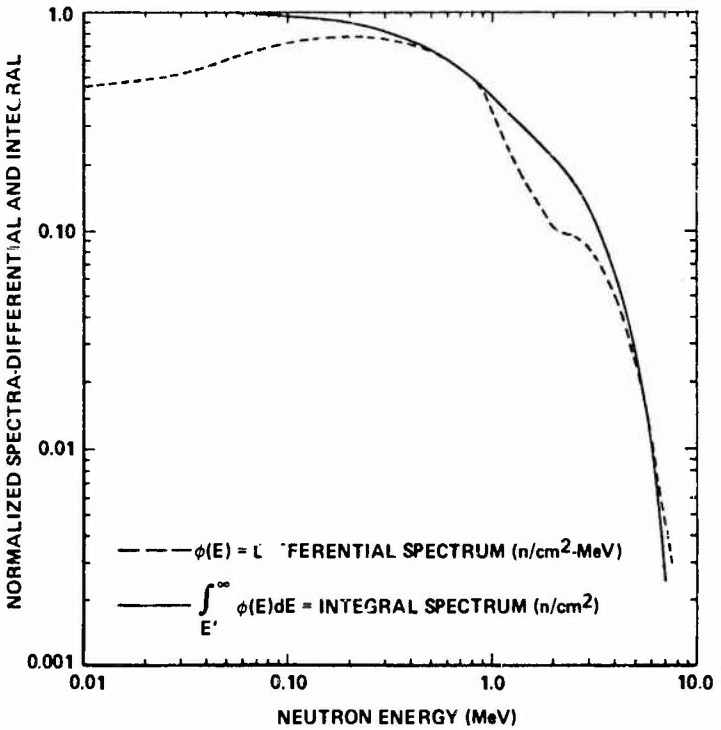

Figure 2-7. SPR-III unperturbed glory hole spectra.

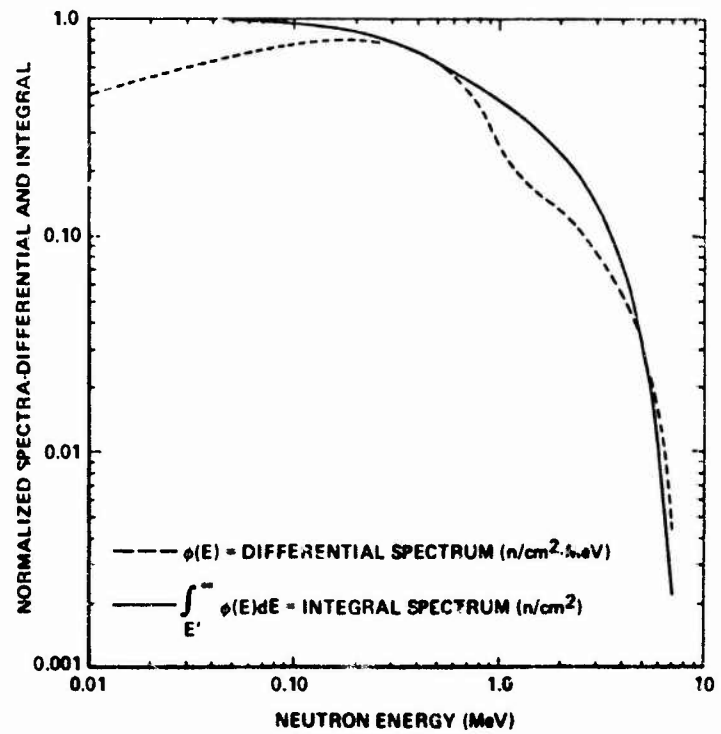

Figure 2-8. SPR-III unperturbed leakage spectra.

Table 2-4. Measured SPR-III neutron spectrum (central cavity, horizontal and vertical center line, free-field).

Group Number	Lower Energy (MeV)	Upper Energy (MeV)	Normalized Group Fraction	Fluence[a] (n/cm^2-MeV)
1	6.5+0	1.0+1	0.00558	1.59+11
2	4.0+0	6.5+0	0.04863	1.95+12
3	2.5+0	4.0+0	0.10410	6.94+12
4	1.5+0	2.5+0	0.12119	1.21+13
5	1.0+0	1.5+0	0.12123	2.42+13
6	6.5-1	1.0+0	0.16189	4.63+13
7	4.0-1	6.5-1	0.16154	6.46+13
8	2.5-1	4.0-1	0.11010	7.34+13
9	1.5-1	2.5-1	0.07502	7.50+13
10	1.0-1	1.5-1	0.03611	7.22+13
11	6.0-2	1.0-1	0.02668	6.67+13
12	4.0-2	6.0-2	0.01190	5.96+13
13	2.0-2	4.0-2	0.01023	5.12+13
14	1.0-2	2.0-2	0.00462	4.62+13
15	5.0-3	1.0-2	0.00111	2.22+13
16	1.0-3	5.0-3	0.00002	5.00+11
17	1.0-4	1.0-3	0.0000003	3.33+10
			1.00000	

[a]Normalized integral fluence = 10^{14} nvt.

The uncertainties associated with any one measurement point are about ±15%. This uncertainty is inherent in any spectral and fluence measurements because of uncertainties relating to detector calibration and positioning, cross-section information, signal measurement, and foil couunting. The uncertainties of the reported Sandia data are typical and representative of the present state of the art.

2.2.4 Support Capabilities

With the exception of radiological and toxicological safety services and the Sandia Laboratories Dosimetry Counting Laboratory, Sandia personnel should not be expected to provide scientific, technical, or engineering consulting services or support to non-Sandia users of the pulse reactor. The primary service provided for the experimenter/user is a nuclear radiation source and/or environment.

The Sandia technical staff is available for consulting services on a limited basis unless special contractual arrangements are made. If experiments involve radioactive or toxic substances, a Sandia health physicist is assigned the responsibility of regulating personnel exposures and ensuring that proper handling procedures are employed.

Utilities available inside the reactor cell include:

1.	Compressed air	4 CFM at 100 psi
2.	Electrical power	40 kVA, 120-V, 1-ϕ ac (15 A/outlet) (220 Vac available upon request)
3.	Water drain	3-in. gravity flow.

Around the inside periphery of the cell are 9 electrical patch panels. Of these, 3 are paired with identical panels outside the cell at trailer parking stations and 4 are connected with panels inside the instrumentation building. The other 2 are used by reactor operations. Each of the 7 experiment boxes provides RG-58B/U coaxial cables, No. 14 signal wires, a ground bus, and an empty 4-in. conduit for the experimenter to pull his own cables when desired.

Near the patch panel at each trailer station, 208-V, 3-ϕ, 100-A electrical power is available through an Appleton AEEA-10476 connector. Also, each trailer station has a 120-V, 1-ϕ ac supply, terminated in four 3-prong convenience outlets. Instrumentation cables, which must be provided by the experimenter, may be laid along the ground between the outer patch panel and the recording trailer. Equipment located within the reactor room must be wired for remote operation since personnel will not be permitted insi the area while the reactor is being operated.

Any cable reaching from the reactor to the patch panel should be a minimum of 20 ft long. Any cable pulled through the patch panel conduit should be a minimum of 45 ft plus the desired length outside the cell.

An instrumentation building located immediately adjacent to the reactor building houses permanently installed analysis equipment. Dual-beam oscilloscopes with automatically actuated cameras, power supplies of various voltage and current ratings, and several types of amplifiers are available. Space is also available for the experimenter to set up his own special equipment. Cables should be 65 ft long to reach from the reactor to equipment in the instrumentation building.

No screen room is available at the facility, but provisions can be made for adequate electrical shielding.

Timing triggers for pre-burst and post-burst and signals relative to burst peak can be furnished if required.

Dosimetry data can be provided by the Sandia Laboratories Dosimetry Counting Laboratory. Standard foil techniques are used for neutron measurements. TLD-400 dosimetry is used for the γ measurements.

Limited calculation facilities are available at the reactor site. The Sandia Laboratories computational laboratory can be made available on a limited basis by prearrangement.

Light machine shop facilities and experiment preparation and setup laboratories are available.

Limited photographic equipment is available. Oscilloscope cameras and film are readily available.

Technical and administrative inquiries related to the use of the SPR-III should be directed to:

Reactor Applications Division
Organization 5451
Sandia Pulsed Reactor Facility
Sandia Laboratories
P.O. Box 5800
Kirtland AFB East
Albuquerque, NM 87115
Telephone: (505) 264-2361 or 264-3304

A final experimental plan must be submitted 4 weeks in advance of the anticipated use of the facility. The format to follow in submitting this plan is shown in Figure 2-9. Scheduling of reactor time is not considered until the contract is approved and the experimental plan is received.

Costs and charges associated with use of the facility are documented and available directly from Sandia Laboratories. The shipping address is:

Supervisor, Organization 5451
Sandia Laboratories
P.O. Box 5800
Kirtland AFB East
Albuquerque, NM 87115

2.2.5 Applicability and Availability

The SPR-III provides a transient radiation environment readily applicable to TREE experiments. The facility is available to agencies of the DoD and to private organizations having Department of Energy (DoE) or DoD contracts requiring the use of the reactor. The reactor is available on the basis of noninterference with Sandia programs.

The reactor facility is located in an isolated experimental area 6 miles south of the main Sandia Laboratory, making it necessary for experimenters to provide their own transportation.

2.2.6 Security Clearance

Security clearances are required to gain unescorted access to the SPR facility. Visitors with a Q-clearance or a DoD Secret clearance with a Restricted

Data certification may have unescorted access to the SPR. Visitors without the above clearances must be escorted while in the security area. Visitor Control must be contacted to arrange for access to the laboratory.

Date_____

TO: J. A. Snyder, 5451 Building 6591 Ext. 264-1272

FROM: _____ Org._____ Ext. _____
(Responsible Project Leader)

Other Participants_____

This experiment has been discussed with SPR personnel and the scheduled dates are:

_____

Title_____

_____

Objective_____

_____

Security Classification_____

Procedures_____

_____

_____

_____

Items to be exposed (qty., wt., mat'ls, dimensions, etc.)

_____

_____

_____

Radiation levels and total number of SPR operations required

_____

_____

Experimenter Signature_____

Reviewed and Approved by
SPR Supervision_____
(Date)

Reviewed by Committee_____
(Date)

Arrange for Area V access and submit plan as soon as possible after scheduled reactor time has been verbally confirmed.

NOTE: EXPERIMENTAL SETUP FOR IRRADIATION, AND REMOVAL, WILL NOT BE DONE BY OPERATIONS PERSONNEL

Figure 2-9. Sandia pulse reactor facility experiment plan.

2.3 U.S. ARMY MATERIAL TESTING DIRECTORATE, ARMY PULSE RADIATION FACILITY (APRF)

2.3.1 Characteristics

The APRF reactor is a highly mobile and versatile all-metal, fueled, unreflected, and unmoderated critical assembly. It is operated in either super-prompt critical pulse or steady-state mode. For the exposure of small objects to high neutron fluence levels, the APRF can be operated with either 39-mm or 106-mm dia., 198-mm high glory holes. The maximum fluence available in a glory hole is 6×10^{14} n/cm^2 (1-MeV equivalent) delivered in a single 45-μs wide pulse. At the reactor-shroud surface the maximum available fluence is 1.5×10^{14} n/cm^2 in a single pulse.

The APRF is also designed for the simulation of tactical nuclear environments and the irradiation of very large objects. The reactor is suspended from a transporter capable of positioning it remotely at various locations inside a 30-m dia., 25-m high silo made of low-scatter materials, as well as at an outdoors test pad. The reactor can be raised from inside a pit to 13 m above floor level, which is borated. A relatively free-field environment simulating an air burst can thus be generated by the reactor.

In the pulse mode the reactor is normally operated to 1.5×10^{17} fissions per pulse. In the steady-state mode the reactor can be operated up to 10 kW for 13 min or continuously at 5 kW.

The reactor is operated in a γ mode through the use of various n/γ converter shields. These are tailored to meet specific criteria up to dose rates of 3×10^9 rad/s with pulse widths ranging from 50 μs to 5 ms. The reactor is also used to produce high thermal fluxes up to 10^{18} n/cm^2-s, with the help of polyethylene flux traps.

Table 2-5 summarizes the irradiation capability of the reactor. Figure 2-10 depicts the reactor and facility building.

2.3.2 Test Parameters

The maximum pulse yield is 2.1×10^{17} fissions. Normal operations are in the range 1.2 to 1.5×10^{17} fissions:

	Pulse Yield		
	1.2×10^{17}F	1.5×10^{17}F	2.1×10^{17}F
Pulse Width (FWHM), μs	52	45	40
Initial Reactor Period, μs	19	17	10

Figure 2-11 shows traces of a typical pulse shape taken with the APRF Data Acquisition System. The reactor can be operated in a wide-pulse mode, obtained by placing suitable moderators near the reactor. Peak γ dose rate versus pulse

Table 2-5. Key APRF performance data.

Exposure Location	Neutron Fluence n/cm^2 (>10 keV)	γ Dose Rad (tissue)	Pulse Width (μs)	Peak γ Rate (rad(Si)/s)	n/γ Ratio (n/cm^2 per rad)
STANDARD CORE					
At Reactor Shroud	1.5×10^{14}	3.3×10^{4}	48	2.6×10^{8}	4.5×10^{9}
In-Core, 38-mm Dia., 198-mm High Glory Hole	5.6×10^{14}	1.75×10^{5}	48	1.3×10^{9}	3.2×10^{9}
External n/γ Converter	2.8×10^{13}	1.1×10^{5}	48	8.5×10^{8}	2.5×10^{8}
	2.8×10^{13}	1.1×10^{5}	400	1.5×10^{8}	2.5×10^{8}
	2.8×10^{13}	1.1×10^{5}	1000	7.7×10^{7}	2.5×10^{8}
REFLECTED CORE/106-mm GLORY HOLE					
In-Core, 106-mm Dia., 198-mm High Glory Hole	5.0×10^{14}	1.6×10^{5}	60	9.7×10^{8}	3.2×10^{9}
In-Core n/γ Converter	3.6×10^{14}	3.9×10^{5}	60	2.4×10^{9}	9.2×10^{8}
	3.6×10^{14}	3.9×10^{5}	400	5.0×10^{8}	9.2×10^{8}

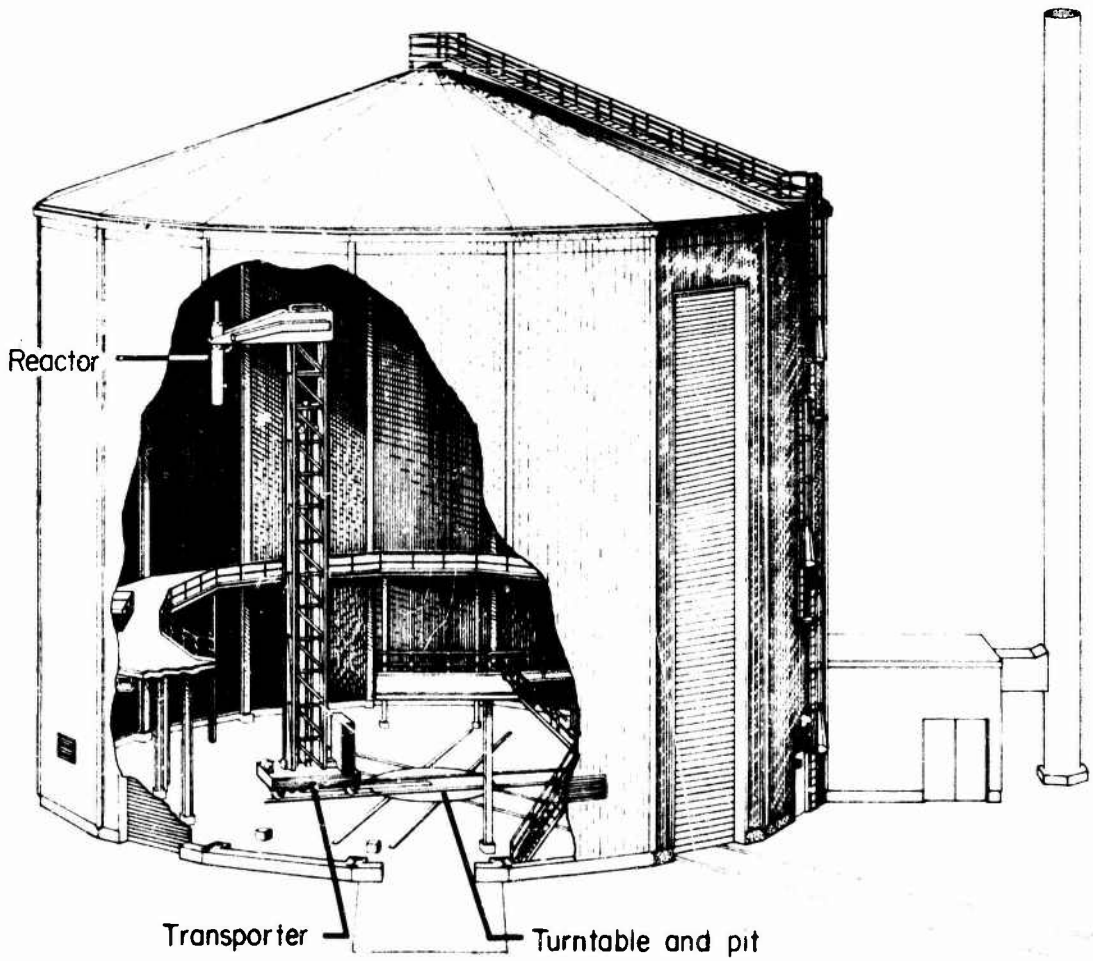

Figure 2-10. Army pulse radiation facility.

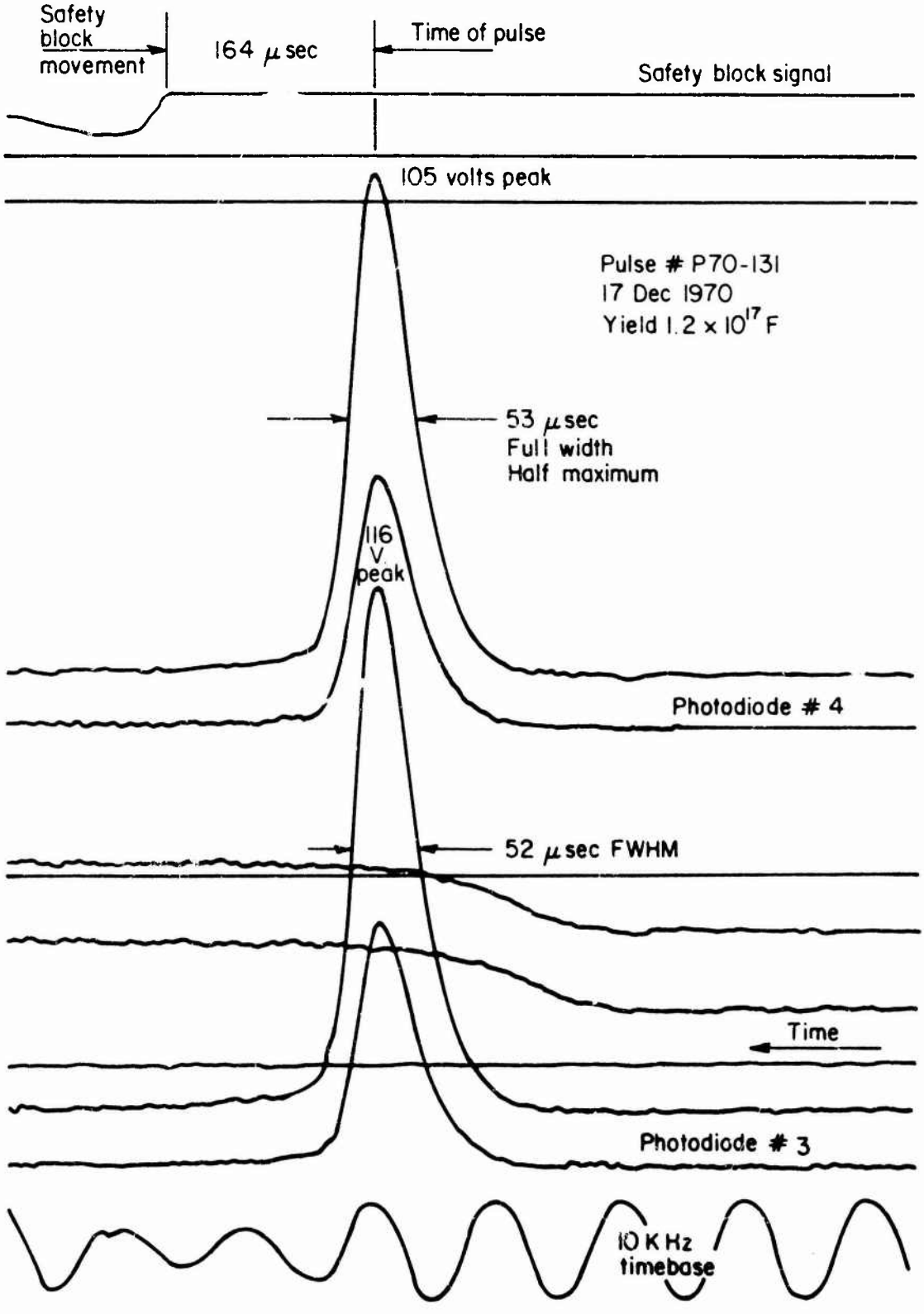

Figure 2-11. Pulse trace.

width at half maximum (PWHM) power for γ converters is shown in Figure 2-12 and peak γ dose rate versus total neutron fluence for γ converters is shown in Figure 2-13.

Maximum temperature rise is approximately 600°C. Cooling time (forced air) is 40 min. Measured temperature-time profiles are available; they depend on pulse and FWHM.

An assessment of sample reactivity worth will be made by the reactor staff for each experiment conducted. The following should be noted:

1. The decoupling shield placed around the core isolates the reactor from reactivity effects of experiments placed external to, but near, the reactor
2. Samples placed within the glory holes have a strong reactivity effect on the reactor and careful reactor control is required
3. Moving experiments, such as burning rocket motors, require detailed reactivity calibrations to determine their effect during a pulse
4. In general, when an experiment's reactivity contribution in the pulse mode is uncertain, its contribution will be evaluated by exposing it or a mock-up to one or several pulses at levels lower than that required for final irradiation.

Peak reactivity insertion rate is $7/s (burst rod).

Typical repetition rate is 105 min between high-level pulses, which includes about 30 min of access to change the experiment as required. For planning purposes, a 2-hr cycle time should be used for typical experiments, although as many as 6 pulses can be obtained in a day.

Pulse reproducibility for a typical experiment is ±2%. In general, changes in the experiment rather than in the reactor determine reproducibility from run to run.

2.3.3 Environment

2.3.3.1 Fluence and Dose Maps

Fluence, dose, and spectrum measurements, as well as calculations, are made by APRF staff. Free-field fluence data are given in Figures 2-14 through 2-20. Intercomparisons and cross calibrations with other facilities have been made and current data are available from the facility.

The neutron fluence is determined from Pu-239 and Np-237 loaded double-fission chambers developed by the National Bureau of Standards (NBS). These chambers are calibrated against a standard Cf-252 spontaneous fission source, also at NBS. The result is a traceable calibration accurate to better than

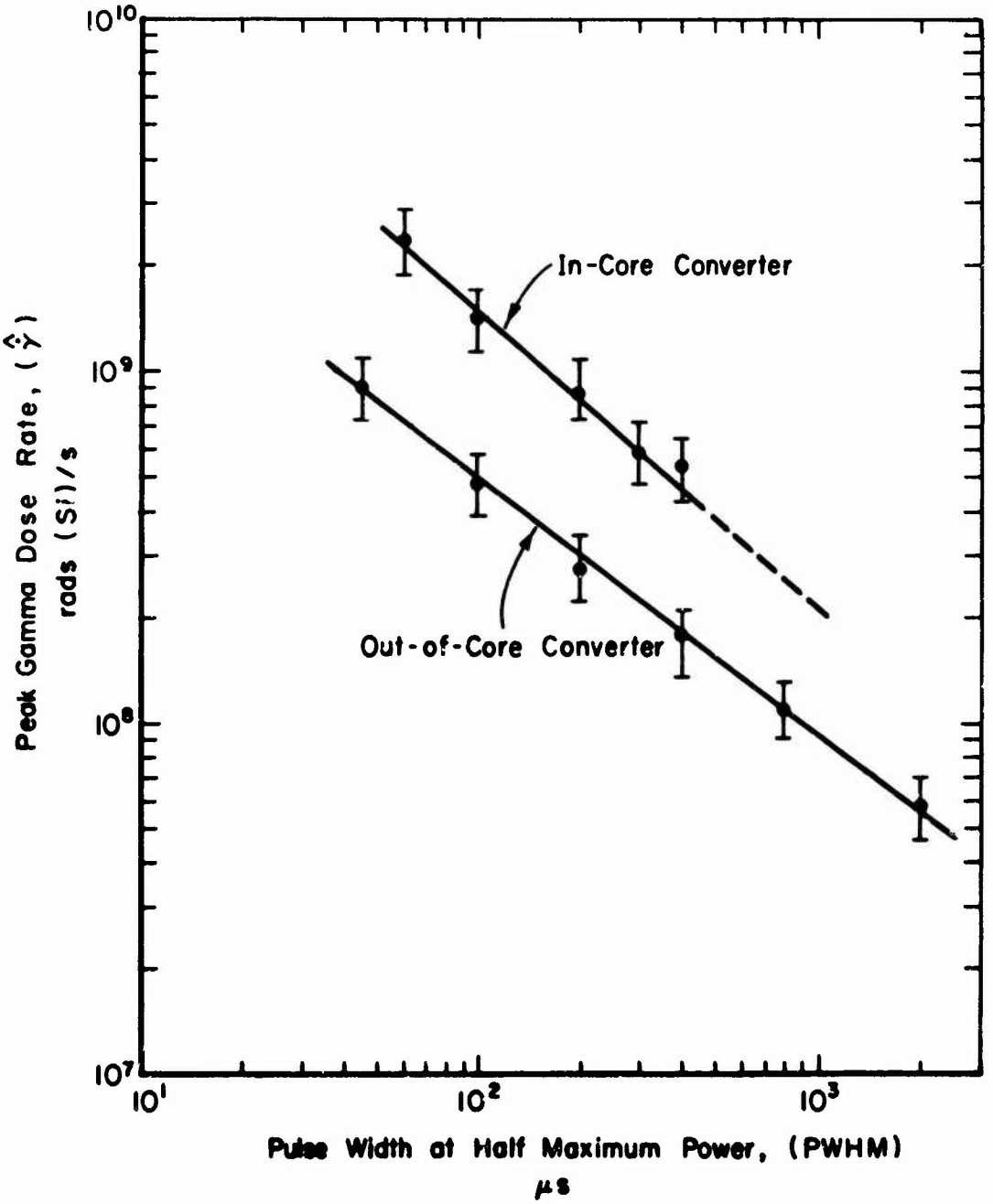

Figure 2-12. Peak γ dose rate versus PWHM for APRF n/γ converters.

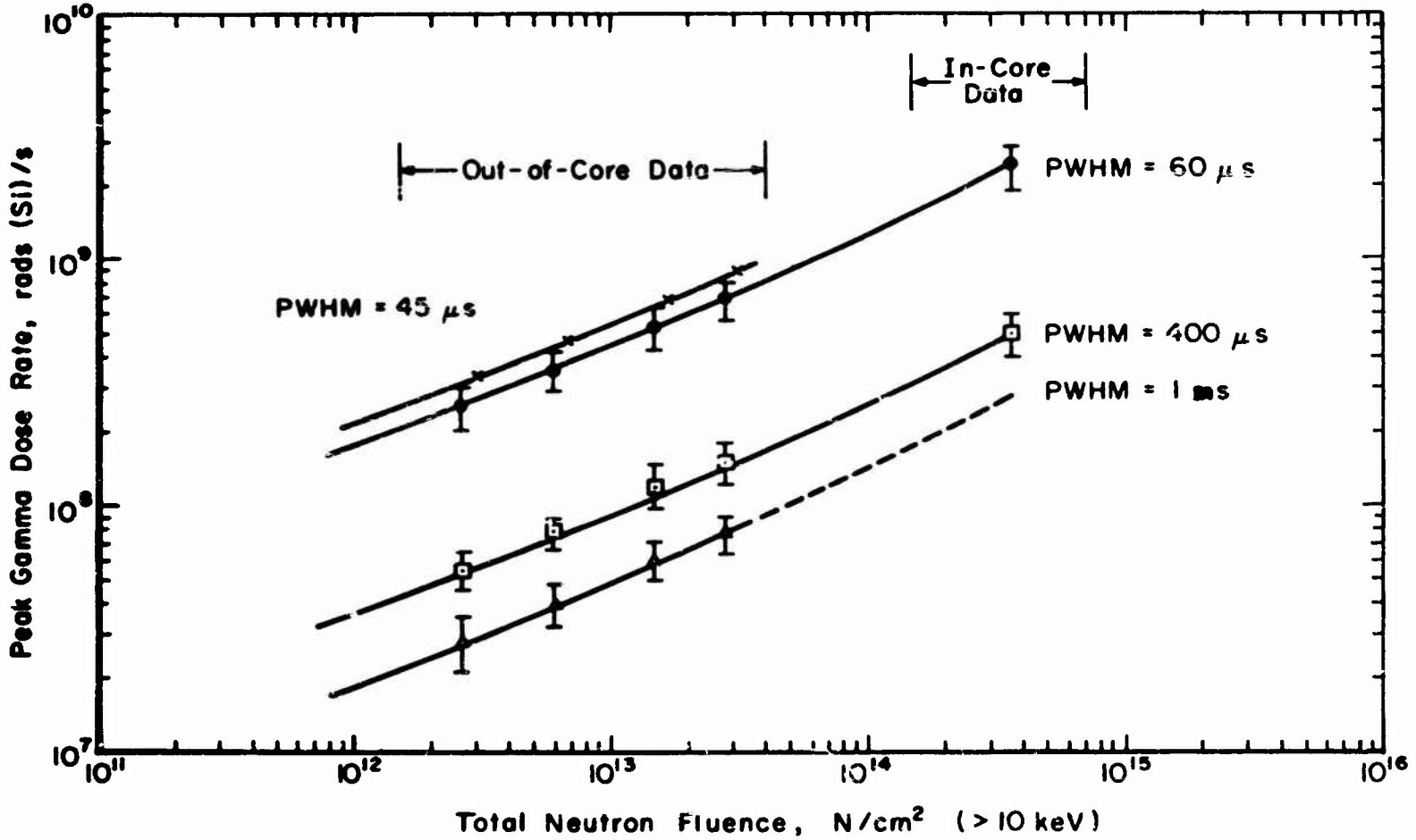

Figure 2-13. Peak γ dose rate versus total neutron fluence for APRF n/γ converters.

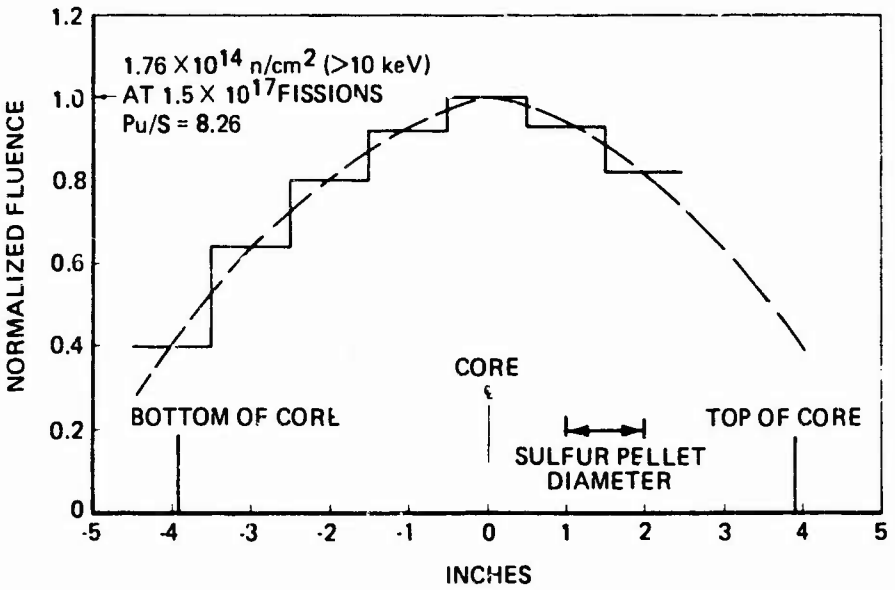

Figure 2-14. Radial fluence traverse.

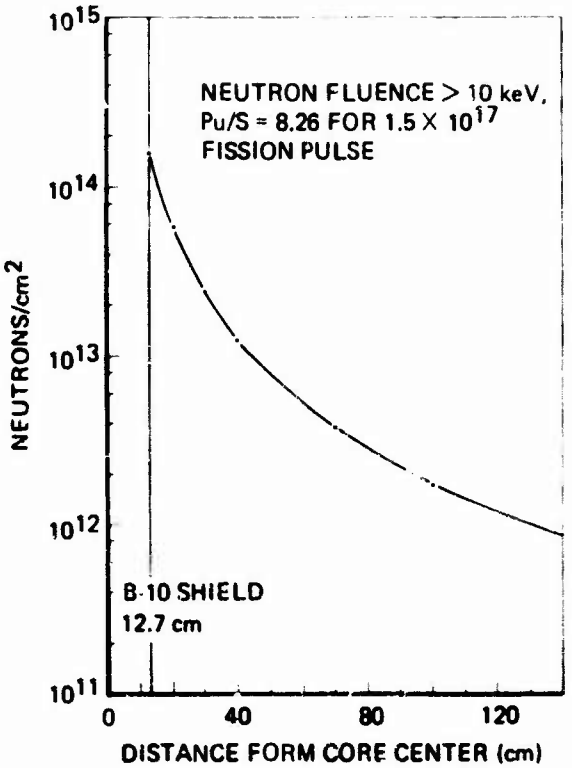

Figure 2-15. Vertical neutron fluence distribution across APRF reactor decoupling shield.

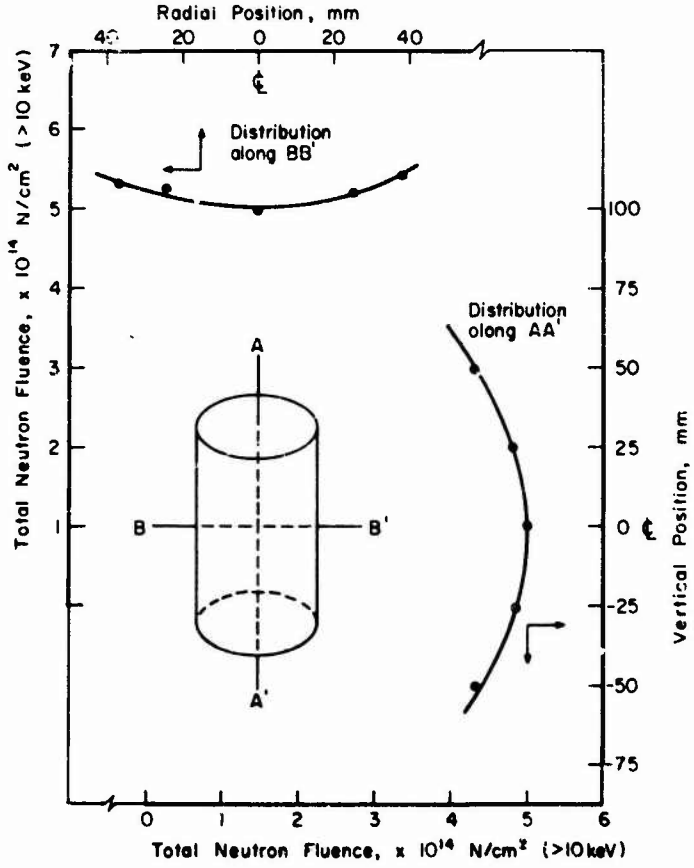

Figure 2-16. APRF 106-mm-dia. glory hole neutron fluence distributions.

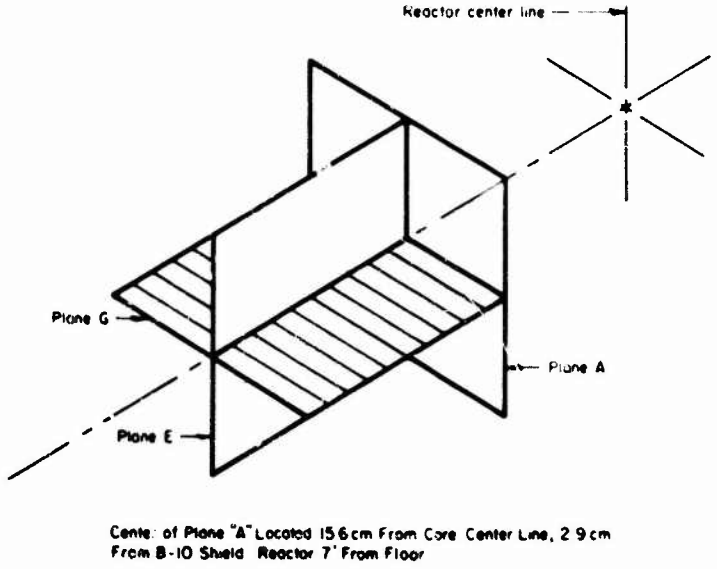

Figure 2-17. Normalized neutron fluence locations.

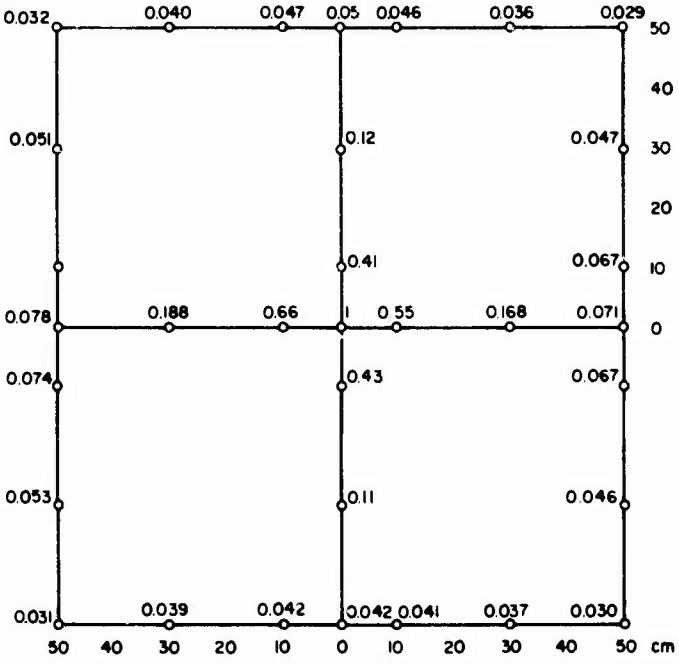

Normalized to center of Plane A. Plane A is 15.8 cm from core ℄. F_γ at CTR = 1.06×10^{14} neutron/cm^2 for a yield of 1.5×10^{17} fissions.

Figure 2-18. Normalized neutron fluence.

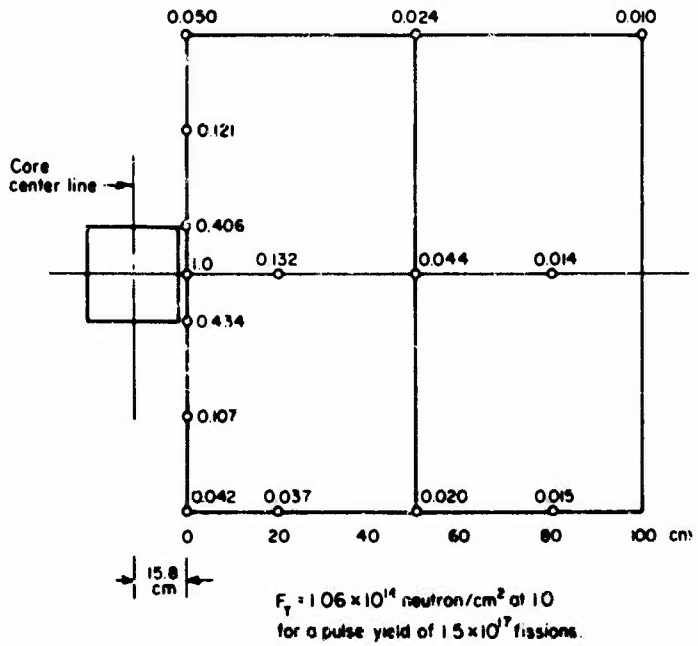

$F_\gamma = 1.06 \times 10^{14}$ neutron/cm^2 at 10 for a pulse yield of 1.5×10^{17} fissions.

Figure 2-19. Normalized neutron fluence.

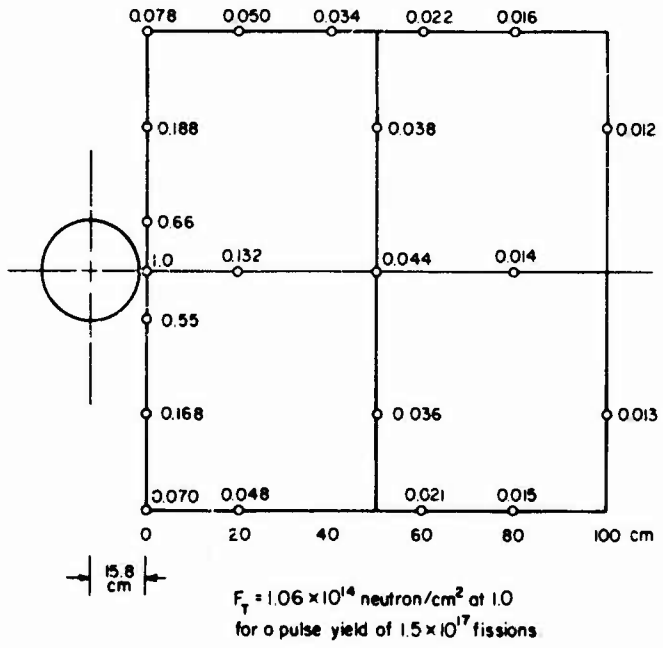

Figure 2-20. Normalized neutron fluence.

5%. Routine dosimetry is performed with S pellets yielding a nominal >3-MeV fluence. The (>10-keV)/(>3-MeV) flux ratio is 8.8 ± 0.6 in both glory holes and 7.4 ± 0.5 for leakage neutrons, respectively. The free-field APRF neutron spectrum is a slightly degraded U-235 fission spectrum and is essentially 1-MeV equivalent.

Figures 2-14 through 2-20 can be used to determine the fluence or flux during steady-state operation using the experimentally verified conversion factor of 1×10^{17} fissions = 56.6 kW-min.

Neutron and γ dose measurements in rad tissue are made with tissue-equivalent and air-equivalent ionization chambers. These range in volume from 0.5 cc to 16 liters and can be used from in-core to a range of several hundred m from the reactor.

Several n/γ converter shields are available at APRF. In these shields, fast neutrons from the reactor are slowed down by use of a moderator such as polyethylene, and the low-energy neutrons are then captured in Cd and Gd to produce captured γ-rays.

To date, two basic out-of-core shields have been developed: a narrow-pulse converter, and a wide-pulse converter. Figure 2-12 shows the measured γ dose rate versus FWHM for both narrow and wide pulses. The converter consists of a box 400 mm wide, 360 mm high, and 380 mm deep, with 76-mm thick walls of converter material consisting of polyethylene impregnated with 20 w/o CdO and 10 w/o Gd_2O_3. The back is open for access. The maximum output is 1.3×10^{17} fissions per pulse for narrow pulses and $\sim 1.8 \times 10^{17}$ fissions per pulse for

wide pulses. From Figures 2-12 and 2-13 it is seen that there is some flexibility in FWHM and neutron fluence and the same dose rate can be obtained over a range of these parameters.

Figure 2-21 shows the neutron and γ doses at the inside center of the converter box for tissue as a function of converter thickness. Figure 2-22 shows the same data for Si. For Si, the neutron contribution inside the converter shield is very small.

APRF has a complete high-resolution neutron and γ spectrum measurement capability centered on proton recoil, NE213 scintillator, and Li-6 solid-state spectrometers. These spectrometers can be used to obtain the spectra when the basic free-field data are inadequate. Measurements are made as far as 450 m from the reactor in simulated tactical nuclear environments. Calculations are made using ANISN one-dimensional and the DOT 3.5 two-dimensional discrete ordinate codes. In general, agreement between calculations and measurements is good. Typical data are shown in Figure 2-23.

APRF has available the routine foil activation and spectrum unfolding techniques for those applications where this is required.

Reference free-field neutron and photon leakage spectral data are given in Tables 2-6 through 2-8. The 90-group spectrum is the most recent determination.

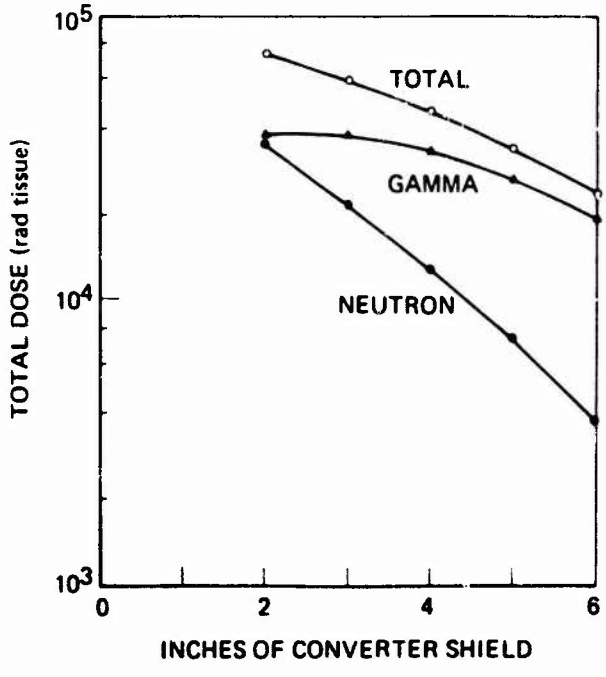

Figure 2-21. Total γ and neutron doses versus converter thickness (rad tissue at 1.3×10^{17}F) (66.3 kW-min).

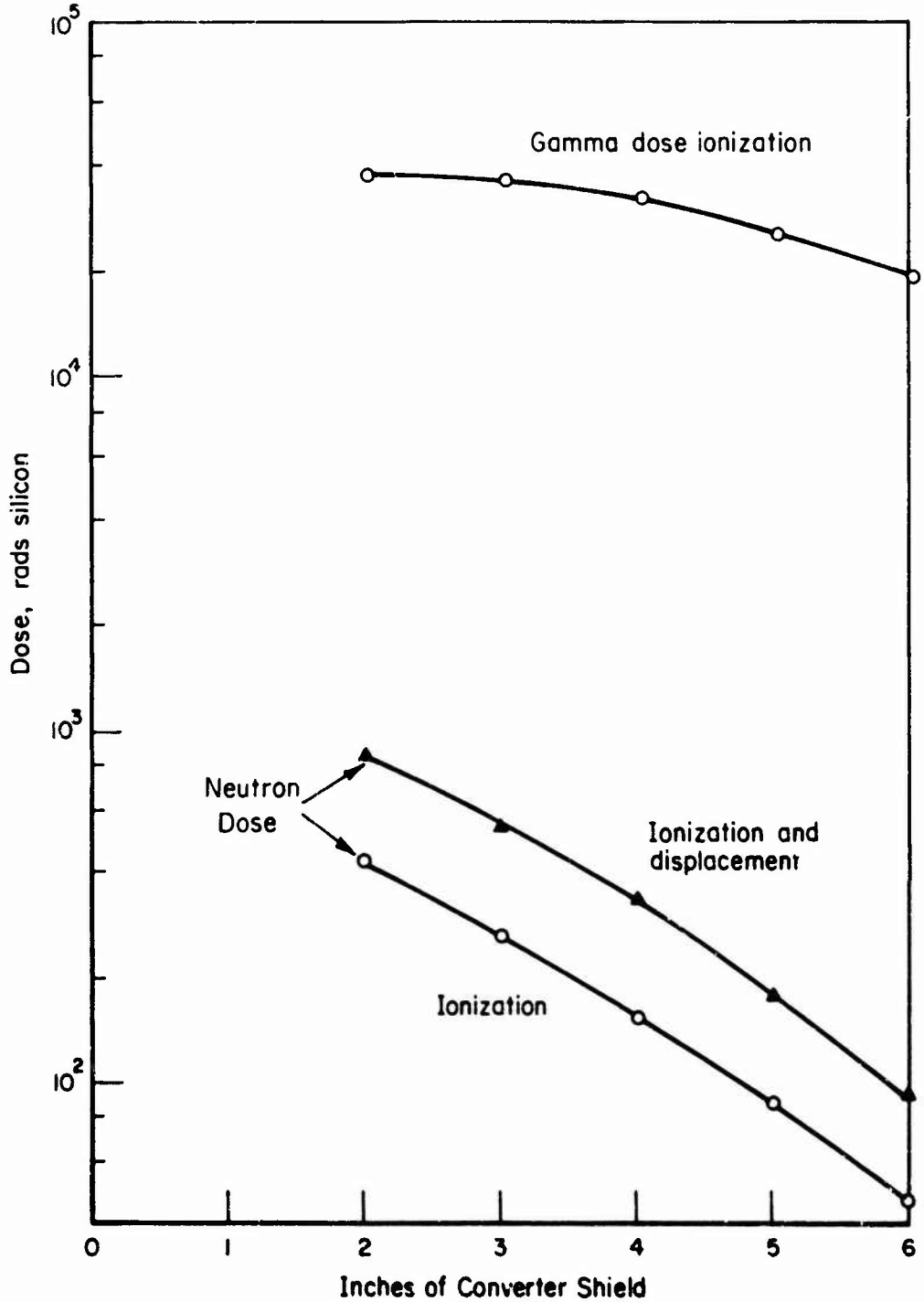

Figure 2-22. Total γ and neutron doses versus converter thickness (rad Si at 1.3×10^{17} F)(66.3 kW-min).

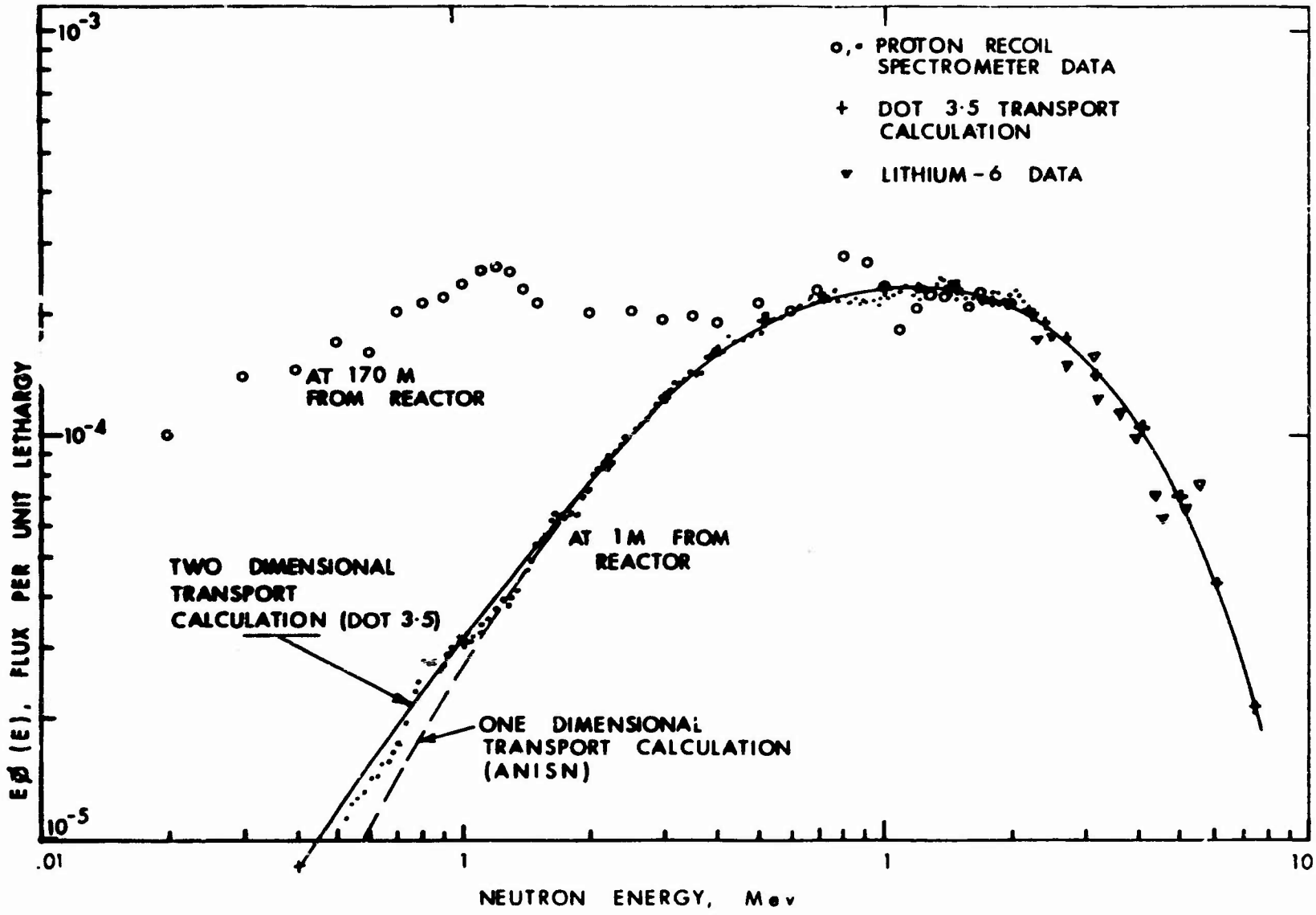

Figure 2-23. APRF neutron spectra.

Table 2-6. APRF reactor leakage neutron spectrum.[a]

Energy Group	Neutron Energy, E lower	Integral Spectrum		Differential Spectrum
		$(n/cm^2)^b$	Relative Spectrum	$(n/cm^2MeV)^b$
	14.92 MeV			
1	10.00	7.66×10^8	0.00064	1.56×10^8
2	6.70	1.02×10^{10}	0.00850	2.87×10^9
3	4.50	5.18×10^{10}	0.04297	1.88×10^{10}
4	3.01	1.42×10^{11}	0.11770	6.09×10^{10}
5	2.02	2.56×10^{11}	0.21247	1.15×10^{11}
6	1.35	4.16×10^{11}	0.34499	2.40×10^{11}
7	0.91	5.93×10^{11}	0.49176	3.97×10^{11}
8	0.55	8.26×10^{11}	0.68550	6.54×10^{11}
9	0.334	9.99×10^{11}	0.82892	8.00×10^{11}
10	0.202	1.10×10^{12}	0.91497	7.92×10^{11}
11	0.123	1.16×10^{12}	0.95883	6.64×10^{11}
12	40.9 keV	1.19×10^{12}	0.99012	4.61×10^{11}
13	11.7	1.20×10^{12}	0.99755	3.07×10^{11}
14	3.35	1.20×10^{12}	0.99927	2.48×10^{11}
15	0.75	1.21×10^{12}	0.99984	2.64×10^{11}
16	0.17	1.21×10^{12}	0.99997	2.78×10^{11}
17	37.3 eV		1.00000	2.43×10^{11}
18	8.32			1.59×10^{11}
19	1.86			6.69×10^{10}
20	0.41			1.60×10^{10}
21	Thermal	1.21×10^{12}	1.00000	9.09×10^8
Sum	--	1.21×10^{12}	1.00000	5.79×10^{12}

[a]Two-dimensional discrete ordinate transport calculation.
[b]Normalized to 1.0×10^{17} fissions at 1 m from core center.

Table 2-7. APRF reactor leakage photon spectrum.[a]

Energy Group	Neutron Energy, E lower	Integral Spectrum		Differential Spectrum
		(photons/cm^2)[b]	Relative Spectrum	(pnotons/cm^{2}MeV)[b]
	10 MeV			
1	8.0	9.01×10^{7}	0.00017	4.51×10^{7}
2	7.0	2.53×10^{8}	0.00046	1.62×10^{8}
3	6.0	6.86×10^{8}	0.00126	4.33×10^{8}
4	5.0	8.56×10^{8}	0.00158	1.70×10^{9}
5	4.0	1.49×10^{9}	0.00274	6.31×10^{9}
6	3.5	9.22×10^{9}	0.01700	1.55×10^{10}
7	3.0	2.10×10^{10}	0.03880	2.36×10^{10}
8	2.5	4.33×10^{10}	0.07988	4.45×10^{10}
9	2.0	8.30×10^{10}	0.15304	7.93×10^{10}
10	1.6	1.36×10^{11}	0.24988	1.31×10^{11}
11	1.2	2.18×10^{11}	0.40233	2.07×10^{11}
12	0.9	2.98×10^{11}	0.54896	2.65×10^{11}
13	0.6	4.01×10^{11}	0.74025	3.46×10^{11}
14	0.4	4.85×10^{11}	0.89110	4.20×10^{11}
15	0.21	5.30×10^{11}	0.97706	2.34×10^{11}
16	0.12	5.41×10^{11}	0.99700	1.20×10^{11}
17	0.07	5.42×10^{11}	0.99997	3.23×10^{10}
18	0.10	5.42×10^{11}	1.00000	2.19×10^{8}
Sum	--	5.42×10^{11}	1.00000	1.93×10^{12}

[a]Two-dimensional discrete ordinate transport calculation.
[b]Normalized to 1.0×10^{17} fissions at 1 m from core center.

Table 2-8. APRF 90-group leakage neutron spectrum.

Group	Lower Energy Boundary (MeV)	Upper Energy Boundary	Group Flux Q(E)[a]
1	1×10^{-5}	1×10^{-3}	2.95×10^{6}
2	1×10^{-3}	2×10^{-3}	2.98×10^{6}
3	2×10^{-3}	5×10^{-3}	3.03×10^{6}
4	5×10^{-3}	1×10^{-2}	3.14×10^{6}
5	1×10^{-2}	2×10^{-2}	3.34×10^{6}
6	2×10^{-2}	3×10^{-2}	3.59×10^{6}
7	3×10^{-2}	4×10^{-2}	3.82×10^{6}
8	4×10^{-2}	5×10^{-2}	4.04×10^{6}
9	5×10^{-2}	6×10^{-2}	4.25×10^{6}
10	6×10^{-2}	7×10^{-2}	4.45×10^{6}
11	7×10^{-2}	8×10^{-2}	4.63×10^{6}
12	8×10^{-2}	9×10^{-2}	4.80×10^{6}
13	9×10^{-2}	1×10^{-1}	4.96×10^{6}
14	1×10^{-1}	1.25×10^{-1}	5.21×10^{6}
15	1.25×10^{-1}	1.50×10^{-1}	5.53×10^{6}
16	1.50×10^{-1}	1.75×10^{-1}	5.78×10^{6}
17	1.75×10^{-1}	2×10^{-1}	5.99×10^{6}
18	2×10^{-1}	2.25×10^{-1}	6.16×10^{6}
19	2.25×10^{-1}	2.50×10^{-1}	6.28×10^{6}
20	2.50×10^{-1}	2.75×10^{-1}	6.38×10^{6}
21	2.75×10^{-1}	3×10^{-1}	6.44×10^{6}
22	3×10^{-1}	3.25×10^{-1}	6.47×10^{6}
23	3.25×10^{-1}	3.50×10^{-1}	6.48×10^{6}
24	3.50×10^{-1}	3.75×10^{-1}	6.47×10^{6}
25	3.75×10^{-1}	4×10^{-1}	6.44×10^{6}
26	4×10^{-1}	4.25×10^{-1}	6.39×10^{6}
27	4.25×10^{-1}	4.50×10^{-1}	6.33×10^{6}
28	4.50×10^{-1}	4.75×10^{-1}	6.26×10^{6}
29	4.75×10^{-1}	5×10^{-1}	6.18×10^{6}
30	5×10^{-1}	5.25×10^{-1}	6.09×10^{6}
31	5.25×10^{-1}	5.50×10^{-1}	5.99×10^{6}
32	5.50×10^{-1}	5.75×10^{-1}	5.89×10^{6}
33	5.75×10^{-1}	6×10^{-1}	5.78×10^{6}
34	6×10^{-1}	6.25×10^{-1}	5.67×10^{6}
35	6.25×10^{-1}	6.50×10^{-1}	5.55×10^{6}
36	6.50×10^{-1}	6.75×10^{-1}	5.43×10^{6}
37	6.75×10^{-1}	7×10^{-1}	5.31×10^{6}
38	7×10^{-1}	7.25×10^{-1}	5.19×10^{6}
39	7.25×10^{-1}	7.50×10^{-1}	5.06×10^{6}
40	7.50×10^{-1}	7.75×10^{-1}	4.94×10^{6}
41	7.75×10^{-1}	8×10^{-1}	4.82×10^{6}
42	8×10^{-1}	8.25×10^{-1}	4.70×10^{6}
43	8.25×10^{-1}	8.50×10^{-1}	4.58×10^{6}
44	8.50×10^{-1}	8.75×10^{-1}	4.46×10^{6}
45	8.75×10^{-1}	9×10^{-1}	4.34×10^{6}
46	9×10^{-1}	9.25×10^{-1}	4.22×10^{6}

(continued)

Table 2-8 (continued).

Group	Lower Energy Boundary (MeV)	Upper Energy Boundary	Group Flux Q(E)[a]
47	9.25×10^{-1}	9.50×10^{-1}	4.11×10^{6}
48	9.50×10^{-1}	9.75×10^{-1}	3.99×10^{6}
49	9.75×10^{-1}	1	3.88×10^{6}
50	1	1.1	3.62×10^{6}
51	1.1	1.2	3.22×10^{6}
52	1.2	1.3	2.86×10^{6}
53	1.3	1.4	2.54×10^{6}
54	1.4	1.5	2.25×10^{6}
55	1.5	1.6	2.00×10^{6}
56	1.6	1.7	1.78×10^{6}
57	1.7	1.8	1.59×10^{6}
58	1.8	1.9	1.42×10^{6}
59	1.9	2	1.27×10^{6}
60	2	2.1	1.14×10^{6}
61	2.1	2.2	1.02×10^{6}
62	2.2	2.3	9.20×10^{5}
63	2.3	2.4	8.32×10^{5}
64	2.4	2.5	7.54×10^{5}
65	2.5	2.6	6.87×10^{5}
66	2.6	2.7	6.27×10^{5}
67	2.7	2.8	5.74×10^{5}
68	2.8	2.9	5.28×10^{5}
69	2.9	3	4.88×10^{5}
70	3	3.1	4.52×10^{5}
71	3.1	3.2	4.20×10^{5}
72	3.2	3.3	3.92×10^{5}
73	3.3	3.4	3.67×10^{5}
74	3.4	3.5	3.38×10^{5}
75	3.5	3.6	3.07×10^{5}
76	3.6	3.7	2.80×10^{5}
77	3.7	3.8	2.55×10^{5}
78	3.8	3.9	2.33×10^{5}
79	3.9	4	2.13×10^{5}
80	4	4.2	1.86×10^{5}
81	4.2	4.4	1.57×10^{5}
82	4.4	4.6	1.32×10^{5}
83	4.6	4.8	1.11×10^{5}
84	4.8	5	9.39×10^{4}
85	5	5.5	7.06×10^{4}
86	5.5	6	4.66×10^{4}
87	6	6.5	3.09×10^{4}
88	6.5	7	2.06×10^{4}
89	7	7.5	1.37×10^{4}
90	7.5	8	9.20×10^{3}

[a]Normalized to a total (E > 10 keV) neutron fluence of 2.83×10^{8} n/cm^2-s-kW at 1 m from core center.

The n/γ dose ratio in rad tissue is 10 for free-field conditions near core surface and 7 in the glory hole with a steel liner. With 150 mm of n/γ converter material, this ratio can be changed by a factor of 50 from 10 to 0.2, as shown in Figure 2-24. In terms of neutron fluence per γ dose, this ratio is 4.48×10^9 n/cm^2 rad for leakage neutrons and 3.23×10^9 n/cm^2 rad in the steel-lined glory hole. This ratio can be varied through proper shielding arrangements, and also varies significantly as a function of range.

Experience has shown that induced electrical noise is not a problem at the APRF. Normal coaxial shielding techniques have proven to be adequate for experiments. However, unusual experiments involving high impedance or gains greater than 1,000 would warrant consultation with the facility staff regarding triaxial signal systems and types of grounds.

2.3.4 Support Capabilities

A professional and technical staff is available to guide, plan, and set up experiments, perform dosimetry, and assist in data acquisition. Each user program is assigned to a project engineer whose responsibility it is to provide technical and administrative consultation so that each program is completed satisfactorily and on schedule. Extensive electronic support equipment and a complete data-recording system are available at the facility. Staff engineering assistance is available so users can make the maximum use of this capability.

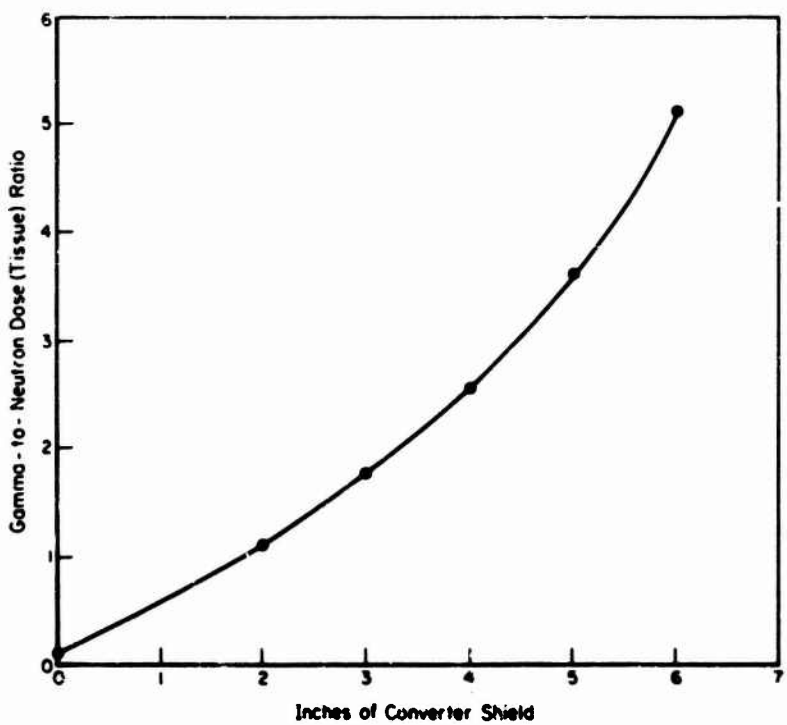

Figure 2-24. γ/n dose (tissue) ratio versus converter shield thickness.

The APRF Transient Data Recording System is designed to record electrical transient data over frequency ranges of dc to 80 kHz and 400 Hz to 700 kHz. The system consists of three 14-track magnetic tape instrument recorders, FM and direct recorder electronics, time code and analog calibration systems, an assortment of signal-processing instrumentation, and an oscillograph for "quick-look" data display. Patch panels are provided in the instrument room for connecting any signal cable to any data channel. Trumpter triaxial patch plugs and cords are used for all low-level signals.

Ten channels of B&F Model 1-700 universal signal conditioners are available to process thermocouple or strain-gage signals. Regulated strain-gage power supplies are rated at 100 mA, 1 to 30 V, and 1 to 50 mA in constant I operation. Three-step calibration relays are provided for automatic calibration. The strain-gage system will accept 1-, 2-, or 4-arm strain gages and up to 8-wire double-shunt calibration.

Signal amplification is provided by 26 dc amplifiers (Dynamics Instrument Company Model 7514B) with the following characteristics:

1. Differential input
2. Input impedance, 10 MΩ
3. Frequency response, dc to 100 kHz, -3db
4. Gain, steps 1 to 1,000
5. Output V, ±10 V.

The analog calibration system will provide a 3-point calibration (including zero) of 50 data channels, simultaneously, prior to a reactor pulse. This calibration system has the following features:

1. Zero, 50%, 100% of full-signal calibration levels
2. Total calibration time less than 6 s
3. Individually adjustable levels from 0.001 to 10 V
4. Manual or automatic stepping through the different calibration levels
5. Square-wave or dc output
6. Shunt resistor calibration for strain gages and mV injection for thermocouples and dc amplifier channels.

Connector panels leading to the data system, with an assortment of cables, are available in the Reactor Building (East, North, and Northwest) and at the outdoor test pad. Each connector panel includes the following connectors and cables:

Connector	Cable	Quantity
BNC	RG-58 C, 50-Ω	20
HN	RG-11 A, 75-Ω	10
BNC	RG-62 B, 93-Ω	5
Triaxial	RG 108A Twinax, 78-Ω	10
Viking 4-pin	2-wire, shielded	20
Viking 13-pin	8-wire, shielded	10

Three 14-track instrumentation recorders are available for the recording of data. They are equipped with medium-band heads giving a direct frequency response of 400 Hz to 700 kHz, and an FM response of dc to 80 kHz using IRIG wideband Group I frequencies. An IRIG-A time-code signal is recorded on each recorder for search and control purposes. One recorder is used for playback into either oscilloscopes or an oscillograph. The oscillograph is equipped with 14 channels to display all data simultaneously on a tape.

No screen room is available. However, provisions can be made for adequate electrical shielding.

APRF supporting electric equipment is as follows:

Item	Quantity Available
556 Tektronix Oscilloscope	3
555 Tektronix Oscilloscope	3
R7912 Tektronix Transient Digitizer	1
PDP 11-05 DEC Computer	1
Digital Lab Peripheral System	1
Nuclear Data 4420 Dual Parameter Multichannel Analyzer System	1
C-19 Oscilloscope Cameras	5
200 Hewlett Packard Audio Oscillator	1
575 Tektronix Curve Tracer	1
56505 Power Designs Power Supplies	4
890A Harrison Lab Power Supply	1
2K10 Power Designs Power Supply	2
261 Keithley Picoampere Source	2
660A Keithley Differential Voltmeter	1
500 Keithley Megohmmeter	2
1210-C General Radio Signal Generator	1
1862C General Radio Megohmmeter	1
Cu-2 Anadex Pulse Generator	1
6613 Texas Instruments Pulse Generator	1
6609 Texas Instruments Pulse Generator	1
5 8A Hickok Tube Tester	1
3440 Hewlett Packard Digital Voltmeter	1
1212D ORNL Pulse Generator	1
184 Tektronix Time-Mark Generator	1

(continued)

Item	Quantity Available
5244L Hewlett Packard Counter/Timer	1
652A Hewlett Packard Sine-Wave Generator	1
3400 RMS Meter	2
241 Keithley Power Supply	1
415B Fluke Power Supply	3
454 Tektronix Oscilloscope	1
531 Tektronix Oscilloscope	1
RIDL 400-Channel Pulse Height Analyzer	1
TC-200 Tennelec Linear Amplifier	2
C-12 Oscilloscope Camera	2

A zero-time pulse is available for external synchronization of circuits and oscilloscopes. The synch pulse is +20-V, 20-Ω source impedance and will drive up to 20 oscilloscopes. The time interval between the synch pulse and the peak of the reactor pulse is approximately 125 μs for a 1.2×10^{17} fissions-yield pulse.

Dosimetry is performed by the facility staff. Various neutron and γ dosimetry systems are available, including S and fission foil counting, high-resolution spectrometers, γ glass microdosimeters and miniature ion chambers, and active dosimeters (including PIN, diodes, and SEMIRAD). Specialized requirements such as spectrum calculations can be arranged for, subject to prior negotiations.

Light machine shop facilities can provide limited service at the site. The APG central shop facilities for heavy mechanical work are available by special arrangement. Extensive experiment preparation rooms/laboratories, including a radiochemistry lab, a metallurgical lab, and a small electronics repair lab, are available. Office space, a small library, a conference room, a main technical library, and a photographic laboratory are also available.

2.3.5 Procedural Information

Address technical and administrative inquiries to:

Commander
U.S. Army Aberdeen Proving Ground
Attn: STEAP-MT-R
Aberdeen Proving Ground, MD 21005
Telephone: Com. (301) 278-4881, 3204, 3970
A/V 283-4881, 3204, 3970

Dr. H.P. Yockey
Dr. A.H. Kazi
Mr. R.C. Harrison

Direct funding transfers to:

Commander
U.S. Army Aberdeen Proving Ground
Attn: STEAP-CO
Aberdeen Proving Ground, MD 21005
Telephone: (301) 278-4520

Approximately 3 months lead time for programs requiring several weeks, including time for approval of a written test plan, is required. Short programs can be accommodated on shorter notice as the schedule permits. It is essential that informal contact with the facility be established as soon as there appears to be a requirement. Cost and charges associated with the use of the reactor and the facility can be obtained directly from the facility.

2.3.6 Applicability and Availability

The APRF was built to support the U.S. Army radiation effects mission. Over the past several years investigations of prime interest have included radiation effects on propellants, ordnance, electronics and chemicals, vehicle shielding, neutron radiography, dosimetry, and health physics. The reactor has been used extensively in TREE experiments.

A full operating staff and a limited professional staff are permanently assigned to the facility. The professional staff is not primarily oriented toward TREE investigations; however, they will provide assistance and technical consultation within the available limits of manpower and funding. The APRF is located at some distance from the main area of Aberdeen Proving Ground and from the nearer motels. The facility is about 1 hr from Friendship Airport in Baltimore and 1½ hr from National Airport in Washington, D.C. It is necessary for experimenters to provide their own daily transportation.

2.3.7 References

1. "Army Pulse Radiation Facility," brochure available directly from APRF.

2. Kazi, A.H., "Fast-Pulse Reactor Operation with Reflector Control and a 106 mm Diameter Glory Hole," *Nuclear Science and Engineering, 60:62-73,* May 1976.

3. Kazi, A.H., T.A. Dunn, R.C. Harrison, and D.O. Williams, "Characteristics of Pulsed Fast Neutron-to-Gamma Ray Converters," *Nuclear Technology, 25:450-463,* March 1975.

4. McGarry, E.D., A.H. Kazi, G.S. Davis, and D.M. Gilliam, "Absolute Neutron-Flux Measurements at Fast Pulse Reactors with Calibration against Californium-252," *IEEE Trans. Nucl. Sci., NS-3, 6:2002,* December 1976.

5. Kazi, A.H., D. McGarry, and D.M. Gilliam, "Standardization of Fast Pulse Reactor Dosimetry," *Proc. International Specialists Symposium on Neutron Standards and Applications, March 28-31, 1977,* National Bureau of Standards Special Application 493, October 1977.

6. Kazi, A.H., G.S. Davis, and C.R. Heimbach, "Spectrum and Dose Calibrations of Controlled Neutron Fields at the APRF Critical Assembly," *Second ASTM-EURATOM Symposium on Reactor Dosimetry,* Palo Alto, California, October 1977.

2.4 ARMY FAST BURST REACTOR FACILITY

The Fast Burst Reactor (FBR) is a Godiva-type reactor that produces a neutron environment approximating a weapon environment. It is an all-metal, unreflected, and unmoderated critical asssembly in the form of a right-circular cylinder 8 in. in dia. and 7.6 in. high. The assembly contains a total mass of 92.4 kg of fully enriched U (93.2% U-235) alloyed with 10 w/o Mo. Samples are irradiated external to the reactor core. Recently, it also has been used as a pulsed γ source. The neutron pulse is nominally 50-μs wide (FWHM) and at the closest approach to the core offers a fast flux of about 6×10^{13} n/cm^2 per burst. When used as a γ source, the pulse may be as wide as several hundred μs.

A small axial cavity has been incorporated into the FBR design. At a later date (after further testing), the use of this cavity will be permitted. It is expected that this cavity will allow experimenters to expose small experiments to doses 5 times larger than exposures external to the core.

A thin-walled steel shroud approximately 8.75 in. in dia. and 10 in. high covers the fuel assembly. The shroud, lined with B, serves a dual purpose by ducting forced cooling air over the fuel system and by diminishing the reactivity contribution of moderating test samples placed external to the core. Typical turnaround time from burst to burst is about 90 min. Minimum turnaround time, without cell entry, is about 45 min.

The FBR may be operated in the pulse mode or at a steady-state power of up to 5 kW. In a steady-state mode, it will produce the dose equivalent to a usual burst in about 15 min.

Figure 2-25 illustrates the reactor and facility building. The reactor is normally operated in a room 50 x 50 x 20 ft. For experiments too large for the reactor cell, the reactor may be moved to an outdoor operating site at a ground-level station. There are no features of the surrounding terrain (trees, hills, etc.) that limit the utility of the outdoor site.

2.4.1 Operating Characteristics

Maximum burst yield is 1×10^{17} fissions and has the following associated with it:

1.	Total leakage neutrons	$\sim 1.5 \times 10^{17}$ n
2.	Neutron fluence 1 in. from reactor shroud	$\sim 7 \times 10^{13}$ n/cm^2 (E > 10 keV)
3.	Peak γ dose	2×10^4 rad*
4.	Peak γ dose rate	1×10^8 rad*/s

Pulse width and initial reactor period results of measurements utilizing fluor detectors placed external to the reactor are:

---

* It is assumed the dose is in air.

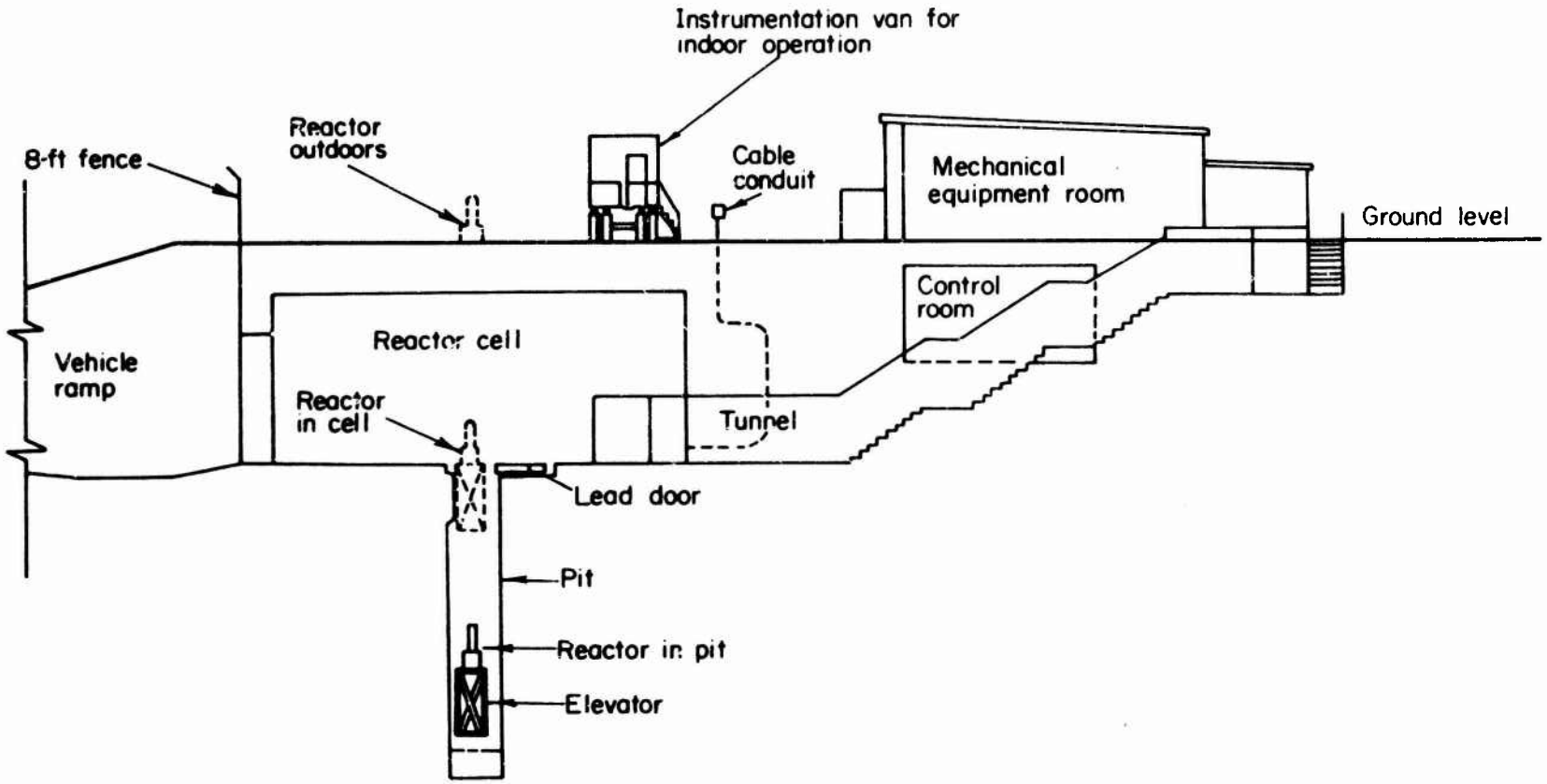

Figure 2-25. Elevation section of FBR control building and reactor cell.

1. Pulse width (FWHM) 48 μs
2. Initial reactor period 16 μs

Temperature characteristics are:

1. Maximum temperature rise 300-500°C
2. Maximum average temperature rise 150-250°C
3. Cooling time (forced air) 45 min

Quantitative data on temperature-time profile are not available.

Experiments having a reactivity worth of up to ~$2.00 can be accommodated. An assessment of sample reactivity worth will be made by the FBR staff for each experiment conducted. Peak reactivity insertion rate is $50/s, burst repetition rate is 1 per 75 min, and predictability is ±5%.

2.4.2 Environment

2.4.2.1 Fluence and Dose Maps

Figures 2-26 through 2-28 are nomographs showing the total fast flux available. The maximum γ dose is about 10^4R at the closest approach to the reactor.

Detailed measurements of the neutron and γ environment generated by the FBR were performed during September 1964 by the Santa Barbara Division of Edgerton, Germerhauser, and Greer, Inc. Neutron fluence and γ dose measurements were made throughout the irradiation cell and in a corresponding volume around the reactor while in an outdoor operating location. Measurements were made in four basic geometries:

1. 6-in. horizontal circle in the geometric midplane of the core and 6-in. vertical semicircles intersecting the vertical core axis
2. 1-m horizontal circle and vertical semicircles
3. Vertical traverses 1 m from the reactor axis
4. Radial profiles from 6 in. to approximately 25 ft from the reactor core center.

All data were normalized to a burst of 1.0×10^{16} fissions (24.3°C ΔT). Data taken from those results are to be used as a guide. If environmental data are required, measurements should be made at the time of the experiment.

Neutron measurements were made using the foils listed in Table 2-9. Results of the neutron measurements are given in Tables 2-10 through 2-19, which tabulate the data as obtained from each of the several foil positions, and Figures 2-29 through 2-41, which graphically display averages of the tabulated data.

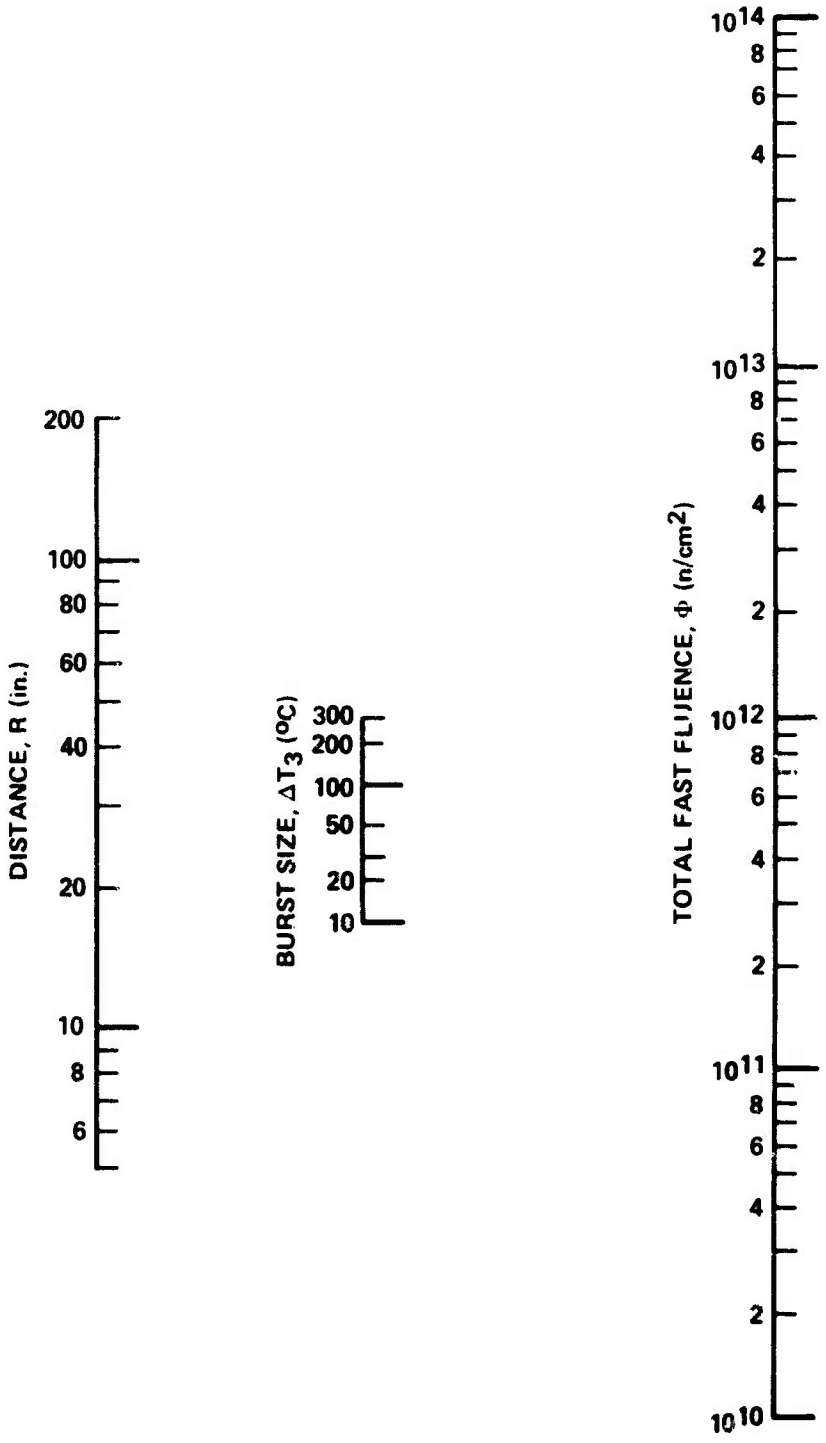

Figure 2-26. Total fast fluence for a given burst size and a given distance at the FBR.

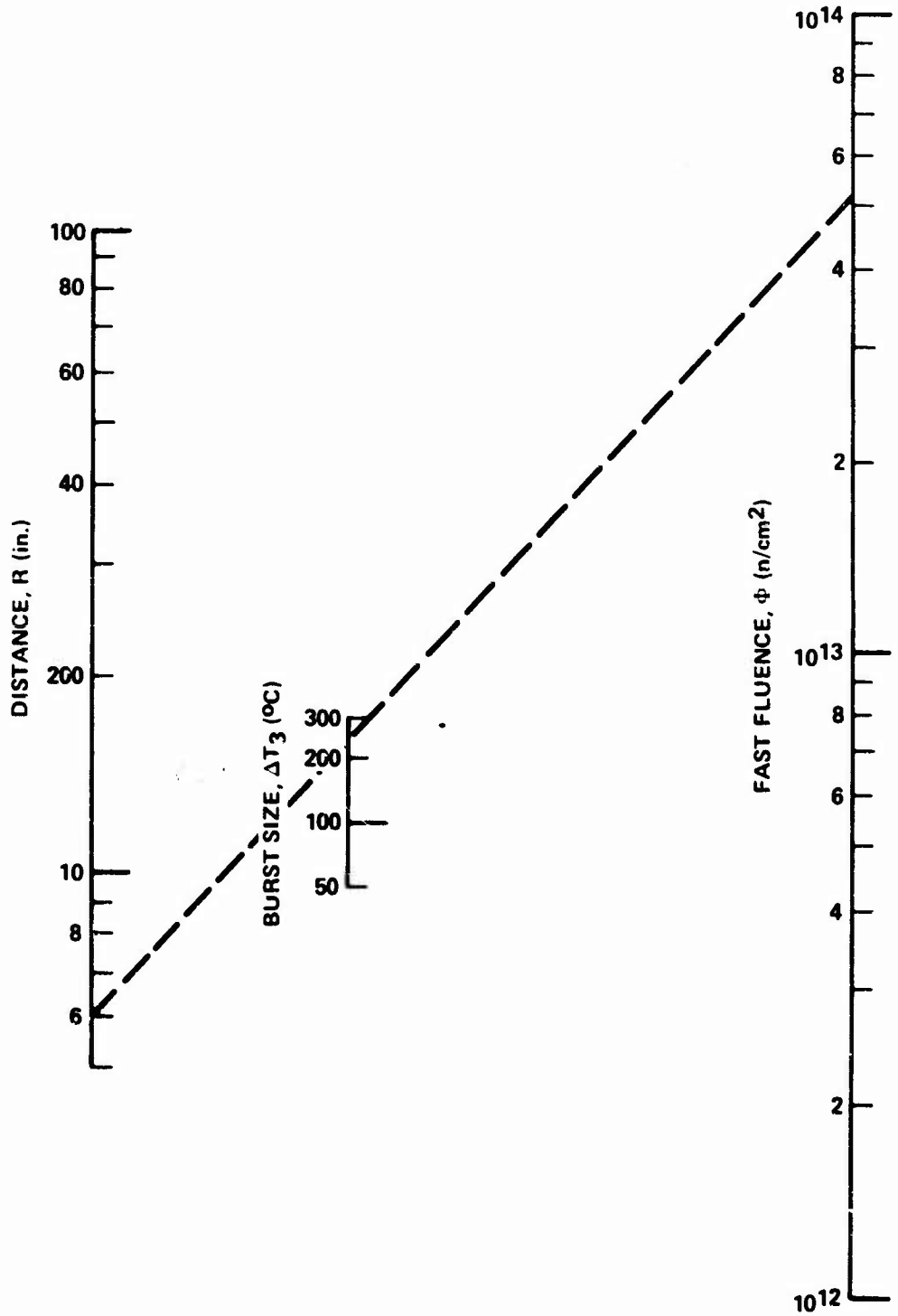

Figure 2-27. Total fast fluence for a given burst size and a given distance at the FBR.

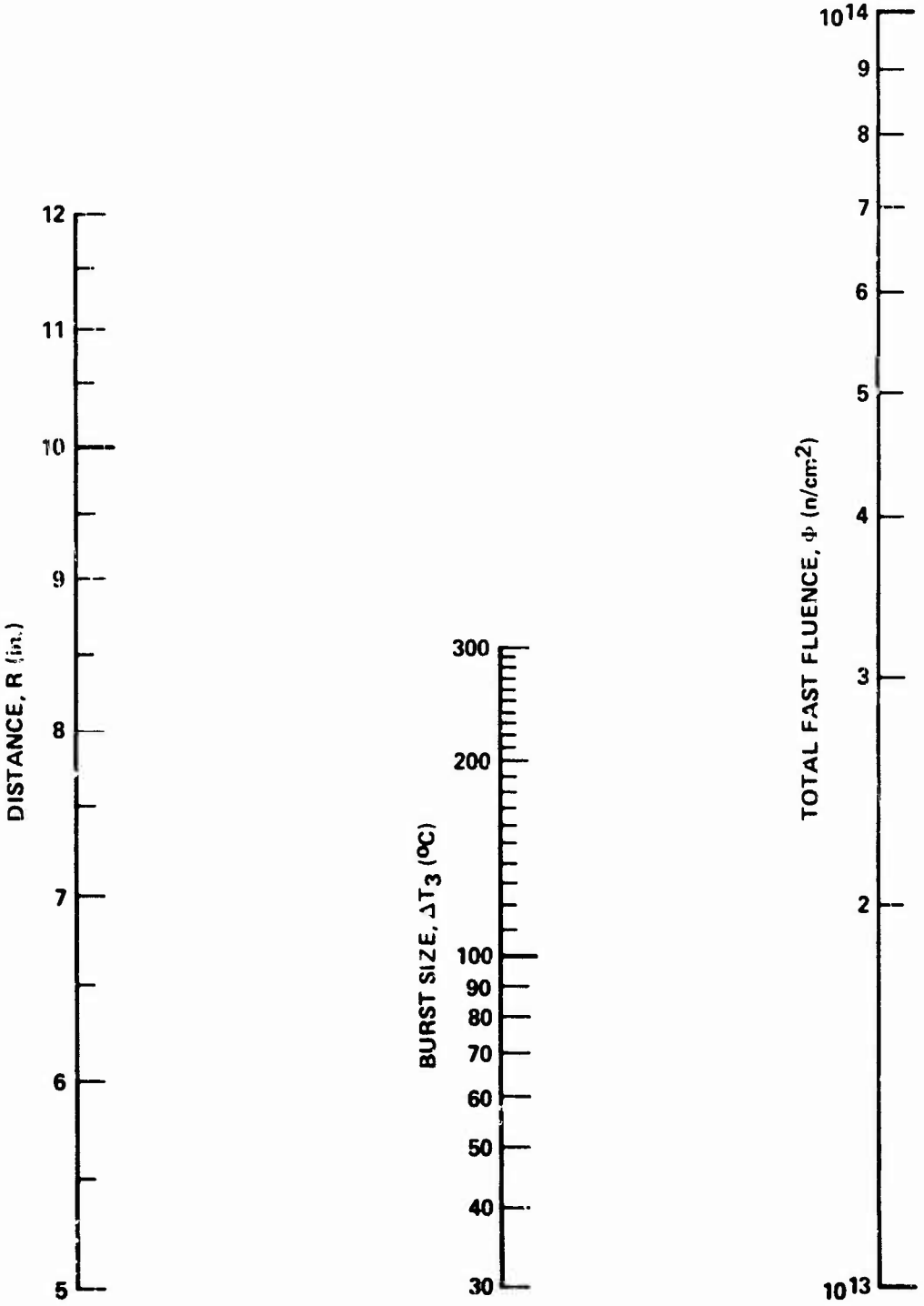

Figure 2-28. Total fast fluence for a given burst size and a given distance at the FBR.

Table 2-9. Neutron threshold detectors.

Material[a]	Reaction	Effective Threshold Energy (E_{eff}) (MeV)	Effective Cross Section (cm^2)
Pu^{239}	$Pu^{239}(n,f)F.P.$	0.010	1.7×10^{-24}
Np^{237}	$Np^{237}(n,f)F.P.$	0.60	1.6×10^{-24}
U^{238}	$U^{238}(n,f)F.P.$	1.5	0.55×10^{-24}
S^{32}	$S^{32}(n,p)P^{32}$	3.0	0.30×10^{-24}
Ni^{58}	$Ni^{58}(n,p)Co^{58}$	3.0	0.29×10^{-24}
Mg^{24}	$Mg^{24}(n,p)Na^{24}$	6.3	0.05×10^{-24}
Al^{27}	$Al^{27}(n,\alpha)Na^{24}$	7.5	0.08×10^{-24}

[a]Fission foils were encapsulated in Cd-coated Cu and irradiated in a B^{10} shield.

Table 2-10. Neutron fluence > 3.0 MeV per 1.0×10^{16} fissions (24.3°C ΔT) on 6-in. horizontal circle.

Position (deg)	Fluence ($\times 10^{11}$ n/cm^2) (E > 3.0 MeV)	
	Outdoor	Indoor
0	7.62	7.67
12	7.46	7.67
24	7.54	7.80
36	7.51	7.80
48	7.26	7.54
60	7.23	7.47
72	7.21	7.47
84	7.18	7.47
96	7.23	7.54
108	7.26	7.47
120	7.56	7.87
132	7.67	8.20
144	7.53	8.14
156	7.34	8.14
168	7.18	7.94
180	7.32	7.94
192	7.04	7.80
204	6.99	7.87
216	7.23	8.00
228	7.54	8.34
240	7.81	8.40
252	7.73	8.47
264	7.62	8.40
276	7.70	8.34
288	7.67	8.14
300	7.45	8.07
312	7.29	7.80
324	7.31	7.67
336	7.15	7.60
348	7.45	7.74
Average	7.40	7.89

Table 2-11. Neutron fluence > 3.0 MeV per 1.0×10^{16} fissions (24.3°C ΔT) on 1-m horizontal circle.

Position (deg)	Fluence ($\times 10^{10}$ n/cm^2) (E > 3.0 MeV)		Position (deg)	Fluence ($\times 10^{10}$ n/cm^2) (E > 3.0 MeV)	
	Outdoor	Indoor		Outdoor	Indoor
0	1.57	1.56	186	1.52	1.55
6	1.59	1.52	192	1.52	1.50
12	1.52	1.51	198	1.52	1.54
18	1.53	1.48	204	1.50	1.52
24	1.53	1.50	210	1.54	1.49
30	1.54	1.51	216	1.55	1.51
36	1.52	1.48	222	1.54	1.50
42	1.59	1.52	228	1.50	1.53
48	1.52	1.49	234	1.54	1.53
54	1.53	1.48	240	1.56	1.48
60	1.49	1.48	246	1.56	1.50
66	1.51	1.50	252	1.57	1.56
72	1.52	1.52	258	1.59	1.54
78	1.55	1.47	264	1.58	1.62
84	1.49	1.48	270	1.55	1.58
90	1.55	1.49	276	1.54	1.58
96	1.55	1.49	282	1.55	1.58
102	1.53	1.49	288	1.51	1.53
108	1.52	1.50	294	1.50	1.50
114	1.52	1.44	300	1.55	1.54
120	1.52	1.51	306	1.53	1.52
126	1.45	1.46	312	1.54	1.51
132	1.52	1.53	318	1.56	1.51
138	1.48	1.51	324	1.51	1.52
144	1.50	1.55	330	1.52	1.52
150	1.48	1.51	336	1.43	1.53
156	1.55	1.58	342	1.55	1.53
162	1.56	1.57	348	1.54	1.53
168	1.53	1.56	354	1.58	1.55
174	1.54	1.55			
180	1.59	1.54	Average	1.53	1.52

Table 2-12. Vertical traverse of neutron fluence > 3.0 MeV per 1.0×10^{16} fissions (24.3°C ΔT) at 1 m from reactor center.

Distance from Floor (in.)	Fluence ($\times 10^9$ n/cm^2) (E > 3.0 MeV)				
	Position 1[a]	Position 2	Position 3	Position 4	Average
Indoor					
6	4.33	4.16	4.07	4.18	4.19
12	5.26	4.73	4.65	4.82	4.86
18	5.88	5.60	5.49	5.72	5.67
24	6.82	6.49	6.21	6.55	6.52
30	8.21	7.75	7.48	7.55	7.75
36	9.60	8.94	9.07	9.40	9.25
42	11.5	10.7	10.7	10.7	10.9
46	12.7	11.8	12.0	12.4	12.2
50	14.0	13.3	13.8	13.3	13.6
54	14.7	14.8	15.2	14.8	14.9
58	15.9	16.4	16.3	15.5	16.0
62	17.1	16.6	16.5	16.6	16.7
65.5	15.2	15.2	15.2	15.2	15.2
72	14.6	13.9	15.0	14.9	14.6
76	13.2	13.2	13.2	13.5	13.3
80	11.9	11.9	12.7	12.6	12.3
84	11.5	11.1	11.1	11.6	11.3
90	9.46	9.39	9.20	8.52	9.14
96	7.53	7.81	7.90	6.76	7.50
102	7.13	6.74	6.70	6.48	6.76
Outdoor					
6	4.12	3.97	3.95	4.24	4.07
12	4.87	4.76	4.54	4.87	4.76
18	5.63	5.51	5.40	5.95	5.62
24	6.64	6.52	6.32	6.70	6.55
30	7.89	7.47	7.81	7.89	7.77
36	9.29	8.83	9.37	9.29	9.19
42	11.0	10.9	10.9	11.0	11.0
46	12.3	11.5	12.3	12.3	12.1
50	13.3	13.0	13.3	13.4	13.3
54	14.8	14.4	14.8	14.7	14.7
58	15.9	15.8	15.6	15.8	15.8
62	16.9	16.9	16.7	16.9	16.9
65.5	15.3	15.3	15.3	15.3	15.3
72	15.0	14.6	14.2	14.5	14.6
76	13.5	13.6	13.5	13.4	13.5
80	12.2	12.4	12.2	12.1	12.2
84	11.0	10.8	11.4	9.02	10.6
90	10.0	9.52	9.83	8.41	9.40
96	8.06	8.18	8.03	8.18	8.11
102	6.62	7.07	6.76	7.87	7.08

[a]The positions referred to here are 90 degrees apart on a circle of 1-m radius and centered at the reactor core. Position 1 is the southeast direction with subsequent positions being located clockwise around the circle.

Table 2-13. Neutron fluence > 3.0 MeV per 1.0 x 10^{16} fissions (24.3°C ΔT) as a function of radial distance from core center, indoor.

Distance From Core Center (in.)	Fluence (n/cm^2) (E > 3.0 MeV)						
	0°[a]	60°	120°	180°	240°	300°	Average
6	7.89 x 10^{11}	7.89 x 10^{11}	7.89 x 10^{11}	7.89 x 10^{10}	7.89 x 10^{11}	7.89 x 10^{11}	7.89 x 10^{11}
7	4.75	4.00	4.75	5.24	5.95	4.82	4.92
8	4.00	3.53	3.98	4.58	4.43	3.98	4.08
9	2.89	2.72	3.15	3.07	3.45	3.15	3.07
10	2.39	2.27	2.41	2.58	2.80	2.52	2.50
11	2.05	2.04	2.02	2.05	2.19	2.04	2.07
12	1.66	1.72	1.67	1.73	1.88	1.64	1.71
13	1.38	1.48	1.50	1.51	1.59	1.45	1.49
14	1.15	1.25	1.27	1.26	1.39	1.24	1.26
15	1.09	1.10	9.25 x 10^{10}	1.12	1.18	1.07	1.08
17	8.27 x 10^{10}	8.31 x 10^{10}	7.65	8.62 x 10^{10}	9.21 x 10^{10}	8.15 x 10^{10}	8.37 x 10^{10}
19	6.69	6.63	6.76	7.02	7.14	7.03	6.88
21	5.59	5.51	5.47	5.91	5.79	5.68	5.66
23	4.40	---	4.90	---	4.67	4.68	4.66
25	3.96	---	4.00	3.87	3.98	4.02	3.96
28	3.14	3.13	3.17	3.21	3.01	3.16	3.14
31	2.58	2.61	2.56	2.37	2.73	2.57	2.57
34	2.09	2.09	2.19	2.20	2.20	2.19	2.14
39.4	1.52	1.52	1.52	1.52	1.52	1.52	1.52
49	1.12	1.12	1.12	1.15	1.10	1.15	1.13
59	7.74 x 10^{9}	7.74 x 10^{9}	7.90 x 10^{9}	7.39 x 10^{9}	7.76 x 10^{9}	7.82 x 10^{9}	7.73 x 10^{9}
69	5.79	5.69	5.84	5.82	6.01	5.75	5.82
93	3.27	3.20	3.35	3.30	3.35	3.14	3.27
117	2.17	1.98	2.12	2.21	2.19	2.09	2.13
141	1.41	1.49	1.49	1.53	1.51	1.47	1.48
165	1.10	1.13	1.11	1.11	1.13	1.01	1.10
189	8.45 x 10^{8}	8.52 x 10^{8}	8.75 x 10^{8}	8.71 x 10^{8}	8.63 x 10^{8}	7.81 x 10^{8}	8.48 x 10^{8}
213	6.70	6.75	7.21	7.13	7.46	6.89	7.02
237	5.86	5.21	5.57	5.55	5.65	5.53	5.56
261	4.60	4.78	5.01	4.59	4.90	5.20	4.85
285	4.81	4.27	4.50	4.57	4.23	---	4.48

[a]Zero degrees lying directly south with subsequent degrees measured in a clockwise manner on a horizontal plane located at the core center.

Table 2-14. Neutron fluence > 3.0 MeV per 1.0 x 10^{16} fissions (24.3°C ΔT) as a function of radial distance from core center, outdoor.

Distance From Core Center (in.)	Fluence (n/cm^2) (E > 3.0 MeV)						
	0°[a]	60°	120°	180°	240°	300°	Average
6	7.40 x 10^{11}	7.40 x 10^{11}	7.40 x 10^{11}	7.40 x 10^{11}	7.40 x 10^{11}	7.40 x 10^{11}	7.40 x 10^{11}
7	4.74	4.68	4.76	4.36	5.61	4.22	4.73
8	4.15	3.69	3.61	3.74	4.28	3.88	3.89
9	3.01	3.01	2.42	2.98	3.15	3.26	2.97
10	2.55	2.38	2.36	2.48	2.63	2.50	2.49
11	2.02	1.89	1.96	1.96	2.07	2.15	2.01
12	1.86	1.66	1.75	1.72	1.90	1.82	1.78
13	1.43	1.47	1.45	1.51	1.61	1.52	1.50
14	1.21	1.18	1.29	1.27	1.33	1.22	1.25
15	1.06	1.06	1.06	9.96 x 10^{10}	1.09	1.07	1.06
17	8.45 x 10^{10}	7.70 x 10^{10}	7.19 x 10^{10}	8.20	---	8.50 x 10^{10}	8.01 x 10^{10}
19	6.39	6.69	6.14	5.83	---	6.89	6.41
21	6.01	5.81	5.64	5.78	5.91 x 10^{10}	5.74	5.81
23	4.78	4.51	4.61	4.78	4.81	4.94	4.74
25	3.87	3.94	4.01	3.97	3.94	3.87	3.93
28	3.32	3.02	3.14	3.18	3.24	3.22	3.19
31	2.49	2.64	2.36	2.42	2.43	2.53	2.48
34	2.00	2.16	2.05	2.20	2.07	2.12	2.10
39.4	1.53	1.53	1.53	1.53	1.53	1.53	1.53
49	1.11	1.15	1.11	1.13	1.23	1.21	1.16
59	7.71 x 10^{9}	7.92 x 10^{9}	7.70 x 10^{9}	7.94 x 10^{9}	8.33 x 10^{9}	8.26 x 10^{9}	7.98 x 10^{9}
69	5.78	5.94	5.70	5.70	6.35	5.70	5.86
97	3.25	3.28	3.18	3.24	3.42	3.25	3.27
117	2.13	2.07	1.96	2.01	2.12	2.16	2.07
141	1.38	1.55	1.45	1.03	1.41	1.45	1.38
165	1.05	1.06	1.07	8.70 x 10^{8}	1.12	1.07	1.04
189	8.05 x 10^{8}	8.03 x 10^{8}	7.68 x 10^{8}	6.40	8.34 x 10^{9}	8.05 x 10^{8}	7.76 x 10^{8}
213	6.16	6.74	5.89	5.23	6.40	6.32	6.11
237	4.99	4.52	4.89	4.42	5.09	5.33	4.87
261	4.24	4.53	3.86	3.90	4.31	4.34	4.20
285	3.49	3.54	3.30	3.52	3.30	3.30	3.41

[a]Zero degrees lying directly south with subsequent degrees measured in a clockwise manner on a horizontal plane located at the core center.

Table 2-15. Neutron fluence above various threshold energies per 1.0×10^{16} fissions (24.3°C ΔT) on four vertical traverses 1 m from core center, indoor.

Distance Above Floor (in.)	Pu^{239} (n/cm^2) (E > 10 keV)	Np^{237} (n/cm^2) (E > 0.60 MeV)	U^{238} (n/cm^2) (E > 1.50 MeV)	S^{32} (n/cm^2) (E > 3.0 MeV)	Ni^{58} (n/cm^2) (E > 3.0 MeV)	Mg^{24} (n/cm^2) (E > 6.3 MeV)	Al^{27} (n/cm^2) (E > 7.5 MeV)	Thermal Neutron (n/cm^2)
Position 1[a]								
12	4.75 (10)[b]	2.67 (10)	1.30 (10)	5.26 (9)	4.58 (9)	6.39 (8)	2.76 (9)	1.37 (9)
24	6.38 (10)	3.59 (10)	1.79 (10)	6.82 (9)	6.69 (9)	1.01 (9)	3.68 (9)	1.37 (9)
36	8.57 (10)	4.95 (10)	2.42 (10)	9.60 (9)	8.24 (9)	1.41 (9)	4.67 (8)	1.31 (9)
54	1.23 (11)	7.24 (10)	3.81 (10)	1.47 (10)	1.32 (10)	2.16 (9)	7.39 (8)	1.51 (9)
65.5	1.31 (11)	8.12 (10)	4.10 (10)	1.46 (10)	1.56 (10)	2.20 (9)	8.19 (8)	1.62 (9)
72	1.32 (11)	8.18 (10)	4.08 (10)	1.52 (10)	1.46 (10)	1.86 (9)	7.39 (8)	1.46 (9)
80	1.17 (11)	7.00 (10)	3.38 (10)	1.19 (10)	1.31 (10)	1.60 (9)	6.09 (8)	1.39 (9)
90	8.70 (10)	5.29 (10)	2.64 (10)	9.46 (9)	1.00 (10)	1.11 (9)	4.34 (8)	1.37 (9)
102	6.53 (10)	3.92 (10)	1.90 (10)	7.13 (9)	7.12 (9)	9.88 (9)	3.19 (8)	1.35 (9)
Position 2								
12	5.01 (10)	2.72 (10)	1.26 (10)	4.73 (9)	3.96 (9)	6.06 (8)	2.29 (8)	1.39 (9)
24	5.93 (10)	3.11 (10)	1.75 (10)	6.49 (9)	5.73 (9)	9.36 (8)	3.51 (8)	1.46 (9)
46	9.79 (10)	5.95 (10)	3.03 (10)	1.18 (9)	1.03 (10)	1.55 (9)	5.06 (8)	1.48 (9)
62	1.36 (11)	8.06 (10)	4.25 (10)	1.66 (9)	1.58 (10)	1.92 (9)	7.74 (8)	1.48 (9)
65.5	1.31 (11)	8.12 (10)	4.10 (10)	1.52 (9)	1.56 (10)	2.20 (9)	8.19 (8)	1.62 (9)
72	1.20 (11)	7.32 (10)	3.95 (10)	1.39 (9)	1.39 (10)	1.95 (9)	7.40 (8)	1.43 (9)
80	1.03 (11)	6.40 (10)	3.21 (10)	1.19 (9)	1.27 (10)	1.61 (9)	5.98 (8)	1.39 (9)
90	8.19 (10)	5.19 (10)	2.63 (10)	9.39 (9)	9.76 (9)	1.14 (9)	4.71 (8)	1.43 (9)
102	6.35 (10)	3.49 (10)	1.89 (10)	6.74 (9)	7.09 (9)	1.00 (9)	3.50 (8)	1.38 (9)
Position 3								
12	.78 (10)	2.36 (10)	1.26 (10)	4.65 (9)	3.90 (9)	5.45 (8)	2.22 (8)	1.39 (9)
36	8.12 (10)	4.40 (10)	2.35 (10)	9.07 (9)	7.89 (9)	1.17 (9)	4.48 (8)	1.39 (9)
54	1.26 (11)	7.74 (10)	3.77 (10)	1.52 (10)	1.36 (10)	1.83 (9)	6.70 (8)	1.40 (9)
62	1.38 (11)	7.97 (10)	4.46 (10)	1.65 (10)	1.52 (10)	2.04 (9)	7.88 (8)	1.42 (9)
65.5	1.31 (11)	8.12 (10)	4.10 (10)	1.52 (10)	1.56 (10)	2.20 (9)	8.19 (8)	1.62 (9)
72	1.25 (11)	7.52 (10)	3.83 (10)	1.50 (10)	1.48 (10)	2.13 (9)	7.80 (8)	1.39 (9)
80	1.14 (11)	6.32 (10)	3.46 (10)	1.27 (10)	1.31 (10)	1.89 (9)	6.13 (8)	1.39 (9)
90	8.77 (10)	5.00 (10)	2.69 (10)	9.20 (9)	9.35 (9)	1.06 (9)	4.35 (8)	1.39 (9)
102	6.23 (10)	3.55 (10)	1.88 (10)	6.70 (9)	6.84 (9)	9.90 (8)	3.32 (8)	1.39 (9)
Position 4								
24	6.35 (10)	3.81 (10)	1.82 (10)	6.55 (9)	6.46 (9)	8.16 (8)	3.32 (8)	1.42 (9)
46	1.07 (11)	6.31 (10)	3.21 (10)	1.24 (10)	1.16 (10)	1.61 (9)	5.77 (8)	1.44 (9)
54	1.28 (11)	7.34 (10)	3.89 (10)	1.48 (10)	1.40 (10)	1.91 (9)	7.17 (8)	1.46 (9)
62	1.40 (11)	8.61 (10)	4.41 (10)	1.66 (10)	1.59 (10)	2.21 (9)	8.30 (8)	1.46 (9)
65.5	1.31 (11)	8.12 (10)	4.10 (10)	1.52 (10)	1.56 (10)	2.20 (9)	8.19 (8)	1.62 (9)
72	1.42 (11)	7.23 (10)	4.16 (10)	1.49 (10)	1.50 (10)	1.96 (9)	7.72 (8)	1.46 (9)
80	1.16 (11)	6.01 (10)	3.64 (10)	1.26 (10)	1.31 (10)	1.72 (9)	6.42 (8)	1.44 (9)
90	9.05 (10)	5.36 (10)	2.82 (10)	8.52 (9)	9.01 (9)	1.19 (9)	4.80 (8)	1.39 (9)
102	5.59 (10)	3.72 (10)	2.08 (10)	6.48 (9)	7.93 (9)	9.92 (8)	3.66 (8)	1.41 (9)
Vertical Traverse Average Values								
12	4.85 (10)	2.59 (10)	1.27 (10)	4.88 (9)	4.15 (9)	5.97 (8)	2.42 (8)	1.38 (9)
24	6.22 (10)	3.50 (10)	1.79 (10)	6.62 (9)	6.29 (9)	9.20 (8)	3.51 (8)	1.42 (9)
36	8.35 (10)	4.67 (10)	2.39 (10)	9.33 (9)	8.06 (9)	1.29 (9)	4.57 (8)	1.35 (9)
46	1.02 (11)	6.13 (10)	3.12 (10)	1.21 (10)	1.10 (10)	1.58 (9)	5.42 (8)	1.46 (9)
54	1.26 (11)	7.44 (10)	3.82 (10)	1.48 (10)	1.36 (10)	1.96 (9)	7.17 (8)	1.45 (9)
62	1.38 (11)	8.21 (10)	4.37 (10)	1.66 (10)	1.57 (10)	2.06 (9)	7.97 (8)	1.45 (9)
62.5	1.31 (11)	8.12 (10)	4.40 (10)	1.52 (10)	1.56 (10)	2.20 (9)	8.19 (8)	1.62 (9)
72	1.30 (11)	7.55 (10)	4.01 (10)	1.46 (10)	1.47 (10)	1.97 (9)	7.58 (8)	1.44 (9)
80	1.20 (11)	6.44 (10)	3.42 (10)	1.23 (10)	1.30 (10)	1.65 (9)	6.15 (8)	1.40 (9)
90	8.68 (10)	5.24 (10)	2.69 (10)	9.14 (9)	9.53 (9)	1.12 (9)	4.55 (8)	1.39 (9)
102	6.18 (10)	3.67 (10)	1.94 (10)	6.76 (9)	7.00 (9)	9.93 (8)	3.42 (8)	1.38 (9)

[a]The positions referred to here are 90 degrees apart on a circle of 1-m radius centered at the reactor core. Position 1 is in the southeast direction with subsequent positions being located clockwise around the circle.

[b]"(10)" = 10^{10}; "(9)" = 10^9; etc.

Table 2-16. Neutron fluence above various threshold energies per 1.0 x 10^{16} fissions (24.3°C ΔT) on four vertical traverses 1 m from core center, outdoor.

Distance Above Floor (in.)	Pu^{239} (n/cm^2) (E > 10 keV)	Np^{237} (n/cm^2) (E > 0.60 MeV)	U^{238} (n/cm^2) (E > 1.50 MeV)	S^{32} (n/cm^2) (E > 3.0 MeV)	Ni^{58} (n/cm^2) (E > 3.0 MeV)	Mg^{24} (n/cm^2) (E > 6.3 MeV)	Al^{27} (n/cm^2) (E > 7.5 MeV)	Thermal Neutron (n/cm^2)
Position 1[a]								
12	4.48 (10)[b]	2.61 (10)	1.26 (10)	4.87 (9)	4.77 (9)	7.32 (8)	2.19 (8)	9.14 (8)
62	1.24 (11)	8.01 (10)	4.01 (10)	1.69 (10)	1.66 (10)	2.27 (9)	8.26 (8)	5.00 (8)
65.5	1.16 (11)	7.08 (10)	3.79 (10)	1.53 (10)	1.49 (10)	2.08 (9)	7.41 (8)	4.7 (8)
76	1.11 (11)	6.95 (10)	3.62 (10)	1.35 (10)	1.10 (10)	1.73 (9)	7.44 (8)	4.1 (8)
96	6.78 (10)	4.21 (10)	2.05 (10)	8.06 (9)	8.18 (9)	1.18 (9)	4.77 (8)	3.5 (8)
Position 2								
46	8.32 (10)	5.39 (10)	2.83 (10)	1.15 (10)	1.07 (10)	1.58 (9)	5.71 (8)	6.15 (8)
65.5	1.16 (11)	7.08 (10)	3.79 (10)	1.53 (10)	1.49 (10)	2.08 (9)	7.41 (8)	4.7 (8)
90	8.03 (10)	5.24 (10)	2.53 (10)	9.52 (9)	8.93 (9)	1.32 (9)	5.12 (8)	3.7 (8)
Position 3								
24	5.36 (10)	3.23 (10)	1.64 (10)	6.32 (9)	5.96 (9)	1.00 (9)	3.03 (8)	7.66 (8)
65.5	1.16 (11)	7.08 (10)	3.79 (10)	1.53 (10)	1.49 (10)	2.08 (9)	7.41 (8)	4.7 (8)
76	1.01 (11)	6.87 (10)	3.22 (10)	1.35 (10)	1.22 (10)	1.67 (9)	6.70 (8)	4.1 (8)
96	6.53 (10)	4.21 (10)	2.11 (10)	8.03 (9)	8.15 (9)	1.00 (9)	4.20 (8)	3.5 (8)
Position 4								
36	8.01 (10)	4.71 (10)	2.36 (10)	9.29 (9)	8.68 (9)	1.34 (9)	4.60 (8)	6.65 (8)
54	1.18 (11)	7.04 (10)	3.64 (10)	1.47 (10)	1.38 (10)	1.90 (9)	8.05 (8)	5.39 (8)
65.5	1.15 (11)	7.08 (10)	3.79 (10)	1.53 (10)	1.49 (10)	2.08 (9)	7.41 (8)	4.7 (8)
90	8.06 (10)	5.06 (10)	2.54 (10)	8.41 (9)	1.06 (10)	1.29 (9)	5.07 (8)	3.7 (8)
Vertical Traverse Average Values								
12	4.48 (10)	2.61 (10)	1.26 (10)	4.87 (9)	4.77 (9)	7.32 (8)	2.19 (8)	9.14 (8)
24	5.36 (10)	3.23 (10)	1.64 (10)	6.32 (9)	5.96 (9)	1.00 (9)	3.03 (8)	7.66 (8)
36	8.01 (10)	4.71 (10)	2.36 (10)	9.29 (9)	8.68 (9)	1.34 (9)	4.60 (8)	6.65 (8)
46	8.32 (10)	5.39 (10)	2.83 (10)	1.15 (10)	1.07 (10)	1.58 (9)	5.71 (8)	6.15 (8)
54	1.18 (11)	7.04 (10)	3.64 (10)	1.47 (10)	1.38 (10)	1.90 (9)	8.05 (8)	5.39 (8)
62	1.24 (11)	8.01 (10)	4.01 (10)	1.69 (10)	1.66 (10)	2.27 (9)	8.26 (8)	5.00 (8)
65.5	1.16 (11)	7.08 (10)	3.79 (10)	1.53 (10)	1.49 (10)	2.08 (9)	7.41 (8)	4.7 (8)
76	1.06 (11)	6.91 (10)	3.42 (10)	1.35 (10)	1.16 (10)	1.70 (9)	7.07 (8)	4.1 (8)
90	8.04 (10)	5.16 (10)	2.53 (10)	8.97 (9)	8.97 (9)	1.30 (9)	5.09 (8)	3.7 (8)
96	6.65 (10)	4.21 (10)	2.09 (10)	8.04 (9)	8.16 (9)	1.09 (9)	4.48 (8)	3.5 (8)

[a]The positions referred to here are 90 degrees apart on a circle of 1-m radius and centered at the reactor core. Position 1 is in the southeast direction with subsequent positions being located clockwise around the circle.

[b]"(10)" = 10^{10}; "(9)" = 10^9; etc.

Table 2-17. Neutron fluence above various threshold energies per 1.0 x 10^{16} fissions (24.3°C ΔT) as a function of radial distance from core center, indoor.

Distance from Core Center (in.)	Pu^{239} (n/cm^2) (E > 10 keV)	Np^{237} (n/cm^2) (E > 0.60 MeV)	U^{238} (n/cm^2) (E > 1.50 MeV)	S^{32} (n/cm^2) (E > 3.0 MeV)	Ni^{58} (n/cm^2) (E > 3.0 MeV)	Mg^{24} (n/cm^2) (E > 6.3 MeV)	Al^{27} (n/cm^2) (E > 7.5 MeV)	Thermal Neutron (n/cm^2)
0°[a]								
6	6.79 (12)[b]	4.31 (12)	2.23 (12)	7.89 (11)	7.85 (11)	1.12 (11)	4.32 (10)	1.1 (9)
9	2.08 (12)	1.48 (12)	8.44 (11)	2.89 (11)	2.80 (11)	3.92 (10)	1.48 (10)	1.35 (9)
12	1.42 (12)	8.55 (11)	4.51 (11)	1.66 (11)	1.71 (11)	2.39 (10)	8.86 (9)	1.43 (9)
15	8.88 (11)	5.14 (11)	2.92 (11)	1.09 (11)	1.10 (11)	1.52 (10)	5.59 (9)	1.39 (9)
21	4.13 (11)	2.36 (11)	1.38 (11)	5.59 (10)	5.31 (10)	7.74 (9)	2.80 (9)	1.40 (9)
28	2.32 (11)	1.32 (11)	7.62 (10)	3.14 (10)	3.08 (10)	4.52 (9)	1.49 (9)	1.42 (9)
39.4	1.31 (11)	8.12 (10)	4.10 (10)	1.52 (10)	1.56 (10)	2.20 (9)	8.19 (8)	1.62 (9)
59	5.56 (10)	3.40 (10)	1.76 (10)	7.74 (9)	7.29 (10)	--	3.86 (8)	1.40 (9)
117	1.80 (10)	1.07 (10)	5.28 (9)	2.17 (9)	1.8 (9)	--	1.26 (8)	1.43 (9)
189	9.04 (9)	4.53 (9)	2.18 (9)	8.45 (8)	--	--	5.4 (7)	1.31 (9)
261	5.49 (9)	2.83 (9)	1.38 (9)	4.60 (8)	--	--	2.4 (7)	1.30 (9)
120°								
6	6.79 (12)	4.31 (12)	2.23 (12)	7.89 (11)	7.85 (11)	1.12 (11)	4.32 (10)	1.1 (9)
9	2.40 (12)	1.56 (12)	8.19 (11)	3.15 (11)	2.88 (11)	4.00 (10)	1.48 (10)	1.37 (9)
12	1.39 (12)	8.86 (11)	4.66 (11)	1.67 (11)	1.68 (11)	2.31 (10)	8.71 (9)	1.40 (9)
15	9.36 (11)	5.68 (11)	3.06 (11)	9.25 (10)	1.08 (11)	1.53 (10)	5.57 (9)	1.41 (9)
21	3.84 (11)	2.32 (11)	1.31 (11)	5.47 (10)	5.57 (10)	7.40 (10)	2.86 (9)	1.38 (9)
28	2.32 (11)	1.40 (11)	7.67 (10)	3.17 (10)	3.02 (10)	4.54 (9)	1.57 (9)	1.38 (9)
39.4	1.31 (11)	8.12 (10)	4.10 (10)	1.52 (10)	1.56 (10)	2.20 (9)	8.19 (8)	1.62 (9)
59	5.81 (10)	3.61 (10)	1.86 (10)	7.90 (9)	7.35 (9)	--	3.79 (8)	1.32 (9)
117	1.86 (10)	1.07 (10)	5.34 (9)	2.12 (9)	1.8 (9)	--	1.05 (8)	1.38 (9)
189	9.57 (9)	4.93 (9)	2.17 (9)	8.75 (8)	--	--	4.2 (7)	1.25 (9)
261	5.61 (9)	3.02 (9)	1.82 (9)	5.01 (8)	--	--	1.6 (7)	1.21 (9)
240°								
6	6.79 (12)	4.31 (12)	2.23 (12)	7.89 (11)	7.85 (11)	1.12 (11)	4.32 (10)	1.1 (9)
9	2.73 (12)	1.73 (12)	8.93 (11)	3.45 (11)	3.46 (11)	4.62 (10)	1.65 (10)	1.36 (9)
12	1.59 (12)	9.81 (11)	5.36 (11)	1.88 (11)	1.92 (11)	2.54 (10)	9.20 (9)	1.34 (9)
15	9.67 (11)	5.56 (11)	3.21 (11)	1.18 (11)	1.16 (11)	1.63 (10)	6.04 (9)	1.43 (9)
21	4.57 (11)	2.68 (11)	1.54 (11)	5.79 (10)	5.61 (10)	8.00 (9)	2.98 (9)	1.42 (9)
28	2.32 (11)	1.33 (11)	7.83 (10)	3.01 (10)	3.22 (10)	4.76 (9)	1.69 (9)	1.43 (9)
39.4	1.31 (11)	8.12 (10)	4.10 (10)	1.52 (10)	1.56 (10)	2.20 (9)	8.19 (8)	1.62 (9)
59	5.76 (10)	3.63 (10)	1.83 (10)	7.76 (9)	7.46 (9)	--	3.86 (8)	1.34 (9)
117	1.96 (10)	1.11 (10)	5.46 (9)	2.19 (9)	1.8 (9)	--	1.09 (8)	1.36 (9)
189	9.16 (9)	4.58 (9)	2.11 (9)	8.63 (8)	--	--	5.3 (7)	1.30 (9)
261	6.57 (9)	2.67 (9)	1.31 (9)	4.90 (8)	--	--	2.3 (7)	1.27 (9)
Radial Profile Average Values								
6	6.79 (12)	4.31 (12)	2.23 (12)	7.89 (11)	7.85 (11)	1.12 (11)	4.32 (10)	1.1 (9)
9	2.40 (12)	1.59 (12)	8.48 (11)	3.16 (11)	3.05 (11)	4.18 (10)	1.54 (10)	1.36 (9)
12	1.47 (12)	9.07 (11)	4.84 (11)	1.73 (11)	1.77 (11)	2.41 (10)	8.92 (9)	1.39 (9)
15	9.31 (11)	5.47 (11)	3.06 (11)	1.06 (11)	1.11 (11)	1.55 (10)	5.73 (9)	1.41 (9)
21	4.18 (11)	2.46 (11)	1.41 (11)	5.62 (10)	5.50 (10)	7.71 (9)	2.88 (9)	1.40 (9)
28	2.32 (11)	1.38 (11)	7.81 (10)	3.10 (10)	3.11 (10)	4.64 (9)	1.58 (9)	1.41 (9)
39.4	1.31 (11)	8.12 (10)	4.10 (10)	1.52 (10)	1.56 (10)	2.20 (9)	8.19 (9)	1.62 (9)
59	5.71 (10)	3.56 (10)	1.82 (10)	7.80 (9)	7.37 (9)	--	3.84 (9)	1.35 (9)
117	1.87 (10)	1.08 (10)	5.36 (9)	2.16 (9)	1.8 (9)	--	1.13 (9)	1.39 (9)
189	9.26 (9)	4.68 (9)	2.15 (9)	8.69 (8)	--	--	4.9 (7)	1.29 (9)
261	5.89 (9)	2.84 (9)	1.51 (9)	5.84 (9)	--	--	2.1 (7)	1.26 (9)

[a]Zero degrees lying directly south with subsequent degrees measured clockwise on a horizontal plane located at the core center.

[b]"(12)" = 10^{12} "(11)" = 10^{11}; etc.

Table 2-18. Neutron fluence above various threshold energies per 1.0 x 10^{16} fissions (24.3°C ΔT) as a function of radial distance from core center, outdoor.

Distance from Core Center (in.)	Pu^{239} (n/cm^2) (E > 10 keV)	Np^{237} (n/cm^2) (E > 0.60 MeV)	U^{238} (n/cm^2) (E > 1.50 MeV)	S^{32} (n/cm^2) (E > 3.0 MeV)	Ni^{58} (n/cm^2) (E > 3.0 MeV)	Mg^{24} (n/cm^2) (E > 6.3 MeV)	Al^{27} (n/cm^2) (E > 7.5 MeV)	Thermal Neutron (n/cm^2)
				0°[a]				
6	6.78 (12)[b]	4.40 (12)	2.22 (12)	7.40 (11)	8.11 (11)	1.10 (11)	4.23 (10)	4.56 (8)
9	2.52 (12)	1.47 (12)	8.22 (11)	3.01 (11)	3.13 (11)	3.92 (11)	1.47 (10)	4.99 (8)
12	1.39 (12)	8.32 (11)	4.57 (11)	1.86 (11)	1.90 (11)	2.48 (10)	9.20 (9)	5.68 (8)
15	1.00 (12)	5.58 (11)	3.02 (11)	1.06 (11)	1.15 (11)	1.56 (10)	6.08 (9)	6.18 (8)
21	4.02 (11)	2.58 (11)	1.34 (11)	6.01 (10)	6.42 (10)	8.58 (9)	2.98 (9)	5.79 (8)
28	2.27 (11)	1.49 (11)	7.63 (10)	3.32 (10)	3.29 (10)	4.62 (9)	1.52 (9)	5.95 (8)
39.4	1.16 (11)	7.08 (10)	3.79 (10)	1.53 (10)	1.49 (10)	2.08 (9)	7.41 (8)	4.7 (8)
59	6.04 (10)	3.61 (10)	1.73 (10)	7.71 (9)	7.55 (9)	9.48 (8)	3.82 (8)	4.5 (8)
117	1.63 (10)	1.15 (10)	4.92 (9)	2.13 (9)	1.5 (9)	3.18 (8)	9.96 (7)	2.5 (8)
189	6.55 (9)	3.81 (9)	1.86 (9)	8.05 (8)	--	--	3.7 (7)	1.6 (8)
261	4.19 (9)	3.00 (9)	1.34 (9)	4.24 (8)	--	--	--	9.4 (7)
				120°				
6	6.78 (12)	4.49 (12)	2.22 (12)	7.40 (11)	8.11 (11)	1.10 (11)	4.23 (10)	4.56 (8)
9	2.36 (12)	1.39 (12)	7.88 (11)	2.42 (11)	2.86 (11)	3.63 (10)	1.37 (10)	4.72 (8)
12	1.21 (12)	7.14 (11)	4.23 (11)	1.75 (11)	1.86 (11)	2.40 (10)	9.40 (9)	5.78 (8)
15	8.54 (11)	5.48 (11)	2.83 (11)	1.06 (11)	1.07 (11)	1.43 (10)	5.28 (9)	5.18 (8)
21	4.24 (11)	2.76 (11)	1.43 (11)	5.64 (10)	5.72 (10)	8.00 (9)	2.90 (9)	5.48 (8)
28	2.18 (11)	1.36 (11)	7.42 (10)	3.14 (10)	3.38 (10)	4.49 (9)	1.44 (9)	5.42 (8)
39.4	1.16 (11)	7.08 (10)	4.10 (10)	1.53 (10)	1.49 (10)	2.08 (9)	7.41 (8)	4.7 (8)
59	5.73 (10)	3.63 (10)	1.82 (10)	7.70 (9)	6.58 (9)	8.69 (8)	3.45 (8)	4.5 (8)
117	1.64 (10)	--	5.00 (9)	1.96 (9)	1.6 (9)	3.14 (8)	8.90 (7)	2.1 (8)
189	6.98 (9)	--	1.75 (9)	7.68 (8)	--	--	4.1 (7)	1.7 (8)
261	2.88 (9)	--	6.81 (8)	3.86 (8)	--	--	--	9.2 (7)
				240°				
6	6.78 (12)	4.40 (12)	2.22 (12)	7.40 (11)	8.11 (11)	1.10 (11)	4.23 (10)	4.56 (8)
9	2.66 (12)	1.65 (12)	9.30 (11)	3.15 (11)	3.55 (11)	4.58 (10)	1.72 (10)	5.68 (8)
12	1.42 (12)	8.81 (11)	4.69 (11)	1.90 (11)	1.94 (11)	2.45 (10)	9.10 (9)	6.08 (8)
15	9.28 (11)	5.96 (11)	3.05 (11)	1.09 (11)	1.21 (11)	1.60 (10)	6.00 (9)	5.63 (8)
21	4.40 (11)	2.86 (11)	1.46 (11)	5.91 (10)	6.22 (10)	8.56 (9)	3.08 (9)	5.92 (8)
28	2.16 (11)	1.40 (11)	7.44 (10)	3.24 (10)	3.26 (10)	4.70 (9)	1.66 (9)	5.38 (8)
39.4	1.16 (11)	7.08 (10)	3.79 (10)	1.53 (10)	1.49 (10)	2.08 (9)	7.41 (8)	4.7 (8)
59	5.87 (10)	3.78 (10)	1.82 (10)	8.33 (9)	8.14 (9)	1.07 (9)	4.04 (8)	4.4 (8)
117	1.84 (10)	1.15 (10)	5.61 (9)	2.12 (9)	1.8 (9)	3.2 (8)	8.1 (7)	3.1 (8)
189	6.89 (9)	3.73 (9)	2.01 (9)	8.34 (8)	6.5 (8)	--	3.3 (7)	1.8 (8)
261	4.06 (9)	2.11 (9)	1.13 (9)	4.31 (8)	--	--	--	7.3 (7)
				Radial Profile Average Values				
6	6.78 (12)	4.40 (12)	2.22 (12)	7.40 (11)	8.11 (11)	1.10 (11)	4.23 (10)	4.56 (8)
9	2.51 (12)	1.60 (12)	8.47 (11)	2.85 (11)	3.18 (11)	3.91 (10)	1.52 (10)	5.13 (8)
12	1.34 (12)	8.12 (11)	4.53 (11)	1.84 (11)	1.90 (11)	2.44 (10)	9.23 (9)	5.83 (8)
15	9.28 (11)	5.67 (11)	2.97 (11)	1.07 (11)	1.14 (11)	1.53 (10)	5.80 (9)	5.65 (8)
21	4.22 (11)	2.74 (11)	1.41 (11)	5.85 (10)	6.12 (10)	8.36 (9)	2.99 (9)	5.73 (8)
28	2.21 (11)	1.41 (11)	7.50 (10)	3.23 (10)	3.31 (10)	4.60 (9)	1.54 (9)	5.59 (8)
39.4	1.16 (11)	7.08 (10)	4.10 (10)	1.53 (10)	1.49 (10)	2.08 (9)	7.41 (8)	4.7 (8)
59	5.88 (10)	3.7 (10)	1.79 (10)	7.91 (9)	7.26 (9)	9.93 (8)	3.77 (8)	4.5 (8)
117	1.70 (10)	1.15 (10)	5.18 (9)	2.07 (9)	1.6 (9)	3.2 (8)	8.9 (7)	2.6 (8)
189	6.78 (9)	3.77 (9)	1.86 (9)	8.02 (8)	--	--	3.7 (7)	1.7 (8)
261	3.72 (9)	2.55 (9)	1.06 (9)	4.14 (8)	--	--	--	8.6 (7)

[a]Zero degrees lying directly south with subsequent degrees measured clockwise on a horizontal plane located at the core center.

[b]"(12)" = 10^{12}; "(11)" = 10^{11}; etc.

Table 2-19. Neutron energy spectrum as a function of radial distance from reactor center expressed in percent of neutrons above threshold energy and normalized to 100% above 10 keV.

Distance From Core Center (in.)	Percent Above Measurement Foil Threshold					
	Pu	Np	U	S and Ni	Mg	
Outside						
6	100	65	33	11.5	1.6	0.6
9	100	64	34	12	1.6	0.6
12	100	61	34	14	1.8	0.7
15	100	61	32	12	1.6	0.6
21	100	65	33	14	2.0	0.7
28	100	64	34	15	2.1	0.7
39.4	100	61	35	13	1.8	0.6
59	100	62	30	13	1.6	0.6
117	100	67	30	12	1.8	0.5
189	100	56	27	12	-	0.5
261	100	68	28	11	-	-
Inside						
6	100	64	33	12	1.6	0.6
9	100	66	35	13	1.7	0.6
12	100	62	33	12	1.6	0.6
15	100	59	33	12	1.7	0.6
21	100	59	34	13	1.8	0.7
28	100	60	33	13	1.9	0.7
39.4	100	62	31	12	1.7	0.6
59	100	62	32	13	-	0.7
117	100	58	29	11	-	0.6
189	100	51	24	9.4	-	0.5
261	100	48	26	8.2	-	0.3
Reference Spectra { Watt	100	83	53	21	2.1	0.8
Reference Spectra { Godiva	100	65	33	13		

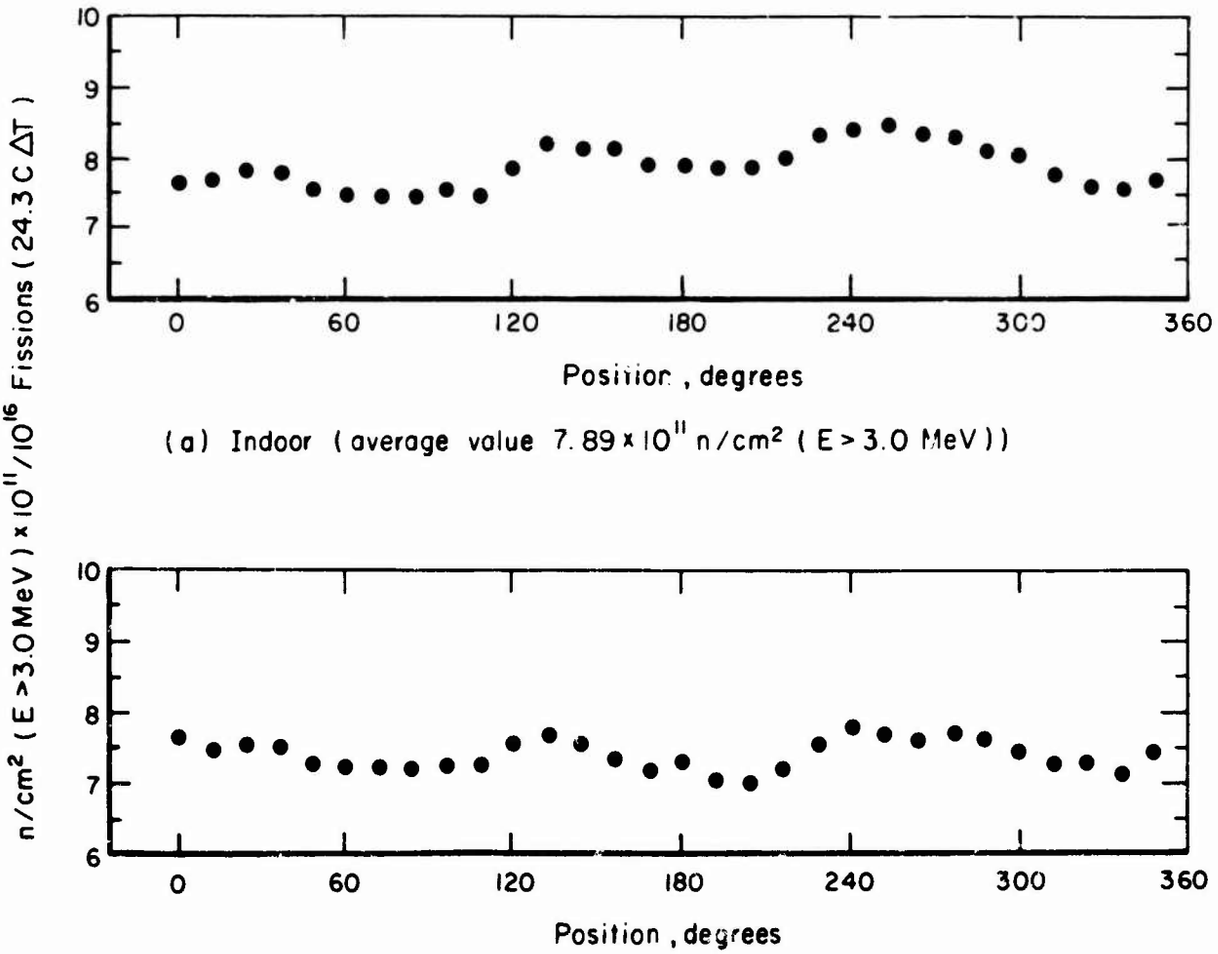

Figure 2-29. Average neutron fluence > 3.0 MeV on 6-in. horizontal circle.

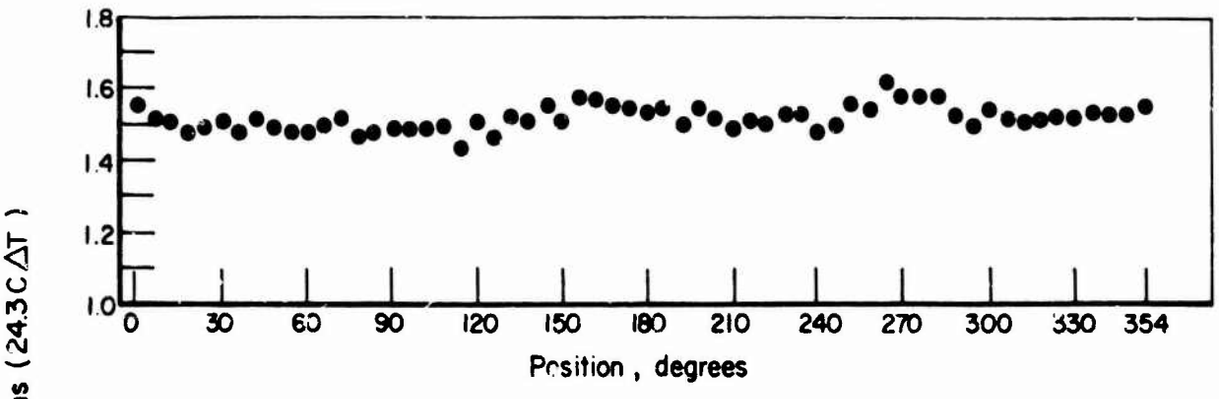

(a) Indoor (Average value 1.52×10^{10} n/cm^2 (E > 3.0 MeV))

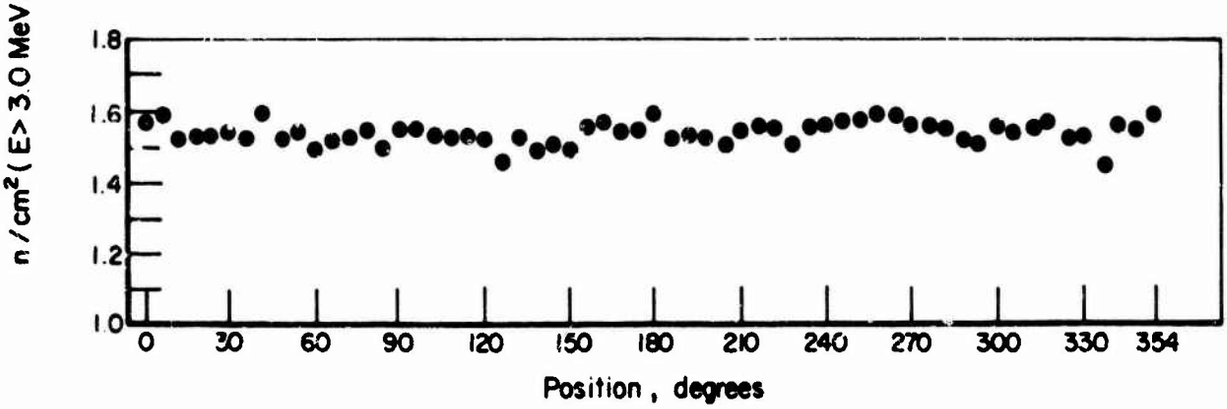

(b) Outdoor (Average value 1.53×10^{10} n/cm^2 (E > 3.0 MeV))

n/cm^2 (E > 3.0 MeV) / 10^{16} Fissions (24.3 C ΔT)

Figure 2-30. Average neutron fluence > 3.0 MeV on 1-m horizontal circle.

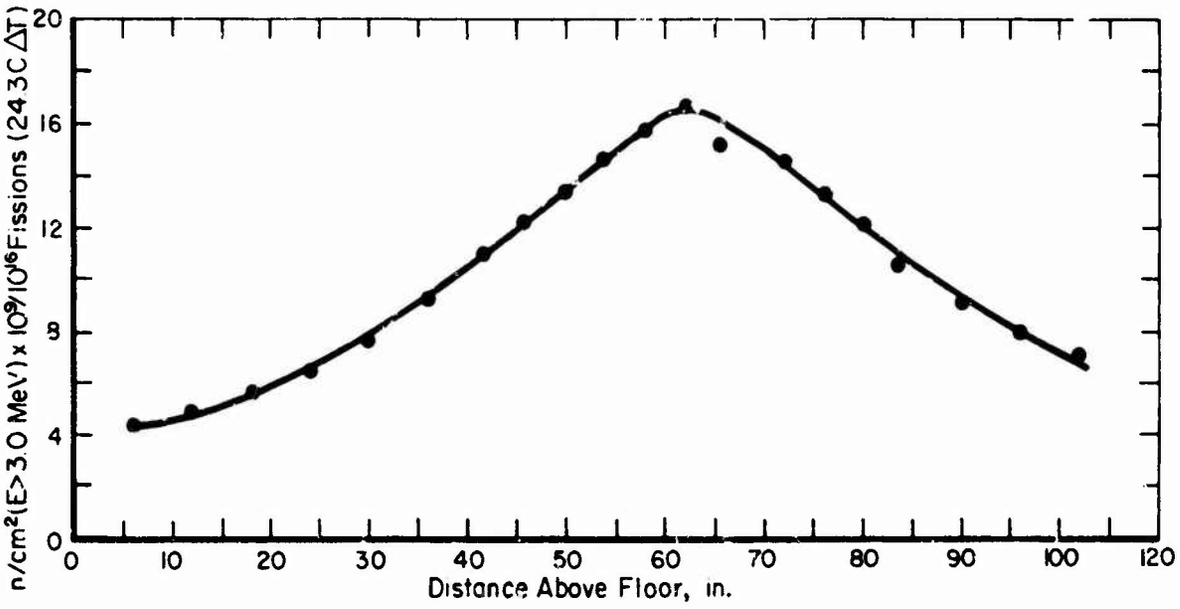

a. Indoor

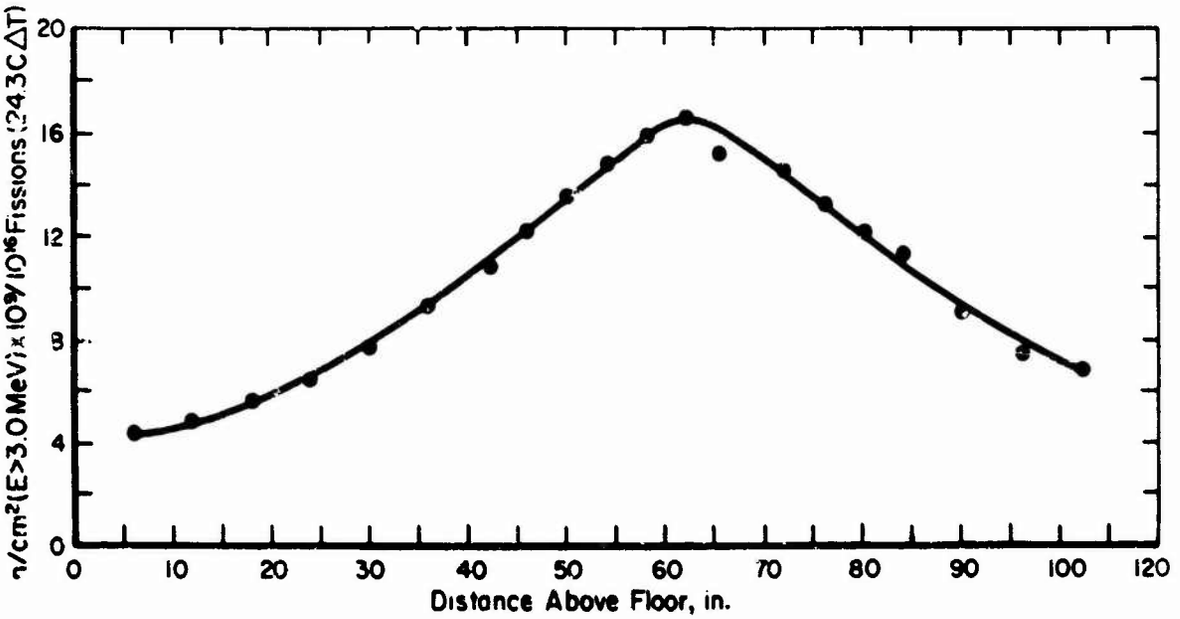

b Outdoor

Figure 2-31. Average neutron fluence > 3.0 MeV vertical traverse at 1 m from reactor axis.

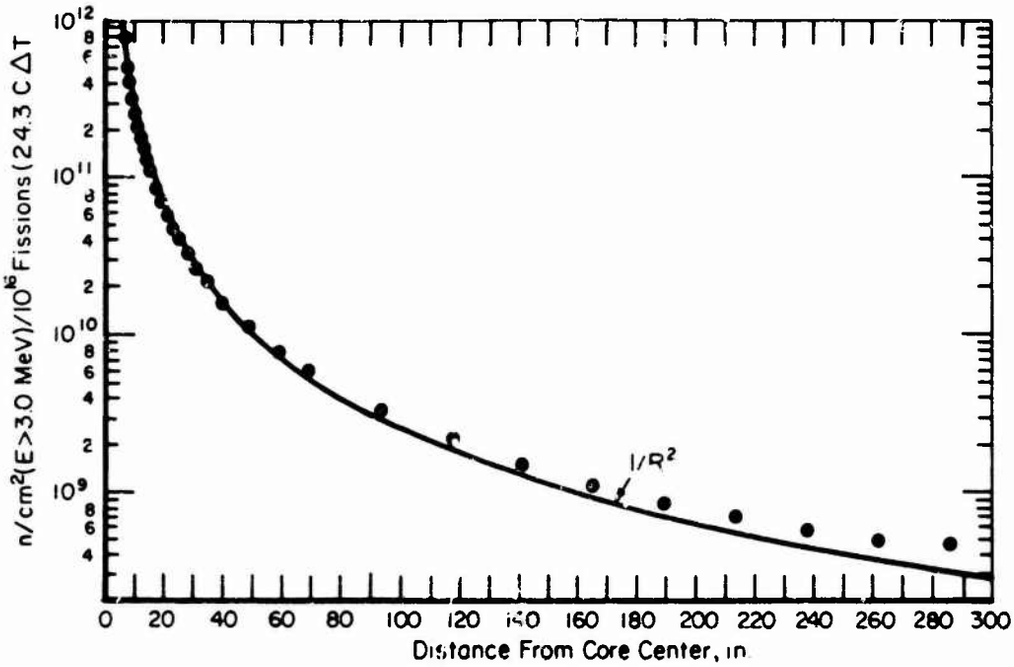

Figure 2-32. Average neutron fluence > 3.0 MeV as a function of radial distance from core center, indoor.

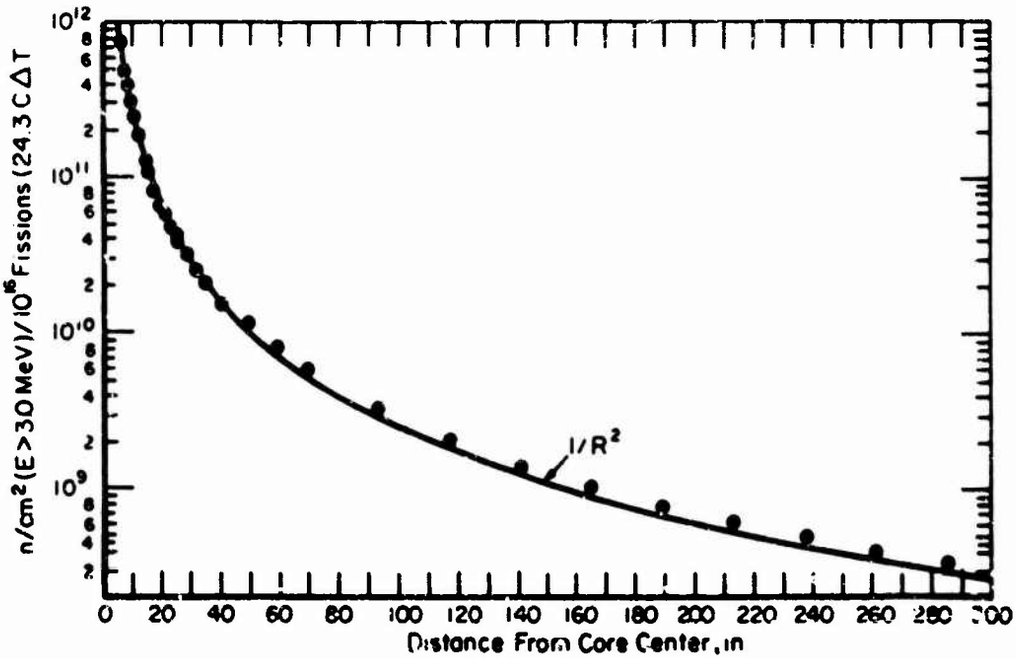

Figure 2-33. Average neutron fluence > 3.0 MeV as a function of radial distance from core center, outdoor.

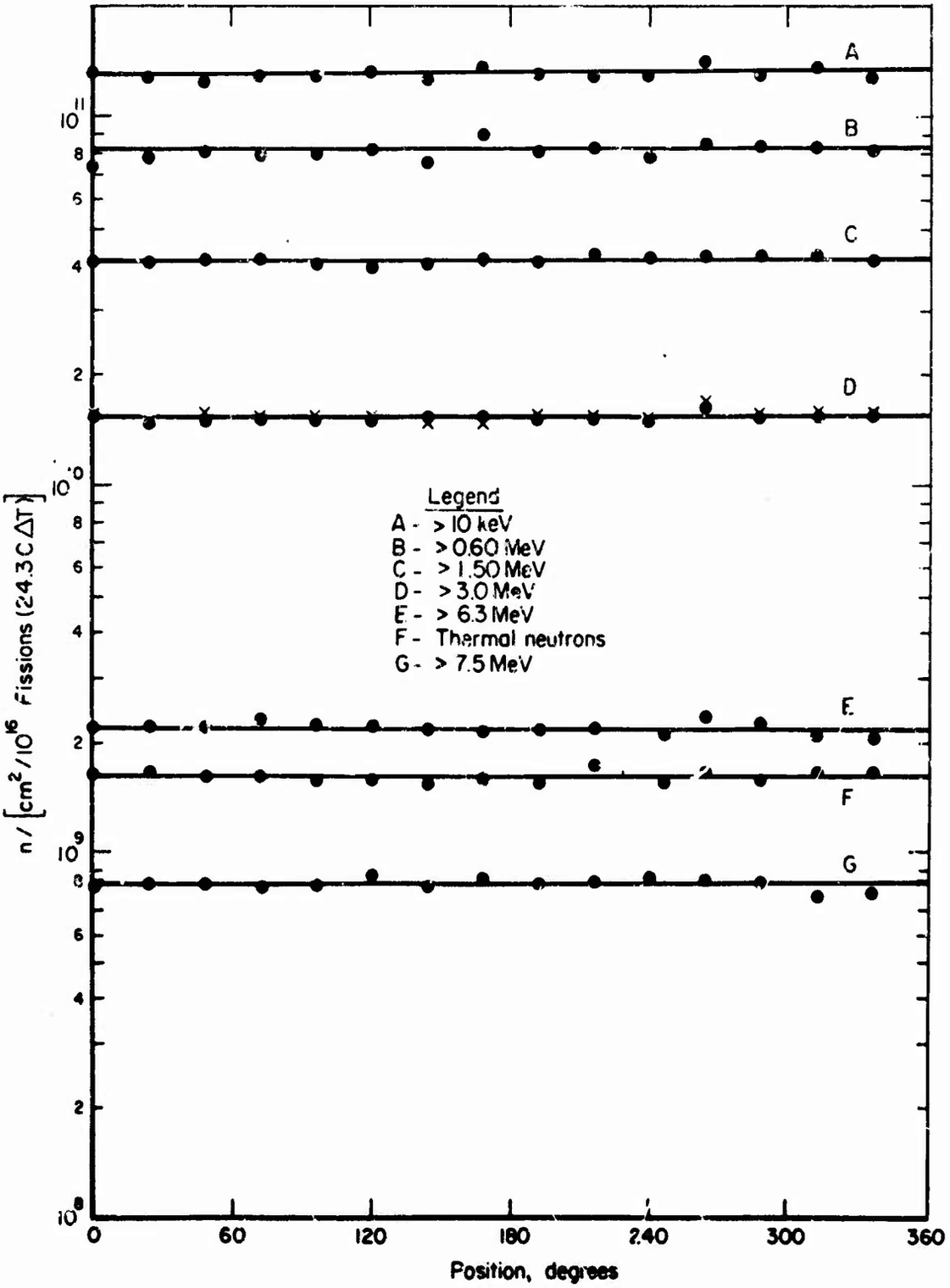

Figure 2-34. Average neutron fluence above various threshold energies on 1-m horizontal circle, indoor.

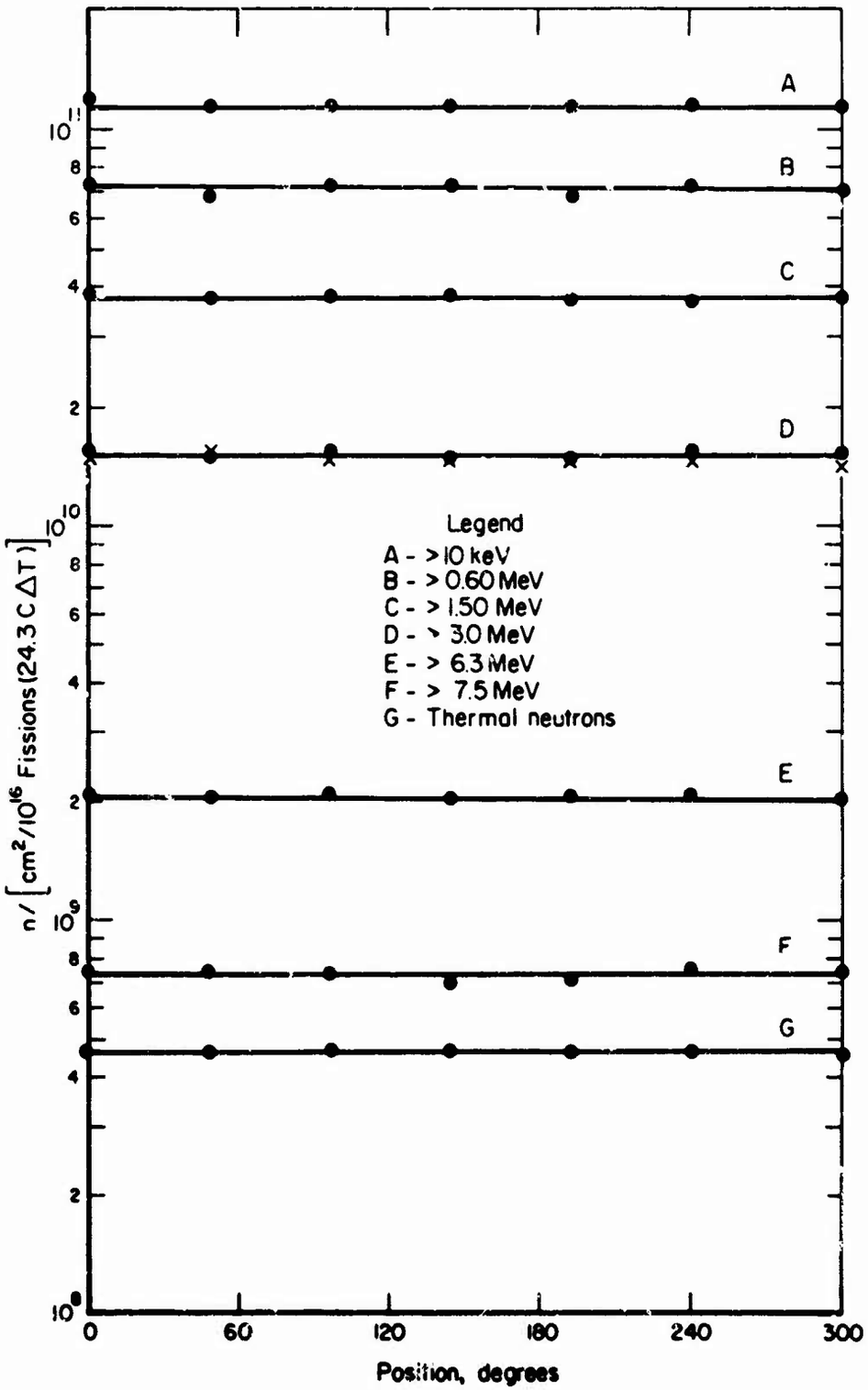

Figure 2-35. Average neutron fluence above various threshold energies on 1-m horizontal circle, outdoor.

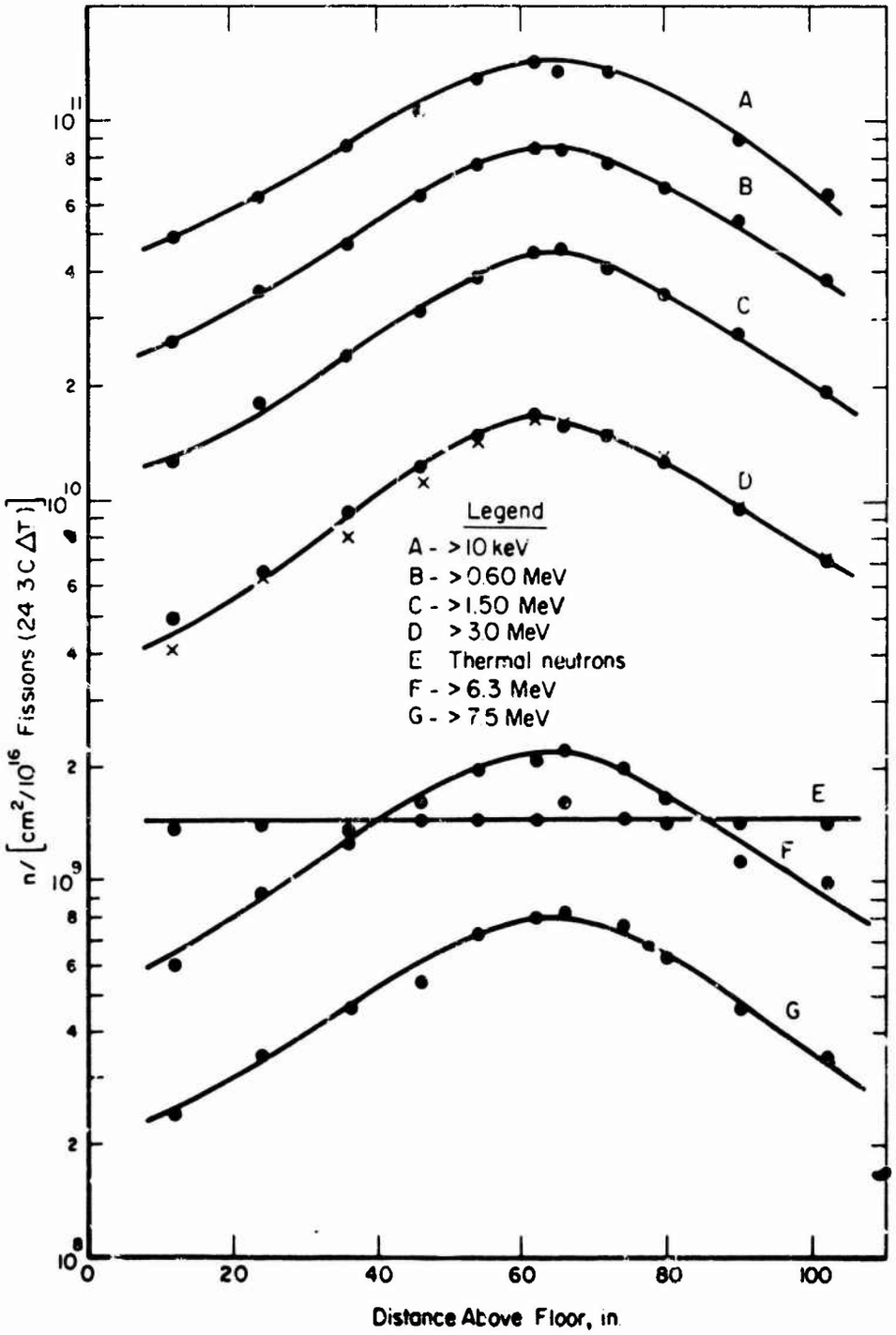

Figure 2-36. Average neutron fluence above various threshold energies on a vertical traverse 1 m from reactor axis, indoor.

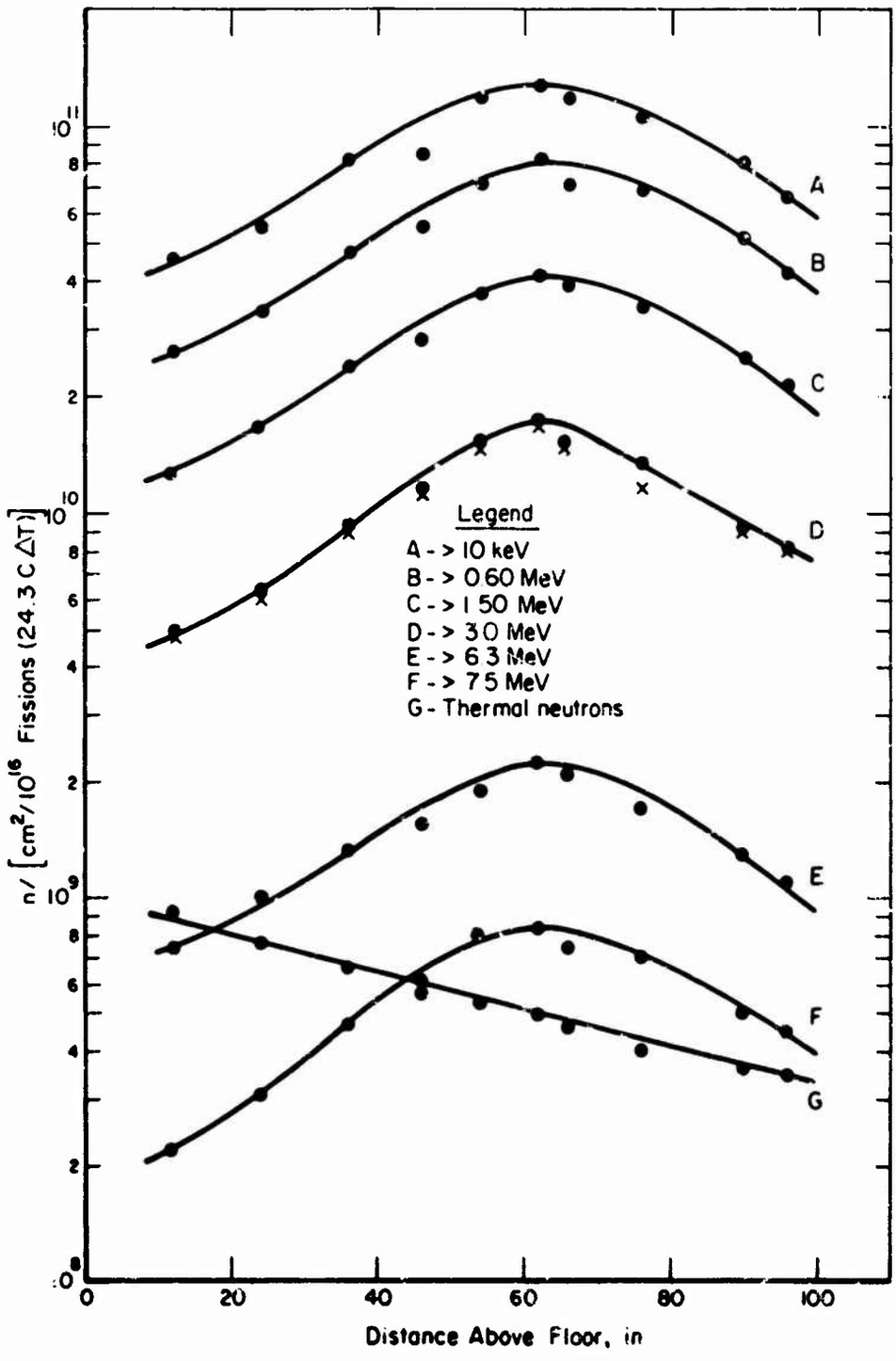

Figure 2-37. Average neutron fluence above various threshold energies on a vertical traverse 1 m from reactor axis, outdoor.

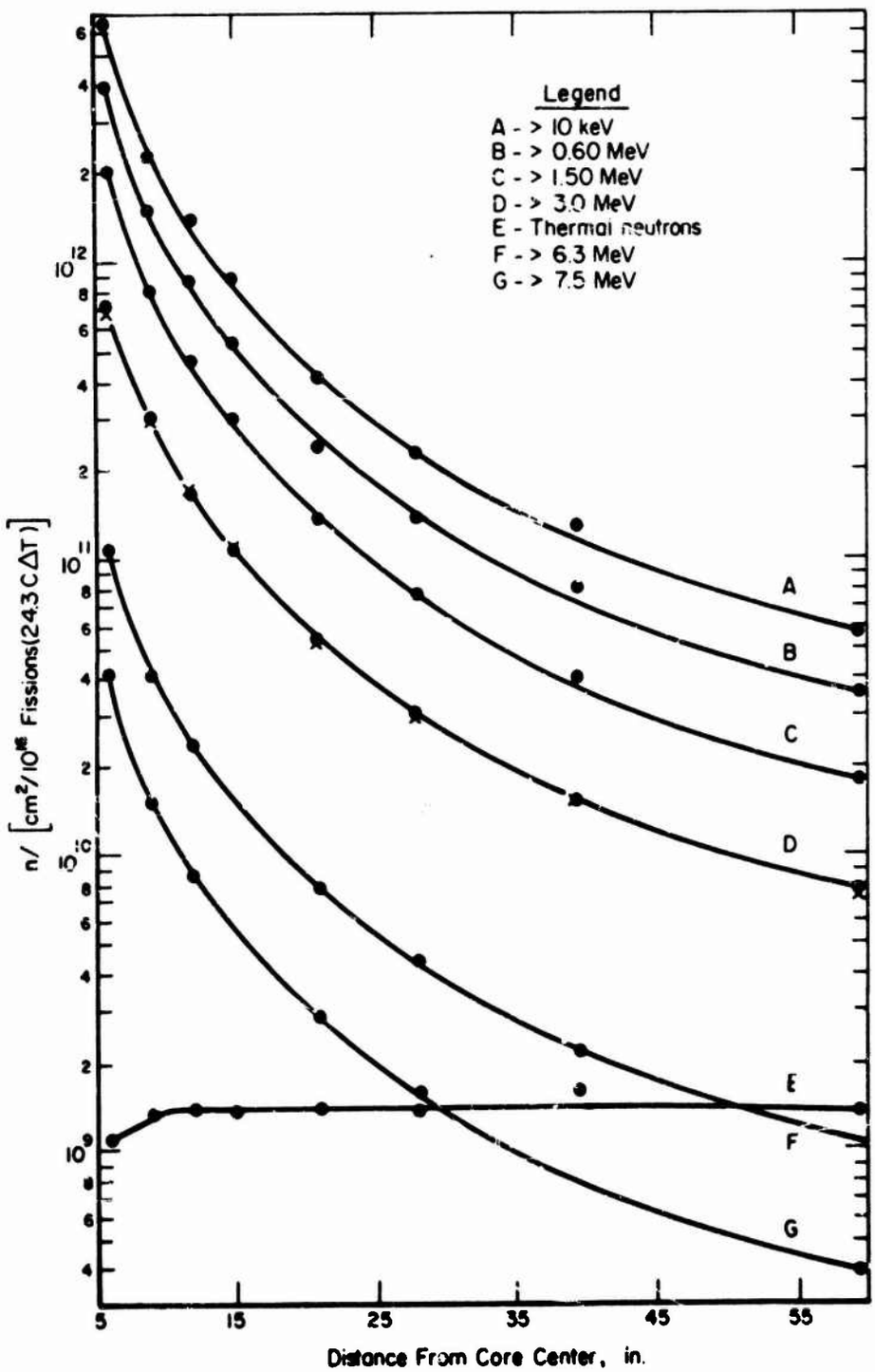

Figure 2-38. Average neutron fluence above various threshold energies as a function of radial distance from core center, indoor.

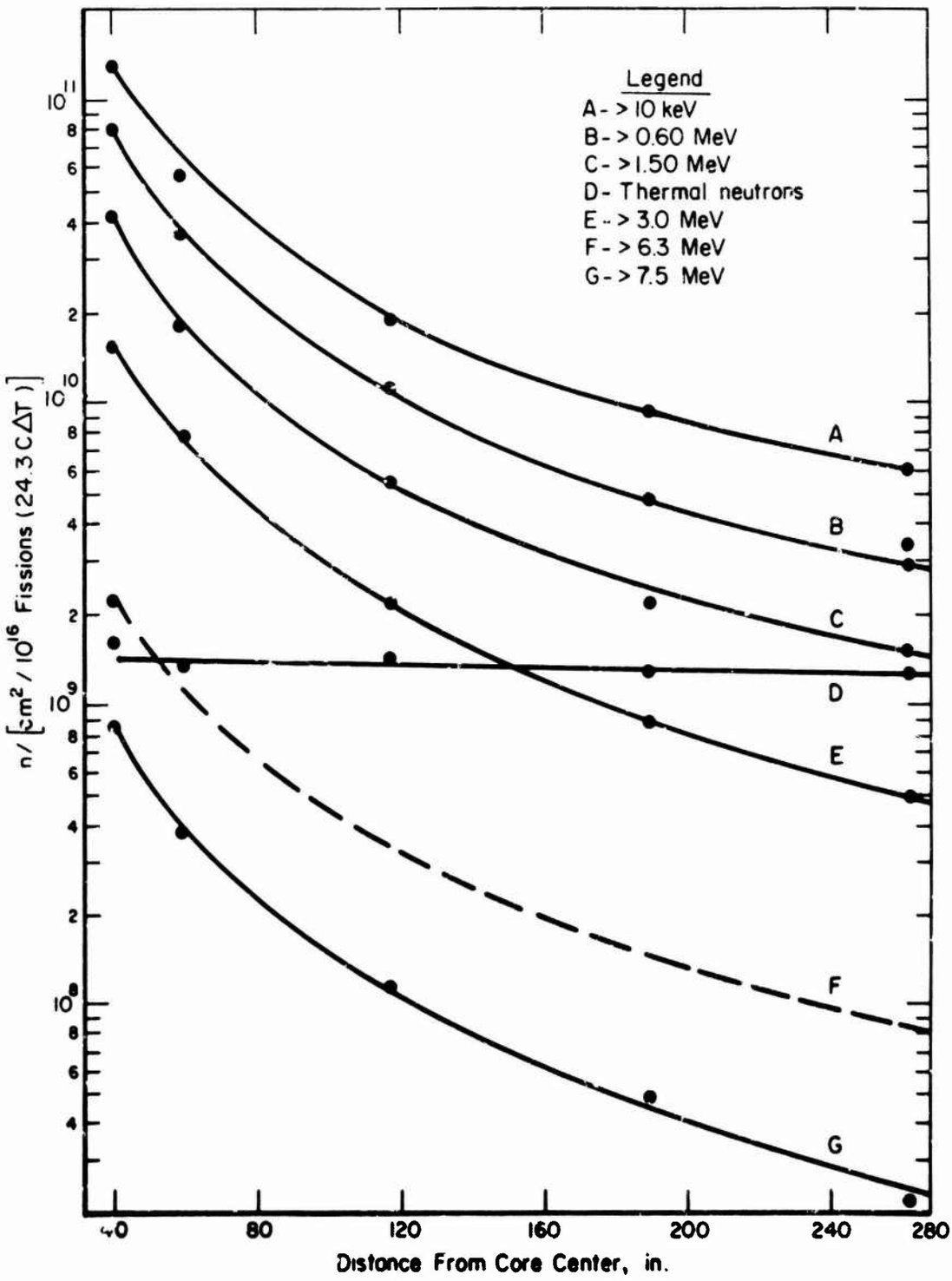

Figure 2-39. Average neutron fluence above various threshold energies as a function of radial distance from core center, indoor.

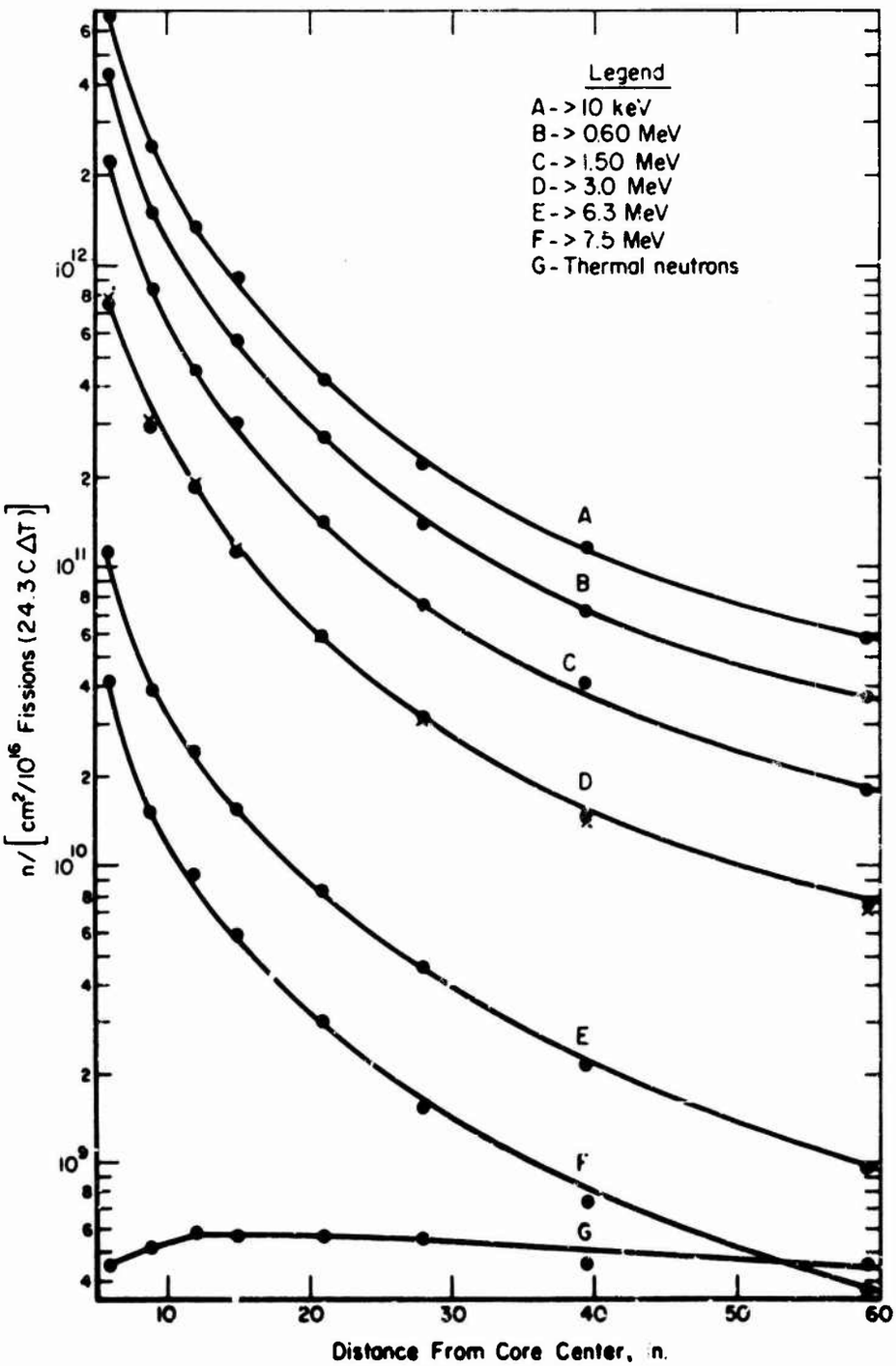

Figure 2-40. Average neutron fluence above various threshold energies as a function of radial distance from core center, outdoor.

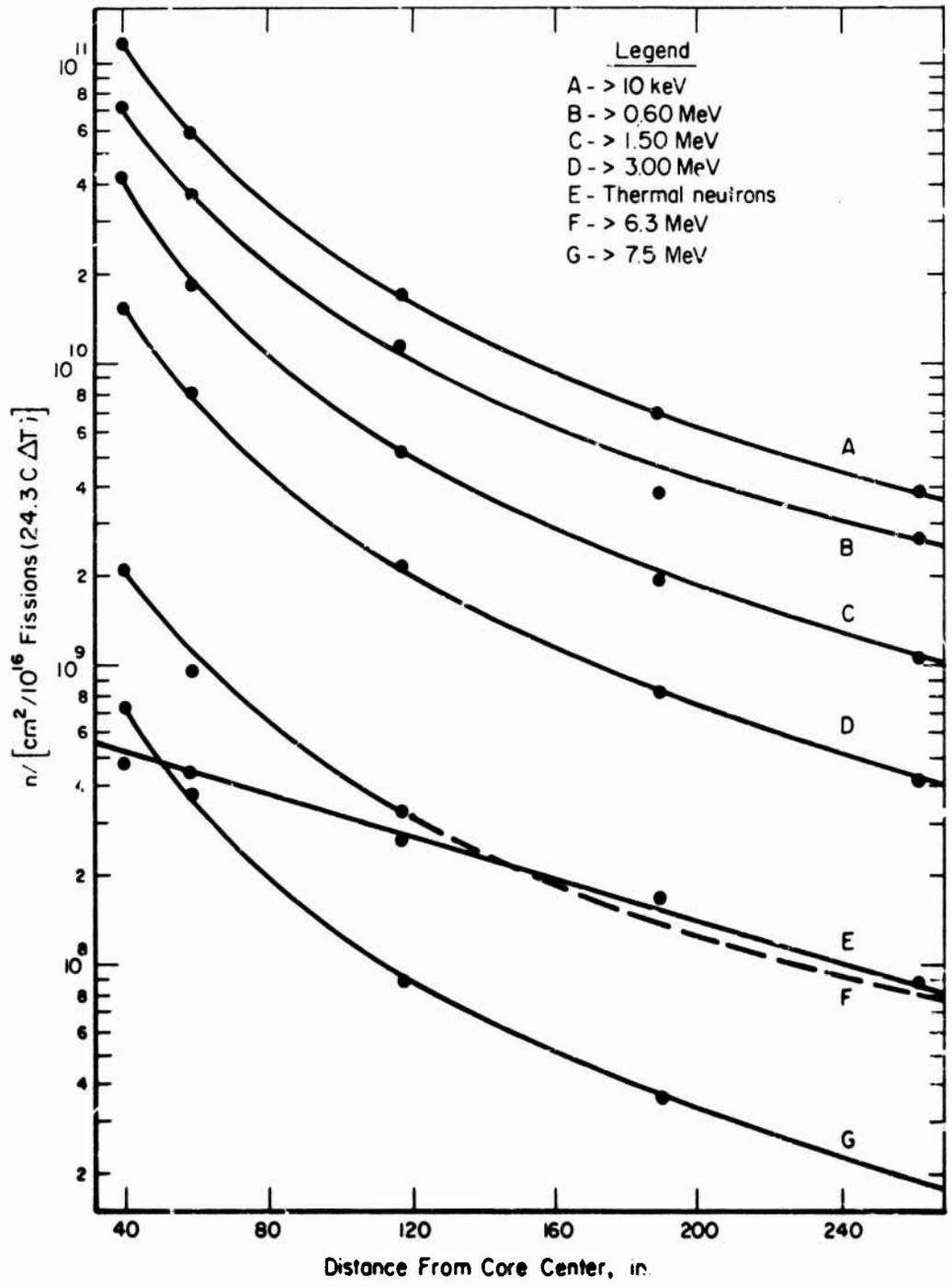

Figure 2-41. Average neutron fluence above various threshold energies as a function of radial distance from core center, outdoor.

Gamma dose measurements were made with TLD dosimeters, Ag-activated phosphate glass-rod microdosimeters, and chemical dosimeters. Measurements were made at positions similar to those used in the neutron measurements. Results are given in Tables 2-20 through 2-25 and Figures 2-42 through 2-46. As with the neutron data, the tables represent the data as obtained from the various dosimeter positions and the curves graphically display averages of the tabulated data.

Spectrum data are not available, but the neutron fluence data in Tables 2-15 through 2-18 and in Figures 2-34 through 2-41 are presented in terms of thresholds from which spectral data can be derived. The fluence measurements were made utilizing 7 different threshold foils. The n/γ ratio is 4×10^9 n/$(cm^2$ (E > 10 keV) rad) and can be varied through the use of proper shielding arrangements.

Quantitative data on background radiation are not available. All cables are protected with suitable shielding. It is the experience of the facility operators that RF background noise poses no serious problems.

2.4.3 Support Capabilities

The prime mission of the laboratory is to provide facilities for U.S. Government agencies or their contractors to conduct experiments that require a nuclear radiation environment. Facility personnel operate the reactor and supply limited operational and working assistance. A professional staff, enhanced by scientific and engineering personnel from university and college faculties, is available to support all experimental programs.

Monitoring of electronic experiments is acomplished by cables run through conduits from the reactor cell, or outdoor site, to an instrumentation room. The cable length from the reactor to the instrument racks in the instrumentation room is nominally 60 ft. Cables are permanently installed, terminating in patchcord panels in both the reactor cell and the instrumentation room. This cable installation consists of 40 RG-58 c/u, 10 RG-59 c/u, and 11 double No. 18 conductors. Extra conduits and cable pulling equipment are available for experimenters to install additional cables as needed.

Small experiments to be exposed between 6 in. and 48 in. from the reactor may be mounted on a table. The top of this table is ¼-in. pegboard. The experiment needs to be fastened so that it is mechanically stable. Large and/or heavy experiments must be supported by experimenter-supplied fixtures and must be mechanically stable. The support fixture should be designed to rest on a concrete portion of the floor.

Experiments containing moving parts, liquids, or explosives require special consideration and, therefore, must be described in minute detail in the test plan.

Various timing signals are available to allow the experimenter to coordinate data taking with the reactor burst.

Table 2-20. γ dose per 1.0×10^{16} fissions (24.3°C ΔT) on 6-in. horizontal circle.

Position (deg)	Exposure (R)			
	Indoor		Outdoor	
	TLD	Glass Rods	TLD	Glass Rods
0		1536		1690
12	1691		2015	
24		1591		1730
36	1665		2009	
48		1500		1670
60	1649		1865	
72		1522		1640
84	1546		1777	
96		1518		1670
108	1674		1839	
120		1594		1690
132	1819		1959	
144		1631		1620
156	1623		1908	
168		1536		1620
180	1674		1796	
192		1500		1610
204	1776		1858	
216		1555		1571
228	1895		1833	
240		1628		1583
252	1836		1783	
264		1620		1567
276	1794		1796	
288		1591		1599
300	1828		1927	
312		1556		1535
324	1639		1733	
336		1522		1604
348	1708		1777	
Average	1674	1561	1858	1627

Table 2-21. γ dose per 1.0×10^{16} fissions (24.3°C ΔT) on 1-m horizontal circle, indoor.

Position (deg)	Exposure (R)				Position (deg)	Exposure (R)			
	TLD	Glass Rods	Chem.	μTLD		TLD	Glass Rods	Chem.	μTLD
0		37.4	31.8	32.0	186	37.8			
6					192		33.3	31.8	31.9
12		36.9	33.3	31.6	198				
18	36.2				204		37.7	30.9	34.3
24		36.3	36.6	32.3	210	35.7			
30					216		32.5	30.5	33.4
36		35.3	32.7	32.4	222				
42	36.2				228		38.5	32.5	36.1
48		34.5	32.2	30.5	234	35.3			
54					240		39.5	32.8	30.4
60		35.7	31.3	31.4	246				
66	38.0				252		37.9	33.5	33.4
72		35.9	33.1	29.3	258	38.0			
78					264		39.7	34.0	36.4
84		37.1	32.1	30.7	270				
90	36.5				276		38.1	34.4	35.2
96		36.7	32.7	30.9	282	35.6			
102					288		37.8	33.3	34.5
108		36.0	30.5	29.7	294				
114	34.6				300		35.6	34.4	31.4
120		35.4	30.7	33.4	306	LOST			
126					312		35.1	33.4	34.3
132		35.1	29.5	31.1	318				
138	36.2				324		37.5	32.9	35.4
144		36.4	32.9		330	34.9			
150					336		35.6	31.6	37.0
156		36.4	35.8	29.5	342				
162	41.5				348		37.3	33.0	36.1
168		37.9	33.5	33.5	354	35.1			
174									
180		34.8	30.9	31.0	AVERAGE	36.6	36.5	32.6	32.7

Table 2-22. γ dose per 1.0×10^{16} fissions (24.3°C ΔT) on 1-m horizontal circle, outdoor.

Position (deg)	Exposure (R)				Position (deg)	Exposure (R)			
	TLD	Glass Rods	Chem.	μTLD		TLD	Glass Rods	Chem.	μTLD
0		39.8	36.7	31.9	186	35.8			
6					192		34.4	35.4	34.4
12		38.9	36.2	31.9	198				
18	39.4				204		41.1	37.0	32.4
24		39.5	35.9	33.0	210	39.0			
30					216		41.7	35.4	30.5
36		38.5	35.2	33.6	222				
42	38.4				228		40.1	35.2	30.9
48		39.5	36.2	34.4	234	37.4			
54					240		37.3	33.3	LOST
60		37.4	35.6	36.7	246				
66	35.6				252		40.4	38.0	34.0
72		41.0	35.4	32.3	258	39.0			
78					264		43.8	33.8	32.4
84		40.0	33.0	34.0	270				
90	36.2				276		38.8	36.7	36.6
96		39.6	35.9	32.3	282	35.5			
102					288		43.4	34.1	29.0
108		41.1	37.7	37.5	294				
114	36.1				300		39.1	32.8	30.5
120		38.3	37.5	34.5	306	36.9			
126					312		40.4	34.1	30.5
132		40.5	36.2	34.1	318				
138	35.5				324		37.9	35.4	33.6
144		LOST	36.7	30.5	330	34.7			
150					336		45.8	38.8	35.6
156		39.3	36.2	33.6	342				
162	40.4				348		37.4	35.9	32.4
168		40.9	38.3	30.5	354	38.1			
174									
180		42.8	36.9	31.3	AVERAGE	37.1	39.9	35.8	32.0

Table 2-23. γ dose per 1.0×10^{16} fissions (24.3°C ΔT) vertical traverse at 1 m from reactor axis.

Distance Above Floor (in.)	Position 1[a]		Position 2		Position 3		Position 4		Average
	TLD	Glass Rods	TLD	Glass Rods	TLD	Glass Rods	TLD	Glass Rods	
Indoor Exposure (R)									
6	11.0			12.8	11.0			12.7	11.9
12		14.2	13.8			13.9	12.2		13.5
18	15.4			17.2	14.7			16.1	15.9
24		18.4	16.6			17.4	17.4		17.5
30	19.2			20.4	19.5			21.2	20.1
36		25.6	23.0			24.9	24.7		24.5
42	29.2			27.6	26.6			28.3	27.9
46		30.9	30.1			34.0	33.7		32.2
50	33.7			32.3	37.0			34.7	34.4
54		34.6	36.2			34.8	36.2		35.4
58	39.2			35.1	36.2			41.0	37.9
62		36.8	38.9			38.7	44.5		39.7
65.5	36.6	36.5	36.6	36.5	36.6	36.5	36.6	36.5	36.6
72	44.5			46.3	41.1			37.4	42.3
76		34.1	38.3			34.1	39.3		36.4
80	33.0			32.5	34.9			33.3	33.4
84		32.5	31.1			30.1	31.7		31.4
90	26.0			30.0	25.3			31.7	28.2
96		20.1	22.0			26.0	20.7		22.2
102	18.9			21.1	17.5			24.4	20.5
Outdoor Exposure (R)									
6	10.1			14.0	No data obtained			20.1	14.4
12		18.4	11.9				14.3		14.9
18	16.4			22.1				16.4	18.3
24		28.1	16.9				18.7		21.2
30	20.1			23.1				24.7	22.7
36		30.1	24.8				27.0		27.3
42	29.1			29.1				32.8	30.3
46		34.8	33.8				37.2		35.3
50	34.7			35.8				37.8	36.1
54		45.1	38.1				38.1		40.4
58	39.8			39.1				44.5	41.1
62		45.5	39.8				44.0		43.1
65.5	37.1	39.9	37.1	39.9	37.1	39.9	37.1	39.9	38.5
72	41.5			49.2	46.0			48.2	46.2
76		42.9	39.6			47.6	43.5		43.4
80	37.8			42.1	44.7			37.3	40.4
84		35.7	34.3			40.5	34.8		36.3
90	29.3			27.8	31.0			30.2	30.4
96		27.8	24.3			30.2	23.9		26.6
102	21.1			18.3	21.5			23.0	20.7

[a]The positions referred to here are 90 degrees apart on a circle of 1-m radius and centered at the reactor core. Position 1 is in the southeast direction with subsequent positions located clockwise around the circle.

Table 2-24. γ dose per 1.0 x 10^{16} fissions (24.3°C ΔT) as a function of radial distance from core center, indoor.

Distance From Core Center (in.)	(R) 0°[a] TLD	0° Glass Rods	60° TLD	60° Glass Rods	120° TLD	120° Glass Rods	180° TLD	180° Glass Rods	240° TLD	240° Glass Rods	300° TLD	300° Glass Rods	Average
6	1674	1561	1674	1561	1674	1561	1674	1561	1674	1561	1674	1561	1618
7		1082	1010			981	1270			1981	1207		1255
8	1041			750	1061			872	1144			1373	1040
9		646	759			672	801			1098	927		817
10	575			461	557			514	649			487	541
11		375	463			425	483			451	463		443
12	413			333	422			357	500			341	394
13		302	365			303	360			326	343		333
14	298			254	306			257	343			261	287
15		241	280			168	298			261	261		252
17	229			131	201			192	236			200	207
19		161	168			149	187			183	177		171
21	145			138	140			130	147			128	188
23		106	114			105	120			116	123		114
25	100			95	106			96	69			97	94
28		91	99			79	73			83	79		84
31	60.2			68	56			92	47			68	65
34		61	56			62	51.2			61	50		57
39.4	36.6	36.5	36.6	36.5	36.6	36.5	36.6	36.5	36.6	36.5	36.6	36.5	36.5
49		24	24.4			23	24.2			24.2	23.6		23.9
59	18.6			17.1	21.8			17.1	18.8			16.9	18.4
69		13.9	13.1			13.4	13.8			13.3	13.4		13.5
93	8.4			8.3	7.8			8.3	8.2			8.5	8.3
117		6.7	5.6			6.5	6.3			7.5	5.8		6.4
141	5.17				4.5				4.9				4.8
165			3.6				4.2				3.7		3.8
189	3.2				3.5				3.2				3.3
213			2.8				3.1				2.7		2.9
237	2.7				2.4				2.6				2.6
261			2.3				2.4				2.4		2.4
285	2.3				2.0				2.3				2.2

[a]Zero degrees lying directly south with subsequent degrees measured clockwise on a horizontal plane located at core center.

Table 2-25. γ dose per 1.0 x 10^{16} fissions (24.3°C ΔT) as a function of radial distance from core center, outdoor.

Distance From Core Center (in.)	(R) 0°[a] TLD	0° Glass Rods	60° TLD	60° Glass Rods	120° TLD	120° Glass Rods	180° TLD	180° Glass Rods	240° TLD	240° Glass Rods	300° TLD	300° Glass Rods	Average
6	1796	1627	1796	1627	1796	1627	1796	1627	1796	1627	1796	1627	1711
7		1533	1239			1312	1432			1738	1219		1412
8	1037			1022	955			929	1331			1014	1045
9		753	823			754	996			967	955		875
10	681			710	640			727	741			717	703
11		587	475			610	549			628	620		578
12	431			396	431			429	444			432	428
13		348	399			337	372			375	393		371
14	321			282	300			313	302			321	307
15		262	282			237	283			273	269		268
17	200			191	178			214	202			211	199
19		156	163			150	151			164	165		158
21	148			130	LOST			152	150			116	139
23		111	114			113	105			116	118		113
25	99			78	137			97	97			93	100
28		75	73			77	77.8			79	73		76
31	63			43.7	60			57.5	56.1			61	56.9
34		51.1	51.2			50.8	53 9			52.5	51.3		51.8
39.4	37.1	39.9	37.1	39.9	37.1	39.9	37.1	39.9	37.1	39.9	37.1	39.9	38.5
49		26.8	25.7			25.7	26.1			28.8	28.3		26.9
59	17.2			19.5	17.9			18.4	18.7			20.1	18.6
69		14.5	13.2			13.7	15.0			14.5	13.6		14.1
93	8.2			8.14	7.28			9.41	7.90			8.9	8.31
117		5.34	5.21			5.47	5.04			5.34	4.99		5.23
141	3.34			4.07	3.47			3.7	3.64			4.8	3.84
165		3.31	2 85			2.54	2.64				2.69		2.80
189	1.96			2.80	2.04			2.0	2.00			2.7	2.25
213		1.53	1.64			1.15	1.55				1.54		1.48
237	1.35				1.22				1.24				1.27
261		1.15	1.13				1.14				0.95		1.05
285	0.90				0.82				0.79				0.84
40 ft.					0.35								0.35
50 ft.					0.23								0.23
70 ft.					0.11								0.11
90 ft.					0.074								0.074
140 ft.					0.035								0.035
190 ft.					0.022								0.022
220 ft.					0.019								0.019

[a]Zero degrees lying directly south with subsequent degrees measured clockwise on a horizontal plane located at the core center.

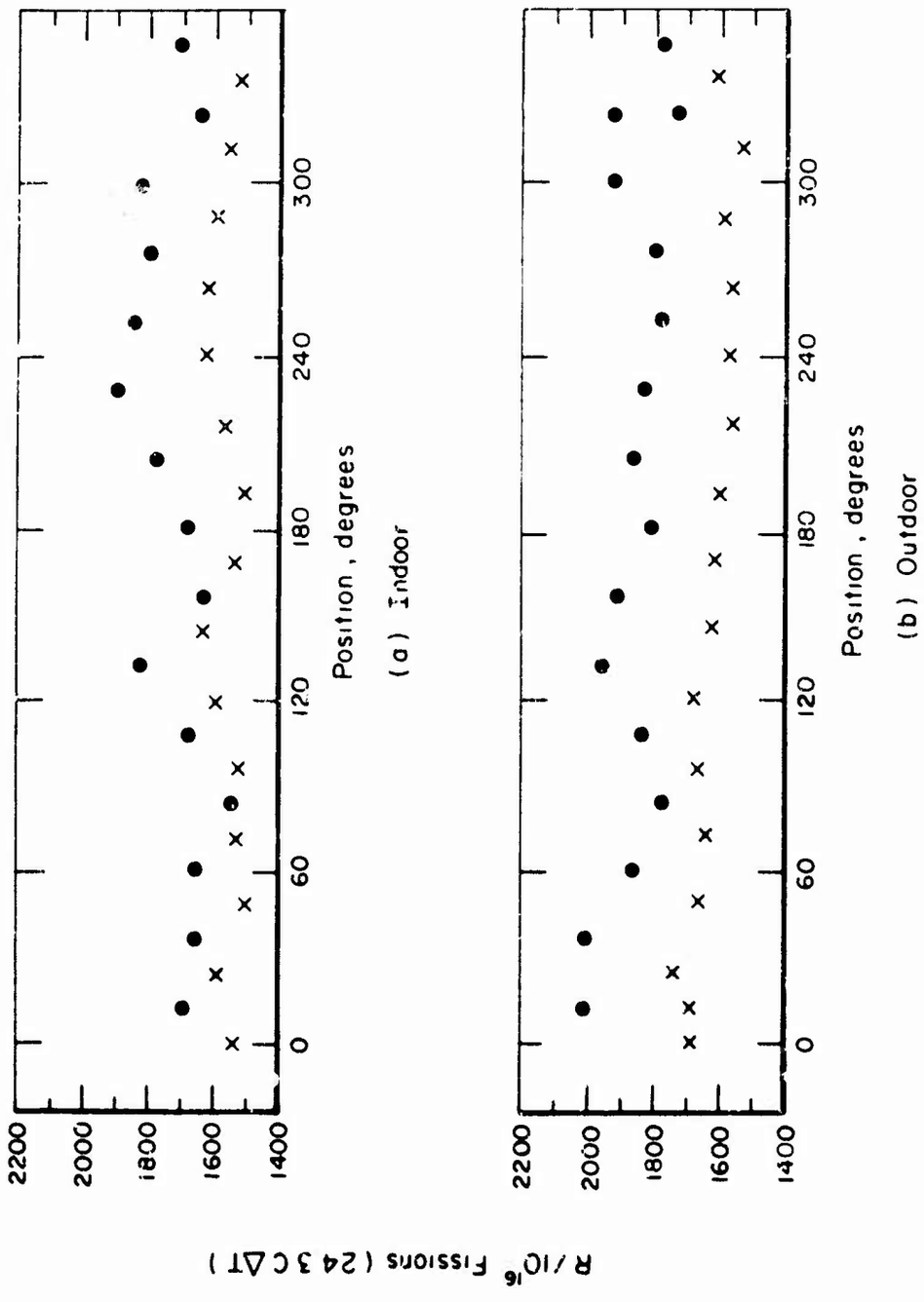

Figure 2-42. γ dose on 6-in. horizontal circle.

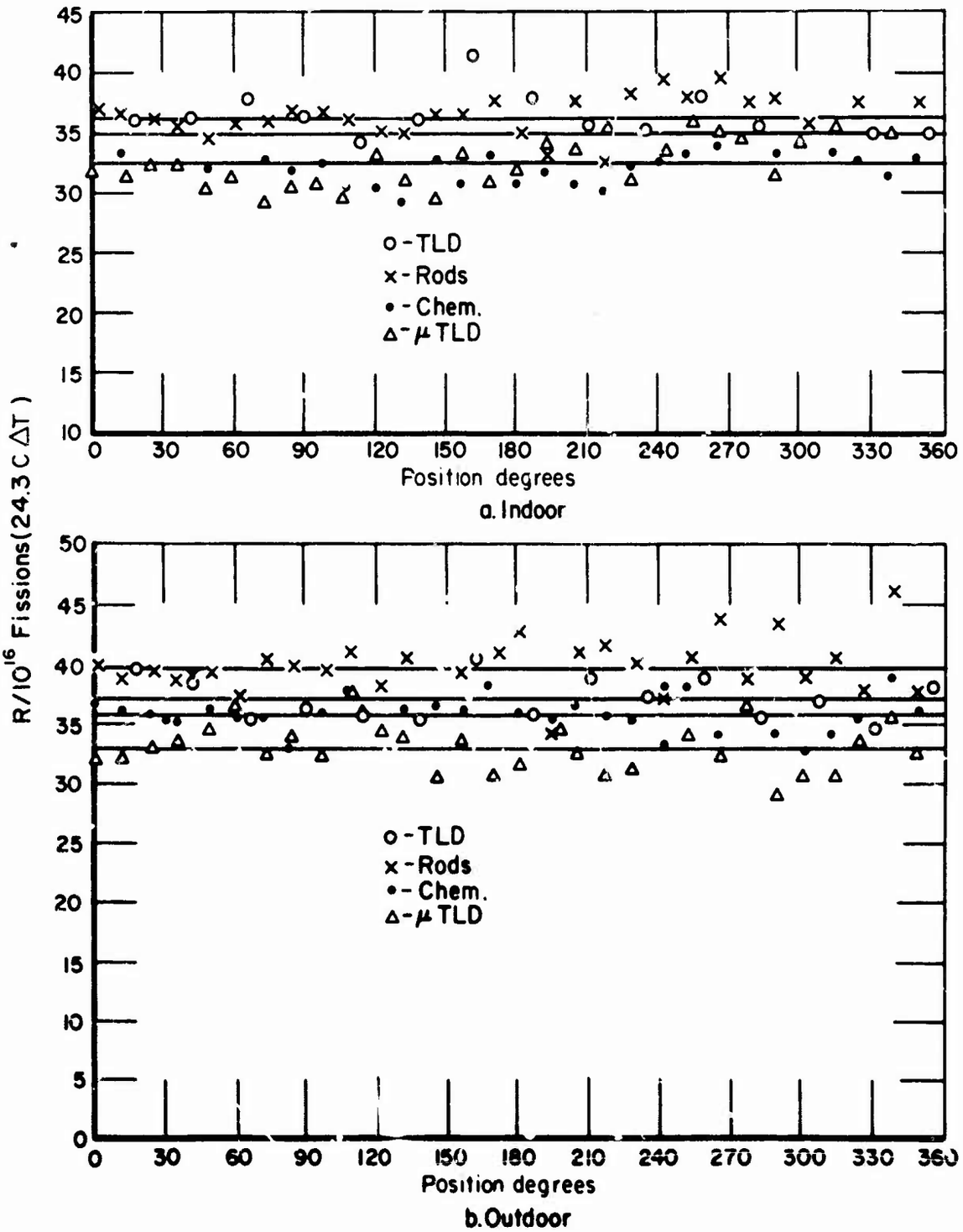

Figure 2-43. γ dose on 1-m horizontal circle.

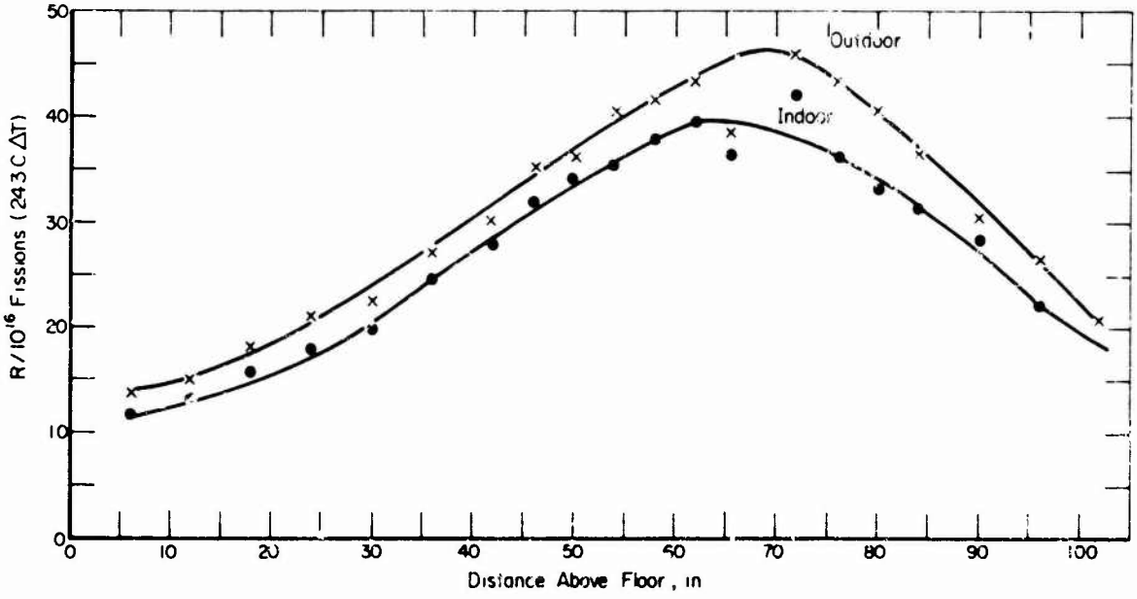

Figure 2-44. γ dose vertical traverse at 1 m from reactor axis.

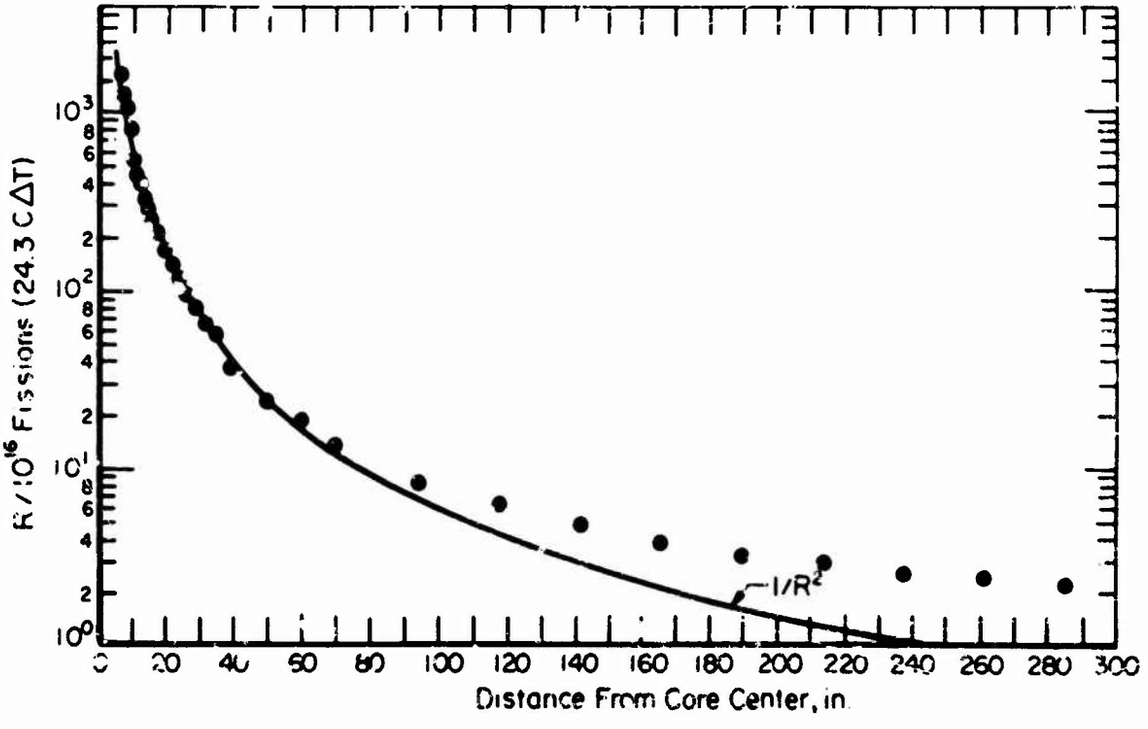

Figure 2-45. γ dose as a function of radial distance from core center, indoor.

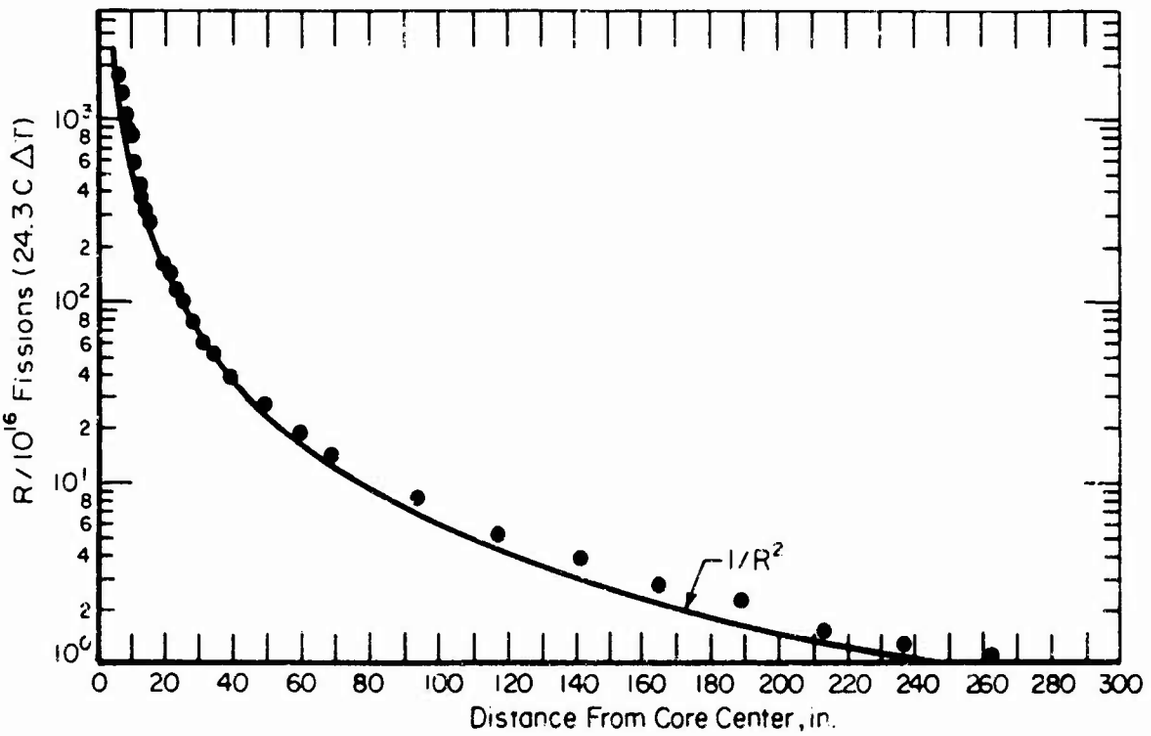

Figure 2-46. γ dose as a function of radial distance from core center, outdoor.

Utilities available at the reactor cell are listed in Table 2-26. Dosimetry equipment and instrumentation for the FBR are described in Table 2-27.

Test requirements, including all the preceding considerations, along with experiment size and exposure levels needed, should be submitted at least 2 weeks in advance of the scheduled test. This allows personnel concerned with the foregoing problems time to contact the experimenter to correct any evident problems before he leaves his facility for the White Sands Missile Range (WSMR). Failure to submit detailed requirements in writing 2 weeks in advance of the scheduled test date could result in delay of the test after the experimenter arrives.

Authorization for photographic support must be obtained from the Missile Range Administration. Professional photographic support is available at the WSMR facility.

2.4.4 Procedural Information

The reactor is operated by the Army Missile Test and Evaluation Nuclear Weapons Effects Branch. Technical and administrative inquiries should be addressed to:

Table 2-26. Utilities available at the reactor cell.

Utility	Description	Quantity	Location
Electrical outlet	208 V, 30 A, 3-ϕ twist lock receptacle	3	Inside
Electrical outlet	125 V, 15 A, duplex receptacle	10	Inside
Electrical outlet	208 V, 100 A, 3-ϕ, 4-pole, Appleton-type receptacle	8	Outside
Electrical outlet	125 V, 15 A, duplex receptacle	12	Outside
Electrical outlet	440 V, 50 A, 3-ϕ, 4-pole, Appleton-type receptacle	1	Outside
Cable conduits	6-in. conduit	9	From reactor cell to outside ground level
Cable conduits	6-in. conduit	4	From reactor cell to instrumentation room
Compressed air	0.5-in. air lines at 15 cfm, 100 psi, with quick-disconnect connectors	2	Outside
Communication	Intercommunication system	4	Outside

Table 2-27. Dosimetry equipment and instrumentation for the FBR.

Item	Quantity
400-channel, 4-input pulse-height analyzer	2
γ-spectroscopy system using a 3-in. x 3-in. NaI scintillation crystal	1
Automatic sample-changing, β-counting system	1
Automatic data printout system	1
2-pi gas-flow counting system	1
Glass-rod microdosimetry system	1
LiF thermoluminescent dosimetry system	1
EG&G thermoluminescent dosimetry system	1
Film dosimetry system	1
Fission and threshold foil counting system with automatic sample changer	Several
Calibration sources	Various
4096-channel pulse-height analyzer	1
Li-drifted Ge solid-state detector	1
Li-6 neutron spectrometer system	1
He-3 neutron spectrometer system	1

Nuclear Effects Directorate
Attention: STEWS-TE-AN
White Sands Missile Range
NM 88002.

Telephone contact can be made with Mr. A. De La Paz or Mr. L.L. Flores at (915) 678-1161.

A lead time of approximately 4 weeks is required for scheduling. However, in advance of a firm scheduling commitment, an experiment test plan must be submitted and approved.

Cost and charges associated with use of the reactor and facility can be obtained directly from the technical coordinator. The shipping address is:

Transportation Officer
Attention: Nuclear Weapons Effects Division
White Sands Missile Range
New Mexico 88002.

Classified mailing and shipping addresses are to be arranged through proper channels on an as-needed basis.

2.4.5 Applicability and Availability

The FBR is one component of a laboratory whose specific mission is to provide facilities for U.S. Government agencies or their contractors to conduct experiments that require nuclear irradiation. The reactor is readily available and amenable to TREE experiments. The laboratory is capable of carrying out, on a project basis, complete or partial experimental programs. A full operating staff is permanently assigned to the facility, although the professional staff is not extensive. However, scientific and engineering personnel from university and college faculties are available to support experimental programs.

The facility is located within the confines of the WSMR. Operations may involve considerable commuting distance between available overnight accommodations and the site. Arrangements for daily transportation must be made by the experimenter. If the facility has to be used during other than normal working hours, such arrangements must be made in advance.

2.4.6 References

1. "Characteristics of Nuclear Effects Branch Radiation Facility and Operational Procedures," memorandum, Army Missile Test and Evaluation Directorate, March 1966.

2. Humpherys, K., W. Quam, C. Rainbolt, R. Durkee, and T. Dahlstrom, *Nuclear Radiation Dosimetry Measurements of the White Stands Missile Range Fast Burst Reactor*, January 1965.

2.5 WHITE SANDS MISSILE RANGE STEADY-STATE NEUTRON GENERATOR

2.5.1 Characteristics

The Neutron Generator (SNG) of the Nuclear Weapon Effects Branch (NWEB) is a Texas Nuclear Corporation Model 9905. It can be used to produce monoenergetic neutrons of either 14 or 2.6 MeV by the use of tritium or deuterium targets. It also can be used in a pulsed mode.

2.5.2 Operating Characteristics

Minimum target-to-sample separation is 5 mm. Multiple (5-target) assembly allows rapid switching to new target and switching between 2.6 and 14 MeV neutrons. Typical target life is 5 mA hr. Steady-state mode operating characteristics are:

	14 MeV	2.6 MeV
High V	150 kV	150 kV
Beam I	2 mA	2 mA
Isotropic output	2×10^{11} n/s	8×10^{8} n/s
Useable flux	1.5×10^{10} n/cm^2/s	6×10^{7} n/cm^2/s

Pulse mode operating characteristics are:

Pulse width (continuously variable)	1 μs to 10^4 μs
Repetition rate (continuously variable)	10 to 10^5 pps
Residual beam	6×10^{-4}% of peak
Beam I	Up to 1 mA
Output at 1 mA	10^{11} n/s
Useable flux (14 MeV)	7×10^{9} n/cm^2/s
Useable flux (2.6 MeV)	3×10^{7} n/cm^2/s

2.5.3 Environment

The SNG can be used for radiation effects testing or as part of a complete activation analysis system, which includes pneumatic transfer systems, with dual two-axis rotator, 400-channel analyzers (RIDL 34-12B and TMC 404), single-channel analyzers, and a radiochemical laboratory. The SNG also can be used for neutron radiography, and a photoprocessing laboratory is available.

2.5.4 Support Capabilities

The prime mission of the facility is to support experimenters and, when available, to provide necessary personnel and equipment for full operational and working assistance. Facility personnel operate the SNG. The limited professional staff, enhanced by scientific and engineering personnel from university and college faculties, is available to support all experimental programs.

Extensive electronic equipment and support components are maintained for use by NWEB SNG experimenters. Instrumentation trailers equipped for monitoring and

recording experimental data are available on a contractual basis. Adequate facilities and space are available for the experimenter to utilize his own instrumentation trailers.

Neutron dosimetry for 14-MeV neutrons (tritium target) is Cu or Al activation foil. At 2.6 MeV (deuterium target), S activation foils are used. The accuracy of the dosimetry is ±10%. Threshold neutron activation foils (Pu, Np, U-235, U-238, Th, S, Ni, Fe, Mg, Al, Mn, Au, Na) are available. For more complete technical details, see Dosimetry Technical Report 69-1, *Fast Neutron Dosimetry for the 150-kV Texas Nuclear Neutron Generator (SNG)*. This report is available from NWEB.

Light machine shop facilities, as well as experiment preparation laboratories, personnel offices, security storage, and conference rooms, are available at the facility.

Authorization for photographic support must be obtained from the Missile Range Administration. Professional photographic support is available at the facility.

The SNG test cell is approximately 6 m x 6 m x 6 m high. Signal cables from the test cell are strung through underfloor conduits to the instrumentation room or a screen room (see Figure 2-47).

Cost and charges associated with use of the NWEB SNG and facility can be obtained directly from the technical coordinator. The shipping address is:

Transportation Officer
White Sands Missile Range
NM 88002
Attention: Nuclear Weapons Effects Directorate

Classified mailing and shipping addresses must be arranged for through proper channels, on an as-needed basis.

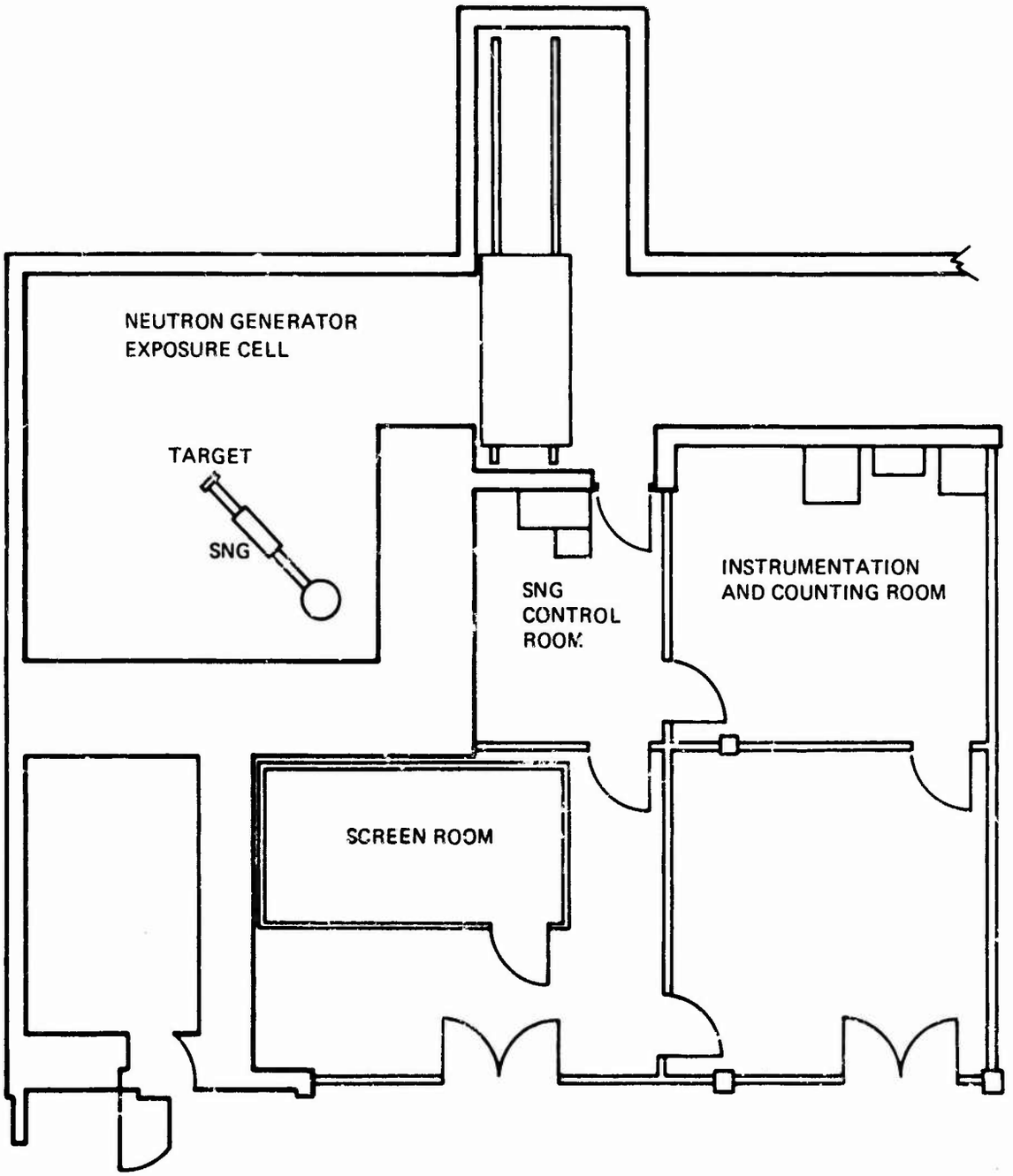

Figure 2-47. WSMR neutron generator.

2.6 SANDIA PULSE REACTOR (SPR-II)

2.6.1 General Characteristics

The SPR-II is an all-metal, unreflected, and unmoderated critical assembly in the form of a right-circular cylinder, 8 in. in dia. and 8.2 in. high. The assembly contains a total mass of 105 kg of fully enriched U (93.2% U-235), alloyed with 10 w/o Mo. A 1.5-in. dia. "glory hole" extends vertically through the center of the core, facilitating internal as well as external irradiation of small test samples. It is at the midplane of the glory hole that the principal performance criterion, $\sim 10^{15}$ n/cm^2 (E > 10 keV) for a maximum yield burst, is defined.

A thin-walled Al shroud approximately 8.75 in. square and 17 in. high covers the fuel assembly. The shroud, coated with B, serves a dual purpose in ducting forced cooling gas over the fuel system, thereby achieving relatively efficient cooling; and, second, it diminishes the reactivity contribution of moderating test samples placed external to the reactor. Cooling reduces the maximum delay time between bursts to 2 hr.

The reactor is capable of operating in either the pulse mode or at a steady-state power of up to 5.0 kW for several hours. Steady-state operation is minimized, however, because it produces large fission product inventories in the core.

Data presented here are from data obtained by Sandia Laboratories in an effort to characterize the output and environment generated by the SPR-II.

2.6.2 Operating Characteristics

The burst energy release is characterized by the temperature rise in the fuel. A standard SPR-II burst produces about a 350° to 400°C temperature rise (maximum). Measured characteristics for a typical (300°C) and various power runs are given in Tables 2-28 and 2-29. Peak power level is approximately 89,000 MW.

Pulse width varies inversely with burst size; the larger the temperature excursion, the narrower the pulse. Figure 2-48 shows the relationship between pulse width and pulse yield. Figure 2-49 depicts 3 different burst profiles, as measured with a photodiode.

Cooling time is approximately 1 hr, depending upon the size of the operation.

Measured data regarding the tolerable reactivity worth of experimental samples indicate the following:

1. The protective shroud around the fuel material isolates the reactor from the experiments placed external to the core.

Table 2-28. Neutron fluences.

Location	Operation	Neutron Fluences >10 keV
GH	Burst[a]	7.25×10^{14}
GH	Power Run (PR)[b]	1.44×10^{15}
6 in. from core	Burst	5.92×10^{13}
6 in.	PR	7.79×10^{13}
12 in.	Burst	1.39×10^{13}
12 in.	PR	1.98×10^{13}
24 in.	Burst	4.74×10^{12}
24 in.	PR	4.88×10^{12}

[a]300°C ΔT burst

[b]4.5×10^6 W/s power run.

Table 2-29. γ dose[a], rad (H_2O).

Location	Operation	TLD 200 (CaF_2 - Mn)	TLD 100 (LiF)	Ag_3PO_4
GH	Burst[b]	1.46×10^5	(1.134×10^5)[e]	1.61×10^5[f]
GH	Power Run 1 (PR1)[c]	2.06×10^5	2.34×10^5	2.14×10^5
GH	Power Run 2 (PR2)[d]	(1.58×10^5)[e]	2.35×10^5	2.36×10^5
0 in. from shroud	Burst	1.92×10^4	2.13×10^4	1.77×10^4
0 in.	PR1	2.35×10^4	3.08×10^4	1.97×10^4
0 in.	PR2	2.66×10^4	3.21×10^4	2.43×10^4
6 in.	Burst	3.12×10^3	5.28×10^3	---
6 in.	PR1	3.50×10^3	6.28×10^3	---
6 in.	PR2	4.01×10^3	6.38×10^3	---
12 in.	Burst	1.34×10^3	(5.02×10^3)[e]	---
12 in.	PR1	1.49×10^3	3.69×10^3	---
12 in.	PR2	1.53×10^3	3.96×10^3	---

[a]Doses for PR1 have been multiplied by 3.0 for ease of comparison.

[b]300°C ΔT burst.

[c]18 kW-min power run.

[d]54 kW-min power run.

[e]Inconsistent with other data.

[f]Corresponds to 1-MeV γ fluence of 3.24×10^{14} γ/cm^2.

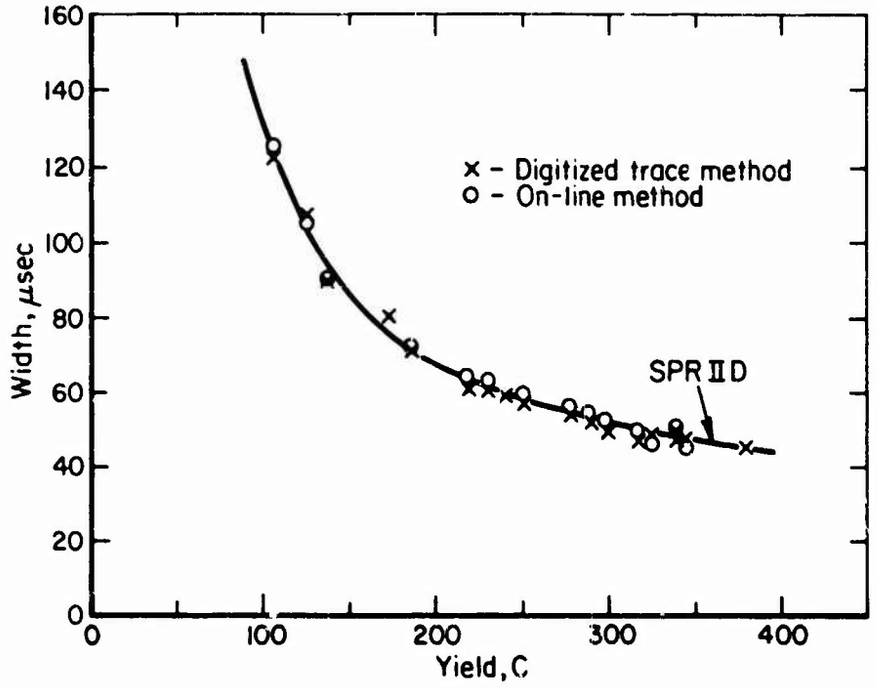

Figure 2-48. Burst width versus burst yield (yield is measured temperature rise).

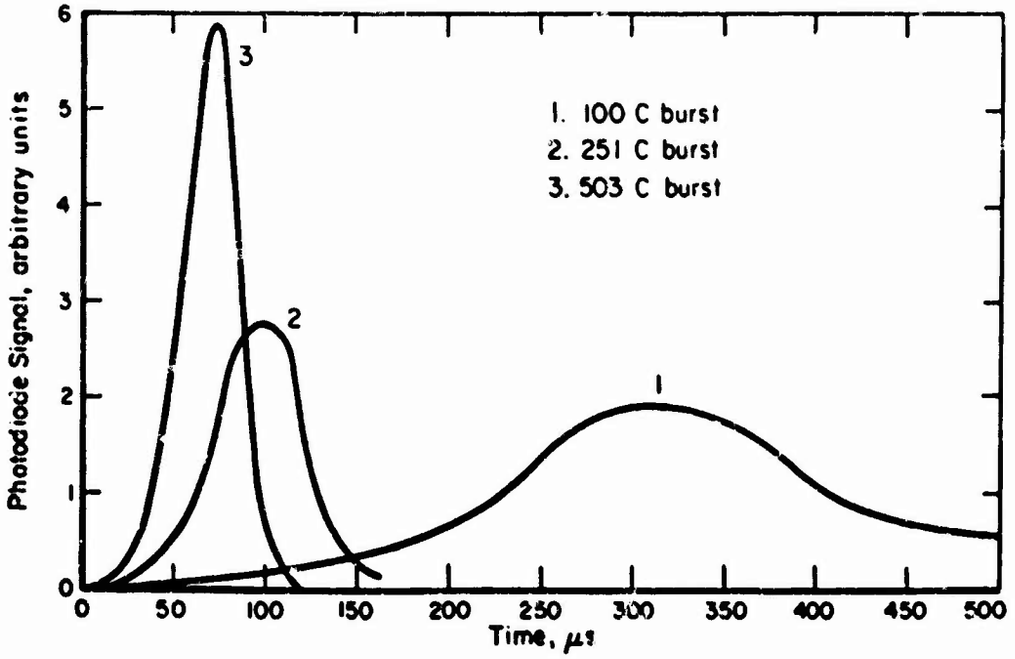

Figure 2-49. SPR-II burst time profiles for various-size bursts, as determined with a photodiode.

2. Samples placed within the glory hole are very strongly coupled to the reactor. Measurements have been made regarding the reactivity worth of various sample materials in this position.

An assessment of sample reactivity worth will be made by the reactor staff for each experiment conducted.

Reactivity insertion rate is approximately $10/s.

Burst frequency is approximately 1 burst/2 hr, depending on the size of the burst.

2.6.3 Environment

Measurements of the neutrons and γs generated by SPR-II in the glory hole and around the outside of the reactor are presented here.

Neutron measurements were made utilizing threshold foils and fission-couple detectors. The results are shown in Figures 2-50 through 2-54 and Table 2-28. The measurements were made essentially in a free-field condition; i.e., there were no spectrum-perturbing experiments near the reactor during the measurements. Therefore, the values given should be representative of any free-field location in the reactor room. Table 2-30 shows the relative uniformity of the fluence at a position 15 in. from core center as shown in Figures 2-55 and 2-56.

Absorbed γ dose measurements were made with Ag_3PO_4 glass. The measured data were corrected for the neutron sensitivity of the glass in the SPR-II spectrum and also corrected to rad (water) using an assumed γ energy spectrum. The results characterizing the SPR-II γ environment are presented in Figures 2-57 through 2-59 and Table 2-29.

Measurements imply that fluence and dose levels are approximately linear with fuel temperature rise.

Neutron spectra measurements were made in the glory hole and outside the core. The results are shown in Figure 2-60 and from foil measurements in Tables 2-31 and 2-32.

Recent measurements show the variation of the n/γ ratio with position and types of reactor operation. Measurements were made using S foils to determine neutron fluence n/cm^2 ($E > 10$ keV), and 3 types of γ dosimetry were used to measure the absorbed dose (see Tables 2-28 and 2-29). Ag_3PO_4 data below 4.4×10^3 rads (at 6 in. and 12 in. from the shroud) could not be resolved. The TLD 100 values are consistently higher than the TLD 200 (Mn-activated) values because of neutron activation of ^6L in the TLD 100 samples. The n/γ ratios are given in Table 2-33. The TLD 200 data and some of the Ag_3PO_4 data from this table are shown graphically in Figure 2-61.

Possible sources of error include positioning error of successive dosimetry packages, shadowing effects, and faulty dosimetry.

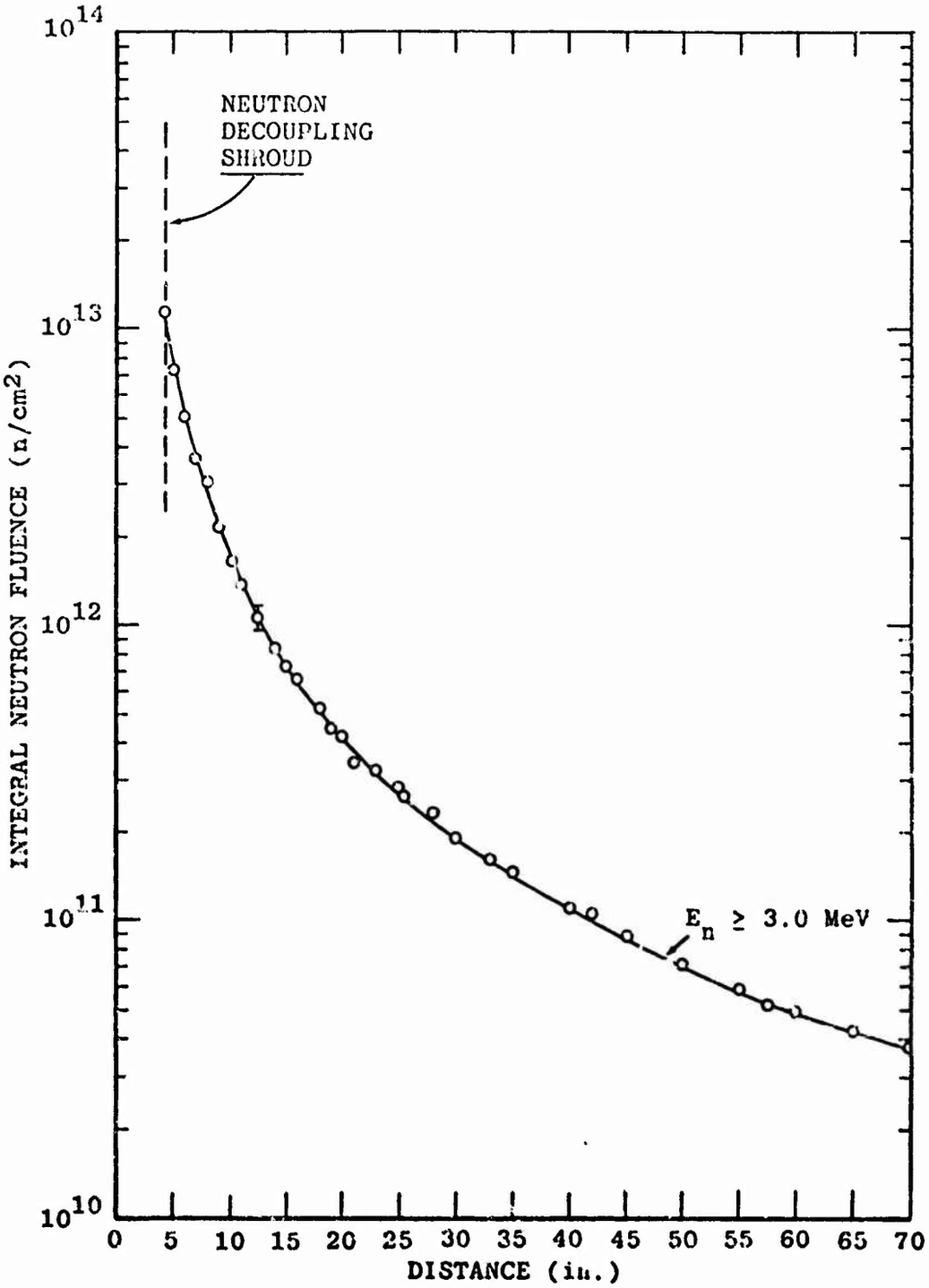

Figure 2-50. Free-field integral neutron fluence as a function of distance from the reactor vertical center line at 57.7 in. above the floor for a 200°C burst.

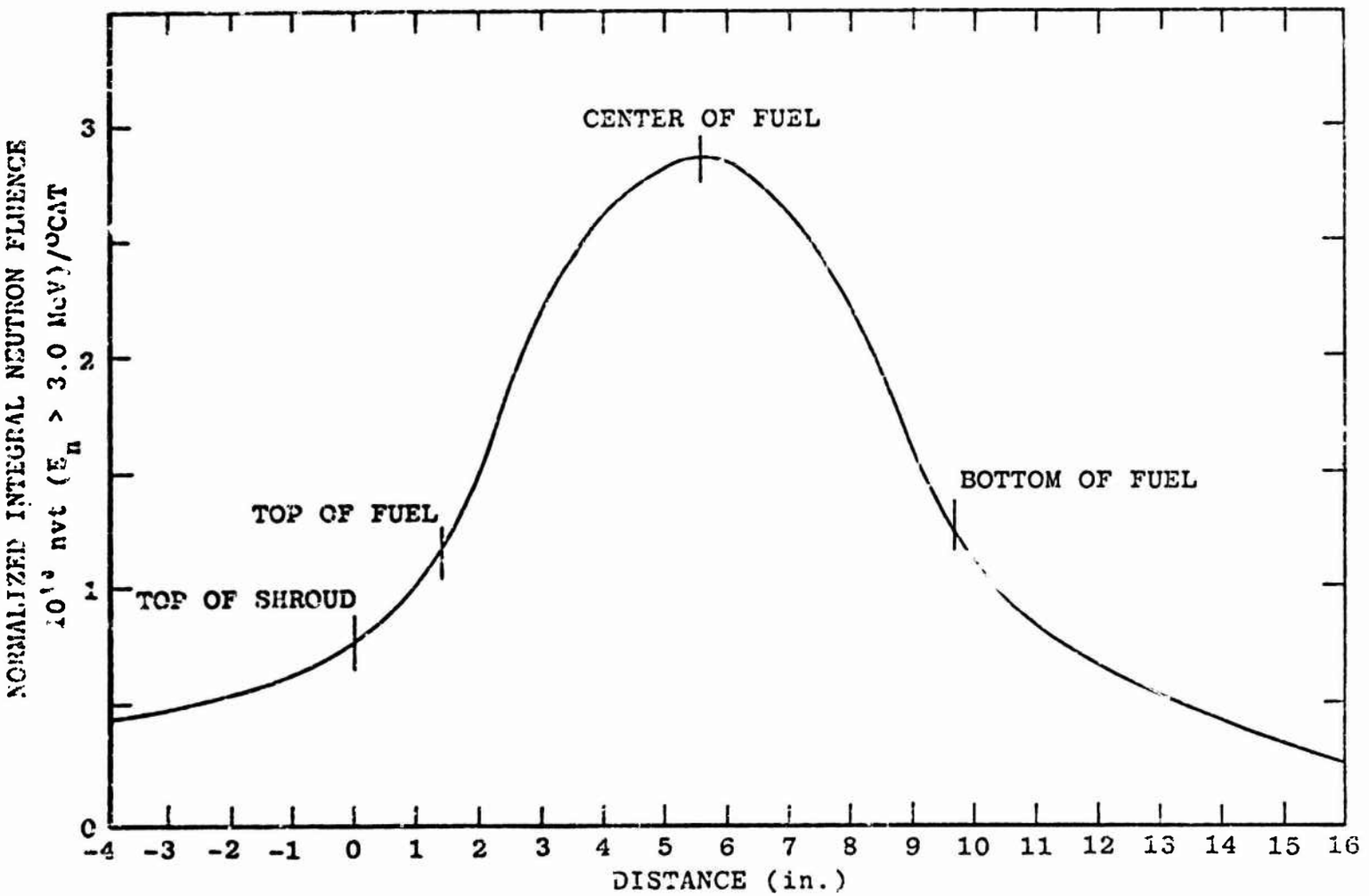

Figure 2-51. Integral neutron fluence ($E_n \geq 3.0$ MeV) on the outside shroud surface normalized to core temperature change as a function of distance from the top edge of the shroud.

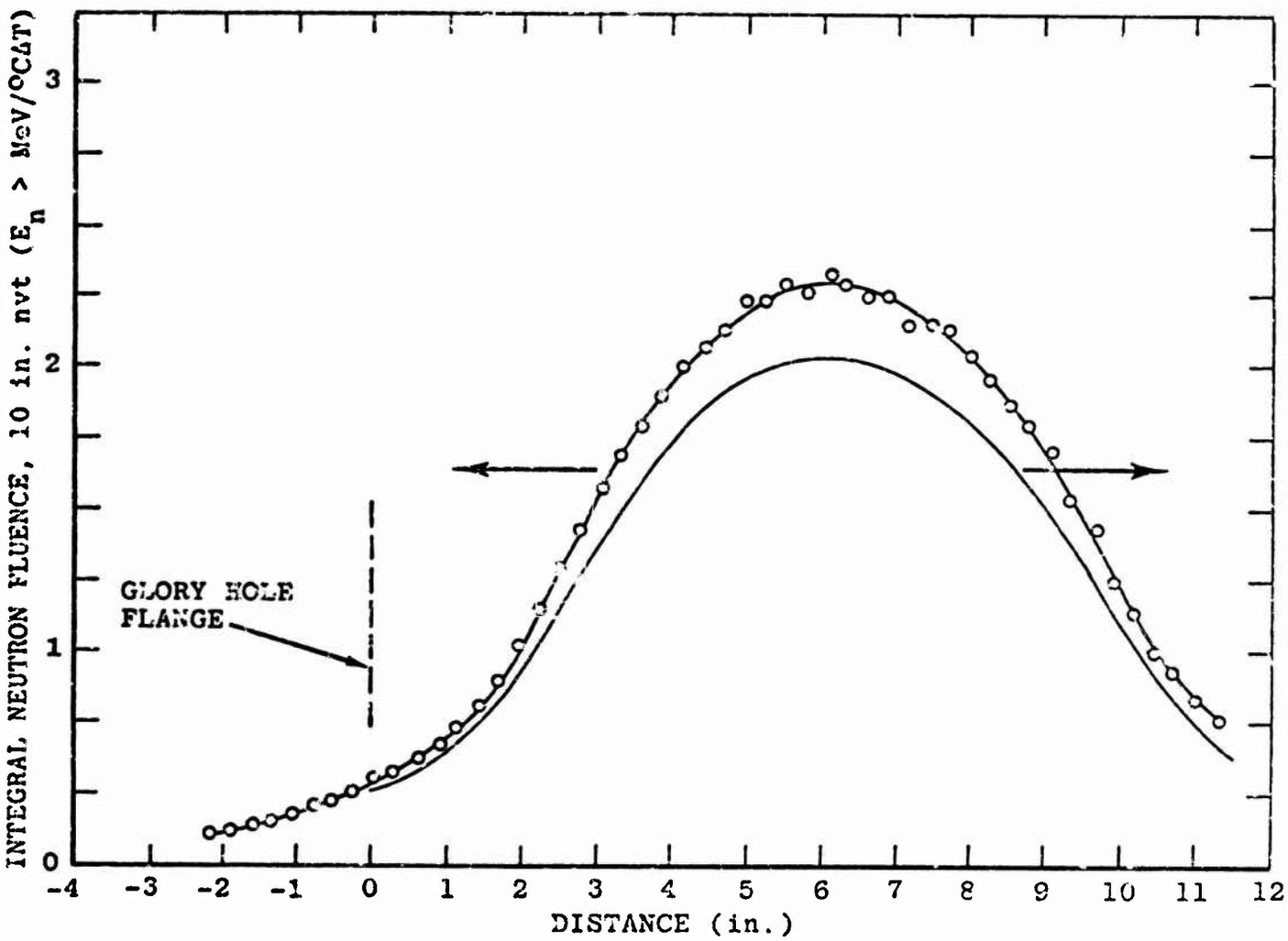

Figure 2-52. Integral neutron fluence ($E_n \geq 3.0$ MeV) normalized to core temperature change for the glory hole center line versus vertical distance from the top of the glory hole flange.

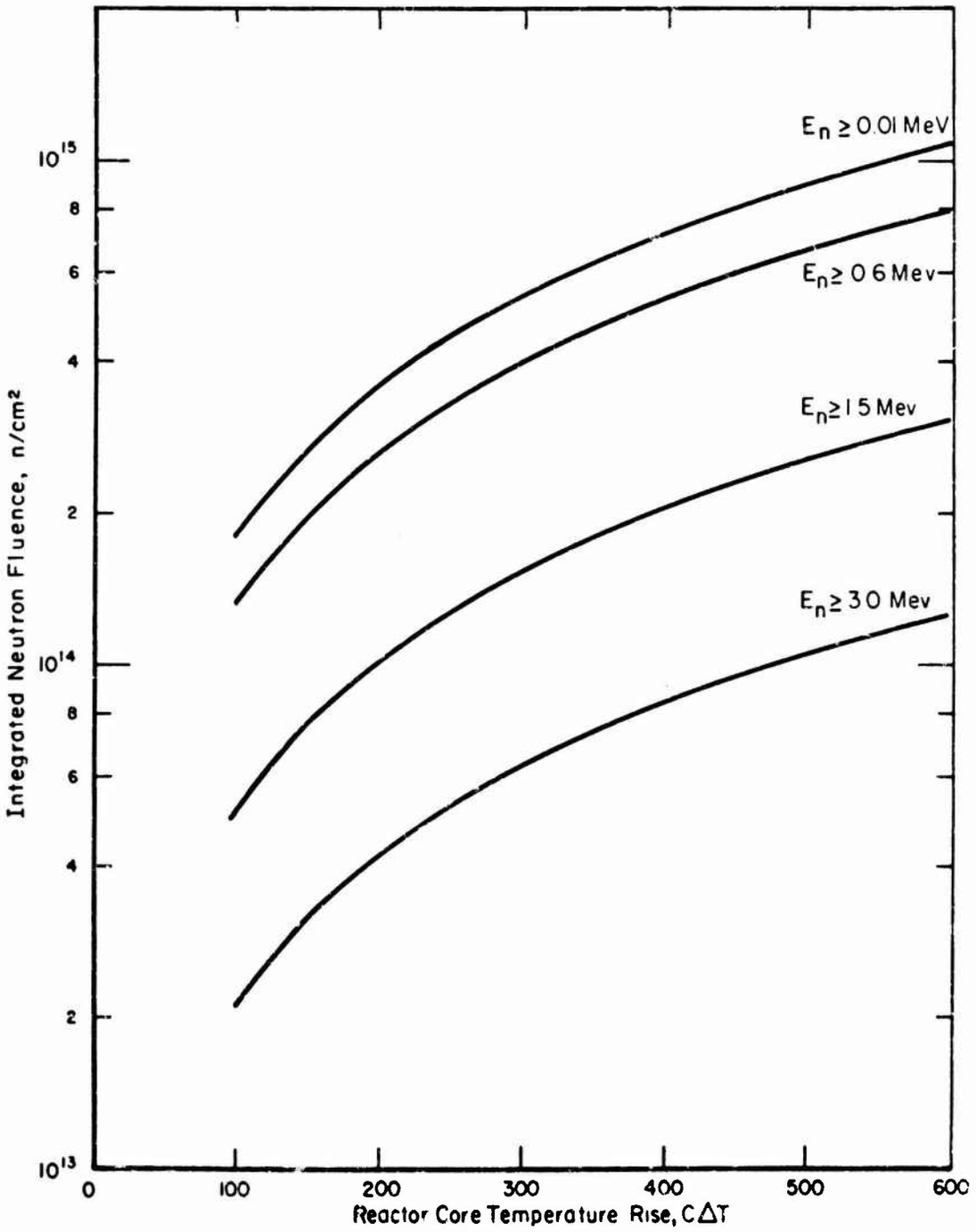

Figure 2-53. Glory hole fluence at the nuclear center of the glory hole versus SPR-II.

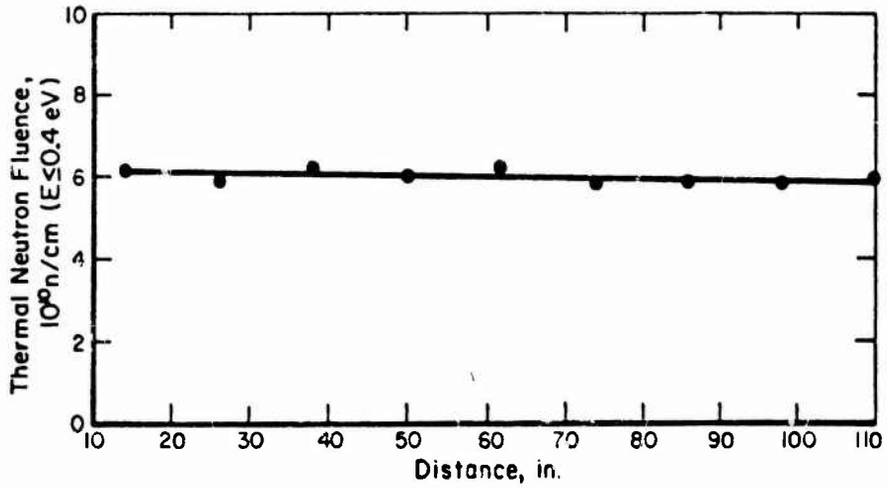

Figure 2-54. Thermal neutron fluence ($E_n \geq 0.4$ eV) as a function of distance from the reactor vertical center line at 57.5 in. above the floor for a 200°C burst.

Table 2-30. Relative fluence profile 15 in. from reactor center line.[a]

Vertical Location (in. from midplane)	Relative Horizontal Location (deg) θ		
	-9.55	0	+9.55
+6	0.740	0.767	0.741
+3	0.862	0.842	0.897
0 Z	0.964	0.925	0.928
-3	0.922	1.0	0.961
-6	0.867	0.878	0.892

[a]Fluence map is symmetrically located with respect to two support posts. It should be emphasized that the geometric volume enclosed by the exposure area and the reactor center line did not include the support posts. The flux is attenuated by as much as 40% at a position directly behind a post.

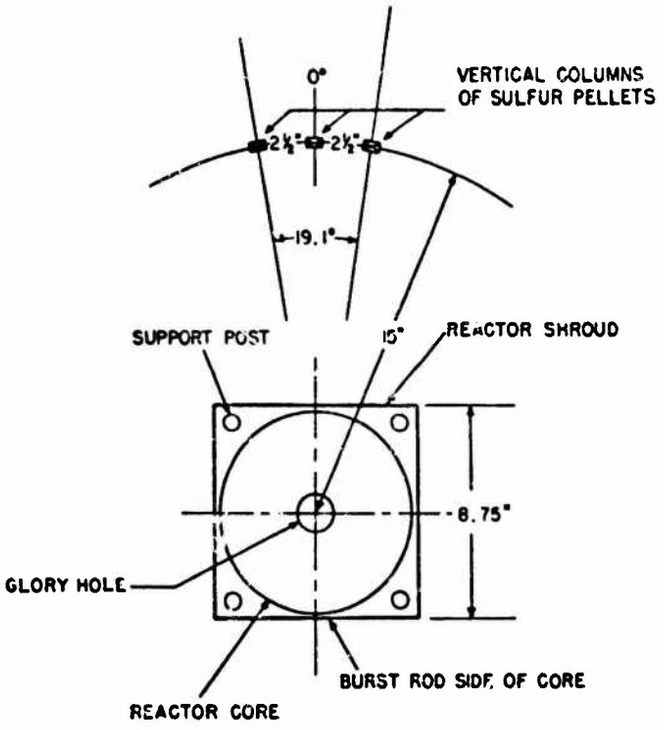

Figure 2-55. Horizontal placement of dosimeters.

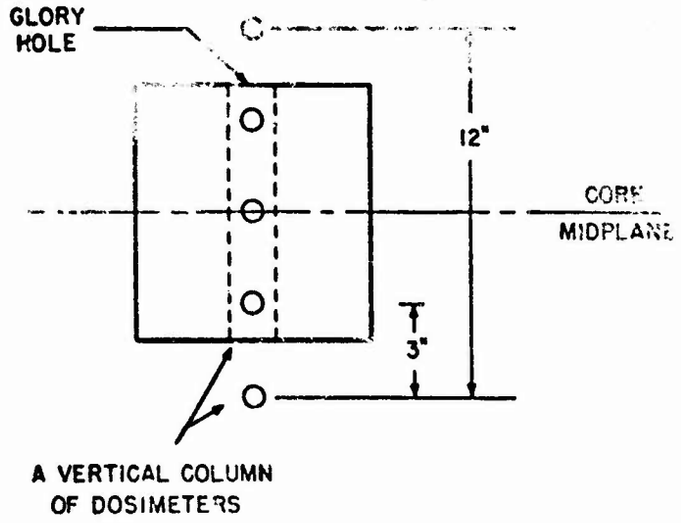

Figure 2-56. Vertical placement of dosimeters.

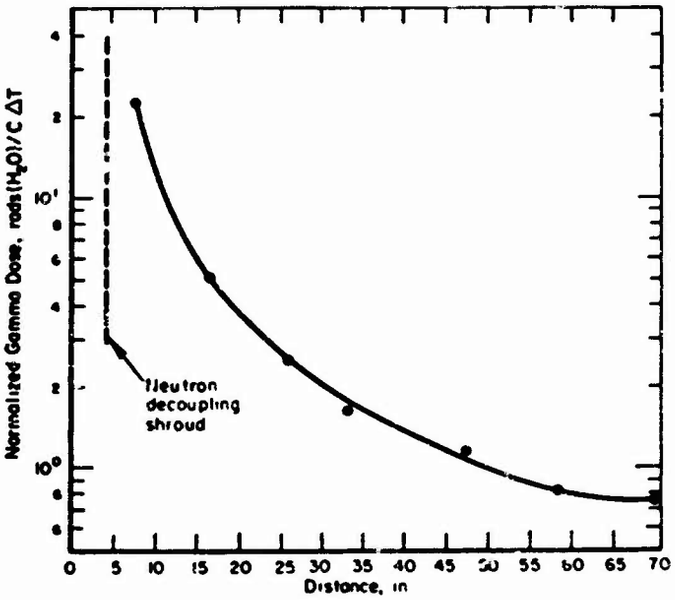

Figure 2-57. Normalized γ dose as a function of distance from the reactor vertical center line at 57.5 in. above floor.

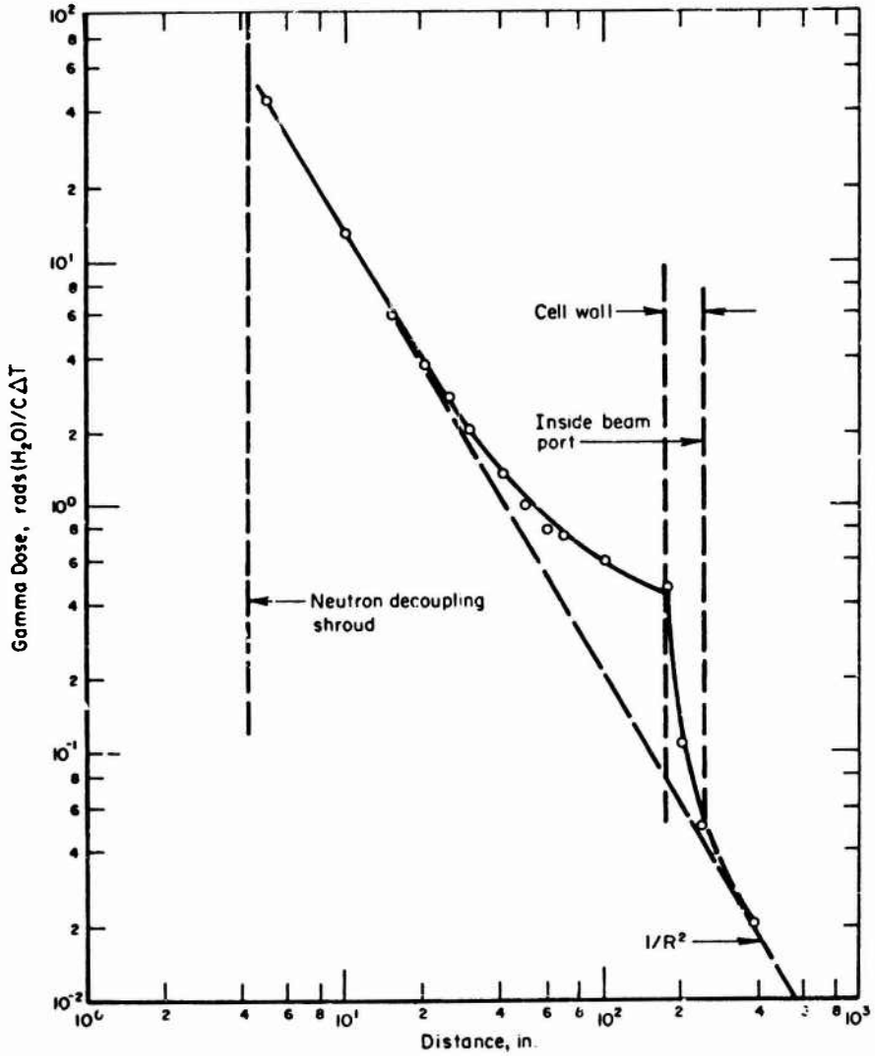

Figure 2-58. γ dose as a function of distance from the reactor vertical center line at 57.5 in. above the floor for a 1°C temperature rise.

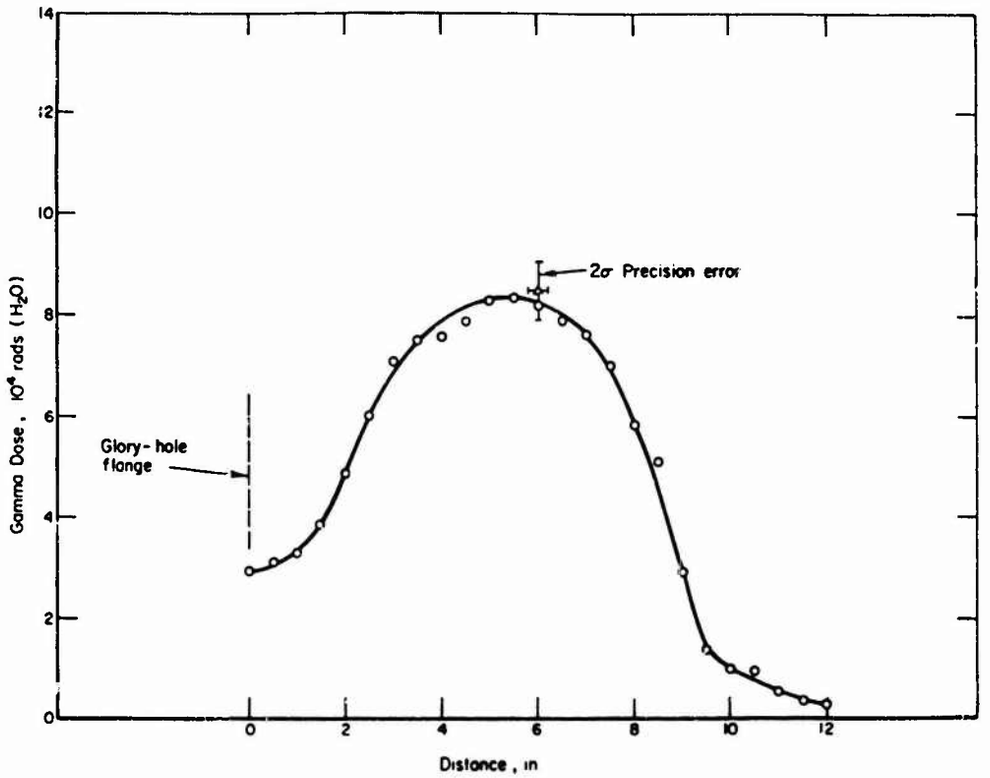

Figure 2-59. γ dose on the glory hole center line as a function of vertical distance from the top edge of the glory hole for a 200°C burst.

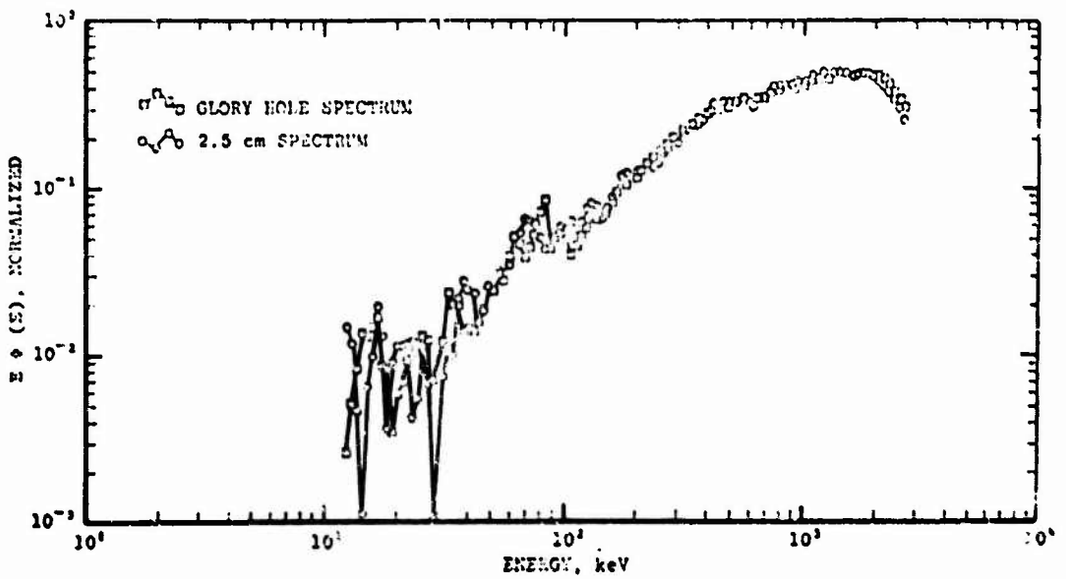

Figure 2-60. Comparison of the glory hole and 2.5-cm spectra, proton recoil measurements.

Table 2-31. Neutron spectrum at external position 1 in. above shroud on vertical center line.

Threshold Energy (MeV)	Fraction of Neutrons Above Threshold Energies
Total fast fluence	1.0
0.6	0.685 ± 0.055
1.5	0.340 ± 0.030
3.0	0.100 ± 0.006

Table 2-32. Glory hole neutron spectrum.

Threshold Energy (MeV)	Fraction of Neutrons Above Threshold Energies
Total fast fluence	1.0
0.6	0.740 ± 0.75
1.5	0.285 ± 0.030
3.0	0.117 ± 0.009

Table 2-33. n/γ ratios (10^9 n/cm^2-γ rad (H_2O)).

Location	Operation	TLD 200 (CaF_2 - Mn)	n/γ TLD 100 (LiF)	(Ag_3PO_4)
GH	Burst	4.18	(5.379)[a]	3.79
GH	PR1[b]	3.09	2.72	2.97
GH	PR2[c]	(4.06)[a]	2.73	2.73
0 in. from shroud	Burst	6.51	5.87	7.06
0 in.	PR1	5.59	4.29	6.70
0 in.	PR2	4.92	4.08	5.39
6 in.	Burst	6.44	3.81	--
6 in.	PR1	5.57	3.11	--
6 in.	PR2	5.04	3.17	--
12 in.	Burst	6.07	(1.62)[a]	--
12 in.	PR1	5.23	2.01	--
12 in.	PR2	5.04	2.06	--

[a]Inconsistent with other data.

[b]18 kW-min power run.

[c]54 kW-min power run.

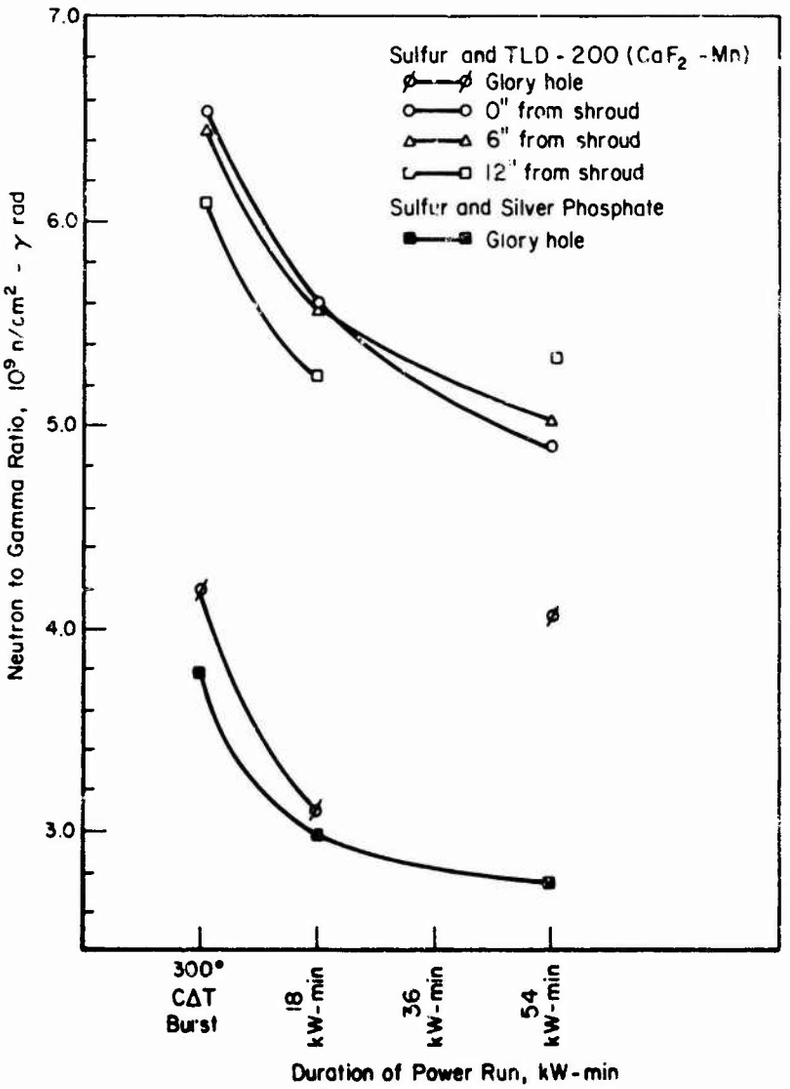

Figure 2-61. n/γ ratios as a function of operation.

At any given experiment location in or around the SPR-II, the n/γ ratio is higher on a burst operation than on a power run of equivalent neutron fluence because of the delayed γ dose associated with the extended exposure time required on a power run. A long power run at low power results in fewer n/γ than a short power run at high power (with the total number of kW-min equal in both cases) because a smaller fraction of delayed γ is emitted during the exposure time of the short power run.

The n/γ ratio on a 1-kW 54-min power run is 21.5 to 24.5% lower than an equivalent burst operation at each location investigated.

The experiment location that provides the highest n/γ ratio is just outside the reactor shroud. This location provides a ratio approximately 55% greater

than in the glory hole. At a position 12 in. from the shroud (on the core midplane), the ratio is 45% greater than in the glory hole.

The experience of the facility operators indicates that RF background noise poses no serious problem.

An analysis of the errors and uncertainties associated with the resulting neutron and γ data was performed by the Sandia Laboratories. This analysis established that the uncertainties associated with any 1 measurement point are at worst ±12%. This uncertainty is inherent in any spectral and fluence measurements because of contributing factors relating to detector calibration and positioning, cross-section information, signal measurement, and foil counting. The singular and overall uncertainties associated with the reported Sandia data are typical and representative of the present state of the art.

2.6.4 Support Capabilities

With the exception of radiological and toxicological safety services of the Sandia Laboratories Dosimetry Counting Laboratory, Sandia personnel should not be expected to provide scientific, technical, or engineering consulting services or support to non-Sandia users of the pulse reactor.

The primary service provided by Sandia for the experimenter/user is a nuclear radiation environment from the pulse reactor. The Sandia technical staff is available for consulting services only on an occasional and limited basis, unless special contractual arrangements are made. If experiments involve radioactive or toxic substances, a Sandia health physicist is assigned the responsibility of regulating personnel exposures and ensuring that proper handling procedures are employed.

Utilities available inside the reactor cell include:

1. Compressed air — 4 CFM at 100 psi
2. Electrical power — 40 kVA, 120 V, 1 ϕ
3. Water drain — 3-in. gravity flow.

Around the inside periphery of the cell are 9 electrical patch panels. Three of these are paired with identical panels outside the cell at trailer parking stations and 4 are connected with panels inside the instrumentation building. The other 2 are used by reactor operations. Each of the 7 experiment boxes provides RG-58B/U coaxial cables, No. 14 signal wires, a ground bus, and an empty 4-in. conduit for the experimenter to pull his own cables when desired.

Near the patch panel at each trailer station, 208-V, 3-ϕ, 100-A electrical power is available through an Appleton AEEA-10476 connector. Also, each trailer station has a 120-V, 1-ϕ, ac supply, terminated in four 3-prong convenience outlets. Instrumentation cables, which must be provided by the experimenter, may be laid along the ground between the outer patch panel and the recording trailer. Equipment to be used within the reactor room must be wired for remote operation since personnel are not permitted inside the reactor room while the reactor is running.

Any cable reaching from the reactor to the patch panel should be at least 20 ft long. Any cable pulled through the patch panel conduit should be at least 45 ft plus the desired length outside the cell.

An instrumentation building located immediately adjacent to the reactor building houses permanently installed data-gathering and analysis equipment. Dual-beam oscilloscopes with automatically actuated cameras, power supplies of various voltage and current ratings, and several types of amplifiers are available. Space is also available for the experimenter to set up his own special equipment. Cables should be 65 ft long to reach from the reactor to the oscilloscopes or tape recorder in the instrumentation building.

No screen room is available at the facility; however, provisions can be made for adequate electrical shielding.

Sandia Laboratories Field Test Organization has located several instrumentation vans in TA-V to support the reactor facilities. This support capability is available to perform data acquisition functions.

Timing triggers for pre-burst and post-burst and signals relative to burst-peak can be furnished, if required.

Dosimetry data can be provided by the Sandia Laboratories Dosimetry Counting Laboratory. Standard foil techniques are used for neutron measurements. Glass-rod dosimetry is used for γ measurements.

Calculational facilities are available at the SPR site. The Sandia Laboratories Computational Laboratory, although not normally available to non-Sandia users of the SPR, may be utilized on a limited basis by prearrangement. A terminal is available in TA-V which inputs the CDC 6500s and 7600 for unclassified programs. Various outputs are available.

The TA-V Data Acquisition and Display System (DADS) is located near the SPR facility. This system, built around the EMR 6130 digital computer, accepts either digital or analog inputs from remote consoles. Digital or analog outputs are available on a CRT display, magnetic tape, or in printed form. The DADS is available to all SPR experimenters. One of the remote consoles is located at the SPR facility.

Light machine shop facilities and experiment preparation and setup laboratories are available. Limited photographic equipment and oscilloscope cameras and film are readily available. Please check with security before bringing photographic equipment into the area.

2.6.5 Procedural Information

Technical and administrative inquiries related to the use of SPR-II should be directed to:

Reactor Applications Division
Organization 5451
Sandia Pulsed Reactor Facility
Sandia Laboratories
P.O. Box 5800
Kirtland Air Force Base (East)
Albuquerque, NM 87115
Telephone: (505) 264-2361 or 264-1272

A final plan of experiment must be submitted 4 weeks in advance of anticipated use of the facility. The format to follow in submitting this plan is shown in Figure 2-62. Scheduling of reactor time is not considered until final approval of the contract and the plan has been received.

Costs and charges associated with use of the facility are documented and available directly from Sandia Laboratories. The shipping address is:

Supervisor, Organization 5451
Sandia Laboratories
P.O. Box 5800
Kirtland Air Force Base (East)
Albuquerque, NM 87115

2.6.6 Applicability and Availability

The SPR-II provides a transient radiation environment readily applicable to TREE experiments. The facility is available to agencies of the DoD and to private enterprises having DoE or DoD contracts requiring the use of the reactor. The reactor is available on the basis of noninterference with Sandia programs. The reactor facility is located in an isolated experimental area 6 miles south of the main Sandia Laboratory, making it necessary for experimenters to provide their own transportation.

2.6.7 Security Clearance

Security clearances are required to gain unescorted access to the SPR facility. Visitors with a Q-clearance or a DoD Secret clearance with a Restricted Data certification may have unescorted access to the SPR-II. Visitors without the above clearances must be escorted while in the security area. Visitor Control must be contacted to arrange for access to the laboratory.

Date_____

TO: J. A. Snyder, 5451 Building 6591 Ext. 264-1272

FROM: _____ Org._____ Ext._____
(Responsible Project Leader)

Other participants_____

This experiment has been discussed with SPR personnel and the scheduled dates are:

_____

Title_____

_____

Objective_____

_____

Security Classification_____

Procedures_____

_____

_____

_____

Items to be exposed (qty., wt., mat'ls, dimensions, etc.)_____

_____

_____

_____

Radiation levels and total number of SPR operations required____

_____

_____

_____

Experimenter Signature_____

Reviewed and Approved by SPR Supervision_____
(Date)

Reviewed by Committee_____
(Date)

Arrange for Area V access and submit plan as soon as possible after scheduled reactor time has been verbally confirmed.

NOTE: EXPERIMENTAL SETUP FOR IRRADIATION, AND REMOVAL, WILL NOT BE DONE BY OPERATIONS PERSONNEL.

Figure 2-62. Sandia pulse reactor facility experiment plan.

2.7 LAWRENCE LIVERMORE LABORATORY SUPER KUKLA PROMPT BURST REACTOR

2.7.1 General Characteristics

Super Kukla is an all-metal unreflected, unmoderated, fast reactor in the form of a hollow right circular cylinder 30 in. in dia. with a variable height which is nominally 37 in. at critical. The hollow core contains a central irradiation cavity 18 in. in dia. and 30 in. high. Samples may be irradiated either within the cavity or at any of several external positions. The top cylinder may be closed with a 6-in. thick W plate which both reflects neutrons and supports an associated sample container. The reactor contains approximately 4,500 kg of enriched U (20% U-235) alloyed to 10 w/o Mo. The reactor was built primarily to provide a pulsed isotropic fast-neutron source throughout a relatively large experimental volume. The low U-235 enrichment and the large core size produce a prompt neutron lifetime that is much longer than for smaller highly U-235 enriched reactors, therefore producing a considerably longer pulse width.

A maximum power burst causes a measured core temperature rise of approximately 285°C and a peak core temperature rise of approximately 500°C. Due to limited core cooling capability, the burst repetition rate for bursts producing a measured core temperature rise in excess of 100°C is limited to 1 burst per day. However, extensive experimentation is conducted utilizing bursts producing measured temperature rises less than 100°C, thereby increasing the burst repetition rate.

2.7.2 Operating Characteristics

Maximum burst yield is 5.0×10^{18} fissions. Maximum burst yields 2.0×10^{15} n/cm^2 (E > 10 keV) fluence isotropically (radial uniformity ±5%) within the exposure cavity, with $\sim 5 \times 10^{18}$ n/cm^2/s peak neutron flux (E > 10 keV). Maximum burst yields 2.7×10^5 rad γ dose in the sample cavity with $\sim 7 \times 10^8$ rad/s peak γ flux.

The pulse width is burst-yield dependent, ranging from ~400 μs to several ms. The corresponding reactor periods may vary from ~100 μs to more than 100 ms. Figure 2-63 depicts typical pulse shapes as a function of burst yield.

Maximum measured core temperature rise is 285°C for a 5.0×10^{18} burst. The relationship between total fissions produced and measured core temperature rise is linear.

The reactor will accommodate test samples having a reactivity worth of up to ±$10.00. An assessment of sample reactivity worth will be made by the Lawrence Livermore Laboratory (LLL) for each experiment conducted. The maximum reactivity insertion rate is $70/s.

Burst repetition rate is determined by the core temperature rise. Maximum burst (285°C ΔT) repetition rate is 1 burst per day. Pulses of less than

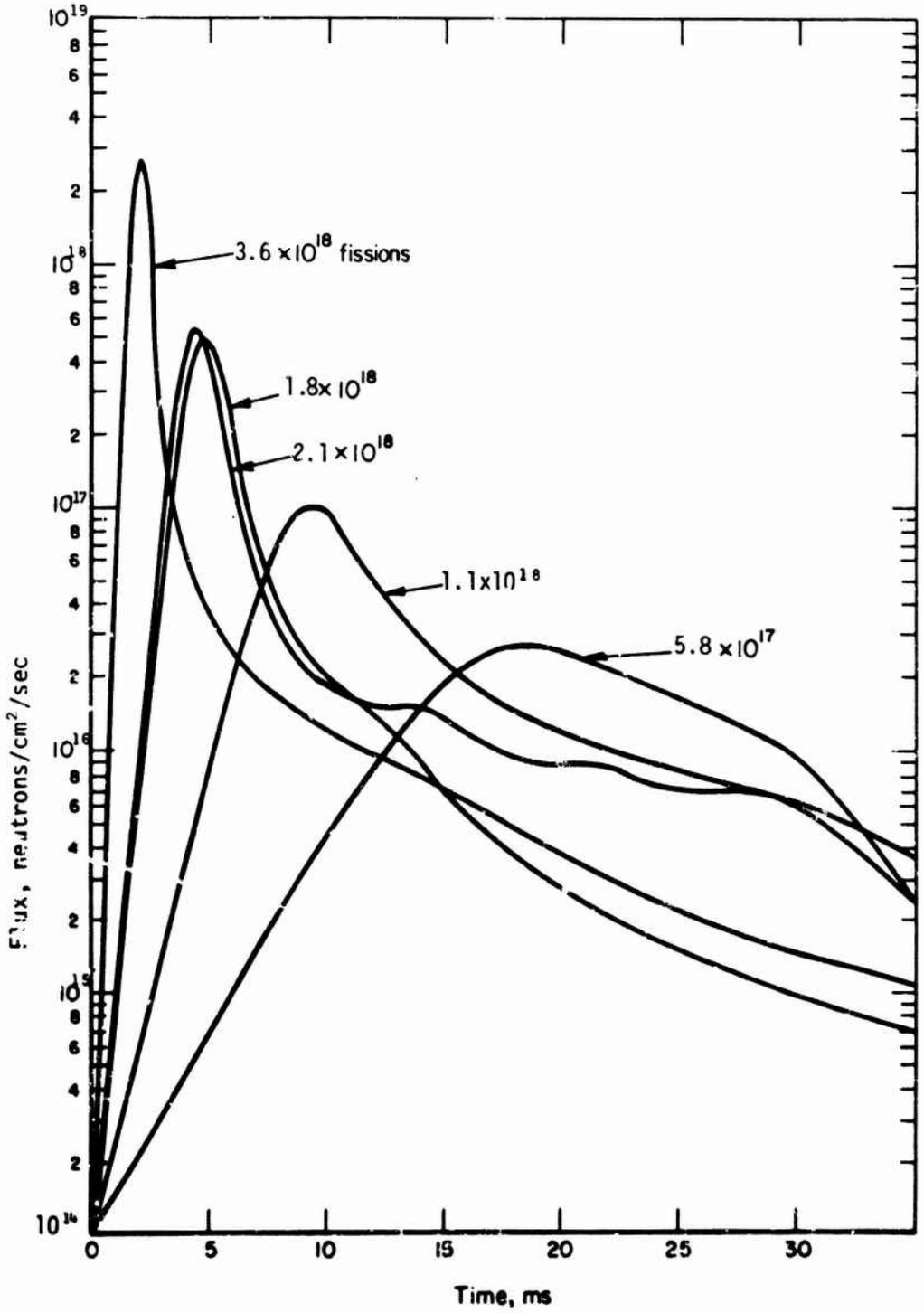

Figure 2-63. Super Kukla pulse shape as a function of burst fission yields.

20°C ΔT require 90 min between pulses. Predictability of the burst characteristics is influenced by the perturbation of the experimental sample. Accuracy of the prediction depends on how many pretest pulses can be made with the sample or a mockup of the sample in the reactor, to experimentally determine the reactor burst kinetics with that sample.

2.7.3 Environment

Because of the perturbing influence of experimental test samples, no quantitative flux or fluence maps have been generated with samples in the reactor. Limited measurements with an empty sample cavity utilizing a U-235 fission probe, Oy fission foils, and Oy wires have been made. Results of these measurements are shown in Figures 2-64 and 2-65.

First-order estimates of the flux at an experimental position are made by extrapolation of the data in Figure 2-64. It is recommended that when precise environmental data are required by an experimenter, such measurements be made concurrently with the experiment.

The bare reactor n/γ ratio is typically 7.4×10^9 n/cm^2/rad. The n/γ ratio delivered to the sample can be varied by using various neutron moderator and absorber materials in the sample assembly.

Neutron spectra and γ dose measurements are given in Tables 2-34, 2-35, and 2-36, and in Figures 2-66 and 2-67.

The average neutron energy is 0.77 MeV and the median neutron energy is 0.45 MeV. The Super Kukla 1-MeV equivalent neutron factor is 0.58. Pulse widths are dependent upon the neutron kinetic characteristics of each reactor sample combination and upon the burst yield. Figure 2-63 shows typical pulse shapes as a function of burst yield with the reactor in a fast kinetics configuration.

All cables are protected with suitable shielding. The experience of the facility operators indicates that RF background noise poses no serious problem when proper electrical isolation and shielding procedures are used.

2.7.4 Support Capabilities

The staff of the Super Kukla facility at Mercury, Nevada, will operate the reactor, associated diagnostics system, and DAS.

The available support staff includes LLL's Super Kukla facility group which is concerned primarily with experimental operations. The group consists of: 1 physicist/nuclear engineer, 1 mechanical technician, 2 electronics technicians, and 1 health physicist.

Immediately adjacent to the reactor bunker is an electronics relay station containing electronic equipment which must be close to the machine, yet out of the intense radiation field. This station contains the necessary electronic equipment to transmit low-level signals over the half mile of buried cables to the control building. The Super Kukla facility has adequate cabling and power.

1. 2"×18" dia 20 % enriched disk - Bottom
   Solid tungsten plug - Top
2. 3"×18" dia depleted disk - Bottom
   Hollow tungsten plug with 13" dia
   20 % enriched disk - Top
3. 3" depleted disk - Solid tungsten plug
4. 3" depleted disk - Open top

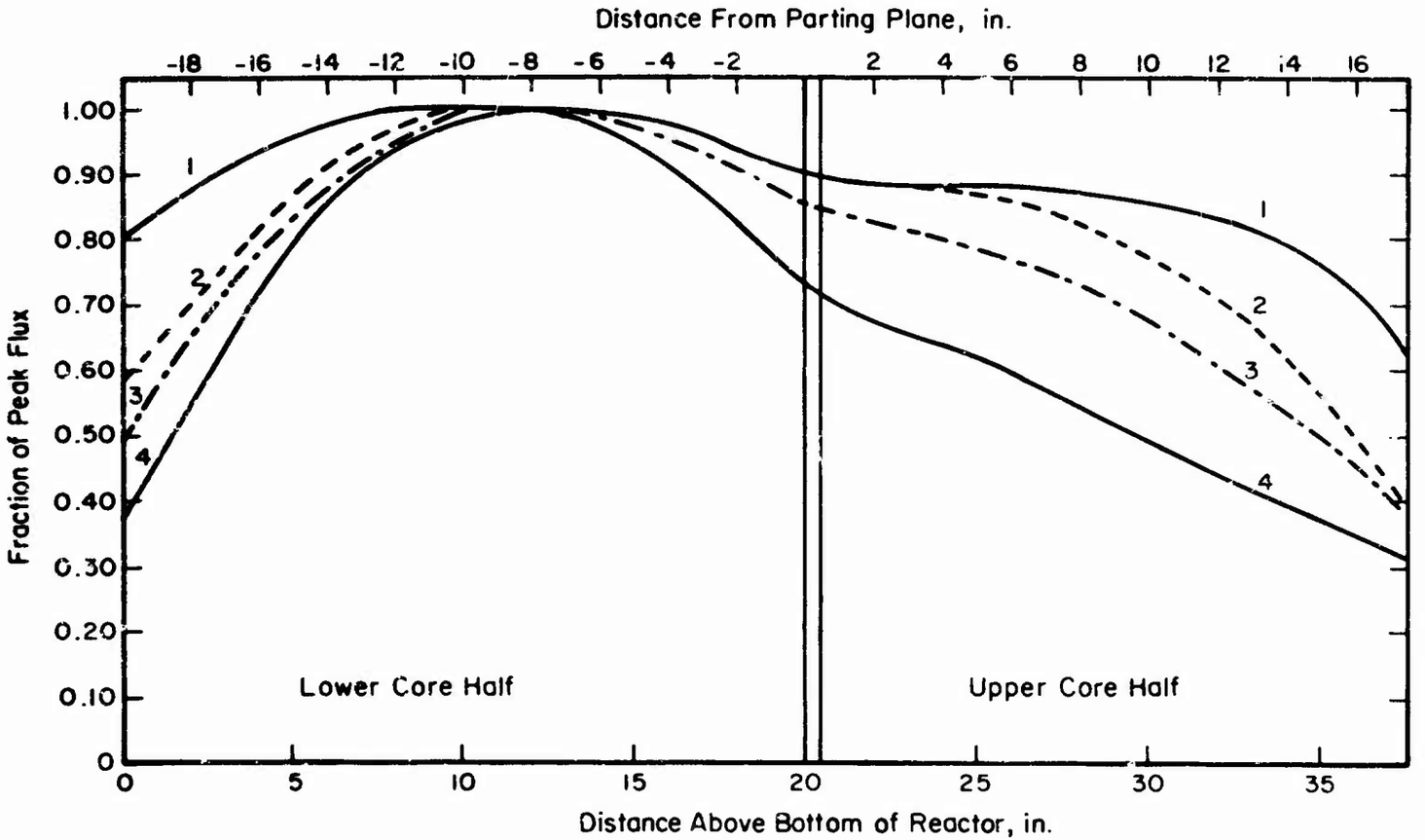

Figure 2-64. Vertical flux profile for Super Kukla.

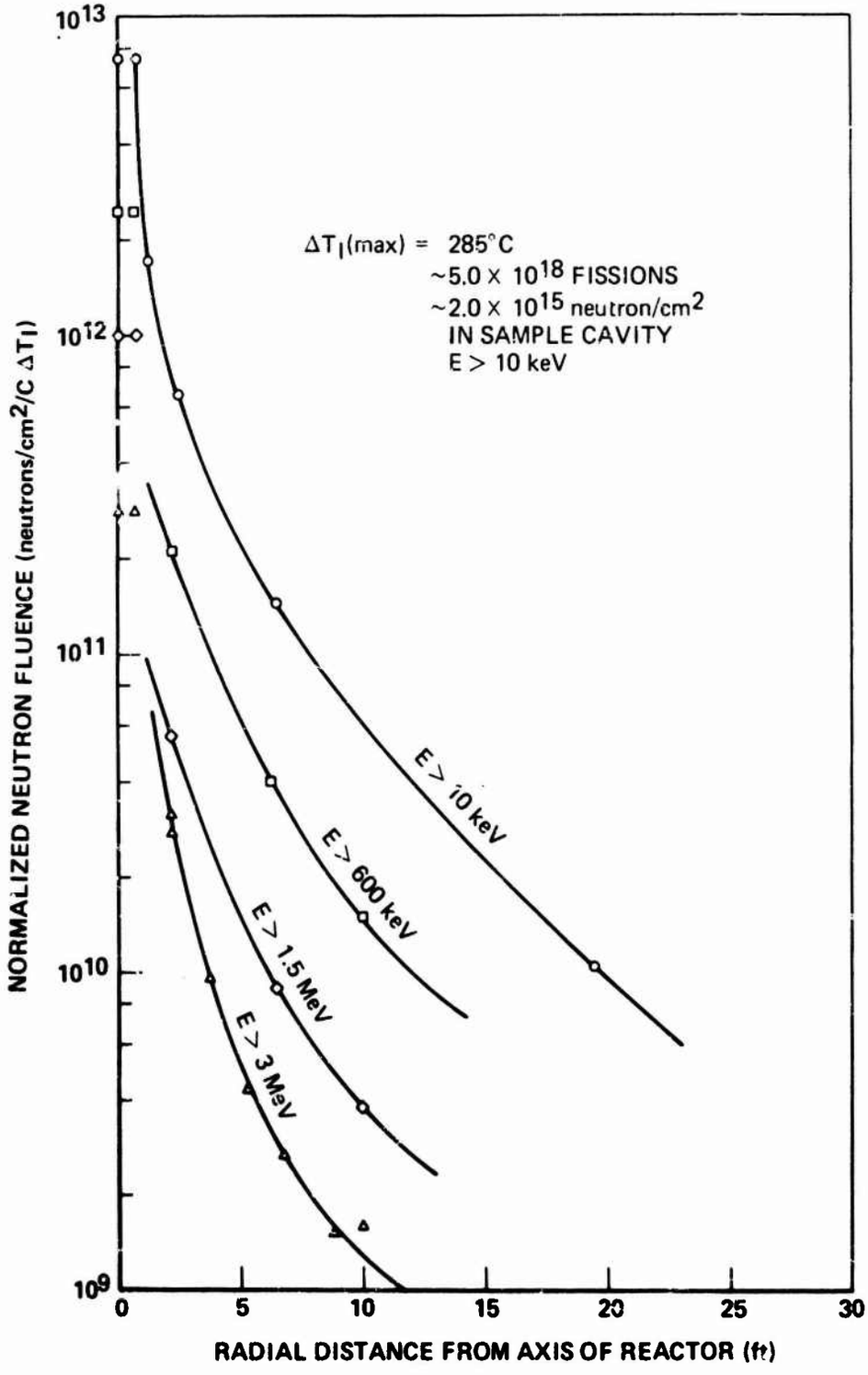

Figure 2-65. Normalized neutron flux versus location from axis of reactor.

Table 2-34. Preliminary Monte Carlo calculations of the Super Kukla neutron spectrum made by LLL utilizing the Sons-Alpha code (date: September 1967)

Group Number	Energy (MeV)	Percent in Group
1-8	0 - 0.0013	0.0
9	0.0013 - 0.0052	0.31
10	0.0052 - 0.0209	0.60
11	0.0209 - (etc.)	1.35
12	0.0471	3.43
13	0.0837	11.39
14	0.1884	21.05
15	0.3349	18.70
16	0.5234	15.71
17	0.7536	9.03
18	1.026	4.90
19	1.340	5.26
20	2.093	4.17
21	3.015	2.22
22	4.103	1.23
23	5.359	0.43
24	6.783	0.09
25	8.29	0.08
26	10.0	0.02

Note: These data are plotted in Figure 2-66. The median of this distribution falls in Group 15, with 11.87% above Group 14 and 6.83% below Group 16.

Table 2-35. Experimental neutron spectrum and γ dose measurements.

Detector Material	Threshold Neutron Energy (E_o)	Cavity Center		1 ft. Outside	
		23.1°C ΔT Burst #250	285°C ΔT Max. Burst	23.1°C ΔT Burst #250	285°C ΔT Max. Burst
Co ratio		1.02			
		n/cm^2 > Threshold			
Pu	10 keV	1.71×10^{14}	2.1×10^{15}	1.51×10^{13}	1.9×10^{14}
Np	0.6 MeV	5.66×10^{13}	7.0×10^{14}	6.35×10^{12}	7.8×10^{13}
U-238	1.5 MeV	2.30×10^{13}	2.8×10^{14}	2.45×10^{12}	3.1×10^{13}
In	1.5 MeV	2.24×10^{13}		2.52×10^{12}	
S	3.0 MeV	6.56×10^{12}	8.1×10^{13}	7.50×10^{11}	9.3×10^{12}
Au	Thermals only	1.9×10^{10}	2.3×10^{11}	1.15×10^{11}	1.4×10^{12}
Co glass	γ dose	2.17×10^{4} γ rad	2.7×10^{5} γ rad	2.02×10^{3} γ rad	2.5×10^{4} γ rad

Table 2-36. Threshold detector results.

Detector Material	Threshold Neutron Energy (E_o)	Percent $E_n > E_o$
22	10 keV	100.
Np	0.6 MeV	39.7
U	1.5 MeV	16.1
S	3.0 MeV	4.5
Au	Thermal neutrons	0.015

Notes: 1. Burst No. 395 on April 27, 1967.
2. W. Quam of Edgerton, Germerhauser, and Greer, letter of May 10, 1967.

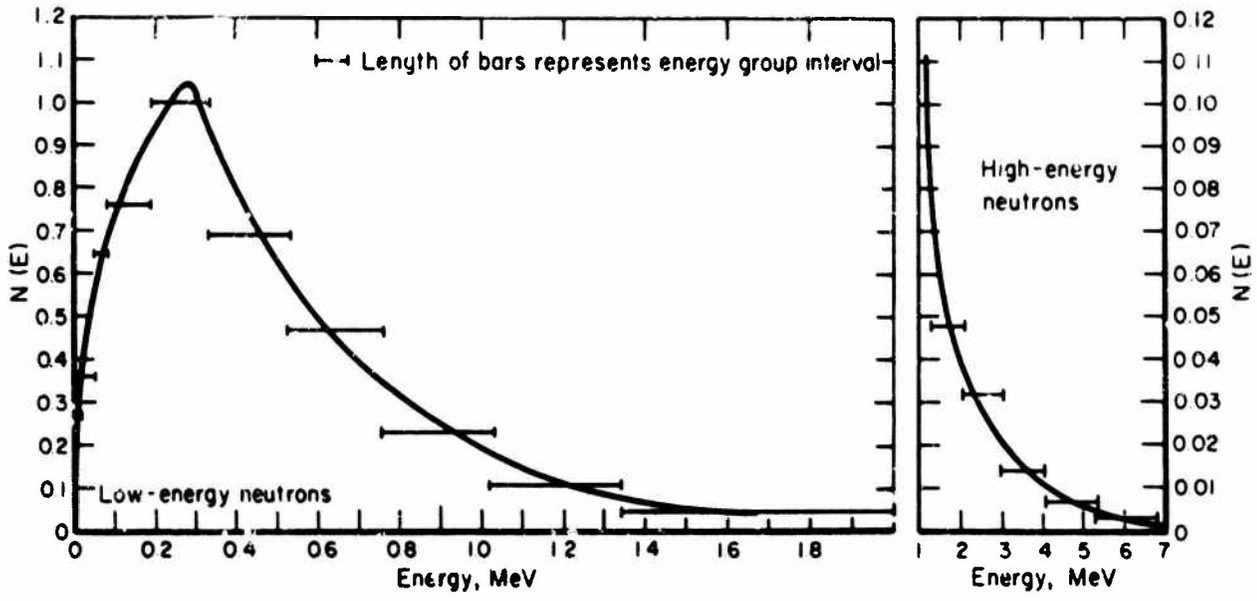

Figure 2-66. Neutron energy spectrum for the Super Kukla.

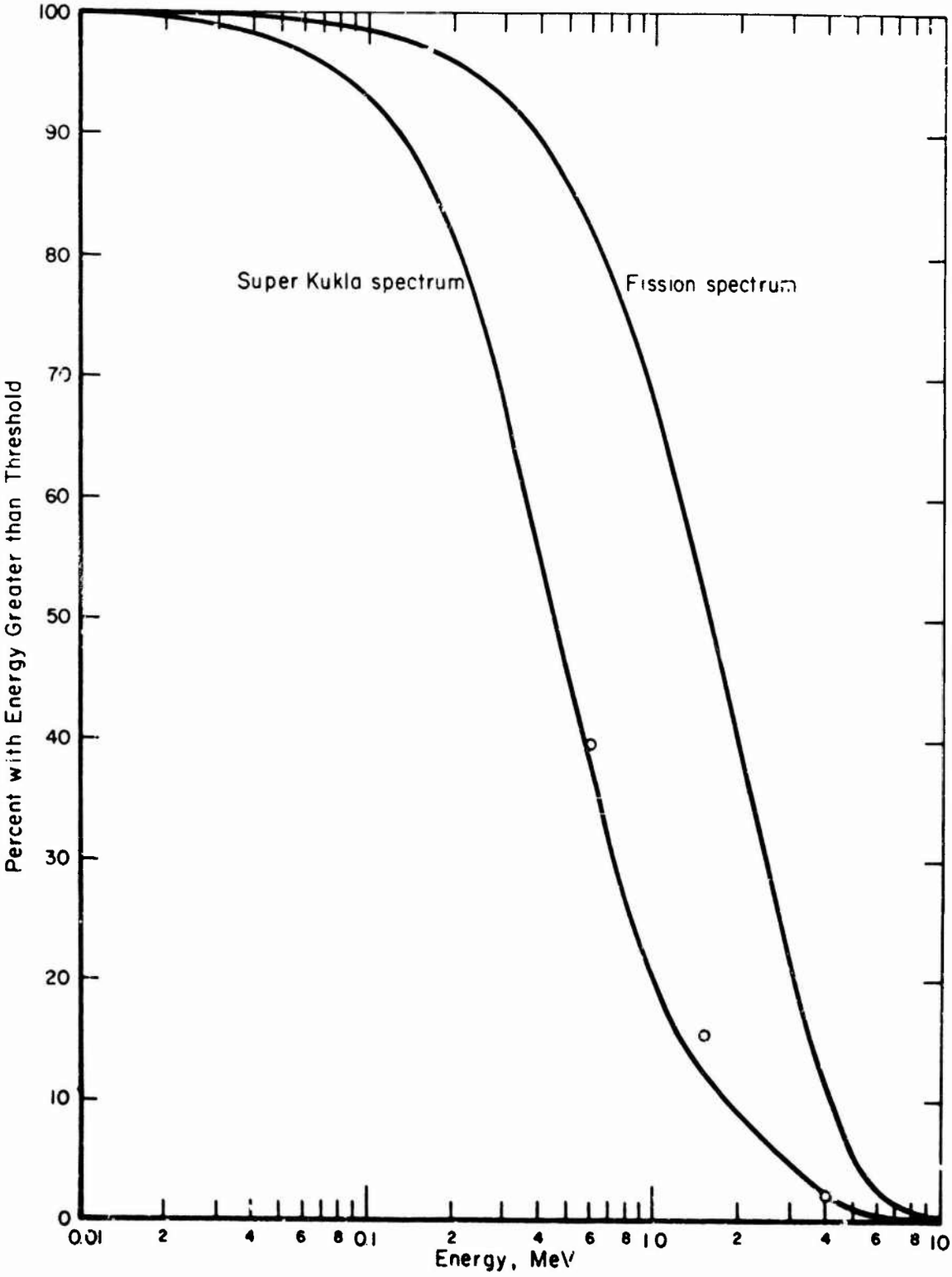

Figure 2-67. Neutron energy spectrum for the Super Kukla.

Adequate space and facilities are available for the use of on-site electronic trailers/vans. No screen room is available at the facility; however, provisions can be made for adequate electrical shielding.

Installed signal cables between the reactor bunker and the electronics relay station include:

200 Belden 8773 (shielded pair)

20 RG/8U (50Ω coax)

10 RG/7U (100Ω coax)

8 RG/22U (125Ω twin coax)

60 RG/108U (125Ω shielded pair)

In addition, 75 pairs of #18 Cu multiconductor control and power cables are installed. Conduits are available for installation of special cables supplied by the experimenter.

IRIG-A time code and pulse generator time markers, in the range of 100 μs to 1 s, as well as operational markers, are available.

Only limited dosimetry is available at the Super Kukla site. The usual practice is for experimenters to provide or contract for dosimetry as needed. A 32-channel FM tape system is the primary data acquisition unit at the facility. Normally, 25 channels with 20-kHz signal frequency response are available for experiment data. The remaining channels are reserved for reactor diagnostic and time-marker data. Cables for additional data channels are available for experimenter-supplied recorders or oscilloscopes. Computational facilities are not available at the Super Kukla facility.

Light machine shop facilities are available on a limited basis by special arrangement with LLL. An above-ground "cold" bay, immediately over the reactor vault, is used for experiment preparation and setup. Additional preparation laboratories are available on a limited basis. Services of the LLL photographic laboratory at Mercury, Nevada, can be used by special arrangement. Polaroid equipment adaptable to standard oscilloscopes is readily available at the Super Kukla site.

2.7.5 Procedural Information

The reactor is operated on an intermittent operating schedule by LLL, University of California, Livermore, California. Technical and administrative inquiries should be addressed to:

Mr. L.R. Peterson
Reactor Facilities
Lawrence Livermore Laboratory
P.O. Box 45
Mercury, NV 89023
Telephone: (702) 647-5201

The reactor can be used by both government and industry by contractual agreement with LLL. To facilitate experimental analysis, as well as the setup and finalization of procedures, a lead time of approximately 3 months is recommended. Costs and charges associated with use of the reactor and facility will be determined by the Business Services Department, LLL.

Unclassified mail to the facility should be directed to:

Mr. L.R. Peterson, Reactor Facilities
Lawrence Livermore Laboratory
P.O. Box 45
Mercury, NV 89023

The unclassified shipping address is:

Lawrence Livermore Laboratory
Warehouse No. 7
Mercury, NV 89023
Attention: Mr. L.R. Peterson

Classified mailing and shipping addresses should be arranged through proper channels at the time needed.

2.7.6 Applicability and Availability

The Super Kukla facility is not primarily TREE oriented. However, it is available for use by special arrangement or in conjunction with the LLL intermittent operating schedule.

The user should be aware that the facility is primarily a DoE installation and is located at the Nevada Test Site (NTS). Operations there involve considerable commuting distances between available overnight accommodations in Mercury, Nevada, or Las Vegas, Nevada, and the Super Kukla site. Arrangements for daily transportation must be made by the experimenter.

A limited operational and technical professional staff is available at the Super Kukla site. Technical and administrative control of the facility is located at Livermore.

2.7.7 References

1. Kloverstrom, F., et al., *Revised Safety Analysis Report for the Super Kukla Prompt Burst Reactor,* UCRL-7695, Rev. 1, February 4, 1954.

2. Kloverstrom, F., *Operating Characteristics of the Super Kukla Prompt Burst Reactor,* UCRL-70138 (Preprint), 1969.

3. Peterson, L.R., and R.E. Kelley, *Super Kukla Operating Experience 1964-1973,* UCRL-74443 (Preprint), 1973.

2.8 NORTHROP REACTOR FACILITY

2.8.1 General Characteristics

The Northrop reactor is a TRIGA MARK F. It uses stainless-steel-clad U-ZrH_2 fuel elements. The reactor pool is 18 ft long and 10 ft wide, with the core located approximately 17 ft below the surface of the water. Irradiations may be carried out in the pool or in the exposure room located at one end of the pool. The exposure room is 8 ft wide, 10 ft long, and 8 ft high, with an access plug door approximately 6 ft^2 opening into the room. A portion of the reactor tank, called the window, projects into one wall of the exposure room. When the reactor is positioned in the window, a minimum thickness of approximately 2 in. of water is between the outer ring of fuel and the exposure-room window. The exposure room enables irradiations to be made without using a watertight container.

An Al access tube of 1.25 in. I.D. can be inserted into the E-ring of the core for in-core irradiations. Experimental devices irradiated around the reactor core may be encapsulated in watertight containers. For in-pool irradiations, the reactor may be operated in any position within the pool. At the opposite end of the pool from the exposure room are 3 horizontal beam ports and 4 pneumatic transfer tubes. The transfer tubes accommodate polyethylene rabbits in which samples are encapsulated for fast transfer in and out of the reactor core. The rabbits have an I.D. of 0.5 in. and are 3.75 in. long. Total transport time through the pneumatic tube is less than 1 s.

The reactor may be operated in the pulse mode or at steady-state powers up to 1 MW. Data presented are primarily associated with the pulse mode. Figure 2-68 illustrates, schematically, the reactor facility.

2.8.2 Operating Characteristics

Characteristics of pulse peak power depend primarily on the reactivity insertion and the fuel loading of the reactor core. Maximum pulse peak power is 1800 MW. Data available here are for a pulse with a reactivity insertion of 024 units, giving a peak power of 1600 MW. Characteristics are:

1.	Prompt energy release	16 MW-s (5×10^{17} fission)
2.	Pulse width (FWHM)	10 ms
3.	Fluence (D-ring position)	
	a. Fast (>10 keV)	6.5×10^{14} n/cm^2
	b. Thermal (<0.4 eV)	4.7×10^{14} n/cm^2

Characteristics of the pulse, including prompt energy release, pulse width (FWHM), and the initial reactor period (as well as peak power) depend primarily on the reactivity insertion and the fuel loading of the reactor core. As a result, pulse characteristics can be varied over a wide range within the licensed operating limits of the facility. Qualitative operating characteristics are shown in Table 2-37 and Figures 2-69 through 2-71.

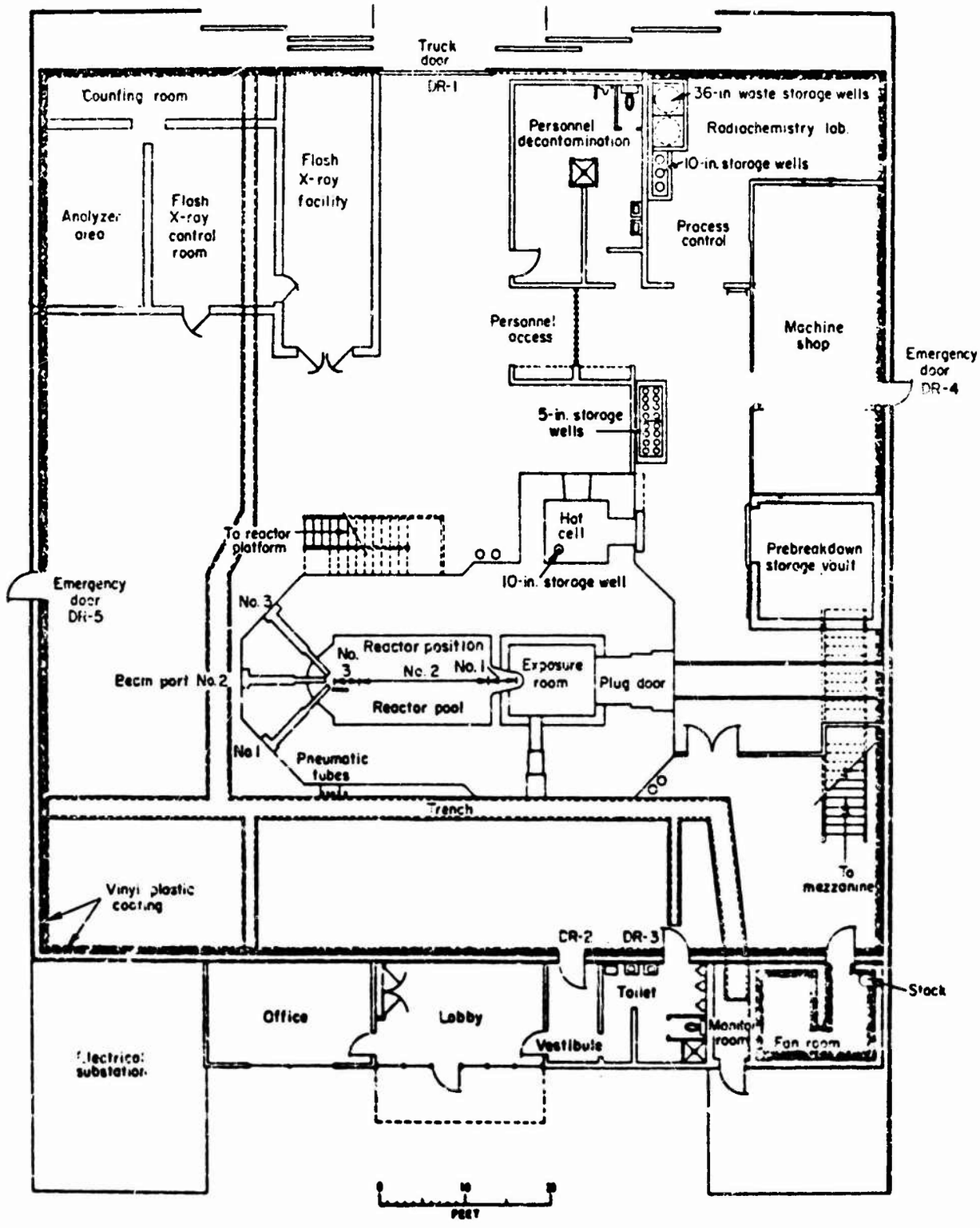

Figure 2-68. Plan view of Northrop reactor facility.

Table 2-37. Northrop reactor performance data.

Location	1 MW Steady-State				16 MW-s Pulse (10 ms Width at Half-Height)			
	Neutron Flux ($n/cm^2 \cdot s$)			Gamma Dose Rate, rad/s (tissue)	Neutron Fluence (n/cm^2)			Gamma Dose, rad (tissue)
	Thermal	E > 10 keV	E > 3 MeV		Thermal	E > 10 keV	E > 3 MeV	
D-ring	2.0×10^{13}	1.9×10^{13}	2.4×10^{12}		4.7×10^{14}	6.5×10^{14}	8.5×10^{13}	
E-ring	1.4×10^{13}	1.4×10^{13}	1.8×10^{12}	1.61×10^{4}	3.5×10^{14}	5.0×10^{14}	6.4×10^{13}	4.3×10^{5}
F-ring	1.2×10^{13}	5.6×10^{12}	7.2×10^{11}		2.7×10^{14}	2.0×10^{14}	2.6×10^{14}	
Dry exposure room (1/4 in. boral)	1.2×10^{12}	1.5×10^{12}	1.8×10^{11}	3.61×10^{3}	1.6×10^{13}	3.3×10^{13}	4.2×10^{12}	9.4×10^{4}
Dry exposure room with 2-in. lead shield and 1/4 in boral shield	6.0×10^{9}	5.5×10^{11}	5.5×10^{10}	5.56	1.3×10^{11}	1.4×10^{13}	1.4×10^{12}	3.5×10^{3}
Pneumatic tubes	7.4×10^{12}	8.0×10^{12}	1.6×10^{12}	1.39×10^{4}	9.0×10^{13}	1.0×10^{14}	2.0×10^{13}	3.5×10^{5}

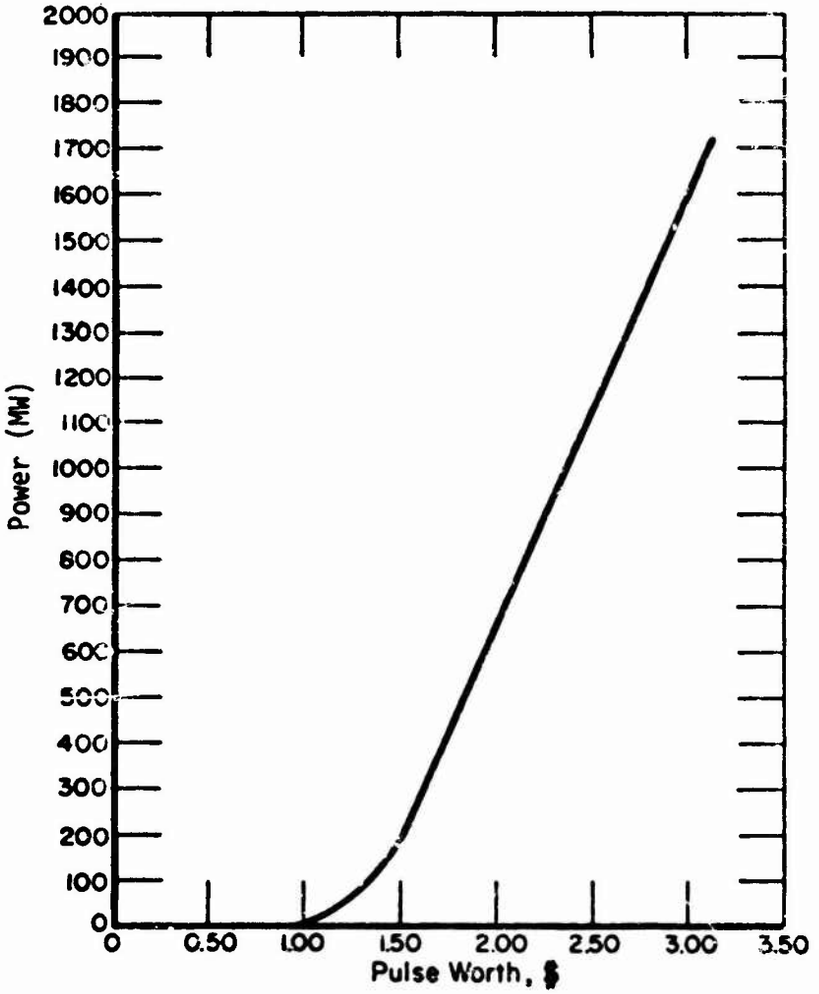

Figure 2-69. Peak power versus pulse worth.

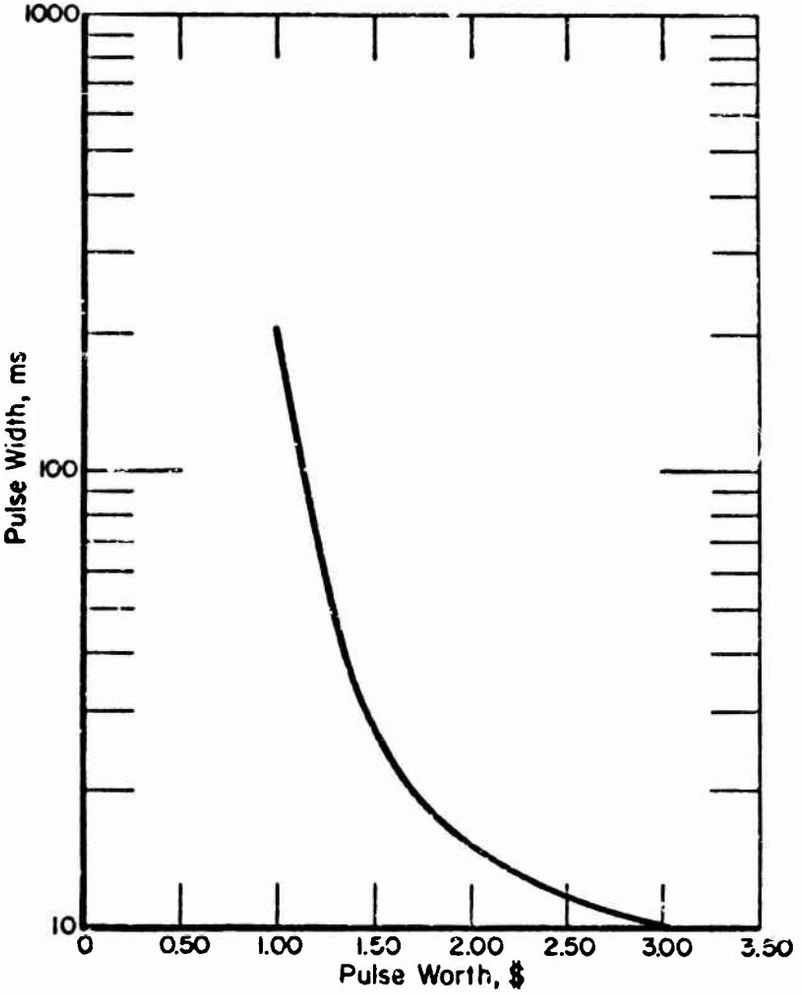

Figure 2-70. Pulse width versus pulse worth.

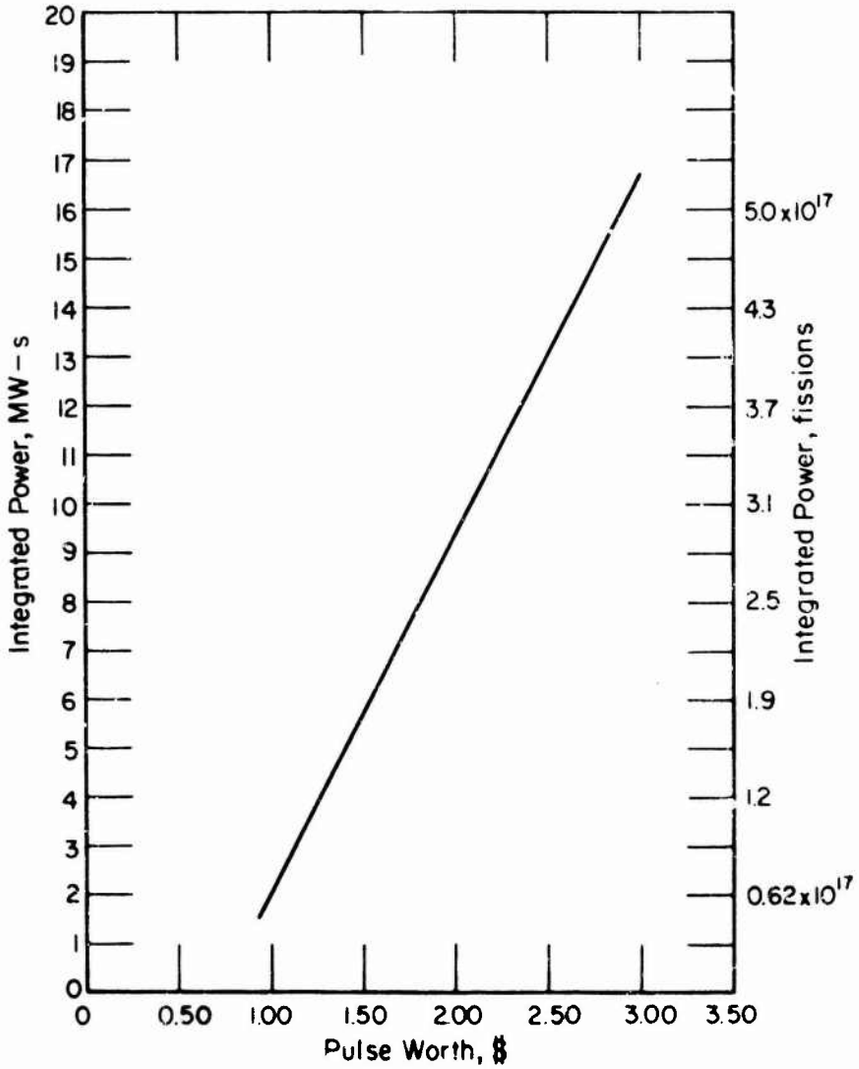

Figure 2-71. Integrated power versus pulse worth.

Except for extreme samples (consisting of fuel material), no limits are expected on the reactivity worth of test samples placed in the exposure room.

Burst repetition rate is several pulses/hr.

2.8.3 Environment

Neutron and γ flux/fluence/dose data are shown in Figures 2-72 through 2-79. Values are given for various locations in the exposure room and in the core. The curves have been normalized to a pulse of $2.97 reactivity insertion.

Data regarding time-dependent spectra are not available. Some insight as to the spectrum as a function of position can be gained from Figures 2-72 through 2-79. The neutron spectrum as measured in the exposure room is shown in Figure 2-80.

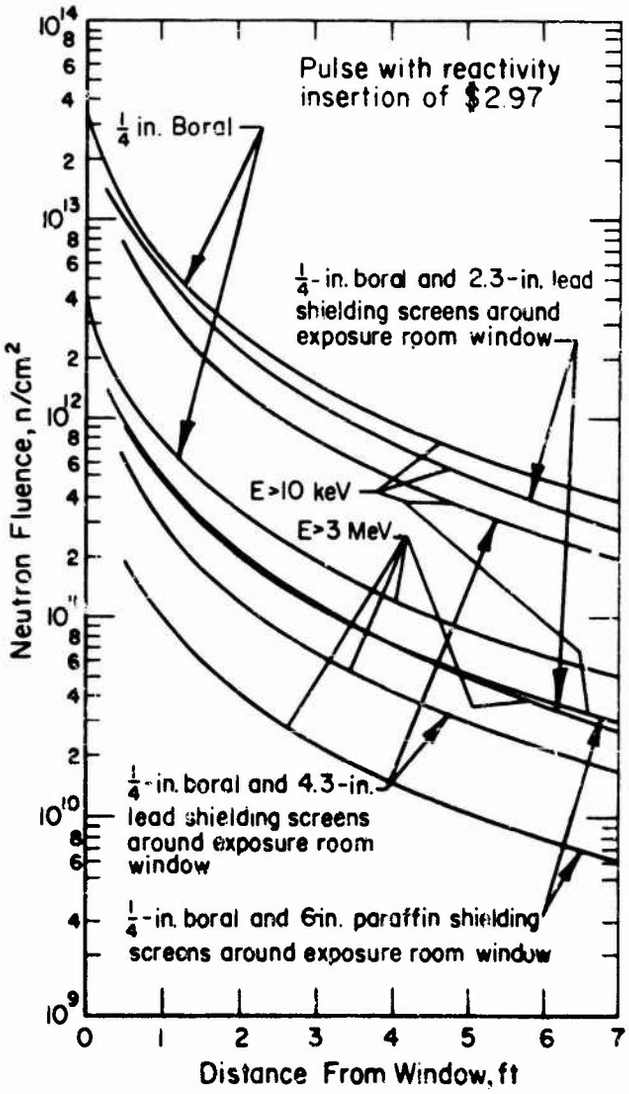

Figure 2-72. Neutron flux versus distance from exposure room window.

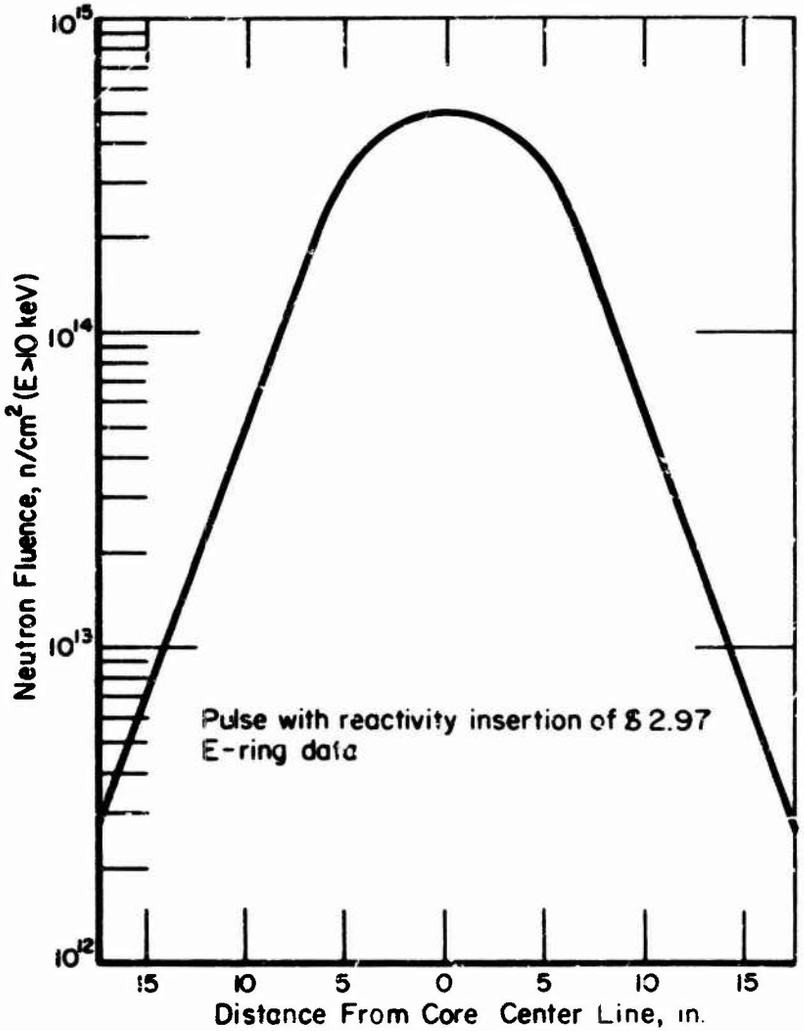

Figure 2-73. Neutron fluence for in-core vertical traverse.

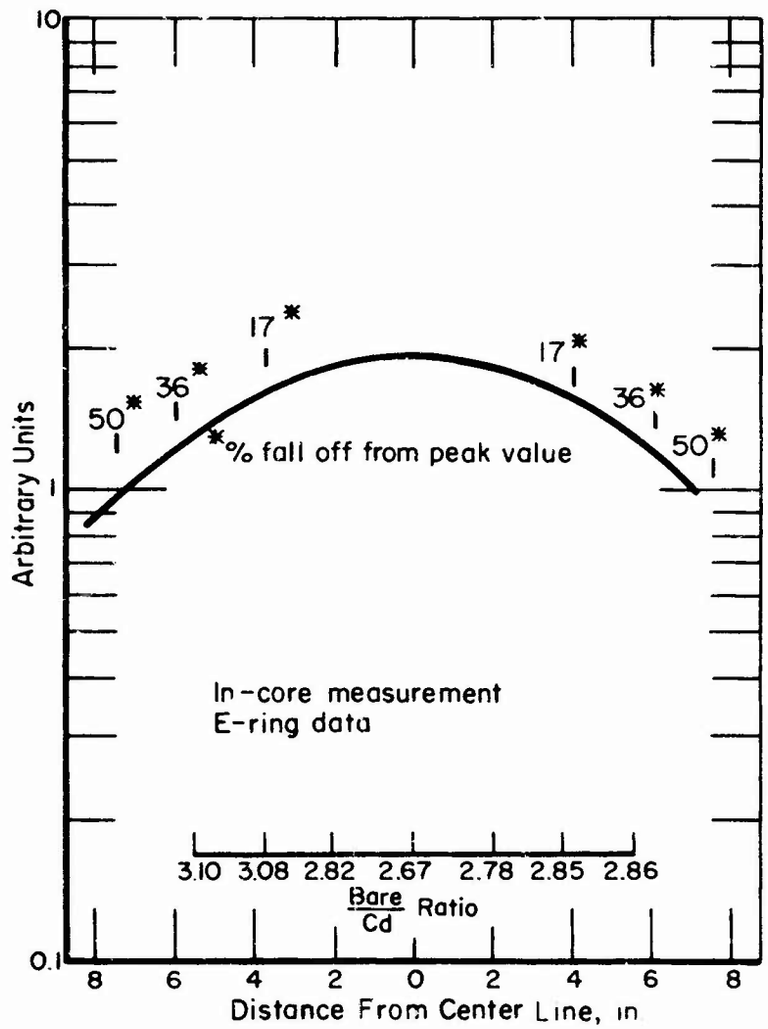

Figure 2-74. Thermal neutrons for in-core vertical traverse.

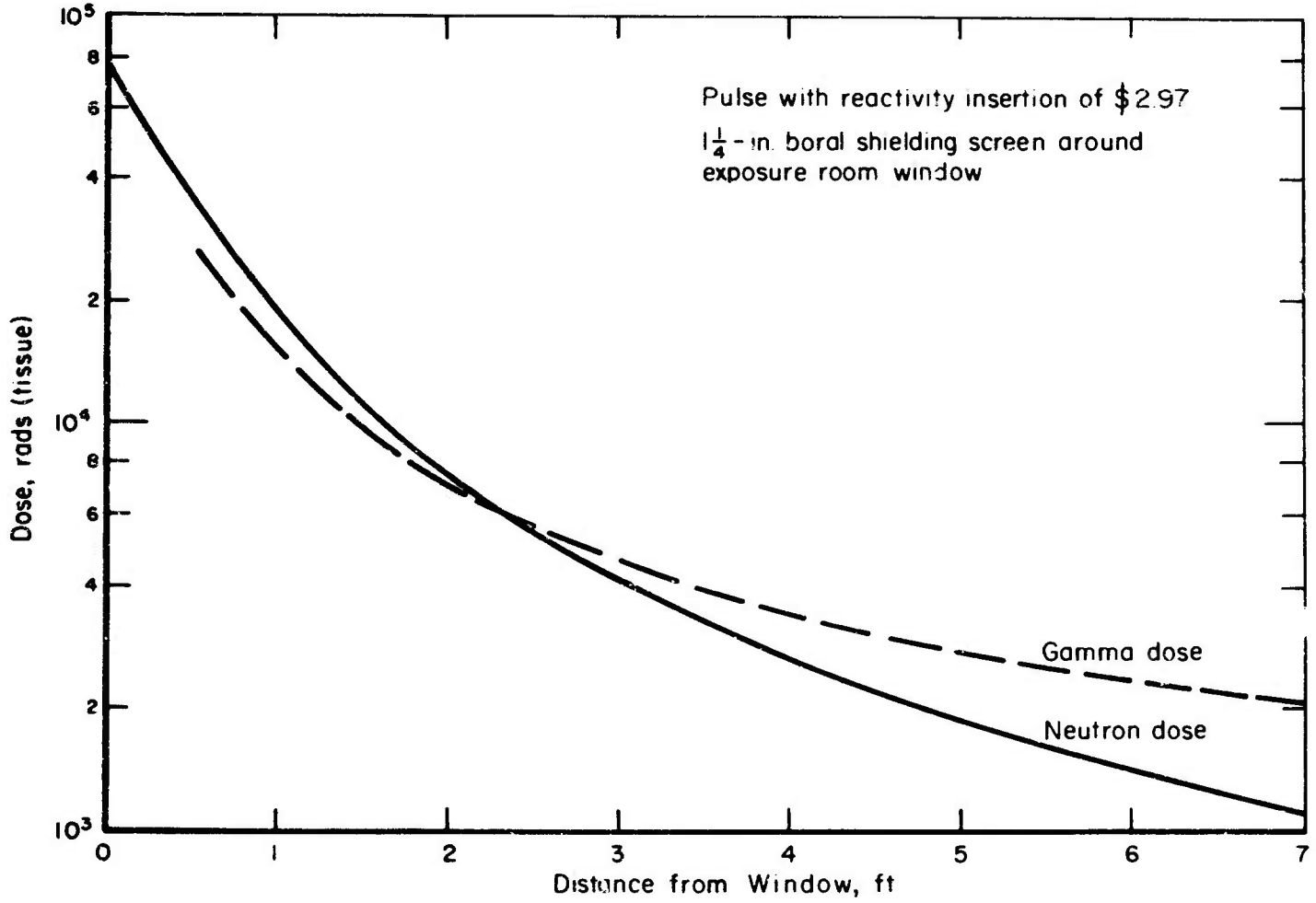

Figure 2-75. Neutron and γ dose versus distance from exposure room window.

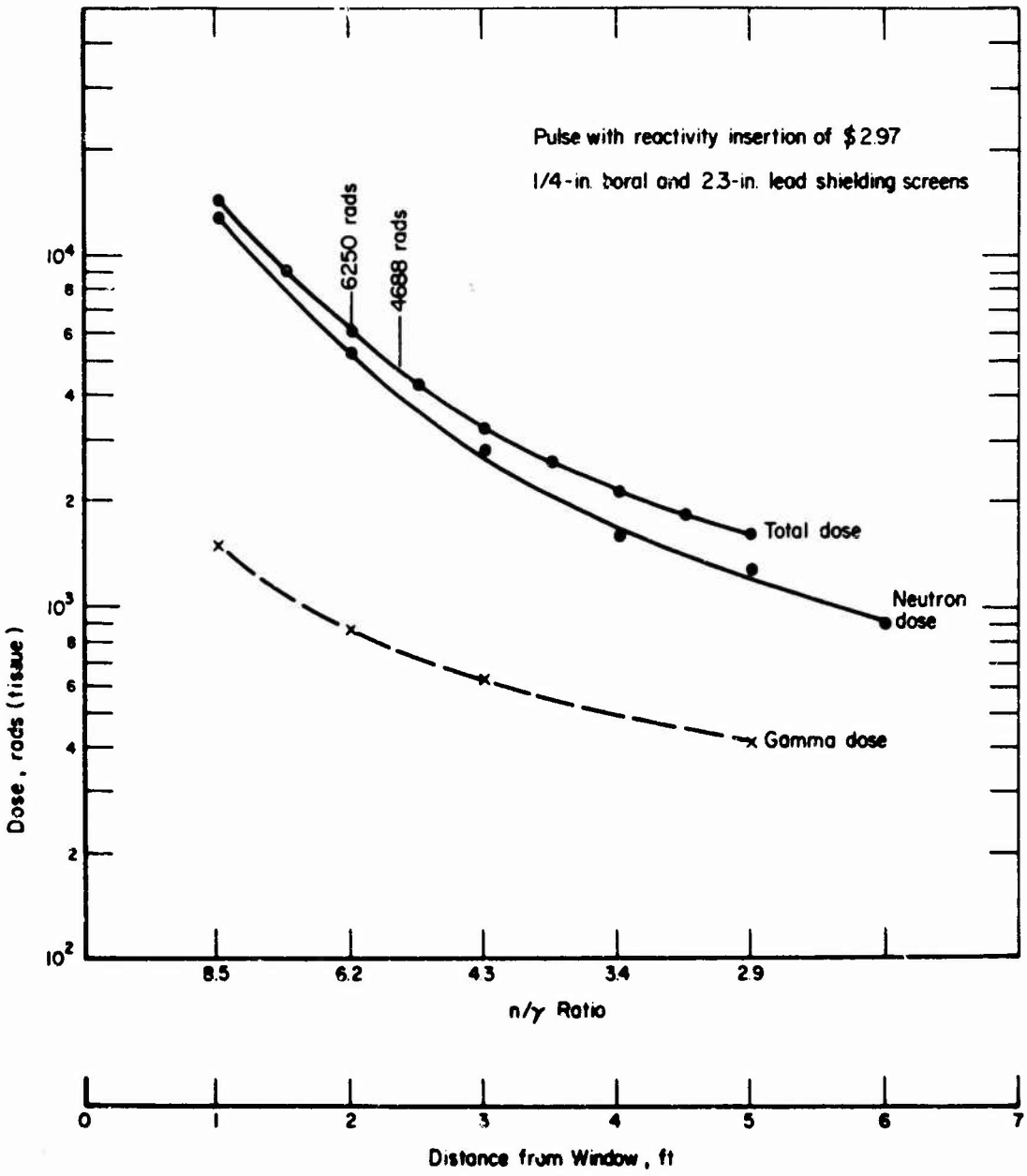

Figure 2-76. Neutron and γ dose versus distance from exposure room window.

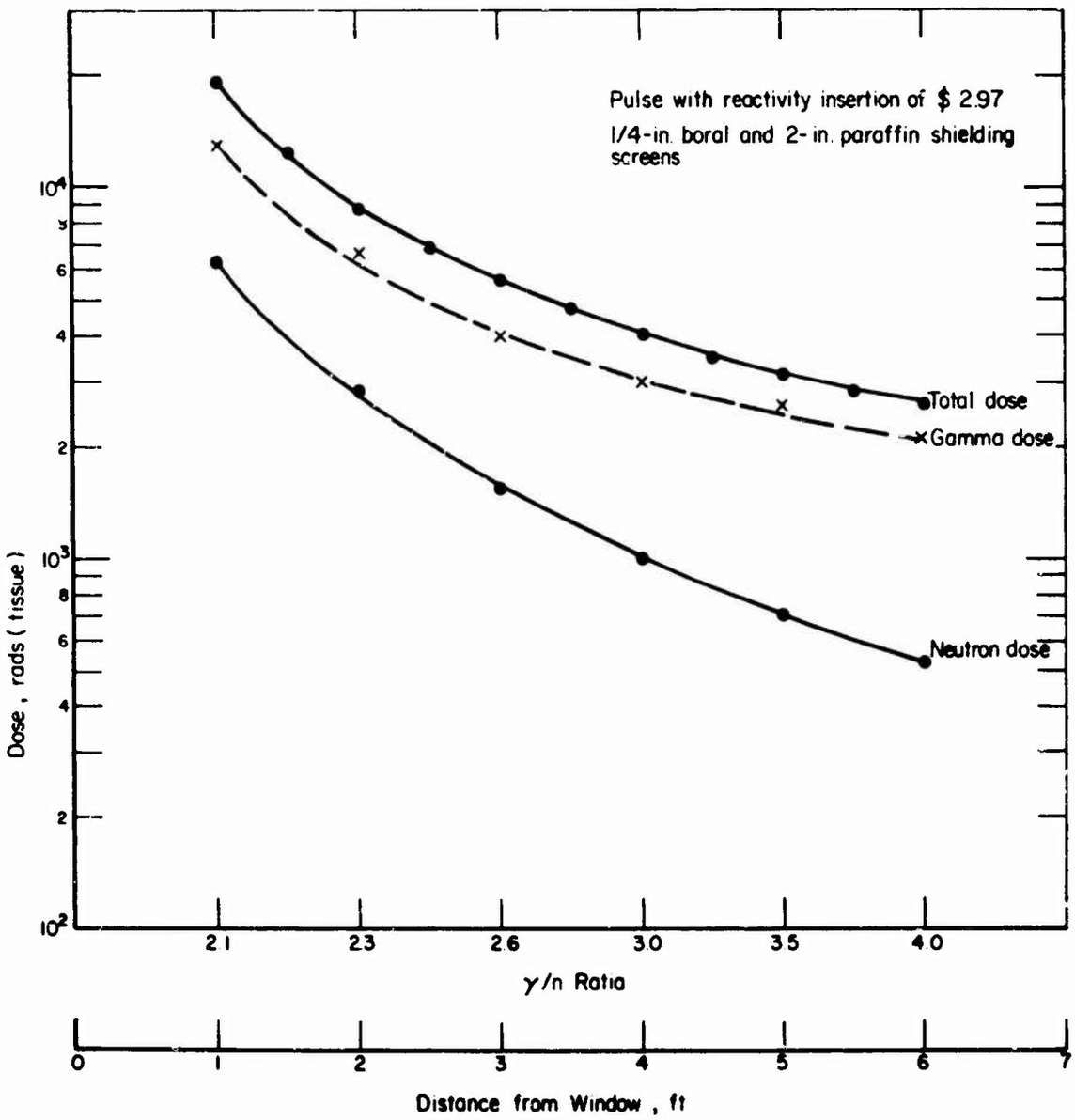

Figure 2-77. Neutron and γ dose versus distance from exposure room window.

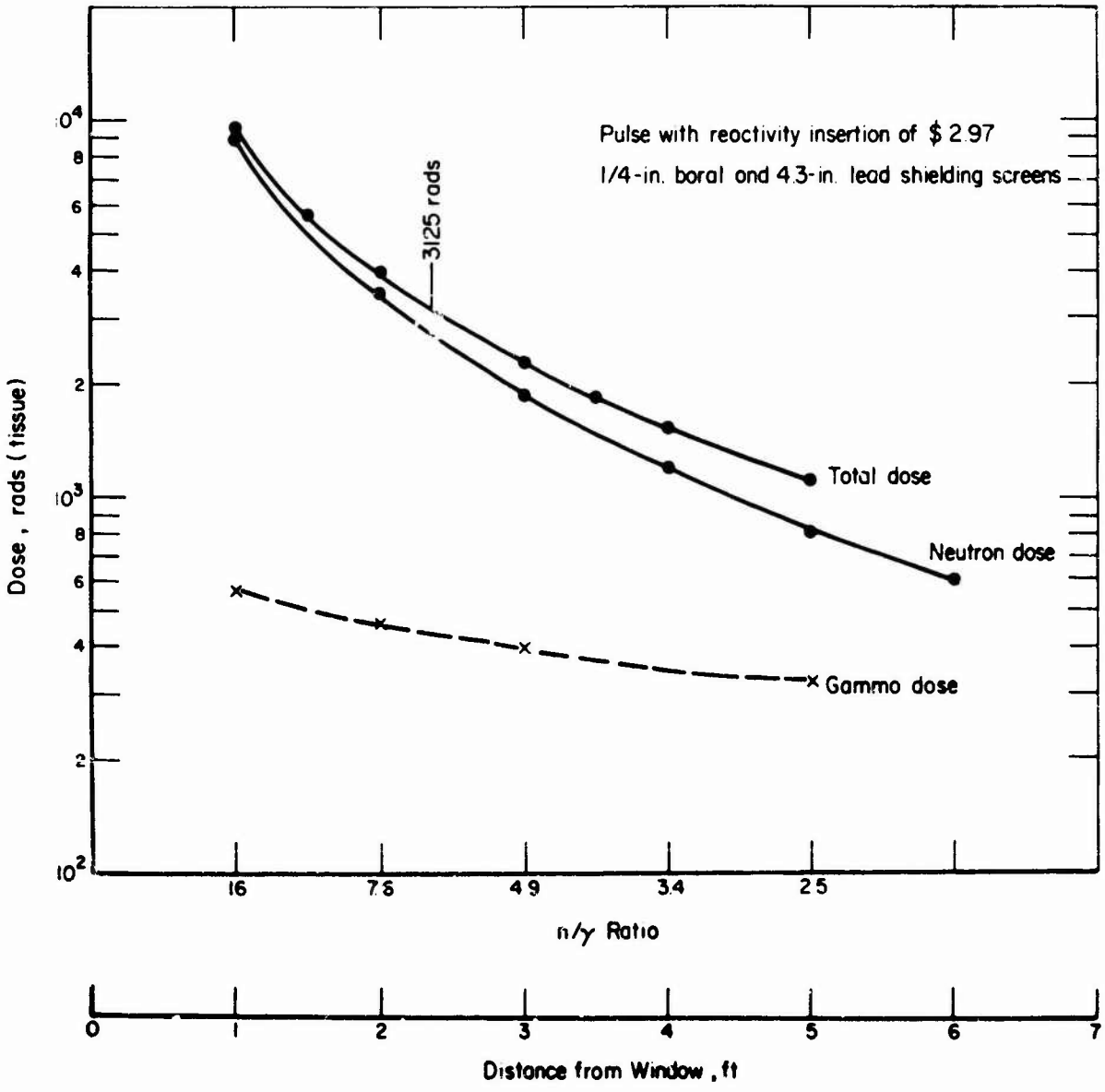

Figure 2-78. Neutron and γ dose versus distance from exposure room window.

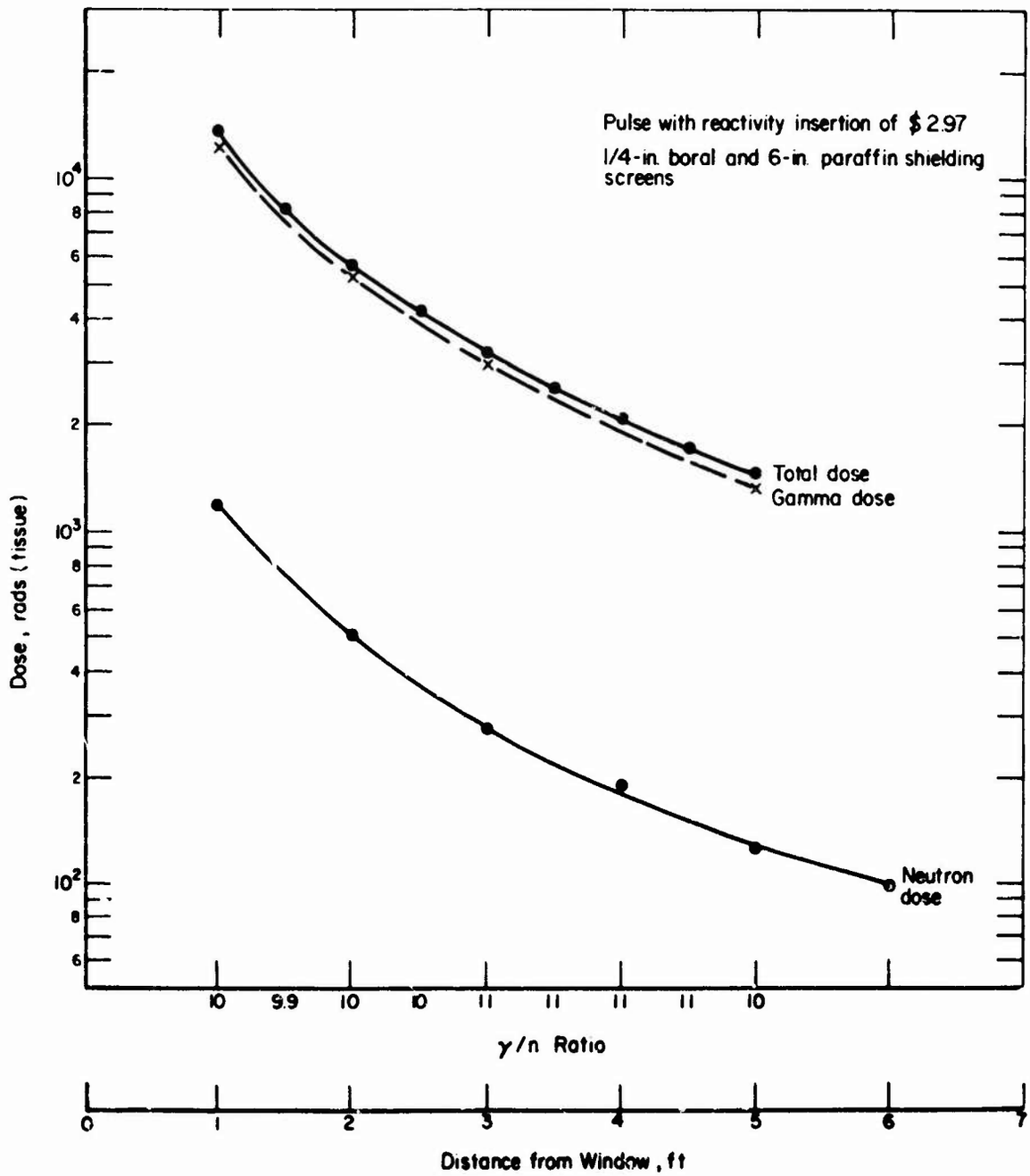

Figure 2-79. Neutron and γ dose versus distance from exposure room window.

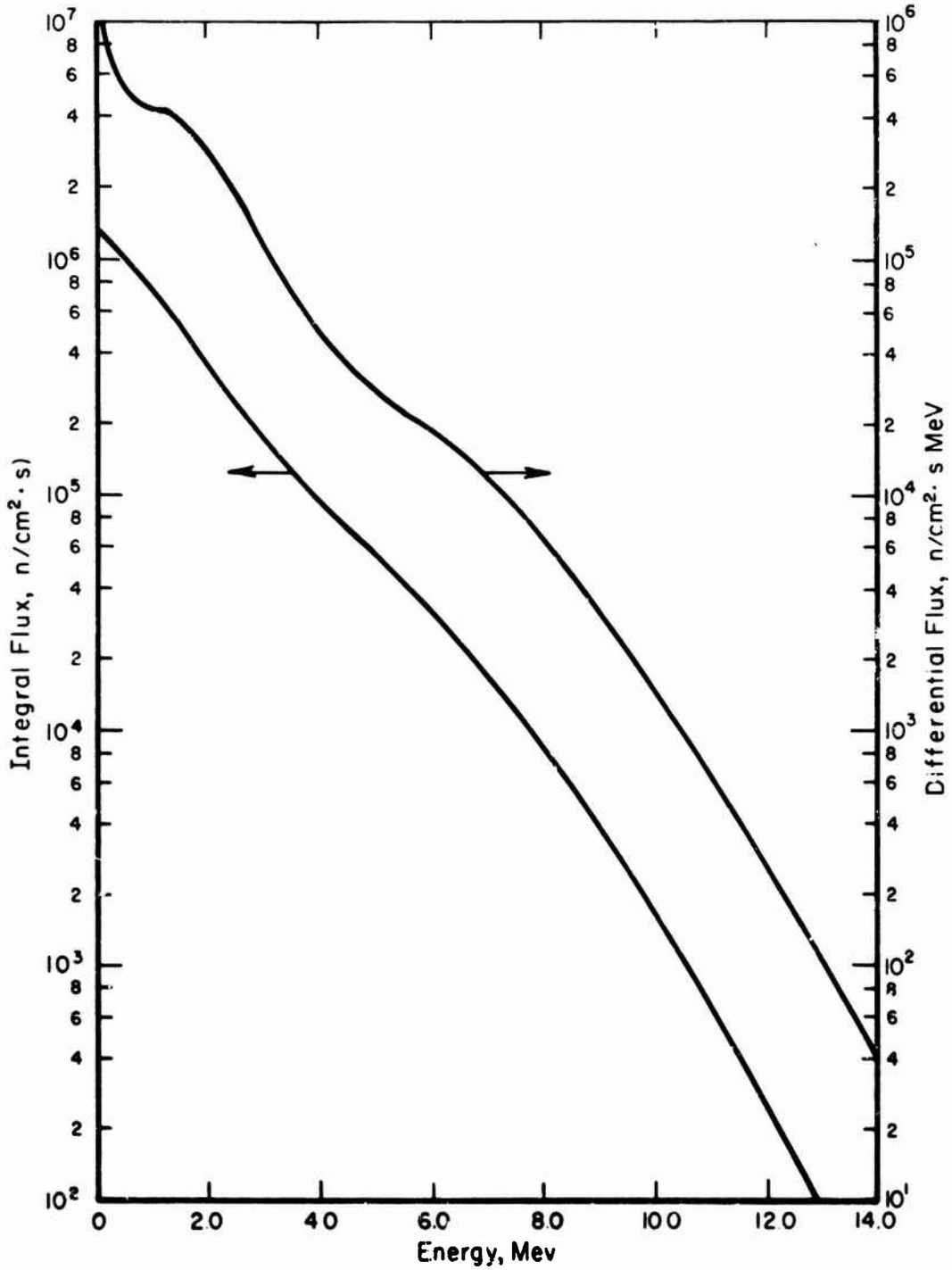

Figure 2-80. Neutron spectrum in exposure room at center of window normalized to reactor power of 1 W.

Typical values of the n/γ ratio for various irradiation positions are presented in Table 2-38. The n/γ ratio in the exposure room can be varied by use of shielding screens available at the facility. The use of screens to vary the n/γ ratio also affects the value of the available fluence/dose.

It is the experience of the facility operators that RF background noise poses no serious problem. A significant post-pulse fission product γ background exists in the exposure room. This can be reduced drastically by moving the core away from the exposure room wall. The Al wall itself becomes activated (half life 2.6 min) and contributes approximately 10 rad/hr into the exposure room.

2.8.4 Support Capabilities

A permanent staff is assigned to the facility to operate the reactor, assist in setting up experiments, perform dosimetry, and lend general support, as required. The professional size of the staff is limited, but they are available for technical consultation.

Limited electronic equipment can be obtained on a noninterference basis. Power outlets are conveniently located and include:

1. 480-V, 3-ϕ, 60 cycle
2. 120-V, 1-ϕ, 60 cycle
3. 120/208-V 3-ϕ (2-ϕ available), 60 cycle
4. 120/208-V, 3-ϕ, 400 cycle
5. 28-Vdc (unfiltered).

Cables or hoses to experimental devices should be a minimum of 40 ft for experiments to be performed in the exposure room or in the pool. A screen room is available at the facility, and the reactor staff has extensive experience in handling RF noise and electrical shielding problems.

Reliable trigger and delayed trigger pulses, initiated by an ionization chamber located in the reactor core, are available. Although the chamber primarily detects the γ radiation, experiments have shown that its signal is also a reasonably accurate representation of the neutron pulse. The trigger and delayed trigger pulses are fast-rise, positive, binary-step pulses. The trigger pulse is initiated by the leading edge of the reactor pulse at a predetermined threshold above the noise level. The delayed trigger output can be externally adjusted to rise anywhere from less than 1 ms to more than 40 ms after the rise of the trigger output.

2.8.5 Dosimetry

Neutron and γ dosimetry equipment and services, including special foil materials, multichannel analyzers, automatic counting systems, and gas flow and scintillation detector systems, are available. Standard foil materials and techniques are used for neutron dosimetry. Thermoluminescent dosimeters (TLDs) are

Table 2-38. n/γ ratio for various irradiation positions.

Position	Neutron		γ	n/γ	
	n/cm^2 (>10 keV)	Rads (tissue)	Rads (tissue)	n/cm^2 (>10 keV) Rads (tissue)	Rad (tissue) Rad (tissue)
Core - Ring E	5.0×10^{14}		4.3×10^{5}	1.2×10^{9}	
Pneumatic Tube	1.0×10^{14}		3.5×10^{5}	2.9×10^{8}	
Exposure Room	3.3×10^{13}		9.4×10^{4}	3.5×10^{8}	
½-in. boral		7.7×10^{4}	5.8×10^{4}		1.3
½-in. boral, 2-in. lead	1.4×10^{13}		3.5×10^{3}	4.0×10^{9}	
½-in. boral, 2.3-in. lead		1.3×10^{4}	1.5×10^{3}		8.5
½-in. boral, 2.6-in. lead		1.22×10^{4}	1.28×10^{3}		9.4
½-in. boral, 4.4-in. lead	1.7×10^{12}	9.0×10^{3}	5.7×10^{2}	1.4×10^{10}	1.6
½-in. boral, 2-in. paraffin		6.3×10^{3}	1.3×10^{4}		4.8
½-in. boral, 6-in. paraffin	9.1×10^{11}	1.2×10^{3}	1.2×10^{4}	7.6×10^{7}	0.1

used for γ dosimetry. Reactor operating personnel can perform or lend assistance in dosimetry measurements.

The Northrop IBM 360-65 computer can be used by special arrangement. In addition, the reactor facility is located near the Control Data Corporation offices, where a CDC 6600 is available on a contract basis. Also available is a RACS tie-in to an IBM 260-40.

Within the reactor building is a radiochemical laboratory, a hot cell, and a complete machine shop capable of constructing special shielding screens and experimental irradiation jigs. The heavy machine shop of the Northrop Corporate Laboratories can be used on a contract basis. Experiment preparation and setup laboratories also are available to the user. Associated with the hot cell is a 2,500-Ci Co-60 irradiation source capable of producing a maximum dose rate of 1.4×10^5 rad(air)/hr.

No photographic laboratory is available. However, Northrop has oscilloscope cameras which may be used.

2.8.6 Procedural Information

Technical and administrative inquiries should be directed to:

Chief, Northrop Reactor
Northrop Research and Technology Center
3401 West Broadway
Hawthorne, CA 90250
Telephone: (213) 970-2297.

The required lead time is dependent upon the type of experiment to be conducted. Routine experiments and irradiations require only nominal advanced planning.

Costs and charges associated with the use of the facility are documented and available directly from Mr. Ray Turner, telephone (213) 970-2297. Address shipments to:

Northrop Reactor
Northrop Research and Technology Center
3401 West Broadway
Hawthorne, CA 90250

The Northrop reactor, which is located within the city of Hawthorne, California, is readily accessible from the surrounding urban area. Tentative schedules can be established and other preliminary arrangements can be completed by contacting Mr. Ray Turner.

2.8.7 Reference

1. Faulkenberry, B.H., and D.H. Rusling, *Northrop Reactor Facility Technical Data*, Northrop Systems Laboratories, Hawthorne, CA.

2.9 PENNSYLVANIA STATE UNIVERSITY BREAZEALE NUCLEAR REACTOR

2.9.1 General Characteristics

The Pennsylvania State University thermal TRIGA Mark III Reactor (PSTR) is a light water-cooled and reflected pool-type reactor, capable of both pulsing and steady-state operation. The reactor is operated in a water-filled pool 14.5 ft wide, 31.5 ft long, and 24 ft deep. The center line of the reactor is located about 20 ft beneath the surface of the water. The reactor is moveable along the length of the pool for flexibility of operation.

The reactor core has a basic shape of a right hexagonal prism containing 6 fuel elements per side. The fuel moderator elements are made up of a fuel region approximately 1.4 in. in dia. and 15 ft long. They consist of a ZrH_2 moderator homogeneously combined with 20% enriched U fuel. Both 8.5 w/o U containing approximately 38 gm U-234 per fuel element and 12 w/o U containing approximately 55 gm U-235 per fuel element are in the core. H in the fuel and water is the moderator.

The reactor is capable of 1,000 kW (thermal) operation with natural convection cooling and can be pulsed repetitively and reproducibly at approximately 15-min intervals to yield a burst having a prompt energy release of up to 24 MW and a peak of 2,000 MW.

2.9.1.1 Horizontal Beam Tubes

Three beam tubes are in use at the present time: one at the pool center line, and one on either side at an angle of 45 degrees with the center tube. The inner section is 6.5 in. in dia. and 3 ft long. The outer section is 7.5 in. in dia. and 2.5 ft long.

2.9.1.2 Central Thimble

The center thimble in the center of the core provides space for the irradiation of samples at the point of maximum flux. The thimble is an Al tube (with an I.D. of 1.33 in.) which extends from the reactor bridge through the center of the reactor core and terminates about 15 in. below the bottom of the core.

2.9.1.3 Pneumatic Tubes

Two pneumatic transfer systems are available to deliver samples to the reactor pool and return them to various laboratories within the building. These systems provide a convenient means of irradiating selected samples at the reactor core either with or without Cd shielding, or in the heavy water thermal column. The transfer time for either system is about 3 s. The polyethylene rabbits in which samples are encapsulated have an I.D. of 0.625 in. and are 4.5 in. long.

2.9.1.4 Pool Irradiations

Experimental devices may be encapsulated in water-tight containers and irradiated in and around the reactor core. In addition, 1.25-in. and 3-in. vertical tubes are available for dry irradiations. A vertical tube is an air-filled Al tube which extends from the reactor bridge to the bottom of the core. It is usually placed against the front face of the core.

A "merry-go-round" capable of rotating as many as 24 samples while they are being irradiated provides a means of simultaneously exposing a large number of specimens in an identical flux.

2.9.2 Additional Irradiation Facilities and Services

2.9.2.1 The Cobalt-60 Gamma-Ray Facility

A γ source composed of 80 sources containing approximately 52 Ci each and 70 sources containing approximately 385 Ci each of Co-60 are available for use in a water-filled pool (computed for May 1, 1978). The pool is 16 ft long by 10 ft wide and 17 ft deep. Several vertical tubes and a bell jar are available to provide dry irradiation areas. Maximum exposure rate as of May 1, 1978 is 6×10^5 rad/hr. This facility can accommodate a wide range of sample sizes, limited mainly by the desired exposure rate. Some examples of the more commonly used configurations are:

1. 1½-in. dia. tube with 80 sources (4.6×10^5 rad/hr)
2. 3-in. dia. tube with 15 sources (6×10^5 rad/hr)
3. 6-in. dia. tube with 25 sources (4.9×10^5 rad/hr)

The exposure rate is fairly constant over a 3-in. height centered about the vertical center line of the souces that surround the tube.

2.9.2.2 The Cockcroft-Walton Neutron Generator

A neutron generator, composed of a 150-kV accelerator, control console and 150-kV power supply which has the capability of supplying a 4-pi yield of 2.5×10^{11} n/s (14 MeV) from a deuterium-triton reaction, is available for research.

2.9.2.3 Subcritical Reactor

A subcritical reactor that has 2,000 kg of natural U contained in 1,289 Al encased slugs and 30,000 lb. of graphite, is capable of being converted into a graphite sigma pile for training and research. In addition, 1,100 kg of 6.9% enriched U are available for subcritical experiments.

2.9.2.4 Hot Cells

Two hot cells with an interior approximately 7.5 ft wide, 5 ft deep, and 13 ft high are available for handling radioactive materials. Each cell contains a

lead-glass window, 2 master slave manipulators, and a remotely operated half-ton hoist. Both cells are designed to handle 100 Ci of Co-60 equivalent radioactive material.

2.9.3 Operating Characteristics

Operating characteristics of the PSTR are as follows:

1. Power Levels
   a. Steady state pulse
   b. 1 MW 2,000 MW (peak power)
2. Temperature-time
   a. Time to peak temperature for a $2.75 pulse is approximately 42 ms
   b. 8.5 w/o fuel peak temperature is approximately 450°C
   c. 12 w/o fuel peak temperature is approximately 480°C.

Maximum allowed excess reactivity of the core is $7. A maximum of $2.86 (2% $\Delta k/k$) reactivity is allowed for experiments. For a $3 pulse, the width of the pulse at half-maximum is approximately 15 ms. Pulses can be repeated every 15 min at a reproducibility of ±10%.

The environment is described in Table 2-39 and Figures 2-81 through 2-85.

2.9.4 Support Capabilities

Several professional and technical support staff personnel are available for activation analysis, reactor experiments, etc. The Radionuclear Applications Laboratory provides researchers with services in activation analysis, radiation counting (including high-resolution γ-ray spectroscopy), radiography, radioisotope production, tracer applications, the design of radiation gaging equipment, and other applications involving the uses of radioactive materials.

Services such as 208-V, 3-ϕ and 120-V, 1-ϕ electrical power are available. Minimum cabling requirements are approximately 35 ft. Time signals are obtained during pulse initiation.

S, Au, In, and Al neutron dosimetry plus γ-ray dosimetry, active, are available. Other foil types have been used for neutron dosimetry but are presently passive.

The Nuclear Engineering facility is available to aid in a wide range of shielding- and reactor-physics-type calculations.

Heavy handling equipment includes a 3-ton capacity overhead crane in the reactor bay, a 5-ton capacity overhead crane in the Co-60 facility, and 2 monorail systems with an attached 3-ton crane which services the loading dock and hot cells. A small machine shop is located within the facility, and electrical

Table 2-39. Description of environment.

Irradiation Facility	Description	Location	1-MW STEADY STATE				Max. Pulse (11 ms width at Half Height)			
			Neutron Flux (n/cm²/s)			γ Flux (r/sec)	Integrated Neutron Flux (n/cm²)			γ Dose (R)
			Thermal	>10 keV	>1.0 MeV		Thermal	>10 keV	>1.0 MeV	
FRONT CORE FACE		B9 3 in. above C	9.4×10^{12}	7.2×10^{12}	3.3×10^{12}	—	—	1.4×10^{14}	6.0×10^{13}	—
		at C	1.1×10^{13}	8.8×10^{12}	3.9×10^{12}	$*1.3 \times 10^{4}$	8.7×10^{14}	2.0×10^{14}	8.5×10^{13}	$*2 \times 10^{6}$
		3 in. below C	1.0×10^{13}	8.5×10^{12}	3.8×10^{12}	—	—	2.2×10^{14}	9.5×10^{13}	—
		B11 3 in. above C	0.4×10^{12}	—	—	—	—	—	—	—
		or at C	9.4×10^{12}	—	—	—	—	—	—	—
		B7 3 in. below C	8.4×10^{12}	—	—	—	—	—	—	—
CENTRAL THIMBLE			—	—	—	—	—	—	—	—
						—	—	—	—	
			—	—	—	—	—	—	—	—
		WET 3 in. above C	—	2.3×10^{13}	9.9×10^{12}	—	—	1.5×10^{14}	6.4×10^{13}	—
		at C	2.5×10^{13}	2.5×10^{13}	1.1×10^{13}	$*9.6 \times 10^{4}$	1.2×10^{15}	2.0×10^{14}	8.6×10^{13}	$*2.2 \times 10^{6}$
		3 in. below C	—	2.2×10^{13}	9.6×10^{12}	—	—	2.1×10^{14}	9.0×10^{13}	—
CENTER BEAM HOLE	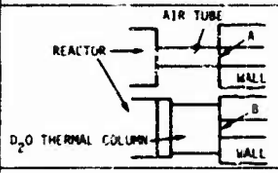	A - Center of 6½ in. beamhole	3.3×10^{9}	5.3×10^{8}	2.2×10^{8}	—	—	—	—	—
		B - Center of 6½ in. beamhole	8.9×10^{8}	—	—	1×10^{3}	—	—	—	—
PNEUMATIC TUBES	Polyethylene Rabbit (Total transport time ~3 s	Bare Rabbit Terminal (E-4)	6×10^{12}	2.4×10^{12}	9.9×10^{11}	$*1.3 \times 10^{4}$	1.5×10^{14}	6.8×10^{13}	3.0×10^{13}	$*3 \times 10^{5}$
		Cd Lined Rabbit Terminal (H-3) (H-3) at Side Core Face	—	2.0×10^{12}	8.6×10^{11}	$*1.3 \times 10^{4}$	8.0×10^{13}	6.1×10^{13}	2.6×10^{13}	$*3 \times 10^{5}$

*γ flux estimated from GA data.

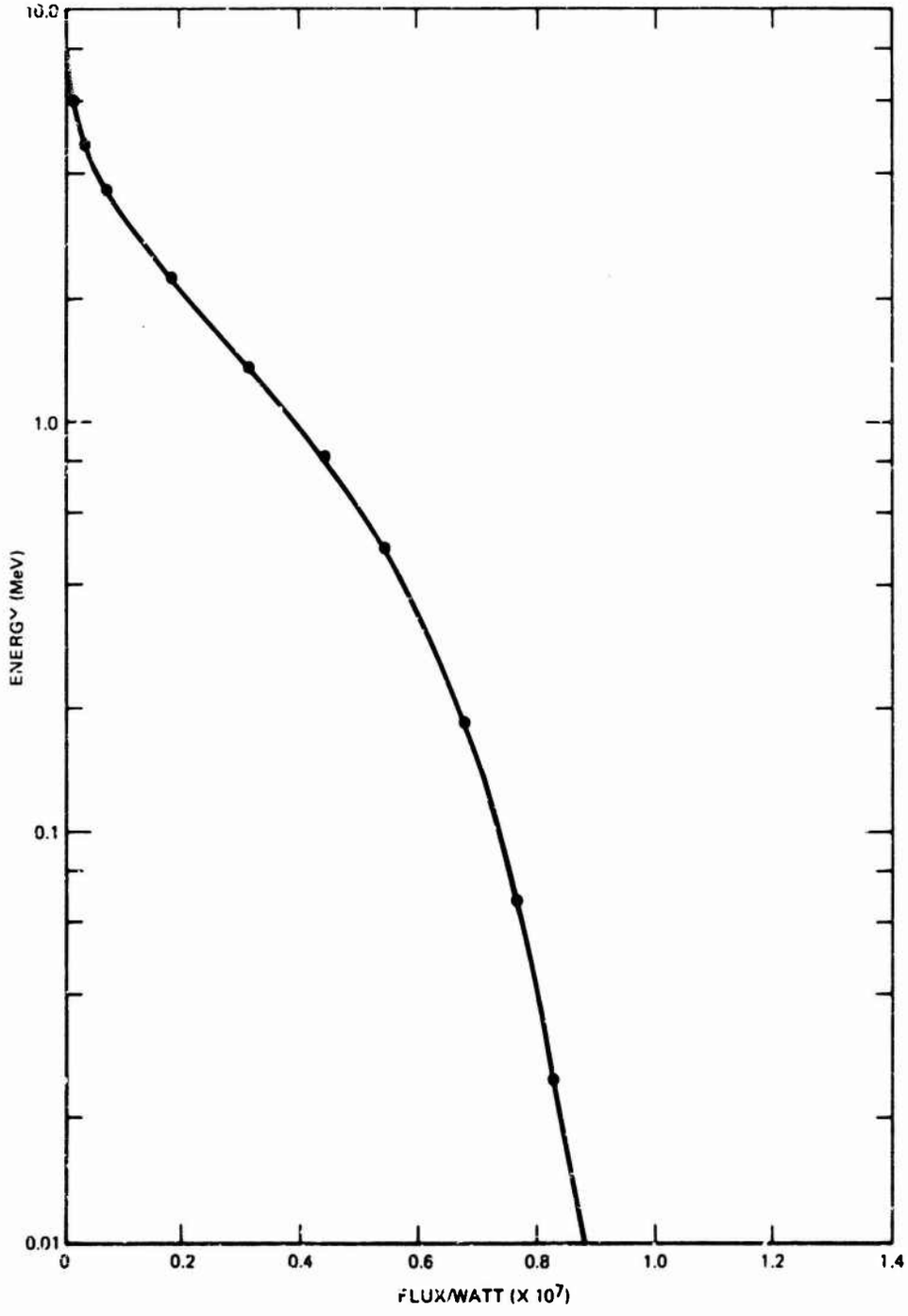

Figure 2-81. Flux intensity with energy greater than E as a function of E.

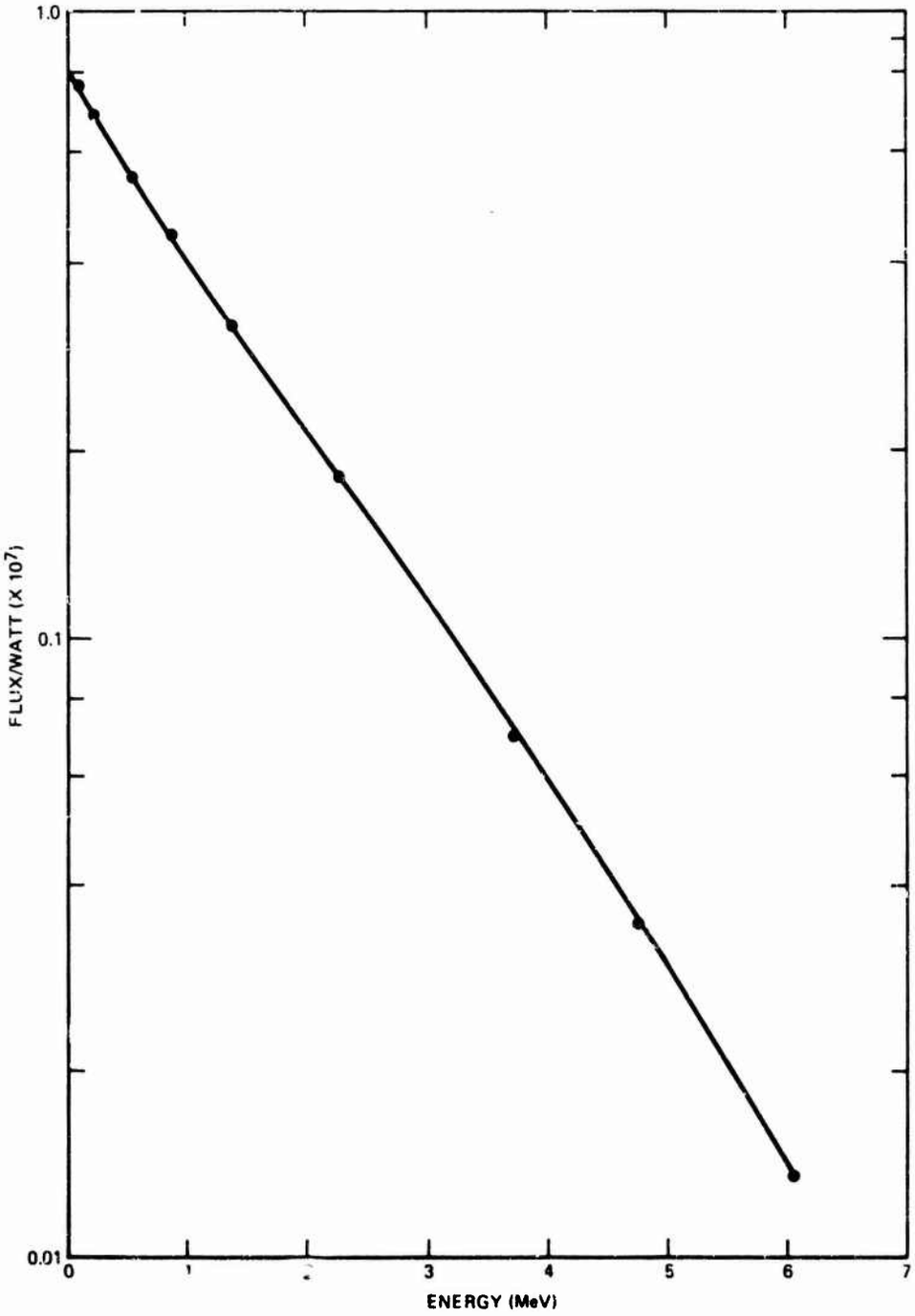

Figure 2-82. Flux intensity with energy greater than E as a function of E.

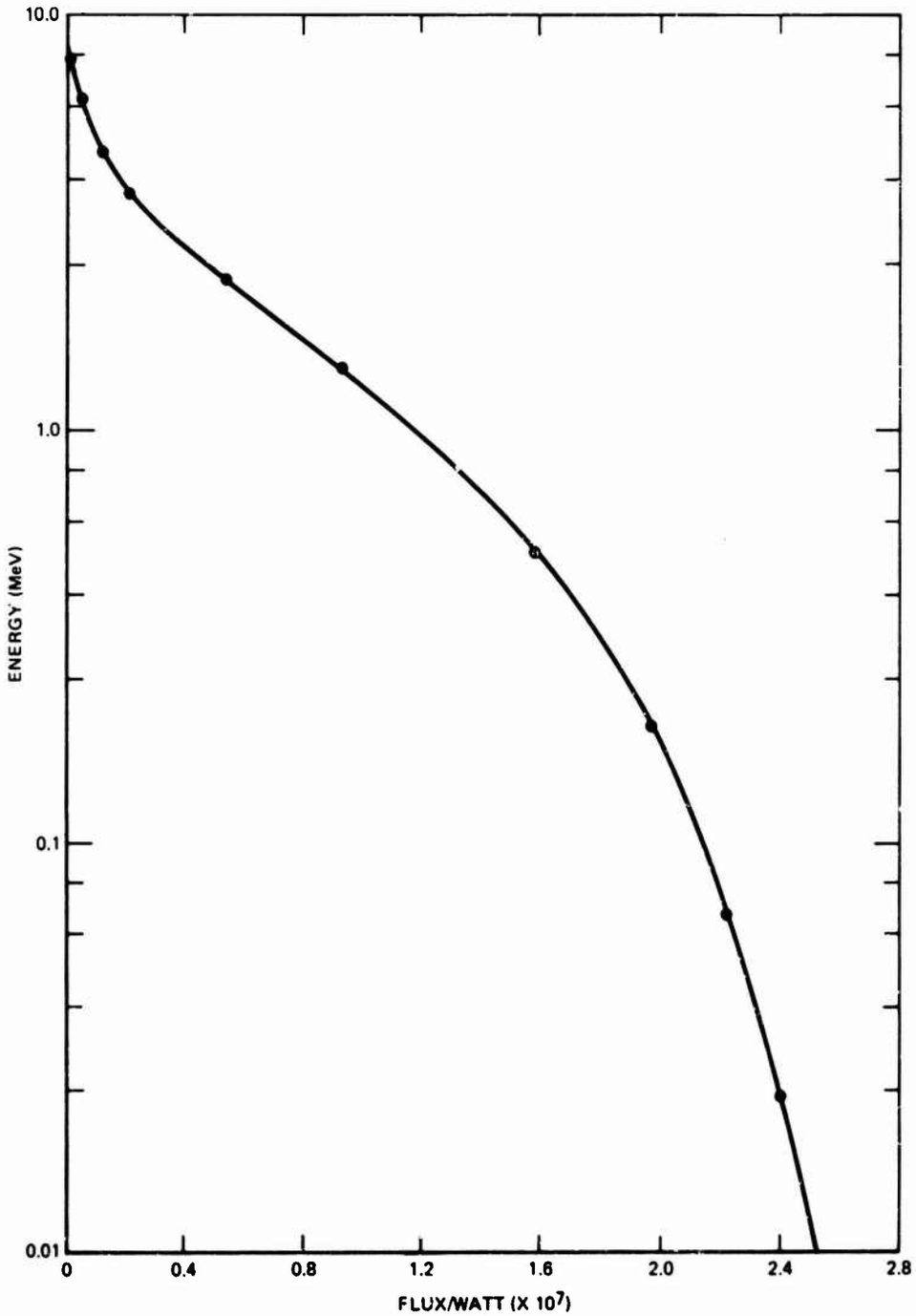

Figure 2-83. Flux intensity with energy greater than E as a function of E.

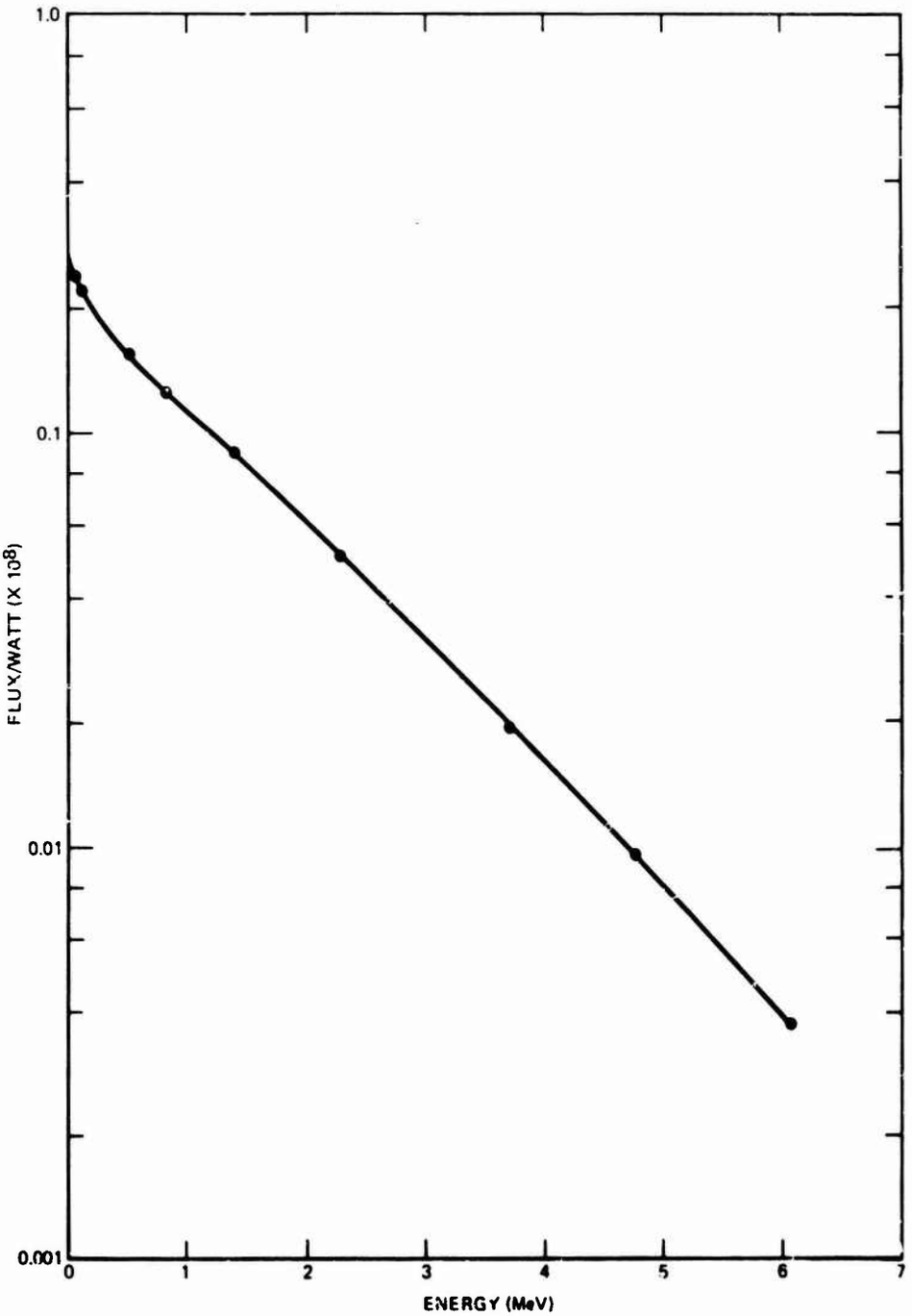

Figure 2-84. Flux intensity with energy greater than E as a function of E.

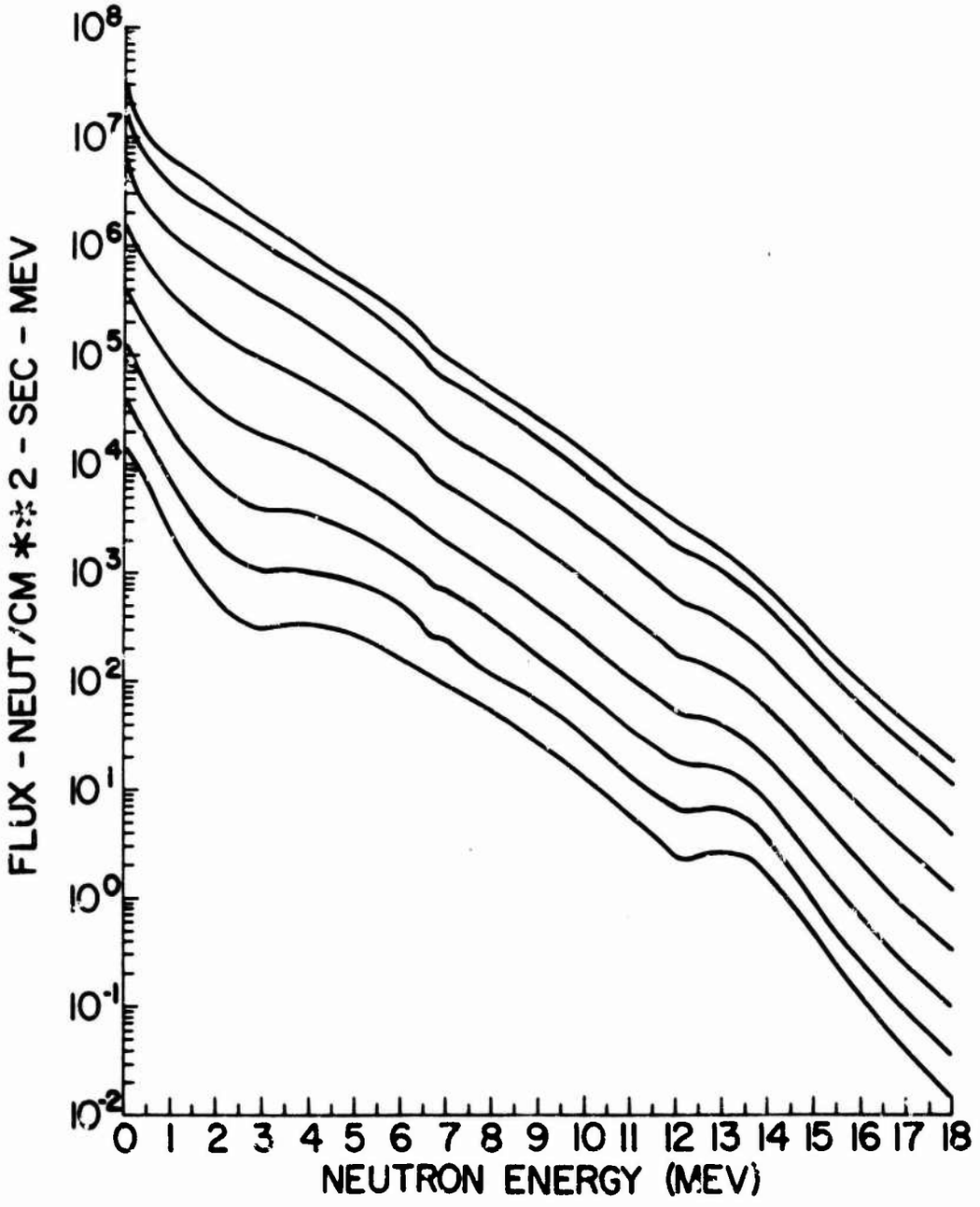

Figure 2-85. Neutron spectra in the TRIGA central thimble with spurious structure eliminated. (The spectra were measured from 2.65 to 23.65 in. above the core center line in 3-in. increments.)

and electronic repair shops are available. In addition to conventional shop equipment, heliarc acetylene and electrical welding equipment are available. The facility also has fume hoods, chemical apparatus, etc., and cameras.

2.9.5 Procedural Information

For additional information, contact:

Director
Breazeale Nuclear Reactor Facility
The Pennsylvania State University
University Park, PA 16802
Telephone: (814) 865-6351

For scheduling, allow 1 to 2 weeks lead time.

Cost of the facilities is $110.00/hr for a prime user; for other users the cost is negotiable. Dosimetry is $55.00/5 points or less. Shipping and handling charges are $55.00.

The shipping address is:

Penn State Breazeale Reactor
University Park, PA 16802.

2.9.6 Reference

1. Schmotzer, J.K., "Unfolding Fast Neutron Spectra and Cross Sections in a TRIGA Reactor," Ph.D. Thesis, The Pennsylvania State University, 1976.

2.10 GENERAL ATOMIC COMPANY TRIGA REACTOR FACILITY

The TRIGA reactor facility at General Atomic (GA) has 2 reactors located in one building: a TRIGA Mark I, and the Advanced TRIGA Prototype Reactor (ATPR). Each reactor is installed in a separate water-filled tank and each has an independent control system which permits simultaneous operation of both. The ATPR and the Mark I are available for TREE experimentation, and are discussed separately in the following paragraphs.

2.10.1 General Characteristics -- TRIGA Mark I

The TRIGA Mark I utilizes Al-clad U-ZrH_2 fuel elements and can be operated in the pulse mode or at a steady-state power of up to 250 kW. The reactor is located in a 6-ft-dia. water-filled circular Al tank with the core approximately 16 ft below the surface of the water. The core is stationary and is surrounded by a 12-in. thick graphite reflector. The open top of the reactor tank is at floor level and permits easy access.

Numerous experiment positions in the Mark I reactor allow for samples of various sizes and shapes. The primary positions are: (1) in-core (made available by removing fuel elements), (2) in, around, and on top of the graphite reflector, and (3) in the water around the core. At the in-core positions, samples up to 6 in. long and 1.25 in. in dia. can be irradiated in a relatively uniform flux (<10% variation). If a uniform flux is not required, specimens up to 24 in. long may be irradiated.

To provide a dry environment, hollow Al tubes, which extend above the surface, are inserted in the desired position. A pneumatic transfer system may be used for fast transfer of small samples in and out of the reactor core. Samples are placed in polyethylene containers 4.5 in. long with 0.68 in. I.D. Travel time from the reactor to the counting room terminus is approximately 3 s. Samples also may be placed in the reflector region of the core, either in radiation thimbles or in the rotary specimen rack.

Irradiation of specimens in other than the standard positions can be accommodated within limits compatible with reactor operations.

2.10.2 TRIGA Mark I Operating Characteristics

Typical of TRIGA reactors, characteristics of the TRIGA Mark I pulse, including peak power, prompt energy release, pulse width and the initial reactor period, depend primarily on the reactivity insertion and the fuel loading of the reactor core. As a result, pulse characteristics can be varied over a wide range within the licensed operating limits of the facility.

Peak power, based on a typical core loading of 70 elements and a routine reactivity insertion of $3.00, is 1,000 MW. Based on a typical core loading of 70 elements and a routine reactivity insertion of $3.00, characteristics are:

1. Prompt energy relase — 18 MW-s (5.6×10^{17} fissions)
2. Pulse width (FWHM) — 16.6 ms

3. Max. fluence (B-ring position):

a. Fast (>10 keV)	9.7×10^{14} n/cm^2
b. Thermal (<0.4 eV)	3.2×10^{14} n/cm^2

Available qualitative operating characteristics are shown in Figure 2-86.

An assessment of reactivity worth and the associated tolerable limit will be made by the reactor staff for each experiment conducted. GA assumes a step insertion of reactivity over a period of approximately 0.1 s. The maximum insertion rate therefore is \$30.00/s.

Burst repetition rate is determined by delayed neutron lifetime, not coolant temperature. The maximum insertion rate therefore is \$30.00/s. The maximum repetition rate is 10 bursts/hr. However, 10 min between bursts is preferred. Burst characteristics are reproducible to within ±5%.

2.10.3 Environment

Quantitative neutron and γ flux/fluence/dose data are available from GA. Extensive measurements were made by Edgerton, Germerhauser, and Greer of the neutron and γ environment generated by the Mark I reactor. Supplementary analyses were made by GA. Standard threshold foil techniques were used for the neutron measurements. γ dose measurements were made using tetrachloroethylene as the dosimeter. This organic liquid, upon exposure to radiation, decomposes into hydrochloric acid. The amount of acid produced is proportional to the γ dose imparted to the tetrachloroethylene. Compensation is made for the slight neutron response of the liquid.

Detailed data for various in-core positions are given in Table 2-40. Dosimetry measurements at the core center line in an air-filled tube (4-in. I.D.) located at the outside edge of the graphite reflector are shown in Table 2-41. Data for typical reactor operations are given Table 2-42. All data are for a core loading of 70 fuel elements and a \$3.00 reactivity insertion pulse.

Spectrum data, as such, are not available. However, the neutron fluence data are presented in terms of thresholds from which spectral data can be derived.

Typical values of the n/γ ratio for various irradiation positions are given in Table 2-42.

2.10.4 Characteristics of ATPR

The ATPR is similar to a TRIGA Mark III. It utilizes stainless-steel-clad U-ZrH_2 fuel elements positioned in concentric rings to form the core. The core is suspended from a movable bridge in a 10-ft dia. by 25-ft deep water-filled pit. The size of the pit allows large experimental devices to be placed near the core, and the open top of the pool permits easy access. The reactor can be operated in the pulse mode or at a steady-state power level of 1,500 kW. Figures 2-87 and 2-88 show the reactor and the ATPR facility.

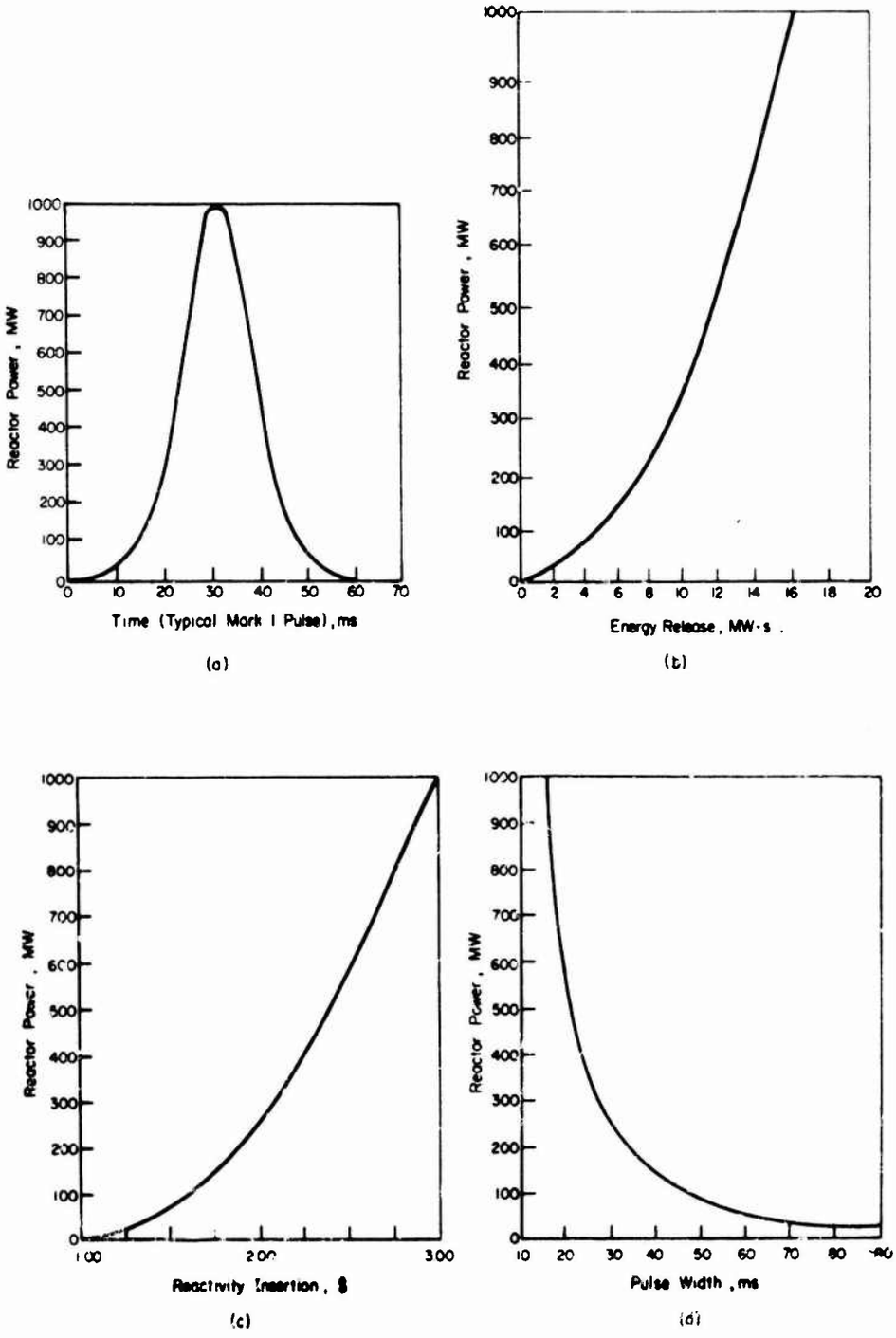

Figure 2-86. Mark I pulsing characteristics.

Table 2-40. Dosimetry values for the TRIGA Mark I reactor (70 fuel elements, $3.00 reactivity insertion).

Position	Neutron Energy	n/cm^2-s-W	n/cm^2, Fluence for 18 MW-s Pulse	n/cm^2-s, Flux for 1,000-MW Pulse
B-ring ($\bar{E}_n$ = 1.1 MeV)	Thermal	1.8×10^7	3.2×10^{14}	1.8×10^{16}
	>10 keV	5.4×10^7	9.7×10^{14}	5.4×10^{16}
	> 0.6 MeV	2.9×10^7	5.2×10^{14}	2.9×10^{16}
	> 1.5 MeV	1.4×10^7	2.5×10^{14}	1.4×10^{16}
	> 3.0 MeV	5.8×10^6	1.0×10^{14}	5.8×10^{15}
C-ring ($\bar{E}_n$ = 1.09 MeV)	Thermal	2.5×10^7	4.5×10^{14}	2.5×10^{15}
	>10 keV	4.9×10^7	8.8×10^{14}	4.9×10^{16}
	> 0.6 MeV	2.4×10^7	4.3×10^{14}	2.4×10^{16}
	> 1.5 MeV	1.3×10^7	2.3×10^{14}	1.3×10^{16}
	> 3.0 MeV	5.2×10^6	9.4×10^{13}	5.2×10^{15}
D-ring ($\bar{E}_n$ = 1.08 MeV)	Thermal	2.1×10^7	3.8×10^{14}	2.1×10^{16}
	>10 keV	4.2×10^7	7.6×10^{14}	4.2×10^{16}
	> 0.6 MeV	1.9×10^7	3.4×10^{14}	1.9×10^{16}
	> 1.5 MeV	1.1×10^7	2.0×10^{14}	1.1×10^{16}
	> 3.0 MeV	4.4×10^6	7.9×10^{13}	4.4×10^{15}
	γ	1.67×10^{-1} rad (air)/s-W	3.0×10^6 rad (air)	1.67×10^8 rad (air)/s
E-ring ($\bar{E}_n$ = 1.04 MeV)	Thermal	1.7×10^7	3.0×10^{14}	1.7×10^{16}
	>10 keV	3.2×10^7	5.8×10^{14}	3.2×10^{16}
	> 0.6 MeV	1.3×10^7	2.3×10^{14}	1.3×10^{16}
	> 1.5 MeV	7.8×10^6	1.4×10^{14}	7.8×10^{15}
	> 3.0 MeV	3.2×10^6	5.8×10^{13}	3.2×10^{15}
F-ring ($\bar{E}_n$ = 1.01 MeV)	Thermal	1.0×10^7	1.8×10^{14}	1.0×10^{16}
	>10 keV	2.1×10^7	3.8×10^{14}	2.1×10^{16}
	> 0.6 MeV	9.1×10^6	1.6×10^{14}	9.1×10^{15}
	> 1.5 MeV	5.2×10^6	9.4×10^{13}	5.2×10^{15}
	> 3.0 MeV	1.5×10^6	2.7×10^{13}	1.5×10^{15}
	γ	6.1×10^{-2} rad (air)/s-W	1.1×10^6 rad (air)	6.1×10^7 rad (air)/s

Table 2-41. Dosimetry values for the TRIGA Mark I reactor at core center line in air-filled tube at outside edge of graphite reflector ($\bar{E}_n$ = 1.22 MeV) (70 fuel elements; $3.00 reactivity insertion).

Neutron Energy	n/cm^2-s-W	n/cm^2, Fluence for 18 MW-s Pulse	n/cm^2-s, Flux for 1,000-MW Pulse
Thermal	2.63×10^6	4.72×10^{13}	2.63×10^{15}
>10 keV	6.8×10^4	1.2×10^{12}	6.8×10^{13}
> 0.6 MeV	2.7×10^4	4.9×10^{11}	2.7×10^{13}
> 1.5 MeV	2.0×10^4	3.6×10^{11}	2.0×10^{13}
> 3.0 MeV	8.4×10^3	1.5×10^{11}	8.4×10^{12}
γ	1.6×10^{-3} rad (air)/s-W	2.8×10^4 rad (air)	1.6×10^6 rad (air)/s

Table 2-42. TRIGA Mark I reactor performance for 250-kW steady-state and 1,000-MW pulsing operation (experimental dosimetry values for a typical core loading of 70 fuel elements).

Experiment Location	Volume With 10 Flux Variation (dia. x length, in.)	250 kW Steady State Operation			1000-MW Pulsing Operati			
					Peak Dose Rate			
		Neutrons, $n/cm^2 \cdot s$			Neutrons, $n/cm^2 \cdot s$			
		Fast (E 10 keV)	Thermal (E 0.4 eV)	rads[b]/s	Fast (E 10 keV)	(E 0.4 eV)	rads[b]/s	
B-ring[c]	1.25 x 6	1.4×10^{13}	4.5×10^{12}	--	5.4×10^{16}	1.8×10^{16}	--	9.
C-ring[c]	1.25 x 6	1.2×10^{13}	6.3×10^{12}	--	4.9×10^{16}	2.5×10^{16}	--	8.
D-ring[c]	1.25 x 6	1.1×10^{13}	5.3×10^{12}	4.2×10^{4}	4.2×10^{16}	2.1×10^{16}	1.7×10^{8}	7.
E-ring[c]	1.25 x 6	8.0×10^{12}	4.3×10^{12}	--	3.2×10^{16}	1.7×10^{16}	--	5.
F-ring[c]	1.25 x 6	5.3×10^{12}	2.5×10^{12}	1.5×10^{4}	2.1×10^{16}	1.0×10^{16}	6.1×10^{7}	3.
Pneumatic transfer system terminus in F-ring	0.5 x 3.8[d]	5.3×10^{12}	2.5×10^{12}	1.5×10^{4}	2.1×10^{16}	1.0×10^{16}	6.1×10^{7}	3.
Rotary specimen rack	40 containers[e]	1.5×10^{12}	1.8×10^{12}	4.0×10^{3}	6.0×10^{15}	7.2×10^{15}	1.6×10^{7}	1.
Reactor pool outside reflector	f	1.7×10^{10}	6.6×10^{11}	4.0×10^{2}	6.8×10^{13}	2.6×10^{15}	1.6×10^{6}	1.
Reactor pool above top of reflector	g	1.1×10^{11}	3.4×10^{11}	--	4.4×10^{14}	1.5×10^{15}	--	7.

[a] Insertion of 2.2 $\Delta k/k$ excess reactivity ($3.00) results in a peak power of 1000 MW, a total integrated energy release of 18 MW

[b] Assumed to be air

[c] A varying number of fuel element positions in the core grid array may be occupied by experiments

[d] In specimen capsule

[e] 0.8-in. I.D. x 3.8-in. each

[f] Volume available has 1.7-ft inside radius and 3-ft outside radius. Flux decreases by inverse square law attenuation with dist

[g] Specimen with a diameter of 1 ft or less placed on top of the reflector will receive a fairly uniform flux

[h] Fast neutron dose is converted from n/cm^2 to rads[b] by multiplying the n/cm^2 value by 2.5×10^{-9} rads[b]/(n/cm^2)

[i] Thermal neutron dose is converted from n/cm^2 to rads[b] by multiplying the n/cm^2 value by 3.25×10^{10} rads[b]/(n/cm^2).

nce for 250-kW steady-state and
xperimental dosimetry values for
fuel elements).

dy State Operation		1000-MW Pulsing Operation[a]						
		Peak Dose Rate			Dose Per Pulse			
$cm^2 \cdot s$		Neutrons, $n/cm^2 \cdot s$			Neutrons			
Thermal (0.4 eV)	rads[b]/s	Fast (E 10 keV)	(E 0.4 eV)	rads[b]/s	Fast n/cm^{2h}	Thermal n/cm^{2i}	rads[b]	n/, (E 10 keV) (n/cm^2)/rad[b]
.5 x 10^{12}	--	5.4 x 10^{16}	1.8 x 10^{16}	--	9.7 x 10^{14}	3.2 x 10^{14}	--	--
.3 x 10^{12}	--	4.9 x 10^{16}	2.5 x 10^{16}	--	8.8 x 10^{14}	4.5 x 10^{14}	--	--
.3 x 10^{12}	4.2 x 10^4	4.2 x 10^{16}	2.1 x 10^{16}	1.7 x 10^8	7.6 x 10^{14}	3.8 x 10^{14}	3.0 x 10^6	2.5 x 10^8
.2 x 10^{12}	--	3.2 x 10^{16}	1.7 x 10^{16}	--	5.8 x 10^{14}	3.0 x 10^{14}	--	--
.9 x 10^{12}	1.5 x 10^4	2.1 x 10^{16}	1.0 x 10^{16}	6.1 x 10^7	3.8 x 10^{14}	1.8 x 10^{14}	1.1 x 10^6	3.4 x 10^8
.9 x 10^{12}	1.5 x 10^4	2.1 x 10^{16}	1.0 x 10^{16}	6.1 x 10^7	3.8 x 10^{14}	1.8 x 10^{14}	1.1 x 10^6	3.4 x 10^8
.3 x 10^{12}	4.0 x 10^3	6.0 x 10^{15}	7.2 x 10^{15}	1.6 x 10^7	1.1 x 10^{14}	1.3 x 10^{14}	2.9 x 10^5	3.8 x 10^8
.6 x 10^{11}	4.0 x 10^2	6.8 x 10^{13}	2.6 x 10^{15}	1.6 x 10^6	1.2 x 10^{12}	4.7 x 10^{13}	2.8 x 10^4	4.3 x 10^7
.4 x 10^{11}	--	4.4 x 10^{14}	1.5 x 10^{15}	--	7.9 x 10^{12}	2.5 x 10^{13}	--	--

n a peak power of 1000 MW, a total integrated energy release of 18 MW·s, and a pulse width of 16.6 ms

d array may be occupied by experiments

radius. Flux decreases by inverse square law attenuation with distance from reflector
the reflector will receive a fairly uniform flux
iplying the n/cm^2 value by 2.5 x 10^{-9} $rads^b/(n/cm^2)$
ultiplying the n/cm^2 value by 3.25 x 10^{10} $rads^b/(n/cm^2)$.

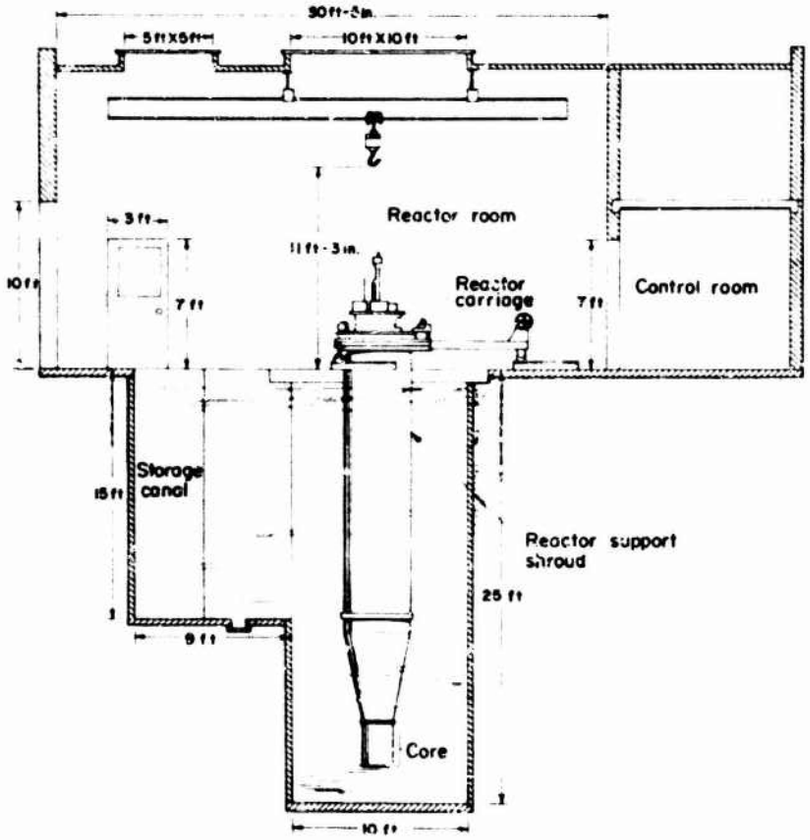

Figure 2-87. Vertical section of ATPR facility.

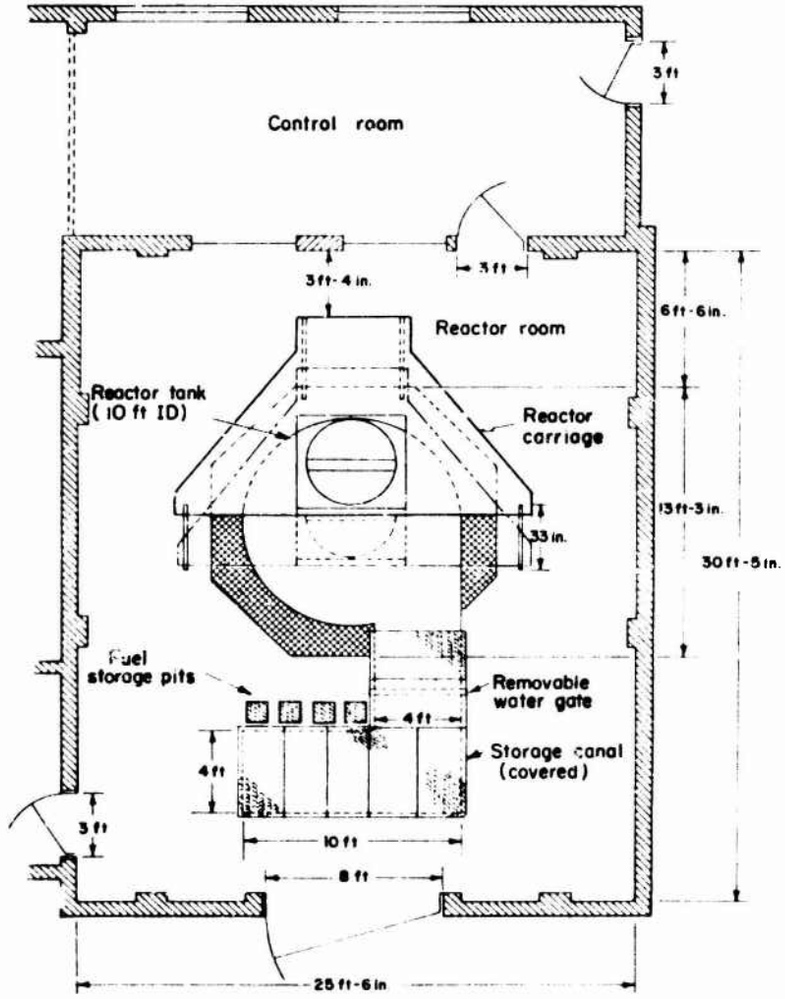

Figure 2-88. Floor plan of ATPR facility.

Samples may be irradiated at in-core positions by removing fuel elements. Samples up to 6 in. long and 1.25 in. in dia. can be tested in a relatively uniform flux (<10% variation). If a uniform flux is not required, longer specimens may be irradiated. To provide a dry environment, hollow Al tubes, which extend above the water surface, are inserted into the desired position. Irradiations also may be performed in a large part of the pool. The reactor core may be centered in the pool, making the entire area around the core available, or the reactor may be moved toward the edge of the pool to permit the installation of extra-large devices. A tube (the "J-tube") can be extended from above the water surface to the reactor core. The J-tube provides fast and convenient access to the edge of the core for samples of medium size. Figure 2-89 depicts the J-tube position relative to the reactor core.

2.10.5 ATPR Test Parameters

Typical of TRIGA reactors, characteristics of the ATPR pulse, including peak power, prompt energy release, pulse width, and the initial reactor period, depend primarily on the reactivity insertion and the fuel loading of the reactor core. As a result, pulse characteristics can be varied over a wide range within the licensed operating limits of the facility.

The ATPR has been safely subjected to reactivity insertions of up to $5.00. Reactivity insertions for typical operating pulses are between $4.00 and $4.60. Normal core loading is 94 to 100 fuel elements. Peak power is 6,400 MW for a typical burst (100 fuel elements and a reactivity insertion of $4.60). Characteristics of a typical burst (100 fuel elements and a reactivity insertion of $4.60) are:

1.	Prompt energy release	43 MW-s (1.3×10^{18} fissions)
2.	Pulse width (FWHM)	6.3 ms
3.	Max fluence (B-ring position)	
	a. Fast (>10 keV)	9.5×10^{14} n/cm^2
	b. Thermal (<0.4 eV)	1.2×10^{15} n/cm^2

Operating characteristics averaged over many experimental measurements are shown in Figure 2-90.

An assessment of reactivity worth and the associated tolerable limit will be made by the reactor staff for each experiment conducted. A step insertion of reactivity over a period of 0.1 s is assumed. The maximum insertion rate therefore is $50.00/s.

Burst repetition rate is determined by delayed neutron lifetimes, not by coolant temperature. The maximum repetition rate is 10 bursts/hr. However, 10 min between bursts is preferred. Burst characteristics are reproducible to within ±5%.

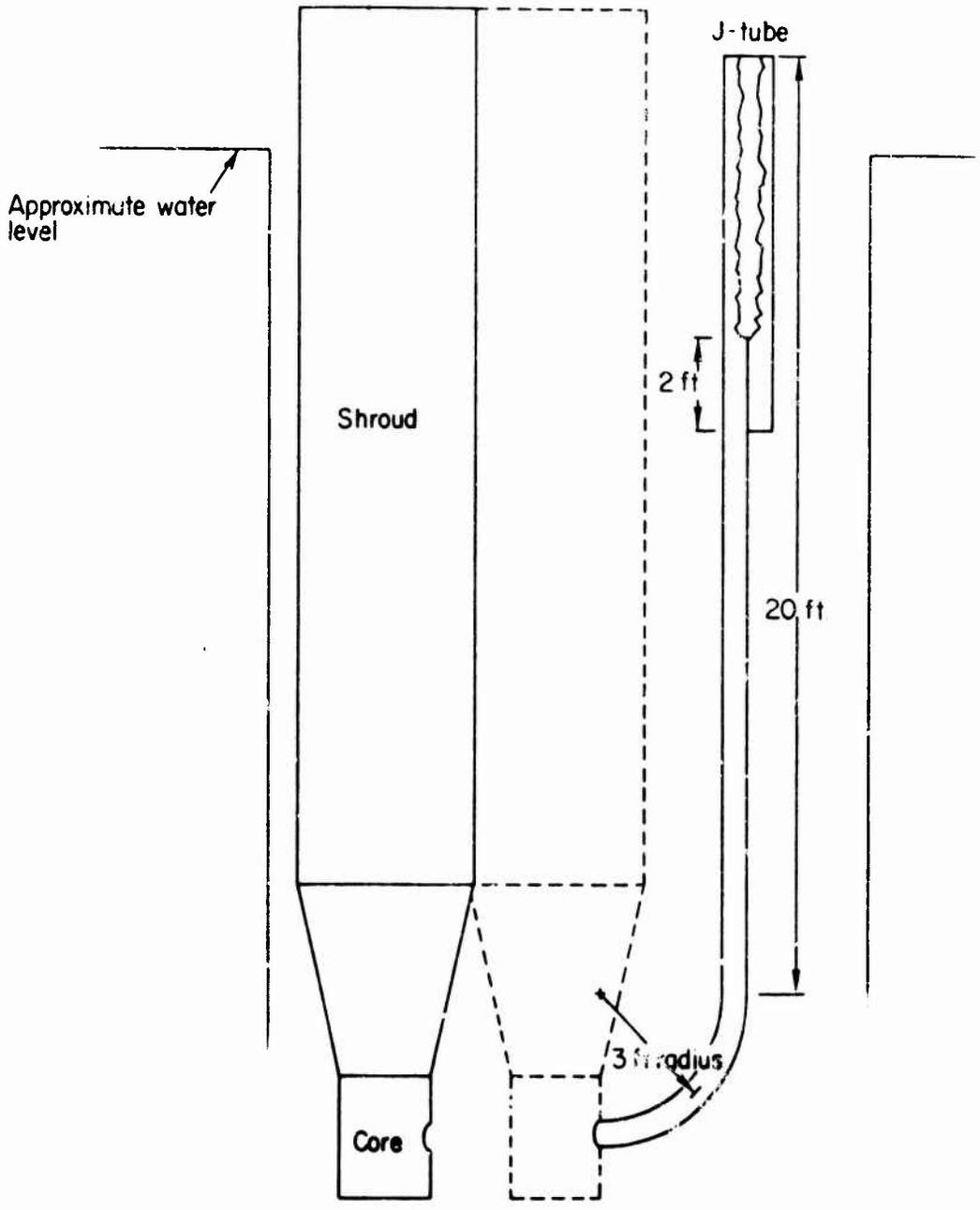

Figure 2-89. J-tube position relative to the reactor core, ATPR.

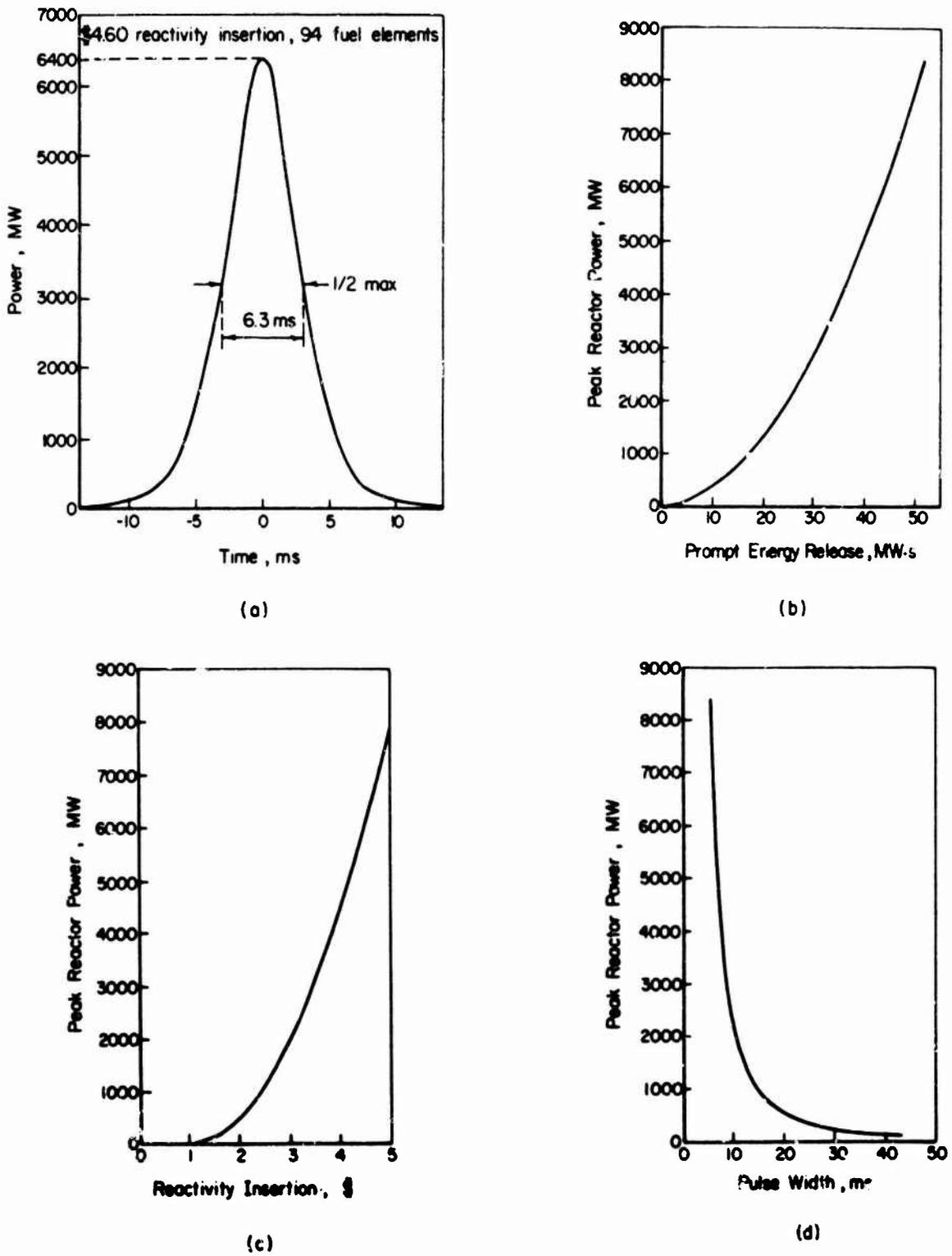

Figure 2-90. ATPR pulsing characteristics.

2.10.6 Environment

Quantitative neutron and γ flux/fluence/dose data are available from GA. Extensive measurements were made by Edgerton, Germerhauser, and Greer of the neutron and γ environments generated by the ATPR. Supplemental analyses were made by GA. Standard threshold foil techniques were used for the neutron measurements. γ dose measurements were made using tetrachloroethylene as the dosimeter. The measurements were made at in-core positions and inside the J-tube. Dosimetry data for the air-filled J-tube are given in Table 2-43.

In-core data (Table 2-44) were taken at the core center line and normalized to doses in air. Figure 2-91 depicts the neutron flux distribution in the vertical plane.

Data for the ATPR are given in Table 2-45 for a $4.60 reactivity insertion and a core loading of 94 fuel elements. Figure 2-92 gives the γ dose in water along the core center line.

2.10.7 Support Capabilities

The TRIGA facility staff consists of nuclear physicists, chemists, and engineers competent in all phases of TREE experimentation.

Members of the professional staff are available for consultation on any phase of a program as well as on specific technical research problems. They can provide guidance in the preparation of experimental programs or can handle programs in their entirety.

A limited amount and type of electronic equipment is maintained by the facility and may be used by experimenters when available. It is recommended that specific equipment required by the experimenter be provided either from his own laboratory or on a rental basis from local suppliers. There is ample space for setting up test and recording equipment and for accommodating instrumentation

Table 2-43. Air-filled J-tube dosimetry data ($\bar{E}_n$ = 0.79 MeV).

Neutron Energy	n/cm^2-s-W	n/cm^2, Fluence for 18 MW-s Pulse	n/cm^2-s, Flux for 1,000 MW Pulse
>10 keV	3.0×10^6	1.2×10^{14}	1.4×10^{16}
> 0.6 MeV	1.7×10^6	6.8×10^{13}	8.1×10^{15}
> 1.5 MeV	1.0×10^5	4.0×10^{13}	4.8×10^{15}
> 3.0 MeV	2.0×10^5	8.0×10^{12}	9.6×10^{16}
γ	1.4×10^{-2} rad (air)/s-W	5.6×10^5 rad (air)	6.7×10^7 rad (air)/s

Table 2-44. In-core dosimetry values for the ATPR ($4.00 reactivity insertion and 100 fuel elements).

Position	Neutron Energy	n/cm^2-s-W)	n/cm^2 Fluence for 40-MW-s Pulse	n/cm^2-s, Flux for 4,300-MW Pulse	n/γ (n/cm^2)/rad (air)
B-Ring ($\bar{E}_n$ = 0.97 MeV)	Thermal	2.9 x 10^7	1.2 x 10^{15}	1.4 x 10^{17}	3.4 x 10^8
	>10 keV	2.2 x 10^7	8.8 x 10^{14}	1.1 x 10^{17}	
	> 0.6 MeV	1.2 x 10^7	4.8 x 10^{14}	5.8 x 10^{16}	
	> 1.5 MeV	6.9 x 10^6	2.8 x 10^{14}	3.3 x 10^{16}	
	> 3.0 MeV	2.5 x 10^6	1.0 x 10^{14}	1.2 x 10^{16}	
	γ	6.6 x 10^{-2}	2.6 x 10^6	3.2 x 10^8	
		rad (air)/s-W	rad (air)	rad (air)/s	
C-Ring ($\bar{E}_n$ = 1.00 MeV)	Thermal	2.3 x 10^7	9.2 x 10^{14}	1.1 x 10^{17}	3.8 x 10^8
	>10 keV	2.1 x 10^7	8.4 x 10^{14}	1.0 x 10^{17}	
	> 0.6 MeV	1.2 x 10^7	4.8 x 10^{14}	5.7 x 10^{16}	
	> 1.5 MeV	6.2 x 10^6	2.5 x 10^{14}	3.0 x 10^{16}	
	> 3.0 MeV	2.3 x 10^6	9.2 x 10^{13}	1.1 x 10^{16}	
	γ	5.5 x 10^{-2}	2.2 x 10^6	2.6 x 10^8	
		rad (air)/s-W	rad (air)	rad (air)/s	
D-Ring ($\bar{E}_n$ = 0.98 MeV)	Thermal	2.0 x 10^7	8.0 x 10^{14}	9.6 x 10^{16}	4.0 x 10^8
	>10 keV	1.8 x 10^7	7.2 x 10^{14}	8.6 x 10^{16}	
	> 0.6 MeV	9.8 x 10^6	3.9 x 10^{14}	4.7 x 10^{16}	
Gold R_{Cd} = 4.28	> 1.5 MeV	5.3 x 10^6	2.2 x 10^{14}	2.5 x 10^{16}	
	> 3.0 MeV	2.0 x 10^6	8.0 x 10^{13}	9.6 x 10^{15}	
	γ	4.4 x 10^{-2}	1.8 x 10^6	2.1 x 10^8	
		rad (air)/s-W	rad (air)	rad (air)/s	
E-Ring ($\bar{E}_n$ = 1.1 MeV)	Thermal	1.7 x 10^7	6.8 x 10^{14}	8.1 x 10^{16}	4.0 x 10^8
	>10 keV	1.3 x 10^7	5.2 x 10^{14}	6.2 x 10^{16}	
	> 0.6 MeV	7.4 x 10^6	3.0 x 10^{14}	3.5 x 10^{16}	
Gold R_{Cd} = 5.31	> 1.5 MeV	4.0 x 10^6	1.6 x 10^{14}	1.9 x 10^{16}	
	> 3.0 MeV	1.5 x 10^6	6.0 x 10^{13}	7.2 x 10^{15}	
	γ	3.3 x 10^{-2}	1.3 x 10^6	1.6 x 10^8	
		rad (air)/s-W	rad (air)	rad (air)/s	
E-Ring ($\bar{E}_n$ = 0.98 MeV)	Thermal	1.5 x 10^7	6.0 x 10^{14}	7.2 x 10^{16}	3.6 x 10^8
	>10 keV	8.1 x 10^6	3.2 x 10^{14}	3.8 x 10^{16}	
	> 0.6 MeV	4.5 x 10^6	1.8 x 10^{14}	2.2 x 10^{16}	
	> 1.5 MeV	2.3 x 10^6	9.2 x 10^{13}	1.1 x 10^{16}	
	> 3.0 MeV	8.6 x 10^5	3.4 x 10^{13}	4.1 x 10^{16}	
	γ	2.2 x 10^{-2}	8.8 x 10^5	1.0 x 10^8	
		rad (air)/s-W	rad (air)	rad (air)/s	
G-Ring ($\bar{E}_n$ = 1.58 MeV)	Thermal	1.6 x 10^7	6.4 x 10^{14}	7.7 x 10^{16}	3.2 x 10^8
	>10 keV	4.4 x 10^6	1.8 x 10^{14}	2.1 x 10^{16}	
	> 0.6 MeV	2.5 x 10^6	1.0 x 10^{14}	1.2 x 10^{16}	
	> 1.5 MeV	1.2 x 10^6	4.8 x 10^{13}	5.7 x 10^{15}	
	> 3.0 MeV	5.2 x 10^5	2.6 x 10^{13}	2.5 x 10^{15}	
	γ	1.4 x 10^{-2}	5.6 x 10^5	6.7 x 10^7	
		rad (air)/s-W	rad (air)	rad (air)/s	

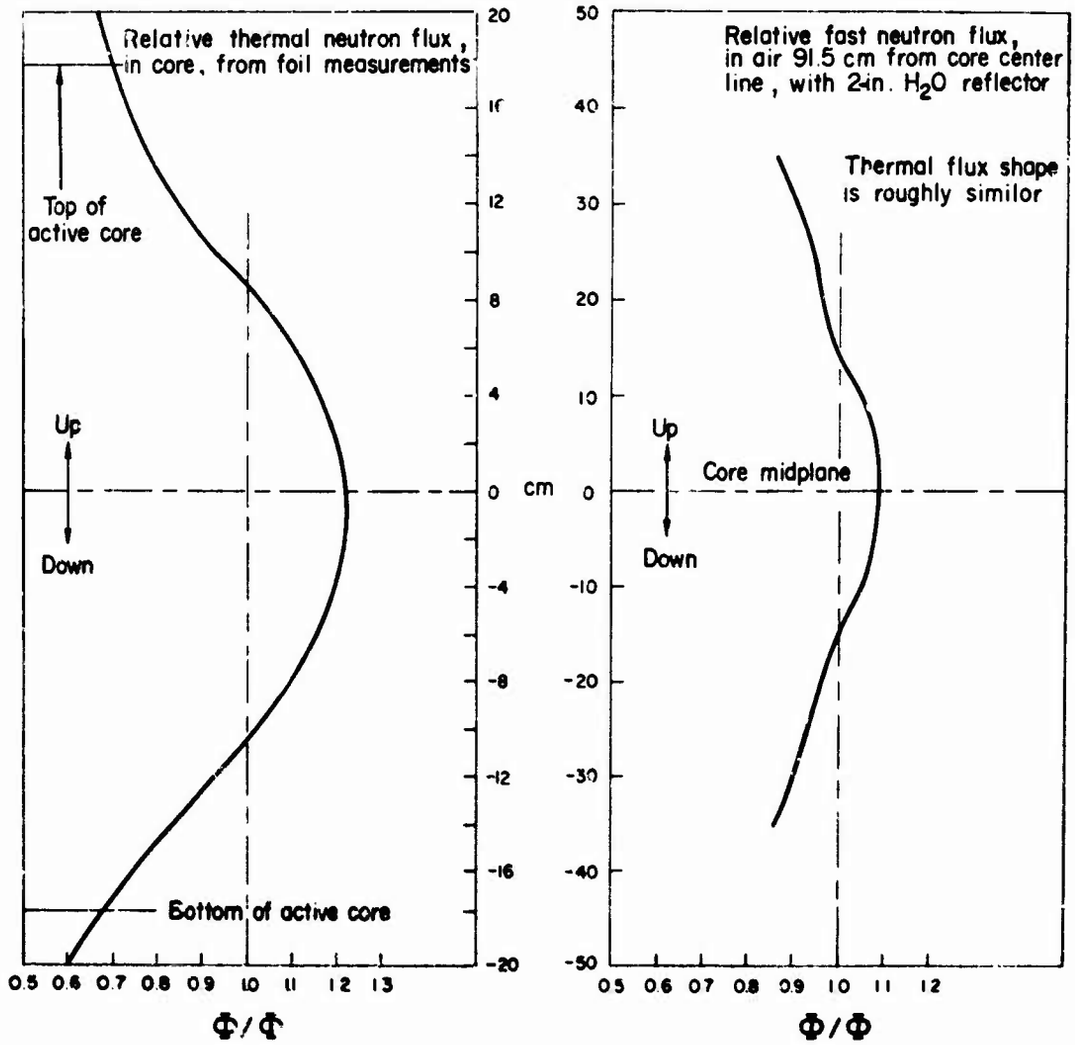

Figure 2-91. Vertical neutron flux distribution.

Table 2-45. Advanced TRIGA prototype reactor performance for 1.5-MW steady-state and 6,400-MW pulsing operation (experimental dosimetry values for a typical core loading of 94 fuel elements).

Experimental Location	Volume With <10% Flux Variation (dia. x length, in.)	1.5-MW Steady-State Operation			6,400 Peak Dose Rate			
		Neutrons, n/cm^2-s			Neutrons, n/cm^2-s			
		Fast (E > 10 keV)	Thermal (E < 0.4 eV)	γ rads[b]/s	Fast (E > 10 keV)	Thermal (E < 0.4 eV)	γ rads[b]/s	(E
B-ring[c]	1.25 x 6	3.3×10^{13}	4.4×10^{13}	9.9×10^{4}	1.4×10^{17}	1.9×10^{17}	4.2×10^{8}	9.5
C-ring[c]	1.25 x 6	3.2×10^{13}	3.5×10^{13}	8.3×10^{4}	1.3×10^{17}	1.5×10^{17}	3.5×10^{8}	9.(
D-ring[c]	1.25 x 6	2.8×10^{13}	3.0×10^{13}	6.6×10^{4}	1.2×10^{17}	1.3×10^{17}	2.8×10^{8}	7
E-ring[c]	1.25 x 6	2.0×10^{13}	2.7×10^{13}	5.0×10^{4}	8.3×10^{16}	1.1×10^{17}	2.1×10^{8}	5.(
F-ring[c]	1.25 x 6	1.2×10^{13}	2.3×10^{13}	3.3×10^{4}	5.2×10^{16}	9.6×10^{16}	1.4×10^{8}	3.5
G-ring[c]	1.25 x 6	6.6×10^{12}	2.4×10^{13}	2.1×10^{4}	2.8×10^{16}	1.0×10^{17}	9.0×10^{7}	1.9
J-tube	5 x 10	4.5×10^{12}	2.4×10^{13}	2.1×10^{4}	1.5×10^{16}	1.0×10^{17}	9.0×10^{7}	1.3
Reactor pool, outside core shroud	[f]	4.2×10^{12}	1.5×10^{13}	1.3×10^{4}	1.8×10^{16}	6.4×10^{16}	5.6×10^{7}	1.2

[a] Insertion of 3.22% Δk/k excess reactivity results in a peak power of 6,400 MW, a total integrated energy release of 43 MW-s, and a

[b] Assumed to be air

[c] A varying number of fuel element positions in the core grid array may be occupied by experiments

[d] The annular volume between the core shroud and the pool tank (10-ft dia.) is available for bulk experiments. Fluxes are given for

[e] Fast neutron dose is converted from n/cm^2 to rads by multiplying the n/cm^2 value by 2.5×10^{-9} rads (air)/(n/cm^2)

[f] Thermal neutron dose is converted from n/cm^2 to rads by multiplying the n/cm^2 value by 3.24×10^{-10} rads (air)/(n/cm^2)

ce for 1.5-MW steady-
rimental dosimetry
el elements).

ion	6,400-MW Pulsing Operation[a]							
	Peak Dose Rate			Dose Per Pulse			n/γ	
	Neutrons, n/cm^2-s			Neutrons, n/cm^2-s				
γ rads[b]/s	Fast (E > 10 keV)	Thermal (E < 0.4 eV)	γ rads[b]/s	Fast (E > 10 keV)	Thermal[b] (E < 0.4 eV)	γ rads[b]	n/cm^2/rads[b] >10 keV	$\frac{rads^b\ (n)}{rads^b\ (\gamma)}$
9×10^4	1.4×10^{17}	1.9×10^{17}	4.2×10^8	9.5×10^{14}	1.2×10^{15}	2.8×10^6	3.4×10^8	0.8
3×10^4	1.3×10^{17}	1.5×10^{17}	3.5×10^8	9.0×10^{14}	9.9×10^{14}	2.4×10^6	3.7×10^8	0.9
6×10^4	1.2×10^{17}	1.3×10^{17}	2.8×10^8	7.7×10^{14}	8.6×10^{14}	1.9×10^6	4.0×10^8	1.0
0×10^4	8.3×10^{16}	1.1×10^{17}	2.1×10^8	5.6×10^{14}	7.3×10^{14}	1.4×10^6	4.0×10^8	1.0
3×10^4	5.2×10^{16}	9.6×10^{16}	1.4×10^8	3.5×10^{14}	6.5×10^{14}	9.5×10^5	3.7×10^8	0.9
1×10^4	2.8×10^{16}	1.0×10^{17}	9.0×10^7	1.9×10^{14}	6.9×10^{14}	6.0×10^5	3.2×10^8	0.8
1×10^4	1.9×10^{16}	1.0×10^{17}	9.0×10^7	1.3×10^{14}	6.9×10^{14}	6.0×10^5	2.2×10^8	0.55
3×10^4	1.8×10^{16}	6.4×10^{16}	5.6×10^7	1.2×10^{14}	4.3×10^{14}	3.7×10^5	3.2×10^8	0.8

MW, a total integrated energy release of 43 MW-s, and a pulse width at half maximum of 6.3 ms

cupied by experiments

s available for bulk experiments. Fluxes are given for a position next to the shroud

value by 2.5×10^{-9} rads (air)/(n/cm^2)

m^2 value by 3.24×10^{-10} rads (air)/(n/cm^2)

2

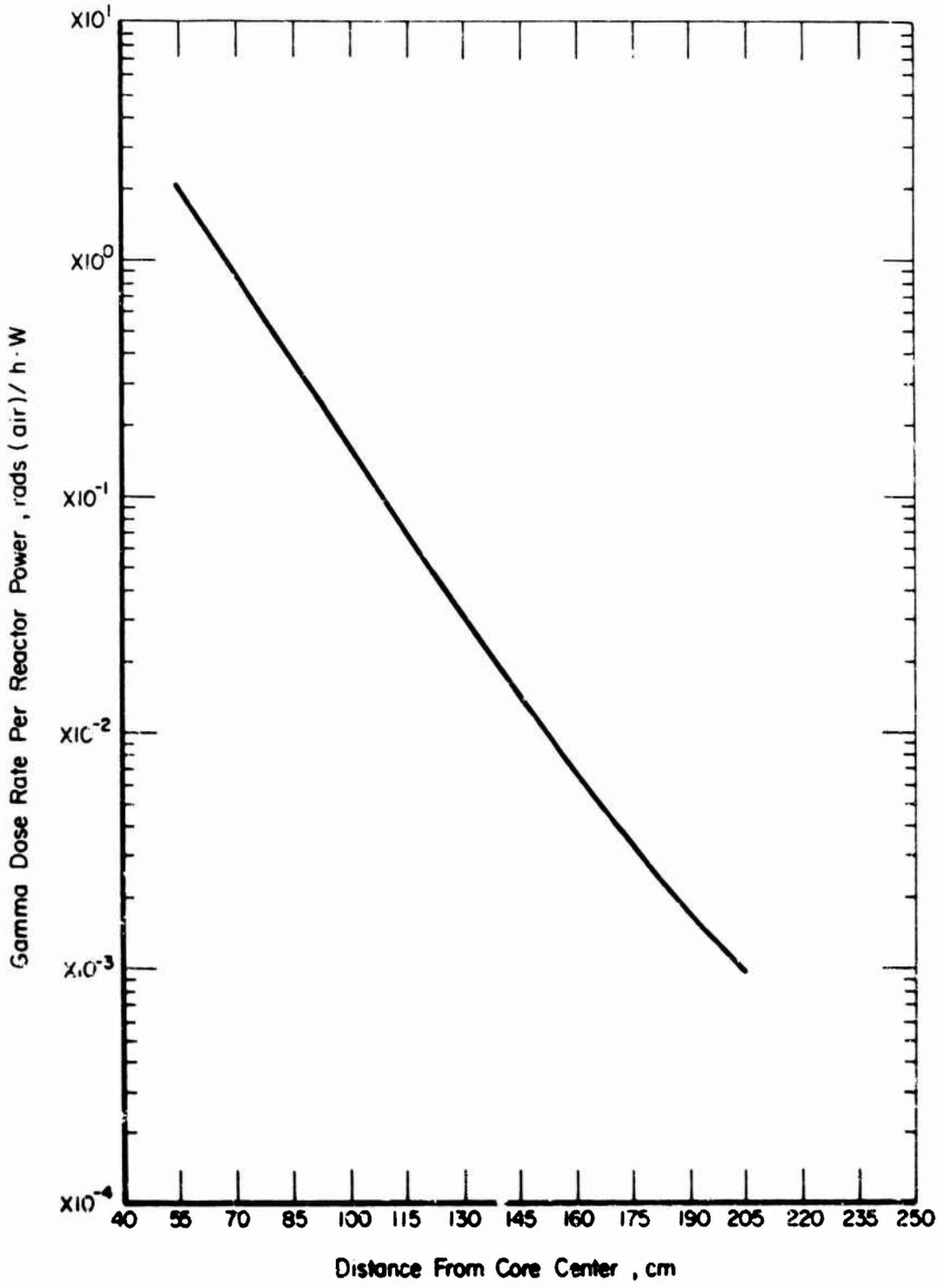

Figure 2-92. γ dose in the water radial from ATPR core.

vehicles and trailers. Power outlets are located throughout the facility. No screen room is available, but experience has shown that RF noise poses no serious problem. Provisions can be made for adequate electrical shielding.

Operating timing signals are available.

The TRIGA facility does not provide dosimetry services but will assist in making subcontracting arrangements.

There is no computer in the reactor building; however, contract arrangements may be made for use of the GA Univac 1108. A light machine shop is available at the facility; GA's heavy machine shop may be used by arrangement. On-site office space and experiment preparation laboratories are available.

2.10.8 Procedural Information

Inquiries related to the use of the TRIGA facility should be directed to:

General Atomic Company
TRIGA Reactor Facility
P.O. Box 81608
San Diego, CA 92138
Telephone: (714) 455-3277
Attn: Mr. J.R. Shoptaugh

A maximum lead time of approximately 3 weeks is required. Costs of using the TRIGA reactors can be obtained directly from GA.

The shipping address is:

General Atomic Company
TRIGA Reactor Facility
10955 John Jay Hopkins Drive
San Diego, CA 92121

The facility is located just a few miles north of San Diego, California. Commuting distances are minimal.

2.10.9 References

1. Coffer, C.O., *Flux Values for the Advanced TRIGA Prototype and TRIGA Mark I Reactors*, Gulf General Atomic Report, GA-6206, Rev., March 15, 1966.

2. *TRIGA Experimental and Irradiation Facilities for Research and Development*, Gulf General Atomic Report, GA-1695, Rev. 5, Nov. 1, 1966.

2.11 SANDIA LABORATORIES ANNULAR CORE PULSE REACTOR (ACPR)

2.11.1 General Characteristics

The ACPR was originally a TRIGA-type reactor; however, it has been recently upgraded to provide improved pulse and steady-state performance (as discussed below). The reactor went critical in April 1978. It is water-cooled and moderated, and fueled with BeO/UO_2 elements arranged in a close-packed lattice. The fuel is enriched to 35% U-235 with 21.5 w/o of UO_2. The height of the core fuel is 52.2 cm with a fuel element dia. of 3.75 cm. The most prominent feature of the facility is a large 23-cm-dia. dry irradiation cavity within the center of the core. The facility also incorporates a large neutron radiography facility external to the core, which is also available to experimenters for irradiation of large items. Samples to be irradiated in the cavity are normally placed within an irradiation container that is 30-cm high and has an I.D. of 20 cm. If an experiment specimen is longer than 30 cm, the upper and lower reflector plugs may be removed. From the horizontal center line of the core to the bottom of the experimental cavity is 117 cm. There is no limitation on the length of experimental samples above the core. Specimens with dia. larger than 23 cm may be irradiated in the radiography facility or outside the reactor core at reduced fluences.

The core structure is located at the bottom of a 3.05-m-dia., 8.50-m-deep stainless-steel water-filled tank. The top of the core is 7.0 m below the surface of the water.

A wide variety of experiment locations may be improvised, and the reactor may be operated in either the steady-state or pulse modes. However, the ACPR is primarily intended to accommodate experiments in the central cavity and operate in the pulse mode, and data presented here are associated primarily with these conditions. If the experimenter requires special conditions, necessary arrangements can be made.

Figure 2-93 shows the reactor building floor plan.

The ACPR is owned by the Department of Energy (DoE) and is operated by Sandia Laboratories in Albuquerque, New Mexico. The reactor is located in Building 6588, Technical Area V of Kirtland (East) Air Force Base. The ACPR is used in a continuing program of fundamental and applied research in radiation effects. Its design is such that a wide variety of experiments can be accommodated.

The main feature of the reactor is the 23-cm-dia. dry-experiment cavity, which occupies the center region of the reactor core. In this large hexagonal cavity, experiments can be exposed to a neutron fluence in excess of 8×10^{15} n/cm^2 in a single pulse. Access to the central irradiation cavity is provided by a vertical loading tube and an offset loading tube which join together in a "Y" fitting about 2.4 m above the core. Both tubes are fabricated from 25-cm-I.D. stainless-steel pipes. The inside of the pipe provides adequate clearance for passage of an experiment 23 cm in dia. through the curved sections. About 30 cm above the core, a transition occurs in the pipe. The cylindrical tube is converted into a hexagonal tube to match the pattern of the fuel elements. Thus, the

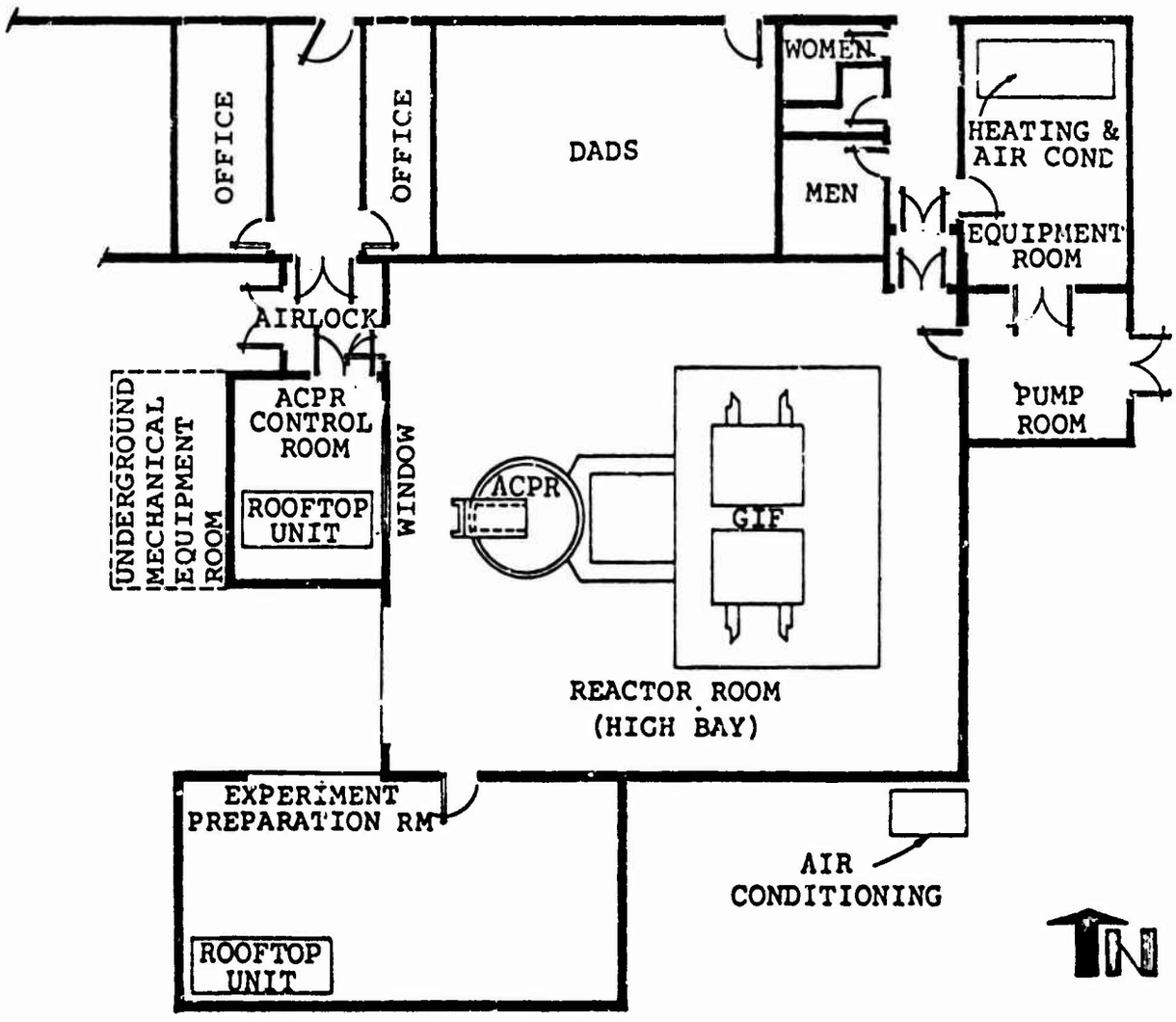

Figure 2-93. Floor plan of Building 6588.

thickness of water between the inner row of fuel elements and the cavity is kept uniformly small to maximize the fast flux.

A facility for post-irradiation experiment storage is located in the upper section of the offset loading tube. This section consists of 4 stainless-steel tubes 25 cm in dia. extended downward approximately 5 m from the upper section of the offset loading tube. Experiments may be stored in this section until sufficient radioactive decay has taken place to allow convenient handling and removal. The storage section provides space to store several experiments at a depth of more than 6.5 m below the water level. Shielding within the storage section is provided by lead plugs which can be located over the storage positions.

The fuel in the ACPR is a BeO-UO_2 sintered ceramic composite material. The fuel is contained in a ribbed Nb liner and sealed in a 0.5-mm-thick stainless-steel cladding. The ribs of the Nb liner maintain inert-gas-filled insulating

gaps between the fuel and the liner and between the liner and the cladding. The fuel elements are 3.75 cm in dia. and have an overall length of 73 cm.

The fuel elements are arranged on a triangular spacing grid to form a hexagonal pattern of fuel surrounding the experiment tube. The operational core loading of the reactor comprises 210 to 220 fuel elements, 6 fuel-followed control rods, 2 fuel-followed safety rods, and 3 adjustable transient rods. Reflector elements of Ni are used to decouple the core from the surrounding water. With this core size, the energy released for a reactivity insertion of $2.70 is about 400 MW-s, with a reactor period of 2.2 ms. Under these conditions, the fuel reaches a maximum adiabatic temperature of 1,400°C.

The principal safety feature of the ACPR reactor is the large prompt negative temperature coefficient of reactivity. This temperature coefficient arises primarily from Doppler absorption in the U-238 resonances and decreased scattering in the BeO matrix resulting from the heating of the fuel material. The coefficient is prompt because the U-235 is intimately mixed with the U-238 and the BeO; thus, the fuel and BeO temperatures rise simultaneously.

In addition to the inherent prompt shutdown process, certain protective features are built into the reactor control system and plant protection system that will automatically limit the power and temperature levels at which the reactor can be operated or which will prevent operation if certain conditions have not been met. These protective features consist of scrams, trips, and alarms which are preset to alarm and/or shutdown the reactor if prescribed limits are approached or exceeded. The scrams and alarms vary with the mode of operation.

The control system permits the operator to manipulate, monitor, and control the reactor. The primary components of the control system are the nuclear channels and the regulating rod drive circuits which permit manual and automatic actuation of the control-rod drives, safety-rod drives, and the transient-rod system, guided by information received from the nuclear instrumentation.

The regulating system has 2 operating regimes: steady-state, and pulse. In the steady-state regime, there are 2 operating modes: steady-state, and positive period. In the pulse regime, there are 5 operating modes: normal pulse, multiple pulse, repetitive pulse, reduced tail pulse, and continuous transient-rod bank withdrawal. Pulse modes permit the reactor power to increase on periods less than the period at prompt critical. Additional modes of operation have been provided for in the design of the console. With additional hardware and safety analyses, these modes will be available. Included are pulse from high steady-state power and high-power, square-wave operation.

Six motor-driven control rods govern the reactor power during delayed critical operations. The control rods are fuel-follower-type rods, wherein the reactivity effect of removing the poison as the rod is withdrawn is augmented by the simultaneous insertion of the fuel-follower section. These control rods pass through and are guided by holes in the top and bottom grid plates. Two motor-driven safety rods are used as safety features and also to reduce the system reactivity in the pre-pulse period.

The adjustable transient rods on the ACPR are actuated by an electro-pneumatic system. The mechanical-drive system permits the transient rods to be used in the steady-state mode as well as in the pulse mode of operation. In the pulse mode, the adjustable drive systems are utilized to adjust reactivity so that any size pulse may be fired, starting with the transient rods in a banked mode.

2.11.2 Operating Characteristics

All of the results presented in this section are calculated results, or results derived from the fuels testing program or early operational data.

2.11.3 Power Level and Energy Release

Peak-pulse power depends primarily on the reactivity insertion. Typical pulse characteristics are as follows:

1.	Reactivity insertion	\$2.95
2.	Peak power	29,500 MW
3.	Pulse width (FWHM)	6.5 ms
4.	Reactor period	1.7 ms
5.	Fluence, cavity	
	a. Fast (>10 keV)	3.7×10^{15} n/cm^2
	b. All energies	6.3×10^{15} n/cm^2
	c. γ dose	3.3 mrad (H_2O)
6.	Maximum fuel temperature	1,400°C
7.	Energy release	400 MW-s
8.	Maximum reactivity insertion rate	>\$50/s

Characteristics of steady-state operation are:

1.	Power	2.0 MW
2.	Flux, cavity	
	a. Fast (>10 keV)	2.3×10^{13} n/cm^2-s
	b. All energies	3.9×10^{13} n/cm^2-s
	c. γ dose rate	2.2×10^{4} rad/s

Figures 2-94 and 2-95 show the peak reactor power and the total pulse energy release as a function of reactivity insertion.

2.11.4 Energy Release

Characteristics of the pulse, including prompt energy release, pulse width (FWHM), the "tail" energy, and the peak power, depend primarily upon the reactivity insertion. As a result, pulse characteristics can be varied over a wide range within the technical specifications of the facility.

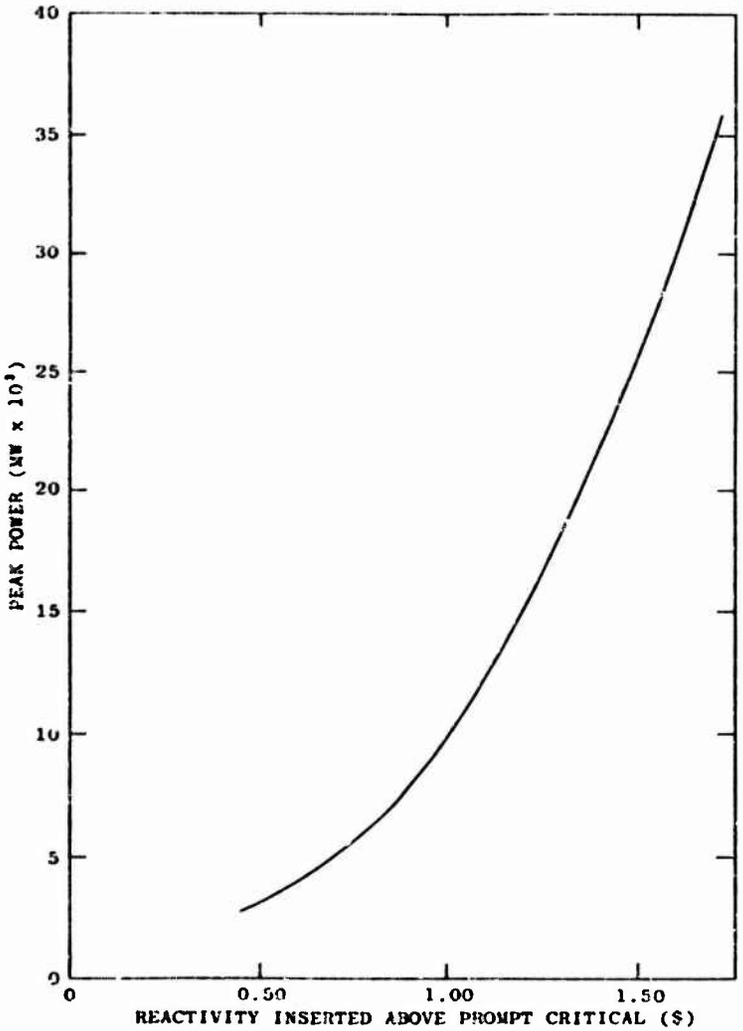

Figure 2-94. Peak power as a function of reactivity insertion.

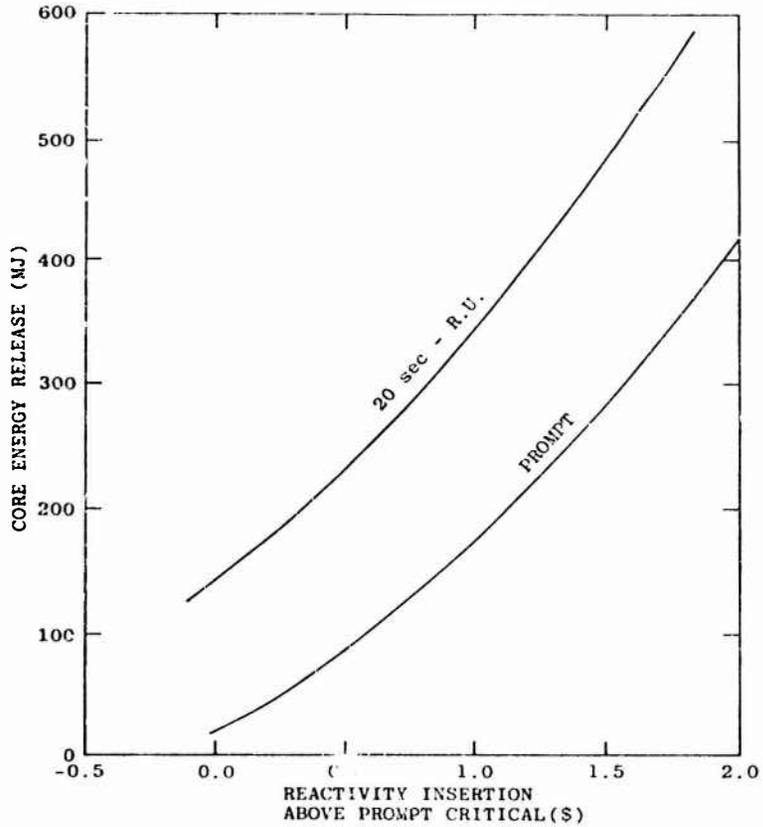

Figure 2-95. Core energy release as a function of reactivity insertion (upper energy release value is calculated for rods held out for 20 s after pulse initiation).

Figures 2-96 through 2-99 summarize these various pulse characteristics. Figures 2-100 and 2-101 give the fuel temperatures as a function of pulse and steady-state operation.

2.11.5 Pulse-Repetition Rate and Pulse Predictability

Pulse-repetition rate is determined by the repeatability required between the first pulse and subsequent pulses. If the experiment can tolerate a $2.70 first pulse, then the repetition rate can be set for the experimenter's particular requirements.

Pulses may be generated as rapidly as every 4 min but at reduced fluence, power, etc. levels. Pulses are predictable to within 5%.

2.11.6 Multiple Pulse Mode

The multiple pulse mode produces 2 or 3 pulses in rapid succession by sequencing the withdrawal of the 3 transient rods. Any combination of rods and timing may be used to achieve the desired fluence and time dependence. The rods may be fired separately or 2 rods may be fired at the same time as a first or second pulse. Figures 2-102 and 2-103 give the power profile and reactor yield for the triple pulse.

2.11.7 Transient Rod Runout Mode

The transient rod runout mode provides the capability to produce high reactor powers over a period of several s. The transient rods are withdrawn using the electro-mechanical drives instead of the pneumatic system. The withdrawal can be pre-programmed to insert the reactivity in a variety of sequences. Figure 2-104 gives the power history for 1 transient rod withdrawal sequence and Figure 2-105 gives the reactor yield for the sequence.

2.11.8 Tolerable Reactivity Worth of Experimental Sample

The maximum available excess reactivity is $12.00. Experiments must be secured if the reactivity worth of the experiment is more negative than $2.70. There is no limitation on reactivity worth of secured experiments. Movable experiments or experiments with movable parts are limited such that combined insertion of experiment and transient rods is less than $2.70.

An assessment of sample reactivity worth and the associated tolerable limit will be made by the reactor staff for each experiment conducted.

2.11.9 Environment

2.11.9.1 Neutron Fluence

Neutron fluence data are quantitatively presented in Figure 2-106. The calculations are free-field, i.e., unperturbed by experiments, etc. The fluence and flux profiles in the cavity for the fast and thermal components of the spectrum are given in Figures 2-107 and 2-108.

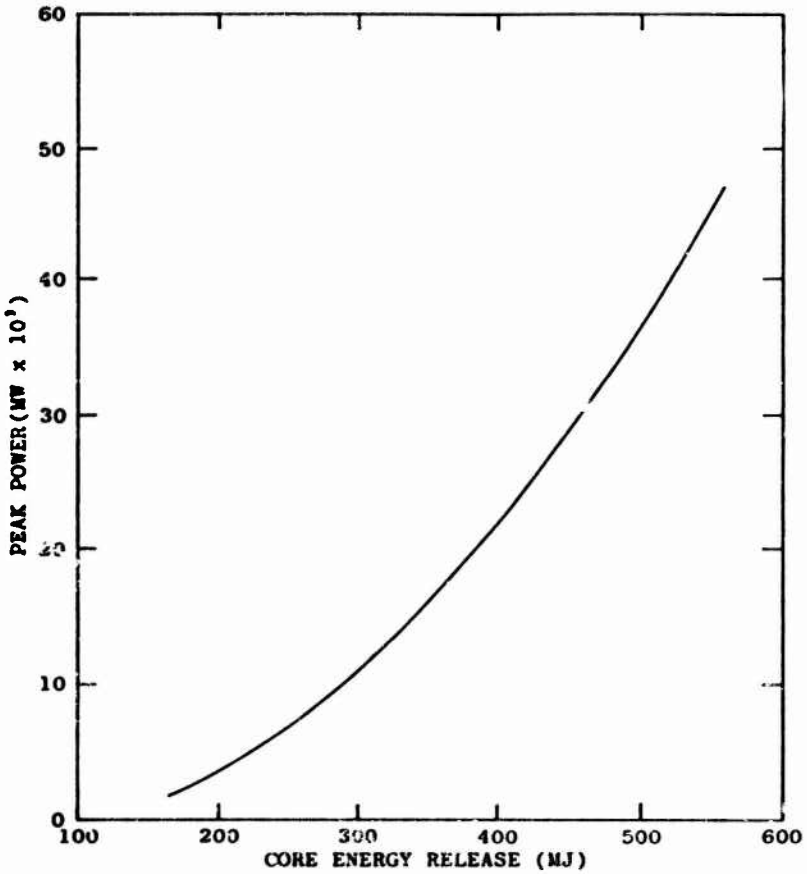

Figure 2-96. Peak power occurring in pulse versus energy release (rods held out for 20 s).

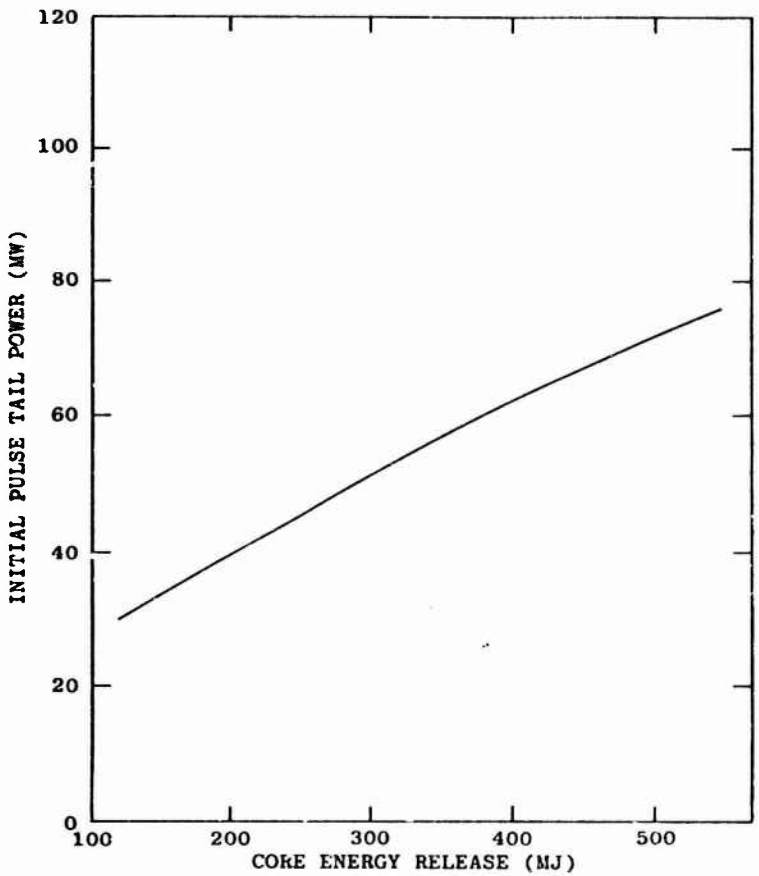

Figure 2-97. Initial power level in pulse tail versus core energy release (rods held out for 20 s).

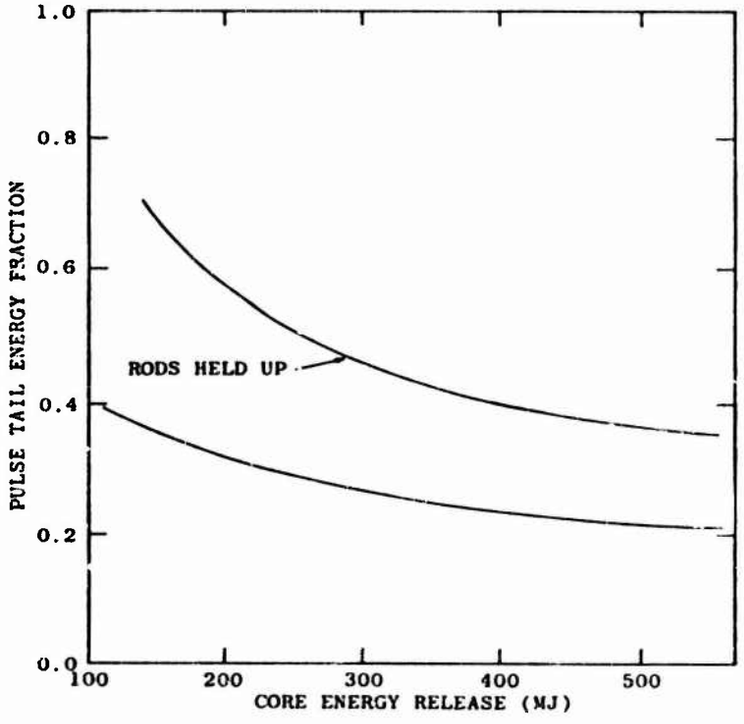

Figure 2-98. Fraction of energy in pulse tail versus total core energy release.

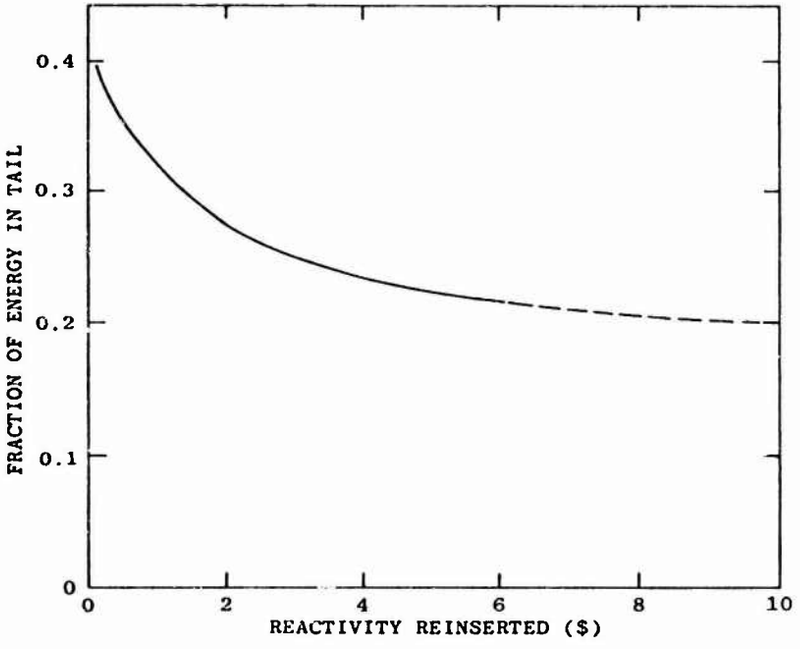

Figure 2-99. Effect of the magnitude of reactivity reinserted in 1.0 s at a delay time of 1.5 s ($2.50 pulse) versus fraction of energy yield in tail.

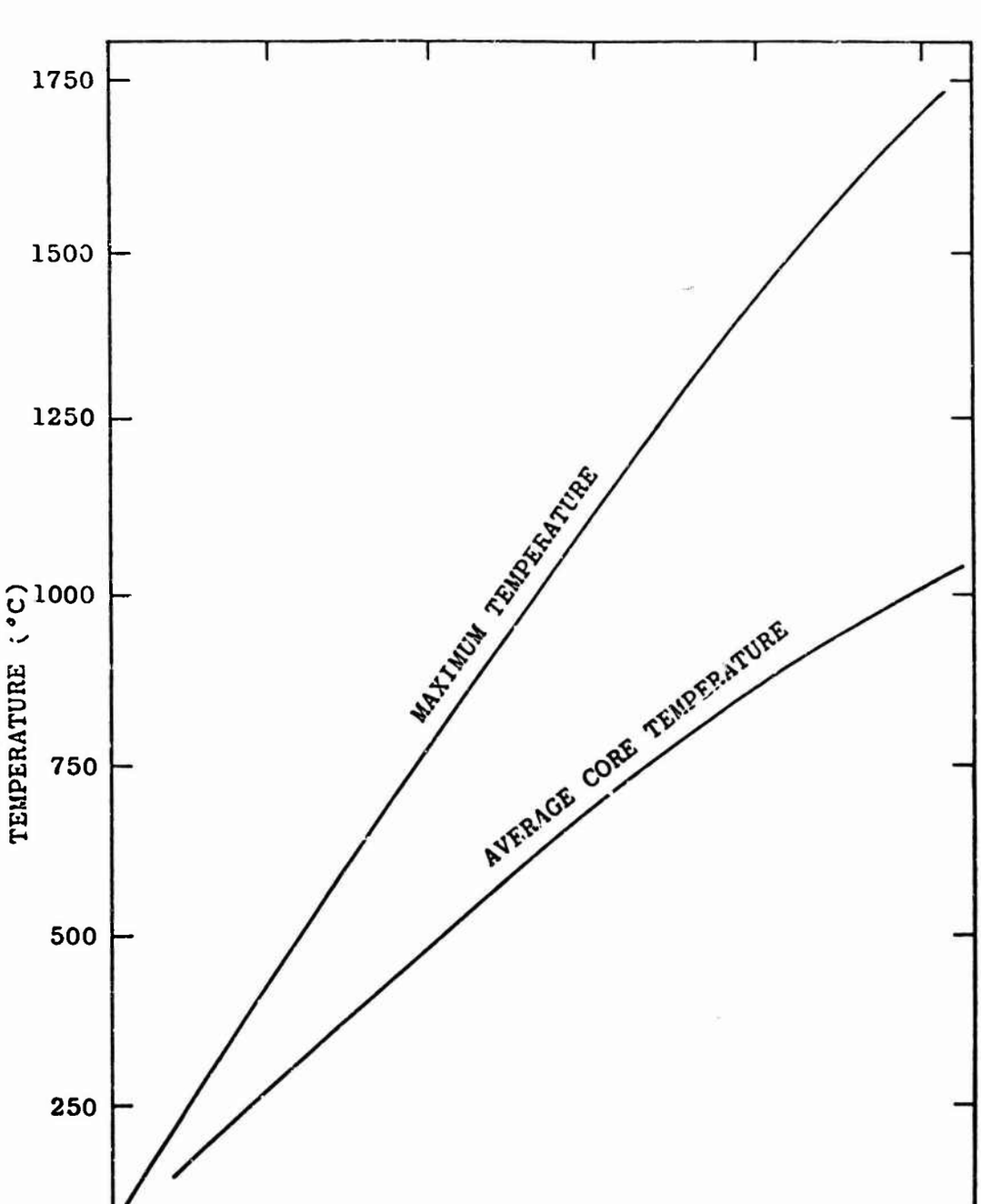

Figure 2-100. Maximum fuel temperature occurring in pulse versus core energy release (rods held out or rods reinserted).

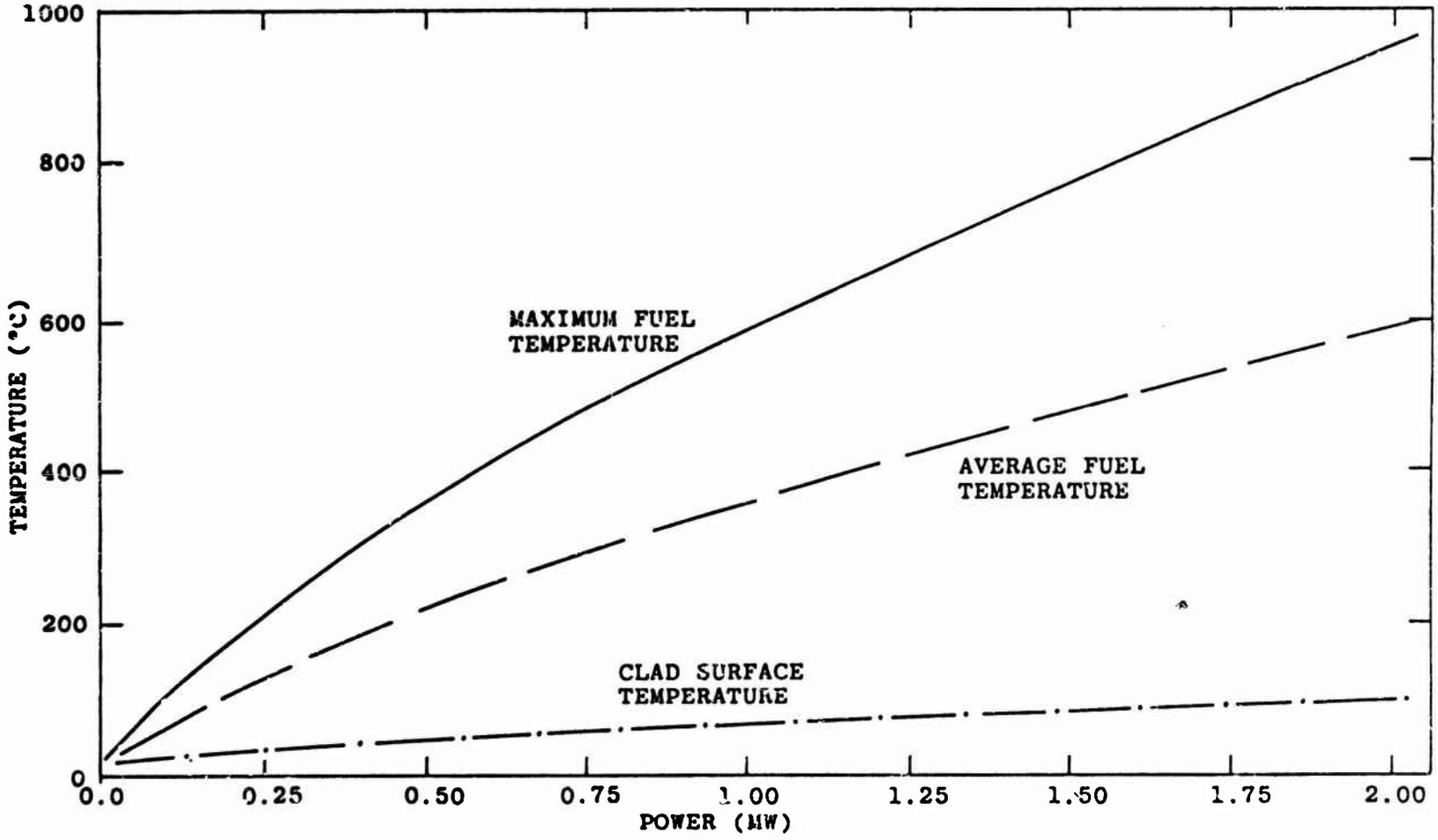

Figure 2-101. Steady-state fuel and clad temperatures.

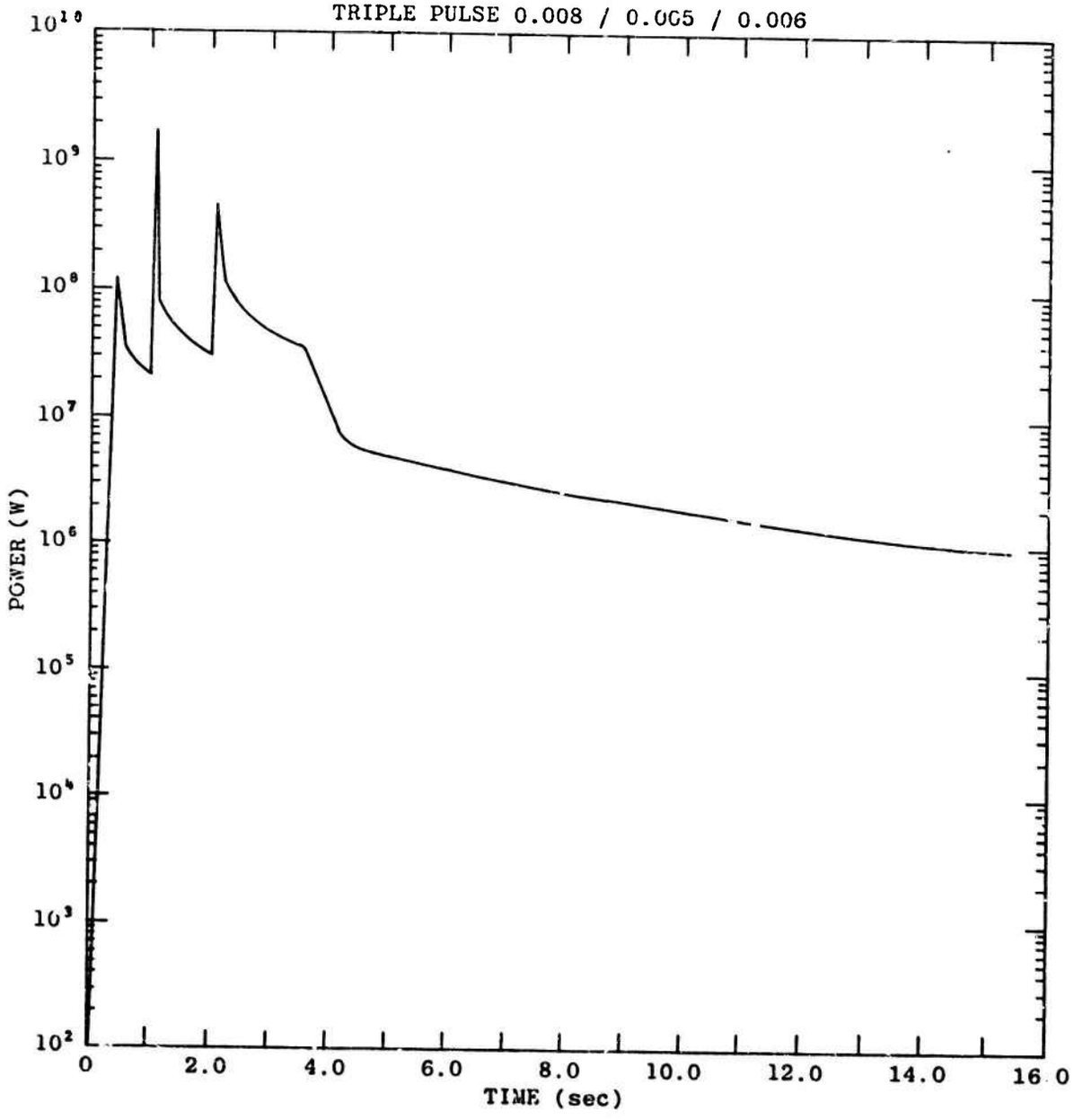

Figure 2-102. ACPR upgrade triple pulse ($1.1/$0.68/ $0.82 α_2, PK1D).

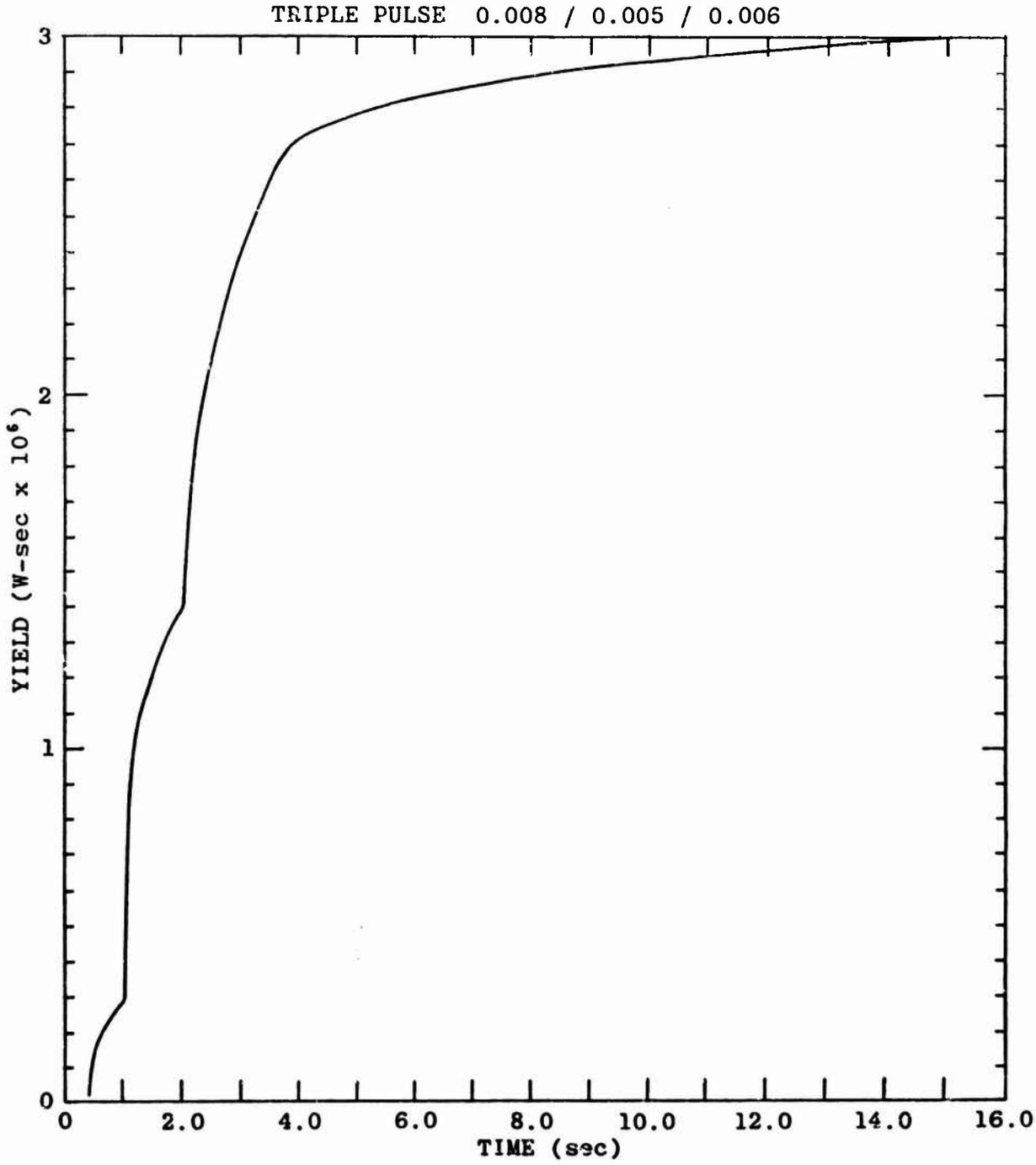

Figure 2-103. Reactor yield versus time for ACPR upgrade triple pulse.

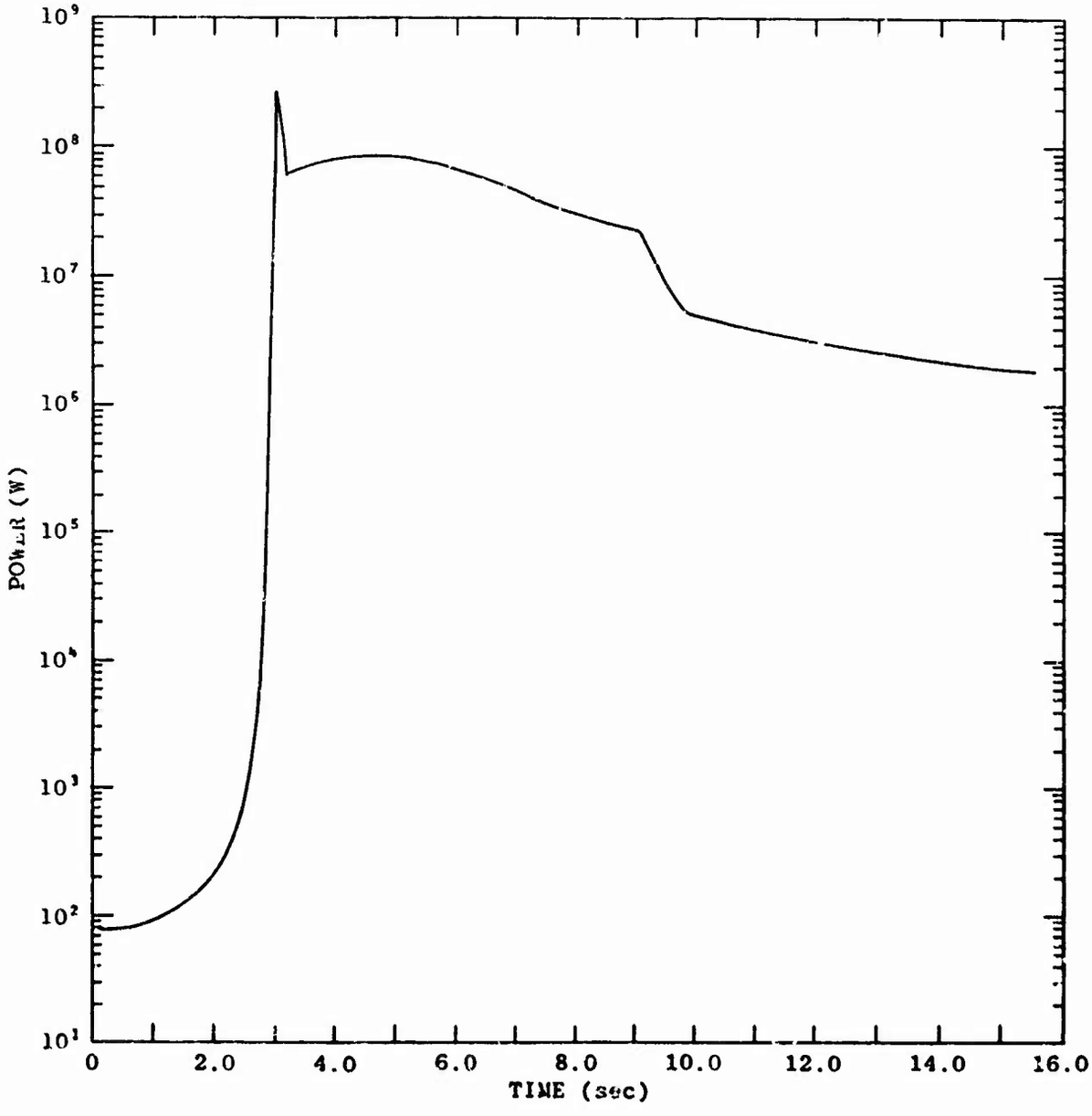

Figure 2-104. Reactor power history for transient rod runout ($3/7 s, BeO-2, PK1D).

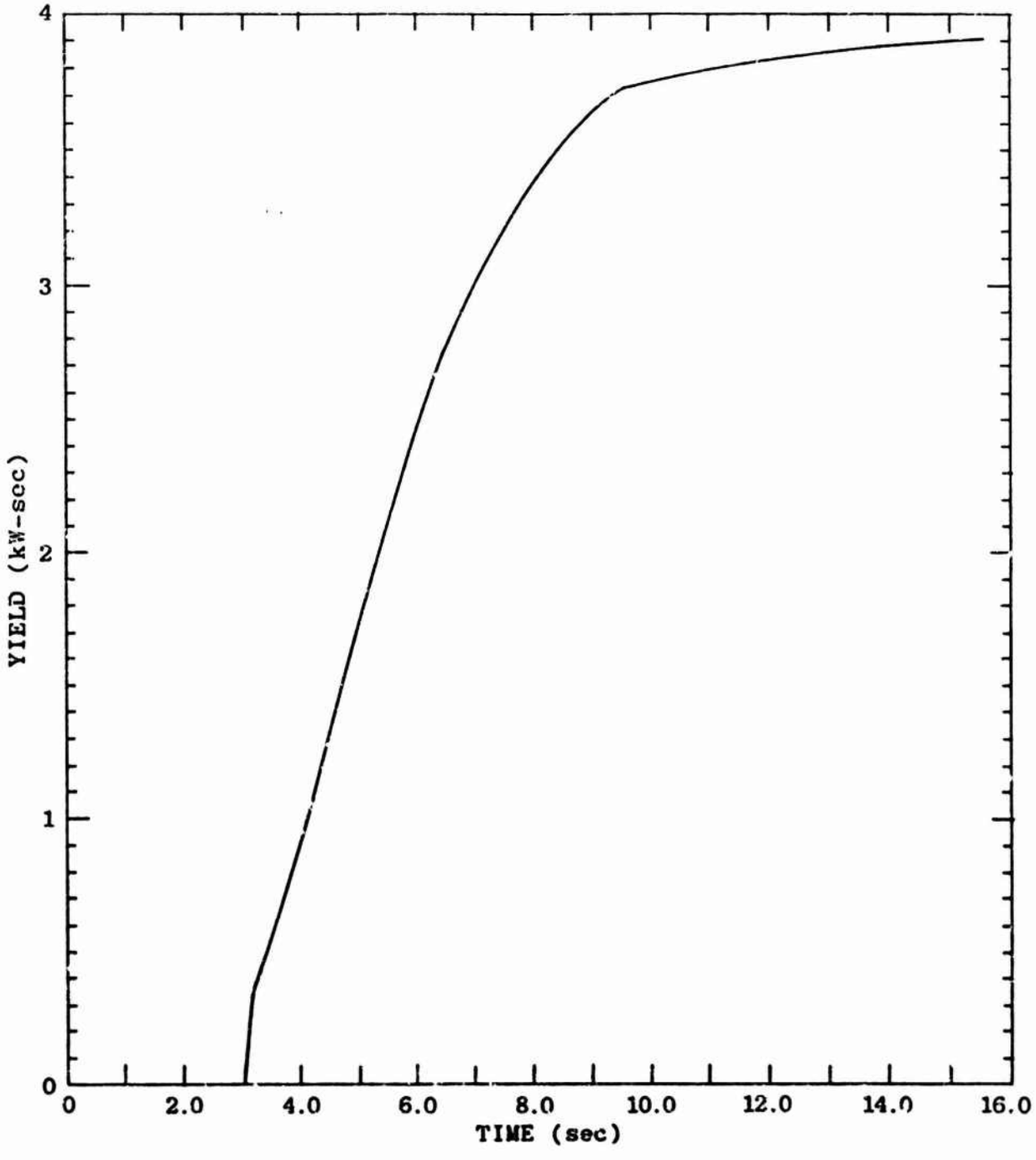

Figure 2-105. Reactor yield versus time for transient rod runout operation.

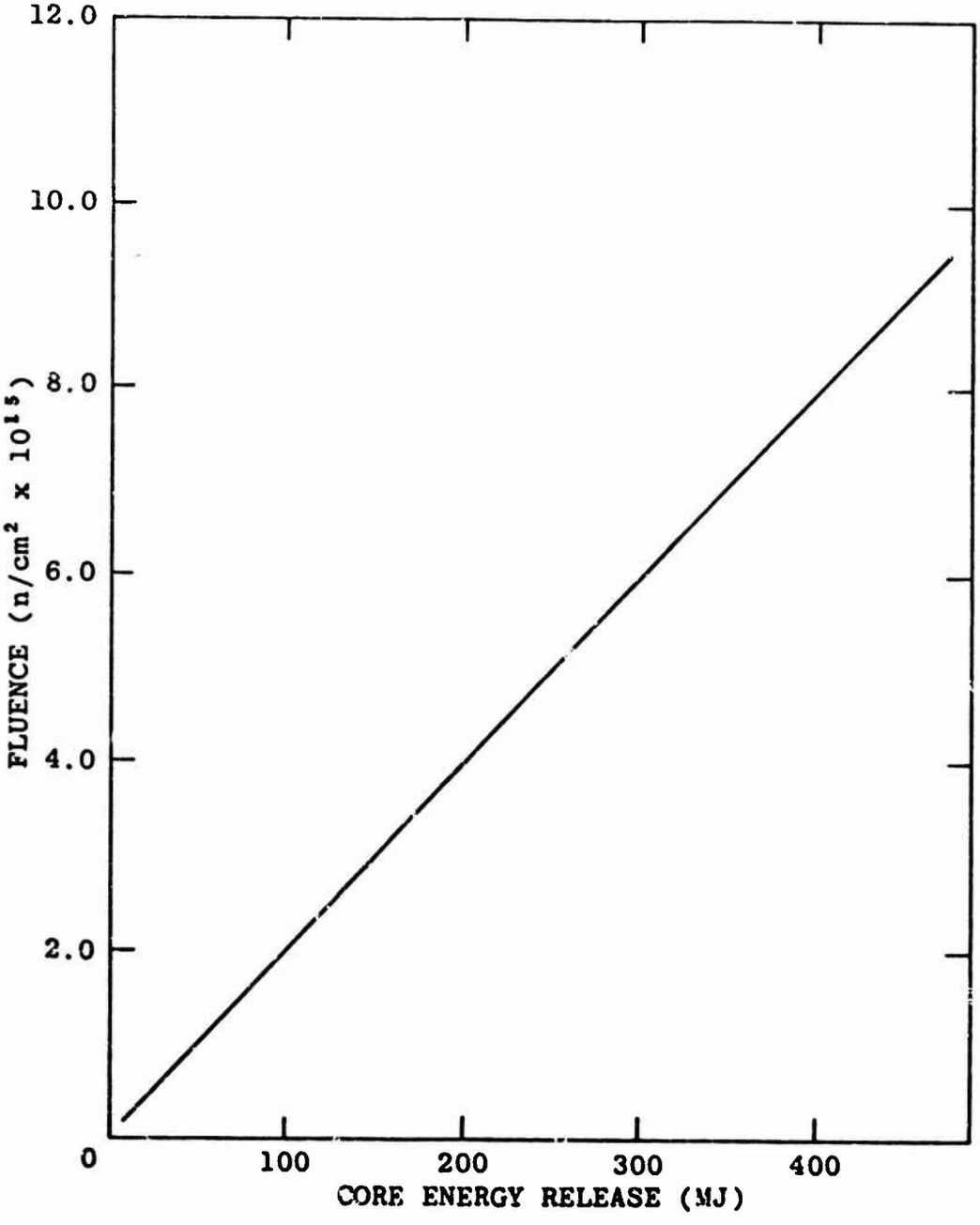

Figure 2-106. Total pulse fluence versus energy release (normalized to S_6 - TH♦TRAN).

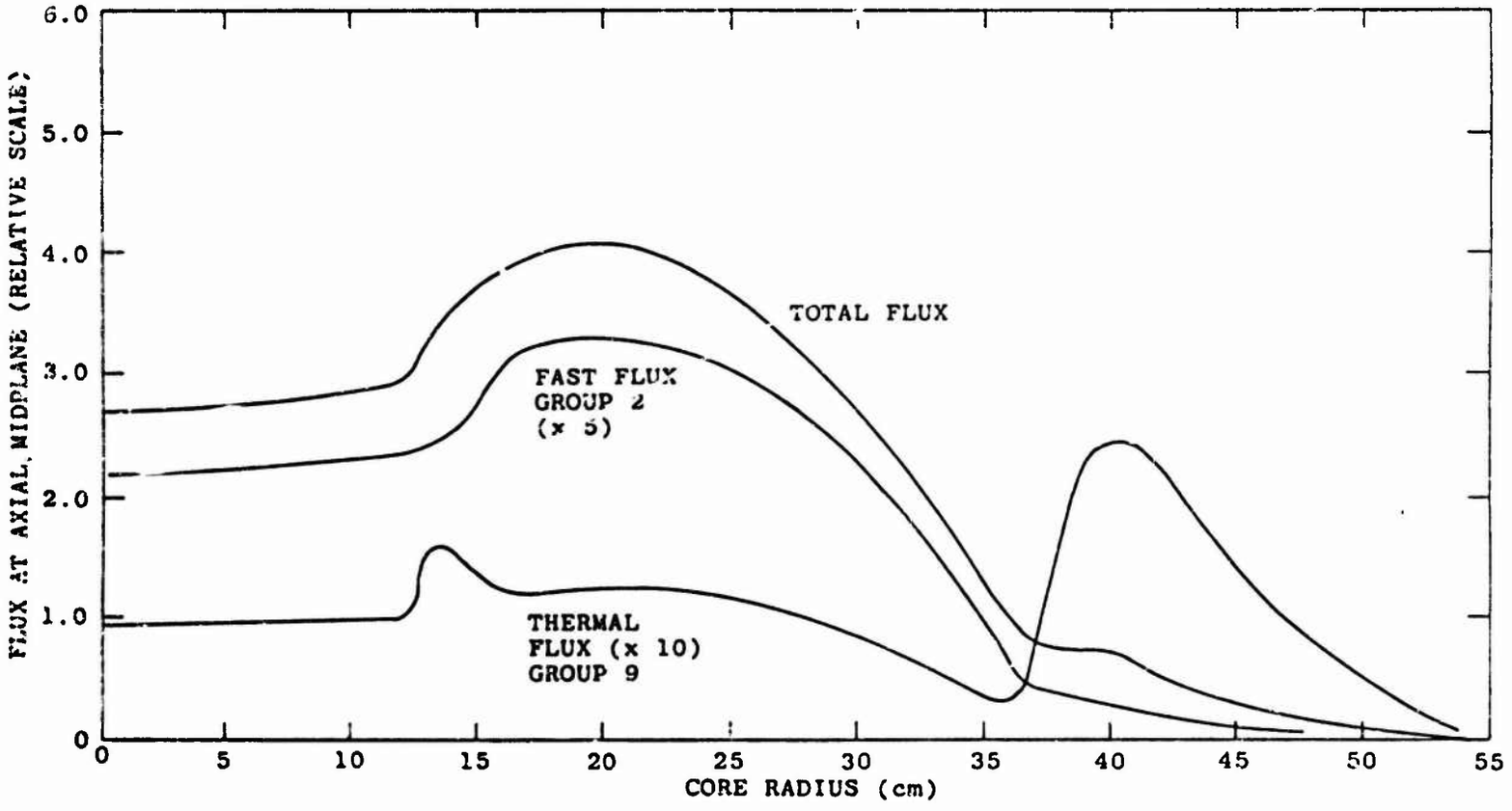

Figure 2-107. Flux at axial midplane in ACPR upgrade (group 1, 14.9 → 1.35 MeV; group 9, 0.005 → 0.06 eV).

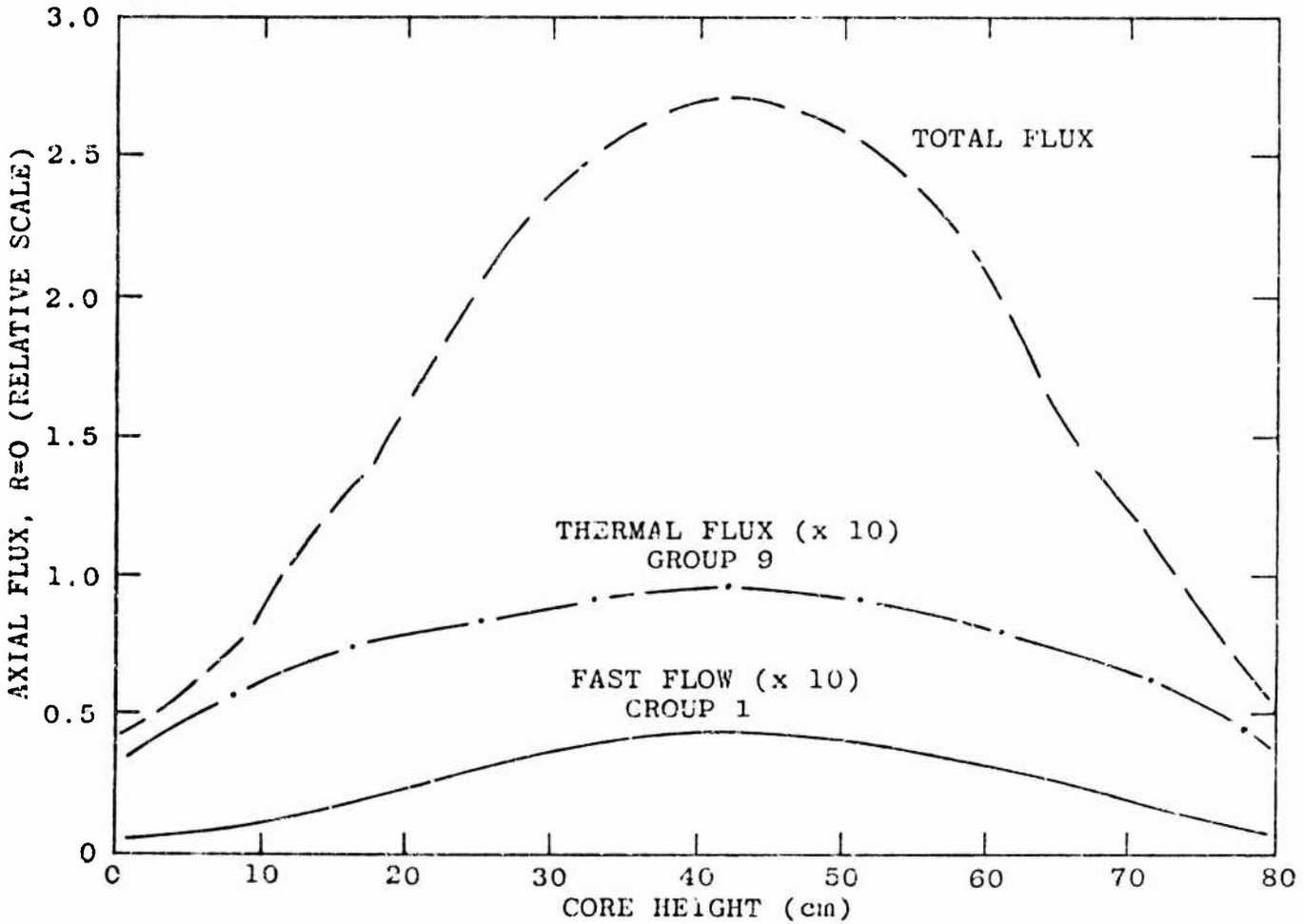

Figure 2-108. Axial flux in cavity of ACPR upgrade.

2.11.9.2 Neutron Energy Spectra

Figure 2-109 shows the integral free-field cavity fluence for all neutron energies. Figures 2-110 and 2-111 give the calculated energy group fractions and the flux per unit energy.

2.11.9.3 Gamma Fluence

No calculations have been made on the γ yield at this time. However, it is estimated that the γ dose will be approximately the same, or slightly less than, the old ACPR (see Figure 2-112 for γ dose data on the old reactor).

2.11.9.4 Background Radiation Doses

Background radiation doses vary from about 1 to 10 rad, depending on core history prior to the experiment run and the length of time the experiment is in the experiment cavity.

2.11.10 Special Capabilities

2.11.10.1 Radiography Facility

The neutron radiography facility is primarily used for nondestructive testing and evaluation of various components, including components containing or composed of high explosives. It is located on the north side of the core and consists of an experiment chamber at core level, a tube with a collimator to bring the neutrons to a stage at the top of the reactor tank, and the support plate and blast shield.

The basic design provides a collimated beam of thermal neutrons such that the flux over the irradiation area is constant. Other features incorporated in the design are the provision for a large irradiation space near the reactor core, and control of the environment inside the tube. The facility is independent of the reactor with respect to mechanical, electrical, and pneumatic functions. All mechanical hardware, such as the vertical tube and upper blast shield, are designed and tested to assure isolation of the reactor safety components from any malfunction of the facility or experiment. It is designed to withstand accidental detonation of an explosive component. The operating limit for the radiography facility is 250 g HE. A safety factor of 4 on material ultimate strain was utilized to determine the operating limit for the facility. The total HE load limit for the High Bay is 500 g HE.

The experiment chamber is constructed of Al plate and has a dry central area with a square cross-sectional area 37.5 cm on a side. From the core horizontal center line to the bottom of the chamber is 46.5 cm. There is no restriction in the upward direction.

The radiography tube is constructed of stainless-steel plate with rib stiffeners. It has 3 sections for ease in fabrication and assembly. A collimator assembly fits down in the radiography tube and has neutron and γ shielding in the form of Cd, Gd, BN, polyethylene, and Pb. A remotely controlled rotatable

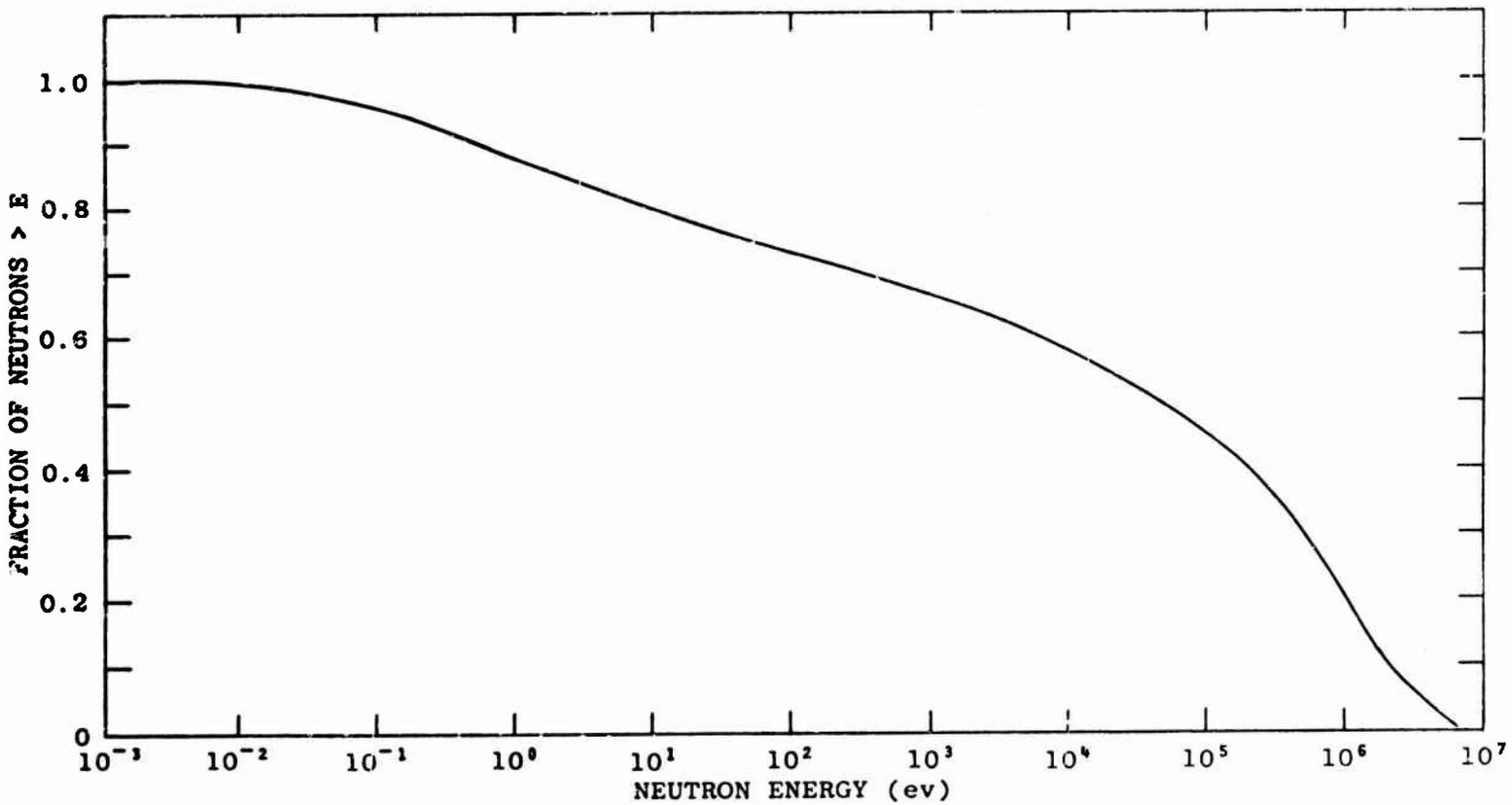

Figure 2-109. Integral neutron spectrum in ACPR cavity.

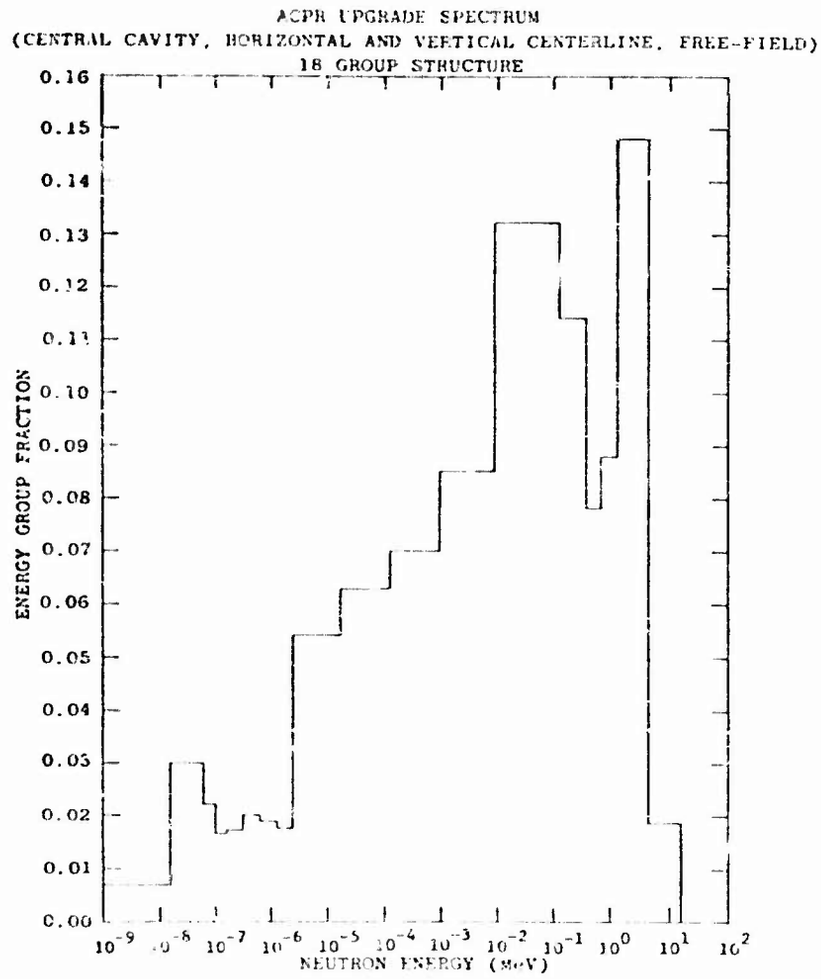

Figure 2-110. Cavity flux spectrum in ACPR upgrade (TWϕTRAN - S_4, P_1, 18 group).

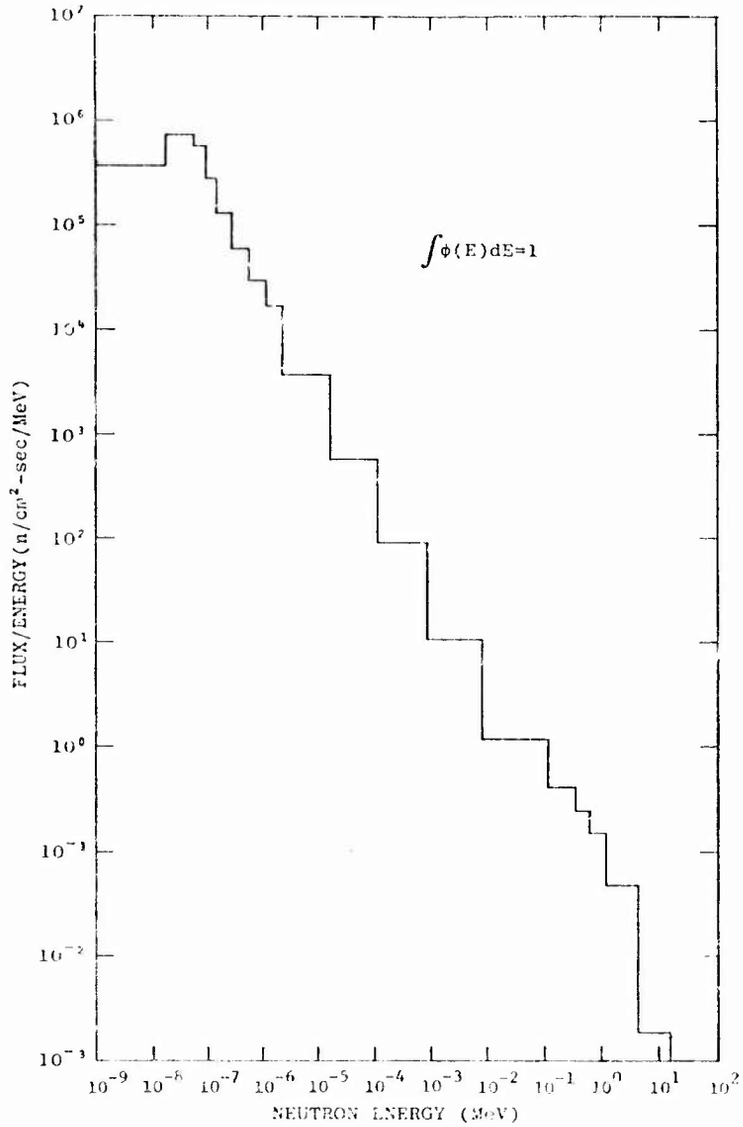

Figure 2-111. Differential energy flux for ACPR upgrade.

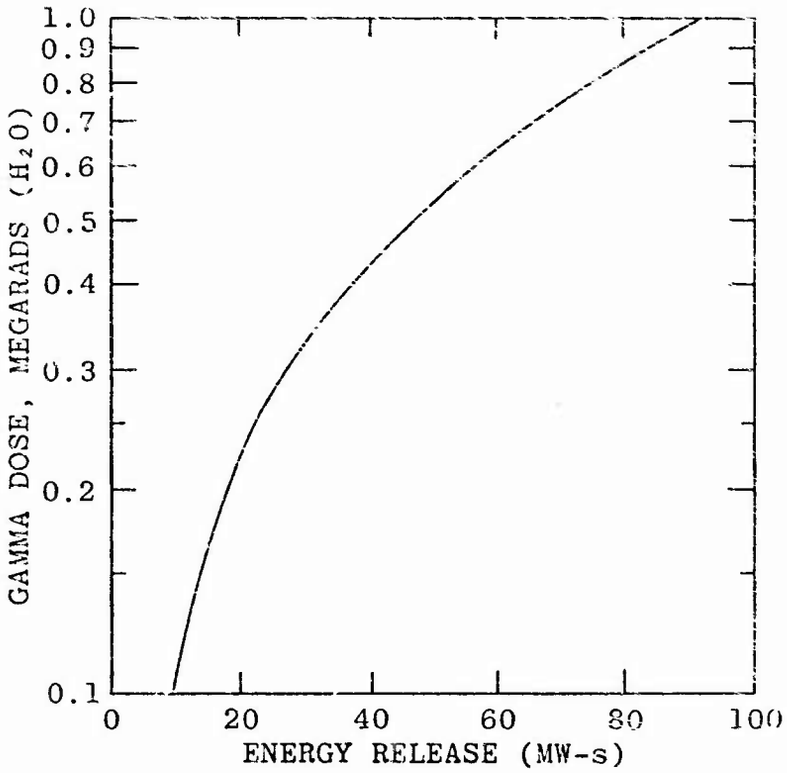

Figure 2-112. Cavity γ dose versus pulse energy release.

cylinder with different size apertures is used to select the desired collimator ratio and to block the neutrons when the system is not in use. The radiography tube is supported by 2 I-beams attached to the tank wall and the transient rod support bridge.

A 2.54-cm-thick steel plate supports the blast shield. The blast shield is constructed of steel plates and I-beams and incorporates a layer of borated polyethylene and a layer of Pb for neutron and γ shielding. The blast shield is approximately 90 cm on a side and covers the upper end of the radiography tube and the stage.

The experiment chamber is equipped with the necessary piping to purge the cavity portion of the experiment chamber to prevent buildup of Ar-41. The experiment chamber exhaust line is connected into the Ar purge system which discharges through a pre-filter, 2 absolute HEPA filters and 2 charcoal filters. The radiography tube is designed to be flooded, gas filled, or evacuated.

The Nondestructive Testing Division is responsible for performing the explosive handling and setup and the film cassette handling and development. To have radiography performed by the ACPR, contact the Nondestructive Testing Division directly and they will perform a safety analysis and schedule the reactor for the required time.

Table 2-46 provides some of the facility specifications. Note that the fluxes are related to a power level of 300 kW which was for the old ACPR. The new ACPR will operate at a power level of 2 MW. So for an approximate value of fluxes, use a factor of 6 for the new reactor. This may tend to give a slightly greater flux than will be measured because the core size has changed significantly and the experiment chamber is somewhat further from the core and has the Ni reflector between it and the fuel elements.

Table 2-46. ACPR radiography facility specifications.

	Collimator Ratio (L/D)			
	65/1	150/1	250/1	500/1
Neutron Beam Flux - Power 300 kW (n/cm^2-s)	1.3×10^7	2.7×10^6	1.1×10^6	2.7×10^5
n/γ Ratio (n/cm^2-mr)	1.6×10^6	1.3×10^6	1.3×10^6	9.3×10^5
Exposure Port Dia. (cm)	15.25	26.4	26.4	26.4
Exposure Area (cm^2)	180	548	548	548
Cd Ratio	15	>15	>15	>15
Resolution for 2.54 cm Object to Film Detector Plane Distance (mm)	0.381	0.170	0.102	0.051
Exposure Time for Single-Coated R Film - Density 3 Background (min)	~4	~60	~90	~300

Notes: 1. All values are for He-filled tube.
2. Exposure time is for ½-mil Gd converter screen.

2.11.10.2 Flexo-Rabbit System

The Flexo-Rabbit system provides a valuable sample delivery facility for the ACPR without requiring any structural modifications. Samples 2.06 cm in dia. by 5.84-cm long can be contained in molded polyethylene shuttle capsules. Flexibility of the system is provided by the design of the irradiation end which can be placed at various locations in the reactor core. Typical applications include neutron activation analysis, study of short-lived isotopes, and exposure of small samples requiring high fluxes of thermal neutrons.

Gas pressure from a standard N gas cylinder operates the Flexo-Rabbit's shuttle capsule. N is preferred over air to prevent the buildup of Ar-41. As a general rule, there is no radioactivity in the N exhaust gas. However, the exhaust gas is dumped into the Ar purge system and exhausted through the filter banks.

The use of gas pressure results in much faster transfer of samples than can be obtained by using a vacuum system for the propelling force. A gas regulator with a large orifice is used to maximize the gas flow and thus minimize the sample transfer time. Under the normal operating pressure of 25 psi, the capsule will travel the 12.2 m from the core to the receiver in about 500 ms. Travel time will vary according to gas pressure, sample weight, and direction of the capsule.

Three basic components make up the Flexo-Rabbit system: the irradiation end piece, the tubing system, and the control unit. These components are described in the following sections.

The 4.57-m-long irradiation end piece is Al throughout. The lower end of the unit has the basic configuration of a fuel element and will fit directly into any fuel element position in the core grid plate with the irradiation end normally located in core position 253. In this location, the fast neutron flux ratio of cavity to rabbit is between 1.60 and 1.70, depending on the control rod positioning. Internal stops assure that the sample is positioned at the core center line. Pb weights encased in Al tubes above the core are used to overcome buoyancy effects. An offset of 15.24 cm in the irradiation end piece prevents direct radiation streaming from the core. The upper end of the unit is joined to the flexible tubing system. Two interconnected flexible tubes, a sample loader, and a dropout receiver make up the tubing system. The larger of the flexible tubes (2.86 cm I.D.) carries the shuttle capsule, while the smaller tube supplies and exhausts the driving gas. Normally, the tubing system is about 12.2-m long, but it can be lengthened to extend the distance from the reactor area to the handling area. Since the irradiation end extends about 4 m above the core before the transition is made from Al to polyethylene, the flexible tubing should not experience any radiation damage. The sample-loading end of the tubing system terminates in a quick-opening loader, which is mounted to a Pb brick so that the top can be opened with one hand. This loader also lends itself to operation by tongs or a remote manipulator.

Returning from the irradiation end, the sample enters the receiver which is especially useful for working with short-lived isotopes. This receiver permits the shuttle capsule to drop out of a tube, thus providing rapid access upon return from irradiation. To minimize the shock of the shuttle capsule returning at high speed, an air cushion has been incorporated into the dropout unit. This permits the sample to slow up momentarily upon its return and then drop out of the receiver under its own weight. Shock to the returning shuttle capsule can be minimized by the air cushion unit if desired, or the speed of the return can be maximized if preferred. The air-cushion and dropout time are controlled by a N-operated valve located on the receiver. Valve operating pressure is about 50 psi. The shuttle capsule normally drops into a large volume box which has a shielding equivalent of 7.6 cm of Pb. Approval of the Environmental Health Group is required before the capsules can be removed from this box.

With the exception of loading the sample, selecting the exposure period, activating the start switch, and recovering the sample from the dropout unit, the operation of the Flexo-Rabbit system is fully automatic. Interruption of the automatic cycle at any time to return the capsule may be accomplished by a switch on the control unit. Manual operation is similar to automatic operation except

the length of the irradiation period is controlled manually rather than by the timer.

Three signal outputs are available from the connectors at the control unit: (1) the start of the irradiation time, (2) the end of the irradiation period, and (3) the arrival of the sample at the receiver. These signals may be used to perform various functions, as might be required.

2.11.11 Support Capabilities

With the exception of radiological and toxicological safety and services of the Sandia Laboratories Dosimetry Counting Laboratory, Sandia personnel should not be expected to provide scientific, technical, or engineering consulting services or support to non-Sandia users of the ACPR facility.

2.11.11.1 Staff

A permanent operating staff is assigned to the ACPR. These personnel are available to assist the experimenter in determining and establishing the correct experiment setup.

The Sandia technical staff, which is competent in all phases of radiation effects, including TREE, is available only for consulting services on an occasional and limited basis unless contractual arrangements are made for special services. If special staff or manpower assistance is required, arrangements for these should be included in contractual negotiations.

2.11.11.2 Electronics

Monitoring equipment for ACPR experiments is normally provided by the user. A limited number of oscilloscopes and visicorders are presently available in the reactor high bay. Sandia Laboratories field test organization has located several instrumentation vans in Technical Area-V (TA-V) to support the reactor facilities. This support capability is available to perform data acquisition functions. However, experiments should not rely on the availability of Sandia equipment unless prior arrangements have been made.

Outlets for 110-V, 1-ϕ, and 220-V, 3-ϕ ac power are located throughout the building. Space is provided for an instrumentation trailer if one is required by the experimenter; however, the experimenter must provide his own trailer. Two Appleton 100-A, 220-V, 3-ϕ female connectors are installed to provide electrical power to the trailer location. Power cables should not be less than 30 ft in length and should terminate in a compatible Appleton connector.

2.11.11.3 Timing Signals

Precise 12-V step-timing signals of from 0 to 1 s from the reactor electrical timer can be furnished, in increments of 1 ms, prior to the pulse. Other timing requirements must be arranged for through prior consultation.

2.11.11.4 Dosimetry

The Sandia Laboratories Dosimetry Counting Laboratory is available for use by all ACPR experimenters. Standard threshold foil techniques are used for neutron fluence measurements. Gamma measurements are made using CaF_2 Thermoluminescent Dosimetry (TLD). Sandia Laboratories will provide detectors for all users and the Counting Laboratory will evaluate results. However, the experimenter has the option of performing his own dosimetry.

2.11.11.5 Computational Facilities

Calculational facilities are available at the ACPR site. The Sandia Laboratories Computational Laboratory, although not normally available to non-Sandia users of the ACPR, may be utilized on a limited basis by prearrangement. A terminal is available in TA-V which inputs the CDC 6600's and the 7600 for unclassified programs. Various outputs are available.

The TA-V Data Acquisition and Display System (DADS) is located near the ACPR facility. This system, built around the EMR 6130 digital computer, accepts either digital or analog inputs from remote consoles. Digital or analog outputs are available on a CRT display, magnetic tape, or in printed form. The DADS is available to all ACPR experimenters. One of the remote consoles is located at the ACPR facility.

2.11.11.6 Shop Facilities

Light machine shop facilities are available at the site.

2.11.11.7 Experiment Preparation Laboratories

The ACPR high-bay area contains floor space of approximately 20 ft x 20 ft immediately adjacent to the reactor pool for experimenter's equipment.

2.11.11.8 Photographic Equipment and Materials

Experimenters normally are required to provide their own photographic equipment and material. Cameras are included, however, with all available Sandia oscilloscopes. Please check with Security before bringing photographic equipment into the area.

2.11.12 Procedural Information

Services of the ACPR facility are available to agencies of the DoE, DoD, and private corporations having DoE or DoD contracts. ACPR availability is on a basis of non-interference with DoE programs. Technical and administrative inquiries related to use of the ACPR should be directed to:

Supervisor
Sandia Laboratories
Reactor Applications Division 5451
P.O. Box 5800

Kirtland Air Force Base (East)
Albuquerque, NM 87115
Telephone: (505) 264-3304 or 8991

2.11.12.1 Scheduling

An experiment-request form (Figure 2-113) must be submitted several weeks in advance. The scheduling of reactor time is not considered until after the experiment-request form is received and final approval of the contract is given.

Ordinarily, experiment plans should be sufficiently detailed to allow effects of the specimen on the reactor characteristics to be determined. However, care should be taken to ensure that the experiment plan contains no classified information.

2.11.12.2 Cost Information

Costs and charges associated with the use of the ACPR have been established and are available directly from the Reactor Applications Division.

2.11.12.3 Shipping Address

Shipments should be directed to:

Supervisor
Sandia Laboratories
Division 5451
P.O. Box 5800
Kirtland Air Force Base (East)
Albuquerque, NM 87115

2.11.13 Applicability and Availability

The ACPR facility provides a transient radiation environment readily applicable to TREE experiments. The facility is available to authorized users on the basis of non-interference with Sandia programs. A competent operating and supervisory staff is permanently assigned to the facility. The technical staff of Sandia Laboratories is competent in all phases of TREE research and experimentation. The experimenter should be aware, however, that this staff does not provide routine assistance to non-Sandia users of the facility.

The ACPR is located in TA-V, which is an isolated experiment area 6 mi south of the main Sandia Laboratory, making it necessary for experimenters to provide their own daily transportation.

2.11.14 Security Clearance

Security clearances are required to gain unescorted access to the ACPR facility. Visitors with a Q-clearance or a DoD Secret clearance with a Restricted Data certification may have unescorted access to the ACPR. Visitors without the above clearances must be escorted while in the security area. Visitor Control must be contacted to arrange for access to the laboratory.

ANNULAR CORE PULSE REACTOR

EXPERIMENT PLAN
(Complete both sides)

To: ACPR Control
Div. 5451
Ext. 264-8991

From: _____ Project Leader
_____ Org.
_____ Ext.

_____ Case No.
_____ Part No.

Title of Experiment: _____

Unusual Requirement: _____

_____

Number of pulses desired and exposure level: _____

_____

Date experiment to be irradiated: _____ Security Classification: _____

Dimensions, maximum overall: _____

Dosimetry Required: (____) Neutron (____) Gamma

Composition of sample (major elements): _____ Mass: _____

Solid ( ) Liquid ( )

Is Liquid: Completely contained? ( ) Yes ( ) No

Unstable in any way? ( ) Yes ( ) No

Approx. melting point: _____ °C

* Is the test item or its associated test gear a safety hazard? i.e., does test item contain toxic materials, fissile materials, explosive material or large energy storage devices, or highly flammable material? (____) Yes (____) No If answer is Yes, complete other side.

		DOSIMETRY DATA		
Date	Requested by	Run	Neutron	Gamma

Experiment Approval:

Operations _____ Health Physics _____ Committee _____

*NOTE: Must be answered.

Figure 2-113. Experiment request plan.

TEST ITEM CONTAINS.

1. Highly flammable material (____) Yes (____) No _____Material

2. Toxic material (____) Yes (____) No _____Material

3. Fissile material_____U235 _____Pu239 _____U233 _____ number of grams

4. Internal electrical power sources

   Specify: (voltage and capacitances)

   _____

5. High internal pressure

   Specify: _____Pressure _____Volume _____Gas

6. Explosive Device name and number_____

   A. Type:

Purpose	Explosive	Grams	Remarks
Primer or IP	_____	_____	_____
Booster	_____	_____	_____
Base charge	_____	_____	_____
Pyrotechnic	_____	_____	_____
Propellant	_____	_____	_____
Total charge	_____	_____	_____

   B. Bridge-wire information:

      Does test item contain a bridge-wire? (____) Yes (____) No

      Is bridge-wire shorted and grounded to case? (____) Yes (____) No

      Nominal bridge-wire resistance:_____ ohms

      Current in amperes_____ No fire _____ All fire

      Power in watts _____ No fire _____ All fire

   C. Initiation sensitivity:

      _____Static _____Spark _____Shock

   D. Quantities: Building 6588 ACPR * _____

      Number to be exposed together _____ (Total Charge:_____)

7. Comment _____

8. Requester Signature _____Org._____Date_____

Approvals:

_____9381

_____3513

_____5451

_____Requester Project Leader

_____Appropriate Reactor Committee

*Usually Bldg. 6588 ACPR will only be used for non-destructive testing and short time storage of radioactive test items.

Figure 2-113. (continued).

2.12 STATE UNIVERSITY OF NEW YORK AT BUFFALO REACTOR

2.12.1 Characteristics

The Nuclear Science & Technology Facility Reactor is a 2-MW, open-tank-type reactor built by AMF Atomics. The present core went critical on June 22, 1964. Fuel is 6% enriched UO_2 clad with zircaloy. A fuel element consists of a bundle of 25 fuel pins in a 5 x 5 array. The minimum critical configuration consists of 16 elements in a 4 x 4 array. A more typical core would consist of 22 elements containing a total of 320 kg of UO_2. Control is attained with 5 blade-type control rods and 1 pulse rod. Moderation and cooling is provided by light water. Core reflection may consist of light water, graphite, aluminum, or a combination of these.

The core is fixed in the center of an approximately 7-ft-dia. tank. The upper half of the tank widens to approximately 7 x 14 ft. Distance from grid plate to top of tank is about 26.5 ft. Two sides of the core are utilized by beam tubes and pneumatic conveyors. A third side is used by the thermal column. The remaining side has a voidable tank which couples the core to the dry exposure chamber.

2.12.1.1 Beam Tubes

Five beam tubes are available. Four 6-in. tubes occupy the north face of the core. The south face has one 6-in. tube. The tubes are at various elevations with respect to the grid plate. The tubes have two steps which increase their size at the outer end to facilitate shielding. The tubes terminate at the outer face of the concrete reactor shield. The total length of the tubes is about 9.5 ft. When not in use, the tubes are sealed with Al cans filled with concrete, a Pb plug, and the remaining space is filled with water. Permanent plumbing provides for venting, filling, and draining of the beam tubes. Normally, no attempt is made to circulate or otherwise control the atmosphere in the beam tubes. Experiments to be placed in a beam tube should be at least 0.25-in. less than the nominal size of the tube to ensure passage. If it is necessary to bring wires or other leads out of the tube, special shielding is required. Slotted plugs are available for the 6-in. tubes, which will accommodate a 1-in.-dia. bundle. Also useful is a Pb shutter that can be hung on the wall over the beam tube. The shutter can be raised vertically and provides 3.5 in. of Pb shielding. A cask is available for either experiment transfer or tube shielding purposes. The cask is mounted on a wheeled dolly. It has an inside volume of 12 in. x 12 in. x 13 in. deep. It provides 3 in. of Pb except for the rear wall which has 3.5 in. Additional shielding can be made from Pb bricks, concrete blocks, or high-density aggregate.

2.12.1.2 Thermal Column

A horizontal thermal column occupies the west face of the core. It is centered and symmetrical about this face. A 5-in.-wide water gap exists between the core and the end of the column. Between the water gap and the tank wall is a graphite-filled pyramidal frustum 2 ft x 3 in. thick. Outside the 0.5-in.-thick Al tank wall there is a 4 ft x 4 ft x 5 ft-deep cavity filled with graphite bars

and surrounded by an Al liner and high-density concrete. A space 23-in. deep is available behind the graphite for locating samples. Access to the column is obtained by removing a 52.5-in.-thick, high-density concrete plug which is motor driven on rails. Four of the graphite bars are removable. The removable bars are in 2 pieces. If the outer piece is removed, a cavity 2-ft deep is created. If both sections are removed, a cavity extends to the reactor tank. Each bar is 4 in^2. The graphite can be entirely removed from the outer section of the column. This gives a higher flux but at the expense of fast-to-slow ratio and increased γ dose. Table 2-47 gives some quantitative data.

Electrical and other leads are easily brought out through the shield, eitner by not closing the plug tightly and coming out underneath the plug, or by using ports in the plug and auxiliary shielding.

Table 2-47. Thermal column fluxes.

Position	Flux ($n/cm^2/s$)
Outer face center	1.47×10^7
Outer face center backed with 4 in. of paraffin	5.68×10^7
2 ft into column backed with graphite stringer	8.77×10^8
At tank wall backed with graphite stringer	3.15×10^{10}
Tube	1.75×10^9

Conditions:
- Reactor Power at 2 MW
- Loading Number 23
- May, 196[illegible]
- Co Foil Detector
- Pb γ shield removed from pool

2.12.1.3 Pneumatic Conveyor

The pneumatic system is used to position small samples at the side of the core. The "rabbit" is made of molded polyethylene and has screw-on end caps. The inside volume is a cylinder 1.25 in. in dia. x 6 in. long. Two systems share a common blower. Conveyor Number 1 has its sending station between Laboratories 103 and 104 on the γ deck. The Pb-shielded return box is also located between the laboratories with a door opening into each laboratory. Both laboratories have fume hoods at the return box for proper handling of the sample. Conveyor Number 2 has its operating station against the tank shield near Laboratory 104 on the γ deck. Again, the return box is shielded and is in a fume hood. Conveyor Number 1

terminates at the north face of the core and Conveyor Number 2 terminates at the south face. The irradiation position is about 3 in. from the core and is about the mid plane. Rabbits are dispatched by push-button and can be returned either manually or by use of a preset timer. Two timers are available; one has a range of 0 to 20 min, and the other has a range of 0 to 5 hr. Return time for a rabbit is less than 3 s for System Number 1 and less than 5 s for System Number 2. Because of radiation damage to the rabbit, single irradiations are normally kept to less than 4 hr. Samples used in a rabbit should be encapsulated. The encapsulation could be a polyethylene bottle, a polyethylene sealed bag, or a quartz ampoule. Unless padded, a sample receives severe mechanical shock at the core and receiving stations. Figure 2-114 and Table 2-48 give some thermal neutron and γ flux data for the rabbit tubes.

2.12.1.4 Fission Plate

A fission plate 13-in. long x 13-in. high x 0.5-in. thick is available for use in the thermal column or square beam tube. It contains 1,040 g of 89.82% enriched U encapsulated in Al.

The conversion ratio of incident thermal flux to emitted fast flux is approximately 1 to 1. The plate is useful in experiments that require a fast flux of known spectral characteristics. Because the plate can be used only at the outer face of the thermal column, only rather low thermal fluxes are available to drive it.

2.12.1.5 Reactor Pulse Characteristics

The Pulstar reactor has the ability to pulse as well as operate at high steady-state levels. This feature is provided by a pulse rod and associated instrumentation systems. Pulsing is presently done using a 20-element core in a 4 x 5 array. The maximum pulse permissible has a peak power of 2,000 MW and an energy release of approximately 35 MW-s. Pulse width at half height is approximately 15 ms; the lower the peak power, the wider the pulse. Total energy released is, therefore, not proportional to peak power. The maximum pulse repetition rate is 3/hr.

Fluence in a pulse can be estimated from the pulse energy released and the known steady-state flux in the position of interest. Experiments can be exposed in any of the normally available facilities, except those located within the core.

2.12.2 Applicability and Availability

The facility is primarily a steady-state reactor. The reactor could be set up for pulsing if the need were sufficiently great. Address inquiries to:

Philip M. Orlosky
Operations Manager
State University of New York at Buffalo
Rotary Road
Buffalo, NY 14214
Telephone: (716) 831-2326

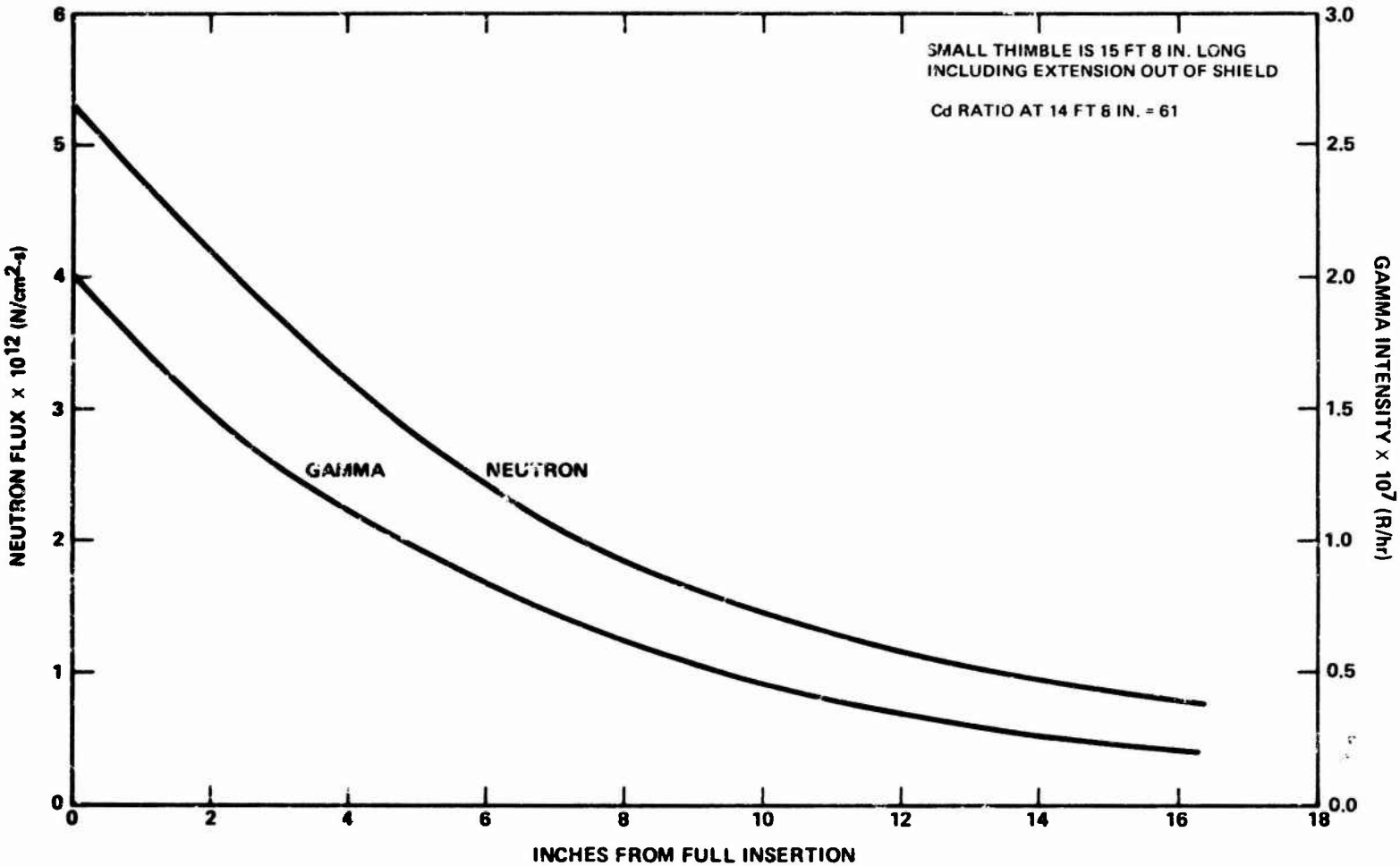

Figure 2-114. Thermal flux and γ intensity in the dry fast rabbit facility.

Table 2-48. Thermal neutron and γ fluxes in the fast rabbit tubes.

Tube	Neutron ($\times 10^{12}$ nv)	Gamma ($\times 10^{7}$ R/hr)
1	2.96	1.90
2	1.15	1.00
3	2.15	1.43
4	3.24	1.79
5	1.07	1.18
6	1.71	1.43

Power: 2×10^{6} watts
Loading: 66-G-4-A
Date: June 24, 1968
Pair combinations: 1-4, 2-5, 3-6

2.13 AFRRI REACTOR FACILITY

2.13.1 Characteristics

The AFRRI-TRIGA is a TRIGA MARK F thermal research reactor installed in 1962 with its original Al-clad fuel. In 1965, stainless-steel-clad fuel was installed, and that core is still in use today. The core consists of 84 TRIGA standard elements and 4 TRIGA-instrumented elements, each containing 3 chromelalumel thermocouples. The fuel material is 8.5 w/o U in ZrH_2, with U maximum enriched to a nominal 20%.

The experimental facilities consist of 2 large exposure rooms, a pneumatic transfer system for irradiation of small samples with a capability to direct the irradiated samples to the hot cell for remote manipulation, and some facilities for in-pool irradiations.

2.13.2 Test Parameters

The TRIGA MARK F can operate at a steady-state power level of 1 MW for extended periods of time, or can be pulsed to provide short bursts of radiation for experimental use. The maximum pulse allowed is $3.28 from a steady-state power level less than 1 kW, with the total power not to exceed 33 MW-s. However, in practicality, the maximum pulse which can be obtained is about $2.90, which provides a rise to 1,800 MW, with a FWHM of about 10 ms. Pulses are generally initiated from a power level of 15 W for consistency, and are generally reproducible within several percent. Depending on the size of the pulse, it takes from 20 min to 1 hr to get set up for another pulse.

2.13.3 Support Capabilities

The reactor facility staff consists of only operations personnel. All support activities such as health physics and dosimetry are consolidated, and support the entire institute. Their services are available to support work at the reactor with prior scheduling and coordination.

2.13.4 Procedural Information

More information can be obtained by contacting Lieutenant Colonel Edwin T. Still at (202) 295-0227. For technical information, contact Captain Ronald E. Schaffer at (202) 295-1290. At least 1 month is required to schedule a new experiment, but after the experiment has been approved, a lead time of 1 week is generally sufficient. The cost of the reactor is $88.00/hr plus an additional 20% for dosimetry support. The address is:

AFRRI
Building 42
NNMC
Bethesda, MD 20014

2.14 UNIVERSITY OF WISCONSIN TRIGA NUCLEAR REACTOR FACILITY

2.14.1 Characteristics

This is a U-ZrH_2 fueled TRIGA-type thermal reactor immersed in a pool with four 6-in. beam ports, thermal column, and in-pool irradiation facilities.

2.14.2 Test Parameters

Test parameters are as follows:

1. 1,000 kW steady state; pulses of up to 900 MW (12.2 MW-s).
2. Excess reactivity is 3.8% $\Delta K/K$; maximum pulse reactivity is 1.4% $\Delta K/K$.
3. 3.8-ms initial period, 15-ms FWHM.
4. Capable of approximately 4 highly reproducible pulses/hr.

2.14.3 Support Capabilities

Typical University Research Reactor staffing and facilities are available. Contact R.J. Cashwell, Reactor Supervisor.

The operating schedule is very flexible. The price list is as follows:

1.	Irradiations	
	a. Pneumatic tube	$ 66.00/hr (Minimum $5.00)
	b. Whale and porpoise tubes	$ 60.00/hr (Minimum $15.00)
	c. Irradiations outside core box, including beamport use and thermal column	$ 55.00/hr (Minimum $12.00)
2.	Use	
	a. Exclusive use	$119.00/hr
	b. For more than 8 hr	$ 95.00/hr
3.	Use of Equipment	
	a. Single-counting channel	$ 3.60/hr
	b. TN-11 multichannel analyzer and sample changer	$ 5.00/hr
4.	Services	
	a. Reactor staff	$ 10.25/hr
	b. Senior operator	$ 15.80/hr
5.	Expendable materials	At Laboratory cost

The shipping address is:

141 Mechanical Engineering Bldg.
University of Wisconsin
Madison, WI 53706

2.15 U.C. IRVINE DEPARTMENT OF CHEMISTRY TRIGA REACTOR

2.15.1 General Characteristics

No current utilization as a burst facility other than for NAA. The U.C. Irvine TRIGA, MARK I, is a 250-kW steady-state reactor. Fuel used is U-235, 20% enriched. Moderator is $ZrH_{1.7}/H_2O$/graphite. Immediate test environment is a water pool (20-ft underwater, access only from top) with dry tubes.

2.15.2 Operating Characteristics

Power level(s) (total fission output/burst) is 1,000 MW peak/15 MW-s pulse; the FWHM is 11 ms. Available reactivity is up to $3.00. The reactivity insertion rate period is about 3 ms. The repetition rate is 6/hr, with good reproducibility.

2.15.3 Support Capabilities

Timing signals are available from pulse fire circuit and rod sensors.

One ion chamber, some calculational capabilities, machine and electronic shop facilities within the School of Physical Sciences, and very limited experiment preparation laboratories are available. Photographic equipment and materials are not available.

2.15.4 Procedural Information

For technical and administrative information, contact:

Dr. George E. Miller
Supervisor
Department of Chemistry
U.C. Irvine
Irvine, CA 92717

Scheduling (lead time) is several months for special experiments. Cost is negotiable. The shipping address is:

Department of Chemistry
U.C. Irvine
Irvine, CA 92717

2.16 WASHINGTON STATE UNIVERSITY REACTOR

The Washington State University (WSU) Nuclear Radiation Center research reactor is a swimming-pool-type reactor originally constructed in 1961 by the General Electric Company for operation at 100 kW thermal power using MTR-type fuel elements. In 1967, the reactor was converted to allow use of TRIGA-type fuel ($U\text{-}ZrH_2$) of 20% enrichment. At that time, the power level was increased to 1 MW and the addition of an electro-pneumatic transient control element allowed pulsing operations of up to $3.15 inserted reactivity.

In 1976, additional instrumentation and control systems were added to allow the use of FLIP-type TRIGA fuel (70% enriched, containing 1.5% Er). At present, the core loading consists of 110 fuel rods in 4-rod clusters of which 35 are FLIP rods and 75 are TRIGA-Standard rods. Pulsing capability after conversion to mixed core was reduced to $2.00 insertions, limiting the average peak power during pulsing to approximately 625 MW.

The experimental program to date has revolved around radioisotope production and beam-type experiments. Pulsing activities have been limited to engineering laboratory studies on pulse characteristics and parameters, test and demonstration pulses, and one short-term experiment involving neutron detector development. Normal reactor operation is 8 hr/day, 3 days/week.

2.16.1 Characteristics

The WSU TRIGA Reactor characteristics are as follows:

1.	Power	
	a. Steady state	1 MW
	b. Pulsed	2,000 MW ($2.50 pulse)
2.	Reactor Core	
	a. Geometry and composition	Lattice of fuel-moderator elements, graphite reflector elements, and control blades in a rectangular grid box, all in water
	b. Grid box dimensions	26 in. x 30 in.
	c. Grid arrangement	7-element x 9-element array
	d. Active lattice height	15 in.
	e. Fuel-moderator composition	8.5 w/o U, 89.9 w/o Zr, and 1.6 w/o H for standard fuel; 8.5 w/o U, 1.5 w/o Er, 1.6 w/o H, and 88.4 w/o Zr for FLIP-type fuel
	f. Fuel enrichment	20% U-235 for standard; 70% U-235 for FLIP
	g. Fuel element construction	4-rod cluster element

h.	Fuel rod dia.	1.41 in.
i.	Fuel H/Zr atom ratio	1.7 to 1 for standard; 1.6 to 1 for FLIP
j.	Metal-to-water ratio	Approximately 0.5
k.	Fuel rod cladding	0.02-in. Type 304 stainless steel
l.	U-235/fuel rod	35 g for standard; 123 g for FLIP
m.	Fuel rod cluster (element) length	37-1/8 in.
n.	Critical mass (cold clean)	3.2 Kg for standard
o.	Core loading for $7 excess K (standard TRIGA only)	103 fuel rods, 26 elements, 3.6 Kg U-235
p.	Neutron source	Sb-Be
q.	Reflector (vertical)	Graphite cylinder 3.5-in. long on each end of fuel rods plus water
r.	Reflector (horizontal)	Graphite bars 3 in. x 3 in. in water

3. Nuclear Parameters

a.	Neutron flux/W (axial average position D-3)	6.85×10^{6} nv/W
b.	Minimum shutdown margin	$0.50
c.	Prompt neutron lifetime	28 μs
d.	Effective delayed neutron fraction	0.0070
e.	Void coefficient	$-\$1.42 \times 10^{-2}$/% void
f.	Prompt temperature coefficient (65% cell inhomogeneity, 15% Doppler effect, 20% core leakage)	$-\$1.36 \times 10^{-2}$/°C

4. Pulsing Parameters (maximum allowable)

a.	Reactivity insertion	$2.00
b.	Fuel temperature in instrumented fuel rod	500°C
c.	Power level to start pulse	2 kW

5. Core Parameters (approximate, dependent upon fuel temperature - all standard fuel)

a.	Neutrons/fission	2.07
b.	Thermal utilization factor	0.696
c.	Resonance escape probability	0.950
d.	Fast fission factor	1.06
e.	Fermi age	22.6 cm^2
f.	Diffusion length squared	2.74 cm^2
g.	Buckling	0.017 cm^{-2}
h.	Infinite multiplication factor	1.45
i.	Fast nonleakage probability	0.722
j.	Thermal nonleakage probability	0.956

2.16.2 Support Capabilities

Facilities available at the Nuclear Radiation Center include fully equipped electronics and machine shops, including professional personnel and experiment preparation laboratories. The reactor staff includes 2 full-time senior operators, 1 full-time operator-technician, and 2 part-time reactor operators.

2.16.3 Procedural Information

Technical and administrative information, including scheduling and charges, may be provided by either William E. Wilson (Associate Director), or Thomas A. Lovas (Operations Manager) at the following address:

Nuclear Radiation Center
Washington State University
Pullman, WA 99164
Telephone: (509) 335-8641

2.17 BERKELEY TRIGA MARK III

2.17.1 Characteristics

This pool reactor is fueled with U-ZrH_2, 8.5 w/o-20% enriched, and moderated with ZrH_2 and H_2O. The immediate test environment is H_2O, graphite, or air.

2.17.2 Test Parameters

Test parameters are as follows:

1.	Power level	Maximum 1,350 MW
2.	Fissions	5×10^{17}
3.	Available reactivity	Maximum $3.00
4.	Reactivity insertion rate	<1 s/$3
5.	Pulse period	2.8 ms
6.	Repetition rate	Approximately 10 min
7.	Pulse	12 ms at FWHM
8.	Temperature-time profile	Gaussian

2.17.3 Environment

Figures 2-115 and 2-116 show neutron fluxes.

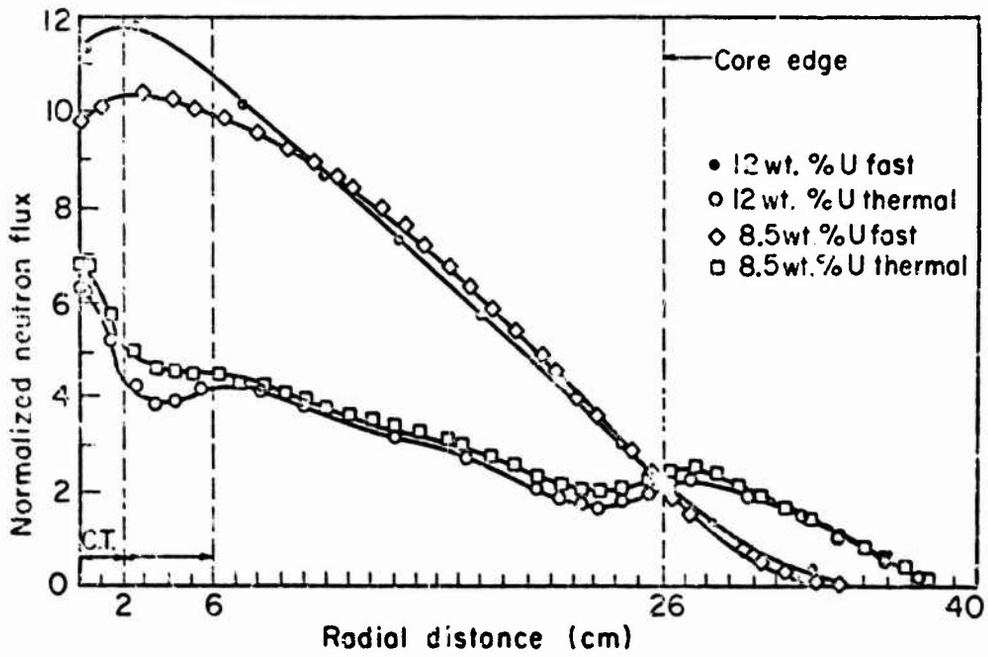

Figure 2-115. Normalized neutron flux versus radial distance.

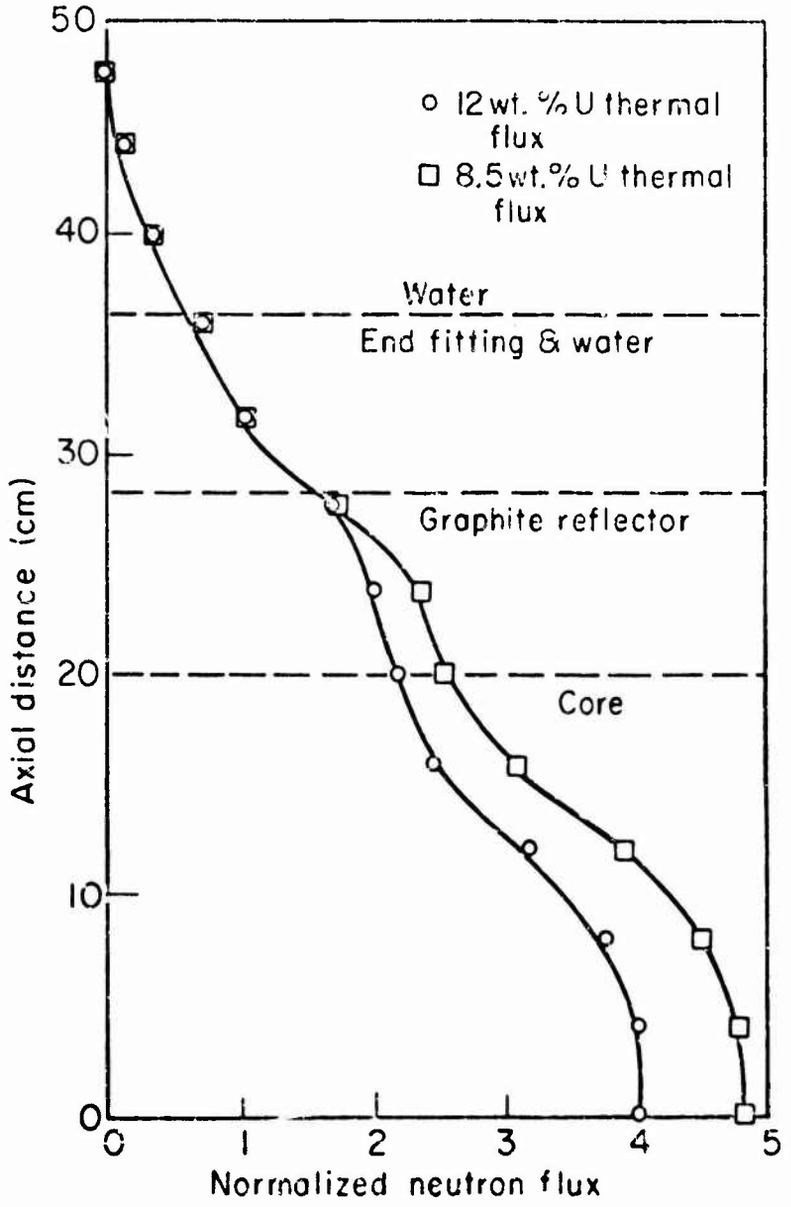

Figure 2-116. Normalized neutron flux versus axial distance.

Background radiation levels are 0 to 50 mrem/hr total Xβγ. There is no background RF, μwave, neutrons, etc. Diagnostic techniques used in the environment measurements are film, TLD, and assorted survey meters. Errors in the environment measurements are ±20%.

2.17.4 Support Capabilities

Professional and nonprofessional technical support staff available are reactor supervisor, reactor health physicist, chief reactor operator, reactor operator, machine and electronic shop personnel, and reactor laboratory secretary.

PG&E and emergency generator, several timing signals, assorted ion chamber and GM/TLD, film and criticality foils, decontamination room, general machine and electronic shop equipment, hoods, capsules, sealer, etc. are available, in addition to a photographic darkroom, enlarger, and chemicals.

2.17.5 Procedural Information

For technical and administrative information, contact T.H. Lim, reactor supervisor. Scheduling lead time is 1 week. The cost is $55 to $110/hr irradiation. The shipping address is:

TRIGA III Berkeley Research Reactor
Department of Nuclear Engineering
University of California
Berkeley, CA 94720

2.18 KANSAS STATE UNIVERSITY (KSU) TRIGA MARK II

2.18.1 General Characteristics

Fuel of this thermal reactor is 20% enriched U in a ZrH_2 matrix, stainless-steel cladding. The moderator is H_2O, graphite. Tests can be performed in core or in beam port.

2.18.2 Operating Characteristics

Power levels are 10^7 J/pulse. Peak power at ambient temperature is 250 MW. Available reactivity is $2.00. The pulse period is 10 ms. Repetition rate is 1/15 min, and reproducibility is ±3% peak power.

2.18.3 Environment

Flux density at peak power is $10^{16} cm^{-2} s^{-1}$ (neutrons, E > 0.2 eV). The pulse width is 35 ms ($2.00). Background is 2.5×10^7 rad/s (γ) in central thimble at peak pulse power. Diagnostic techniques are foil counting and in-core ion chambers.

2.18.4 Support Capabilities

The staff consists of 3 professionals, 3 support personnel, plus full resources of the Nuclear Engineering Department faculty, staff, and facilities.

Timing signals are available. The dosimetry is full range, active and passive. An IBM 370-158 provides calculational capabilities. Shop facilities consist of a machine shop and an electronics shop. Experimental preparation laboratories also are available. Photographic equipment available includes a fully equipped darkroom and professional equipment.

2.18.5 Procedural Information

For information regarding the use of this facility contact:

Richard E. Faw, Director
KSU Nuclear Reactor Facility
Ward Hall
Kansas State University
Manhattan, KS 66506

Scheduling requires a 30-day lead time. Costs are available upon request. For shipping, the address is as listed above.

2.19 UNIVERSITY OF TEXAS AT AUSTIN
TRIGA MARK I

2.19.1 Characteristics

Fuel rods are 28-in. long x 1.5-in. dia., of 0.020-in. stainless-steel cladding. The fuel is U-ZrH_2, with 20% enriched U-235. The reflector is graphite and light water. The moderator is light water, graphite, and ZrH_2.

2.19.2 Support Capabilities

Figure 2-117 is a sketch of the reactor floor plan. Other experimental devices available at the laboratory are a subcritical assembly, a 2,000 Ci Co-60 irradiator, a Nuclear Chicago Sodium Iodide coincidence counting system, a neutron beam irradiation facility, and numerous proportional and Geiger-Mueller detection and counting systems.

2.19.3 Procedural Information

For information concerning the use of the facility, contact Dr. E.L. Draper, Jr., or Mr. Joseph A. Burack at the following:

The University of Texas Main Campus
Taylor Hall 131
Austin, TX

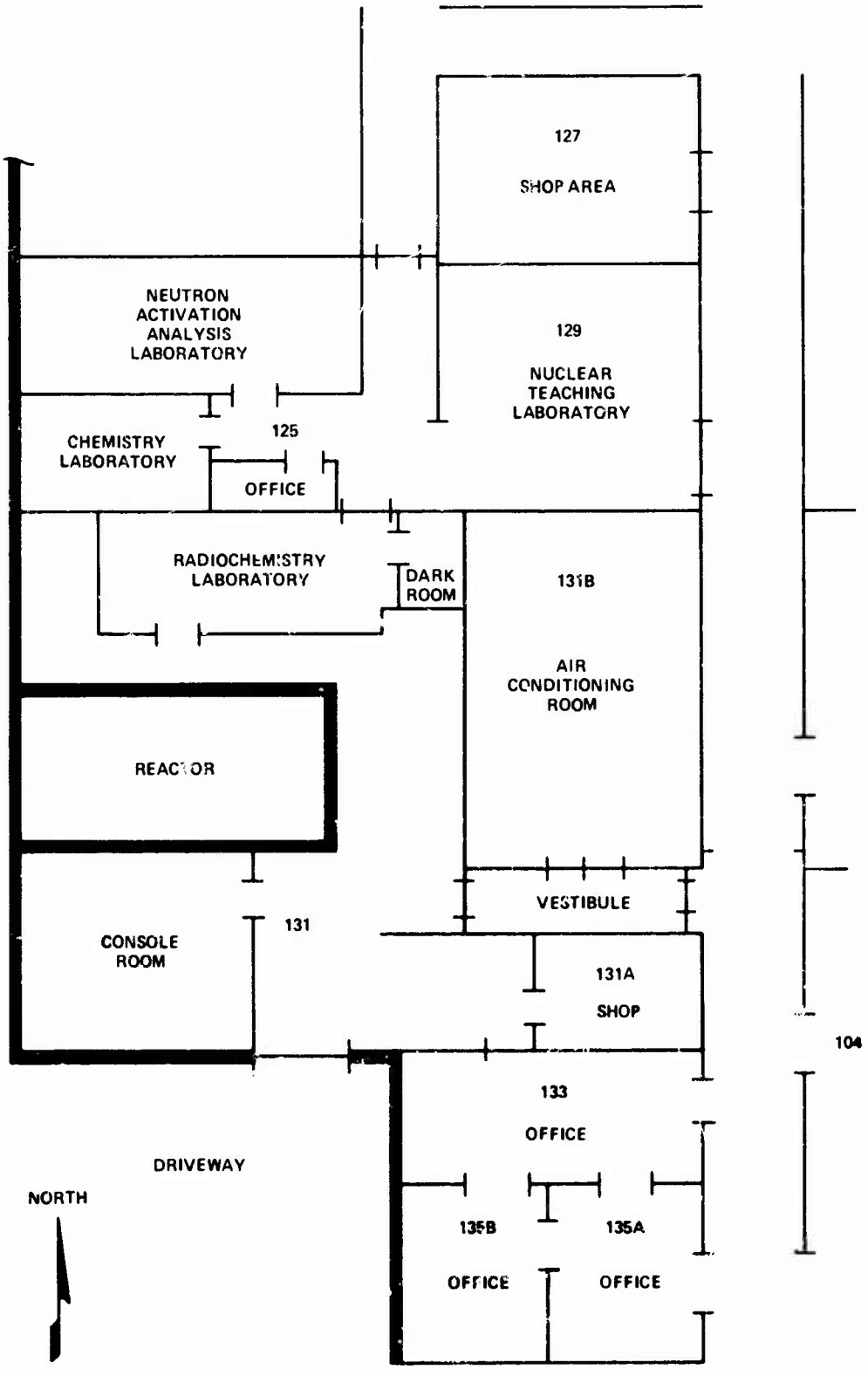

Figure 2-117. Floor plan of University of Texas reactor laboratory complex.

SECTION 3

FLASH X-RAY MACHINES

3.1 INTRODUCTION

In these machines, electrons generated by discharge of stored electrical energy through a cold cathode tube are converted to x-rays. They also are referred to as electron-beam generators since the electrons themselves can be used directly for irradiation studies.

Flash x-rays have high dose rates over a relatively large volume. A wide range of beam intensities, energies, and spatial distribution profiles may be obtained by varying machine design factors such as stored charge, charging V, circuit parameters, ca[illegible] geometry, and target material. However, for a given machine, the pulse widt[illegible] is essentially fixed and only limited variations of photon energy and dose rate are possible.

Machines presently available for TREE studies cover a wide range of operating parameters. The amount of energy a particular machine can deliver is generally proportional to its physical size. They have the disadvantage that for any given pulse the electrical discharge can occur in an unpredicted, abnormal mode, delivering an output pulse unlike that expected. This problem is encountered much more frequently in the large machines than in the smaller ones. The fidelity of a given pulse is not guaranteed and sufficient diagnostics should be employed to monitor each shot.

At each facility, the staff operates the machine, assists in setting up the experiment and determining dosimetry, and is available for technical consultation.

Flash x-ray (FXR) facilities were requested to supply data emphasizing quantitative descriptions of the electron and x-ray fields and the accuracy to which these values are known. Requests were also made for data characterizing the predictability and reproducibility of the environment on a pulse-to-pulse basis. Figure 3-1 is a copy of the form sent to the individual facilities.

I. Electron-beam mode, environment

A. Total beam energy versus voltage

B. Beam geometry (area, spread, pressure in beam region, etc.)

C. Output wave form versus time for different voltages

D. Beam-energy density versus position (axial and plan view) subject to perturbation by experimental equipment

E. Electron-energy spectrum as a function of voltage, position, and time

F. Characteristic deposition in Si, Au, etc.

G. Repetition rate and pulse reproducibility/predictability

H. Diagnostic techniques used in the environment measurements

I. Discussion of errors in the environment measurements

J. Electrical noise mapping (experimental configuration dependent)

II. High-voltage flash x-ray mode, environment (quantities dependent upon anode-cathode geometry and charging voltage)

A. Dose as a function of position (both axial and plan view, data to be presented as isodose contours)

B. Dose rate as a function of position (both axial and plan view of isodose rate lines)

C. Output wave form versus time as function of voltage and position

D. Photon spectrum versus time as function of voltage and position

E. Pulse-timing jitter (pre-pulse and trigger) and pulse delay

F. Repetition rate and pulse reproducibility

G. Diagnostics techniques used in the environmental measurements

H. Discussion of error bars and reproducibility

I. Electrical noise mapping (experimental-configuration dependent)

III. Support capabilities

A. Professional and/or nonprofessional technical support staff available

B. Screen room

C. General electronics available: power, cabling, and minimum cabling requirements

D. Timing signals

E. Dosimetry available (active and/or passive)

F. Calculational capabilities available

Figure 3-1. Outline of data requested from FXR facilities.

G. Shop facilities

H. Experiment preparation laboratories

I. Photographic equipment and materials

J. Test area and configuration available

IV. Procedural information

A. Contact (technical and administrative)

B. Scheduling (lead time)

C. Cost information if available and/or releasable

D. Shipping address

Figure 3-1. (continued).

3.2 FEBETRON 705 ELECTRON-BEAM SYSTEM

3.2.1 Characteristics

The output characteristics of various Field Emission Corporation (now Hewlett Packard) FEBETRON 705 systems are similar, and only one description is given. Support facilities of the individual laboratories: Northrop Research and Technology Center, Kaman Sciences Corporation, Lockheed Palo Alto Research Laboratory, and EG&G are described further on in this section.

An electron beam is generated by discharging the Marx generator through a field-emission cathode vacuum tube. The electron beam impinges upon and passes through a thin Ti window which serves as the tube anode. The tube discharge V (600 kV to 2.3 MV) can be adjusted continually over the operating range by changing the charging V and the gas pressure of the containment tank.

A magnetic coil around the discharge tube produces a magnetic field which focuses the electron beam. This field is internal to the containment tank and during normal operation has a field strength of approximately 4,000 G. This magnetic field may influence the experimental apparatus placed immediately adjacent to the tank wall or face.

X-rays are produced by placing a W (or other suitable material) target at the external focus of the electron beam.

3.2.2 Test Parameters

Operating characteristics of the FEBETRON 705 are:

1.	Maximum charging V	35 kV
2.	Tube V (maximum electron energy)	2.3 MeV
3.	Average electron energy	1.4 MeV
4.	Total beam energy/pulse	400 J
5.	Peak electron-beam I	5,000 A
6.	Number of electrons/pulse	$\sim 2 \times 10^{15}$
7.	Pulse width (FWHM)	
	a. Electron mode	20 to 50 ns
	b. X-ray mode	20 ns
8.	Peak electron energy fluence/pulse	
	a. At tube face (anode)	~ 25 cal/cm^2
	b. 30 cm from tube face	~ 0.1 cal/cm^2
9.	X-ray intensity/pulse	
	a. At target	$\sim 7{,}000$ R
	b. 30 cm from target	~ 25 R

These data are not definitive and are meant only to be used as a guide.

Because of the finite rise and fall times of the accelerating V pulse, the output electrons are continuously distributed from zero to the maximum energy. The electron-beam dia. is dependent upon discharge V and magnetic field strength. Typically, the beam dia. (80% peak intensity at edge) is less than 0.8 cm. The peak x-ray intensity is available over only a very small area, and the maximum usable dose is somewhat less than this value. Total beam energy as a function of charging V and focusing magnetic field strength is given in Figures 3-2 and 3-3.

The beam pinches to the geometric center line a short distance in front of the tube and then diverges. The exact shape of the contour and the value of its maximum vary with machine parameters such as charging V, magnetic focusing field, type of electron-beam tube, and distance from the anode.

Maximum pulse repetition rate (with a special power supply) is 10 pulses/s.

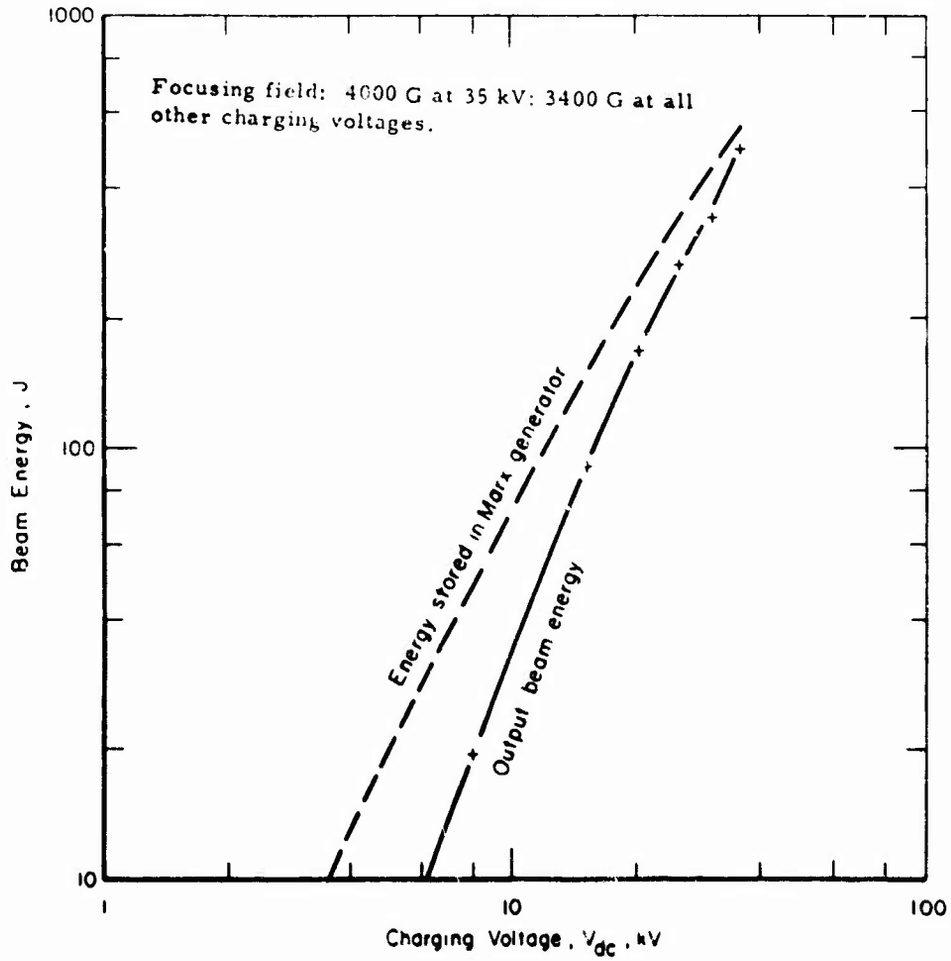

Figure 3-2. Total output beam energy, E, versus charging V (V_{dc}) for the FEBETRON 705/tube 545C.

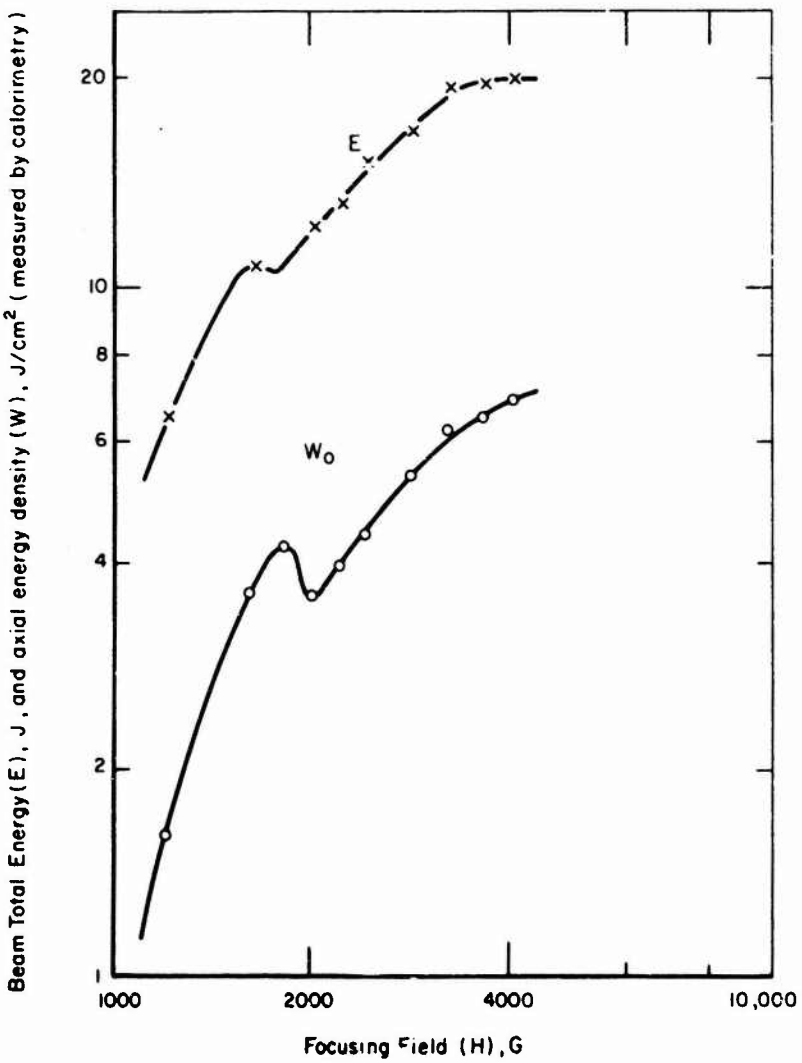

Figure 3-3. Beam energy, E, and energy density (fluence), W_0, at the tube face versus focusing field, H, at 8 kV for the FEBETRON 705/tube 545A.

Figure 3-4 is a superposition of 6 output I waveforms (no Al filter). Experience has shown that center-line dose values are reproducible to within 5%. The actual spatial orientation of the dose center line is not necessarily coaxial with the tube center line, and varies from tube to tube. The dose center-line position may be established by taking dosimetry measurements each time the discharge tube is changed, and occasionally during the life of the tube.

Noise measurements by the manufacturer indicate RF noise is less than 5 mV across 50 ohms at the pulser face, and can be reduced to 1 mV by appropriate shielding.

Electron-beam measurements are made using calorimeters and Faraday cups. X-ray measurements are made using TLDs, cellophane and glass dosimeters, and photodiodes.

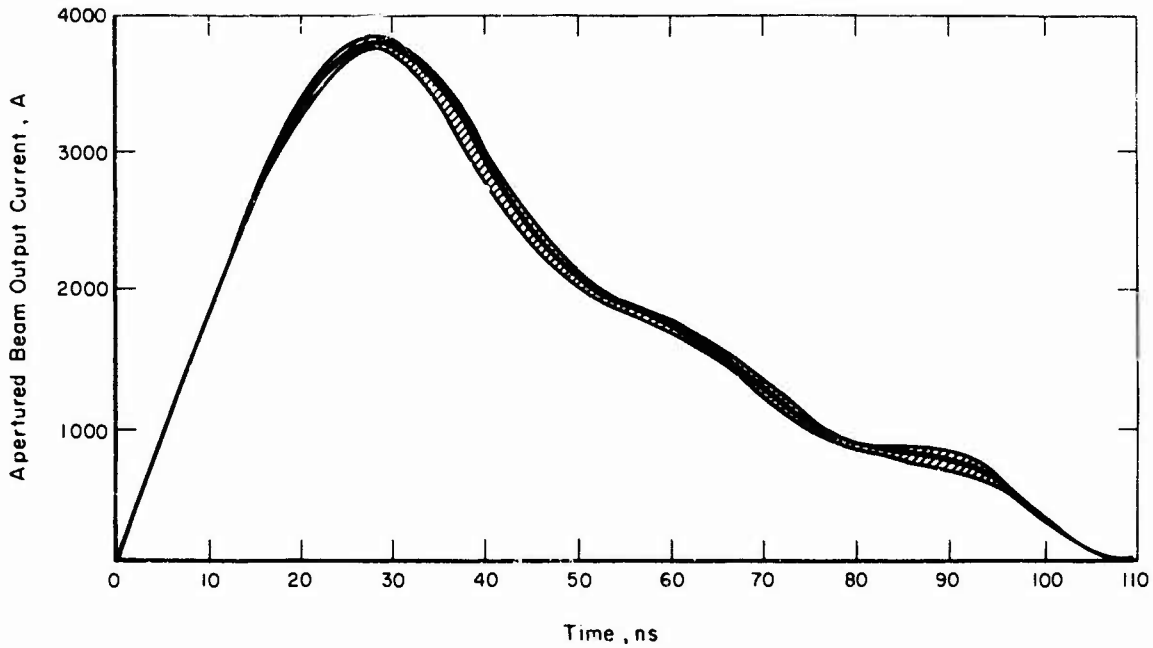

Figure 3-4. Pulse-to-pulse repeatability test for the FEBETRON 705/tube 545C.

3.2.3 Environment for Electron-Beam Mode

Beam profiles are given in Figures 3-5 through 3-7. Electron-beam energy fluence maps are given in Figures 3-8 through 3-10. Waveforms of the output beam are shown in Figures 3-11 and 3-12.

The electron energy spectrum was determined by analyzing the dependence of the output I waveform on the thickness of Al absorbers in the range of 0 to 175 mil. From these waveforms, the transmitted I, as a function of absorber thickness and time, was determined and the output electron energy, as a function of time, was derived. This curve, along with the time-dependent output beam I curve, is shown in Figure 3-13. Analysis of these data led to the electron energy spectrum curves shown in Figures 3-14 and 3-15. In Figure 3-14 it is assumed that the instantaneous electron spectrum is a delta function in energy. The charge in the 3/4-in.-dia. output beam used for spectrum determination is 194 μC. Total charge in the output beam is 320 μC (2×10^{15} electrons).

Figure 3-16 is a dose-depth profile for Al as measured using blue-cellophane dosimetry foils. Analytically determined deposition profiles for carbon are given in Figures 3-17 and 3-18.

3.2.4 Environment for X-Ray Mode

X-ray exposure maps derived from experimental data and analytical calculations are given in Figures 3-19 through 3-21. Figure 3-22 depicts the uniformity or useful region of the beam as a function of x-ray exposure. The x-ray output waveform, as determined from a photodiode detector, is shown in Figure 3-23.

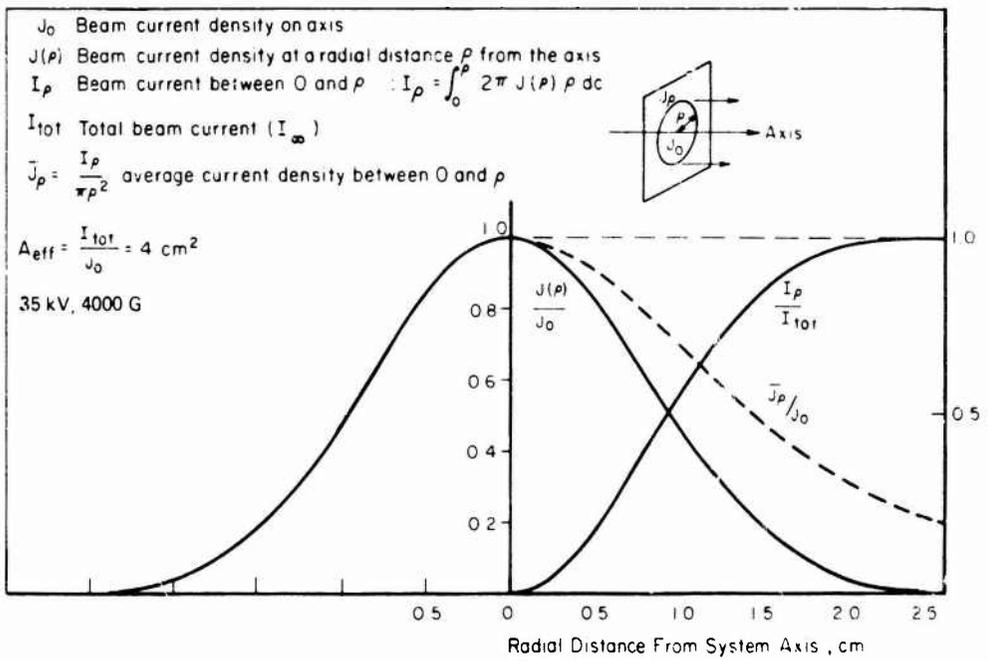

Figure 3-5. Electron-beam intensity profile in plane 0.5 in. from tube face for the FEBETRON 705/tube 545C.

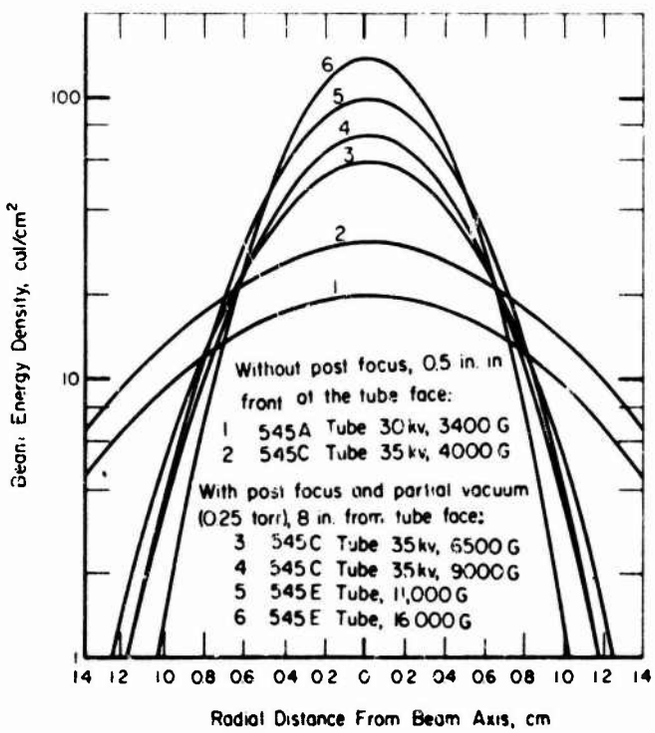

Figure 3-6. Beam energy density profiles for various operating conditions for the FEBETRON 705.

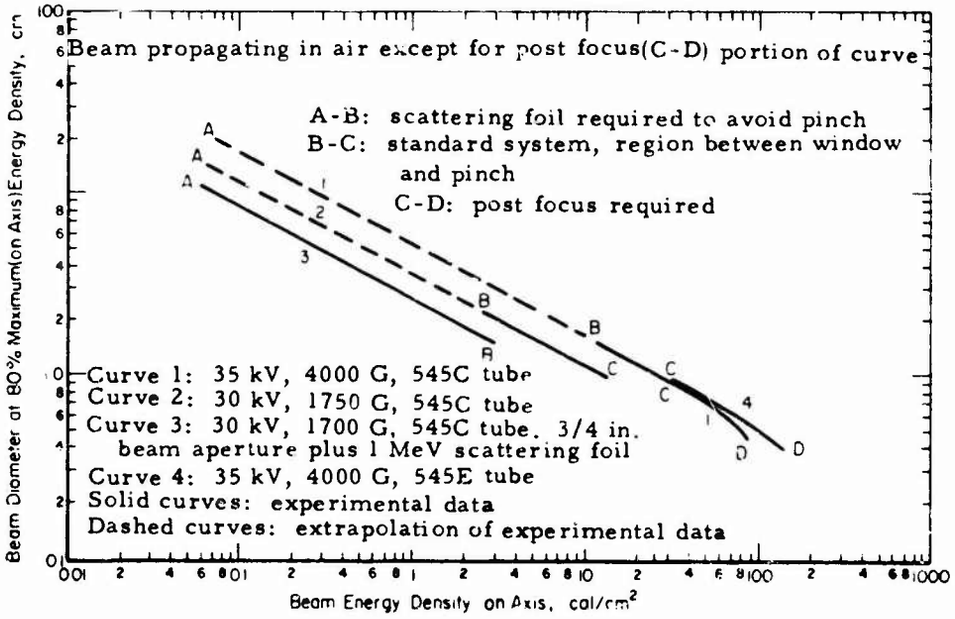

Figure 3-7. Diameter of "useful beam" (energy density at edges equal to 80% of maximum energy density at center) versus beam energy density on axis for the FEBETRON 705.

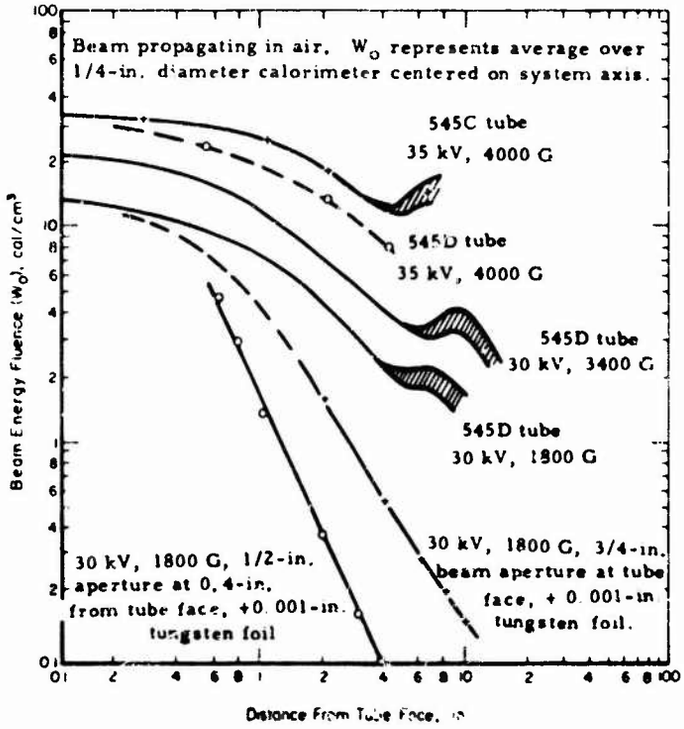

Figure 3-8. Beam energy fluence, W_0, versus distance, r, from tube face.

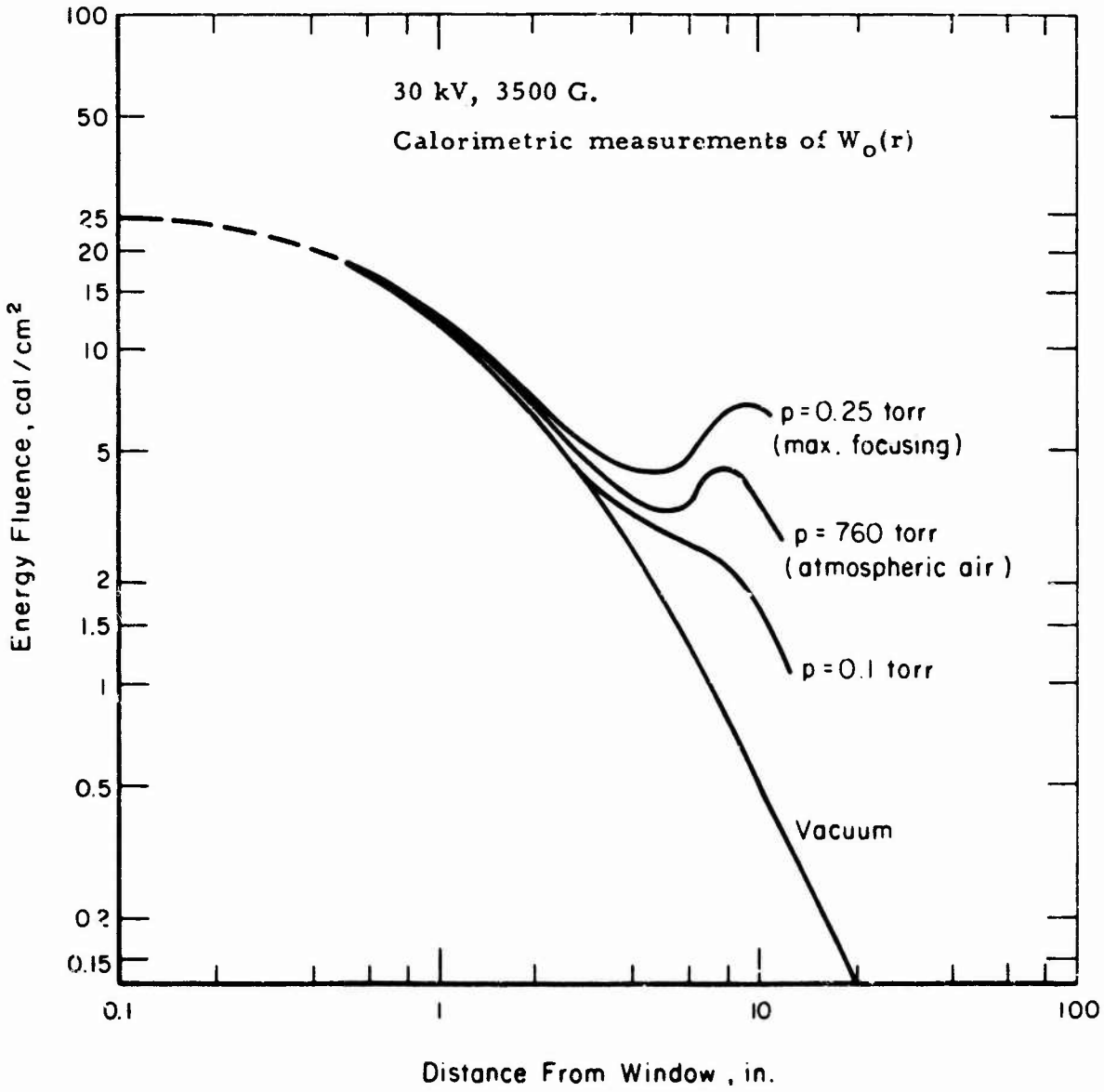

Figure 3-9. Energy fluence, W_o, versus distance, r, from window for FEBETRON 705/tube 545D.

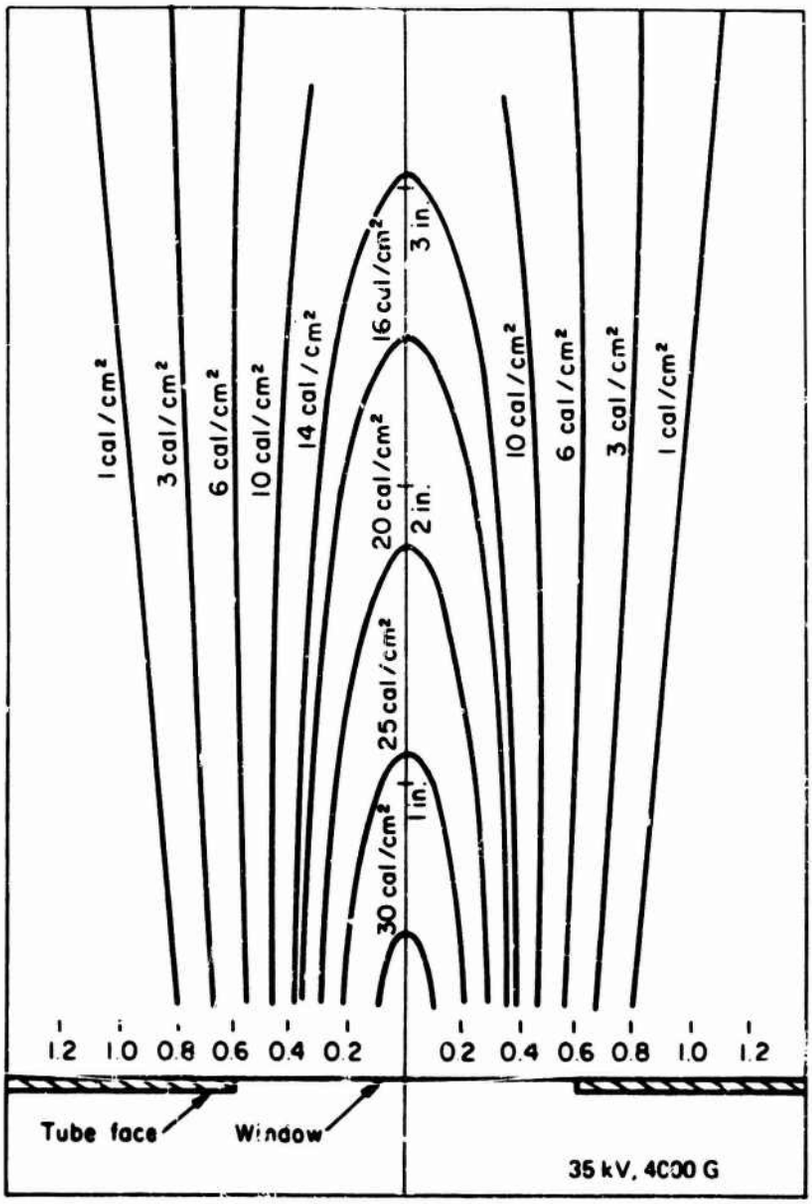

Figure 3-10. Electron-beam energy fluence map for the FEBETRON 705/tube 545C.

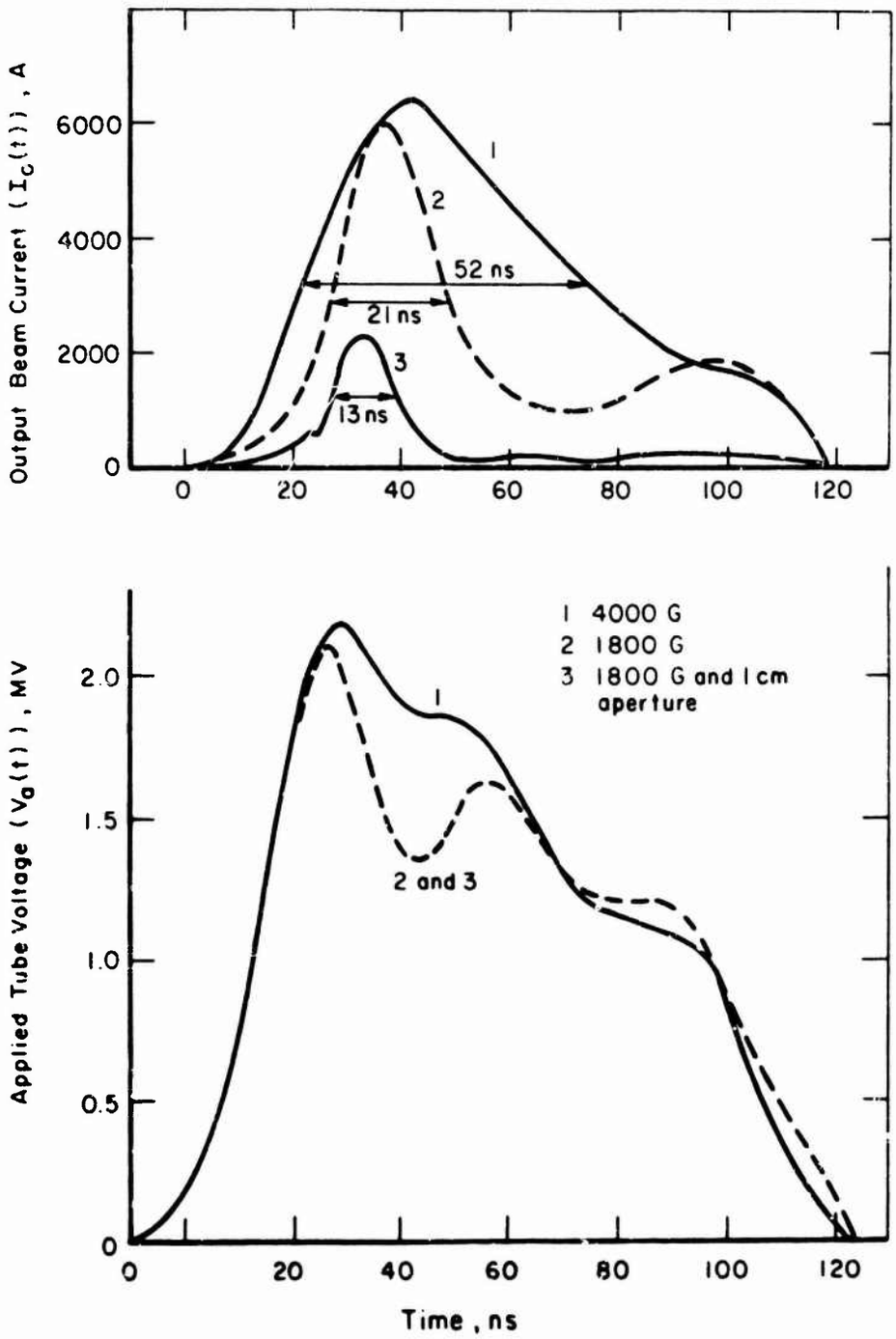

Figure 3-11. Applied tube V, $V_a(t)$, and output beam I, $I_o(t)$, at 35-kV charging V for the FEBETRON 705/tube 545C.

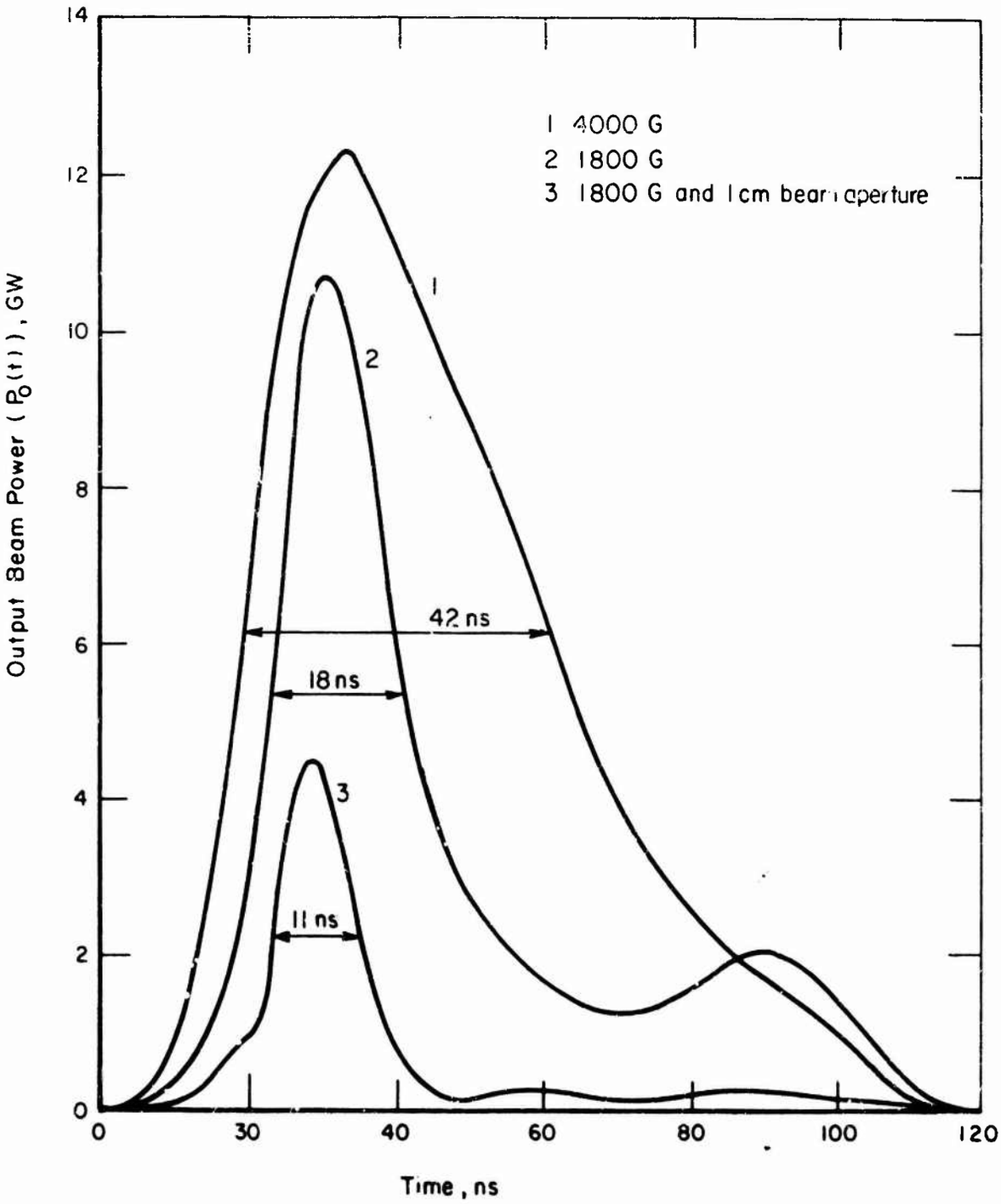

Figure 3-12. Output beam power waveform, $P_0(t)$, at 35-kV charging V for the FEBETRON 705/tube 545C.

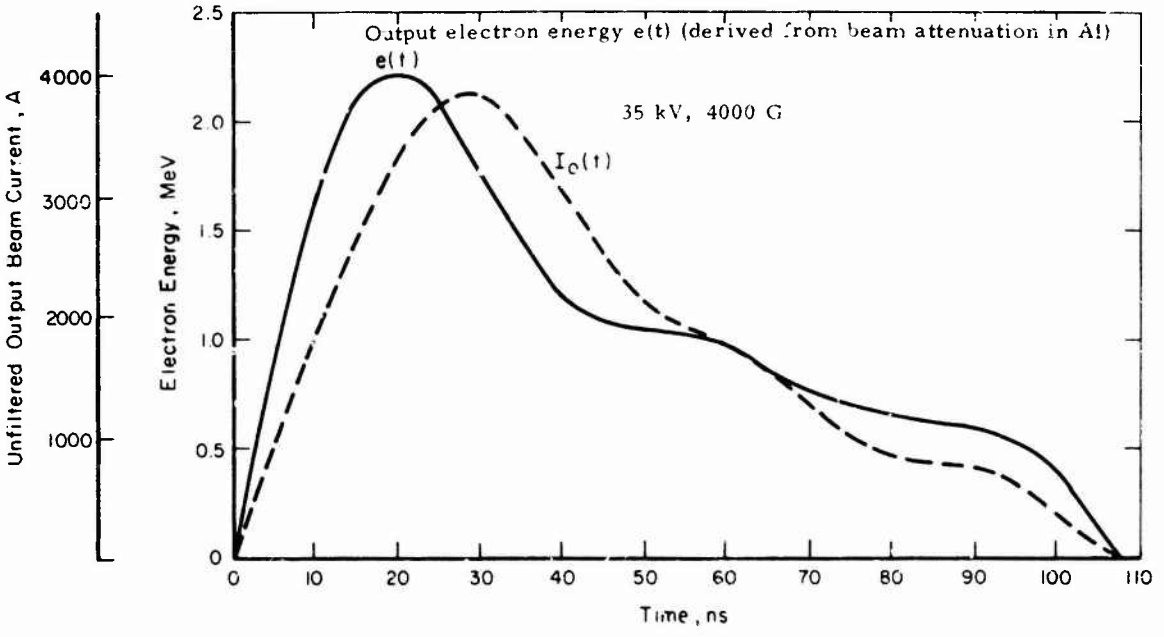

Figure 3-13. Energy spectrum determination for the FEBETRON 705/tube 545C.

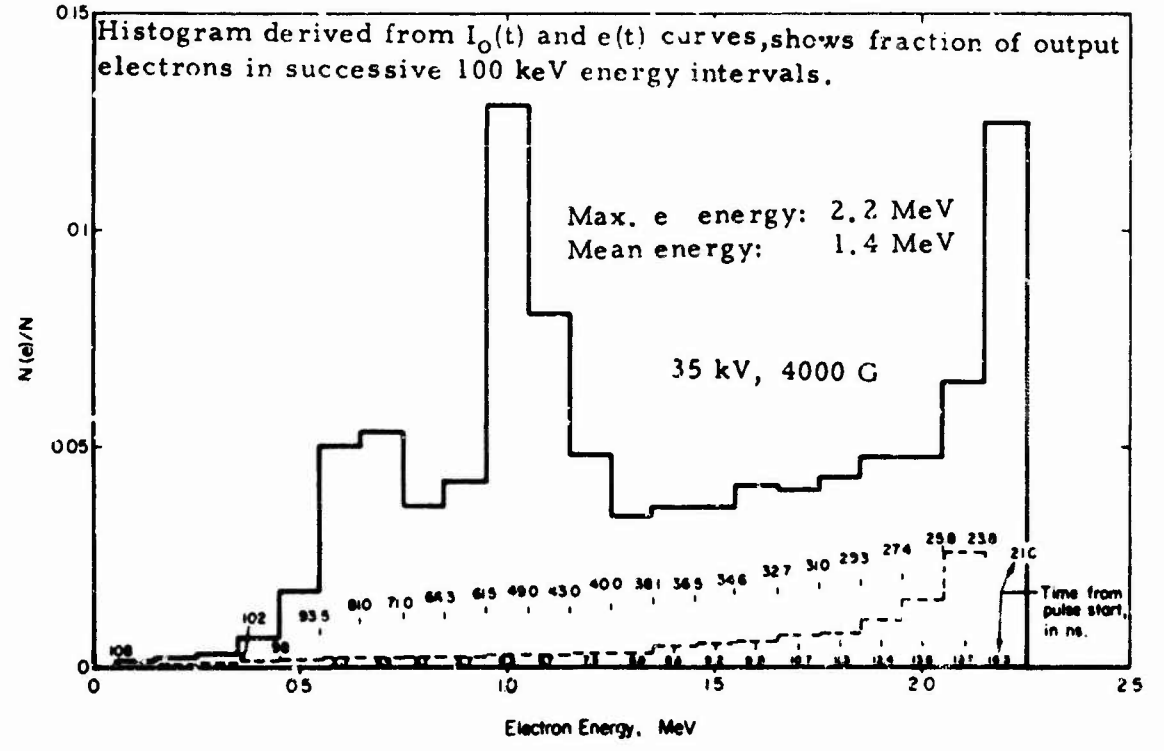

Figure 3-14. Time-resolved electron energy spectrum for the FEBETRON 705/tube 545C.

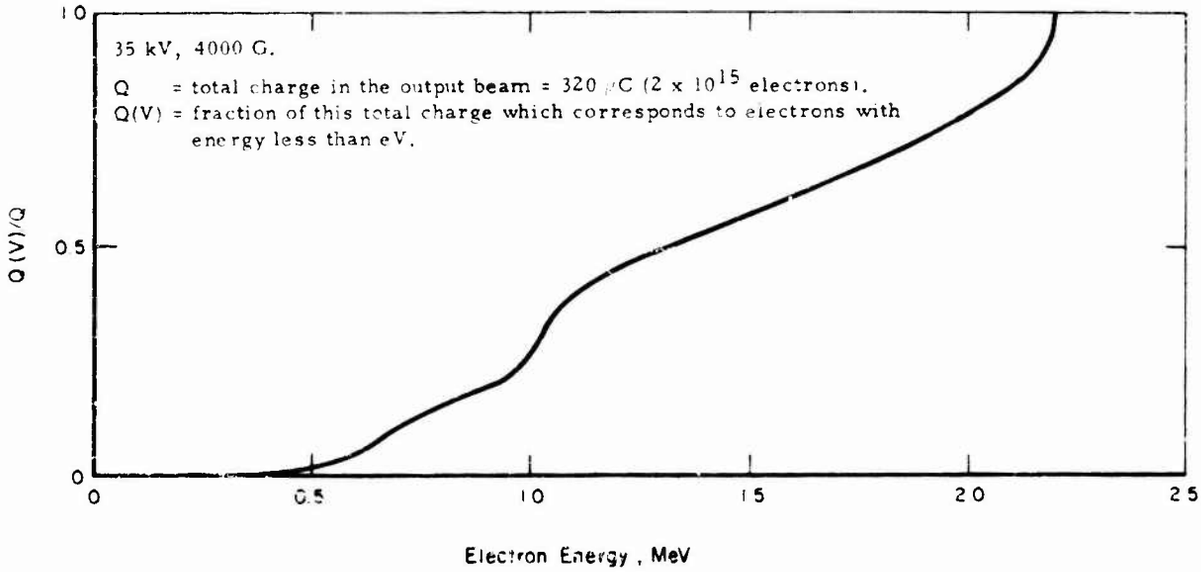

Figure 3-15. Integral electron energy spectrum Q(V)/Q for the FEBETRON 705/tube 545C.

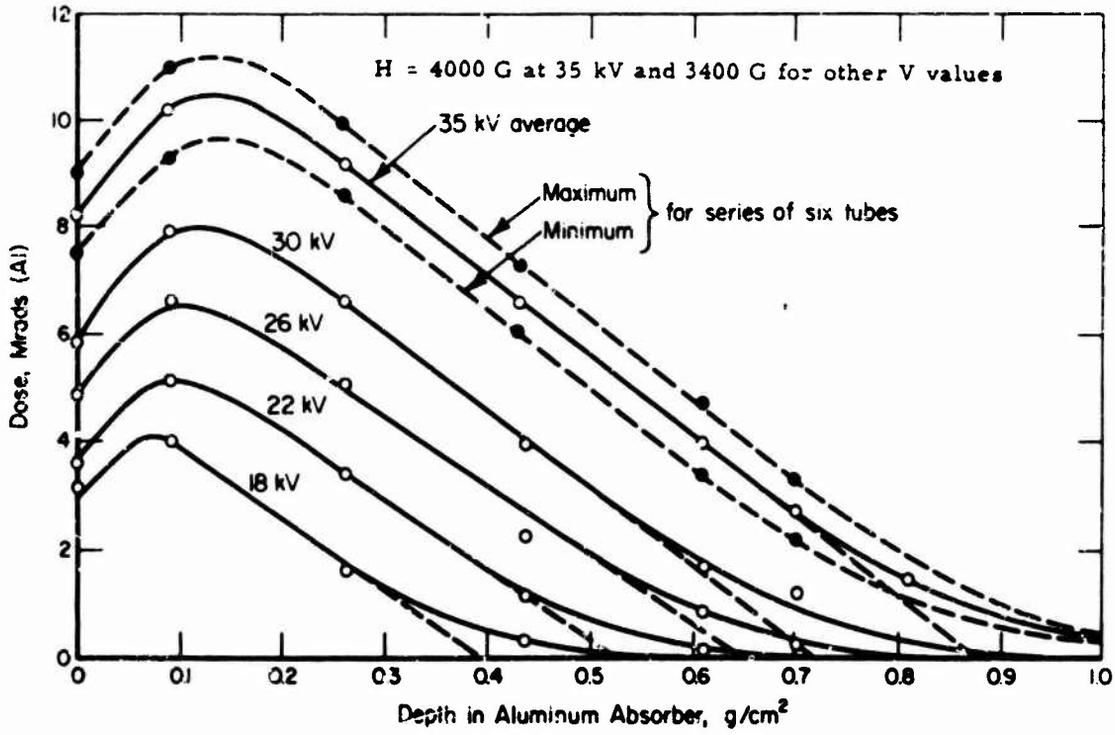

Figure 3-16. Dose versus depth in Al at 4 in. from tube face, versus charging V for the FEBETRON 705/tube 545C.

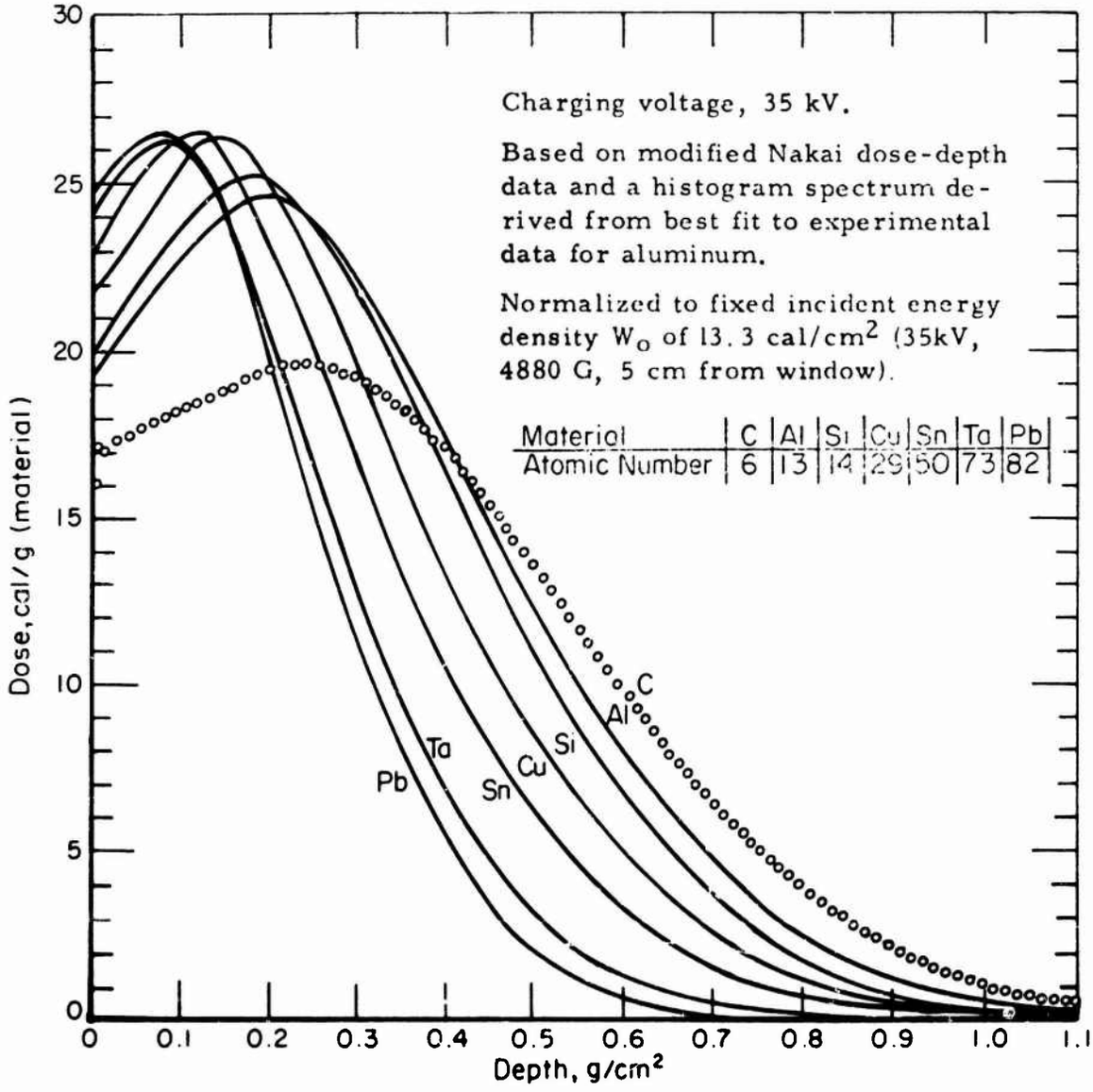

Figure 3-17. Dose deposition in several materials for FEBETRON 705 incident beam.

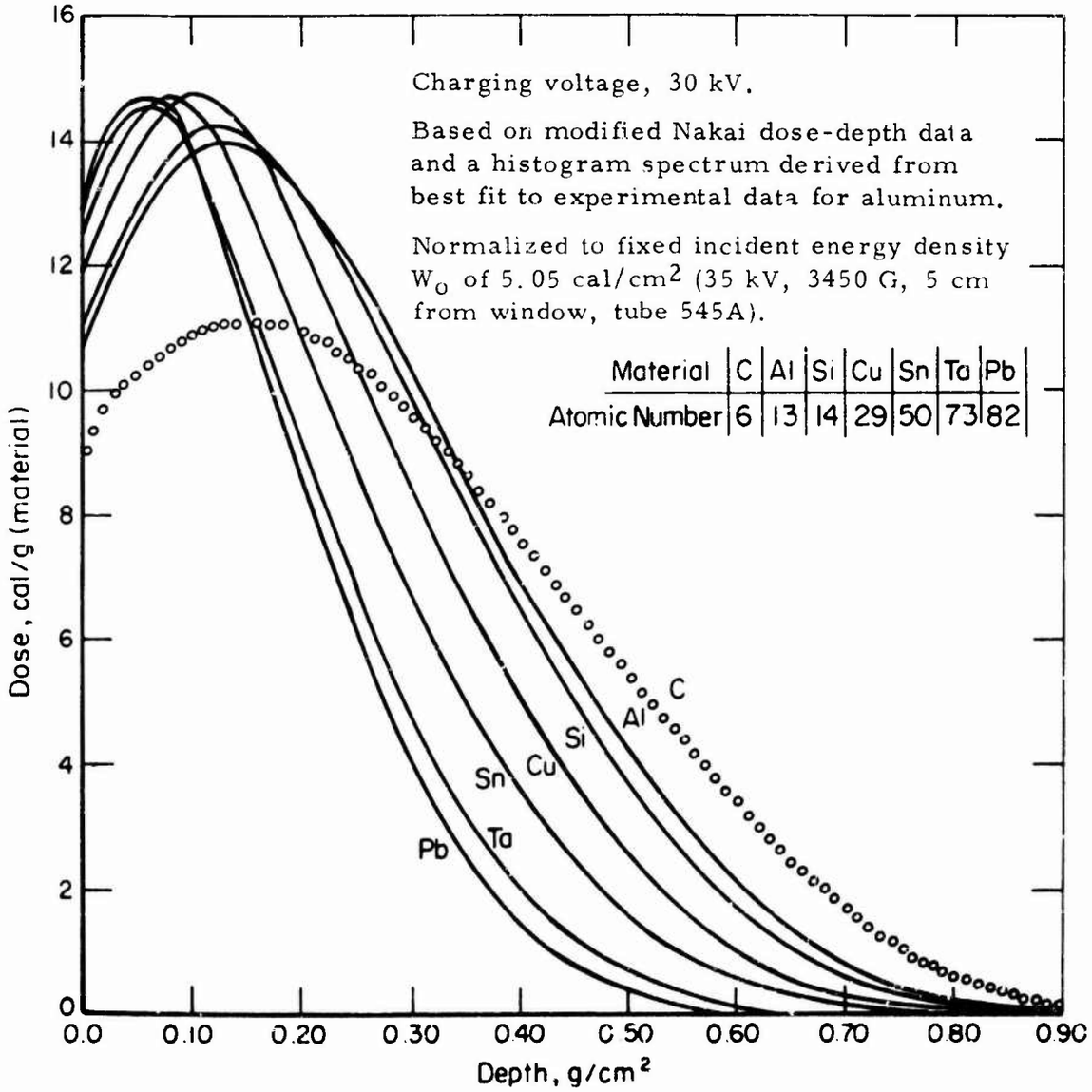

Figure 3-18. Dose deposition in several materials for FEBETRON 705 incident beam.

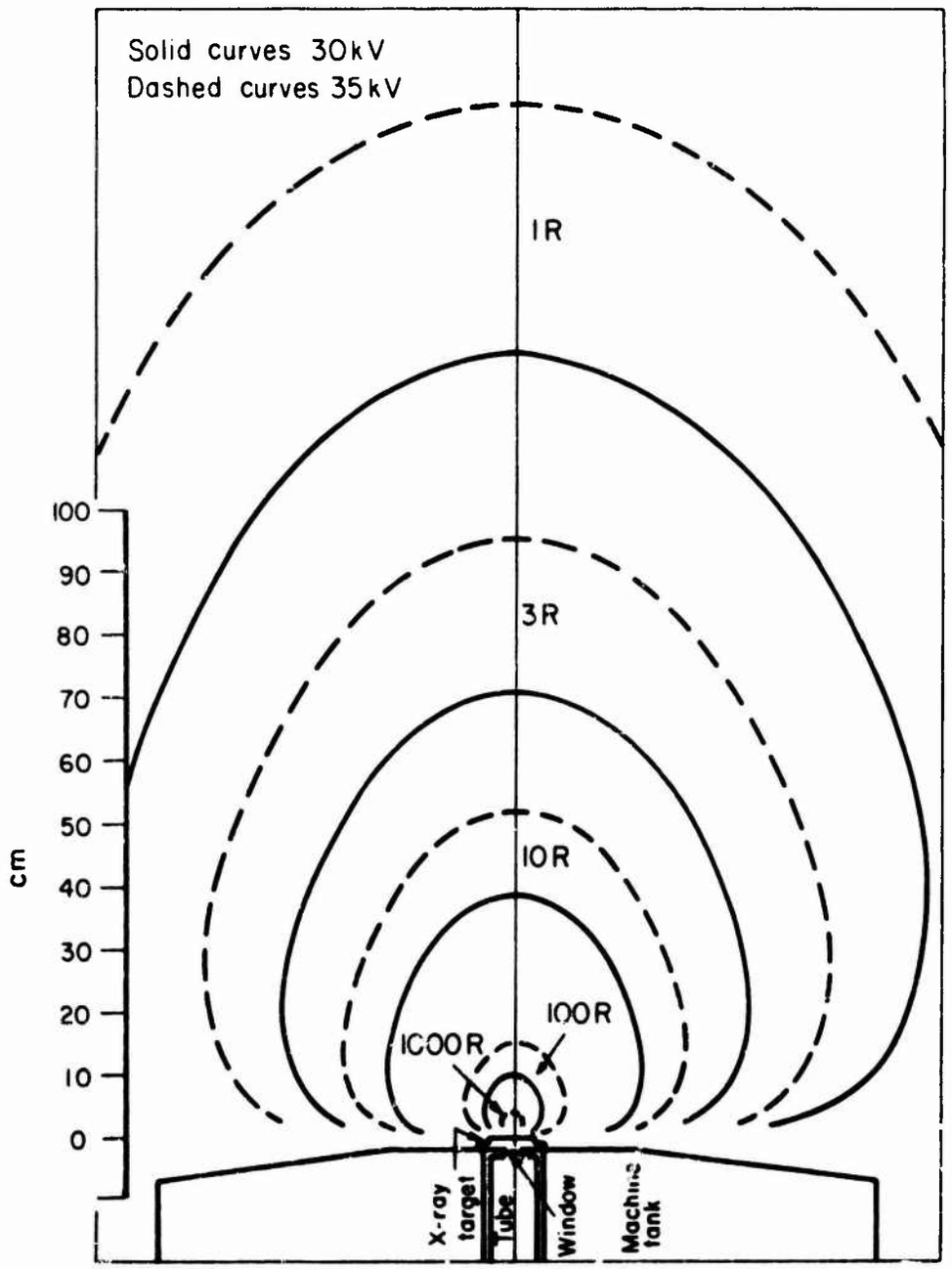

Figure 3-19. X-ray exposure map (in R) for FEBETRON 705/ tube 545C, 30- and 35-kV incident beams.

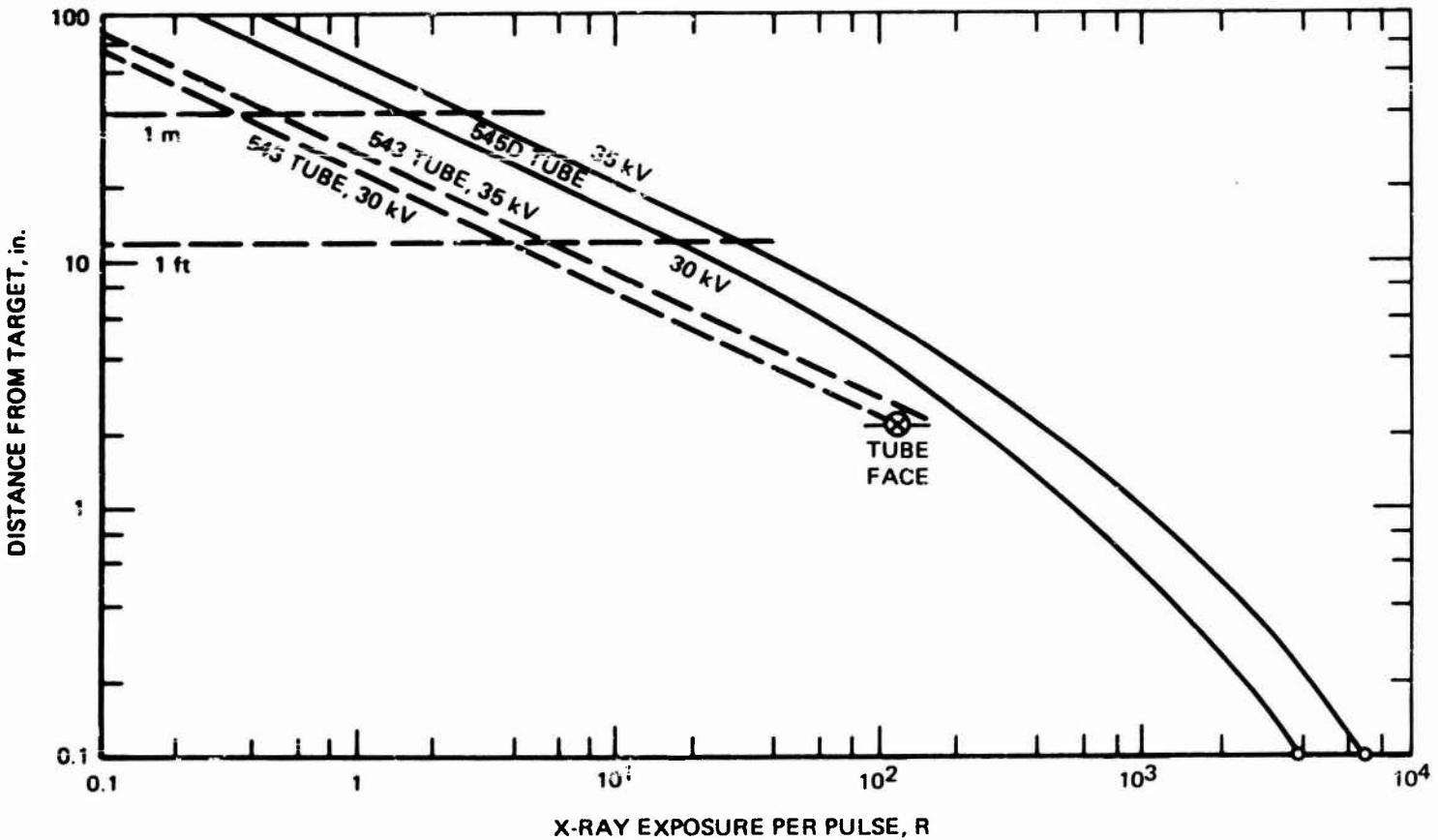

Figure 3-20. X-ray exposure per pulse versus distance from x-ray target for the FEBETRON 705.

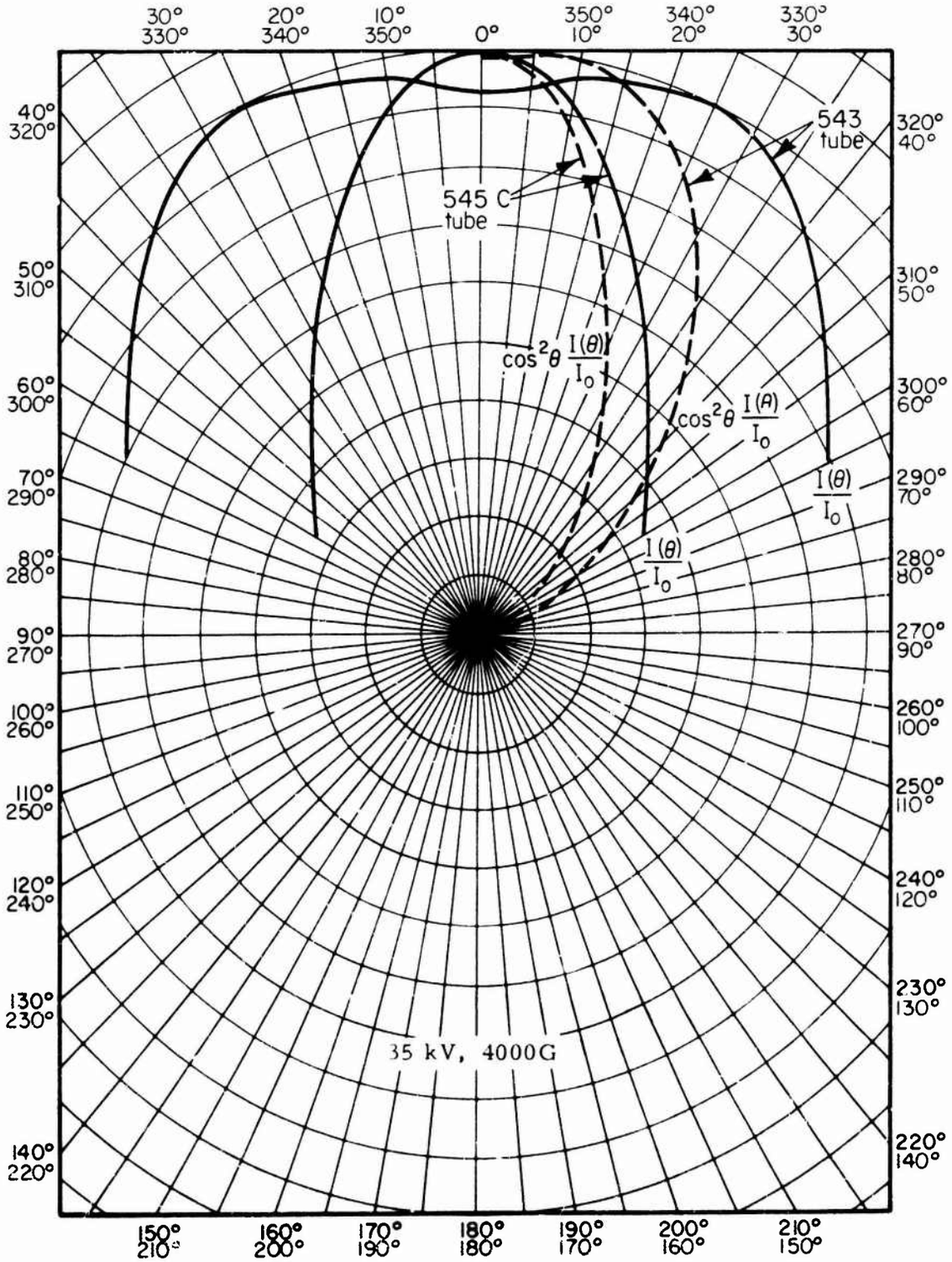

Figure 3-21. Angular distribution of x-ray exposure at large distances from the target for the FEBETRON 705.

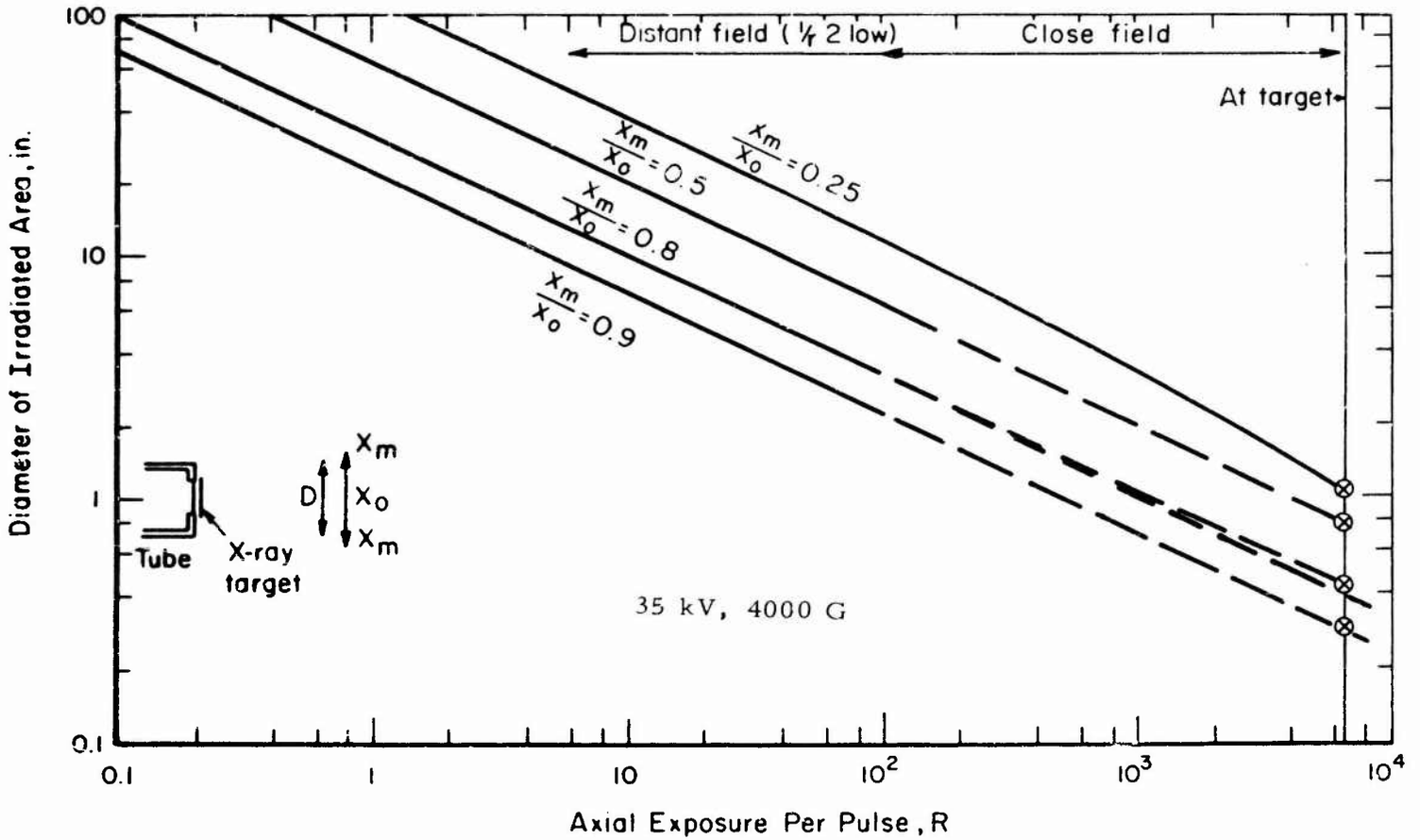

Figure 3-22. Diameter of circular area which can be irradiated with uniformity versus exposure at center of area for a FEBETRON 705/tube 545C.

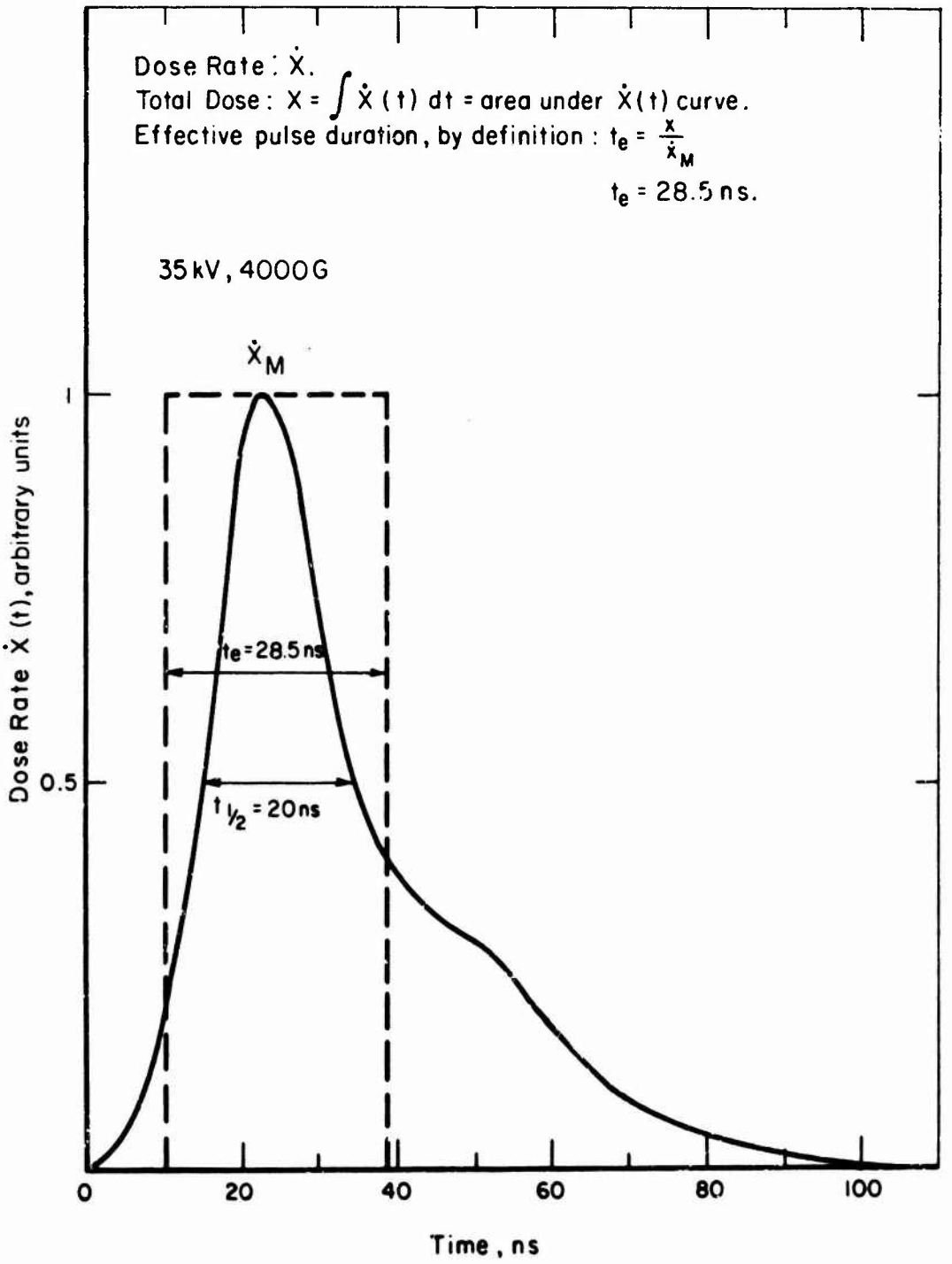

Figure 3-23. X-ray dose rate waveform for the FEBETRON 705/tube 545C.

The photon spectrum has been estimated analytically based upon various assumptions regarding the electron spectrum. Results are given in Figure 3-24.

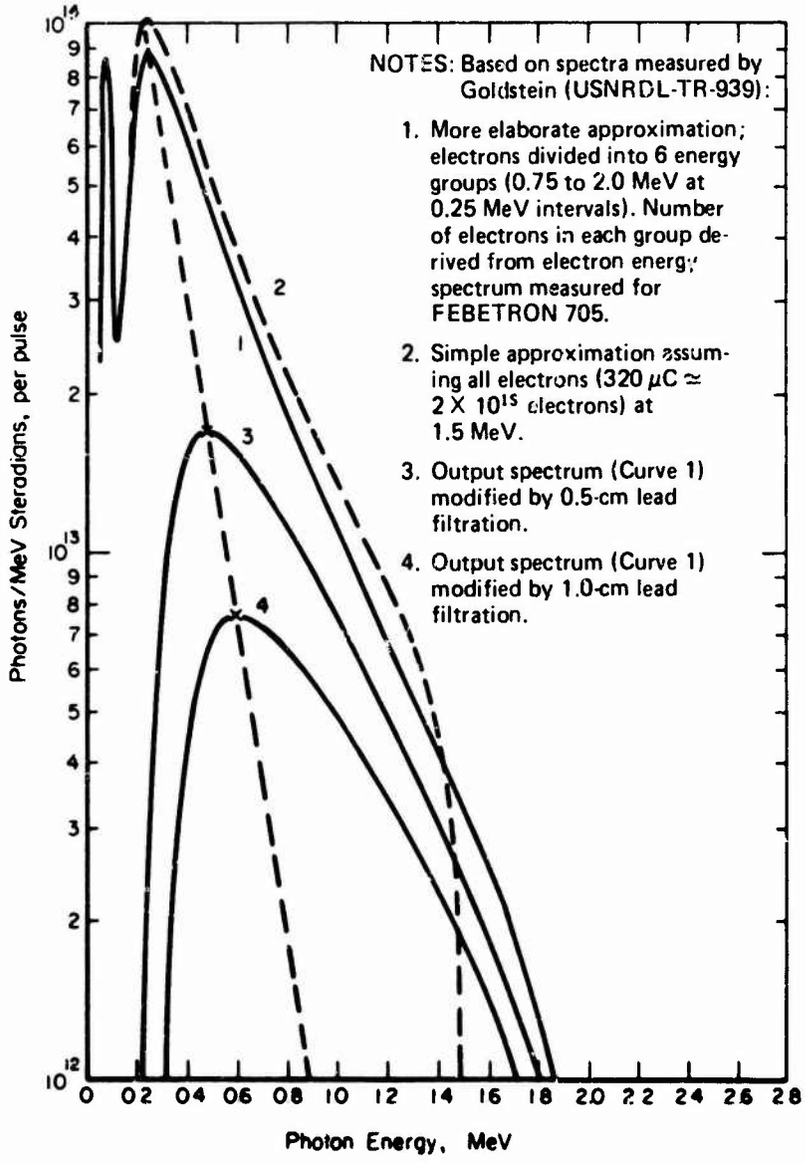

Figure 3-24. Estimated x-ray energy spectrum for the FEBETRON 705.

3.3 FEBETRON 706 ELECTRON-BEAM SYSTEM

3.3.1 Characteristics

Support facilities of the Field Emission Corporation (now Hewlett Packard) FEBETRON 706 are: Lockheed, EG&G, Triangle Institute, and Westinghouse.

FEBETRON tubes are field emission-diodes characterized by large I and small size. Instead of an internal anode, they have a thin window through which the electron beam is transmitted for external use.

3.3.2 Test Parameters

The 2 tubes which operate in the 706 system have nearly identical waveforms (Figure 3-25). Their very short pulse length, approximately 3 ns, enhances the excitation and observation of very fast transient phenomena. The 2 tubes have different beam densities and beam profiles to accommodate different applications. The total beam energy is nearly the same in both cases. The electron energy can be varied over a broad range. Maximum recommended pulse rate is 1 pulse/min. The characteristics given correspond to the maximum warranted output. Electron-beam output and x-ray output specifications for the 706 system are given in Tables 3-1 and 3-2, respectively.

The Model 5510 electron-beam tube accelerates electrons in a vacuum and transmits the beam through a thin window. It has high transmitted I (7,000 A), 500-keV beam energy by penetration, and provides 10 J/pulse with reproducibility of ±3% rms.

The Model 5515 electron-beam tube is for maximum beam density and minimum source size.

A high-V power supply is used to charge the pulser rated at 5 mA, adjustable V from 0 to 30 kV.

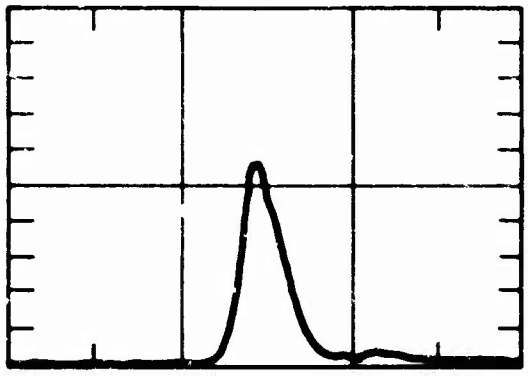

10 ns/cm

(Redrawn from scope picture)

Figure 3-25. Wavefcrm of transmitted electron I.

Table 3-1. 706 system electron-beam output specifications.

Parameter	Tube 5510	Tube 5515
Total Output Beam Energy	10 J	12 J
Maximum Beam Energy Density	4 J/cm^2	8 J/cm^2
Surface Dose in Al	2 Mrad	4 Mrad
Linear Extrapolated Range in Al equivalent electron energy	160 mg/cm^2 500 keV	200 mg/cm^2 600 keV
Pulse Rate		1/min

Table 3-2. 706 system x-ray output specifications.

Parameter	Tube 5515 (external target)		Tube 5290 (internal target)
	Full Beam	Apertured Beam	
X-ray Source Dia.	8-mm effective	4 mm	2.8 mm
X-ray Dose 12 in. from Tube Face Maximum	 60 MR 100 R		 25 MR 7 R
Maximum X-ray Dose Rate	4×10^{10} R/s		2×10^{9} R/s
Penetration in Al	2 in. at 6 ft	2 in. at 2.2 ft	2 in. at 3.5 ft
Pulse Rate	1/min		

The solid curve in Figure 3-26 shows the measured electron dose versus depth in thick Al absorber located 0.5 in. from the tube face. It is quite similar to published data for 500-keV monoenergetic electrons (dashed curve). The surface and maximum doses in Al are 2.6 and 3.4 Mrad, respectively. The peak dose rate reaches 10^{15} rad/s. Integration of the area under the dose-versus-depth curve yields an energy density of 3.6 J/cm^2. Energy density profiles across the beam are shown in Figure 3-27 for two distances (0.125 and 1.5 in.) from the tube face. At the closer distance, a peak density of 5.5 J/cm^2 and a beam half-width of 8 mm are suited to the intense irradiation of small objects. At the larger distance, a broader beam allows nearly uniform irradiation of larger areas.

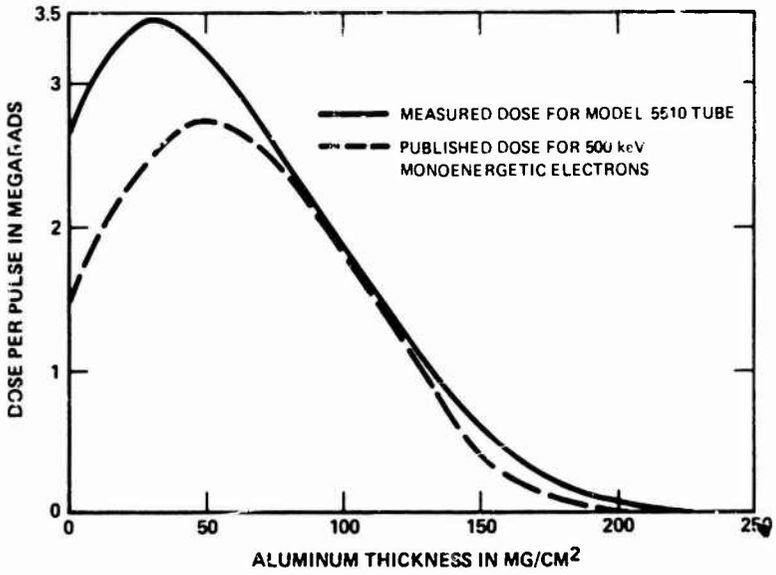

Figure 3-26. Measured electron dose versus depth in thick Al absorber 0.5 in. from the tube face.

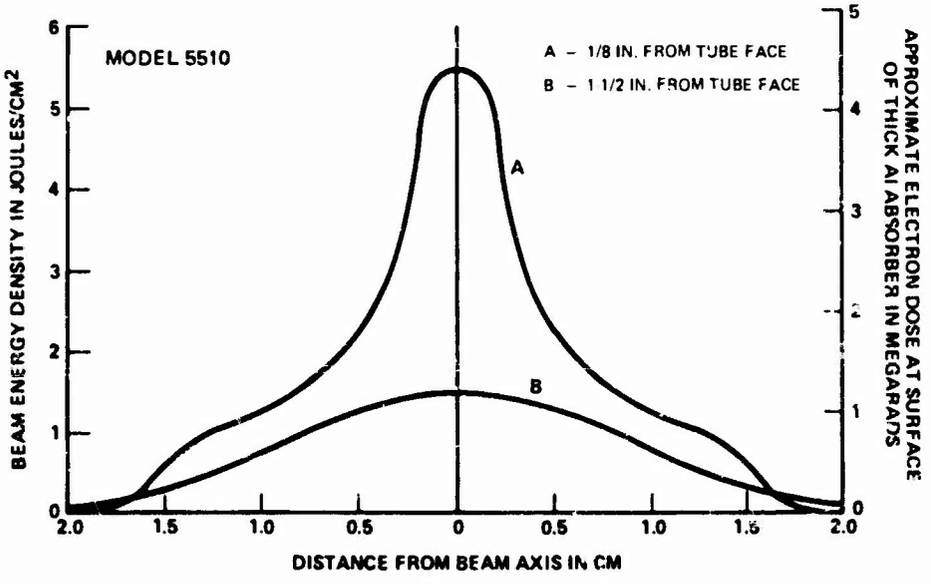

Figure 3-27. Energy density profiles across the beam.

Figure 3-28 shows the beam energy density near the axis as a function of distance from the tube face; the values shown are the average energy density over a 0.25-in.-dia. calorimeter centered on the axis. Peak values on the axis are somewhat higher, as indicated by the dosimetry check point. The beam expands in vacuum and the energy density follows a $1/r^2$ law at distances greater than 1 in. However, in other media the beam propagation characteristics are affected by the medium. In air, the beam expansion is considerably reduced and actually converges at 3 in. from the tube, at least near the axis.

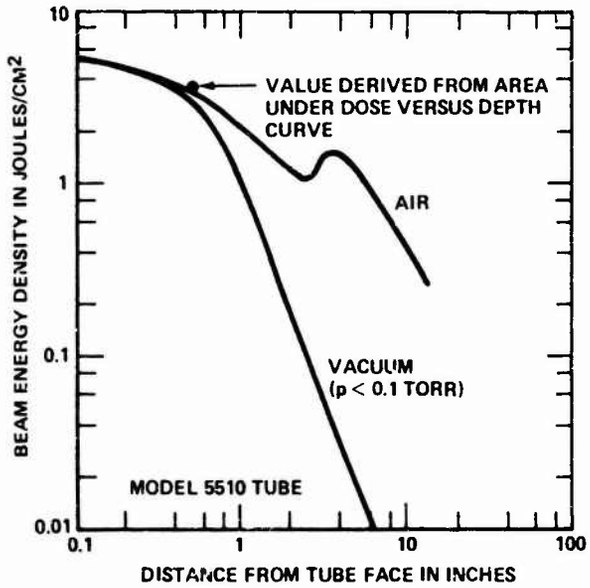

Figure 3-28. Beam energy density near the axis as a function of distance from tube face.

Figure 3-29 shows a complete mapping of the electron beam in the region near the tube window, derived from the data of the previous 2 figures. Both energy density and surface Al dose scales are shown.

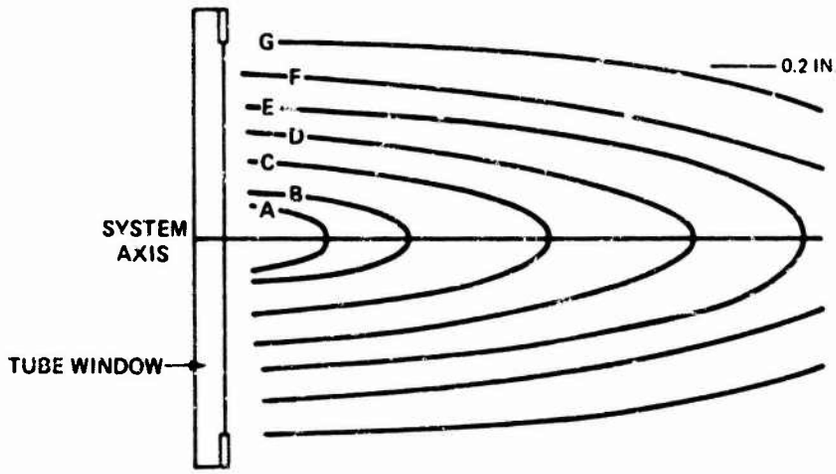

	BEAM ENERGY DENSITY (joules/cm^2)	SURFACE DOSE (megarads)
A	4	3.2
B	3	2.4
C	2	1.6
D	1.5	1.2
E	1.25	1.0
F	1.0	0.5
G	0.5	0.4

Figure 3-29. Map of electron beam in region near the tube window.

Calorimetric measurements of the total beam energy in 100 successive pulses and statistical analysis yields an rms fluctuation of 3% in the total beam energy for tube 5510. Similar measurements with a portion of the beam (0.25-in.-dia. calorimeter) show a mean fluctuation on the order of 5% in energy density near the window (air or vacuum). Comparable fluctuations are expected in the local dose.

The solid curve of Figure 3-30 shows the electron dose versus depth in Al at 0.5 in. from the 5515 tube face; the dotted curve shows the dose versus depth for tube 5510 for comparison.

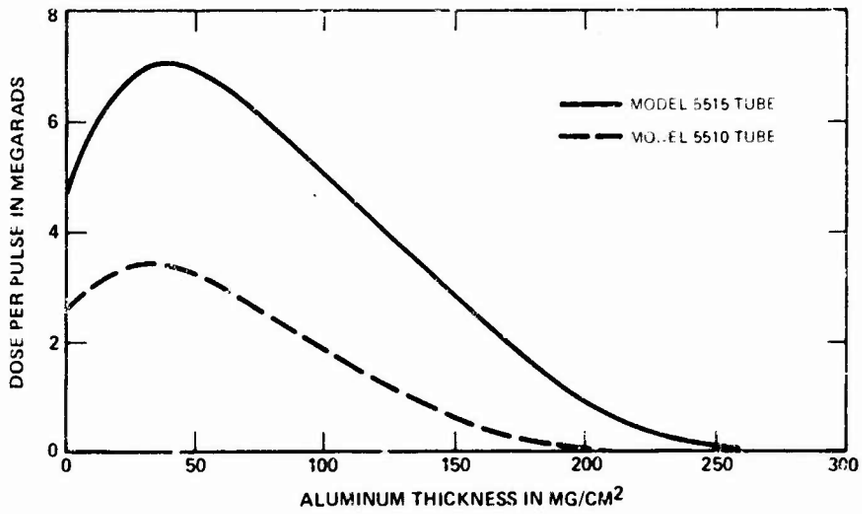

Figure 3-30. Electron dose versus depth in Al at 0.5 in. from 5515 tube face.

Nominal peak dose for tube 5515 is 7 Mrad and the linear extrapolated range of 214 mg/cm^2 is equivalent to that of 620-keV monoenergetic electrons. Measurements of the peak I density at 0.125 in. from the tube face, using a fine aperture Faraday cup, yield a value of 4,000 A/cm^2.

Figure 3-31 compares the energy-density profile for the 2 tubes in the plane 0.125 in. from the tube face. The effective beam cross-sectional area is smaller for tube 5515.

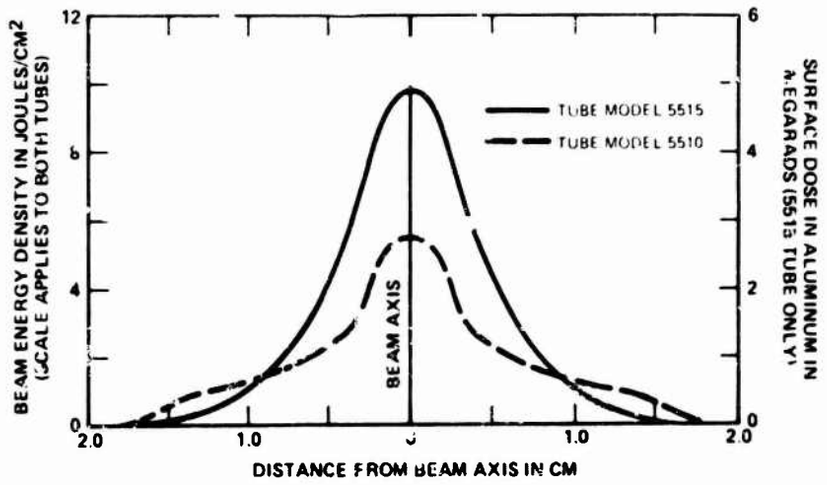

Figure 3-31. Energy-density profiles of 2 tubes in a plane 0.125 in. from the tube face.

Figure 3-32 shows graphs of beam-energy density versus distance from the tube face in air and in a vacuum. Solid curves are for the 5515 tube; dotted curves are for tube 5510.

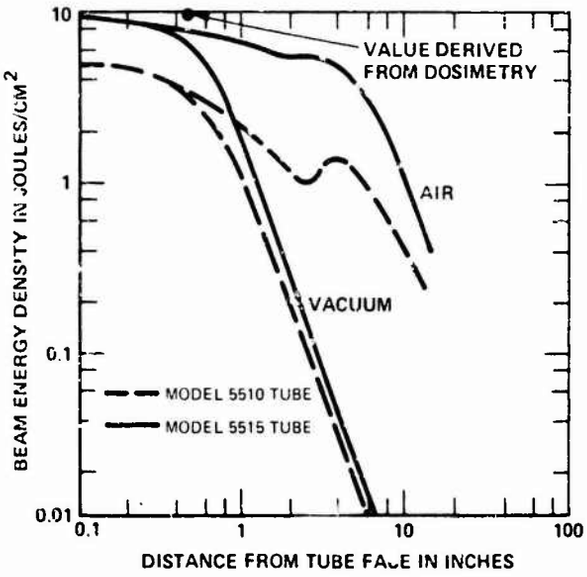

Figure 3-32. Beam-energy density versus distance from tube face in air and in a vacuum.

Energy density is much higher with tube 5515 near the tube face, but the difference decreases at large distances from the tube face since both tubes have comparable values of total beam energy and scattering and traverse energies.

The beam-energy density in air is much higher than that found in a vacuum, although details of the curve differ because of detailed differences in the characteristics of the injected beam. The fact that the beam energy for tube 5515 remains high for some distance is useful in applications requiring a finely apertured electron source, particularly where the tube must be protected from possible damage by the event under study, since it permits location of the tube several inches behind the beam-defining aperture.

For tube 5515, the surface and maximum doses in Al, in Mrad, are approximately 0.5 and 0.8 times the energy density in J/cm^2.

Dose and energy density for tube 5515 are approximately symmetrical about the tube axis. Isodose curves have radii from the axis that are typically constant within 10% near the tube and within 5% at 1.5 in. from the tube.

The pulse-to-pulse reproducibility and beam symmetry for tube 5515 are similar to those for tube 5510. Deviations from symmetry and reproducibility are slightly larger.

An external target converts the FEBETRON's electron beam to an x-ray source. Model 5515 tube provides an x-ray source with the penetration shown in Figure

3-33. The full-output beam has a source size of 8 mm, which can be quite useful at large film-to-source distances (e.g., shadowgraphs of bomb fragments). The x-ray beam is sufficiently broad (about 30 degrees) to cover usefully large areas.

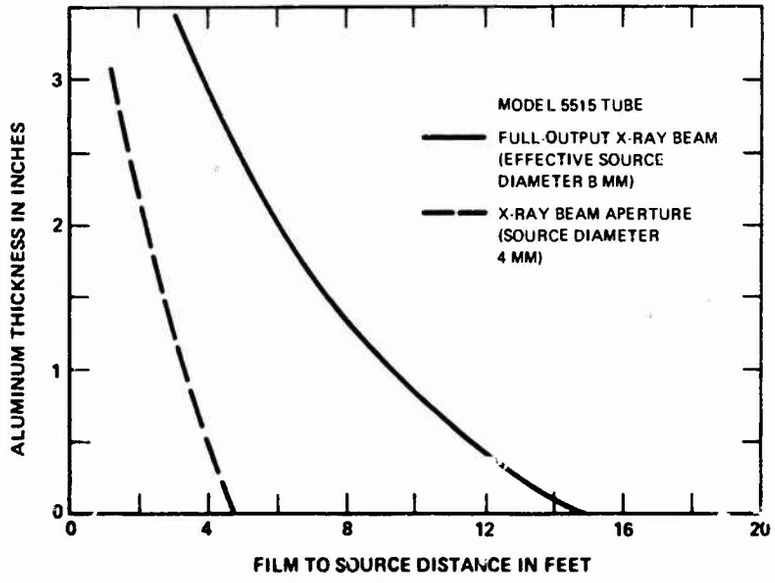

Figure 3-33. X-ray penetration of Model 5515 tube.

Tubes 5510 and 5515 with an external target also can be used as ns x-ray sources for high dose-rate radiation-effects studies. Figure 3-34 shows the dose-per-pulse measured on the axis of tube 5515. Near the target, the dose exceeds 100 R and the dose rate 4×10^{10} R/s. At a given distance from the tube, the x-ray dose for tube 5510 is about 70% of that for tube 5515.

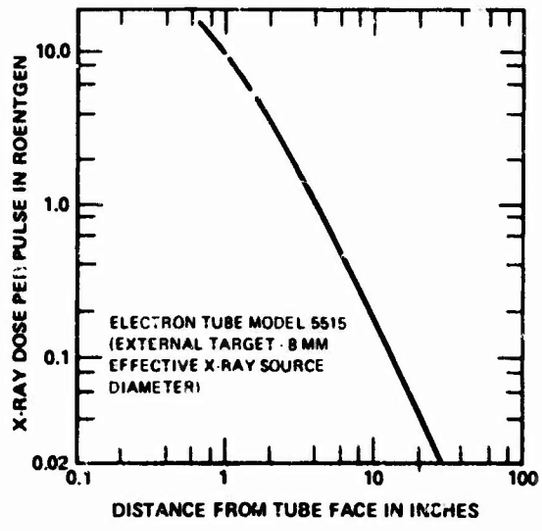

Figure 3-34. X-ray dose versus distance for Model 5515 tube.

3.3.3 Northrop Research and Technology Center FXR Facilities

The Northrop Research and Technology FXR facility (Figures 3-35 and 3-36) is a FEBETRON 705. It is located in the Northrop reactor building, where it is attached to one wall of a shielded enclosure (Topatron Model 7222), and is operated from a console in the control room adjacent to the machine cell. Instrumentation, signal, and power cables, which run from the control room into the shielded room, are routed through four 3.5-in. steel tubes which have 90-degree bends to prevent radiation streaming into the control area.

3.3.3.1 Environment for Electron-Beam Mode

Electron-beam dosimetry measurements were made utilizing calorimeters constructed of 0.125-in.-dia., 0.01-in.-thick Al disks with a chromel-alumel thermocouple unit in the center. Figure 3-37 is a typical electron-beam response curve averaged over the data obtained in this manner.

At full charging V and maximum magnetic field focusing, the electron pulse width (FWHM) is approximately 55 ns.

An external focusing magnet assembly is available to produce electron-beam levels of up to 120 cal/cm^2. The test specimen size at this level is limited to a dia. of ~3/16 in. A magnetic field of up to 16,000 G is present in the target area.

3.3.3.2 Environment for X-Ray Mode

A 0.025-in.-thick Ta target is used to generate x-rays. CaF_2 TLDs are used for x-ray dosimetry. The detectors are calibrated with the Northrop Co-60 source. Table 3-3 gives the results of x-ray dosimetry measurements made in the geometry depicted in Figure 3-38. A typical x-ray response curve averaged over the existing experimental data is given in Figure 3-39.

At full discharge V and maximum (4,000 G) internal field strength, the x-ray pulse width is 20 ns.

3.3.3.3 Support Capabilities

Northrop-owned equipment is available on a noninterference basis. Power is available from 3 wall-mounted 1-ϕ electrical raceways in the control room (20 A), and one in the analyzer area (30 A), which require standard 115-Vac, 3-prong, straight safety plugs. Cable lengths of at least 20 ft are required for positioning of test specimens or fixtures in front of the radiation beam. Additional cable lengths should be anticipated and added if low-level testing is performed with the specimen spaced at greater distances from the machine face. The screen room's primary power is 115-Vac, 1-ϕ, 60-cycle, 15-A. Additional power can be connected to the screen room through permanently installed RFI filters, and includes: 480-V, 3-ϕ, 60-cycle, 30-A; 120/208-V, 3-ϕ, 400-cycle, 30-A; 28-Vdc, 50-A. A scope triggering signal actuated by the tube discharge is available.

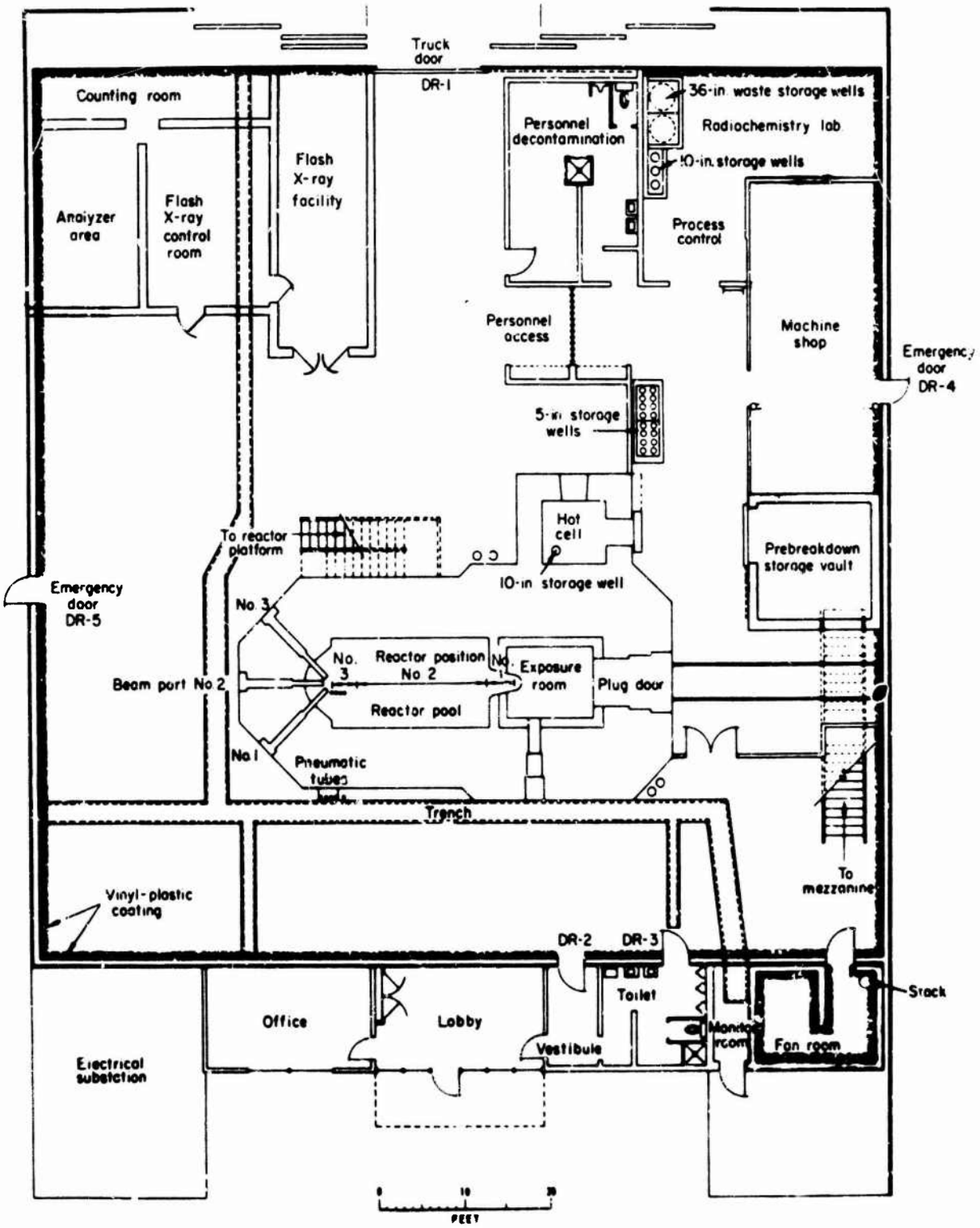

Figure 3-35. Plan view of Northrop reactor facility.

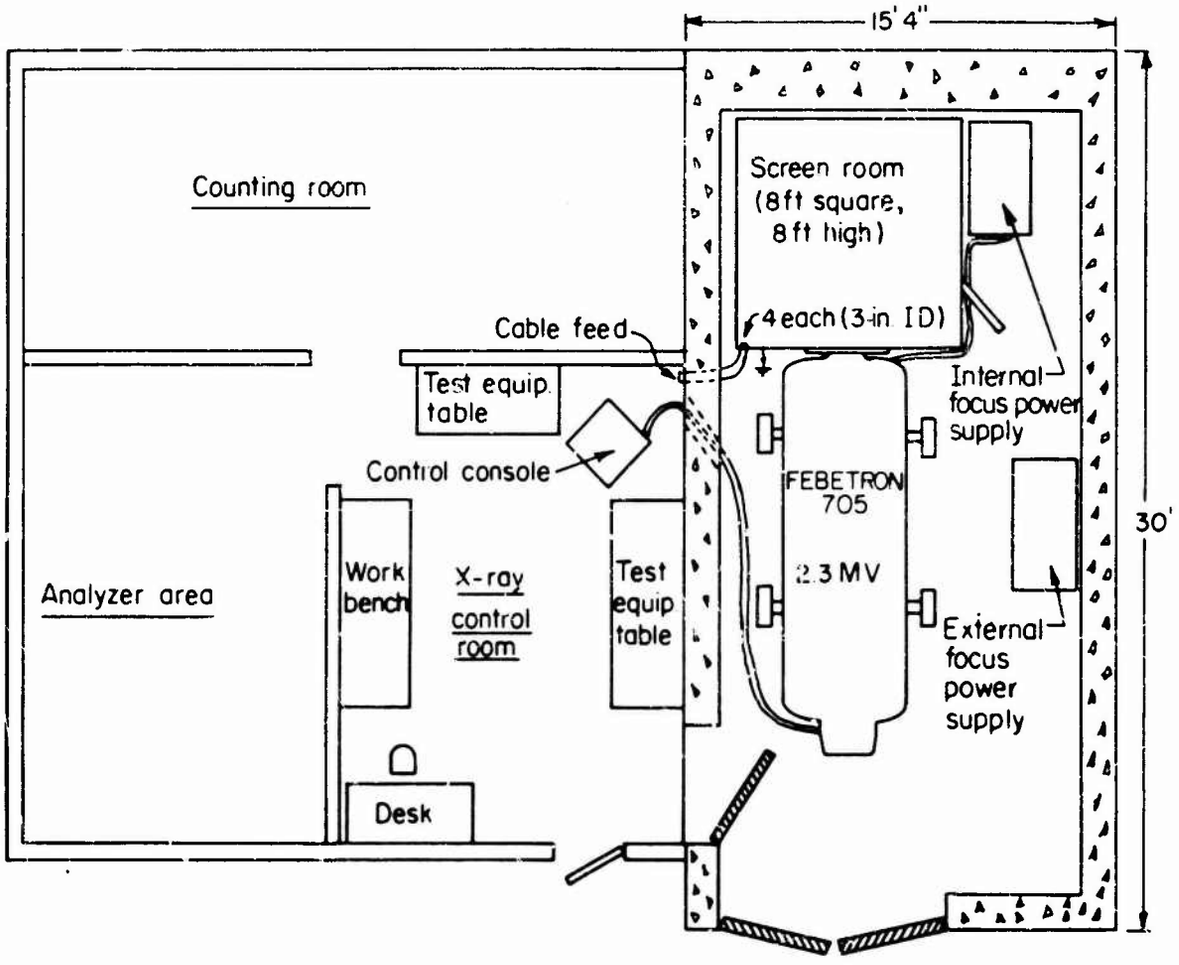

Figure 3-36. Northrop Research and Technology Center 2.3-MV FXR facility.

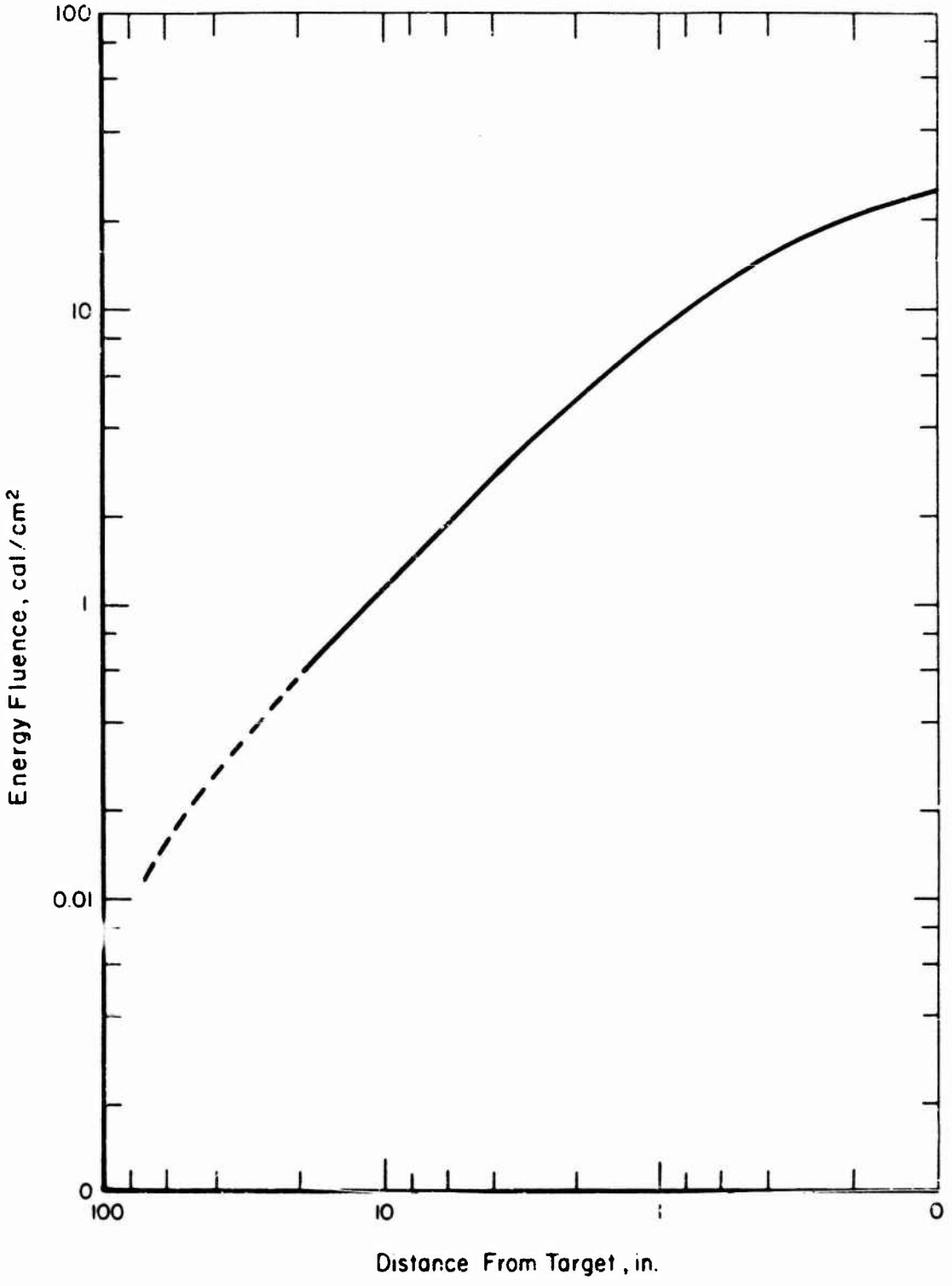

Figure 3-37. Typical electron-beam response of the Northrop FEBETRON 705.

Table 3-3. Northrop FEBETRON 705/tube 545C x-ray beam map.

Dose at a Distance From the Target (rad (Si))							
Position Number	1-in.	2-in.	3-in.	Position Number	1-in.	2-in.	3-in.
1	1290	495	226	18	309	187	136
2	984	436	199	19	256	180	136
3	1030	466	210	20	265	191	146
4	1050	515	218	21	273	191	143
5	1110	418	218	22	290	195	142
7	1040	432	218	23	290	191	146
8	941	418	225	24	367	210	146
9	950	413	211	26	400	203	157
10	499	326	178	27	345	187	155
11	490	336	178	28	370	187	154
12	539	346	194	29	294	178	154
13	625	307	213	30	289	187	131
14	607	311	198	31	299	187	121
15	593	283	189	32	284	187	126
16	523	271	181	33	274	187	129
17	455	267	172				

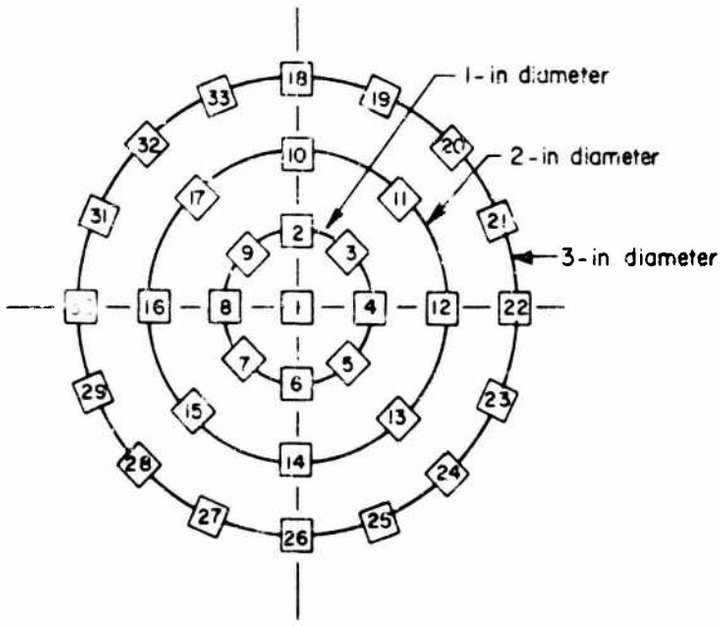

Figure 3-38. TLD fixture positions for Northrop FEBETRON 705/tube 545C x-ray beam map.

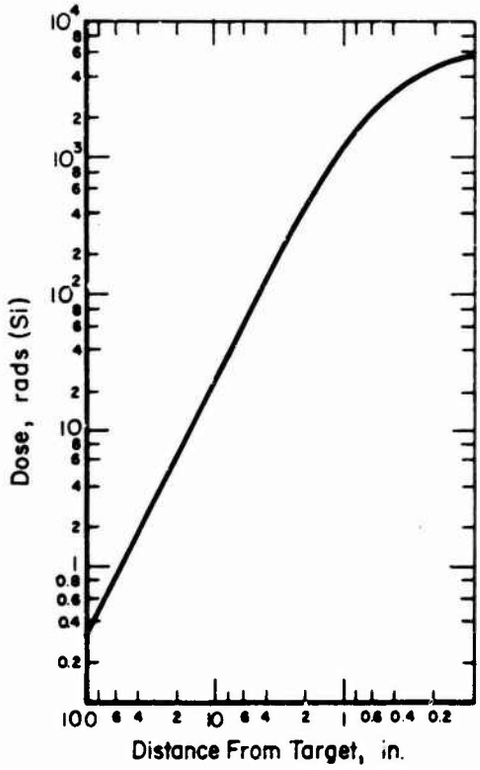

Figure 3-39. Typical x-ray response of the Northrop FEBETRON 705/tube 545C.

Dosimetry equipment and services include multichannel analyzers, automatic counting systems, and gas flow and scintillation detector systems. CaF_2 TLDs are used for x-ray dosimetry.

Northrop's IBM 360-65 computer may be used by special arrangement. Nearby Control Data Corporation's CDC 6600 and a remote tie-in to an IBM 360-40 is available on a contract basis.

Located within the building are a radiochemical laboratory, a hot cell, and a complete machine shop with capability for construction of special shielding screens and experimental irradiation devices. The heavy machine shop of the Northrop Corporate Laboratories is available on a contract basis. Experiment preparation and setup laboratories are available to the user. Associated with the hot cell is 2,500-Ci Co-60 source with a maximum dose rate of 1.4×10^5 rad/hr. Also, a limited amount of photographic equipment can be made available.

Test samples are manually placed within the screen room. An adjustable 24-in. x 30-in. specimen-support table positioned in front of the beam runs on tracks which span the 8-ft room and are parallel to the beam access. The table top is adjustable in height from 30 to 48 in. above the floor level and will support 1,000 lbs. Table-top adjustment from side to side is approximately 4.5 in. either side of center. The center of the radiation beam is 42.5 in. above floor and the bottom cable feedthrough tube is 50 in. above the floor level.

A vacuum chamber, 12 in. in dia. and 22 ft long, is available for special applications.

3.3.3.4 Procedural Information

Technical and administrative inquiries should be directed to:

Northrop Research and Technology Center
Chief, Northrop Reactor
3401 W. Broadway
Hawthorne, CA 90250
Telephone: (213) 970-2297.

The lead time required is dependent upon the type of experiment to be conducted. Routine experiments and irradiations require only nominal advanced planning.

Costs and charges associated with the use of the facility are documented and available directly from Northrop. The shipping address is:

Northrop Research and Technology Center
Flash X-Ray Facility, Northrop Reactor
3401 N. Broadway
Hawthorne, CA 90250
Telephone: (213) 970-2297.

The Northrop FXR facility is primarily a research facility but it can be made available for TREE experiments as the work load permits.

3.3.3.5 Reference

1. "Northrop Corporate Laboratories 2.3-MV Flash X-Ray and Electron Beam Facility," unpublished report available directly from Northrop.

3.3.4 Kaman Sciences Corporation FXR Facilities

The Kaman Sciences FEBETRON 705 is housed in a 24-ft x 31-ft underground laboratory. Access for large or heavy items of equipment is provided by a hydraulic lift with a 4-ft x 6-ft platform.

3.3.4.1 Test Parameters

The charging V of the machine is 15 to 30 kV, although it may be modified to accept a maximum of 35 kV. The minimum charging V is set by the firing characteristics of the machine as controlled by the spark gap. The maximum energy stored at 30 kV is 400 J, and is scaled as the square of the charging V.

Normally, a Field Emission Corporation model 545A electron-beam tube is utilized. The maximum energy density available varies from tube to tube and is 20 to 25 cal/cm^2.

Figure 3-40 is a plot of the total energy as a function of charging V. Figure 3-41 is a typical normalized electron-beam energy density contour.

Steady-state repetition rate is 1 pulse/3 min for continuous operation. For up to 5 pulses, the machine may be operated at 1 pulse/10 s.

Calorimetric measurements indicate that the electron-beam energy density at a given spatial point is reproducible to 2.5% rms pulse-to-pulse.

Pulse timing jitter is less than 10 ns. The pulse also may be delayed over the range of 1 ms to 100 ms, continuously variable in 5 ranges. Using a delayed pulse adds to the timing jitter by less than 0.2% of the delay setting.

To minimize electrical noise, the device under test and associated electronics are placed in an RF shield and tied to the facility ground by a heavy copper braid. Circuit ground is located in the RF box and is isolated from facility ground. Connecting leads from the RF box to a screen cage containing instrumentation are coaxial cables enclosed in a copper wire-mesh shield. This shield is grounded at a point close to the target end of the machine. Using the above grounding and shielding, electrical noise is typically <5 mV when low impedance (50Ω) driving circuits are used.

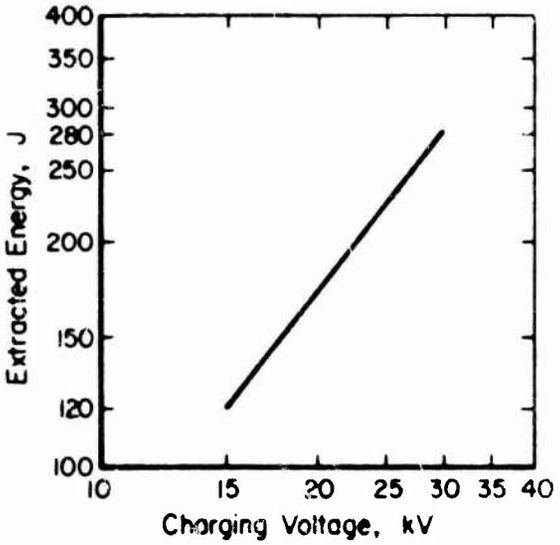

Figure 3-40. Extracted beam energy of Kaman Sciences FEBETRON 705, electron-beam mode.

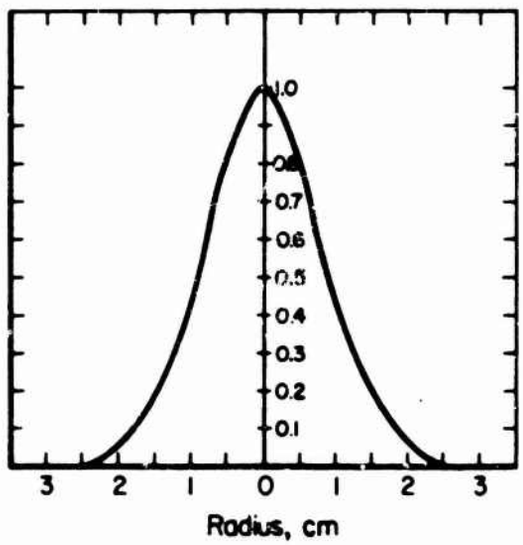

Figure 3-41. Normalized typical beam energy density contour (measured at 1 cm from anode) of Kaman Sciences FEBETRON 705, electron-beam mode.

X-ray diagnostics utilize LiF TLDs and scintillation detectors. The dosimeters are calibrated by means of a Co-60 source.

3.3.4.2 Environment for Electron-Beam Mode

Figure 3-42 is a typical electron-beam center-line energy-density curve for the 545A tube. The curve represents summarized data taken from a large number of total absorbing Al calorimeter measurements.

Typical output power waveforms are shown in Figure 3-43 for 2 charging V.

Figure 3-44 depicts the electron energy spectrum, determined from considerations of V and I time-dependent waveforms. The data have been corrected for electron losses in the thin window anode of the 545A tube. The spectrum is used in Monte Carlo electron transport calculations in conjunction with the thin window tube anode. Of the several methods which may be used to determine an energy spectrum, this method has been found to give results which are in excellent agreement with experimental dose-depth measurements.

Experimentally determined dose-depth profiles for several metallic elements are given in Figure 3-45. The data are normalized to 1 cal/cm^2, and were obtained at a distance of 5 cm from the anode. Calorimetric measurements are accurate to ±6%, with a maximum error of ±10% when beam fluctuations are included.

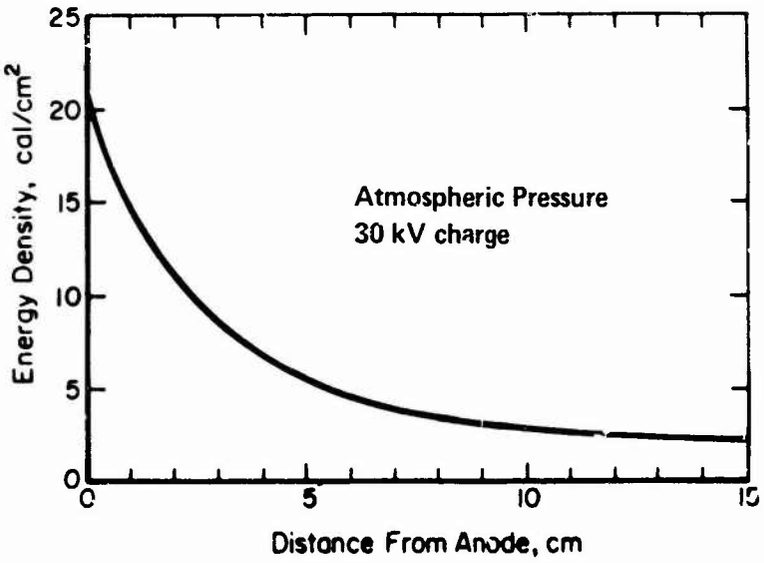

Figure 3-42. Center-line beam energy density (typical) for Kaman Sciences FEBETRON 705/tube 545A, electron-beam mode.

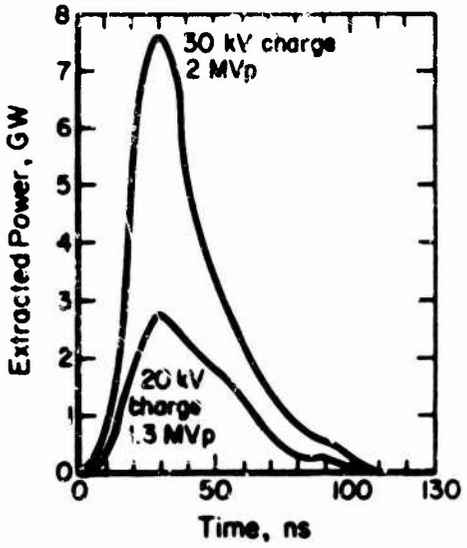

Figure 3-43. Instantaneous beam power for Kaman Sciences FEBETRON 705/tube 545A, electron-beam mode.

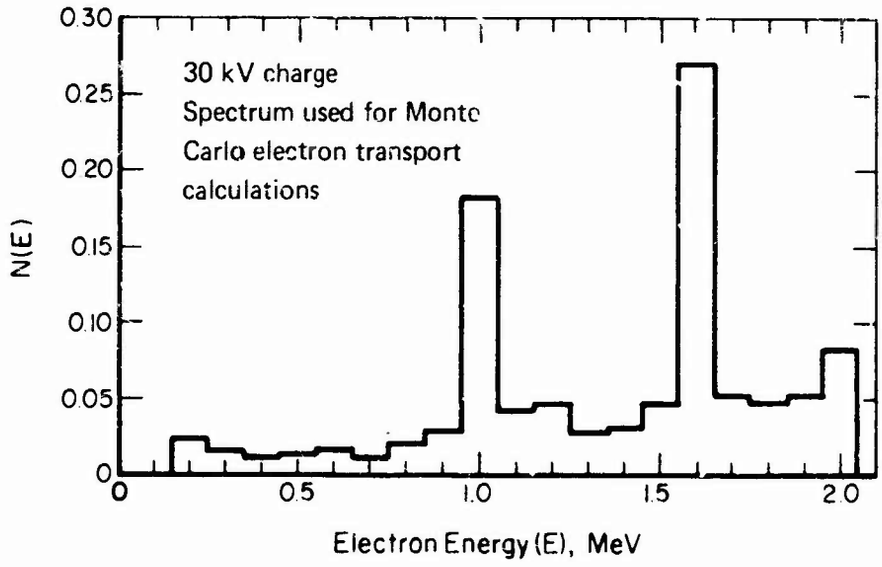

Figure 3-44. Electron energy spectrum N(E) for Kaman Sciences FEBETRON 705/tube 545A.

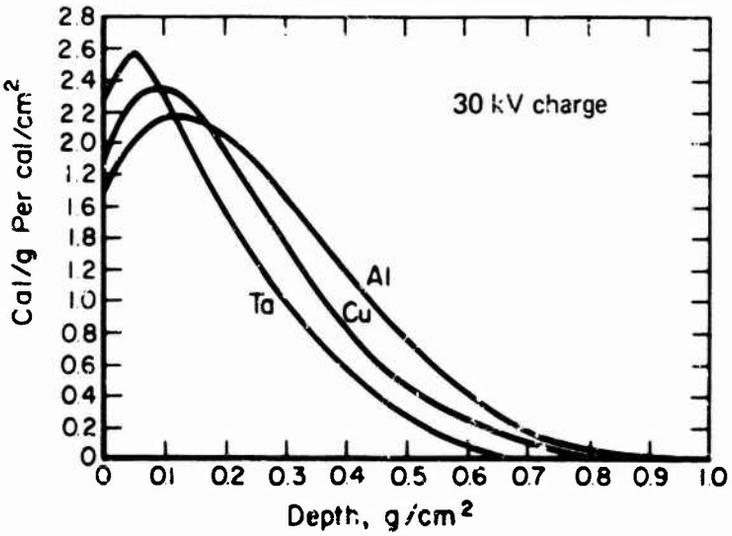

Figure 3-45. Normalized deposition in metals for Kaman Sciences FEBETRON 705/tube 545A, electron-beam mode.

3.3.4.3 Environment for X-Ray Mode

A Ta bremsstrahlung target is utilized for the generation of x-rays.

Figures 3-46 and 3-47 summarize the experimental dose data. Figure 3-48 depicts a typical x-ray mode waveform. The pulse width (FWHM) is 20 ns. A typical photon energy spectrum is given in Figure 3-49.

3.3.4.4 Support Capabilities

Electronic equipment available for experimental diagnostics and analysis includes Tektronix 519, 546, and 555 oscilloscopes, a Tektronix 575 curve tracer, several low-V electronic power supplies, a waveform generator, and equipment for color photomicrography. Space is available external to the laboratory for accommodating instrumentation trailers.

Trigger pulses are available for times ranging to 1 ms before and after machine firing.

Limited dosimetry equipment and services are available. Electron dosimetry is performed by calorimetric and colorimetric techniques. LiF TLDs and electron scintillation techniques are employed for x-ray dosimetry. Personnel from the operating staff are available to lend assistance in dosimetry measurements.

The Kaman Sciences CDC 6400 computer with expanded 65,000-bit memory is available. Operational circuit analysis codes include KNCAC (modified ECAP) and SCEPTRE. Also operational is the specialized FEBETRON Monte Carlo electron transport and energy deposition code EPIC.

Complete machine-shop facilities capable of constructing experimental apparatus, and experiment preparation and setup laboratories, as well as limited office space and conference room, are available.

Oscilloscope cameras for the Kaman oscilloscopes, a dark room, and a limited amount of photographic laboratory equipment may be used.

3.3.4.5 Procedural Information

Technical and administrative inquiries should be directed to:

Kaman Sciences Corporation
1500 Garden of the Gods Road
Colorado Springs, CO 80907
Attn: Dr. Donald H. Bryce, Flash X-Ray Facility
Telephone: (303) 598-5880.

The lead time required depends upon the type of experiment to be conducted. Routine experiments and irradiations require only nominal advance planning. A lead time of 1 week is usually advisable.

The Kaman equipment is government-owned and is available at no cost to qualified users. Users must bear the cost of expendable items such as electron-beam

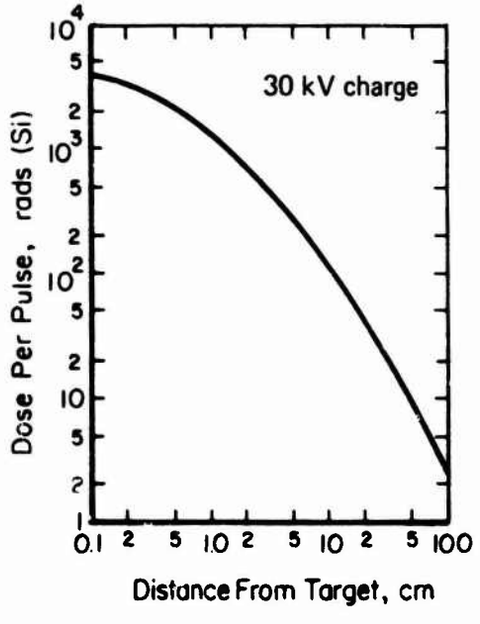

Figure 3-46. Dose per pulse for Kaman Sciences FEBETRON 705/tube 545A, FXR mode.

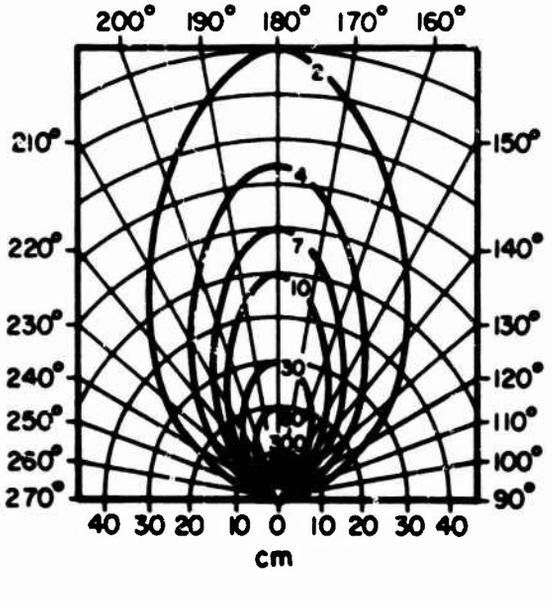

Figure 3-47. Dose contours, rad(Si), for Kaman Sciences FEBETRON 705/ tube 545A, FXR mode.

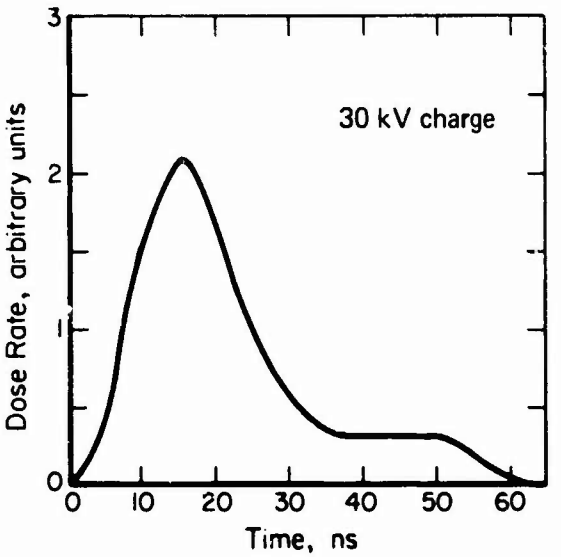

Figure 3-48. Nominal dose rate for Kaman Sciences FEBETRON 705/tube 545A, FXR mode.

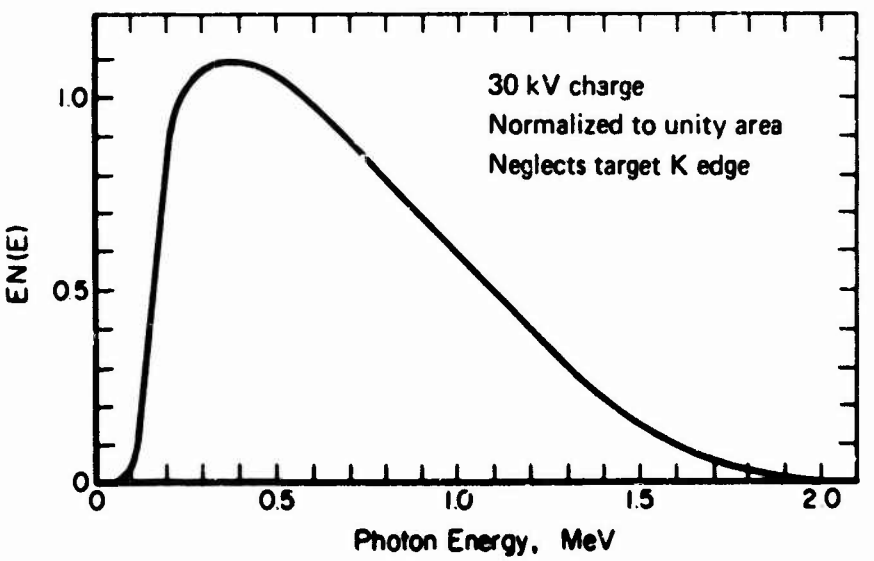

Figure 3-49. Photon spectrum for Kaman Sciences FEBETRON 705/tube 545A, FXR mode.

tubes and films and the cost of any labor. There is no facility use charge. Exact cost quotations may be obtained from the Director.

3.3.5 Lockheed Palo Alto Research Laboratory FXR Facilities

The Lockheed Palo Alto Research Laboratory (LPARL) has a FEBETRON 705 and a FEBETRON 706, both with 5510 and 5515 tubes.

Over 175,000 pulses were fired on the FEBETRON 705, primarily in the electron-beam mode (approximately 80%), with the remainder in the x-ray mode. The machine is available for operation in either mode. The electron beam is most often used directly in air; however, a small vacuum chamber is available. Beam geometry varies with parameters such as charging V, magnetic focusing field, type of electron-beam tube, and distance from the machine anode.

The machine is operated on a manual charge-fire basis with firings every 40 s. The rate of fire may be increased to 6/min for a few (4 to 5) pulses. More than 400 shots per standard 8-hr work shift are commonly achieved.

Normally, for any given tube, pulses are reproducible to within a few percent of each other at a distance of less than 10 cm from the tube window. Pulse delay is variable up to 1 ms, with jitter in the trigger posing no problem since normal experimental work uses an external radiation trigger when required. Pulse width (FWHM) may be modified (although the output is reduced) by appropriate choice of apertures, filters, or magnetic field strength.

Available electrical noise data are limited. A photomultiplier (producing MV of signal) placed in close proximity to the FEBETRON 705 has been used to monitor events spectroscopically 300 ns after the pulse and later. In the adjacent screen room, photocurrents as low as 1 mA may be measured.

Electron-beam measurements are made with various calorimeters, with stainless steel being the standard. Faraday cup, stacked blue cellophane, and red Cinemoid dosimeters are also used.

X-ray dosimetry techniques rely primarily on the use of TLDs calibrated against a Co-60 source. Shot-to-shot reproducibility is within the accuracy of the TLDs.

3.3.5.1 Electron-Beam Mode Environment

Oscilloscope traces of the V monitor for both the x-ray mode of the 705 and 706* and the electron-beam mode of the 705 are given in Figure 3-50. The V monitor is a capacitive V divider from the Marx line. Electron-beam spectral data and energy deposition data are given in References 1 through 3.

---

*Waveform included for 706 x-ray pulse.

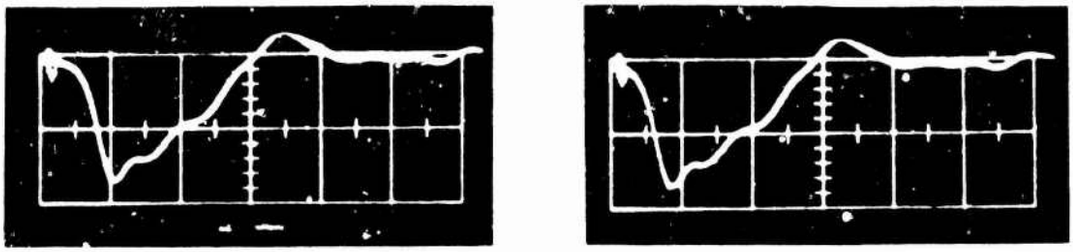

a. Electron-beam mode b. X-ray mode

Notes: Tektronix 519 oscilloscope.
50 ns/division.

Figure 3-50. Lockheed FEBETRON 705 V waveforms.

A post-focus mode is capable of producing approximately 120 cal/cm^2. Sample size is limited to 3-mm dia. at this level.

A number of super-radiant phosphors are available which emit extensively (10^{16} photons/pulse), at discrete wavelengths, from 345 to 735 nm. If activated by the FEBETRON 706, the photon pulse width is less than 3 ns. Fluence measurements are accurate to ±5%.

3.3.5.2 X-Ray Mode Environment

An oscilloscope trace of the bremsstrahlung output taken with a photodiode detector is given in Figure 3-51.

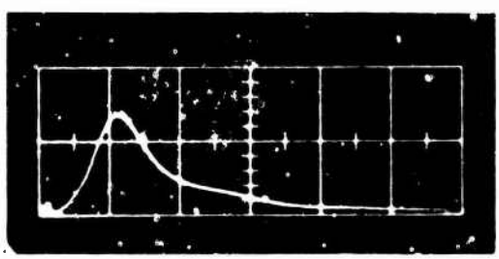

Notes: Scintillator/photodiode.
Tektronix 519 oscilloscope.
20 ns/division.

Figure 3-51. Lockheed FEBETRON 705 bremsstrahlung waveform.

The 706 is equipped with a low-jitter trigger amplifier that produces an accurate firing time (±7 ns) relative to an external trigger signal. The maximum repetitive rate is 1 pulse/m, the energy output is reproducible with ±5% rms, and it is normally operated at 30-kV charging V.

An oscilloscope trace of the x-ray output with the 5510 tube taken from an x-ray detector is given in Figure 3-52.

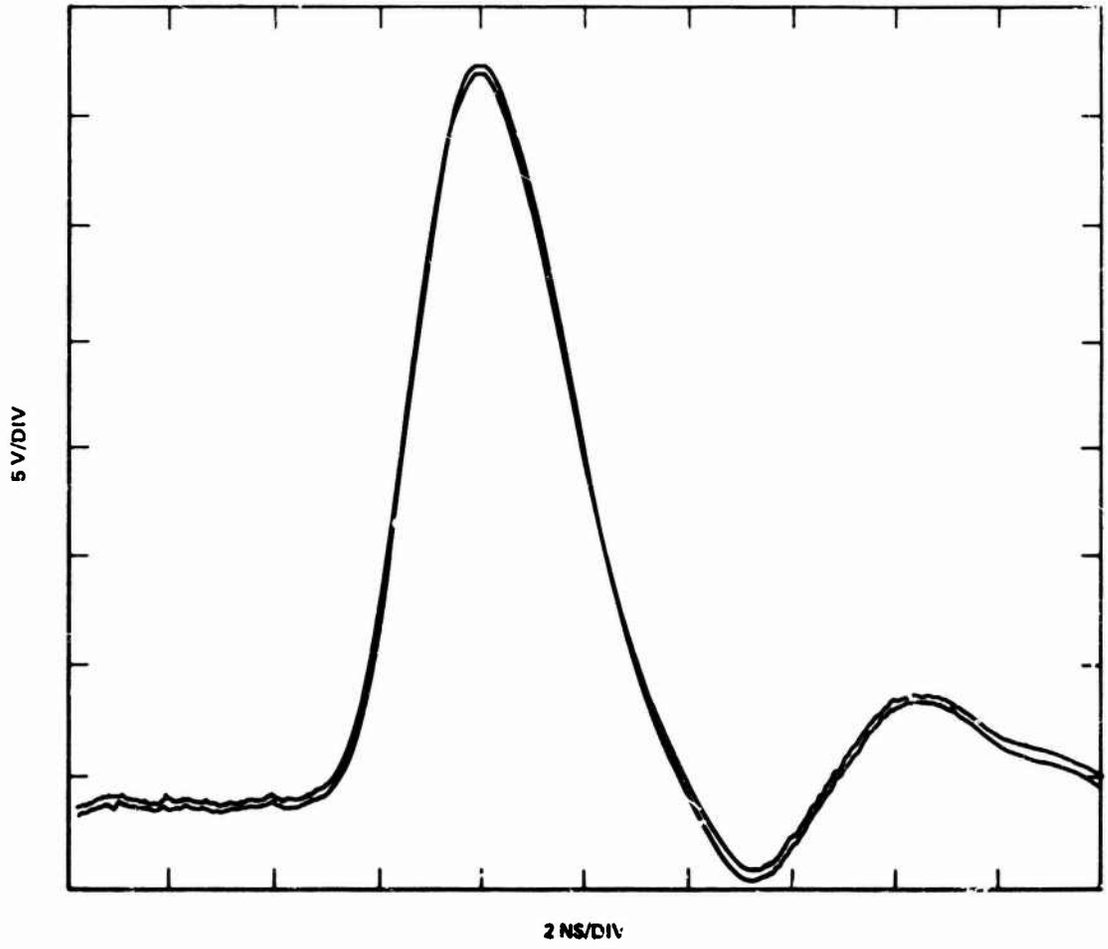

Figure 3-52. FXR pulse from FEBETRON 706. (#3060 detector at 50-cm distance on tube axis. Scales: 5 V/div, 2 ns/div.)

3.3.5.3 Support Capabilities

Electronic equipment is available for complete diagnostics of the machine operation as well as for measurements of material and electronic test sample responses. An instrument pool is located in the same building as the test facility. Space is available external to the facility laboratory for accommodating instrumentation trailers.

Timing signals, including trigger delay up to 1 ms, can be provided from the control room. Radiation triggers are available as standard facility service. TLD

and steel calorimeters, photodiode monitors, and complete diagnostic dosimetry are available.

The Lockheed Research Laboratory computational facility, although not a standard part of the FEBETRON facility, may be used by arrangement. Machine shop facilities capable of constructing experimental apparatus of medium complexity may be used. More extensive facilities are available by arrangement.

Onsite experiment preparation and setup laboratories, limited office space, and a conference room are available. Oscilloscope cameras for the Lockheed oscilloscopes are provided. Complete photographic facilities can be provided, including equipment for microscopic examination and documentation of test specimens. A positioning table and screen room are normally used in the experimental area. The primary test position is approximately 10 cm in front of the beam exit window, with the beam extracted directly into the test specimen in air.

Inquiries concerning operation and use of the facility should be directed to:

Lockheed Palo Alto Research Laboratory
3251 Hanover Street
Palo Alto, CA 94304
Attn: J.F. Riley, 52-11, B/203
Nuclear Sciences Laboratory
Telephone: (415) 493-4411, Ext. 45153.

Scheduling use of the facility generally requires 30 days. Costs and charges are negotiated on an individual basis. Details can be obtained from Lockheed.

The shipping address is:

Flash X-ray Facility, B/205
Lockheed Palo Alto Research Laboratory
3251 Hanover Street
Palo Alto, CA 94304.

3.3.5.4 References

1. Rauch, J.E., "Electron Spectra Produced by the 705 FEBETRON at 10, 12, 15, 20, 30, and 35 kV Charging and the Resultant Dose Depositions in Metallic Elements Ranging from Beryllium to Uranium," LMSC/6-78-69-3, January 13, 1969.

2. Rauch, J.E., "The Determination of Mega-Volt Electron Spectra from Dose Deposition Profiles," *IEEE Transactions on Nuclear Science, 322-325, NS-15*, 1968.

3. Rauch, J.E., "Calorimetric Measurement of Dose Deposition in Aluminum, Copper and Tantalum from High Intensity, Pulsed Electron Beams," *IEEE Transactions on Nuclear Science, 325-335, NS-15*, 1968.

3.3.6 EG&G FXR Facilities

EG&G has a FEBETRON 705 and a FEBETRON 706. Experimenters interested in using the facility should contact:

Lonnie P. Hocker
EG&G Inc.
130 Robin Hill Road
Goleta, CA 93017
Telephone: (805) 967-0456.

3.3.7 Research Triangle Institute FXR Facility

Research Triangle Institute has a FEBETRON 706 with a 5515 tube. Experimenters interested in using the facility should contact:

Dr. Mayrant Simons
P.O. Box 12194
Research Triangle Park, NC 27709.

3.3.8 Westinghouse Electric Corporation FXR Facilities

Westinghouse has a FEBETRON 706 with a 5515 tube, and #1563 low-jitter trigger amplifier system.

The normal specimen test region is a 1-ft^3 airspace, surrounded on 5 sides by a 2-in.-thick layer of Pb bricks for personnel protection. No electromagnetic shielding is presently incorporated into the facility, so experimental measurements are limited primarily to pre-burst and post-burst properties of the test specimens.

Primary diagnostics include a #1653 Faraday cup, a #3060 pulsed radiation detector, and a Tektronix 519 fast-rise oscilloscope for dose-rate information. Total dose measurements are accomplished with a Teledyne Isotopes TLD system, presently active with LiF-Teflon and LiB-Teflon dosimeters.

The Westinghouse Research Laboratory is well equipped with facilities for glassblowing, machine work, and data acquisition, reduction, and analysis.

For information regarding use of the facility, contact:

Westinghouse Electric Corporation
Beulah Road
Pittsburg, PA 15235
Attn: John Hicks
Telephone: (412) 256-3246.

3.4 ION PHYSICS CORPORATION FX-35 ELECTRON-BEAM GENERATOR

3.4.1 Characteristics

The Ion Physics Corporation (IPC) FX-35 pulsed electron accelerator has a characteristic pulse width of 25 ns or less at the half maximum of the power curve; rms output variation at the diode is ±5% or less. The FX-35 can be used either as a stopped beam bremsstrahlung source, or as a direct producer of electron streams.

The FX-35 Electron-Beam Generator operating characteristics are summarized in Table 3-4.

Table 3-4. Operating characteristics of FX-35.

Mean Energy Range (MeV)	Total Beam Energy (cal)	Peak Fluence (cal/cm^2)	Pulse Width (ns)	
			Electron Beam	X-ray
0.4-2.5	400	220	35	20

The FX-35 was designed for use as an FXR machine and is therefore used primarily at V of 1 MV or more, but can be mismatched down to about 400 keV, if necessary.

3.4.2 Test Parameters

The beam is annular at the anode, pinches to the geometric center line at approximately 5 cm, then diverges under vacuum conditions. This is shown in Figure 3-53. The beam is very stable at the 5-cm pinch position. Detailed characteristics of the beam are dependent upon pressure in the drift chamber. The pressure dependence of the beam energy, as determined from calorimeter measurements, is depicted in Figure 3-54. The flux level is determined by the initial pinch position and adjustments are made by regulating the drift-tube pressure. Beam response to these variables is well documented by IPC, and beam control can be maintained for a given experiment configuration. The maximum repetition rate is 2 pulses/min.

An estimate of the pulse predictability can be obtained from Figure 3-55, which shows consecutive bremsstrahlung traces for the FX-35 taken with a pilot-B phosphor and a fast photodiode. Although not definitive, these curves do indicate the reproducibility of these quantities from pulse to pulse. As seen from Figure 3-54, a slight change in pressure causes large changes in deliverable dose for certain pressure regions which slightly degrade electron-beam predictability. The x-ray mode of operation does not utilize a drift tube and the reproducibility is a machine function only.

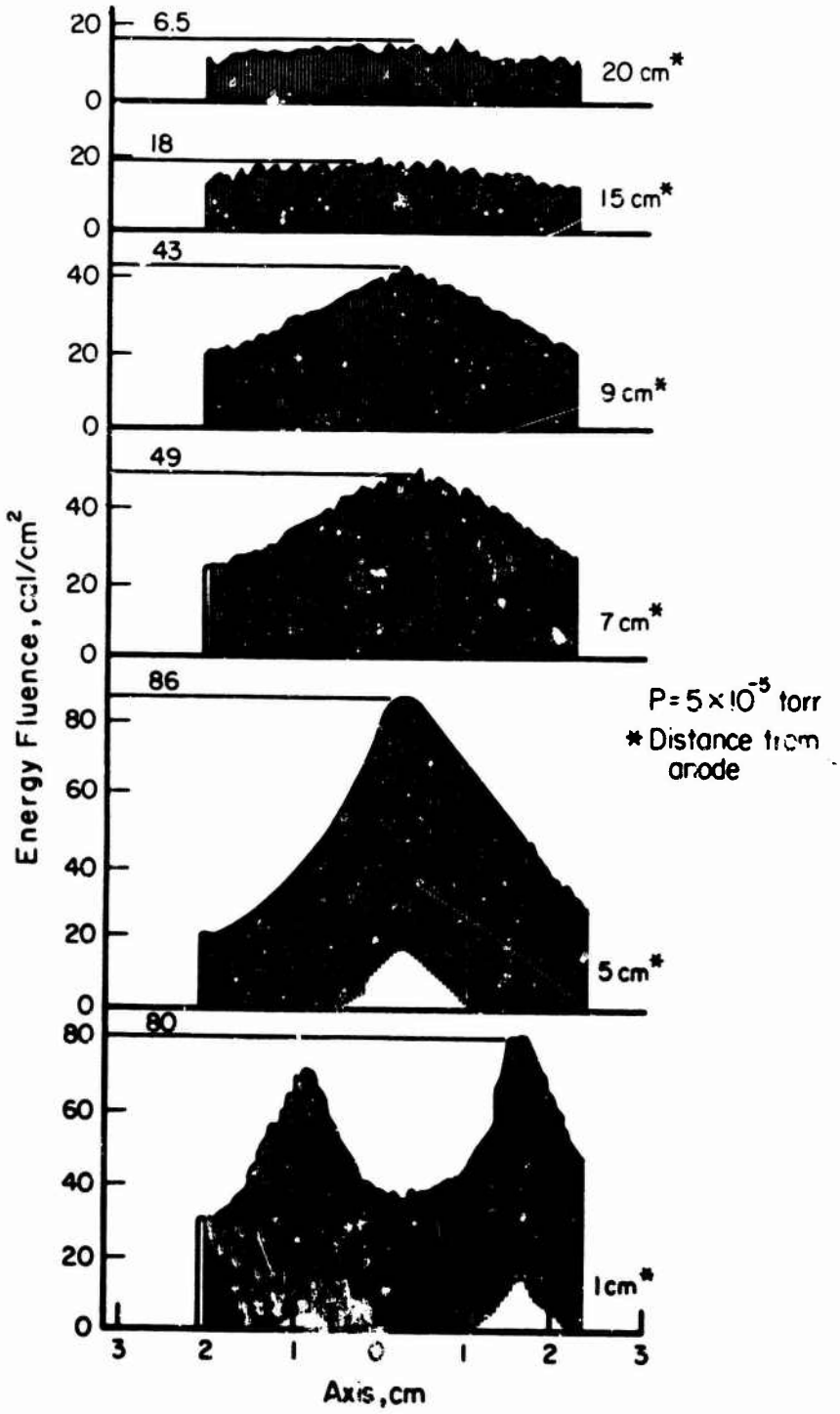

Figure 3-53. FX-35 beam mapping.

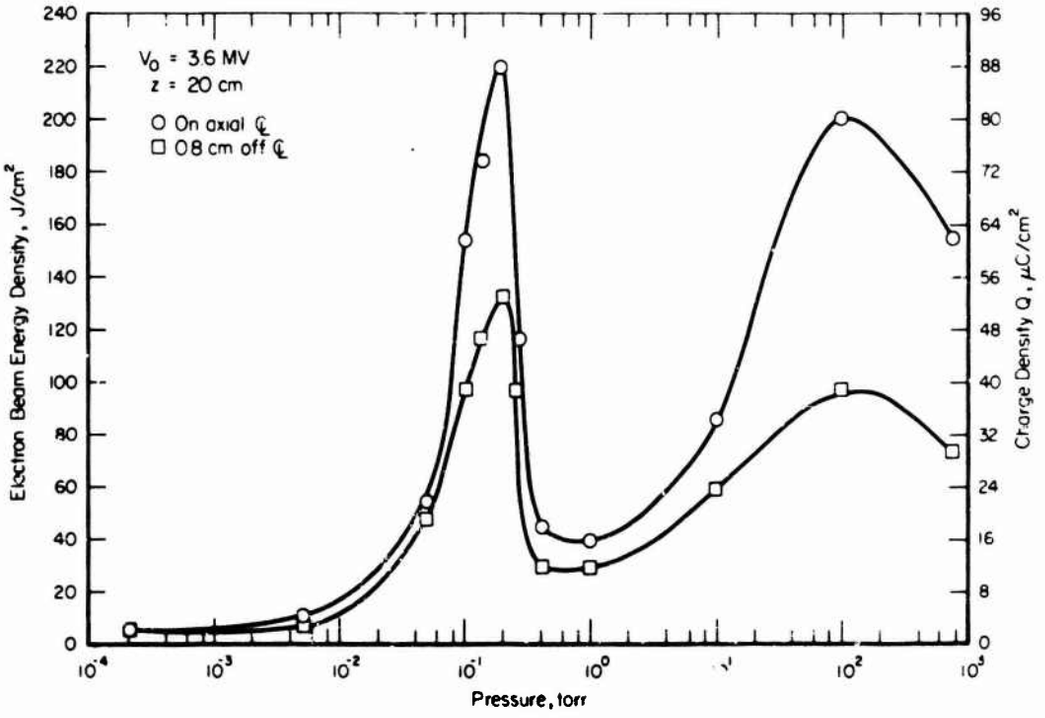

Figure 3-54. Pressure dependence of electron-beam energy monitored calorimetrically 20 cm from entrance window.

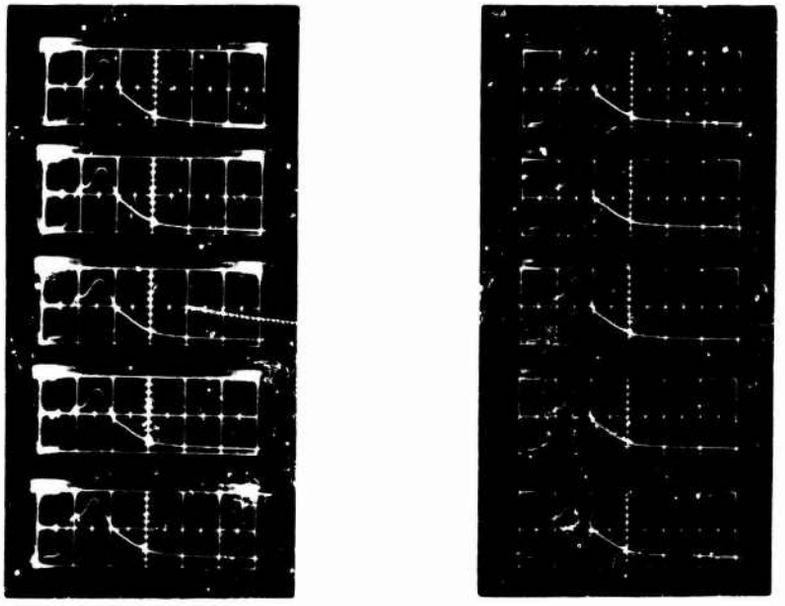

Note: 20 ns/cm.

Figure 3-55. FX-35 bremsstrahlung traces.

The output pulse delay associated with the FX-35 is 500 ns. This delay is defined as the time interval between the command pulse to the spark gap triggering light source and discharge of V at the anode. A Gaussian distribution of jitter is associated with the delay. Data taken for 120 pulses are shown in Figure 3-56. Zero time corresponds to the nominal 500-ns delay.

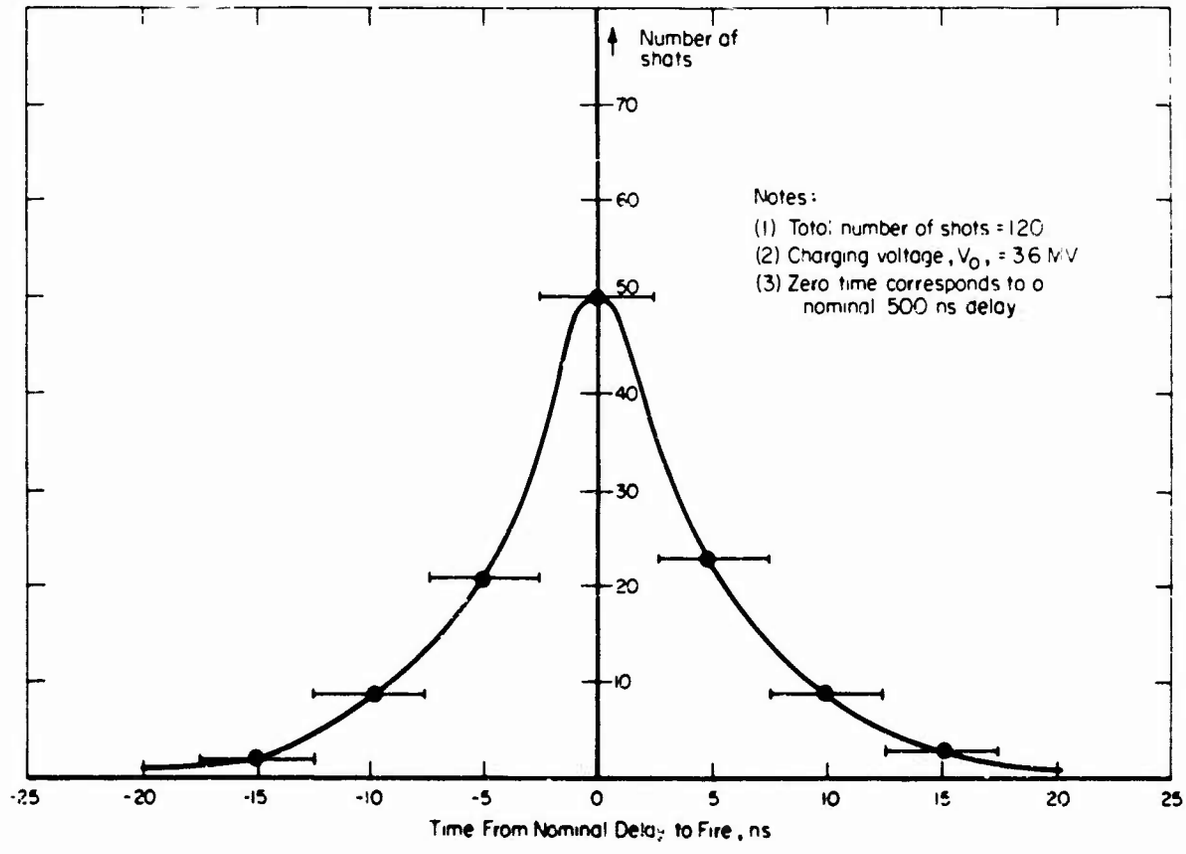

Figure 3-56. FX-35 electronic-trigger performance.

Standard electrical noise measurements were made by IPC using a terminated line placed in the anode plant at both the center-line position and 40 cm off the axis. They showed the Compton replacement I spike followed by RF noise. These measurements, although not absolute, indicate that the FX-35 is inherently quiet. Noise levels are associated with the x-ray and electron beams themselves. Under these operating circumstances, a screen room is not needed, but is available for those experiments particularly sensitive to noise interference. If desired, specific noise measurements can be made concurrent with the experiment.

The monitoring of I and V pulses is the basic diagnostic technique used to indicate machine performance.

Pilot B scintillation measurements are made for every x-ray pulse. The data are used for pulse shape measurements only. TLD dosimetry techniques are used to obtain absolute dose data.

3.4.3 Electron-Beam Mode Environment

Measurements of electron-beam fluence have been made at many pressures and distances. As an example, results of calorimetry measurements of a 2.2-MeV electron beam in vacuum from the FX-35 are given in Figure 3-57. FX-35 V and I waveforms for a single-point and a 20-point cathode are given in Figure 3-58. Performance characteristics of the FX-35 in the electron-beam mode are listed in Table 3-5.

Electron-beam energy spectra have been measured using a 180-degree fixed-field magnetic spectrometer. (The magnetic spectrometer is calibrated by an internal conversion electron source and is accurate to within ±10%.) Representative data using this technique are shown in Figures 3-59 through 3-62 for the FX-35. A time-resolved spectrum, as measured on the FX-35, is given in Figure 3-63.

Time-dependent and integrated spectra for given experimental conditions can be measured by IPC on a routine basis. Spectral measurement techniques are well established.

A measured electron-beam energy deposition profile in Al for the FX-35 is given in Figure 3-64. The measurement was made using thermocouple junctions between Al laminates.

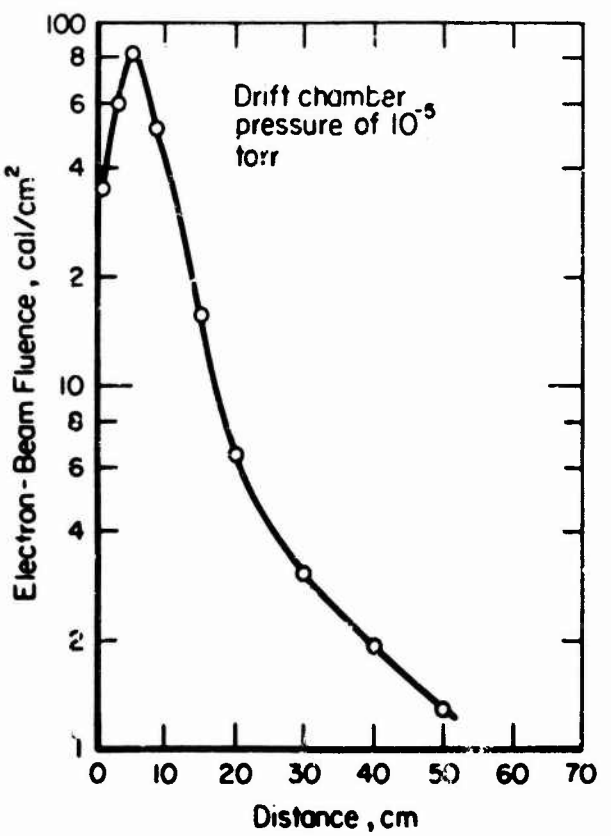

Figure 3-57. FX-35 beam map.

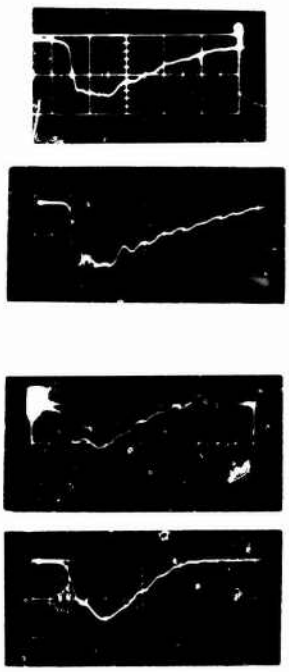

1.7 MV/division
20 ns/division

1/8-in. dia. hemispherical cathode, 2.7-cm gap

13 kA/division
20 ns/division

1.7 MV/division
20 ns/division

20-point cathode, 2.0-cm gap

26 kA/division
20 ns/division

Figure 3-58. FX-35 V and I pulses.

Table 3-5. Performance characteristics of FX-35 in electron-beam mode.

	Average Electron-Beam Energy (MeV)	Total Beam Energy (cal)	Peak Energy Fluence (cal/cm^2)	Pulse Width (ns)	
				Electron Beam	X-ray
(Charging Voltage 4 MV)	0.4	100	80	35	20
	1.3	240	80		
	1.6	300	110		
	2.0	350	150		
	2.5	400	220		

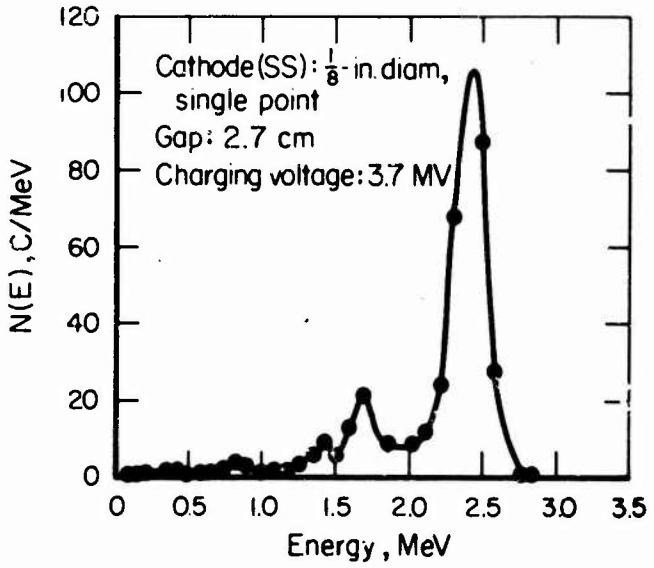

Figure 3-59. FX-35 electron-beam energy spectrum.

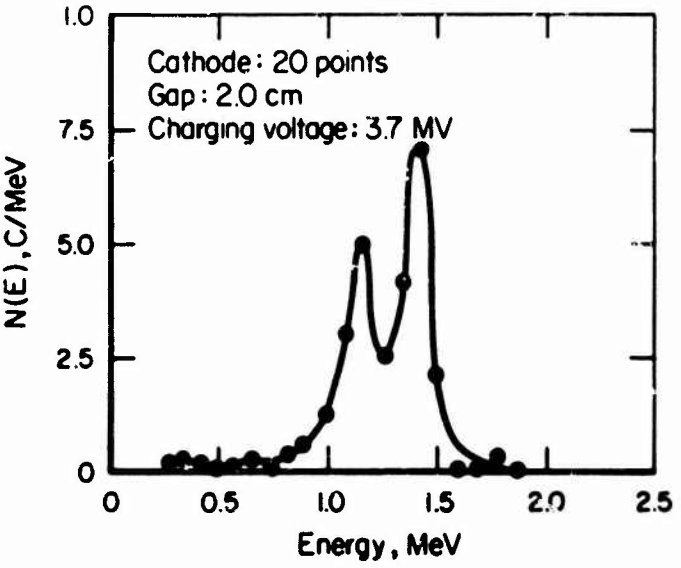

Figure 3-60. FX-35 electron-beam energy spectrum.

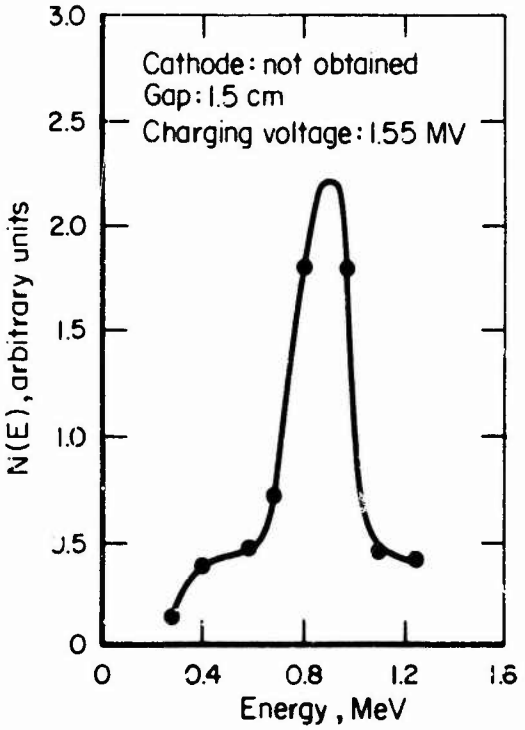

Figure 3-61. FX-35 electron-beam spectrum.

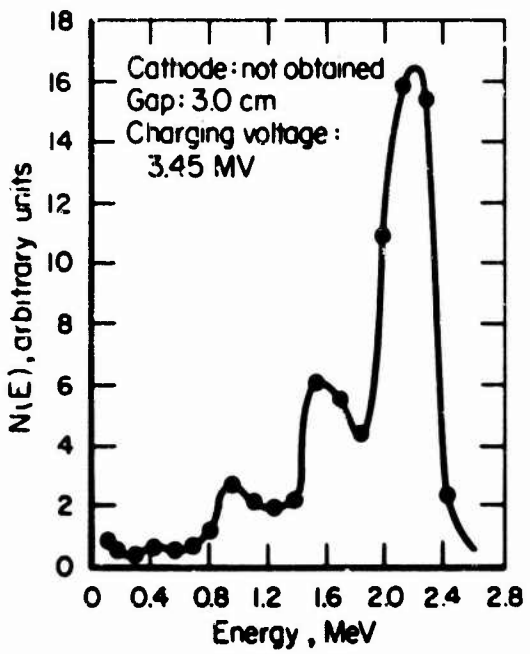

Figure 3-62. FX-35 electron-beam spectrum.

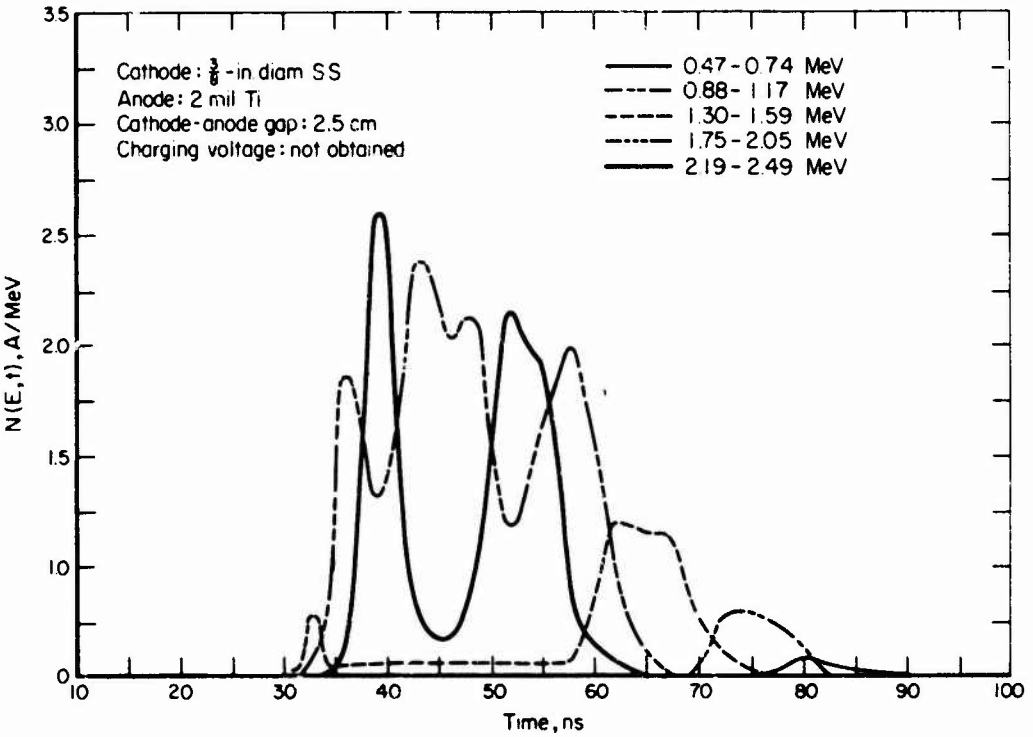

Figure 3-63. Time-resolved spectral measurements on FX-35.

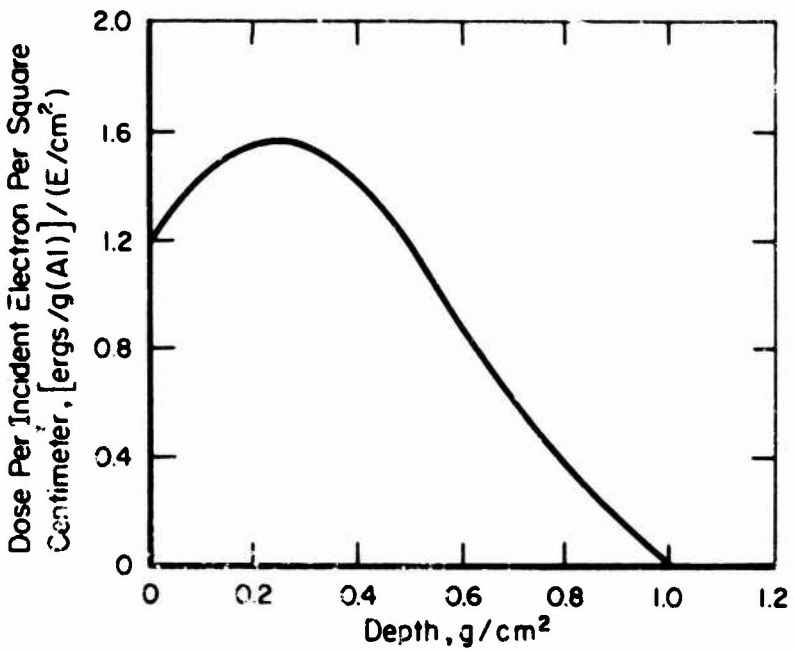

Figure 3-64. 2.0-MeV electron-beam energy deposition profile in Al for FX-35.

3.4.4 X-Ray Mode Environment

A 15-mil Ta bremsstrahlung target (electron range = 2 MeV) and a single-point cathode are used in the x-ray mode. Figure 3-65 consists of smooth curves of TLD capsule data measurements made for numerous x-ray pulses. The dose at a given experimental position is proportional to the fourth power of the charging V.

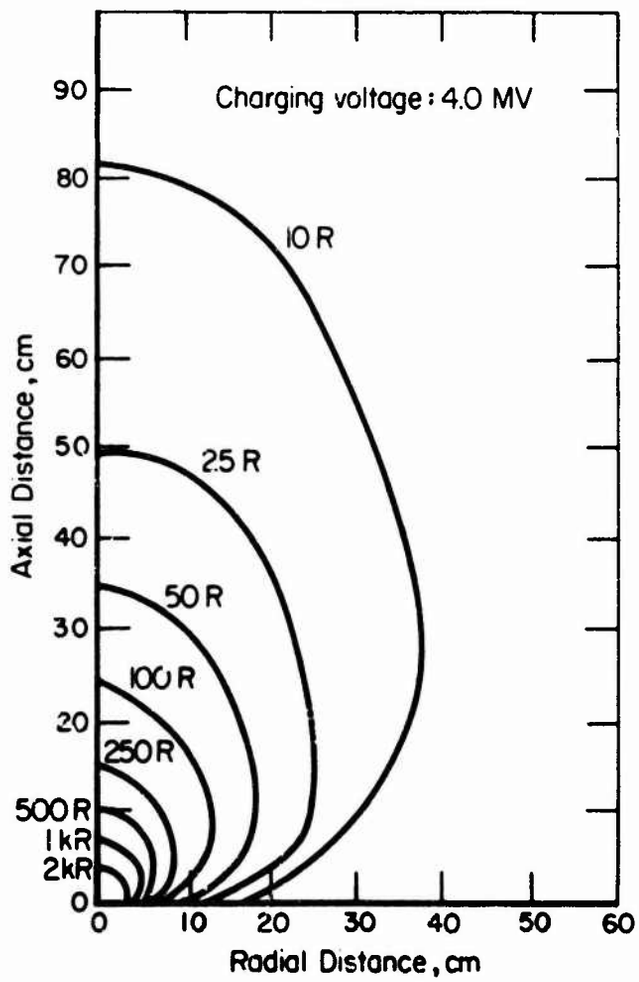

Figure 3-65. FX-35 exposure map.

X-ray spectral measurements have not been made. Calculations of thick-target bremsstrahlung spectra are used as a guide. Figure 3-66 is a plot of such a calculated spectrum.

3.4.5 Support Capabilities

Extensive electronic equipment is available for experimenter use. Included are oscilloscopes, recorders, power supplies, electrometers, pulse generators, oscillators, and various radiation-measuring and analyzing equipment. An

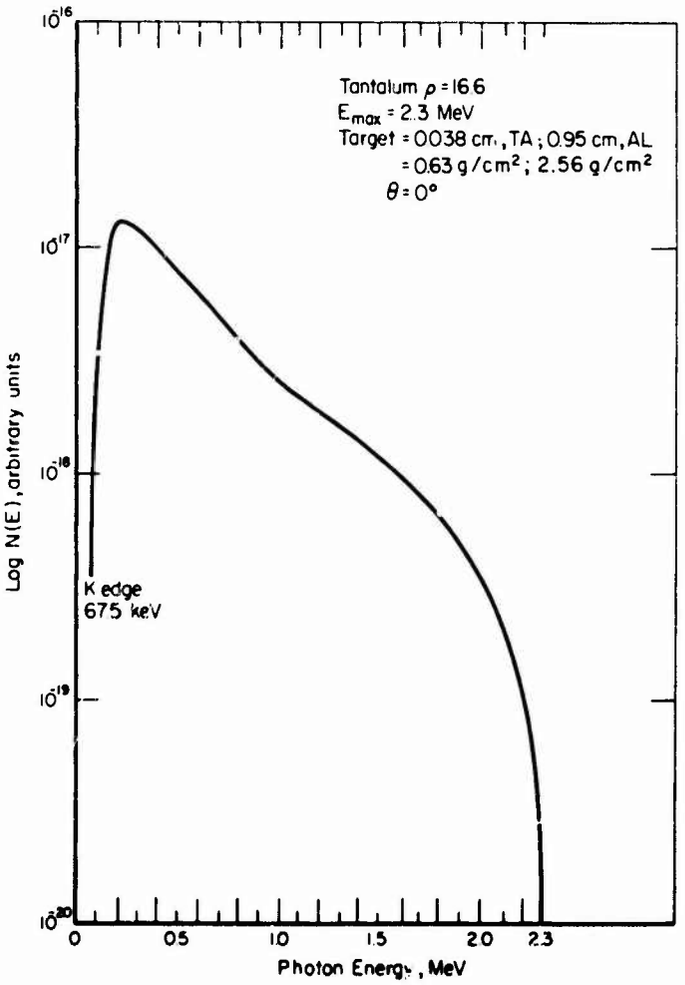

Figure 3-66. FX-35 bremsstrahlung spectrum.

extensive calibration laboratory also may be used. Space for instrumentation trailers or specialized electronic components is available. A complete listing of the test equipment at the IPC laboratory is available upon request. Standard 60-cycle, 100- to 400-V power outlets are located throughout the laboratory. Various cables are available for experimenter use. A minimum distance of 20 ft is required between experimental positions and shielded operating locations. Triggering signals referenced to machine command signals and scintillator signals monitoring radiation output are available.

Dosimetry services, including interpretation of the dosimetry data, are available. Calibrations are made at the laboratory and are based on National Bureau of Standards (NBS) References. Complete CaF_2 TLD dosimetry systems, including powder, microrods, and disks, can be used for x-ray dosimetry. A complete electron-beam dosimetry capability is also available. Beam definition is accomplished by blue-cellophane optical density techniques. Absolute beam measurements are made using thin foil or carbon total-stopping calorimeters. Complete analyses of the calorimetry data are performed at the laboratory. It is estimated that dosimetry techniques are accurate to ±10%.

To record the characteristics of shock waves developed in target materials struck by an electron beam, IPC can provide the following diagnostic instrumentation: X-cut quartz gages, 50-ohm manganin gages, 50-ohm carbon gages, and laser interferometry. Background noise levels for measurements of the first 3 types correspond to about 0.25 kbar. The laser interferometer can be set up to operate in any one of the following configurations, with setup time proportional to the complexity of the arrangement:

1. Displacement mode only
2. Displacement mode plus reflectivity monitor
3. Displacement and velocity modes
4. Velocity mode plus reflectivity monitor
5. Velocity mode only.

The IPC laser interferometer is described in detail in the References.

AVCO Corporation IBM 360, a time-sharing terminal to a GE 430, or a CDC 6600 computer may be used. The following computer programs in FORTRAN are available for experimenter use:

1. ELTRAN-Electron energy deposition
2. ELTRAP-Electron transport in dielectrics
3. PUFF, GENRAT-X-ray deposition
4. PUFF 66
5. One-dimensional elastic stress codes.

The staff of the Analytical Section of the IPC Radiation Effects Division is available, by arrangement, for consultation on analytical problems.

The laboratory has complete machine shop facilities capable of constructing experimental apparatus. In addition, the IPC Model Shop may be used by arrangement. Experiment setup and preparation laboratories are on the premises. Isolated and controlled access laboratories suitable for conducting classified experiments are also available. Office space and conference room facilities are readily available for experimenter use. Polaroid cameras, film, and associated photographic equipment, including various industrial cameras and a Kerr cell framing camera, are available.

The standard electron-beam drift tube is 6-in. I.D. x 10 ft or less length. No drift tube is used in the x-ray mode of operation. In addition, there is an Al vacuum test chamber measuring 18.5 x 18.5 x 28.5 in.

3.4.6 Procedural Information

Technical and administrative inquiries should be made to:

Ion Physics Corporation
P.O. Box 416
South Bedford Street

Burlington, MA 01803
Attn: Mr. Robert D. Evans, Manager
Radiation Effects Section
Telephone: (617) 272-2800, Ext. 292

or, Dr. Helmut Milde, Vice President.

A minimum of 2 weeks between initial contact and initiation of the experimental program is normally required.

Charges and costs associated with the use of IPC facilities are established and published, and are available directly from IPC.

3.4.7 References

1. Evans, R.D., and Ottesen, J.A., *Development of a Velocity Interferometer for Stress Wave Recording in Electron Beams,* IPC Report 7202-TR-410, February 1972.

2. Evans, R.D., *Simultaneous Stress Time and Impulse Measurements Using a Laser Velocity Interferometer and Ballistic Pendulum,* IPC Report 7204-TR-418, April 1972.

3.5 BOEING FX-75 ELECTRON-BEAM GENERATOR

The Boeing FX-75 is an IPC FX-75 high-energy electron-beam generator which has a maximum charging V of 7 MV. It produces a maximum electron-beam energy of 5.2 MeV. Figure 3-67 is a diagram of the facility layout.

In the direct electron-beam mode, the I accelerated from the cathode emitting surface passes through a thin-foil anode window into a low-pressure experimental chamber. The pressure of the residual gas in the drift chamber affects the charge balance in the region of the drifting electron beam and offers a means of controlling the competing forces (electrostatic repulsion and magnetic compression) that determine the beam size and energy density. Particular care must be taken in an electron-beam experiment to arrange experimental apparatus and test samples in a way that they will not interfere with the beam transport. The Boeing Radiation Effects Laboratory (BREL) has two available multipurpose drift chambers; a special chamber may be designed for a particular test series.

In the x-ray mode, the I accelerated from the cathode-emitting surface is directed onto a Ta target to produce an intense burst of high-energy bremsstrahlung.

3.5.1 Test Parameters

Operating characteristics of the Boeing FX-75 are as follows:

1. Charging V	4 to 7 MV
2. Terminal impedance	32 Ω
3. Field emission tube impedance	90 Ω
4. Peak electron-beam energy	5.2 MeV at 7-MV charging V
5. Pulse width (FWHM)	29 ns
6. Charging system capacitance	680 pF
7. Stored energy (at 680 pF, 7 MV)	16 kJ
8. Total electron-beam energy per pulse	~9 kJ at 7-MV charging V
9. Electron-beam I	60,000 A (peak)
10. Peak I density	3,000 A/cm^2

These data are not definitive and are meant to be used only as a guide.

At 5-MV charging V, the total beam energy is 4.4 kJ. At 6.5 MV, the total beam energy is 7.5 kJ. Total beam energy varies as the square of both the electron-beam V and the charging V.

The energy density delivered to a test sample may be varied by adjusting the chamber pressure and the anode-sample distance. Typical fluence distribution curves for a 3.5-MeV beam and a 900-KeV beam are given in Figure 3-68. Energy

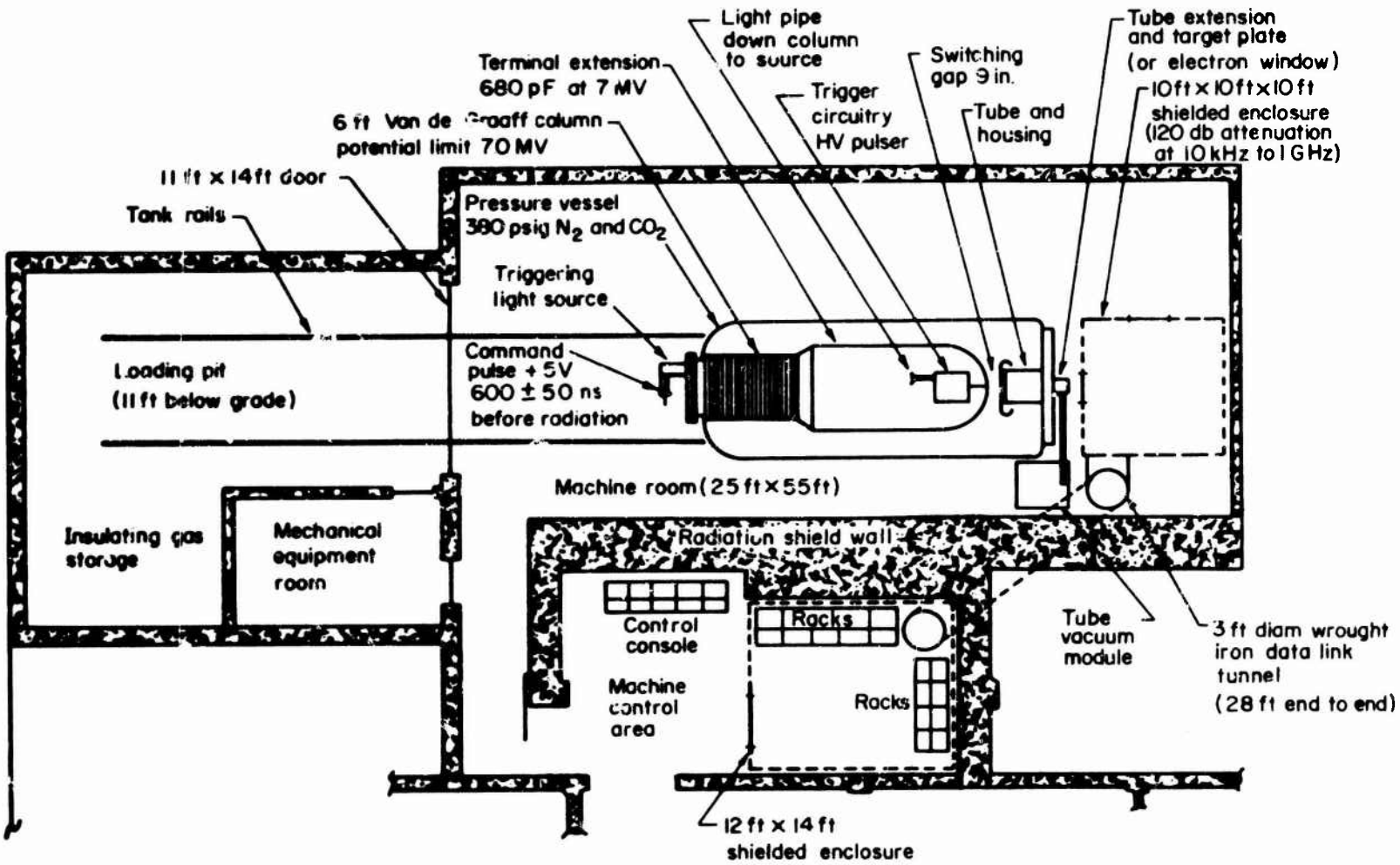

Figure 3-67. BREL FXR facility.

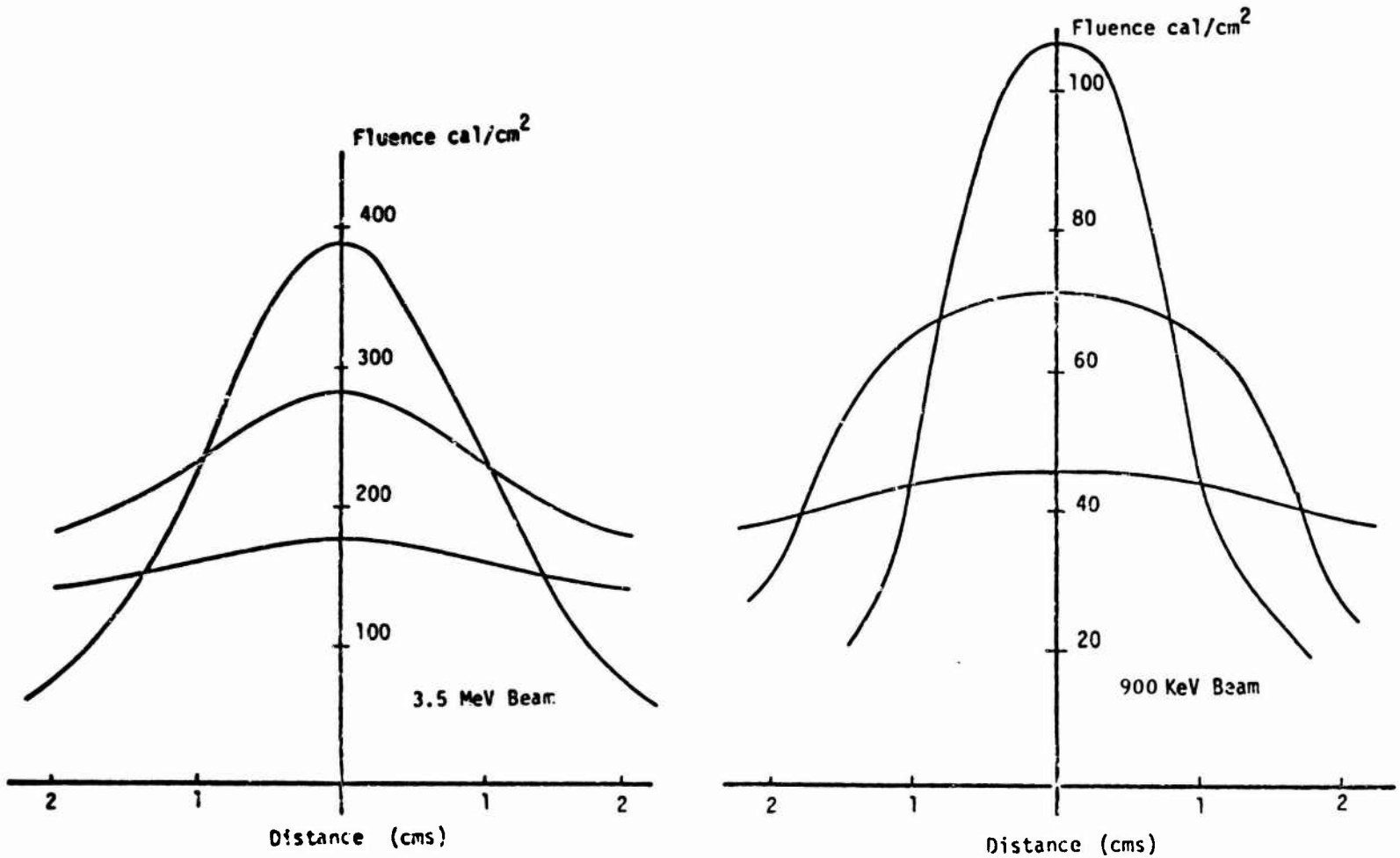

Figure 3 68. Typical fluence distribution curve.

fluences from less than 0.1 cal/cm^2 to greater than 400 cal/cm^2 have been measured. The total electron-beam energy may be varied from about 500 cal to about 2,000 cal. Electron-beam dosimetry is normally done with thin-foil calorimeters in line over a test sample. The lab is equipped to read out 12 channels of calorimeter data, and a range of calorimeter types and arrays are available.

Maximum repetition rate is 1 pulse/2 min. Sample charging and chamber pressure stabilization time usually limits electron-beam testing to 20 shots/day. Normal operating delays limit 5-MV x-ray operation to 120 shots/day. Increased target maintenance limits 6.5-MV x-ray operation to 40 shots/day.

The energy-flux distribution of repetitive electron-beam mode pulses, with the same vacuum test chamber pressure and charging V, is reproducible to ±10%. Reproducibility of x-ray peak rate is ±10%; total dose is ±5%. Pulse predictability is within a factor of 2 for these values. Figure 3-69 shows scope traces of the bremsstrahlung pulse from 10 consecutive FX-75 pulses. These traces show the reproducibility of the pulse.

Pulse delay is 600 ns. This delay is defined as the time interval between the command pulse to the spark-gap triggering light source and discharge of V at the anode. A Gaussian distribution of jitter is associated with the delay. The 3-σ spread in the jitter is ±50 ns.

3.5.1.1 Electrical Noise

Serious operating difficulties are encountered with both electric and magnetic probes inside the electron-beam test chamber. Quantitative data are available upon request.

Two RF-shielded test and instrumentation rooms are provided. The noise environment has not been mapped within these enclosures. BREL reports that the conducted noise from power lines is less than 1 V peak-to-peak, and cable responses (terminated and open) are approximately 20 mV peak-to-peak (for cables in the test area and out of the beam).

Extensive electric- and magnetic-noise measurements were made external to the shielded enclosures. Conducted noise on power lines was measured at 50 V peak-to-peak. Response on terminated RG-9 cable out of the beam was 70 mV peak-to-peak. Noise spectrum is peaked at approximately 30 MHz. Figures 3-70 and 3-71 summarize the noise-measurement data.

3.5.1.2 Diagnostic Techniques

Diagnostic techniques for the electron-beam and x-ray modes are as follows:

1. Electron-beam mode:
    a. Two view cameras for test chamber stereophotography
    b. Metal foil and graphite total-stopping calorimeters for beam mapping and sample irradiation dosimetry

Notes: 10 consecutive shots at 6.0-MV charge voltage.
Exposure at 1.0 m, 70 R.
Time base, 20 ns/cm.
Integrated areas were within 3%.

Figure 3-69. Oscilloscope traces of 10 consecutive bremsstrahlung output pulses.

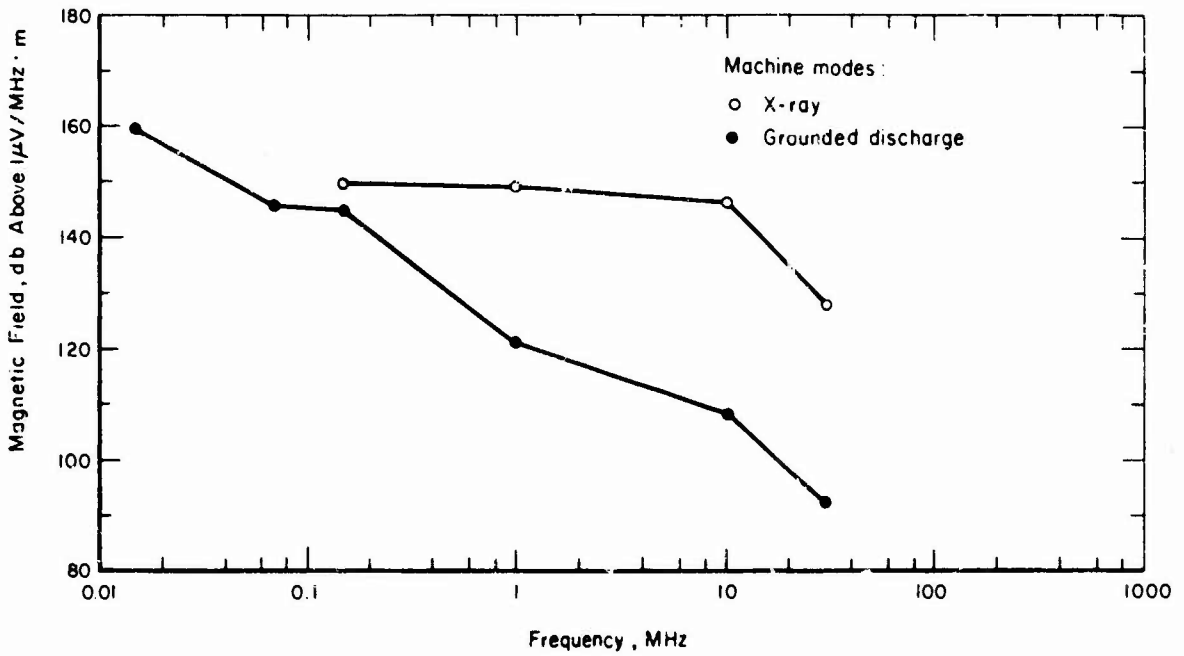

Figure 3-70. Composite magnetic field level in the BREL x-ray room (non-shielded room).

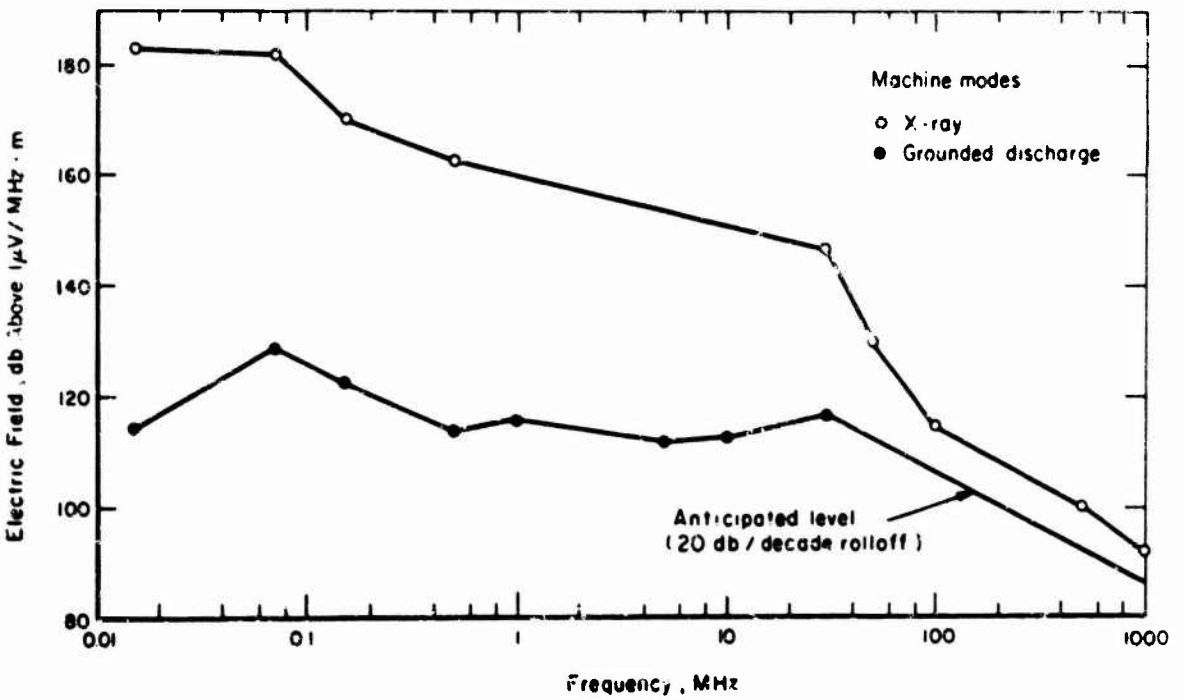

Figure 3-71. Composite electric field level in the BREL x-ray room (non-shielded room).

c. Fast Faraday cup for time-resolved I measurements

d. Deposition profiles--stacked metal foil calorimeters

e. A time-resolved magnetic spectrometer.

2. X-ray mode:

a. Waveform and peak rate determined from calibrated scintillator/photodiode measurements

b. Dose maps and routine dosimetry measured with LiF TLDs (TLDs are Co-60 calibrated and accurate to ±15%)

c. Energy deposition measurements made with TLD-loaded depth-dose arrays

d. Target beam spot observed with a polyvinyl chloride (PVC) intensifying screen and standard open-shutter photographic techniques.

Electron-Beam Mode Environment. Quantitative data of beam energy density versus position are available upon request.

The electron-beam flux delivered to an experimental sample in the vacuum test chamber can be smoothly varied from 1 to 200 cal/cm^2. The spatial distribution of the flux is roughly Gaussian about the beam center line with the geometric shape dependent upon chamber pressure. For very high dose deposition studies, care should be taken to design axial symmetry into the test sample holders.

Figure 3-72 is oscilloscope traces of the electron-beam V and I outputs.

A 10-channel, time-resolved magnetic spectrograph with resolution of 0.25 M has been used to generate electron-beam spectra for several cathode configurations. The spectra are sensitive to the cathode emission surface and anode-cathode gap. There is also spatial dependence on the anode plane. Center-line spectra for 2 typical operating configurations are shown in Figure 3-73. Information on the time history of the spectrum, as well as the dependence of cathode geometry, is available upon request. Energy deposition data are given in Figure 3-74.

X-Ray Mode Environment. Figures 3-75 through 3-82 are x-ray exposure and exposure-rate maps for various charging V. These data are the result of LiF TLD measurements. They are meant to be used only as a guide.

Figure 3-83 is a scope trace of a bremsstrahlung pulse output as measured with a liquid scintillator/photodiode system. Peak height varies as the fourth power of the charging V.

X-ray spectra for 5-MV and 6-MV charge V are shown in Figure 3-84. Figure 3-85 depicts x-ray deposition profiles in Al, Cu, and Pb.

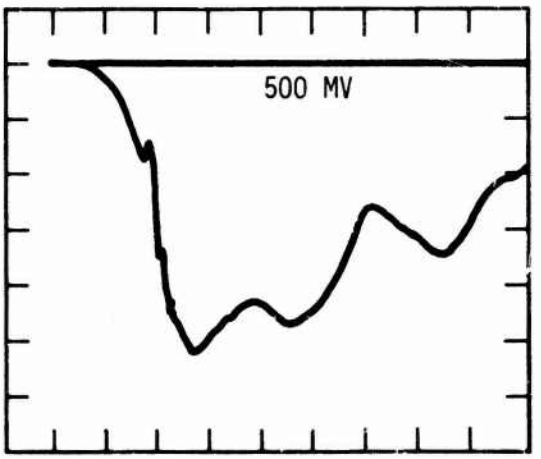

Electron-Beam Current

Notes: Fast, low impedance vacuum shunt outside beam window.
10 ns/cm.
Peak current range, 25,000 to 50,000 A for 4-7 MV charge.

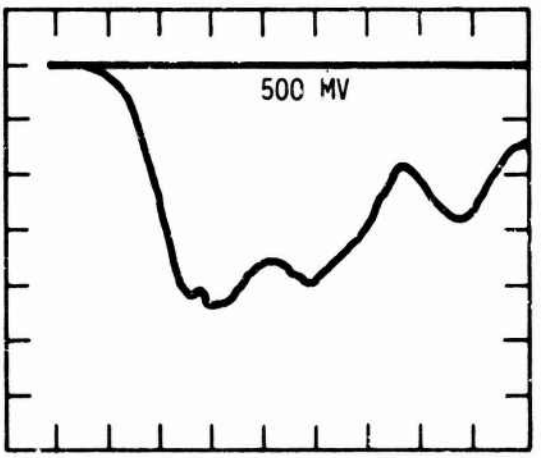

Electron-Beam Voltage

Notes: Capacitive divider voltage monitored inside electron gun.
10 ns/cm.
Peak voltage, approximately 0.7 charging voltage.

(Redrawn from scope pictures)

Figure 3-72. Oscilloscope traces of electron-beam V and I.

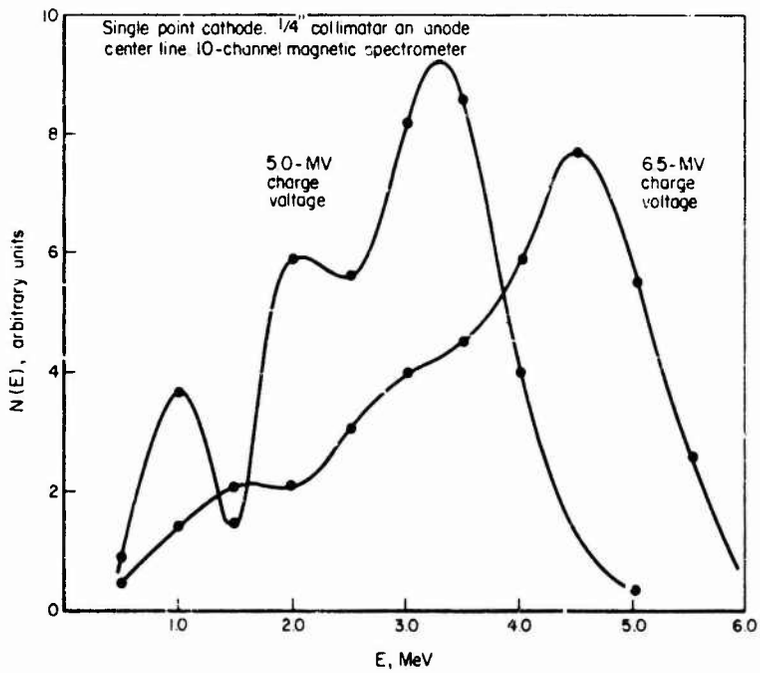

Figure 3-73. Electron-beam spectra for 2 typical operating configurations.

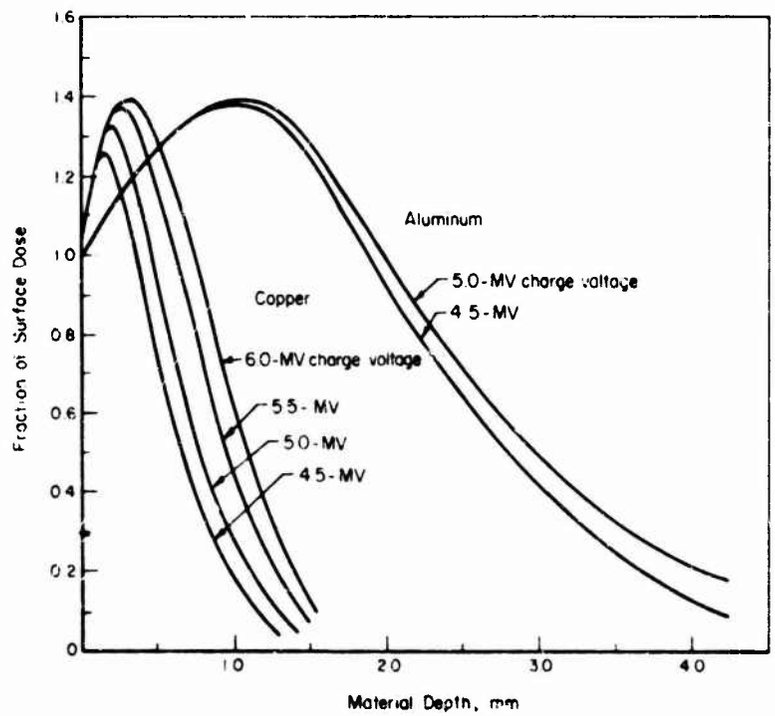

Figure 3-74. Energy deposition profiles for FX-75 electron beam.

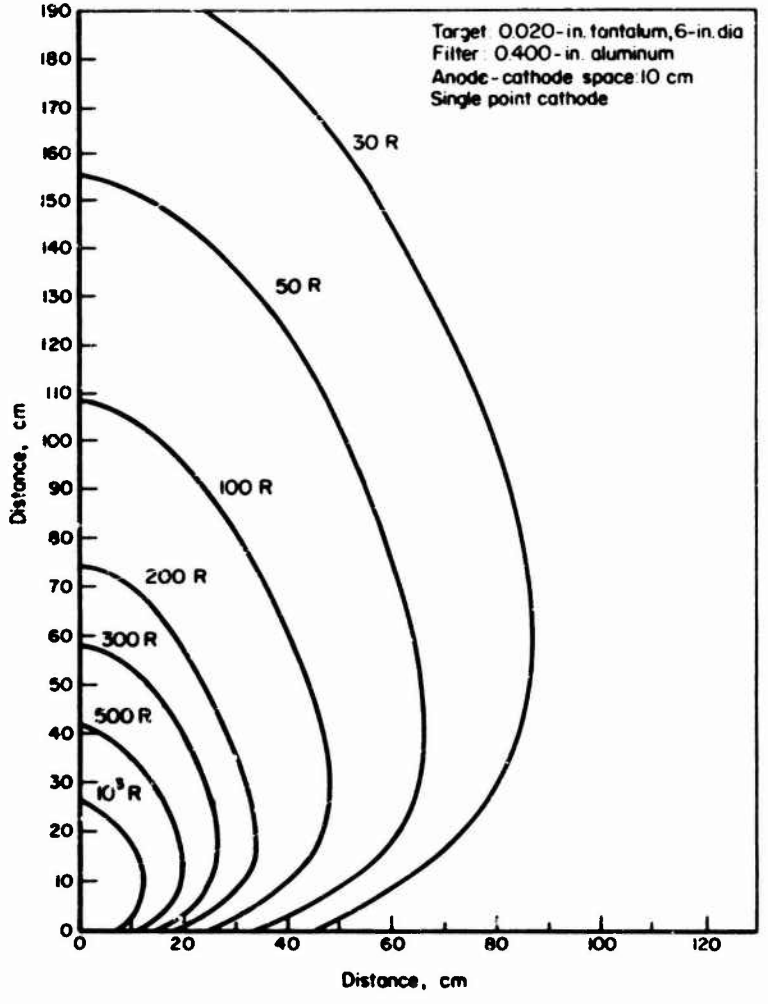

Figure 3-75. X-ray exposure map at 6.5-MV charging V (far field).

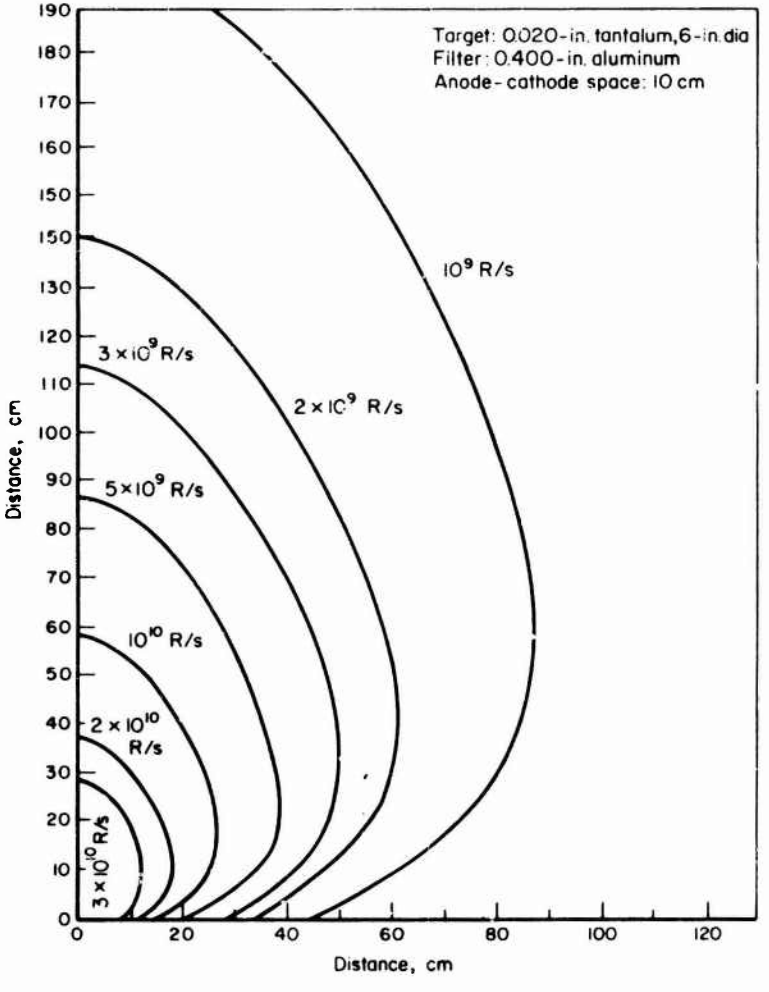

Figure 3-76. X-ray exposure rate map at 6.5-MV charging V (far field).

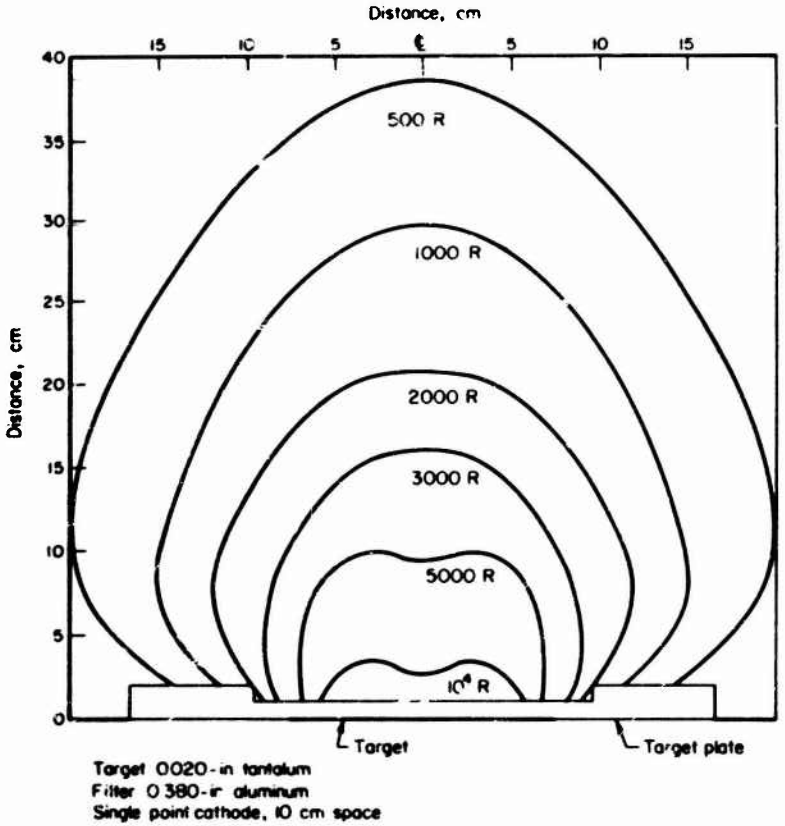

Figure 3-77. X-ray exposure map at 6.5-MV charging V (near field).

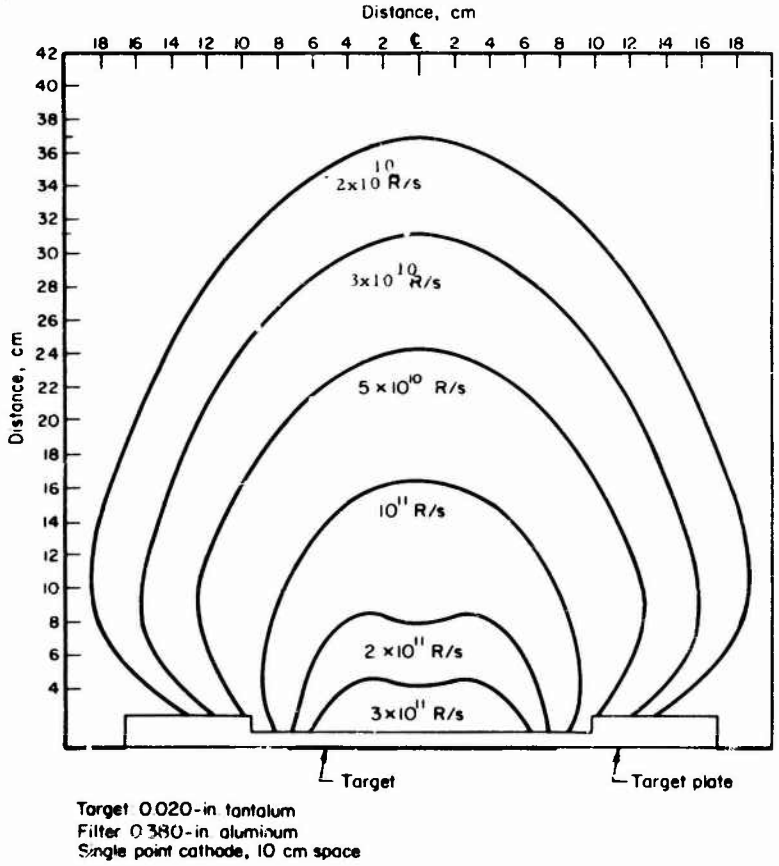

Figure 3-78. X-ray exposure rate map at 6.5-MV charging V (near field).

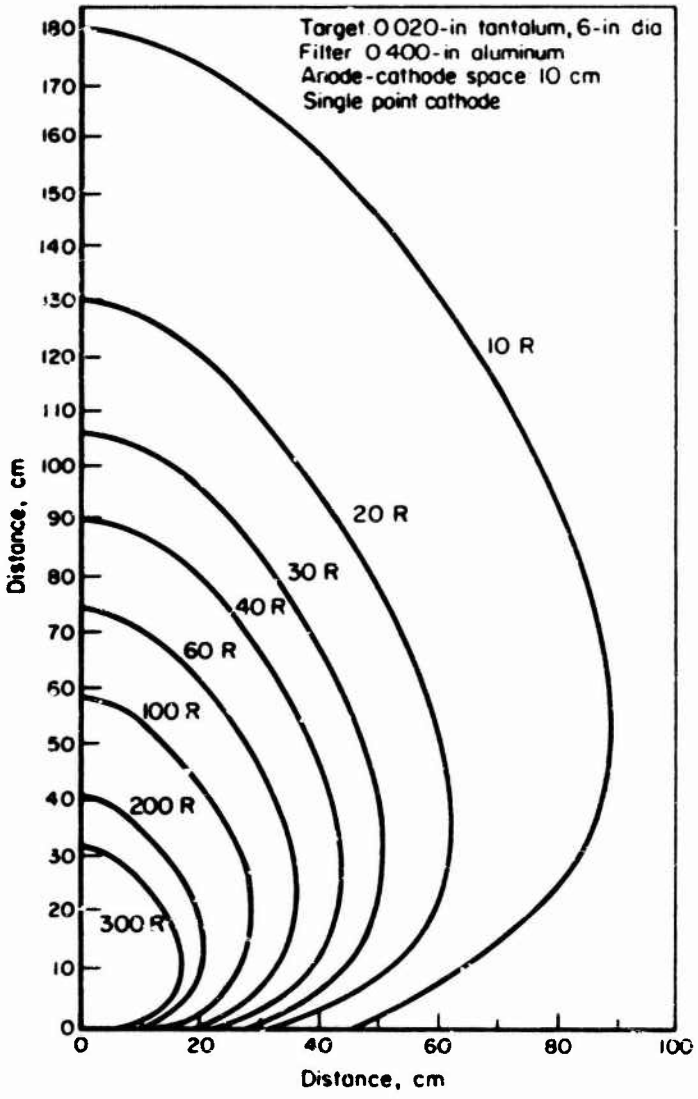

Figure 3-79. X-ray exposure map at 5.0-MV charging V (far field).

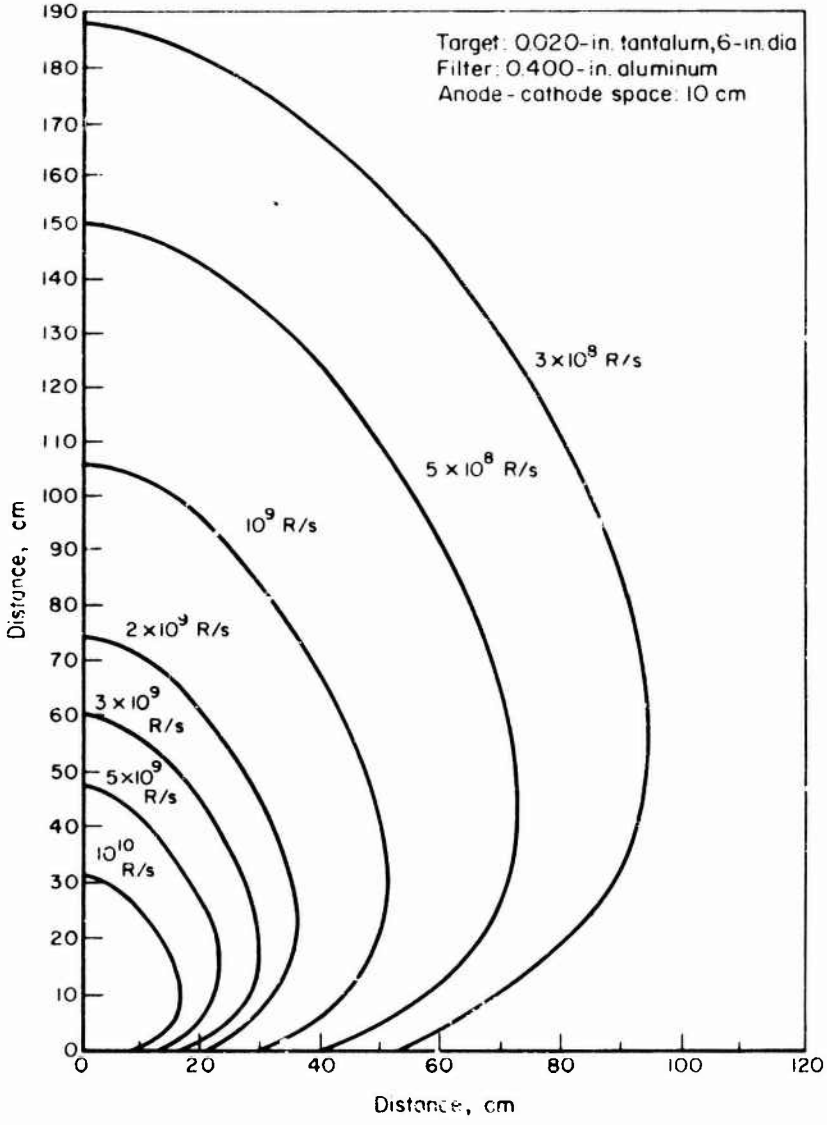

Figure 3-80. X-ray exposure rate map at 5.0-MV charging V (far field).

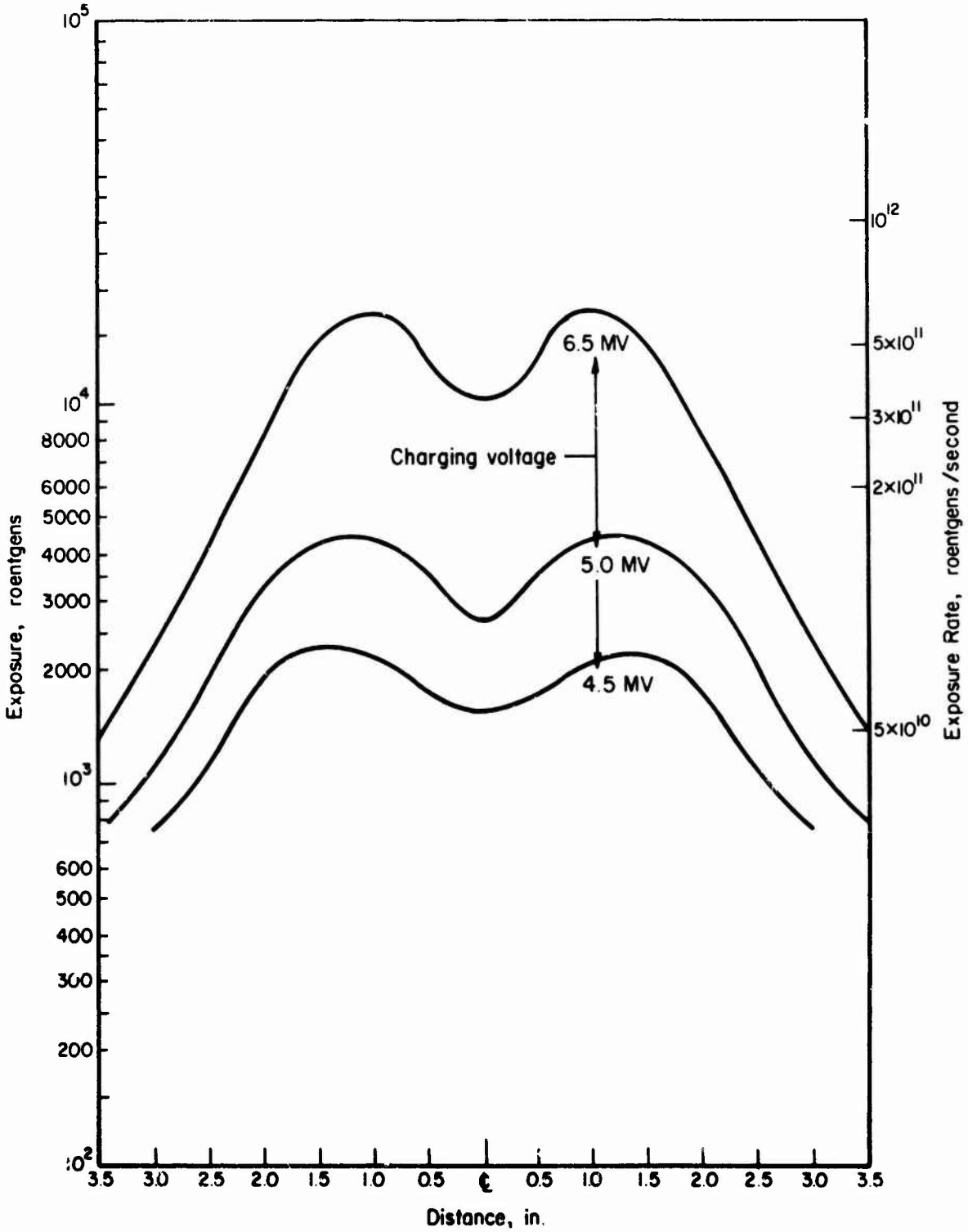

Figure 3-81. X-ray faceplate field map.

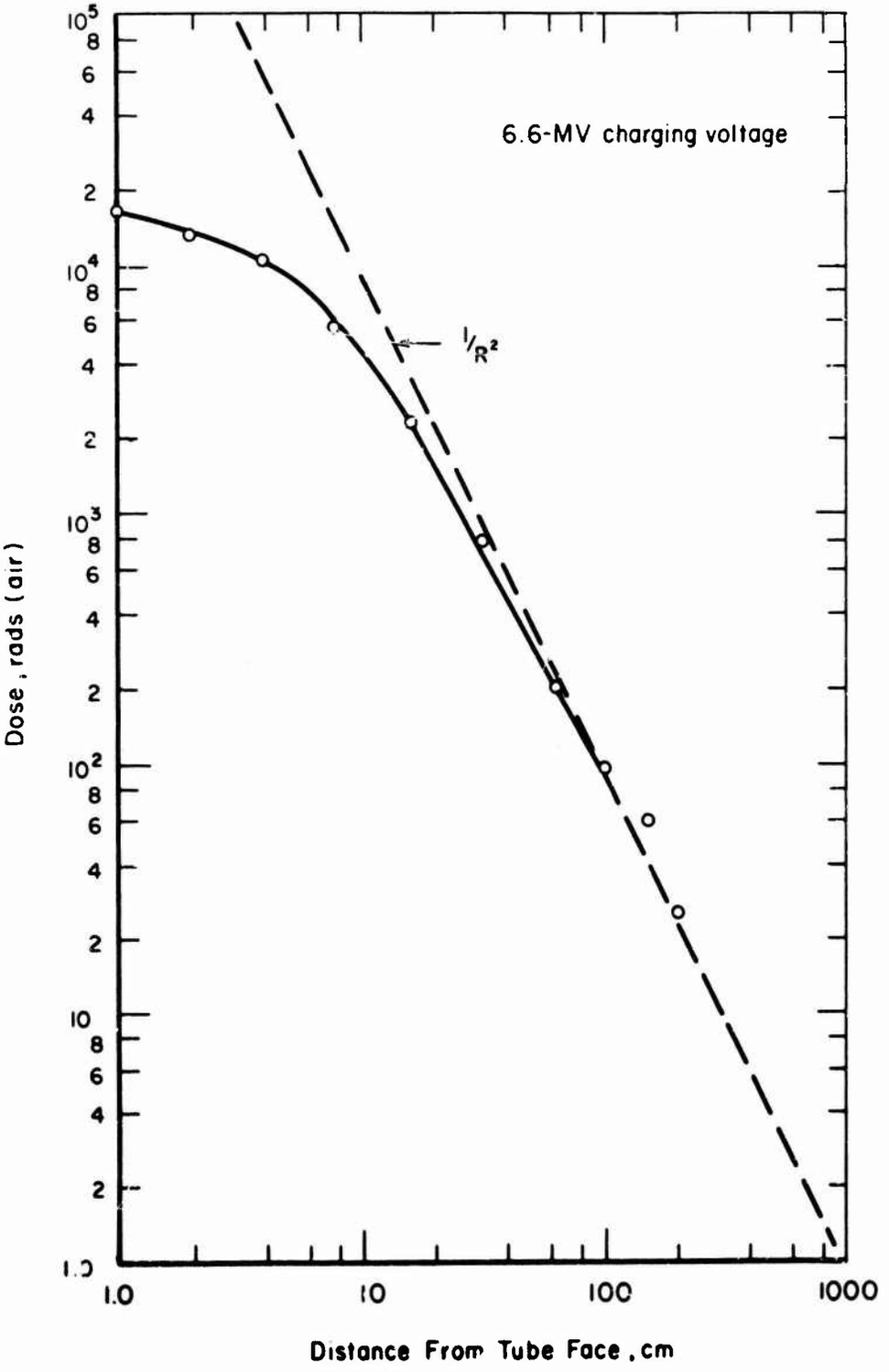

Figure 3-82. X-ray dose versus distance from tube face for the PEL FX-75.

Notes: (1) Liquid scintillator and planar ITT FW 114 photodiode

(2) 20 ns/cm.

Figure 3-83. Oscilloscope traces of bremsstrahlung pulse output.

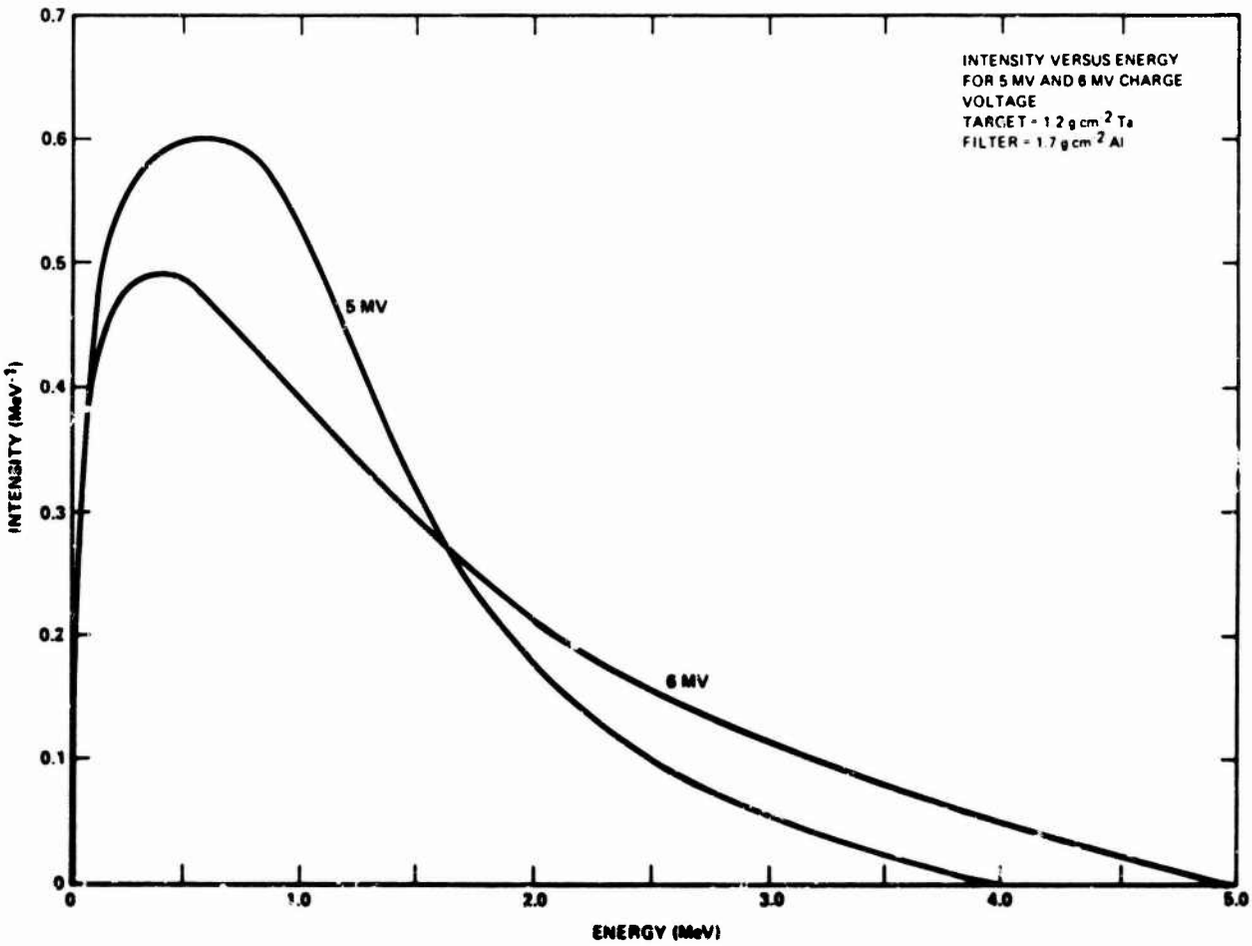

Figure 3-84. Bremsstrahlung pulse output.

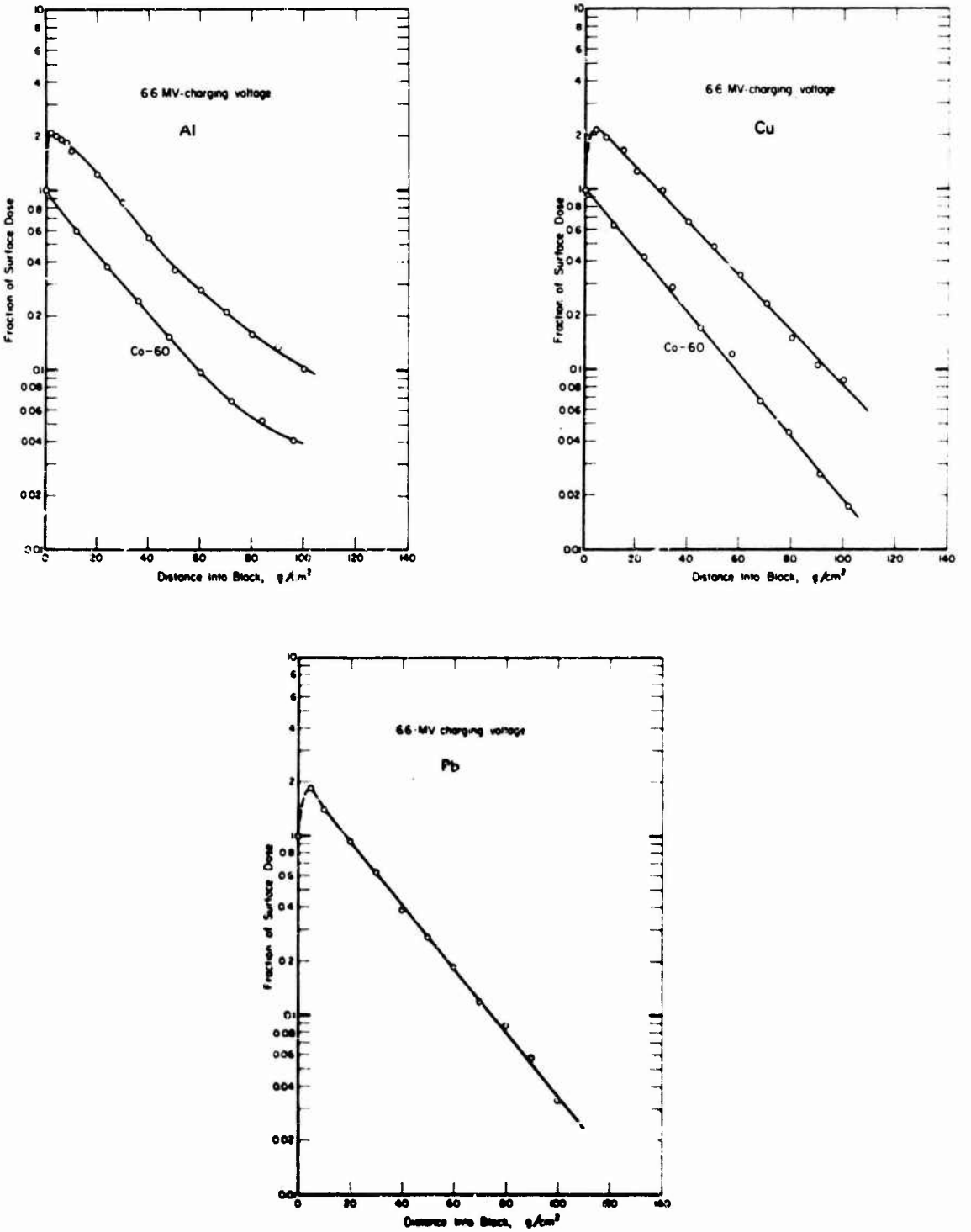

Figure 3-85. X-ray deposition for the BREL FX-75.

3.5.2 Support Capabilities

Electronic equipment for experimental use includes:

1. Instrumentation:
   a. Three Tektronix 519 oscilloscopes
   b. Four Tektronix 7844 oscilloscopes
   c. One Tektronix 7904 oscilloscope
   d. 10-channel HP7100 strip charts
   e. Recorders for calorimetry
   f. Additional equipment including oscilloscopes, power supplies, pulsers, etc. may be obtained from the Boeing test equipment stores.
2. Power:
   a. 120-Vac, 3-ϕ, 60-cycle, 50-kVa in each shielded enclosure
   b. 28-Vdc, 1 kVA.
3. Cables:
   a. Signal and power cables (minimum cable length between test and oscilloscope is 60 ft; special cable bundles are easily accommodated in the 3-ft-dia. cable duct or bulkhead connected to the instrumentation shield room).

Triggering signals responding to machine command signals are readily available. An arrangement of fixed delays makes possible a wide range of trigger timing signals.

Two RF-shielded enclosures are provided: a 10- x 10-ft radiation test room, and a 12- x 14-ft instrumentation room. The enclosures are integrally connected by a 3-ft-dia. wrought-iron data-link tunnel (cable duct) through the radiation shielding wall. The rooms have a specified attenuation of 120 db for both electric and magnetic fields in the frequency range 10 kHz to 1 GHz. Filtered power of 50 kVA is available in each enclosure. A shielded optical link is provided for laser probing apparatus.

X-ray dosimetry techniques include a LiF TLD and calibrated scintillator/photodiode systems. Electron-beam dosimetry is performed by means of transmission foil and total absorbing calorimeters. Instrumentation includes 12 resistance bridges, 12 dc differential amplifiers, and 12 oscillograph channels.

There is a complete dosimetry laboratory for specialized problems. Arrangements can be made for use of the Boeing computer center. Complete machine shop facilities capable of constructing experimental apparatus are readily available at the laboratory.

A 20- x 30-ft bay adjoining the FXR instrumentation room may be used by the experimenter. Office and conference room facilities are limited.

BREL maintains a complete photographic laboratory and dark room with a full complement of equipment. Oscilloscope cameras, two 4 x 5 view cameras, and 2 high-speed image converter cameras with complete accessories are readily available.

Electron-beam experiments are usually carried out within a 3- x 3- x 4-ft electron-beam test chamber or a drift tube 25 in. long with an I.D. of 13.75 in. Both the test chamber and drift tube are partially evacuated.

3.5.3 Procedural Information

Technical inquiries should be directed to:

The Boeing Aerospace Company
Mail Stop 2R-00
P.O. Box 3999
Seattle, WA 98124
Attn: E.M. Costello, Boeing Radiation Effects Laboratory
Telephone: (206) 655-2954

Administrative inquiries should be directed to:

The Boeing Aerospace Company
Research and Engineering Division, Contracts Dept.
P.O. Box 3999
Seattle, WA 98124
Attn: H.M. Kilborn, M/S 8C-26
Organization 21143
Telephone: (206) 773-3449

Scheduling is arranged on an individual basis through the BREL technical contact. It is expected that only nominal lead times are required. Costs and charges may be obtained directly from the BREL administrative contact. The shipping address is:

Boeing Radiation Effects Laboratory
1420 South Trenton Street
Building 15-10
Seattle, WA 98108

3.6 HARRY DIAMOND LABORATORIES (HDL) FX-45 ELECTRON-BEAM GENERATOR

The HDL FX-45 is an IPC FX-45 high-energy electron-beam generator (HIFX) (Reference 1). It has a maximum charging V of 5.0 MV, which produces an electron beam whose mean energy is 3.0 MeV. Figure 3-86 is a diagram of the facility and Figure 3-87 is a detailed diagram of the exposure area, shielded instrument room, and control room.

3.6.1 Test Parameters

The operating characteristics of the HDL FX-45 are as follows:

1. Maximum charging V — 5.0 MV
2. Mean electron kinetic energy (4.1-MV charge):
   a. High-impedance mode — 2.4 MeV
   b. Low-impedance mode — 0.3 to 1.1 MeV (depending on gap size)
3. Pulse width (FWHM) — 25 ns
4. Stored energy (5.0-MV charge) — 2.5 kJ
5. Peak electron-beam I (4.1-MV charge):
   a. High-impedance mode — 23 kA
   b. Low-impedance mode — 30 to 45 kA (depending on gap size)

Maximum repetition rate is 1 pulse/7 min in the x-ray mode and as required by the experimenter in the electron mode.

Measurements made on 25 pulses indicate the standard deviation in on-axis exposure at 12 in. from the target is approximately 4%. Pulse delay (or advance) jitters within 50 ns can be achieved. The jitter using the mechanical trigger is about 40 ms. The typical RF EMP is a damped oscillation at 30 MHz, lasting 0.5 μs with an amplitude (12-ft dipole 50 ft away) of a few hundred mV. This noise signal amplitude is a linear function of machine charging V and is inversely proportional to distance from the machine.

Experimenters will not normally experience any noise problems when their signals are detected with instruments located in the RF-shielded instrument room.

Scintillator-photodiode, V-monitor, and I-monitor profiles can be supplied with any given shot, although these measurements are not made routinely.

Energy stored with the system is proportional to the square of the charging V and is delivered to the electron beam with an efficiency of ~70%. Calculated values of the beam energy in the high-impedance mode as a function of charging V are given in Table 3-6.

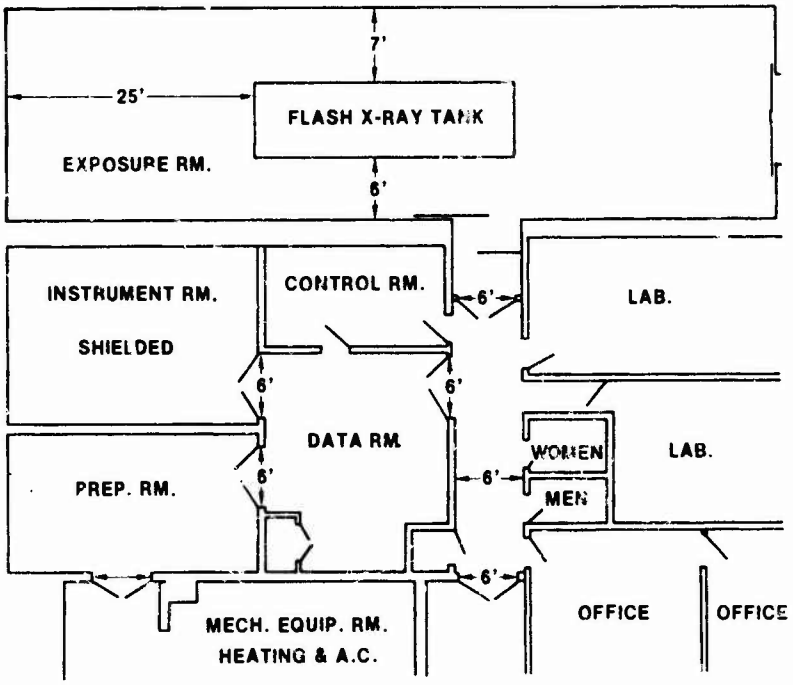

Figure 3-86. HIFX facility layout.

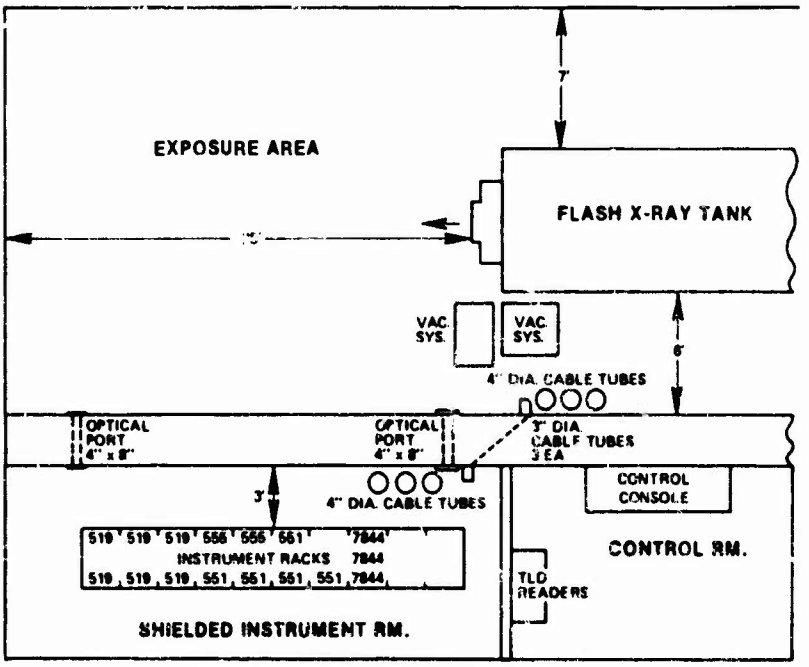

Figure 3-87. Detailed layout of HIFX exposure area, instrument room, and control room.

Table 3-6. Calculated values of the beam energy as a function of charging V for HDL FX-45.

Charging V (MV)	Total Energy (kJ)	Total Beam Energy (kJ)
3	0.9	0.6
4	1.6	1.1
5	2.5	1.7
6	3.6	2.5

Note:

Values are based on a machine capacitance of 198 pF and idealized operation conditions.

The burn pattern of the beam on a bremsstrahlung target is a solid circle about 1.5 in. in dia. In the electron mode, as the beam propagates away from the anode it pinches onto the geometric axis at 1 or more locations which depend on the beam energy and the ambient pressure. After the last pinch the beam diverges. Characteristic data for the high-impedance mode are presented in Table 3-7.

Table 3-7. Beam geometry for HDL FX-45.

Charging V (MV)	Ambient Pressure	Pinch Location (distance from anode)
4.6	1 atm	~5 cm and 10 cm (2 pinches)
5.0	1 atm	~5 cm and 13 cm (2 pinches)
5.7	190 μm Hg	~3 cm, 9 cm, and 20 cm (3 pinches)

The flux level is determined by the initial pinch position and adjustments are made by adjusting the drift-tube pressure. Standard operating modes are utilized for which beam predictability and reproducibility are good. The beam is monitored for each pulse to determine the energy delivered to the test sample.

3.6.1.1 Electron-Beam Environment (High-Impedance Mode)

Measurements to determine beam energy density versus position, utilizing a total absorption Cu calorimeter, have been made. Results are given in Figure 3-88.

Figure 3-89 shows oscilloscope traces of beam V and I and γ-ray intensity. The V and I traces were made with a calibrated capacitor divider V monitor and

a calibrated low-impedance shunt I monitor (References 2 and 3). The γ-ray traces were made with a scintillator-photodiode combination. The latter is uncalibrated, but its response is linear in γ-ray intensity. The time scales of each of the 3 traces for each charge V (V_c) have been synchronized to an accuracy of about 2 ns.

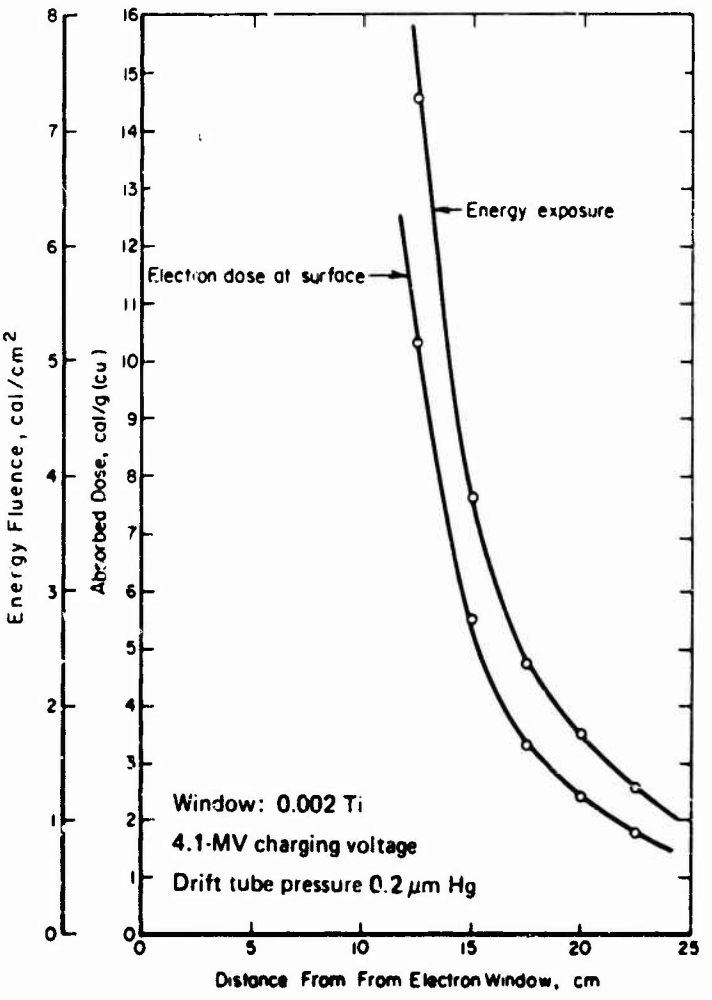

Figure 3-88. Electron-beam energy density versus position (total absorbing Cu calorimeter).

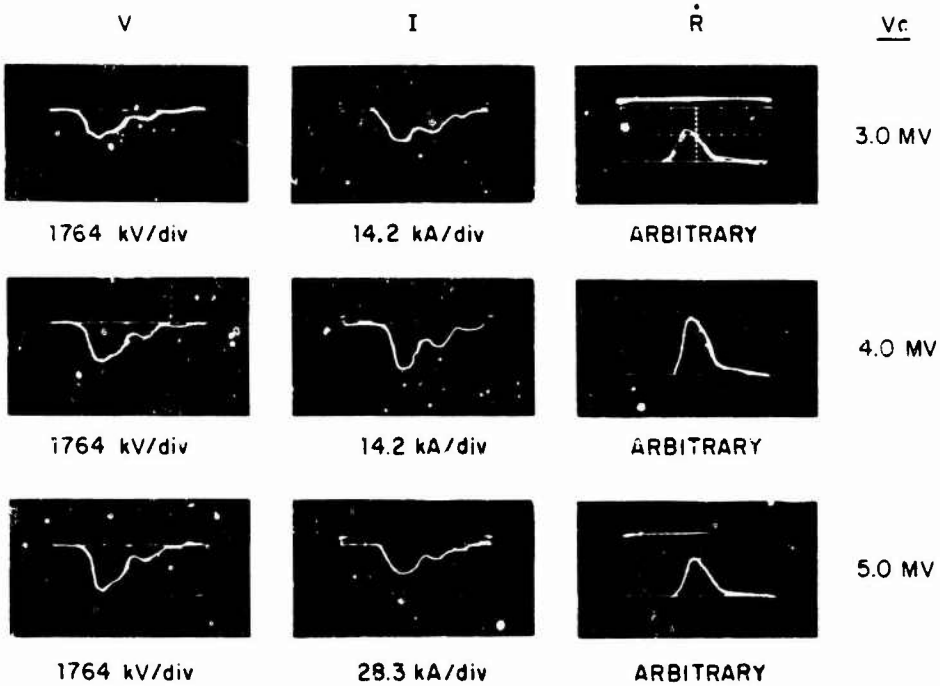

Figure 3-89. V, I, and R traces for high-impedance electron mode (Y scale as labelled; X scale: 20 ns/div).

Electron-beam energy spectra obtained with a magnetic spectrometer are shown in Figure 3-90. In addition, electron-beam energy spectra based on V and I monitor profiles, such as those in Figure 3-89, are shown in Figure 3-91.

Extensive deposition measurements have been made at HDL. Typical depth-dose profiles are shown in Figure 3-92.

3.6.1.2 Electron-Beam Environment (Low-Impedance Mode)

Fluence measurements of the low-impedance mode electron beams have been made utilizing total absorption graphite calorimeters. Average fluence as a function of axial position in the drift chamber for 1 of these beams at 250-μm Hg and 1,000-μm Hg ambient pressure (air) is shown in Figure 3-93. High-resolution fluence distribution maps for this beam at the same ambient pressures 4 cm and 10 cm from the anode are shown in Figure 3-94.

Figures 3-95 and 3-96 show common-axis plots of V and I pulses using the same type of monitors as for the high-impedance mode (Figure 3-89). The lower trace in Figure 3-95 shows a check of the time axis synchronization in which the I monitor pulse was input to both scopes.

Electron-beam energy spectra based on V and I monitor traces like those of Figure 3-91 are shown in Figure 3-97.

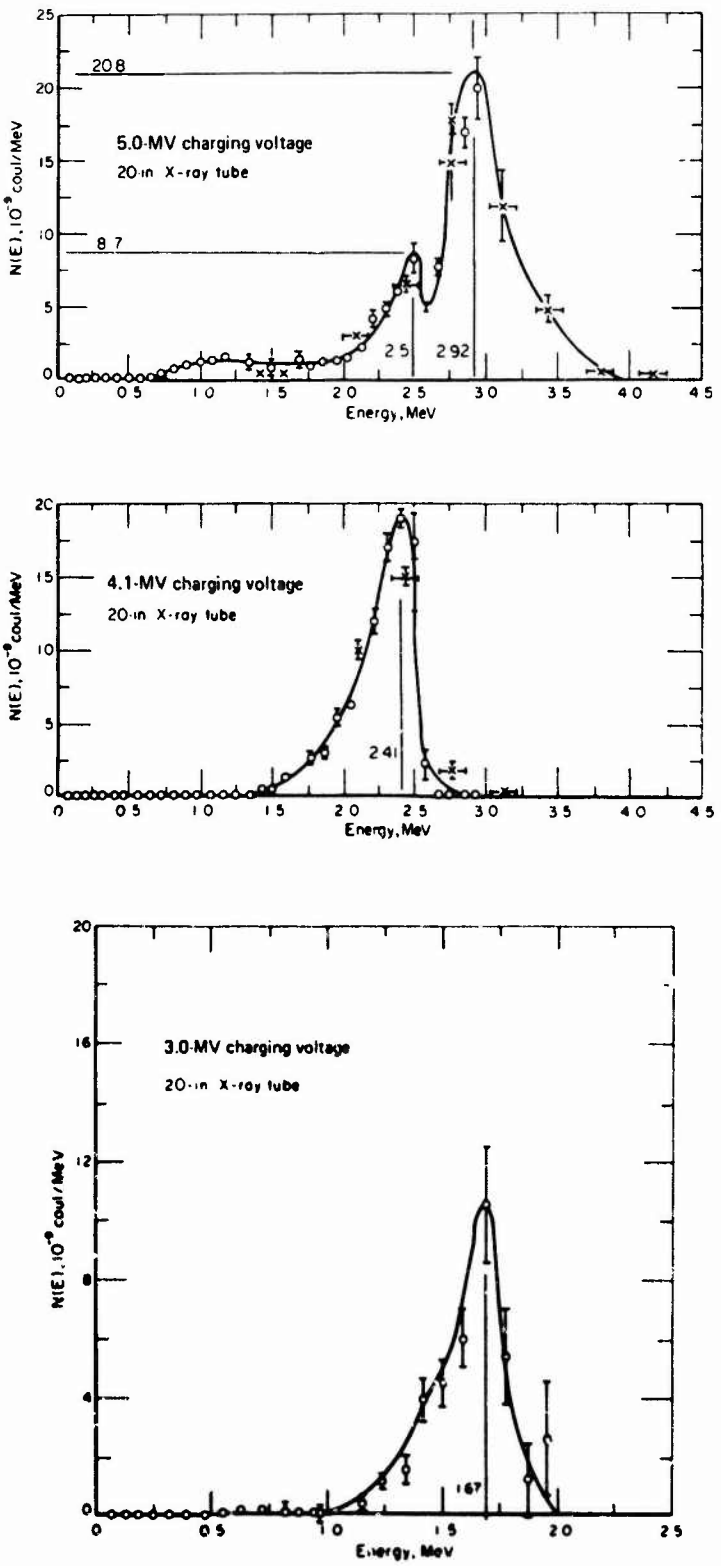

Figure 3-90. HDL FX-45 electron-beam energy spectrum.

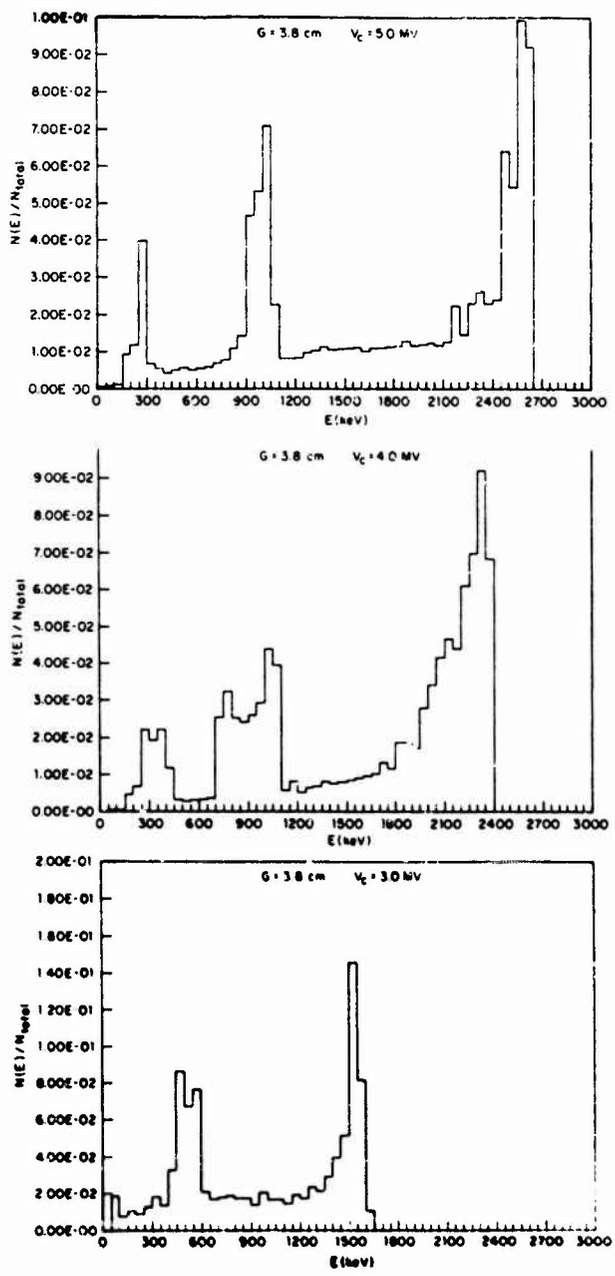

Figure 3-91. Electron energy spectra for high-impedance mode based on V and I monitor traces.

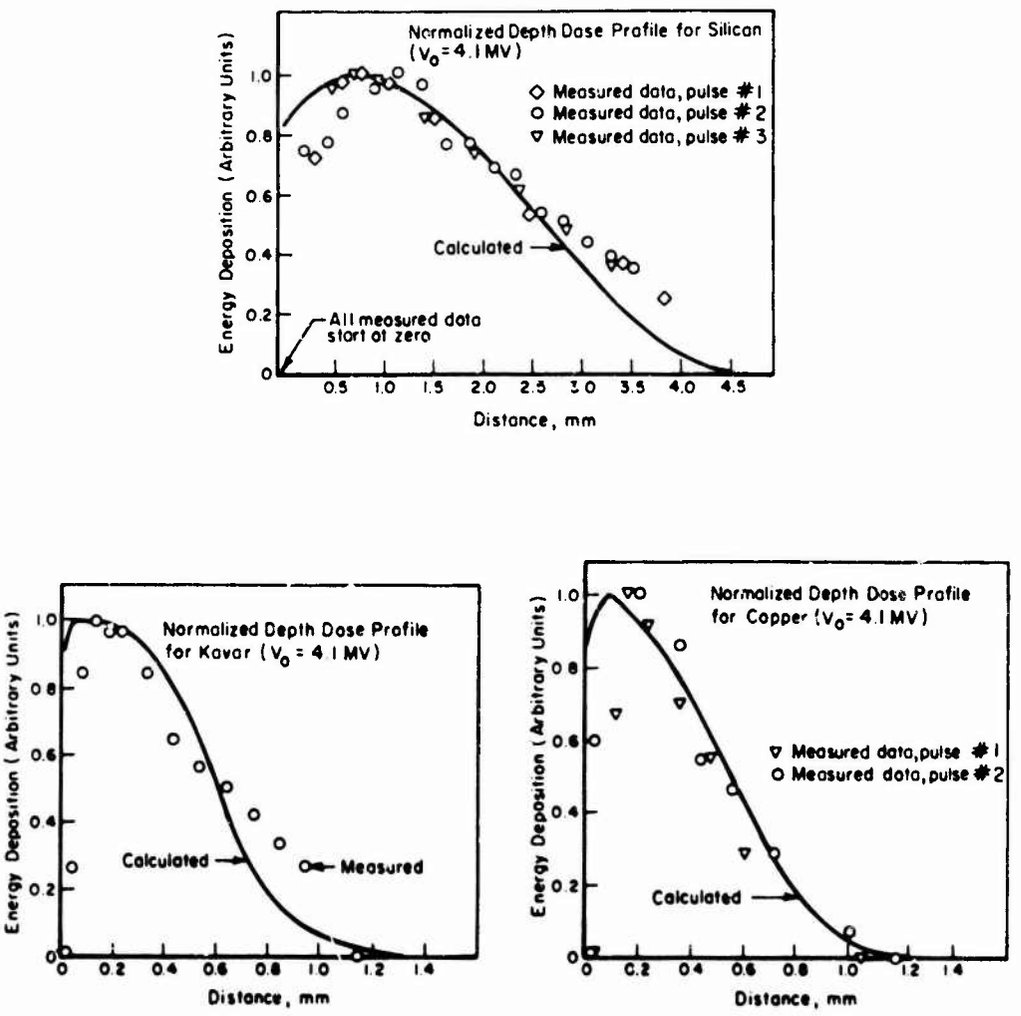

Figure 3-92. HIFX depth-dose profiles.

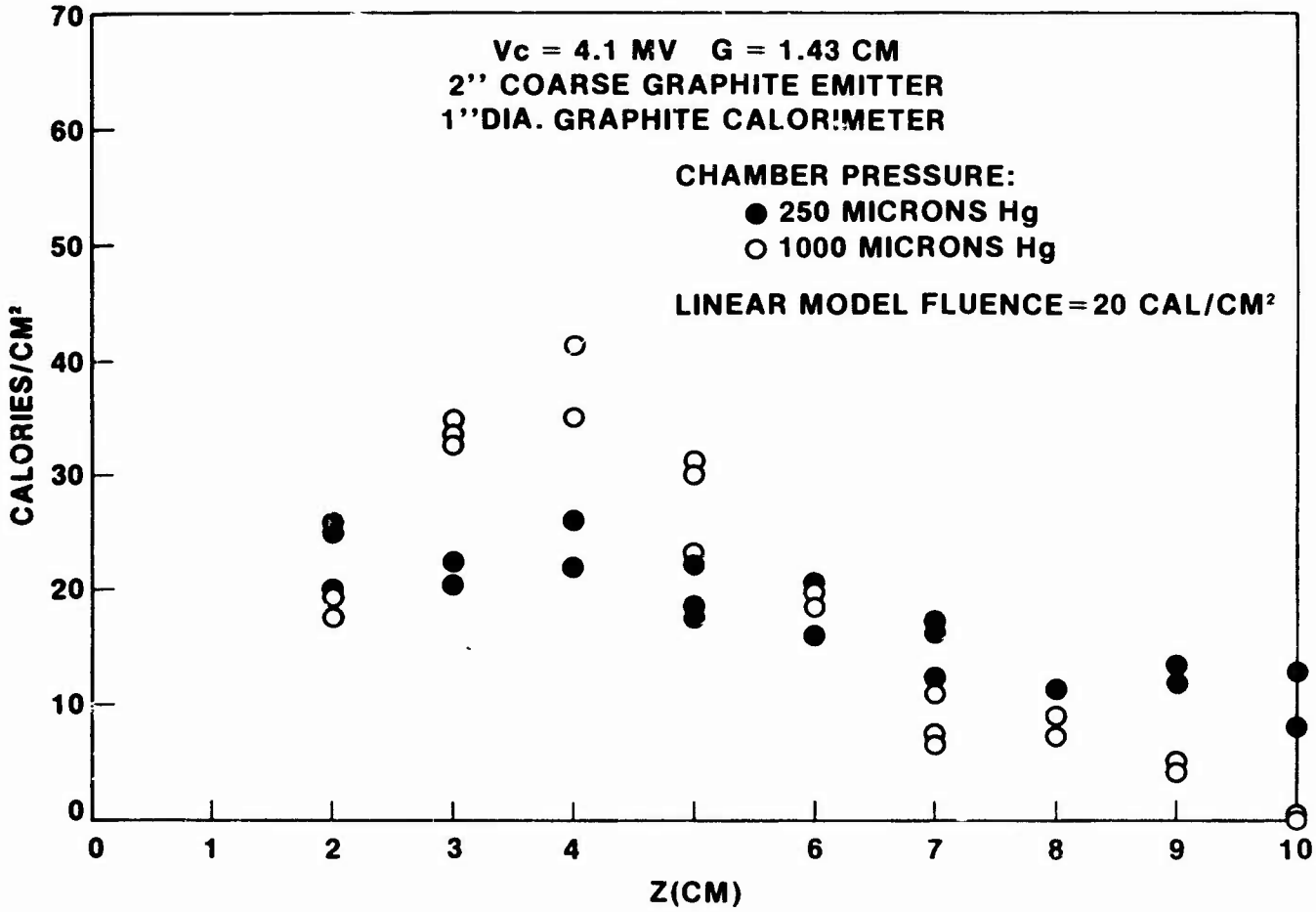

Figure 3-93. Low-impedance mode fluence versus axial position.

HIGH RESOLUTION FLUENCE CALORIMETER

CALORIES PER SQ CM

Vc = 4.1 MV G = 1.43 CM

DIA. = 2 IN.

PEAK DOSE = 4 CAL/GM PER CAL/CM²

2		2		1
	28	16	6	
6	26	28	34	3
	22	18	11	
2		2		2

¼" 1/32"

Z = 4 CM

P = 250μ

2		3		2
	12	15	5	
5	25	50	6	2
	10	18	6	
3		3		2

Z = 10 CM

2		6		1
	18	29	11	
14	38	74	24	5
	22	33	16	
3		8		7

Z = 4 CM

P = 1000μ

3		2		3
	3	3	2	
3	4	3	2	2
	2	3	2	
3		1		2

Z = 10 CM

Figure 3-94. High-resolution fluence distribution maps for low-impedance mode electron beams.

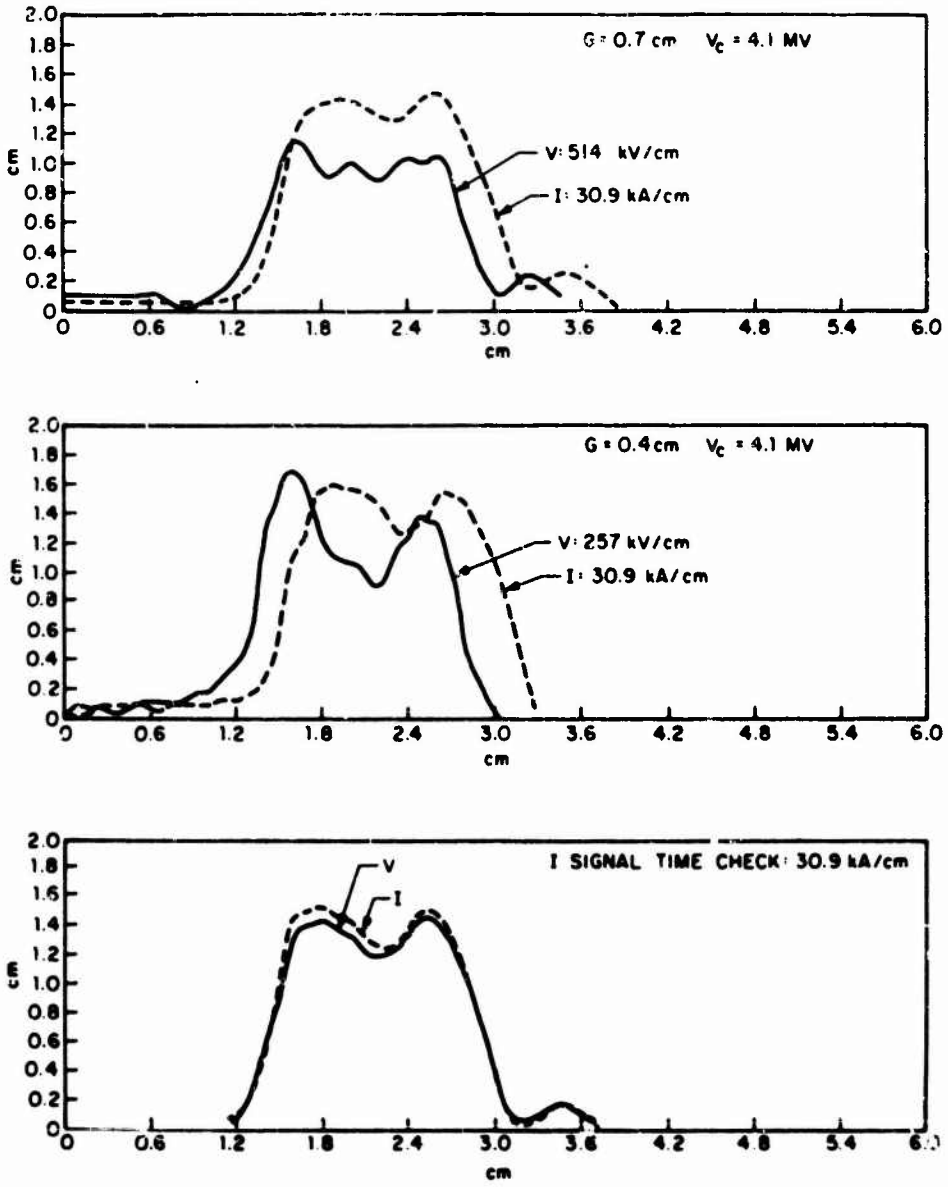

Figure 3-95. V and I monitor traces for low-impedance mode.

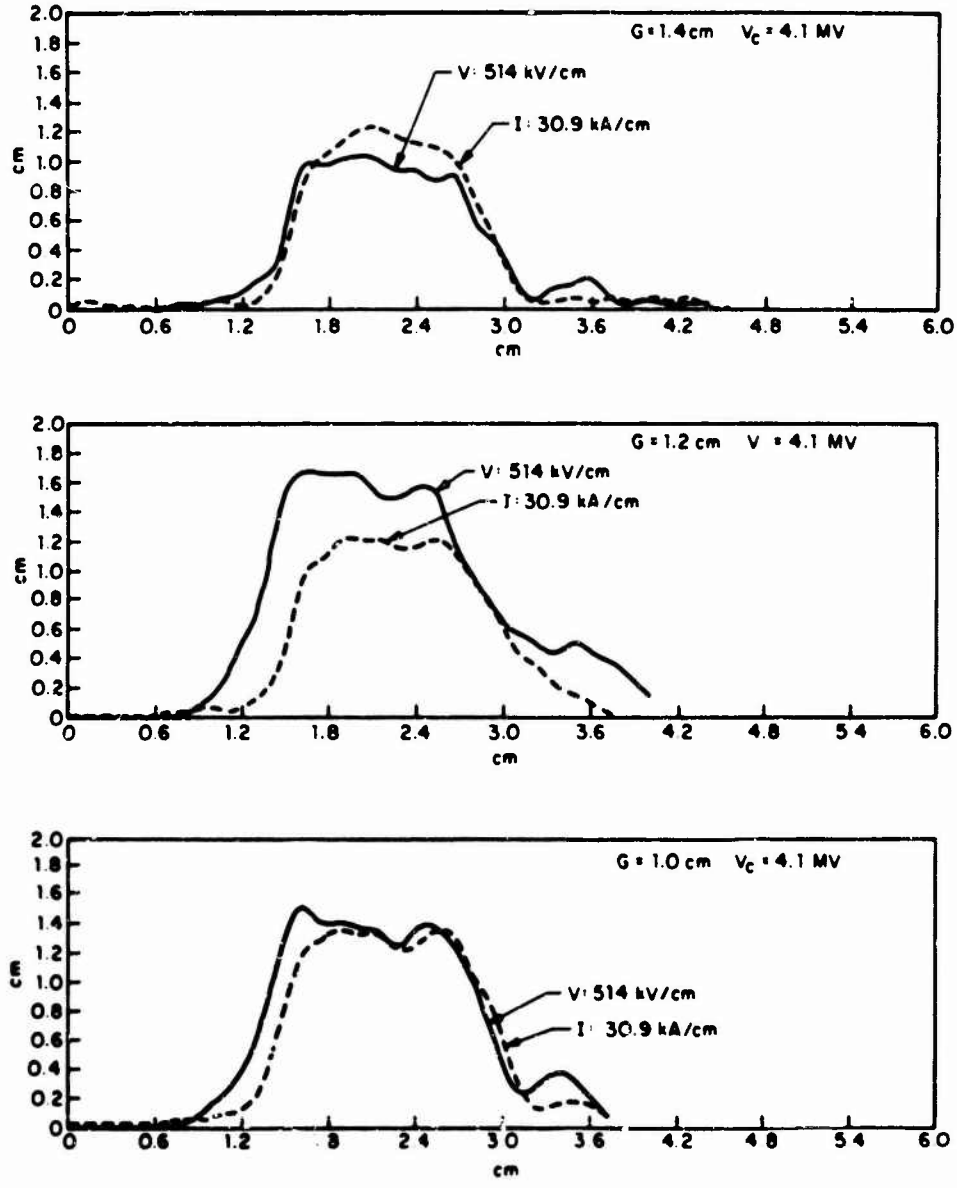

Figure 3-96. V and I monitor traces for low-impedance mode.

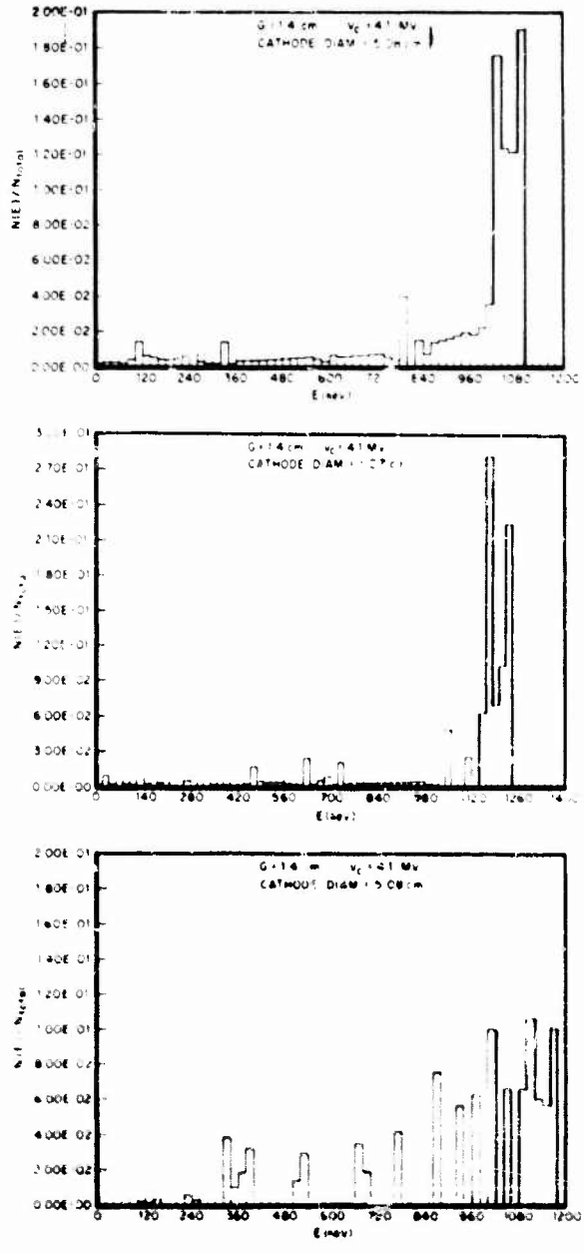

Figure 3-97. Electron energy spectra for low-impedance mode based on V and I monitor traces.

3.6.1.3 X-Ray Mode Environment

Data as obtained are shown in Figure 3-98. The values of x-ray exposure obey the inverse square law for distances greater than 6 in. from the target.

Oscilloscope traces for charging V of 4.1, 5.0, and 5.6 MV are shown in Figure 3-99. The pulse length is adjustable by electrically truncating the discharge to clip the trailing edge. A truncated pulse is also shown in Figure 3-99. The traces are scintillator/photodiode responses to the bremsstrahlung radiation. The measurements were made only to monitor the pulse shape; time scale is 10 ns/cm. A blowup of an oscilloscope trace of the x-ray pulse measured with a Compton diode is shown in Figure 3-100.

Quantitative x-ray spectrum measurements have not been made. Calculations of thick-target bremsstrahlung spectra are used as a guide. Figure 3-101 depicts such a calculated spectrum.

It is reported that by exercising care to select and calibrate the x-ray dosimeter-reader system, the 3-σ standard deviation in absolute accuracy can be reduced to 15%. Reproducibility of the dosimeter-reader system to identical exposures of Co-60 radiation is reported to be ±2%.

3.6.2 Support Capabilities

Three Tektronix 7844, 6 Tektronix 519, 6 Tektronix 551, and 2 Tektronix 555 oscilloscopes and oscilloscope cameras are available for experimenter use. A machine firing sequence is routinely available to actuate cameras and oscilloscopes and to trigger the system.

HDL provides dosimetry services. CaF_2 TLD dosimeters and readers are available for γ dosimetry, as well as Cu and graphite calorimeters for electron dosimetry. Other calorimeter materials and depth-dose calorimetry as well as more elaborate dosimetry, such as ballistic pendulum and laser interferometry, could be made available by arrangement.

The HDL IBM-370 computer may be used by arrangement.

The HIFX facility has an experiment setup and preparation laboratory and a conference room that can be used by experimenters. A drill press and hand tools for small work are available. The HDL machine shop also is available by arrangement. Cameras and film are provided for the oscilloscopes permanently located in the instrument room. Other photographic equipment and materials might be available from the HDL photographic laboratory by arrangement.

Technical and administrative inquiries should be made to:

Harry Diamond Laboratories
Branch 290
Adelphi, MD 20783
Attn: J.D. Silverstein, Flash X-ray Facility
Telephone: (202) 394-2238

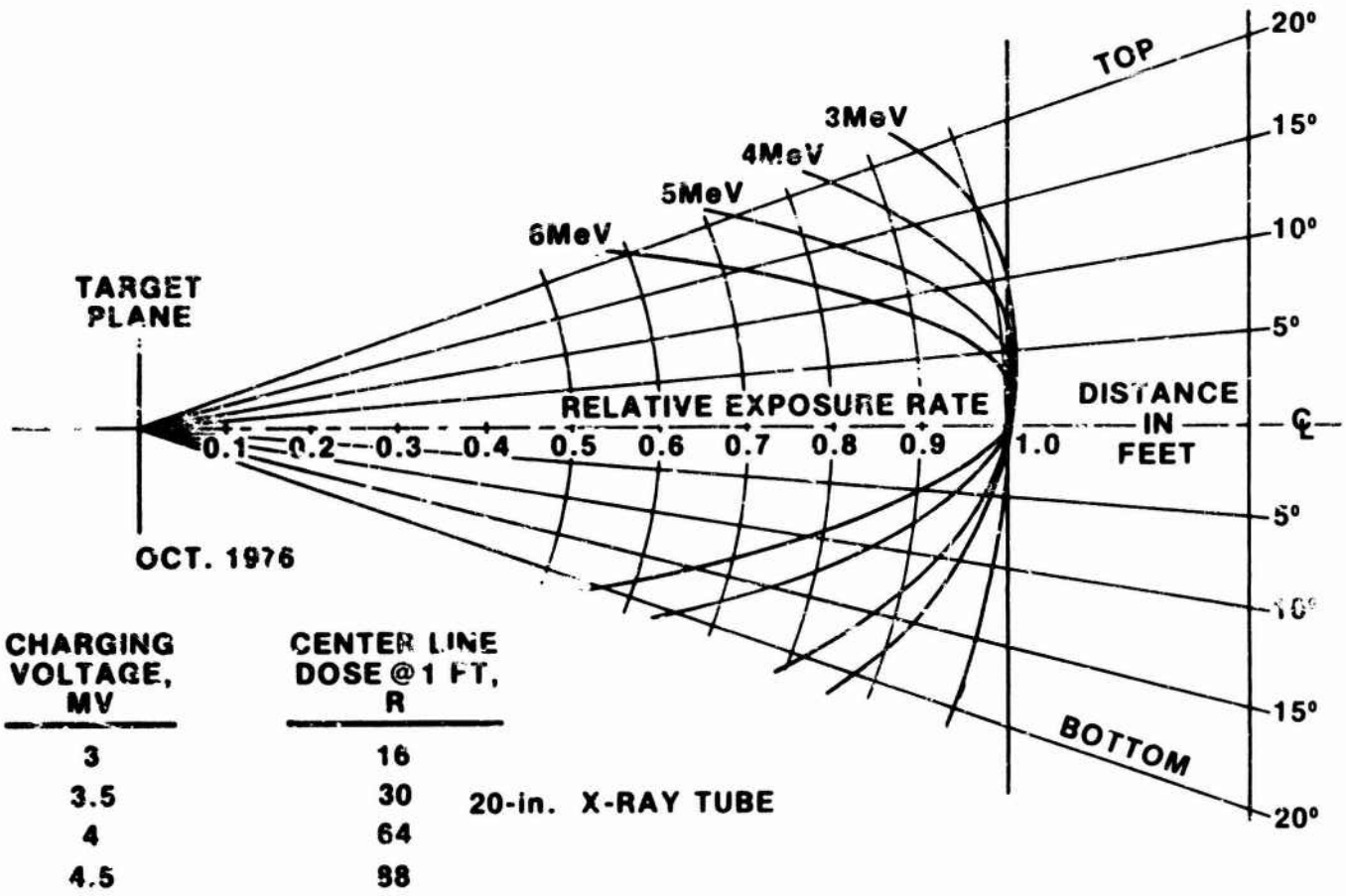

Figure 3-98. X-ray angular distribution in the vertical plane.

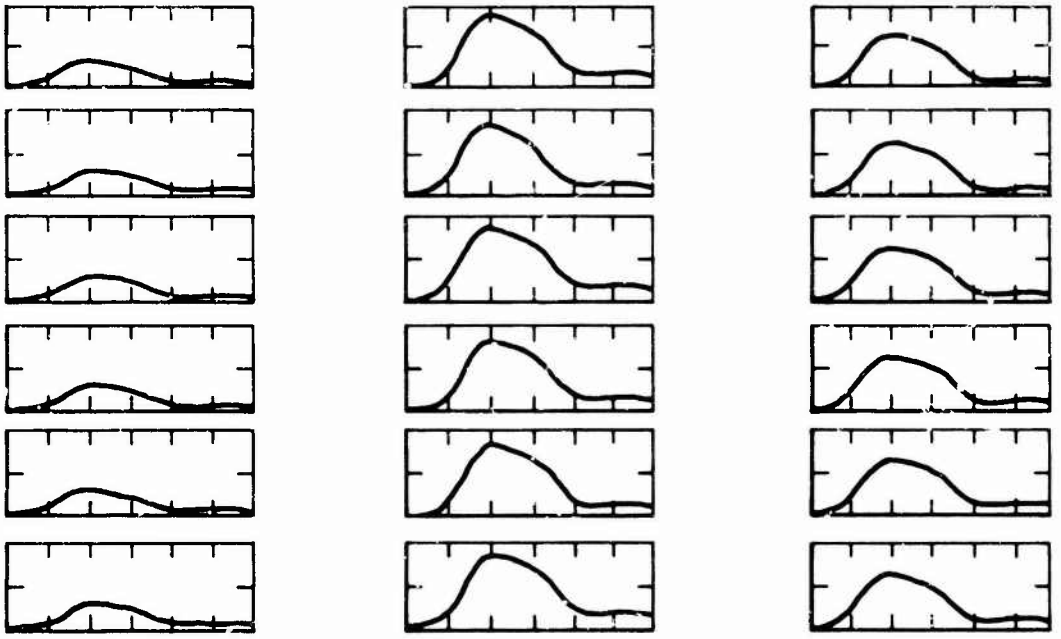

4.1 MV charging voltage

5.0 MV charging voltage

5.6 MV charging voltage

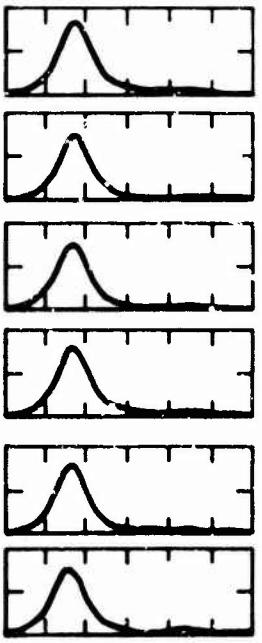

Time scale: 10 ns/cm

(Redrawn from scope pictures)

Crowbar, 5.0 MV charging voltage

Figure 3-99. Oscilloscope traces of HDL FX-45 x-ray waveforms (photodiode scintillator measurements; time scale is 10 ns/cm).

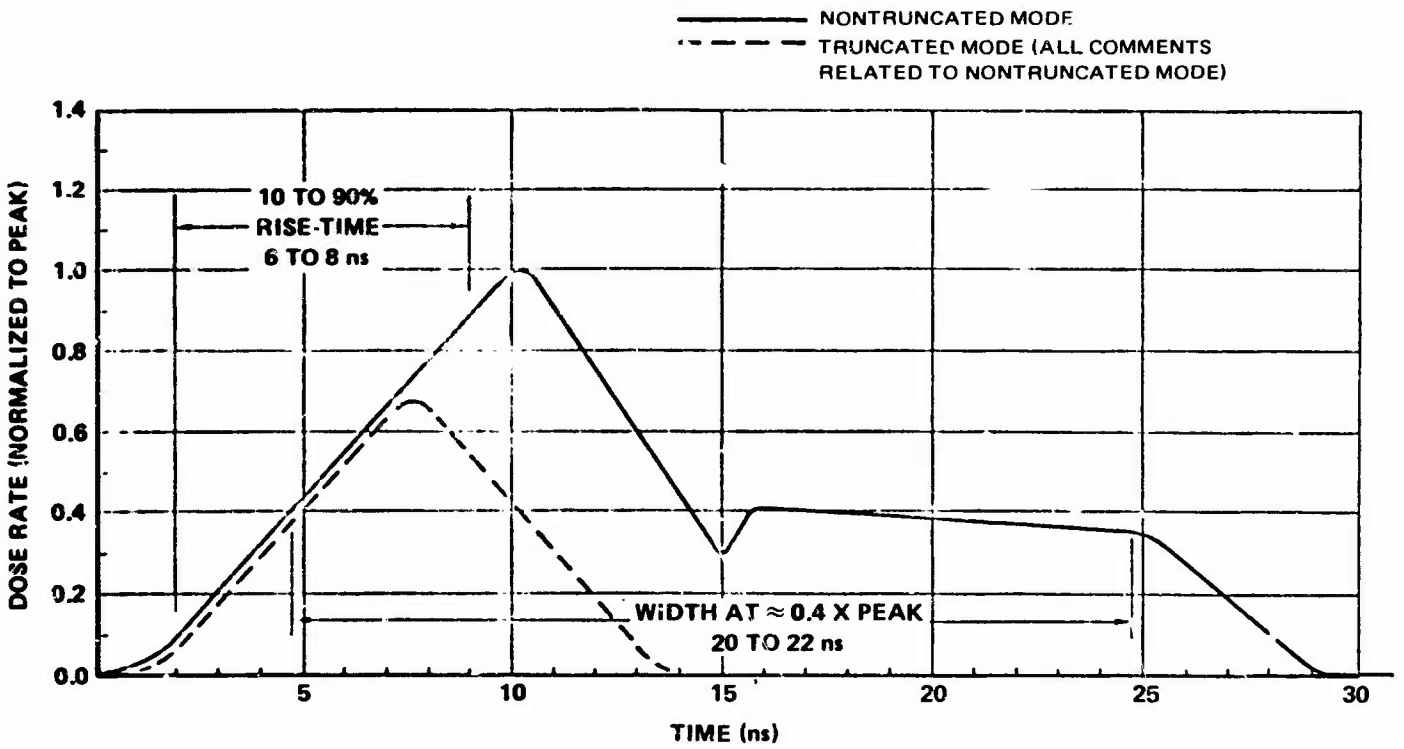

Figure 3-100. X-ray waveform from Compton diode.

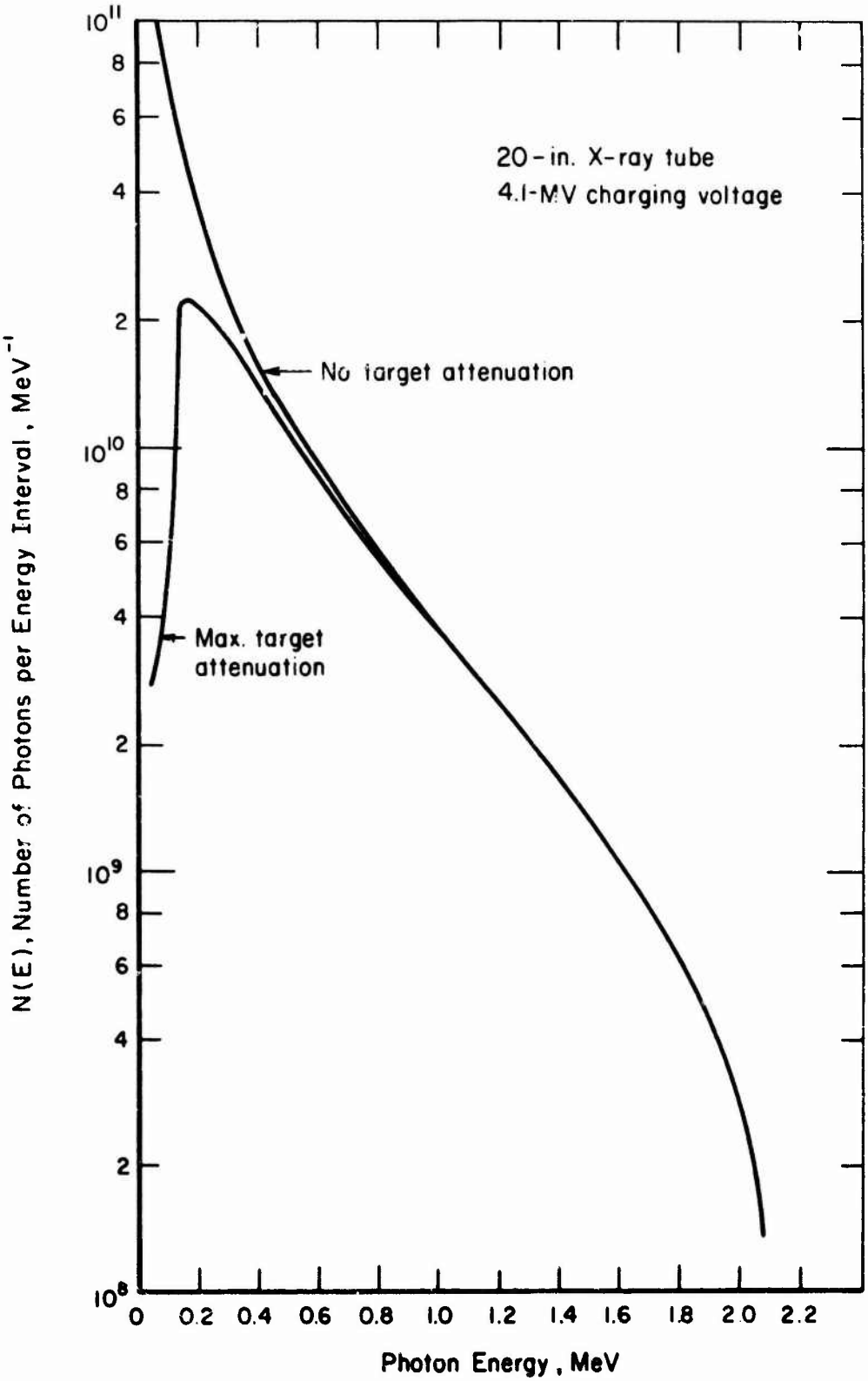

Figure 3-101. Calculated bremsstrahlung spectrum.

A minimum lead time of 3 to 6 months is normally required to schedule use of the facility. An application must be filed by the experimenter in the form shown by Figure 3-102.

Charges and costs associated with use of HDL facilities can be obtained directly from the laboratory. The shipping address is:

Harry Diamond Laboratories
Flash X-ray Facility
Bldg. 504
Adelphi, MD 20783

3.6.3 References

1. *Super Flash X-Ray System--Final Report,* report submitted to HDL by Ion Physics Corporation.

2. Sazama, F.J. and A.G. Stewart, *Design and Testing of a Current and Voltage Monitor for HIFX,* HDL-TR-1558, August 1971.

3. Silverstein, J.D., *Voltage and Current Measurements in HIFX Diodes,* HDL-TM-77-6, August 1977.

TO: Harry Diamond Laboratories, 2800 Powder Mill Road, Adelphi, MD 20783
ATTN: J.D. Silverstein, Br. 290, Bldg. 504 (submit two copies)

FROM: _____
(organization performing test)

ADDRESS: _____

REQUEST PREPARED BY _____ PHONE _____

PERSON IN CHARGE OF MEASUREMENT _____ PHONE _____

FUNDED BY ARMY ____ NAVY ____ AIR FORCE ____ DASA ____ OTHER ____

Contractors must submit authorization from funding agency. Funding agency must forward MIP

DATE OF APPLICATION _____

---

1. Descriptive Title of Proposed Measurement:

   Attach detailed--UNCLASSIFIED--description of proposed measurement. Include:

   a. Purpose of test
   b. System to which test is applicable
   c. Security requirements
   d. Approach
   e. Block diagram of cabling, etc.
   f. Size and weight of package to be exposed
   g. Special requirements, e.g., compressed gases, vacuum, triggering, etc.
   h. Any large apparatus you are bringing
   i. Explosives, noxious materials, etc.
   j. Probability of follow-on tests
   k. Anything else we should know that would help us assure the success of your measurement or that would make our lives easier.

2. Recording channels required: Tektronix 551 ____ 7844 ____
   555 ____ 519 ____

   Number of oscillograph channels _____

3. Type and number of cables required from exposure room to instrumentation room: RG214 ____
   1/2" foam ____
   Other ____

4. Length of time required to set up, prior to use of machine _____

5 Type of pulses: Gamma ____ Electrons ____ Low Impedance Mode ____

6. Charge voltage required: ____ MV

7. Experiment cannot be performed without low jitter (≤50 ns) machine firing feature of electronic trigger: YES ____ NO ____

8. Approximate number of gamma dosimeters required per pulse _____

9. Estimated number of days you will be at the HIFX Facility _____
   (note that we require at least 7 minutes between gamma pulses)

10. Preferred starting date _____ No. of people participating _____

Figure 3-102. Application for use of HDL-HIFX facility.

3.7 PHYSICS INTERNATIONAL PULSERADS 225W, 738, 1150, OWL II, AND PITHON II

3.7.1 Characteristics

There are 5 pulsed electron-beam facilities at Physics International (PI), with electron energies ranging from 100 keV to over 6 MeV. Three are owned by PI and 2 are operated by PI for DNA (OWL II and PITHON II). Although the generators differ in exact configuration, they all operate according to the same basic principles. Energy is stored on a capacitor bank (the Marx generator) of each machine. On a signal, the Marx generator is "fired" (i.e., the capacitor stages, initially connected in parallel, are switched to a series configuration) and a high V is developed on the output end of the Marx generator. This output end is connected directly to the high-V electrode of the pulse-forming line(s) and is used to "pulse-charge" the line(s) in 1 to several μs. The output pulse duration is approximately equal to twice the single transit time of the pulse-forming line. The "generator type" data shown in Table 3-8 give the basic pulse-forming line configuration for each facility and an indication of the type of output switch.

It is useful to consider the general output characteristics of the generators in both the FXR and electron-beam modes. The general shape of the time-integrated electron-energy spectrum incident on the anode plane is given schematically in Figure 3-103. The spectra are peaked at high energy and fall rapidly to zero at the maximum electron V. Electron energy deposition versus depth profiles can be approximated (for experiment planning purposes) by assuming monoenergetic electrons at the mean energy. Figure 3-104 shows approximate deposition profile characteristics over the V range covered by the PI accelerators. These parameters vary somewhat, depending upon the target atomic number and beam transverse energy. Specific deposition profiles can be found in later parts of this section.

For x-ray mode operation, an x-ray "converter" is placed at the anode plane of the diode. This converter can take many forms, the most common of which is a high-Z foil, backed by a thick low-Z plate which stops all the remaining electrons and contains any debris. This configuration, commonly known as a conventional converter, optimizes x-ray output dose. Other converter configurations could be provided to minimize x-ray self-attenuation in the converter and, hence, increase the spectral intensity at low photon energies. Characteristic x-ray spectra are shown in Figure 3-105 for a conventional converter. Unlike the electron-energy spectra incident on the converter, the x-ray spectra are peaked at low photon energies and fall slowly to zero at $h\nu$ = peak incident electron energy. The sharp intensity falloff at low $h\nu$ is due to self-absorption of x-rays in the converter material. X-ray yield (defined as total energy in x-ray pulse/total energy in the incident electron pulse) is strongly dependent on initial electron energy. Approximate yields are given in Figure 3-106. The angular distribution and source area must be taken into account to define the accessible x-ray levels accurately.

For electron-beam mode operation, the electron-beam is injected through a thin, low-Z anode foil into a "drift" chamber, where it is directed to the

Table 3-8. Summary of pulsed electron-beam generator characteristics.

Generator	Type	Peak Electron Energy Range[a] (MeV)	Maximum Total Diode Energy[b] (kJ)	Power Pulse Duration (FWHM) (ns)
OWL II (DNA)	4-Ω water-dielectric coaxial pulse-forming line, transformed to 2-Ω output impedance. Water output switch.	0.4 to 1.4	110	110
1150 Pulserad	35-Ω oil-dielectric coaxial Blumlein pulse line. Oil switch.	2.0 to 6.0	40	60
PITHON II[c]	1.3-Ω water-dielectric coaxial pulse-forming line. Water output switch.			
225W Pulserad	5-Ω water-dielectric coaxial pulse line. Gas output switch.	0.2 to 1.0	10	65
738 Pulserad	8-Ω oil-dielectric coaxial pulse line. Gas output switch.	0.25 to 1.1	6.0	50

Notes:

[a]Mean electron energy is typically 70% of peak value.

[b]Refers to energy delivered into a matched load.

[c]All PITHON output parameters and impedance (except output power) are CONFIDENTIAL; all other data in this table are UNCLASSIFIED.

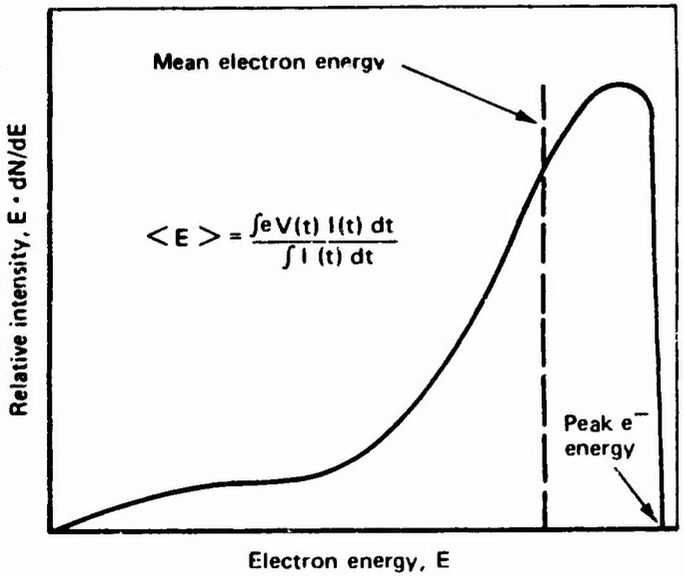

Figure 3-103. Schematic shape of time-integrated electron energy spectra.

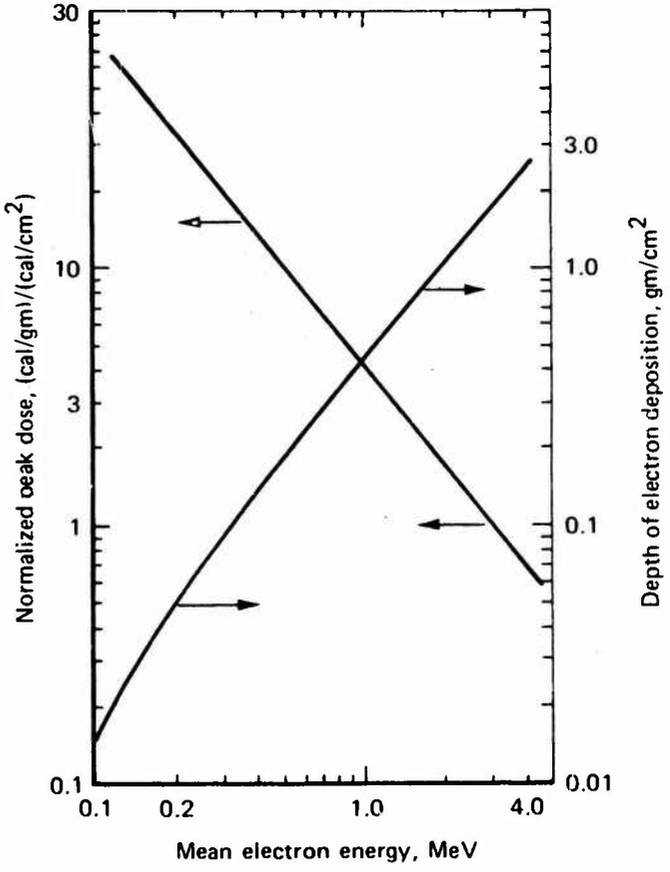

Figure 3-104. Electron deposition depth and peak energy deposition versus mean electron energy.

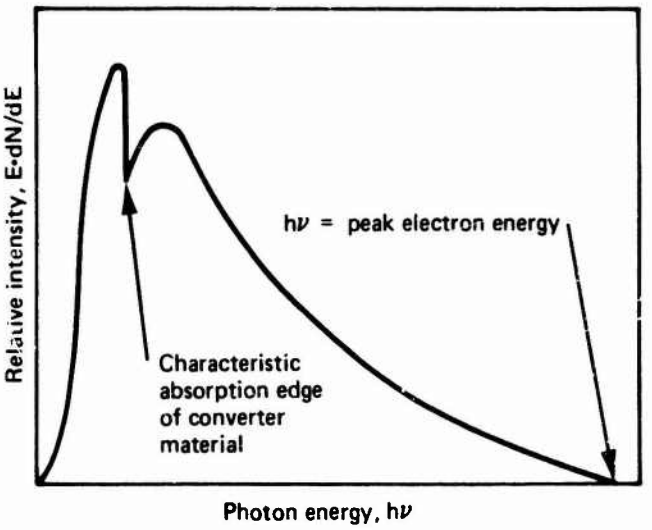

Figure 3-105. Characteristic shape of flash-bremsstrahlung spectra produced by pulsed electron accelerators.

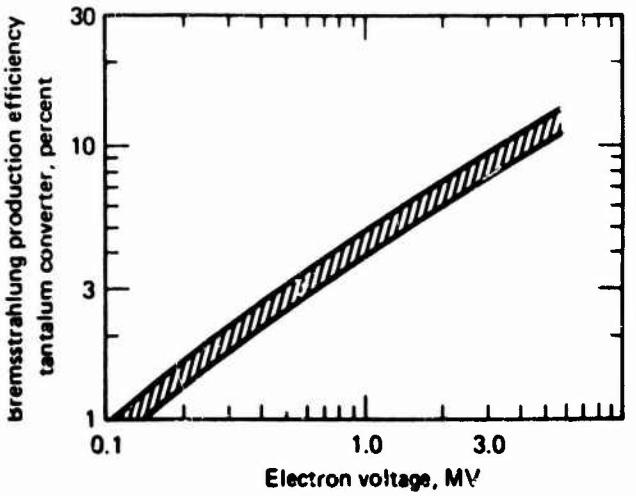

Figure 3-106. Approximate bremsstrahlung yield from conventional Ta converters.

target. In general, it is not possible to deliver 100% of the diode I to the target in a usable (e.g., uniform fluence) beam, although in some cases it is possible to uniformly irradiate targets at the anode. Two commonly used means of beam transport and control at PI are the neutral gas focussing/metallic guide cone technique, used for lower I beams, and the externally applied magnetic (B_z) guide field technique, required at the higher I levels.

3.7.2 Generator Diagnostics

Each facility is equipped with V and I diagnostics, which are used during every pulse. Pulse charge V (the V on the pulse-forming line) is monitored with a resistive divider. Tube V (across the tube insulator envelope) is monitored either with a resistive divider (738, 1150, and 225W) or with a capacitive divider (OWL II). The diode (accelerating) V can be obtained from the tube V waveform by subtraction of the induced V component, proportional to L(dI/dt) within ±10%. This is accomplished by use of a dI/dt monitor whose output is calibrated against the tube V monitor during short-circuit pulses, where the electron accelerating V = 0. Diode I is measured either by use of a B_θ field probe near the diode or by a self-integrating Rogowski coil encircling the beam. Many of these monitors are described in References 1 through 4.

In addition to providing a complete record of generator performance during a series of tests, the generator diagnostics (particularly the V and I waveforms) are a useful complement to both the electron-beam and x-ray diagnostics.

3.7.3 Electron-Beam Diagnostics

Electron-beam environments are characterized in terms of fluence (time-integrated energy flux) and energy deposition versus depth profile. In many cases, these data can be directly measured by calorimetric methods. Segmented graphite fluence calorimetry is available in the following standard configurations (in both 0.79-cm and 1.27-cm thicknesses):

1. 0.5- x 0.5-cm blocks
2. 0.5- x 1.0-cm blocks
3. 5.0- x 5.0-cm blocks

} Square array of 25 blocks

Special block configurations can be provided. Temperature rise in each block is sensed by thermocouples and monitored on a Vidar Data Acquisition system at the rate of 20 channels/s printed on paper tape, or fed directly into a Tektronix SPS Model 62 computer. Calorimetry data, in the form of thermocouple V readings, is promptly computer-analyzed to generate a fluence map. Depending on fluence levels, the accuracy of fluence measurement is typically ±10%.

Energy deposition versus depth measurements are made by means of a stack of thermally isolated foils, each monitored with a thermocouple. These data are also recorded by the Vidar. Accuracy is ±10%. Foil stacks of various metals are available in different thicknesses, the choice depending on the electron energy and dose range of interest. Al foils are most commonly used; graphite foils have been used at dose levels beyond the melting point of most metals. Calorimetry provides the simplest and most direct characterization of electron-beam

environments, but it becomes inadequate as dose levels approach the damage threshold in graphite. In addition to the limitation imposed by graphite vaporization, problems of radiative heat loss versus thermal equilibration times limit present direct (calorimetric) fluence diagnostics to dose levels of 1,000 cal/g. Mechanical problems in graphite depth dosimeters presently limit their application to less than 500 cal/g.

Diagnosis at high-dose levels is accomplished by less direct means. In these cases, the diagnostics are commonly the diode V monitor and a high-I Faraday cup (which measures the energetic electron-beam I at the target). Fluence is computed as $\int eV(t)J(t)dt$, where J is the measured beam I density. This technique has been cross-checked at low-dose levels by comparison with direct fluence calorimetry.

Deposition versus depth profiles in the high-dose region are also obtained by the Monte Carlo transport code. The electron spectrum (from measured V and I waveforms) and angle of incidence at the sample location is the input data. Nonnormal electron incidence is due to electron scattering in the anode foil and to the self-magnetic field of the beam in the diode (References 5 and 6), and is measured by the filtered Faraday-cup technique. Experimental measurements of I transmission versus target thickness have been used to check the deposition calculations. Although other direct techniques for fluence and deposition profile measurement at high-dose levels are under development, they are not presently available.

3.7.4 X-Ray Diagnostics

In the pulsed x-ray environments, use is made of photodiode response (which permits time resolution of pulses and calculation of PWHM), and calorimetry and TLD results. Calorimeter measurements are made with 3 specially designed instruments: a portable calorimeter for measuring fluence and front surface dose simultaneously (Reference 7); a depth-dose calorimeter for high intensity, low-V machines (Reference 8); and an array of small combination calorimeters for measuring areal distribution of fluence and front surface dose (Reference 9). The resulting measurements have been in good agreement with other dosimeter measurements. Also, calculated calorimeter response is verified by exposure to a 400-Ci Cs-137 γ-ray source. Comparison of the measurements of the x-rays from the pulsed machines indicates that absolute values are accurate to within 5 to 10%.

The TLD most commonly used at PI is powdered LiF. These TLDs are used for making faceplate maps and mapping exposure as a function of position. Dosimeter precision is ±3%. Comparison of measurements with those made by commercial customers of the Pulserad Facility agree within the experimental errors of the dosimetry systems. PI maintains a complete TLD readout facility and can provide TLDs in the form of polyethylene or Al jackets filled with LiF powder, or LiF-impregnated teflon discs (±10% accuracy). TLD instrumentation is calibrated regularly against in-house radiation sources.

3.7.5 Noise Levels

Shielded rooms are provided at each of the 5 facilities. Noise levels inside vary somewhat, depending on the facility. Systems are available to reduce noise levels to a few mV when required. These systems can be installed upon request. The Pulsed Radiation Facilities Manager should be contacted at least 1 month in advance of pulsing dates for this provision.

3.7.6 OWL II Data

The OWL generator was constructed in 1971 as a developmental coaxial water line. In 1973, it was upgraded to higher total energy levels as part of a DNA-funded program to develop high-energy electron beams. The machine has a 360-kJ Marx generator which charges a 4-Ω water-filled coaxial pulse-forming line. The line is switched (by a triggered water switch) into a transformer section to provide a 2-Ω output impedance. At the present time (February 1979), the diode insulator is being redesigned to improve reliability at peak V and to reduce I risetime by reducing inductance. This modification is not expected to appreciably alter the time-integrated electron and x-ray environments, although reproducibility should be improved.

Total energy output in excess of 100 kJ (≈25 kcal) is available with a diode of 400 cm^2 area, as shown in Figure 3-107. This diode and its associated hardware are referred to as the "large-area beam system." An 80-cm^2 diode also has been developed for the "small-area beam system," which has produced up to 75-kJ beams.

3.7.6.1 Electron-Beam Environments

Beam transport on OWL II is accomplished by using magnetic guide fields. Table 3-9 indicates the wide range of electron environments attainable. The beam chamber (from anode to target) is N-filled at 1-torr pressure. Representative energy deposition profiles in carbon are shown in Figure 3-108. Dose in carbon of up to 3,000 cal/g is attainable with the small-area beam system. Figure 3-109 shows the interrelationship of dose, fluence, area, and target position in that system, and Figure 3-110 documents the fluence uniformity statistics. The Gaussian curve superimposed on the data in Figure 3-110 shows that the bulk of the data has an rms distribution of about ±8%, although non-Gaussian low-amplitude "wings" are in evidence. Corresponding data on fluence uniformity in the large-area beam system are given in Figure 3-111, which has a different format to show the radial structure of beam fluence. The calorimeter block readings are plotted for 4 pulses as a function of distance from the center of the array. For the higher fluence levels, some fall-off is seen at the beam edge, which is due to the fact that for these levels the outmost blocks were only partially illuminated by the beam. (The 2 outermost sets of blocks extend to 5.4 in. and 5.6 in., respectively, from the center of the array.)

In Figure 3-112, the average fluence in the large-area beam system is shown as a function of the cathode-to-target distance and normalized by the total beam energy. Superimposed on the data points is a plot of the magnetic guide field strength, in arbitrary units, versus cathode-to-target distance. The normalized

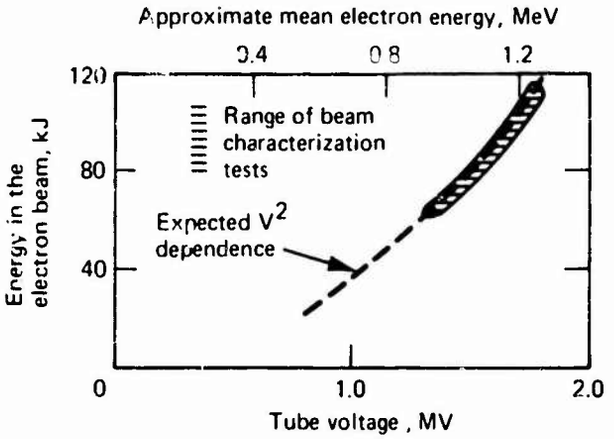

Figure 3-107. Total diode energy versus tube V and mean electron energy, OWL II.

Table 3-9. Typical electron beams, OWL II generator.

Mean Electron Energy (MeV)	Fluence (cal/cm^2) Areas Are Shown in Parentheses	Beam Transport Mechanism
0.570	400 (15 cm^2)	Magnetic lens[a]
0.770	470 (15 cm^2)	Magnetic lens[a]
0.520	5 to 50 (150 cm^2)	Magnetic lens[b]
0.850	5 to 50 (150 cm^2)	Magnetic lens[b]
0.850	135 (55 cm^2)	Magnetic lens[b]
0.850	520 (20 cm^2)	Magnetic lens[b]
0.950	10 to 50 (400 cm^2)	Magnetic lens[b]

Notes:

[a]Converging B_z 4:1.

[b]Converging/diverging B_z.

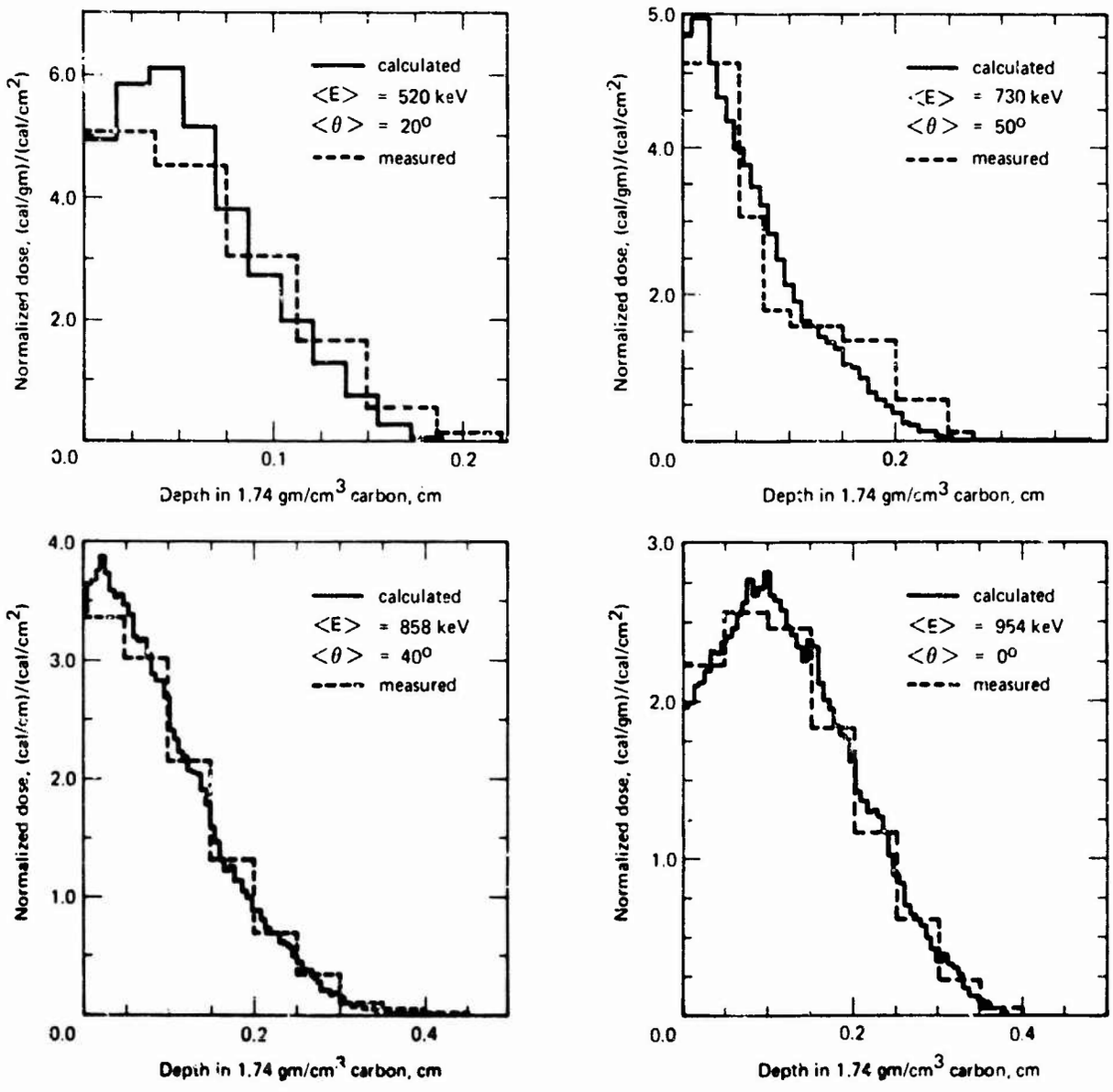

Figure 3-108. Typical electron energy deposition profiles for OWL II.

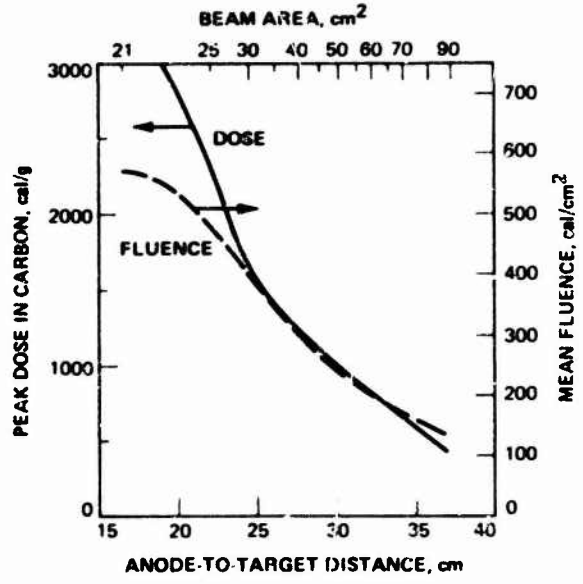

Figure 3-109. Electron environment characterization of the OWL II small-area beam system, for 50-kJ diode energy.

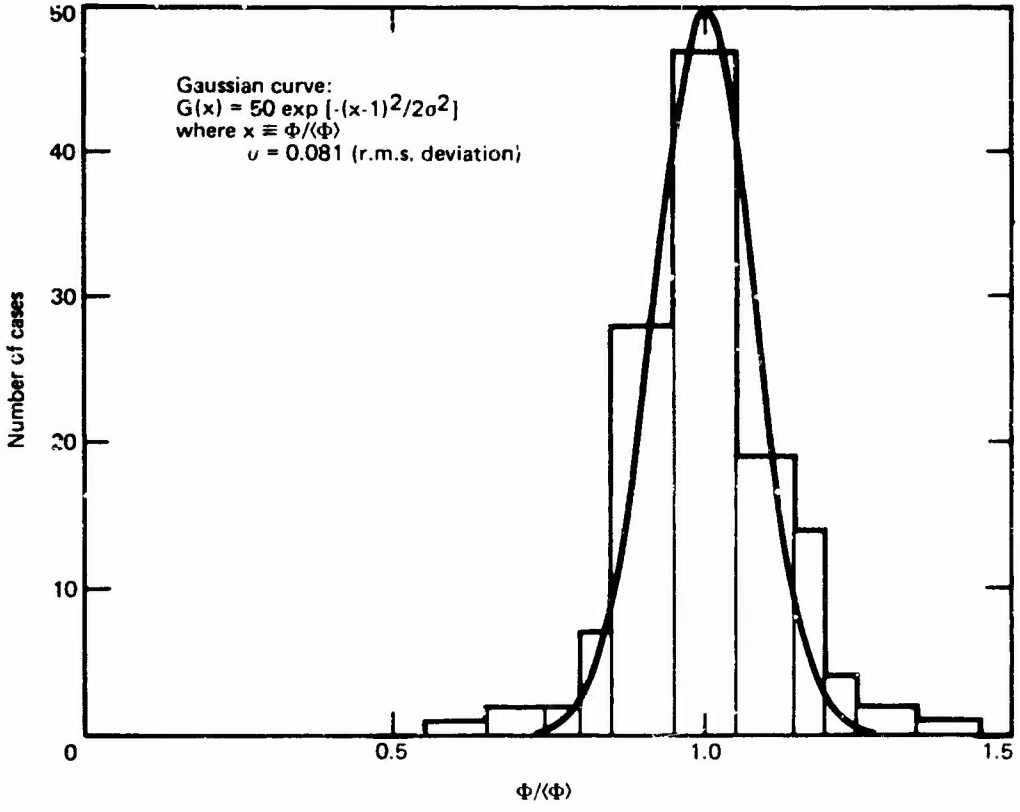

Figure 3-110. OWL II small-area beam system fluence uniformity statistics. (Calorimetry data from 6 pulses are represented. Each "case" is 1 calorimeter block's fluence reading on 1 pulse, relative to that pulse's mean fluence value. A total of 125 cases are included.)

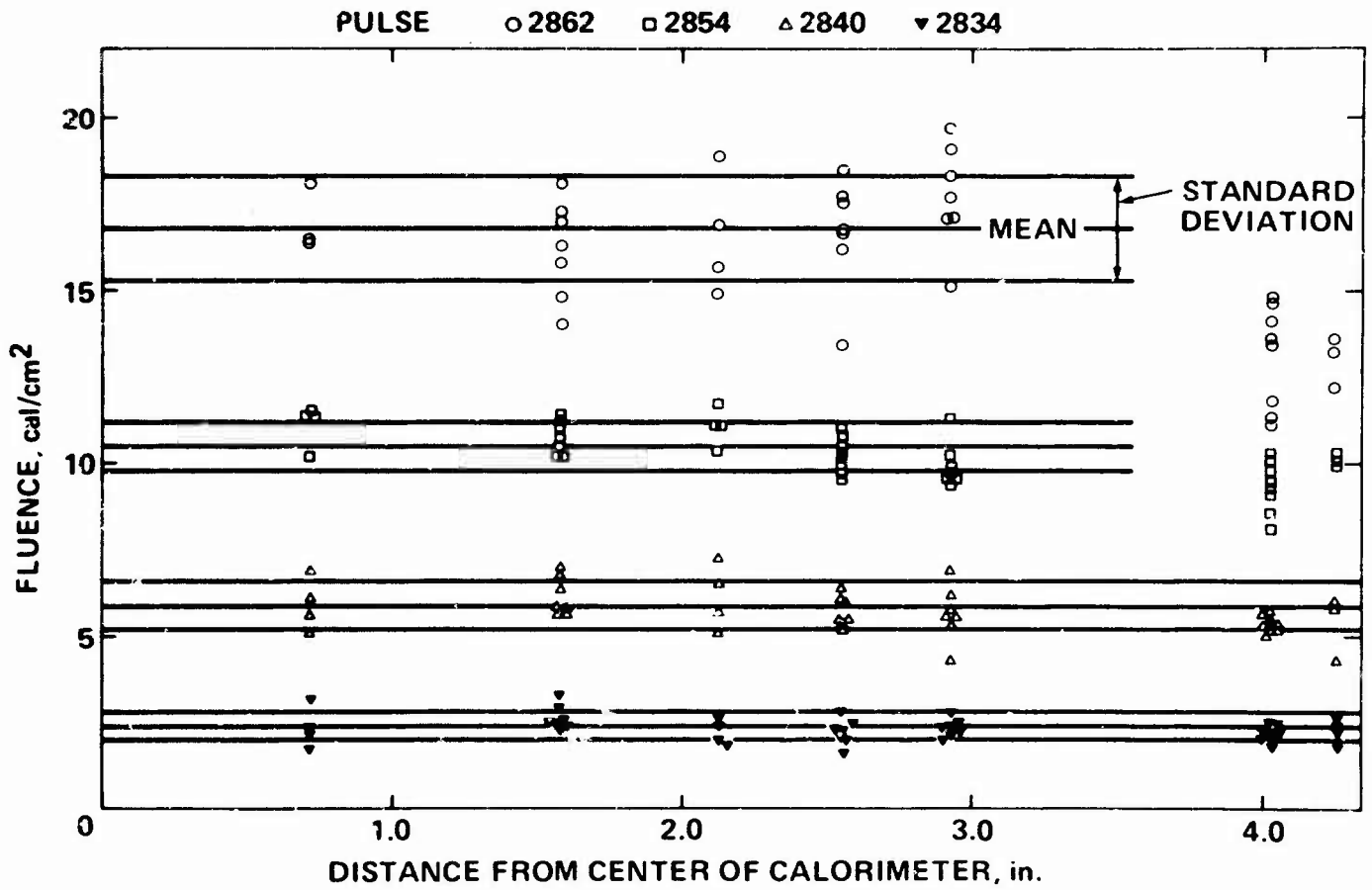

Figure 3-111. Fluence uniformity on OWL II large-area beam system.

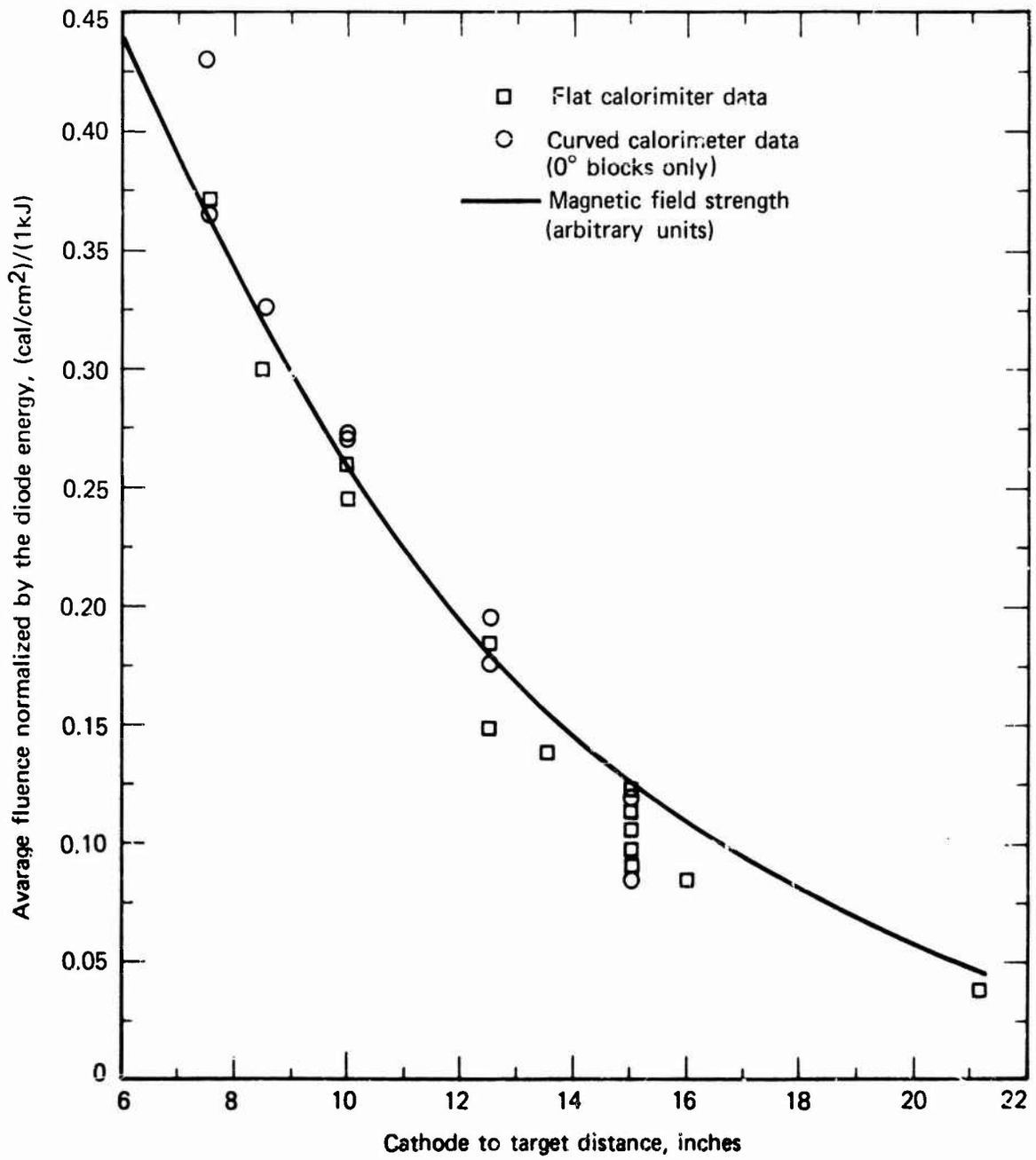

Figure 3-112. Normalized fluence versus distance from cathode, OWL II large-area beam system.

fluence is seen to follow the field strength, in accordance with the simple model of adiabatic single-electron motion in the guide field.

3.7.7 Model 1150 Pulserad Output Data

The 1150 Pulserad is a 35-Ω oil-dielectric coaxial-Blumlein generator with an output V range of 2 to 6 MV and 5 to 40 kJ (1,200 to 9,000 cal) total beam energy.

3.7.7.1 Electron-Beam Environments

Because the 1150 Pulserad is a high-V machine, the anode does not have to be replaced after every pulse. This reduces the turnaround time and allows for a higher pulse repetition rate. Table 3-10 lists typical electron beams from the 1150 Pulserad and Figure 3-113 shows fluence versus target position for the particular conditions indicated. Neutral gas transport in a large drift chamber (60-cm dia. x 60-cm length) is used for beam control. Fluence levels can be varied by choice of diode configuration and target distance from the anode. Additional data are available for other beam conditions.

Measured energy deposition profiles at mean electron energies of approximately 2 and 4 MeV are given in Figure 3-114.

3.7.7.2 X-Ray Environments

The maximum pulse repetition rate is 1 every 3 min. Exposures available on the Pulserad 1150 range from a few R at 3 m to <50,000 R at the faceplate (Figure 3-115). The radiation pulse width is 60 ns at half maximum. The exposure to 50,000 R, combined with the 60-ns pulse time, gives dose rates of approximately 10^{12} rad/s in Si absorbers. This high exposure rate is available only over a few cm^2 at the faceplate (Figure 3-116). Figures 3-117 and 3-118 give curves of the angular distribution of x-ray intensity at 0.5 m and a dose profile showing lines of equal dose. Exposures of 10^{11} rad/s can be obtained over an area of 300 cm^2 (Figure 3-119).

The electron bremsstrahlung spectrum has been calculated with the BSPEC code. Figure 3-120 shows the calculated γ-spectrum emerging from the converter (including attenuation in the converter) for 5-MeV peak electron energy. Figure 3-121 shows this γ-spectrum transmitted through the 0.5-in.-thick Al plate normally used between the converter and the irradiated targets. The mean photon energy is ~1.05 MeV, with a peak intensity at ~350 keV. Qualitative validation of the spectrum shape has been indicated by experimental measurement of energy deposition in a 2-element γ-calorimeter. The calorimeter consists of a 0.3-mil Ta foil backed by a [illegible]-thick block of W. The two elements are thermally isolated and temperature rises are monitored by a thermocouple (on the foil) and a thermistor (embedded in the block). The γ-spectrum in Figure 3-121 predicts a ratio of

$$\frac{\text{Absorbed dose in 0.3-mil Ta}}{\text{Absorbed dose in 1.0-cm W}} = 3.66 \ .$$

Table 3-10. Sample electron beams from the 1150 Pulserad.

Mean Electron Energy (MeV)	Fluence (cal/cm^2)	Beam Area for ±10% Uniformity (cm^2)
4.5	50	35
4.5	100	15
2.0	50	10
2.0	100	5

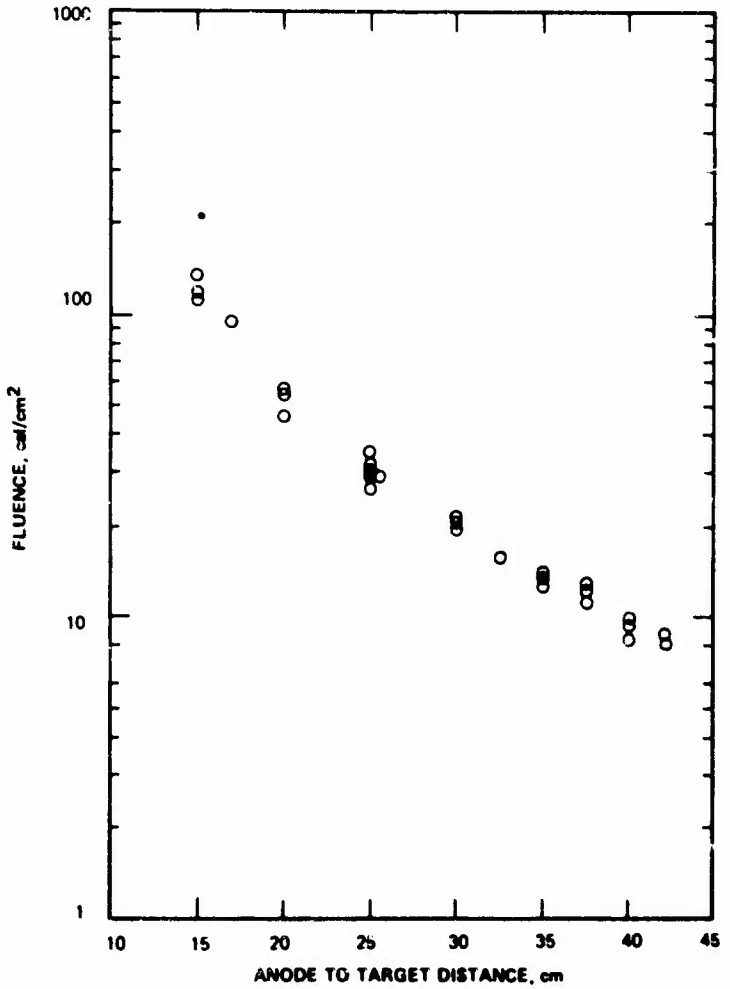

Figure 3-113. Fluence versus target position, 1150 Pulserad. (Peak diode V, 5 MV; chamber pressure, 0.70 torr N_2; 7.6-cm-dia. C cathode. Each circle represents mean fluence in 9-cm^2 area at beam center, an average of nine 1-cm x 1-cm calorimeter block readings.)

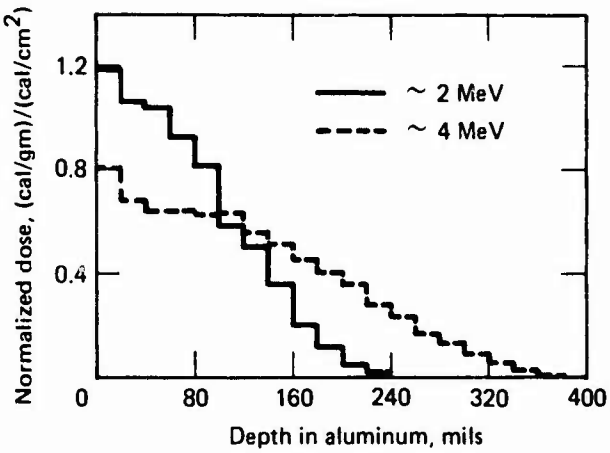

Figure 3-114. Energy deposition profiles from 1150 Pulserad.

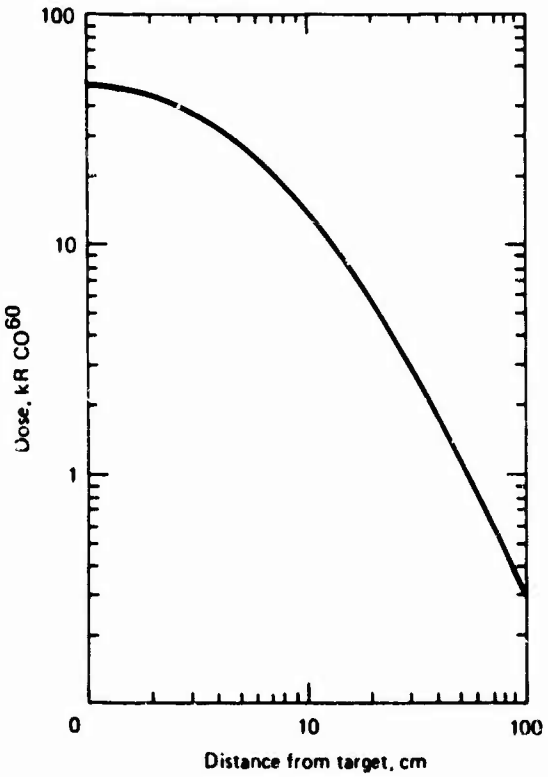

Figure 3-115. On-axis dose as a function of distance from target, 1150 Pulserad.

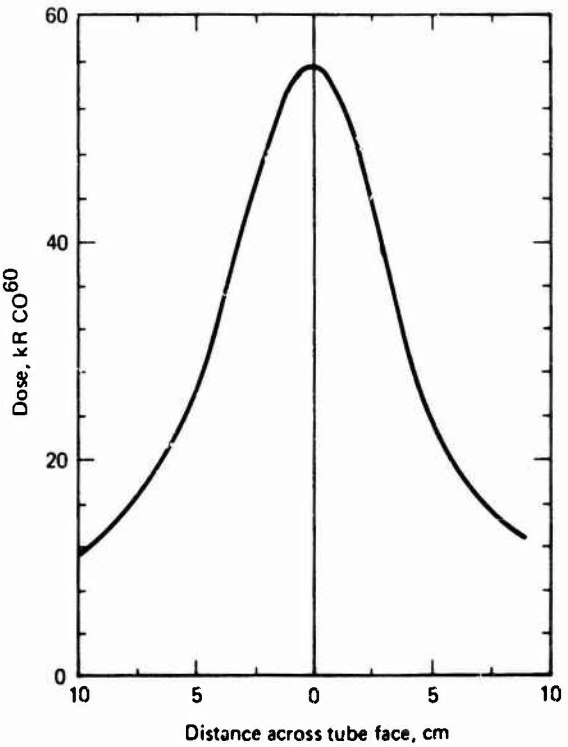

Figure 3-116. Dose profile across tube face, 1150 Pulserad.

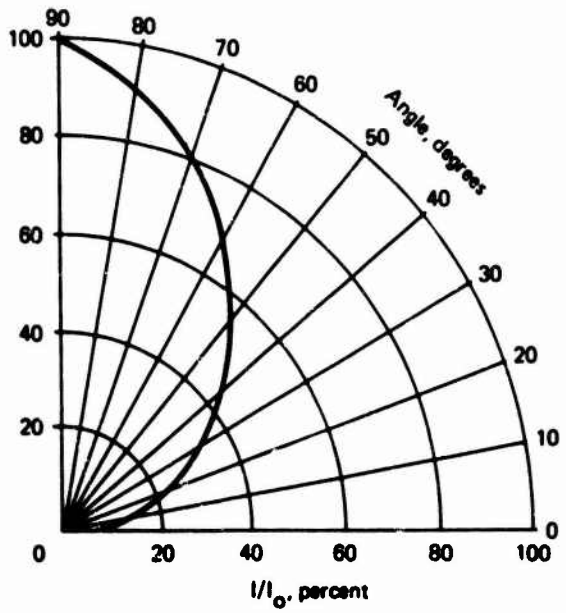

Figure 3-117. Angular distribution of x-ray intensity at 0.5 m, 1150 Pulserad.

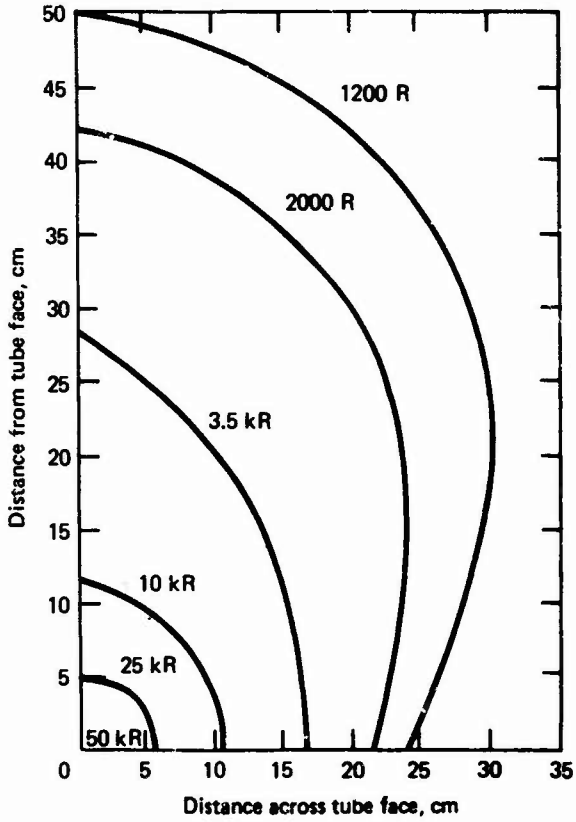

Figure 3-118. Dose profile showing lines of equal dose, 1150 Pulserad.

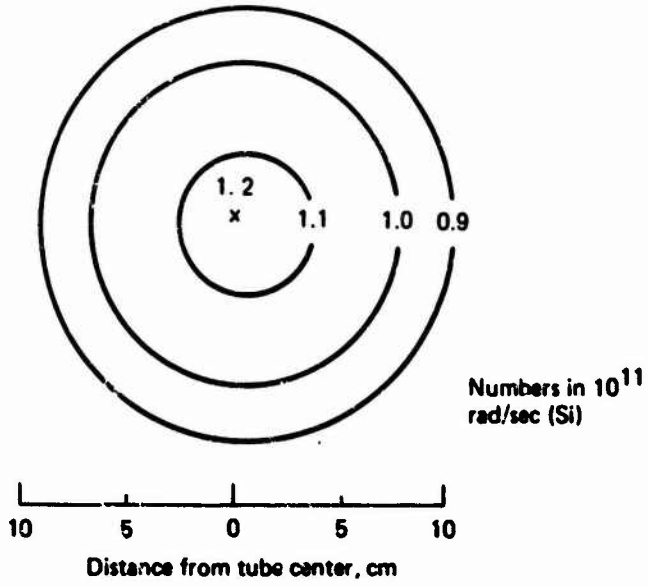

Figure 3-119. Faceplate dose contours for torus cathode.

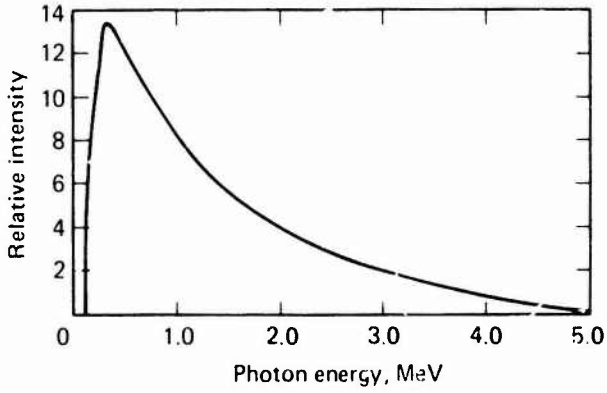

Figure 3-120. BSPEC calculation of thick-target γ-spectrum, including self-absorption in Ta converter, 1150 Pulserad at 5-MeV peak electron energy.

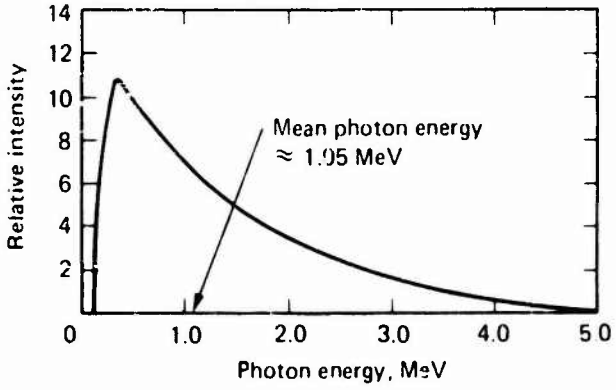

Figure 3-121. γ-spectrum of Figure 3-120 computationally transmitted through 0.5-in. Al.

The measured value of 3.0 ± 0.2 is in reasonable agreement with the calculation.

3.7.7.3 Long-Pulse Environments

The Pulserad 1150 is converted to the long-pulse mode by removing the Blumlein and output switch and adding a parallel L-C filter section, which, with the Marx generator, makes a 2-stage, type A pulse-forming network. The Marx generator consists of 50 0.5-μF and 0.5-μH capacitors. The values of inductance and capacitance in the filter were chosen to give a pulse with FWHM of 1.7 μs into a constant resistive load. The filter is made of 15-nF, 50-kV tubular capacitors in a folded series-parallel configuration, arranged like spokes of a wheel extending

out to V grading rings. Many parallel capacitor strings allow easy trimming of the wave shape to compensate for the decreasing impedance-time history of a real diode. The inductance is provided by a coil wound on the axis. Typical diode waveforms are shown in Figure 3-122. The maximum beam values obtained in the diode tested were 2-MV peak tube V, 35-kA peak I, and 50-kJ beam energy. The 1150 long-pulse generator (LPG) has not been used yet to irradiate targets. Applications should be discussed with PI personnel.

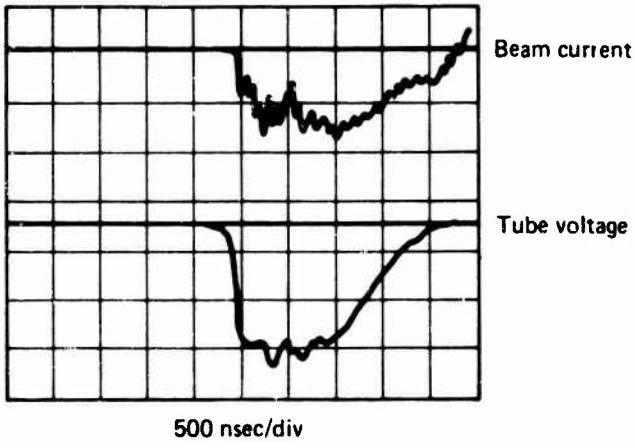

Figure 3-122. Typical V and Faraday-cup waveforms for a low-V shot, 1150/LPG Pulserad.

3.7.8 PITHON II Data

The PITHON II facility uses a 1 MJ Marx generator to charge a 1.3-Ω pulse-forming line through an intermediate pulsed electrostatic store. At the present time (February 1979), the PITHON I modifications which comprise PITHON II are near completion. Electron beams have been generated in PITHON diodes under various diode study programs, but extracted beams have not been developed and are not presently under development. Electron environments are therefore not yet available from this facility.

3.7.8.1 X-Ray Environments

Intense x-ray pulses are available on PITHON II from both the standard electron-beam diode and from imploding plasma loads.

3.7.8.2 Imploding Plasma X-Ray Mode

Intense x-ray pulses in the 2- to 5-keV range are generated on PITHON II by using a fine wire array or puffed gas jet as the machine load to produce an imploding plasma x-ray source. It is expected that source intensities will be enhanced when PITHON II becomes fully operational in the near future.

The x-ray environment has been characterized by a bent-crystal spectrograph, x-ray diodes, and differentially filtered calorimeters and TLDs. A representative spectrum is shown in Figure 3-123. Filters eliminate photons below 1 keV. The line spectrum is hydrogen- and helium-like, with continuum radiation extending upward in energy. The effective photon energy was determined by analyzing the calorimeter and TLD data with the assumption of monoenergetic photons. The radiation source is line-shaped (on-axis), 3 to 4 cm and less than 0.1 cm in dia.

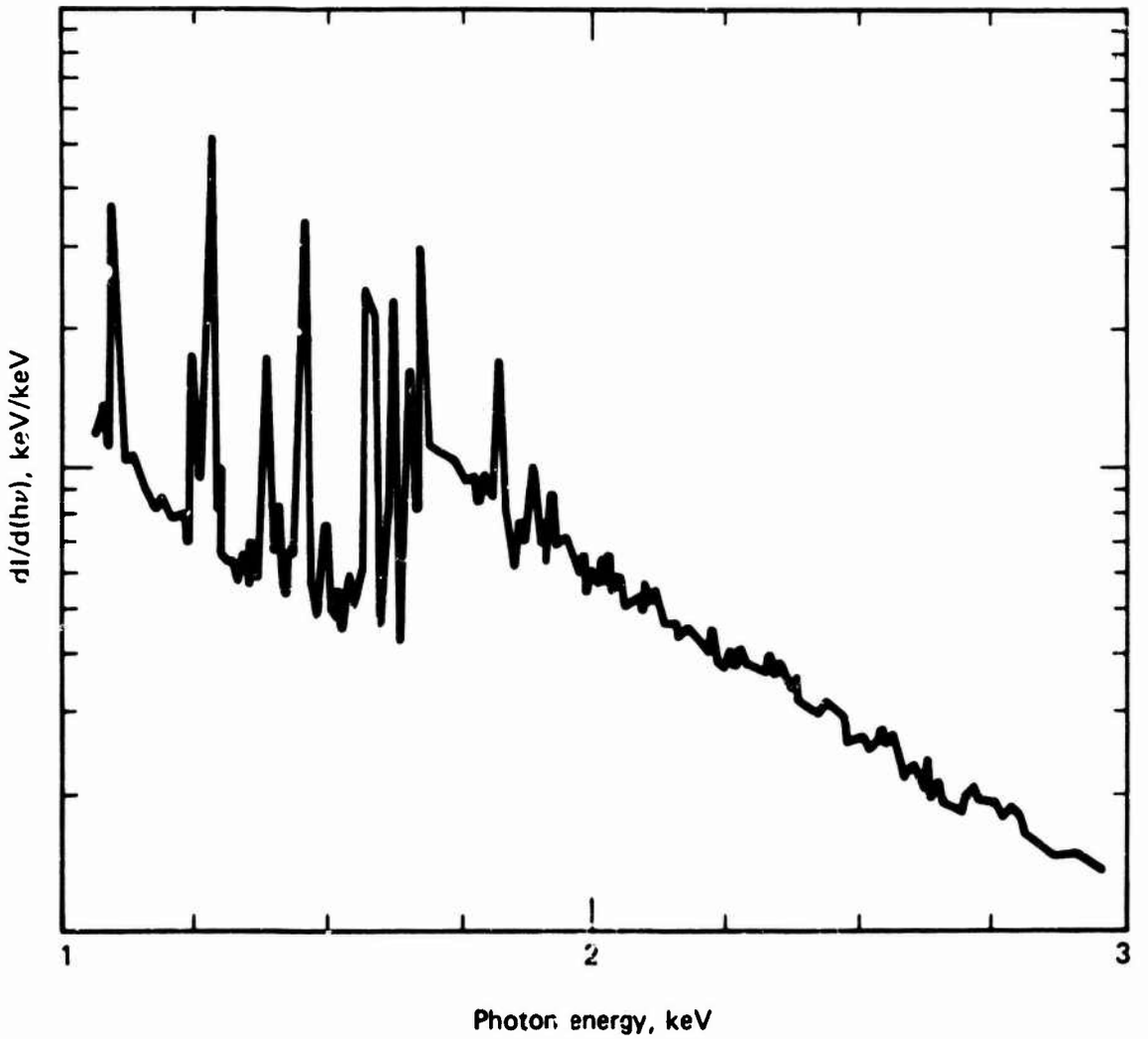

Figure 3-123. Typical Al spectrum at 3.5 TW on PITHON.

3.7.9 Pulserad 225W Output Data

The Pulserad 225W is a 5.25-Ω water-dielectric coaxial-line pulser with 10 kJ available to a matched load in a 65-ns FWHM pulse.

3.7.9.1 Electron-Beam Environment

Representative I and V waveforms are shown in Figure 3-124. The available range of mean electron energy and the corresponding total diode energy (assuming matched load) are given in Table 3-11. The electron environments to date have utilized magnetic guide fields for beam transport. Table 3-12 lists data for a peak electron energy of 0.67 MeV. Other environments can be developed for specific applications.

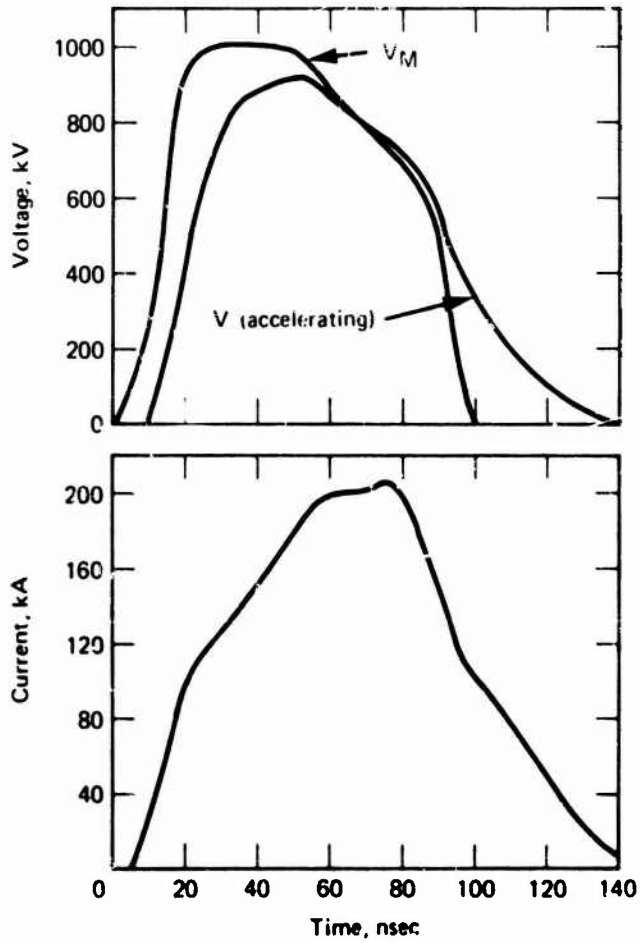

Figure 3-124. V and I traces, 225W Pulserad.

Table 3-11. Pulserad 225W total diode energy versus mean electron energy (assuming matched load).

Mean Electron Energy (MeV)	Total Diode Energy (kJ)
0.80	10
0.60	5.5
0.40	2.5
0.25	1.0

Table 3-12. Representative Pulserad 225W electron environment parameters.

Peak Electron Energy (MeV)	Peak Diode Current (kA)	Beam Energy (kJ)	Beam Area (cm^2)	Fluence[a] (cal/cm^2)	Peak Dose[b] (cal/g)	Peak Dose/Fluence[b] (cal/g)/(cal/cm^2)
0.67	130	5.9	5	250	1875	7.5
			12	100	620	6.2
			50	25	135	5.5

Notes:
[a]Fluence uniformity is nominally ±10% MSD over the area indicated.
[b]In carbon.

3.7.9.2 X-Ray Environment

X-ray environments generated using the standard x-ray mode are available on the Pulserad 225W at intensities up to 30 kR. At that level, the environment uniformity is nominally ±25% over 12.5 cm^2, mean photon energy is approximately 330 keV, and the dose-to-fluence ratio is approximately 2.1 (cal/g)/(cal/cm^2). The dose-area product is 375 kR • cm^2.

3.7.10 Pulserad 738 Output Data

The Pulserad 738 is an 8-Ω oil-dielectric coaxial-line pulser with up to 6 kJ available to a matched load. Overall performance for both electron and x-ray environments is very similar to that of the Pulserad 225W except that at equal peak electron energies, the Pulserad 738 produces 60 to 65% of the electron or x-ray flux generated by the 225W. Use of the older 738 machine is on a time-and-materials basis.

3.7.11 Available Support Services

The Pulservice Center is primarily a simulation facility. Both professional and non-professional technical support staff are available to assist in exposures and analyses. The professional staff includes scientists experienced in the field of simulation exposures and pulsed radiation. The non-professional staff includes trained technicians with experience covering a complete range of support activities. Support level can vary from customer liaison and coordination to complete performance and reporting of the experimental tests, depending on the customer's desires.

Screen rooms for the diagnostic electronics are a permanent part of the set-up. Electronic equipment is available for diagnostic and test measurements. Camera-equipped oscilloscopes are provided as part of the experimental program. Fast oscilloscope traces of radiation pulse shape are available if requested. Other special test equipment is also available and arrangements can be made for its use. Power is available from 120-V and 108-V single-ϕ and 440-V 3-ϕ outlets. Diagnostic signal cables are provided in lengths that reach from the target room to the diagnostic room (~40 ft). Triggering signals responding to machine command signals are readily available. The experimenter has the option of command-firing the machine by providing a trigger pulse or a contact closure. The command signal may be positive or negative with an amplitude of 0.5 to 50 V.

X-ray exposures are monitored using passive TLDs. Dosimeters are read out and readings are available immediately after the exposure so that results can be evaluated before the succeeding shot. Various types of calorimeters are also available for measuring absorbed dose in specific materials.

Calorimetric and Faraday-cup techniques are used to measure the electron beam. For doses below 1,000 cal/g in carbon, multiple small graphite absorbers determine the spatial distribution of electron energy. Data are recorded in digital form on a 100-channel Vidar unit. At higher doses, the multilayered (or filtered) Faraday-cup technique is used to simultaneously measure incident electron I and angle(s), and dose is computed from these data plus the diode V measurement (References 10 and 11).

Up to 15 channels of oscilloscope data can be stored on Tektronix R7912 digitizing oscilloscopes. The data can be processed online using PI Data Acquisition System (DAS) to obtain the time-dependence of the following parameters and other relationships: mean V, power, energy, impedance, integral of trace, derivative of trace, plot of one trace versus another, Child's Law I, parapotential I, and critical I. A manual digitizing tablet can be used to access the DAS. Calorimeter data can be fed directly into a Tektronix SPS Mod 62 to obtain fluence maps and energy deposition profiles (including cooling curve analysis).

Computer facilities, including PI's library of Monte Carlo electron transport and photon deposition codes, are accessible. Finite difference material response codes are also available for calculation of stress-wave propagation and attenuation. Machine shop, welding shop, vacuum laboratory, and electronics shop area,

and adequate experiment set-up and preparation rooms, as well as open floor space, can be provided. A conference room and limited office space are also available. Polaroid cameras are provided with all oscilloscopes, and polaroid film is stocked. Other photographic services, such as film processing, printing, and photography of experimental set-ups, are also available. A TRW image converter camera can be provided (Government-furnished Equipment) for qualifying projects.

3.7.12 Procedural Information

Administrative and technical inquiries should be directed to:

Physics International Company
2700 Merced Street
San Leandro, CA 94577
Attention: Facilities Manager
Telephone: (415) 357-4610, Ext. 572

For scheduling of machine time, a lead time of 2 months is preferred. A purchase order should be sent at least 2 weeks prior to the start of irradiations to confirm reserved dates. Earlier confirmation may be requested of a user with a tentative reservation in case another request for the same date has been made. Inquiries regarding scheduling details should be directed to the Pulsed Radiation Facilities Manager. Use of the DNA facilities should be cleared through DNA, RAEV, Washington, D.C. with PI Contracts Department assistance.

Detailed costs and charges associated with use of the PI Pulserad facilities are available and can be obtained from the Pulsed Radiation Facilities Manager and from PI's Contracts Department.

The shipping address is:

Physics International Company
2700 Merced Street
San Leandro, CA 94577

All shipments of experimenter's equipment to and from PI must be arranged for and prepaid by the user.

The facilities are located in an industrial area of San Leandro, California. The plant is readily accessible from the surrounding urban area and within easy commuting distance of the Oakland, San Francisco, and San Jose airports. (The Oakland Airport is the nearest.) Overnight accommodations with 10 min commuting time are available in Oakland and San Leandro.

3.7.13 References

1. Pellinen, D., *Rev. Sci. Instr. 41, No. 9, 1347*, 1970.

2. Pellinen, D. and S. Heurlin, *Rev. Sci. Instr. 42, No. 6, 824*, 1971.

3. Pellinen, D., *Rev. Sci. Instr. 42, No. 5, 667*, 1971.

4. Pellinen, D. and P. Spence, *Rev. Sci. Instr. 42, No. 11, 1699*, 1971.

5. Spence, P., *Bull. Amer. Phys. Soc. II, Vol. 14, No. 11*, 1969.

6. Yonas, G., P. Spence, et al., DASA 2426, 1969.

7. Wood, D.S., *Rev. Sci. Instr. 43, 908*, 1972.

8. Wood, D.S., *Rev. Sci. Instr. 43, 1094*, 1972.

9. Pellinen, D., *Rev. Sci. Instr. 43, 1181*, 1972.

10. Childers, K. and J. Shea, *A Faraday Cup with Multiple Internal Filters and a Primary Current Monitor for Characterizing High Dose Pulsed Electron Beams*, AFWL-TR-76-132, October 1976.

11. Ecker, B., et al., *Intense Electron Beam Generation and Compression: Advances in High-Dose Diagnostics and Theory*, DNA 4523F, January 1978.

3.8 MAXWELL BLACKJACK 3 AND BLACKJACK 3 PRIME

BLACKJACK 3 and BLACKJACK 3 Prime are DNA-owned pulsed electron-beam accelerators built and operated by Maxwell Laboratories. Both machines are operated from the same Marx generator. However, by switching between the BLACKJACK 3 or BLACKJACK 3 Prime intermediate storage and pulse-forming lines, the x-ray pulse width may be varied between 60 and 30 ns for the 2 machines, respectively. The energy in the electron beam for either machine is 30 kJ. To maintain the same electron-beam energy between the 2 machines, the peak beam potential is 1.0 and 1.5 MeV for BLACKJACK 3 and 3 Prime, respectively. BLACKJACK 3 has been operational for several years and has undergone numerous upgrades to take advantage of recent advances in pulsed-power technology. BLACKJACK 3 Prime was scheduled to be fully operational in August 1978.

3.8.1 Test Parameters

The total beam energy of BLACKJACK 3 is typically 30 kJ, as measured from the electron-beam potential and I. This technique has been confirmed over many shots in which a graphite calorimeter was placed near a thin transmission anode. The peak electron-beam potentials are 1.0 and 1.5 MV for BLACKJACK 3 and BLACKJACK 3 Prime, respectively. These values may be varied over a considerable range by varying the Marx charge potential and the cathode/anode spacing.

The turnaround time for BLACKJACK 3 is about 45 min. This period of time is required to clean the debris from the diode diaphragm, re-oil the diode interior surfaces, replace the cathode, anode, and converter (if in the x-ray mode) and pump the diode to a pressure of less than 6×10^{-4} torr. On any given shot, this time is usually extended because of the interaction with users and the setup of the experimental hardware. For example, 30 machine firings were obtained during a 5-day period when operating BLACKJACK 3 for Northrop. The average turnaround time for all 30 shots was 1.2 hr. In the same sequence of 30 shots, the x-ray dose at 1.3 cm from the Ta converter was measured with a TLD array and the results were given as equivalent dose in 0.02 g/cm^2 Ta. The peak dose at this position was 3.6 ± 0.6 cal/g Ta. The x-ray pulse width (FWHM) was 59 ± 4 ns.

In another series of experiments in which the machine was operated in the electron-beam mode for Effects Technology, Inc., the diode data were analyzed on 20 consecutive machine firings (Reference 1). The power FWHM was 58 ± 6 ns, diode beam energy was 32 ± 4 kJ, and the mean and peak electron beam potential was 720 ± 30 keV and 990 ± 60 keV, respectively.

Timing signals may be taken from a variety of sources. For lowest jitter applications, the signal from a PIN or photodiode may be used as the scope trigger with an appropriate delay in the signal from the experiment. More typically, the trigger signal is obtained from the diode V monitor which occurs about 10 ns ahead of the diode I or x-ray pulse. The jitter is about 1 ns in this case. The oscilloscope trigger signal thus produced may be used to generate a fiducial signal, which in turn may be added to each oscilloscope trace in the system for accurate time correlations between signals.

Electrical noise was measured on BLACKJACK 3 in conjunction with an x-ray test series run for the General Electric Company (Reference 2). These measurements were made in air and in vacuum with and without a Faraday cage. Also, x-ray shields of varying thicknesses were placed in front of the probes. Outside the Faraday cage in air, a 50-ohm terminated cable picked up a 40-V peak-to-peak signal of about a 30 Mcycle frequency which lasted for a time exceeding the 1-μs measurement period. This type of noise is generated from the discharge of electrical energy through the BLACKJACK 3 system due to switching and higher mode electrical oscillations. Inside the Faraday cage behind the x-ray shield within a few cm of the diode, with or without the Faraday cage evacuated, the noise in an open-circuited 50-ohm cable is less than 20 mV peak to peak. Again, the noise had a 30-Mcycle characteristic frequency which lasted for an extended period. Without the x-ray shield, the unterminated cable picked up a 2-V signal in vacuum which followed the x-ray signal. This 2-V signal was reduced to a 0.5-V signal when the Faraday cage was operated at 1 atm air.

3.8.1.1 Diagnostic Techniques

The diode potential is monitored with an electron-field probe that produces a signal proportional to $\dot{E}$, which is passively integrated in the screen room to obtain the diode potential. The diode I is measured with an annular inductive cavity which produces a signal proportional to $\dot{I}$, integrated in the screen room to obtain the electron-beam I. The electron-beam potential is obtained by assuming that a simple inductive correction may be made to the diode potential, i.e.,

$$V_B = V_C - L_D \frac{dI}{dt} \quad ,$$

where V_B is the beam potential, V_D is the diode potential, L_D is the diode inductance and I is the electron-beam I. The beam potential is recorded directly by subtracting from the diode potential the dI/dt signal with the correct time-phasing and amplitude attenuation of the dI/dt signal to acount for the diode inductance. Both the signal time-phasing and the inductance measurements are made with a shorted diode.

The general policy for the operation of BLACKJACK 3 is that the facility offer the diode electrical measurements and an x-ray PIN diode measurement. Other diagnostics should be supplied by the user. This policy was made to keep the basic use cost of BLACKJACK 3 low. However, Maxwell can furnish, and has furnished, a variety of diagnostics to complement those used by the experimenter at an additional cost. Standard x-ray dose measurements are made with TLDs and Ta foil calorimeters. Maxwell uses LiF-impregnated teflon disks made by Teledyne/Isotopes, i.e., SD-LiF-7-0.4. These disks are 0.79 cm in dia. and 0.041-cm thick, with a density of 2.18 g/cm^3. These TLDs are read on a Harshaw Model 2000 Reader. Other types of TLD materials may be used, if required. Maxwell Laboratories makes Ta-foil calorimeters for dose measurements. The standard configuration of this calorimeter is rugged and can tolerate a high shock environment provided the Ta foil is not physically touched by debris or other material. Ta foils have been used ranging in thickness from 0.0084 to 1.7 g/cm^2, although the standard thickness for this work is 0.042 g/cm^2. Other calorimeters may be used upon request.

X-ray spectra measurements have been made such as those made for Northrop (Reference 3) using a series of filters and TLD detectors. PIN diodes with selected filters also may be used for these measurements. However, these measurements lack spectral sensitivity above about 300 keV. Under the proper diode operating conditions, the x-ray spectrum calculated from the electron-beam potential and I spectrum yields the same spectrum as measured with a filtered/PIN spectrometer or other spectral measurement technique (Reference 3). Selected machine waveforms can be digitized and used to generate the electron-beam spectrum and the x-ray spectrum at the request of the user. Electron-beam measurements can be made upon request using stacked C-foil calorimeters, total-beam, C-block calorimeters, or segmented C-block calorimeters.

3.8.1.2 Electron-Beam Mode Environment

A schematic of the standard experimental configuration and magnetic field profile for the electron-beam mode is shown in Figure 3-125. To prevent pinching in the electron beam, the diode is immersed in an applied axially directed magnetic field using solenoids. Cathodes ranging from 5 to 20 cm in dia. have been used to produce beam fluences between 25 and 500 cal/cm^2 at the diode. Since the diode is immersed in the fringe fields of the solenoid, magnetic compression further increases the beam fluence. About 70% of the beam energy can be passed through a 4:1 compression, so that fluences over 1,000 cal/cm^2 are achievable.

A highly compressed electron beam typically contains all velocity angles between 0 and 90 degrees so that it is not useful for materials testing when close computational comparisons are desired. To facilitate comparisons with theory the beam is "cooled" by passing it through a magnetic expansion region. For example, a 2:1 expansion tends to reduce the maximum velocity angle to 45 degrees. At this expansion ratio, measurements with a C-calorimeter foil depth-dose stack have confirmed that the mean angle of incidence of the electrons lies between 20 and 30 degrees (Reference 1).

A thin graphite cloth has been placed in the region of the peak magnetic field to suppress hot spots in the electron beam via scattering and to minimize the contamination of target material blowoff impulse measurements from anode debris. Using this graphite cloth technique, measurements with 4 separate calorimeters at 90-degree intervals at each of several radial locations have shown that the beam uniformity is within ±20% of each other for each radial location (Reference 1).

Except for losses in the electron beam during the compression stage, the electron energy fluence is proportional to the radial magnetic field shown in Figure 3-125. Using a 10-cm dia. cathode, a 120-cal/cm^2 electron beam was measured 70 cm from the anode on axis. The beam was slightly hollow in that 145 cal/cm^2 was measured at a radius of 1 cm. Electron beams of 110, 80, and 30 cal/cm^2 were measured at 2-, 3-, and 4-cm radii, respectively (Reference 1).

Figure 3-126 illustrates typical electron-beam potential and I waveforms which were measured on shot 1632. The peak beam potential was 904 MV and the peak beam I was 580 kA. The diode energy was 34 kJ and the FWHM of the power waveform was 53 ns.

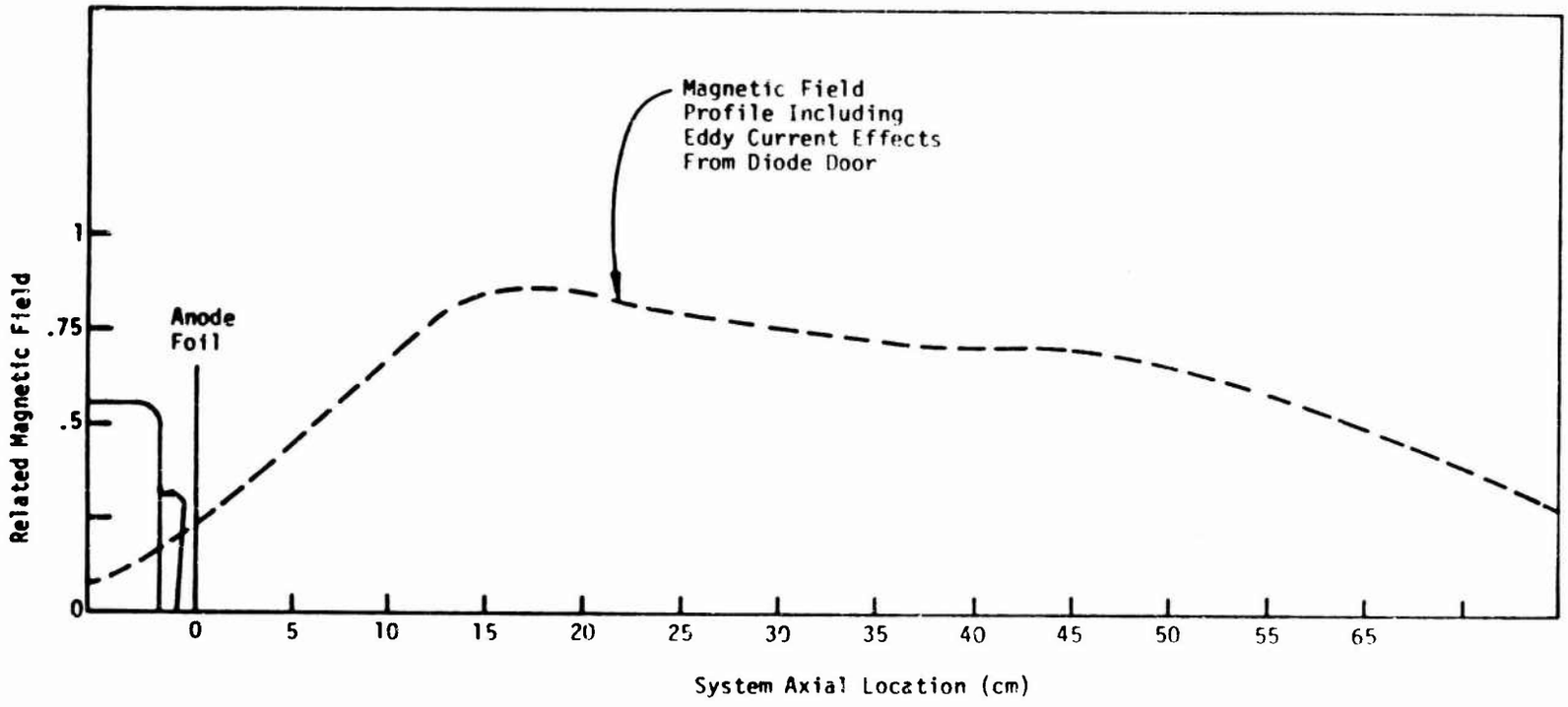

Figure 3-125. BLACKJACK 3 magnetic field profile used for materials testing.

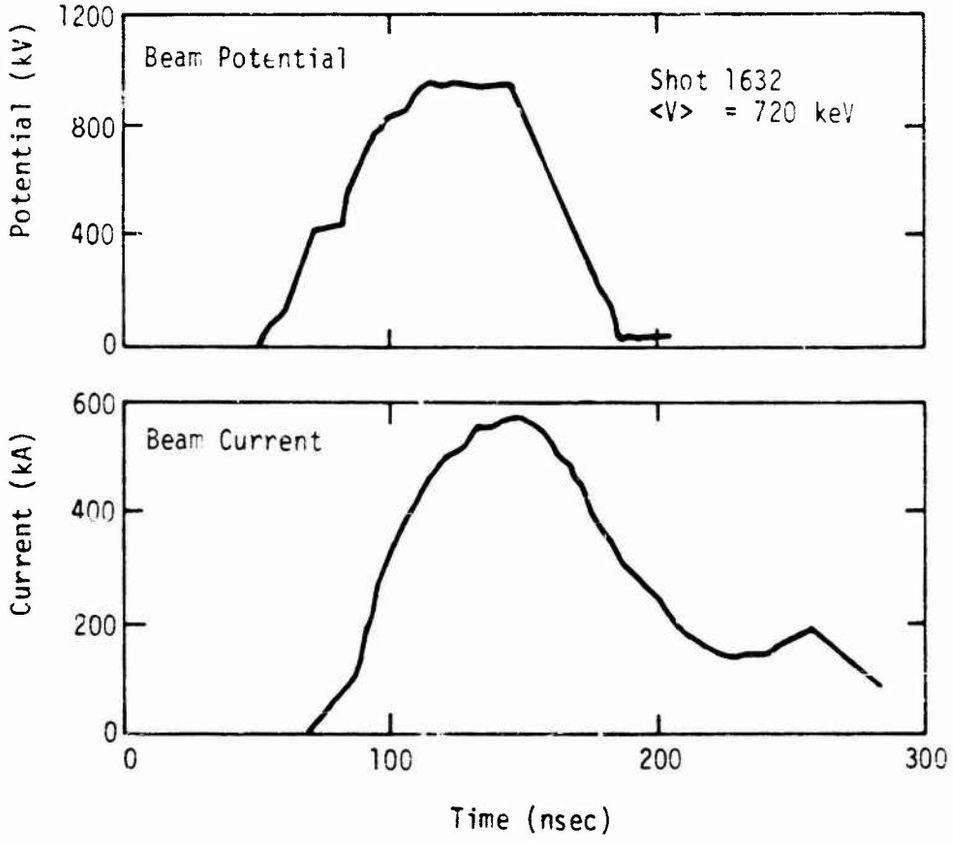

Figure 3-126. Electron beam potential and I waveforms for shot 1632 (the inductive V drop has been subtracted from the diode envelope potential).

Figure 3-127 illustrates a typical energy spectrum for BLACKJACK 3 using shot 1632. The spectrum was calculated from the waveforms shown in Figure 3-126. Figure 3-128 illustrates a measured energy deposition profile in C 70 cm from the transmission anode for shot 1629 (Reference 1). Also shown on Figure 3-128 are Monte Carlo electron deposition calculations run from the electron spectrum calculated for this shot. The 3 curves represent electron incidence angles of 20, 30, and 40 degrees from the normal to the C surface. The effective angle of incidence is about 30 degrees.

3.8.1.3 Environment Measurement Errors

Measurement of the electrical waveforms are accurate to ±5%. The I monitor may be calibrated by physically measuring the dimensions of the cavity. The V monitor must be calibrated by using a pulsed-charge technique. Oscilloscope measurements are only good to ±3% of full scale, at best.

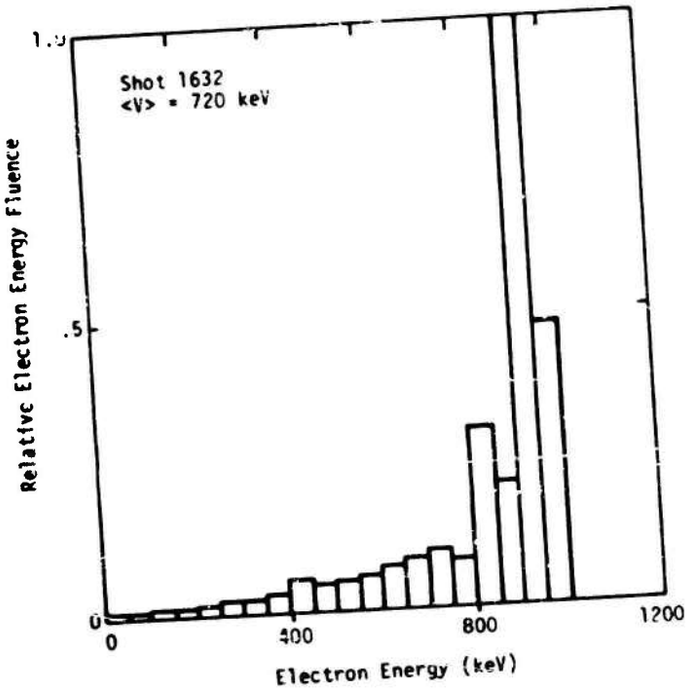

Figure 3-127. Representative electron beam spectrum.

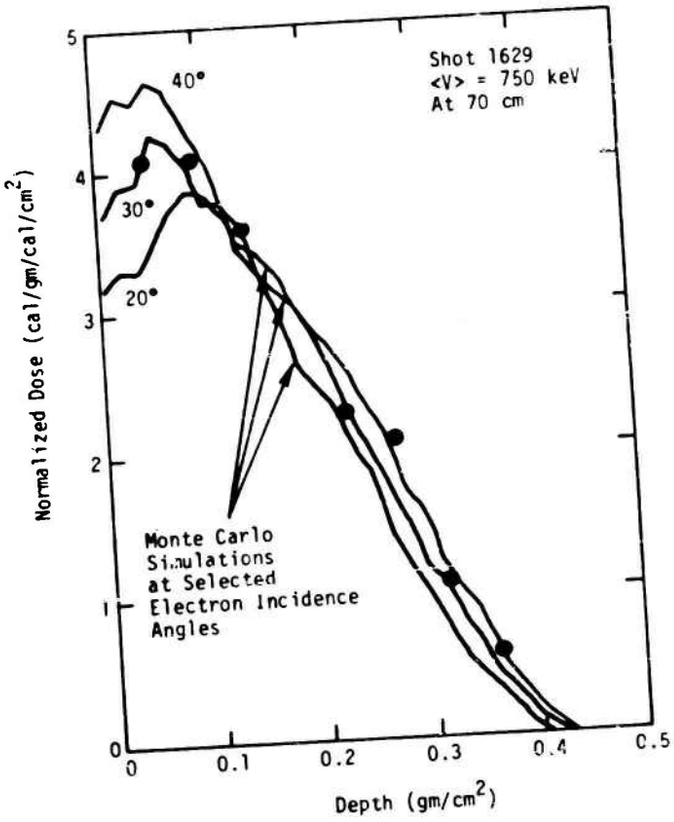

Figure 3-128. Measured depth dose in C for Shot 1629.

The electron-beam fluence and dose measurements were made with ATJ graphite, for which the specific heat was calculated using the following relationship:

$$C_p = 0.150 + 7.82 \times 10^{-4}T - 7.51 \times 10^{-7}T^2 + 2.78 \times 10^{10}T^3 \quad ,$$

where C_p is in cal/g/°C and T is in °C. It is generally believed that this relationship is valid within ±10% from room temperature to 1,000°C. The cooling curve for each measurement was digitized and the resulting data were fitted to an analytic form. The analytic curve was extrapolated to shot time to obtain the temperature rise in the samples. The temperature rise obtained by this technique should be within ±5% of true value, using a calibration visicorder. Hence, the dominating error is in the knowledge of the graphite specific heat.

3.8.1.4 X-Ray Mode Environment

Although BLACKJACK 3 may be operated in several modes, the pinched-beam mode provides an FXR field without the use of an external magnetic field. Since recent users of BLACKJACK 3 have needed to operate without interferences from the external B_z field, most of the beam characterization has been made in this mode. It should be apparent that x-rays may be generated from the electron beam described under the electron mode. Hence, the electron beam could be transported into the magnetic compression region and then into the expansion region. This would allow one to calculate the bremsstrahlung spectrum more accurately since the effective angle of incidence of the electrons may be controlled.

An experimental Faraday cage is mechanically coupled to the front of BLACKJACK 3 through a thick G-10 isolation plate. However, it is just as easy to position the experimental cage next to the machine without any physical contact and avoid the mechanical shock which amounts to deflections with an amplitude of 1 cm over several oscillation periods of 50 ms. The Faraday cage is an extension of the screen room and the signal cables may be placed inside the conduit between the cage and the screen room so that the outer conductor of the cable does not touch ground except at the oscilloscope. The Faraday cage can be evacuated independently of the diode.

The radial variation of x-ray dose has been measured over several experiments using a cathode of inner and outer radii of 5 and 10 cm, respectively, and a 3-degree taper. These data are summarized in Table 3-13. The radial variation of dose follows a gaussian distribution at least down to a value about 25% of the peak dose on axis. Hence, the radii at 50% dose are 2.4, 30, and 77 cm for axial distances of 1.3, 2, and 10 cm, respectively. The variation of axial dose is also given in Table 3-13. The dose in 0.02 g/cm^2 Ta is 3.6, 2.2, and 0.17 cal/g for axial positions of 1.3, 2.0, and 10 cm, respectively. For axial distances greater than 10 cm, the dose decreases as $1/R^2$ and the radial falloff also may be estimated from the $1/R^2$ relationship.

Figure 3-129 illustrates typical electron-beam potential and I waveforms obtained in the pinched beam mode of operation using the cathode described in the previous section. Figure 3-130 gives the time-integrated electron spectrum for this same shot. Figure 3-131 illustrates a typical PIN diode waveform measured for this shot. The x-ray pulse (FWHM) for this shot was 58 ns.

Table 3-13. Radial dose variation from BLACKJACK 3.

Axial Distance Converter (cm)	Gaussian Parameter[a] (cm)	Radius at 50% of Peak Dose (cm)	Area at 50% Dose (cm^2)	Dose Area Product (cal/g)(cm^2)
1.3	0.352	2.36	17.6	67
2	0.279	3.0	28	61
10	0.108	7.7	186	32

Note:
[a]The gaussian parameter is defined as

$$a = \frac{\sqrt{\ln \frac{D}{D(x)}}}{x} ,$$

where D(x) is dose at the radial distance x.

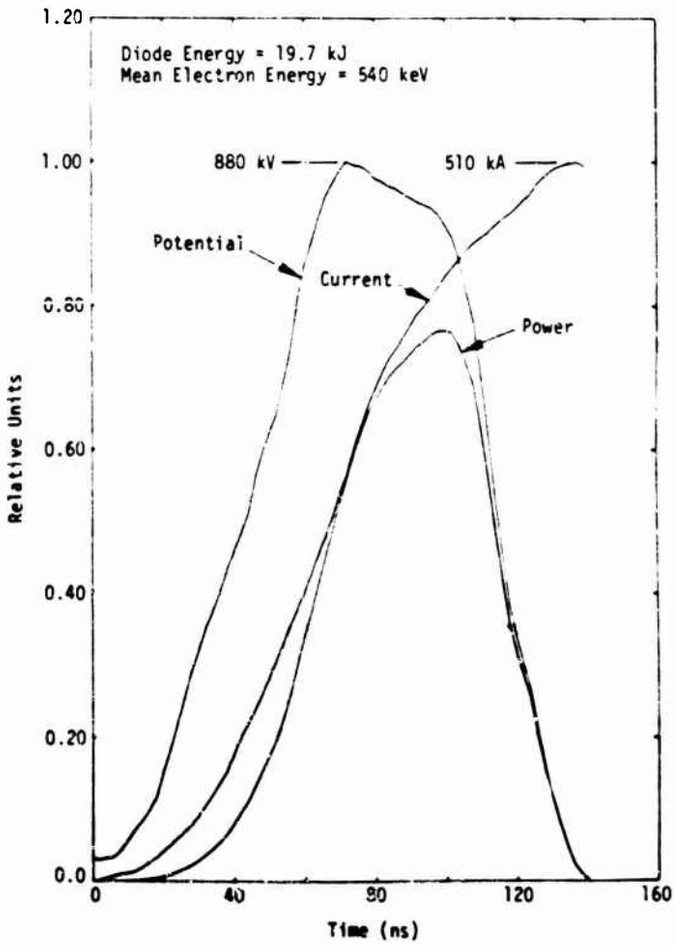

Figure 3-129. Electron beam potential I and power for BLACKJACK 3 shot #1534.

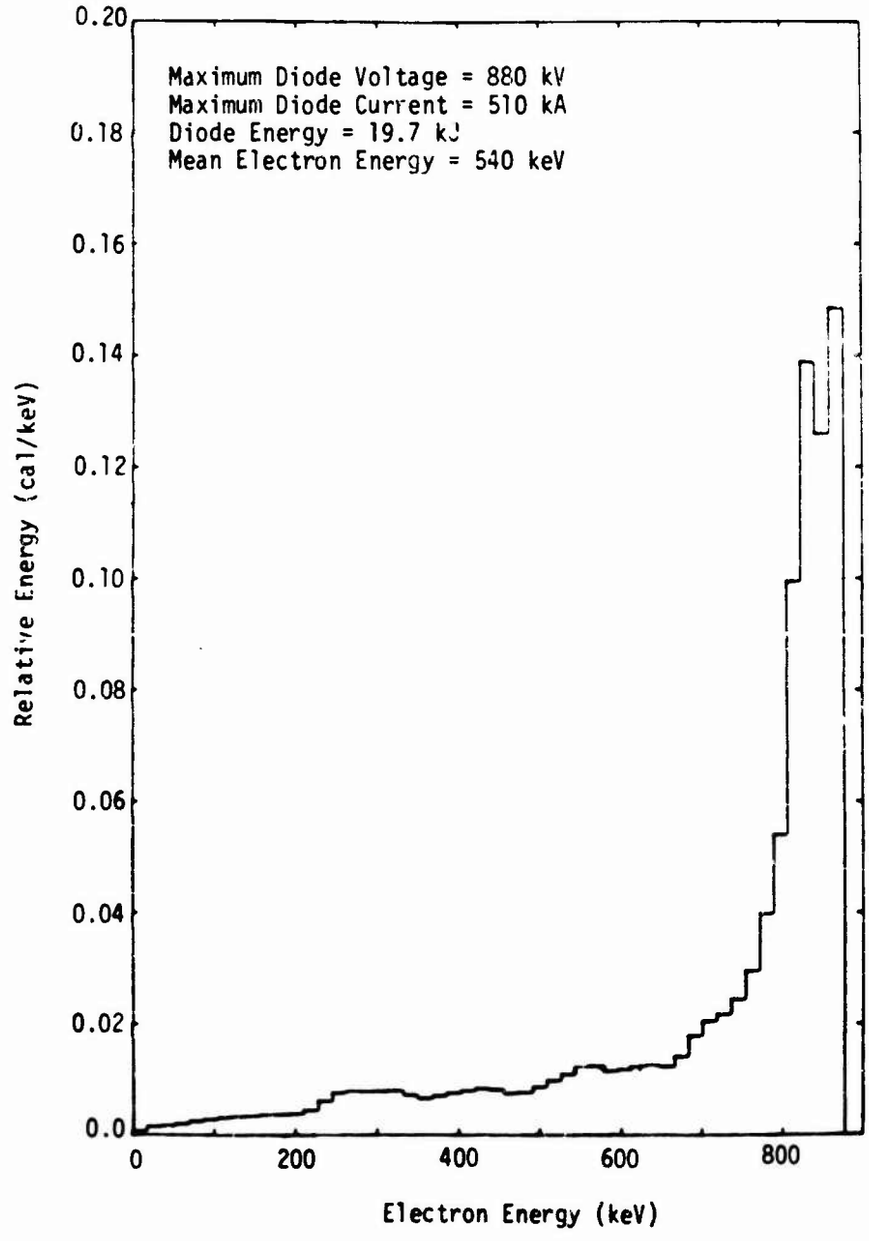

Figure 3-130. Electron energy spectrum for BLACKJACK 3 shot #1534.

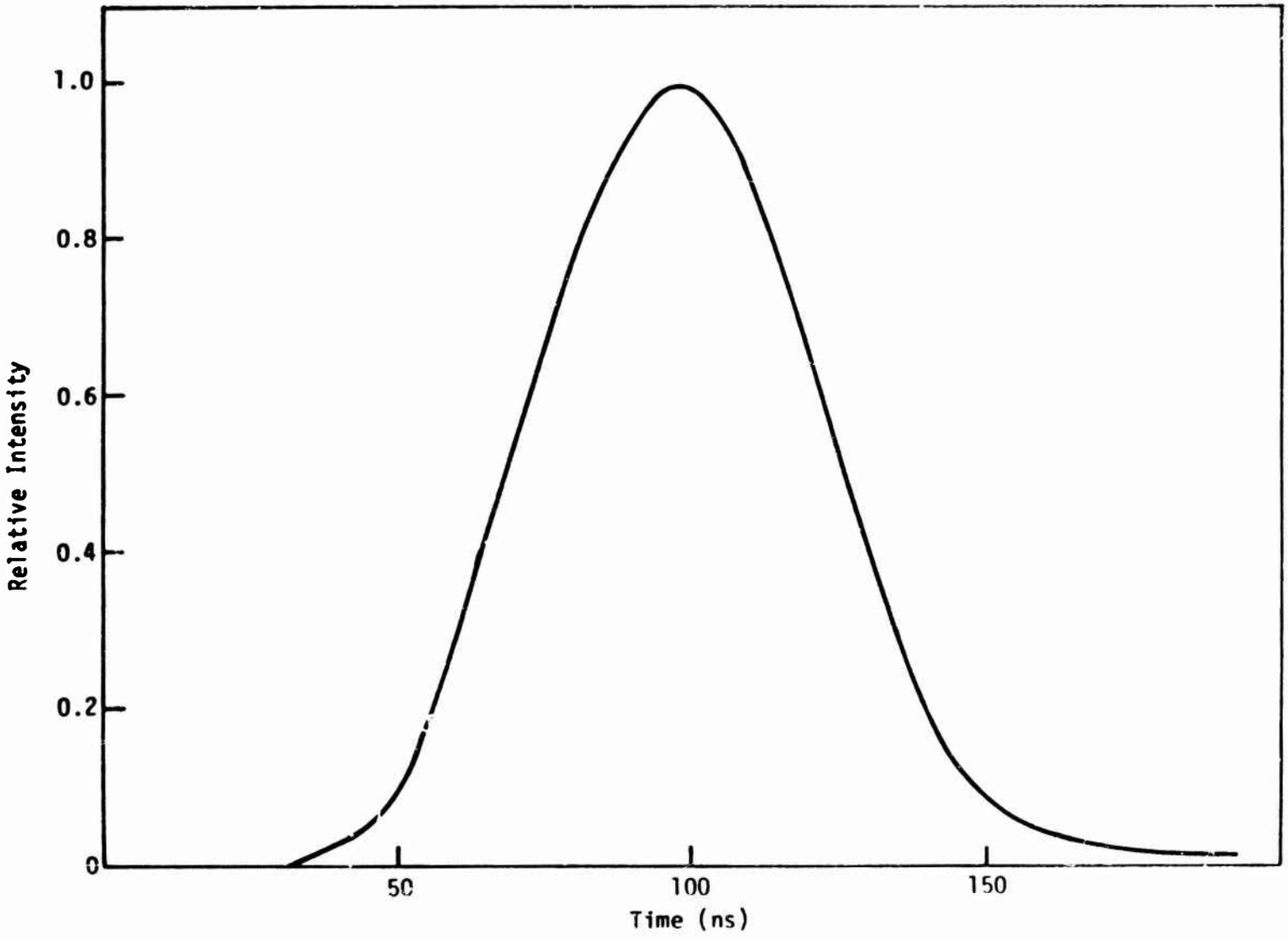

Figure 3-131. PIN diode signal measured on Shot #1536.

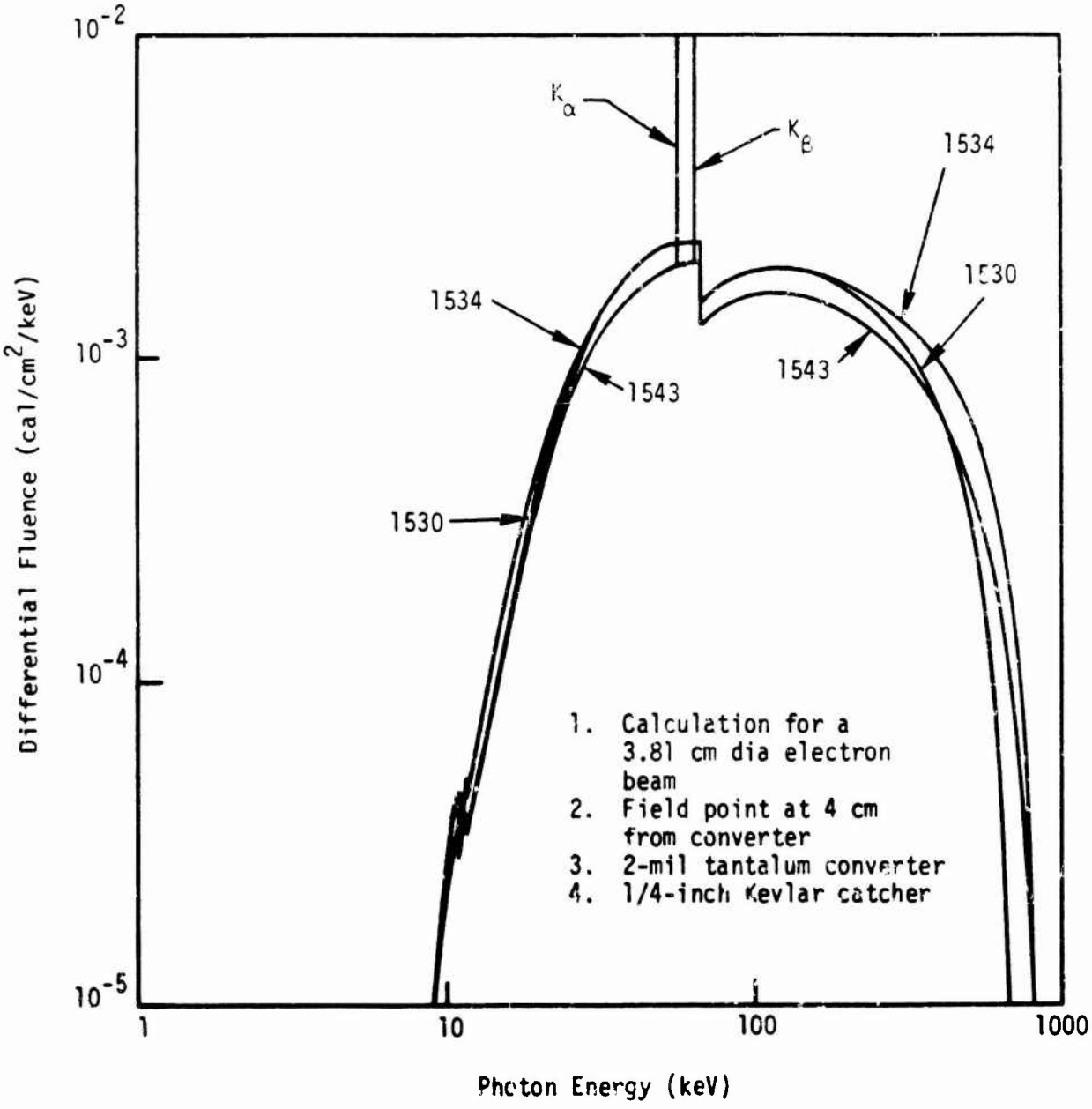

Figure 3-132. Comparison between the calculated bremsstrahlung spectra for BLACKJACK 3 shots 1530, 1534, and 1543.

Detailed measurements of the x-ray spectrum have been compared with the x-ray spectrum calculated from the time-integrated electron spectrum. The results show that the measurements are consistent with the calculated spectrum within the accuracy of the measurements (Reference 3). The calculated spectra for 3 typical BLACKJACK 3 shots in the pinched-beam mode are shown in Figure 3-132. About 6% of the fluence may be attributed to K fluorescence.

3.8.1.5 Environment Measurement Errors

The same comments on the machine electrical waveforms which were given in the section on electron-beam mode are also applicable here. The measurement of dose in Ta using a foil calorimeter is dependent upon the knowledge of the specific heat of Ta, the properties of the thermocouple, heat loss mechanisms, and the accuracy of the recording technique. The values of the specific heat of Ta and the thermocouples are well known and do not affect the accuracy of the measurements. For calorimeters less than 0.04 g/cm^2 (0.0025 cm) thick, corrections must be made for the heat loss down the thermocouple leads. The uncertainty in this correction increases as the foil thickness decreases. The main uncertainty, however, is most likely due to extrapolation of the recorded signal to shot time. This can be made to an accuracy of about ±7% under ideal conditions.

The TLD system (LiF-impregnated in teflon disks) has an inherent repeatability of ±10%, i.e., identically exposed TLDs will have a ±10% standard deviation. The TLDs are calibrated with a Co-60 source versus an ionization chamber which has an accuracy of ±5% traceable to the National Bureau of Standards (NBS).

3.8.2 Support Capabilities

The standard crew consists of two technicians capable of preparing the diode, setting up the screen room, and operating the machine. A senior staff engineer is provided to ensure overall machine performance. Additional machine shop, component assembly, and computational support can be arranged for if necessary.

Up to 4 Tektronix 555 and 6 Tektronix 519 oscilloscopes are available. Any number of trigger-generated fiducials (up to 300 V) can be provided. The fiducials can be sent to the user scopes at any time relative to the main pulse.

Signal entrance to the screen room may be made by a variety of methods. A large 4-in. dia. conduit acts as an extension of the screen room, and this conduit extends into the diode area of the block house. Cables also may be run to the screen wall and coupled to the screen via feedthroughs. These include 19 RG214/U and 18 50-ohm Foamflex (RG 331/U) cables. A long pipe extends through the roof of the screen room for optical signals. The screen room has 100-V, 60-cps power capabilities of 3 kVA available.

Unless specifically requested, dosimetry is the responsibility of the user. However, upon request, TLD and foil-calorimeter measurements of x-ray dose, dose-depth measurements for X-spectrum, and C calorimeters for electron fluence and dose measurements can be provided.

A wide range of computational facilities are available upon request. A Hewlett Packard 9820 desk-top calculator is available at no cost on a noninterference basis. This calculator is complemented by peripherals such as a digitizer, plotter, and magnetic tape cassette reader. This calculator may be used for beam waveform analysis or extrapolation of calorimeter data to shot time. A Data

General 230S Eclipse minicomputer with 64K word storage capability is also available. This minicomputer has several peripherals such as a Hamamatsu optical scanner which may be used for rapid waveform digitization. A Joyce-Lebel Mark 3C microdensitometer also may be used with the minicomputer. The minicomputer may be used to communicate with outside larger commercial computers or the computer complex at the Air Force Weapons Laboratories in Albuquerque, New Mexico. Consequently, users may use the Maxwell computer facilities to reach a computer which could have their own programs, or the user could request the staff at Maxwell Laboratories to make analyses from simple diode waveform analysis using in-house codes or make more sophisticated calculations using SANDYL or other large codes.

Maxwell Laboratories has complete machine shop capabilities, and can machine components up to 6 ft in dia. An in-house welder and technicians experienced in microfabrication techniques are available. Sufficient laboratory benches and desks are available in the main experimental building for users. A photographer and related camera facilities are available to meet all user requirements from witness plate records to experimental hardware configuration documentation.

The BLACKJACK 3 diode is housed in an 8-ft high concrete blockhouse. The width of the blockhouse is about 14 ft and the distance from the diode to the back of the blockhouse is 18 ft. The diode center line is about 4 ft above the concrete floor. The diffusion pump and other diode support hardware is arranged to minimize interference with user hardware. Their locations can be modified if necessary. For information concerning use of the Maxwell facility contact:

Dr. John E. Rauch
Mawell Laboratories, Inc.
9244 Balboa Avenue
San Diego, CA 92123
Telephone: (714) 279-5100, Ext. 199

Maxwell Laboratories offers the use of the BLACKJACK 3 generator for a 5-day, 40-hr week with a guaranteed 15 usable shot minimum at the 25-kJ level with magnetic beam extraction. This includes senior staff supervision of the operation of the facility and 2 full-time technicians. Maxwell Laboratories will make all data available to users (waveforms, calibration, etc.). No data analysis or final report will be furnished under this task.

The fixed price rate schedule for use of the Maxwell facility is as follows:

1 Week (40 hours)	Electron Beam Mode	FXR
Basic Service	$6,600	$7,200
Shot Surcharge	$75/shot over 20 shots; $1,500 maximum	$100/shot over 20 shots; $2,000 maximum
Rebate	$440/shot for under 15 shots*	$480/shot for under 15 shots*

2 Weeks (80 hours)	Electron Beam Mode	FXR
Basic Service	$12,000	$13,200
Shot Surcharge	$75/shot over 40 shots; $3,000 maximum	$100/shot over 40 shots; $4,000 maximum
Rebate	$400/shot for under 30 shots*	$440/shot for under 30 shots*

Pulsing sessions of less than 1 week duration will be booked only under special circumstances, at negotiated rate, with no guarantees provided as to a minimum number of shots.

Pulsing sessions of more than 1 week, but less than 2 weeks, will be prorated at the weekly rate for the entire period, when available. Pulsing sessions of more than 2 weeks duration will be booked at the prorated 2-week rate for the entire period, when available.

Maxwell will endeavor to allow the user to set up experiments prior to the pulsing period. When the facility must be provided on an exclusive basis for user setup during a working week, a charge of $1,000/day (8 hrs) will be levied. This will include the services of the 2 technician/operational crew. If the facility is utilized during the week prior to a customer's pulsing period and setup can be accomplished on a noninterference basis, no charge will be levied. For experiments requiring setup over a weekend, a fee of $500 per (8-hr day) Saturday or $650 per Sunday or holiday (8-hr day) will be levied. This will include the services of 1 technician.

3.8.2.1 Optional Time and Material (T&M) Support

Maxwell Laboratories, Inc. will provide optional T&M support on an as-required basis. (Experience to date has shown extremely little actual effort is necesary.) The T&M effort would be directed only by the user On-Site Manager to the Maxwell BLACKJACK Program Manager.

Consultation services will be provided at the rates indicated below. Any materials will be charged at cost plus 20% handling expense.

1. Senior Staff Engineer $60/hr
2. Machinist $30/hr
3. Senior Technician $29/hr.

Services provided on an overtime basis will be computed on a time-and-a-half or double-time basis, as may be applicable.

The user must provide full workman's compensation and employer's liability insurance, as well as automobile and general liability insurance for his employees and representatives. The user also must provide the prime contract number

*Rebates apply to failure to perform based on Maxwell Laboratories delays.

and agency, along with security clearances for all personnel who will visit Maxwell's site. The shipping address is:

Maxwell Laboratories, Inc.
9110 Balboa Avenue
San Diego, CA 92123
Attn: John E. Rauch

The BLACKJACK 3 and BLACKJACK 3 Prime facility may be used for a wide variety of experiments from materials response studies in the electron-beam mode to transient ionization and SGEMP studies in the x-ray mode. Dose-rate studies may be made by switching between the nominal 60-ns BLACKJACK 3 to the 30-ns BLACKJACK 3 Prime machine.

Use of the BLACKJACK 3 is scheduled on a noninterference basis with ongoing DNA-sponsored experiments. Resolution of scheduling conflicts in the use of the facility are made through DNA if the programs are both DNA sponsored. Normally, a minimum of 60 days of advance notice is required for use of the machine with a valid purchase order or contract received 30 days in advance of the scheduled experiment.

3.8.3 References

1. Froula, N., *Preliminary Characterization of the BLACKJACK III Pulse Electron Beam for Material Response Studies,* CAP-TR-77-11, October 23, 1977, Corrales Applied Physics Co., Corrales, New Mexico (draft report submitted to Effects Technology, Inc., Santa Barbara, California).

2. Phelps, D., and J. Rauch, *General Electric Tunnel Diode Amplifier X-Ray Diode Tests Using BLACKJACK 3, January 9 through 24, 1978,* MLR-716, February 24, 1978, Maxwell Laboratories, Inc., San Diego, California.

3. Phelps, D., and J. Rauch, *BLACKJACK 3 Flash X-Ray Measurements, April 29 - May 6, 1977,* MLF-666, May 27, 1977, Maxwell Laboratories, Inc., San Diego, California.

4. *BLACKJACK 3 Flash X-Ray Facility,* Maxwell Laboratories, Inc., Engineering Bulletin 1021, June 16, 1978.

3.9 TRW VULCAN AND FEBETRON 705 X-RAY FACILITY

TRW Systems Group Vulnerability and Hardness Laboratory has a VULCAN FXR and a Field Emission Model 705 FEBETRON; some of the characteristics of the Field Emission Model 705 are described in Section 3.2.

3.9.1 FEBETRON 705

Because of its excellent reproducibility and high repetition rate, TRW's FEBETRON 705 is used extensively for production latchup screening and for development radiation testing of piece parts.

The FEBETRON facility has a 3-axis automatic-positioning exposure table, a remote TV-viewing system, a fully equipped shielded instrument room, and a sophisticated fully automated electronics system for production "go, no-go" screening testing. With this facility, TRW has screened over 150,000 digital and linear integrated circuits (ICs) for radiation-induced latchup.

3.9.1.1 Machine Specifications

The FEBETRON 705 specifications are:

1. Gamma
   - a. Peak dose — 7,000 rad(Si)
   - b. Pulse width — 20 ns (FWHM)
   - c. Maximum repetition rate — 1 pulse/min
2. Electron
   - a. Average electron energy — 2 MeV
   - b. Peak I — 5,000 A
   - c. Pulse Width — 25 ns (FWHM)
   - d. Maximum dose rate — 10^{14} rad/s
   - e. Maximum fluence (w/ext. magnet) — 140 cal/cm^2

TRW has been performing latchup screening on production parts since 1969 and has built up an inventory of load boards and test procedures for more than 100 different part types; thus, a significant screening cost reduction is realized since the creation of these items comprises much of the initial test cost.

Each IC is individually monitored using a diode radiation detector to demonstrate that radiation dose is within the specified levels. These diodes are calibrated daily or before each new test setup against TLDs which are calibrated against standard radioisotope sources. The calibration of these sources is traceable to NBS primary standards.

3.9.2 VULCAN

The VULCAN facility, in operation in Building 84 of the TRW Systems Group, Redondo Beach, California (Figure 3-133) since November 1973, is available for part-time use by outside customers. VULCAN incorporates a PI 950 pulse-rad machine of advanced design. It is 11 ft wide by 11 ft high at the energy storage end, and 9 ft in dia. at the fast-energy storage end. The total system (50 ft long), including vacuum diode and target, is mounted on railroad tracks so that it can be easily moved for maintenance or for incorporation of the electron-beam drift chamber. The machine projects into a large 40- by 40-ft high ceiling vault which has 18-ft high walls of concrete thick enough to reduce radiation levels well below existing standards. A 10-ft high double-walled steel screen room, certified to 100-db magnetic and electric field attenuation, is centered in front of the target end of the machine. Clearance for lighting restricts the height of test objects to 9 ft, 4 in. above the floor. This room is 28 ft long and 16 ft wide. A 4-ft^2, 0.25-in. thick Al plate, which is part of the rfi/emi screen room closure, is positioned immediately in front of the target, and the machine is butted against the plate, allowing test objects to be placed as close as 0.25 in. to the machine external target face.

The electron/x-ray beam axis is 6 ft from the floor of the screen room. A heavy wooden test table rolls on rails for 28 ft along the beam axis, from the rear of the room to the Al faceplate. The table is supplied with several horizontal flat surfaces, or steps, 3 ft wide by 5 ft deep, for holding test objects and lead shielding. The steps can be adjusted to heights of 4.2 in., 10.5 in., 19.5 in., and 23.7 in. below the beam center line.

The exposure screen room can be entered either through a large 8- by 8-ft double door, or through a conventional door 3.5 ft wide by 7 ft high. The double door, used for large-system entry, is usually kept closed. The smaller door is interlocked with the console so that screen room integrity will be assured during firing.

A second double-walled steel screen room, also certified to 100-db magnetic and electric field attenuation, houses the instrumentation necessary to support experiments. Located behind a 6-ft thick concrete shield forming the west side of the vault, the room is 12 ft wide by 16 ft long by 8 ft high. Welded-steel 6-in. dia. conduits connect the 2 screen rooms, the machine console, the machine, and a parking area beyond the east wall of the building. Protection from x-radiation is provided for the cabling by running the conduits underground.

The machine is made up of several functional subsystems. The basic machine consists of a 50-stage hybrid Marx generator, followed by a folded, oil Blumlein pulse-forming line which, in turn, is followed by a vacuum field-emission diode. For x-ray work, an internal Ta target/anode is used. For electron-beam work, a transmission anode allows the beam produced in the vacuum diode to pass into a vacuum chamber which has an adjustable pressure control for beam density. Sample exposures are made in this chamber.

The machine has an energy storage capability of 100 kJ. This energy is transformed into an extremely intense burst of x-rays to higher than 10^{12} rad/s in

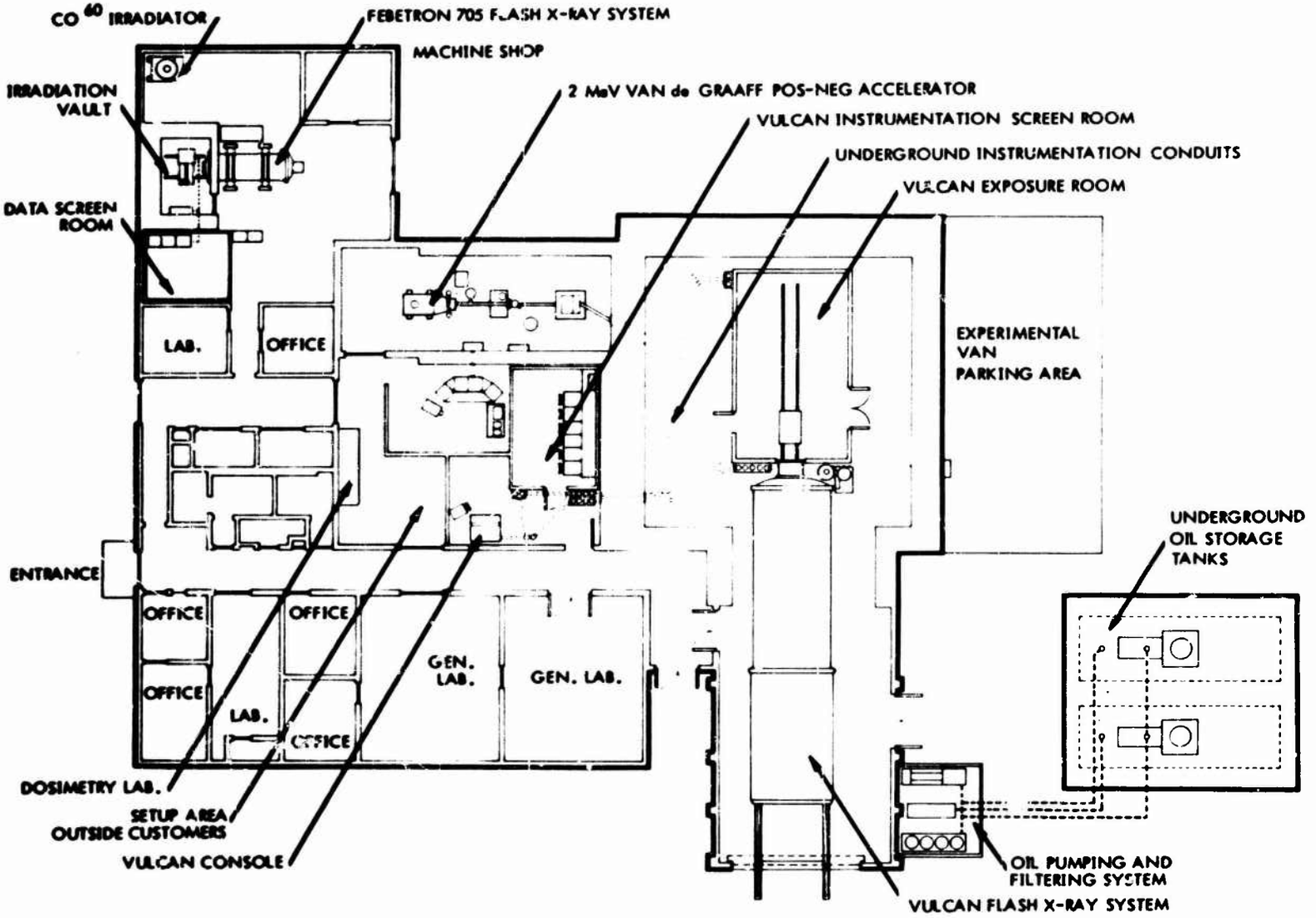

Figure 3-133. VULCAN facility floor plan.

the γ mode or to an electron beam of higher than 5×10^{11} W intensity in the electron mode. The pulse length is typically 45 ns measured as FWHM dose. The field-emission diode consists of a cathode and an anode separated by a high vacuum. For VULCAN, a number of cathode configurations are used: for high dose at the faceplate and into the far-field regions, a multineedle cathode is used; for the production of a relatively uniform dose over a large volume, a large toroidal cathode is used at the expense of high dose at the faceplate.

For x-ray bremsstrahlung production, the anode is made up of a sandwich of 3 sheets of 0.002-in. stainless steel backed by 3 sheets of 0.015-in. Ta backed by 0.625 in. Al beam stopper and vacuum closure. For users in the exposure screen room, the 0.25-in. Al plate required to preserve screen room integrity must be added as additional absorber. For external electron-beam production, other forms of a cathode are used, depending on the beam shape desired; and the anode and target are replaced by a thin Ti window, allowing the beam to enter an auxiliary vacuum chamber.

3.9.2.1 Performance Characteristics

VULCAN performance characteristics for the γ and electron modes are.

1. γ Mode:

a.	Peak x-ray energy	7.5 MeV
b.	Peak dose per pulse	60 krad(Si)
c.	Dose at 1 m	450 rad(Si)
d.	Dose at 28 ft	<3 rad(Si)
e.	Timing jitter	22 ns rms
f.	Maximum repetition rate	1 pulse/5 m

2. Electron Mode:

a.	Average electron energy	4 MeV
b.	Peak I	100,000A
c.	Pulse length	48 ns (FWHM)
d.	Fluence (over 10 cm^2)	>150 cal/cm^2
e.	Front surface dose rate	10^{15} rad(Si)/s
f.	Total useful beam energy	>15 kJ

X-Ray Mode. The dose at the front face from the machine bremsstrahlung, when the needle cathode is used, has a pulse-to-pulse reproducibility better than 16% rms. Beam center wander is less than 0.5 cm.

Volumetric maps are given for the use of the needle cathode in Figures 3-134 and 3-135, and for the toroidal cathode in Figure 3-136. The dose-rate pulse shape as measured by a silicon PIN dosimeter located in the room is shown in Figure 3-137. FWHM has been measured as 45 ± 4 ns.

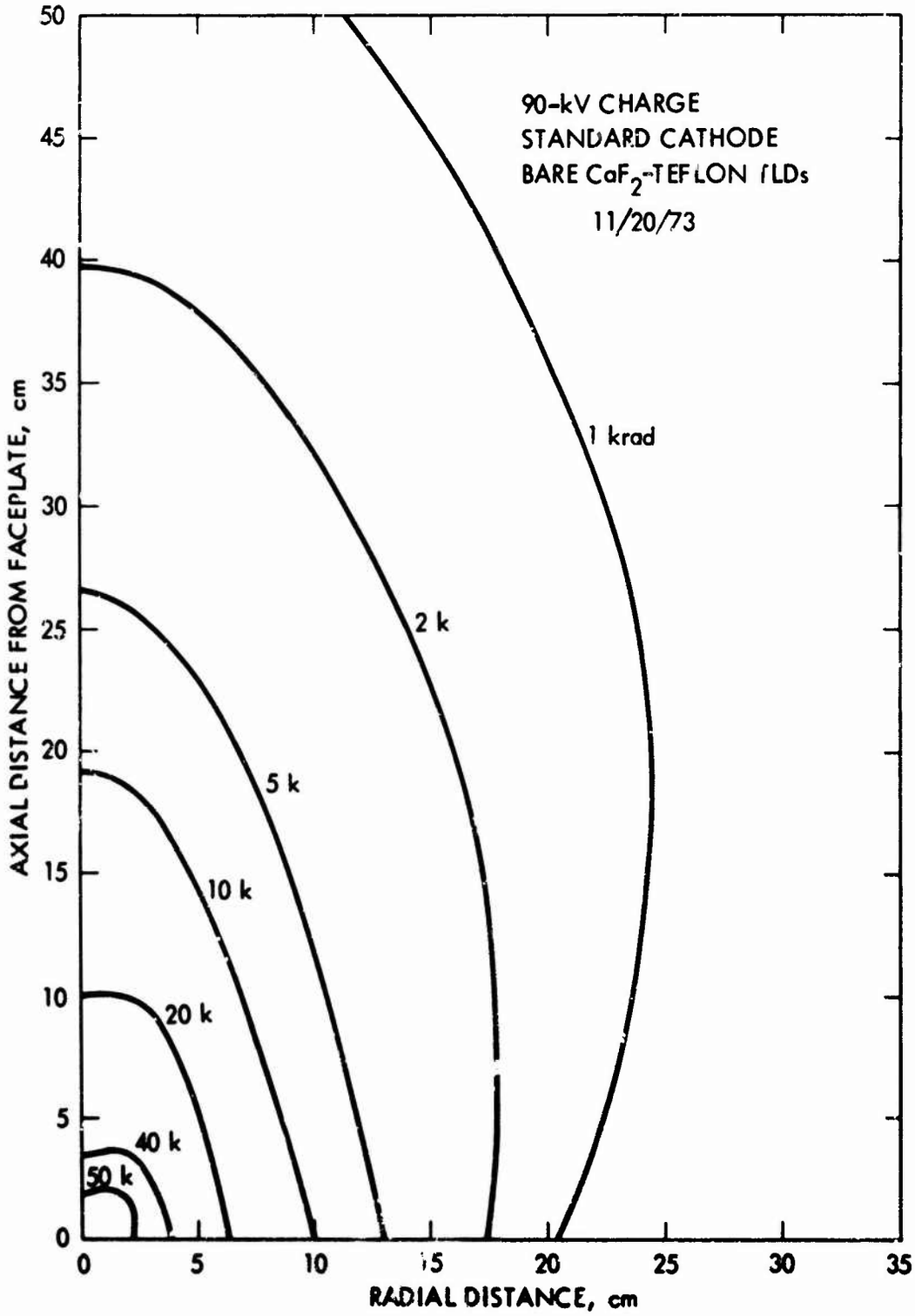

Figure 3-134. VULCAN dose map, 90-kV charge.

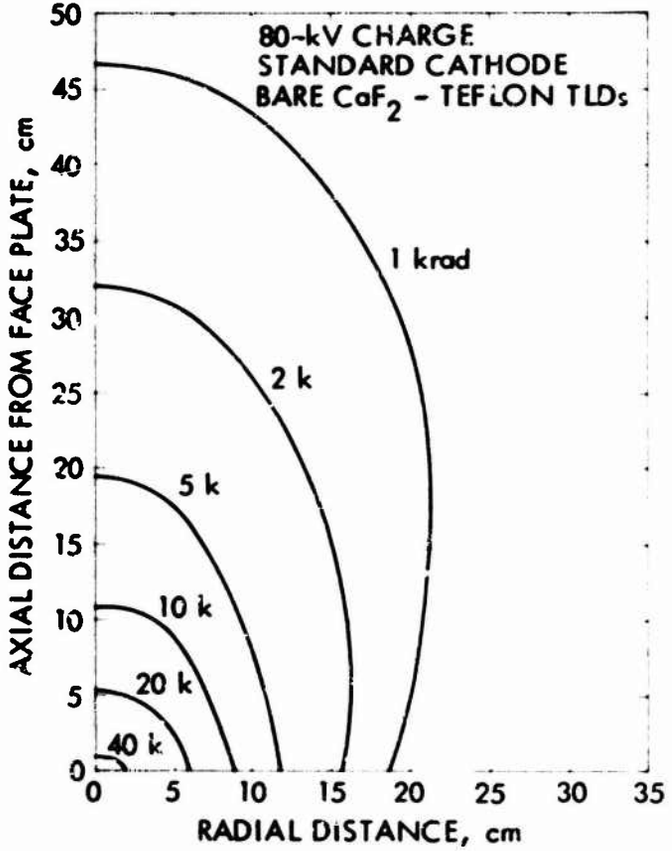

Figure 3-135. VULCAN dose map, 80-kV charge.

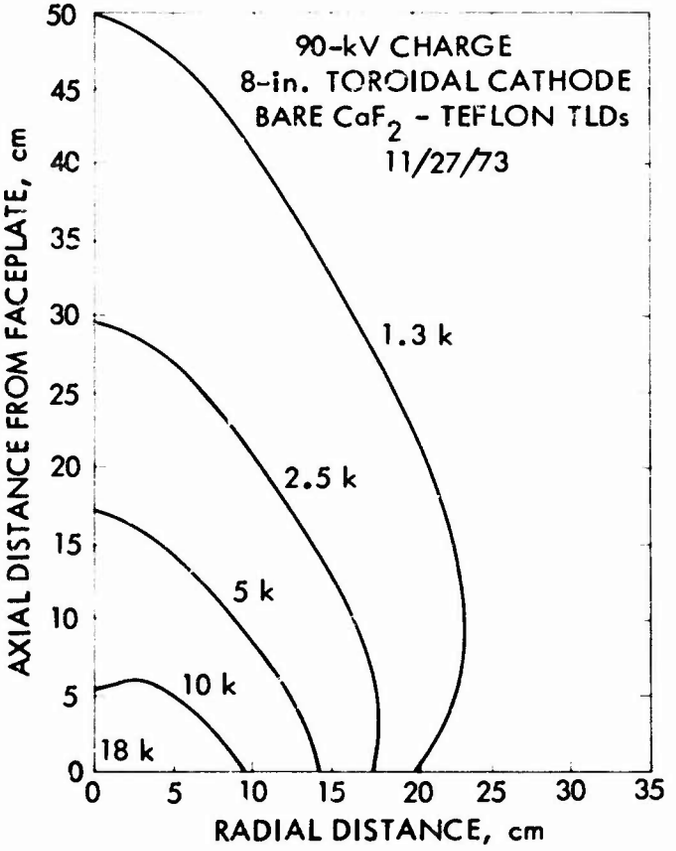

Figure 3-136. VULCAN dose map, toroidal cathode.

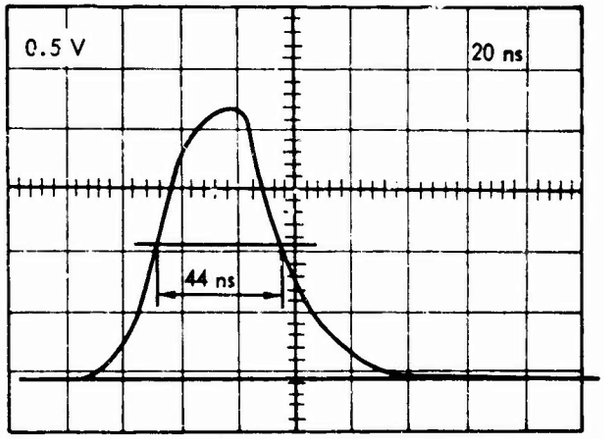

VULCAN PULSE SHAPE
p-i-n DIODE SILICON DOSIMETER
90-kV CHARGE, STANDARD CATHODE

Figure 3-137. VULCAN pulse shape.

The x-ray spectrum from the machine has not been measured. The maximum x-ray energy is about 7.5 MeV at 90-kV charging. As some indication of the effective energy, a plot of CaF_2-teflon disc dosimeter response versus Al sandwich thickness is given in Figure 3-138.

Shot rate is, in general, limited to about 1 shot every 15 min. If no access to the exposure room is required between shots, this time can be reduced to 10 min. Dosimetry readout time requires about 2 min per dosimeter. If a large number of dosimeter readouts is required before the next shot, the shot rate may be limited by dosimeter readout time.

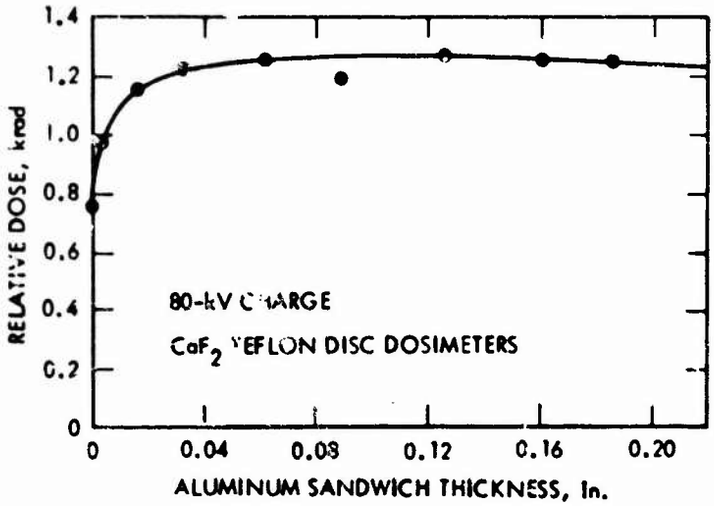

Figure 3-138. VULCAN equilibrium thickness study.

Electron-Beam Mode. In the electron-beam mode, the maximum electron-beam energy is about 4.5 MeV, and the delivered energy to an external target or test device is 15 to 20 kJ. About 10 kJ can be focused to a spot of 1 cm^2 or less, through the use of Bennett pinching in a pressure-controlled vacuum chamber extension.

Instrumentation. The instrumentation screen room is set up for performing a variety of testing programs. Cabling is installed in 4 connecting conduits leading to the exposure screen room: 3 are filled with RG-214 cables to the front of the room, and 1 is filled with RG-214 cables to the rear of the room. All cables are terminated with 50-ohm General Radio type GF-874 connectors at the entrance to each screen room. Cable lengths and routings in the conduits are listed in Table 3-14. In the instrumentation room, RG-214 cables distribute signals from the entry of the instrumentation screen room to patch panels located conveniently close to oscilloscopes on each rack of equipment, terminating also in GF-874 50-ohm connectors. Typical V standing-wave ratio (VSWR) through the patch panels from the devices in the target screen room through the patch panels in the instrument room has been measured at better than 1:10.

Additional empty conduits are provided for expansion, and for users who would rather use their own cables than the installed cables (see Table 3-14). The noise levels during test will, however, be somewhat higher than if the installed cables are used. The conduit running to the van area outside the building is also empty at present, and capped.

A second conduit from the van area connects directly to the instrumentation screen room. Another conduit, used to provide trigger signals from the machine console to the room and from the room to the console, connects directly from the instrumentation room to the console area. These signals pass into the room through coaxial lines but are being replaced by optical trigger links. Additional "go, no-go" information can be passed by way of this conduit. An intercom system connects the console, both screen rooms, and the machine bay.

All 60-cycle power is provided on 1 ϕ. Adequate power is available to operate not only the 6 racks of equipment committed to the room at present, but also at least 5 more racks of equipment and most subsystem test sets, for which there are four 3-prong 50-A Hubbell outlets located around the room.

Air-conditioning is piped directly, partly to the committed racks and partly to the general room area. The system capacity is adequate to handle a load of double the present amount of equipment.

The exposure screen room is supplied with a number of 3-prong Nema outlets arrayed around the room for 110-Vac service. There are also two 3-prong 50-A Hubbell outlets for supplying test sets and other arrrays of support equipment. Instrumentation committed to the instrumentation room is listed in Table 3-15.

All cameras and oscilloscopes are hooked into a completely automatic sequencing system which puts graticules and baselines on each photo frame, oscilloscopes to READY, and opens and closes the shutters at the appropriate time.

Table 3-14. Conduit routing.

Conduit	Routing		Cable			Connector Type
	From	To	Length (ft)	Number	Type	
1	Exposure room, front	Instrument room	44	Empty		
2	Exposure room, front	Instrument room	44	10	RG-214	GF-874
3	Exposure room, front	Instrument room	44	10	RG-214	GF 874
4	Exposure room, front	Instrument room	44	10 4	RG-214 RG-214	GF-874 HN
5	Exposure room, front	Instrument room	40	10 4	RG-214 RG-214	GF-874 HN
6	Exposure room, front	Instrument room	40	Empty		
7	Exposure room, rear	Instrument room	65	10 1	RG-214 RG-214	GF-874 HN (Committed to PIN detector radiation)
8	Exposure room, rear	Instrument room	65	10 4	RG-214 RG-214	GF-874 HN
9	Exposure room, front	Parking lot	38	Empty		
10	Instrument room	Parking lot	70	Empty		
11	Machine console	Instrument room	22	1[a]	RG-214	
12	Machine console	Machine, front	55	--[b]		

Notes:

[a]Not available. For triggering only.

[b]Machine operation and diagnostic cables.

Table 3-15. Committed instruments, instrumentation screen room.

Number of units	Item	Manufacturer and Model Number
6	Oscilloscope with horizontal and vertical amplifier gain readout on the trace, 175 MHz[a]	Tektronix 7704
6	Vertical amplifier plug-in	Tektronix 7A16A
4	Vertical amplifier plug-in	Tektronix 7A21N
2	Vertical amplifier plug-in	Tektronix 7A12
2	Vertical differential amplifier plug-in	Tektronix 7A13
5	Time-base plug-in	Tektronix 7B71
2	Time-base plug-in	Tektronix 7B70
6	Oscilloscope, dual beam, 50 MHz[a]	Tektronix 556
2	Vertical amplifier plug-in	Tektronix L
2	Vertical differential amplifier plug-in	Tektronix 1A5
8	Vertical amplifier plug-in	Tektronix 1A1
13	Oscilloscope cameras, automatic	Tektronix C-52
1	Trigger delay generator (generally committed to operations)	TRW Instruments Company 46A
1	Digital voltmeter	Dana 4530
1	Digital voltmeter	Hewlett-Packard 344A
1	Electronic counter with all plug-ins	Hewlett-Packard 5245L
	Power supplies -- wide variety	

Note:
[a]All oscilloscopes have P11 phosphor tubes.

TRW Systems maintains a large inventory of available equipment such as additional oscilloscopes -- including several Tektronix 7904 systems, magnetic tape recorders, light beam and heat stylus multichannel recorders, and a large variety of timing and digital readout equipment.

Several triggering capabilities are available for operations.

1. A fast radiation trigger is available in the screen room. This trigger is taken from the output of a number of diodes in series which are placed against the faceplate of the screen room and are connected through a shortened cable to the instrumentation room. The diode output can be used directly to trigger oscilloscopes or can be used through a pulse generator.

2. A trigger is available from the console which is taken from the firing pulse to the machine. Delay from the receipt of this trigger to the receipt of the radiation pulse into the instrumentation room is about 1.4 ms with a measured jitter of 22-ns rms. This trigger can be, and generally is, passed through a TRW Instruments Company pulse generator in the room, for a fanout to the oscilloscopes.

3. The machine can be command-fired from the instrumentation room. A 10-V signal into a 50-ohm cable is required for positive triggering. As before, the radiation pulse will be received back in the screen room in about 1.4 ms after the trigger is initiated. A variable-time-delay pulse generator is available in the screen room to provide a wide range of delayed firing times.

Grounding-Shielding-Noise Suppression. A key feature in the specified design of the x-ray machine was that there be no exit points for rfi/emi radiation from inside the machine. The machine, accordingly, has an exceptionally low level of noise output. During operations, the exposure screen room is connected directly to the machine at the interface of the target with the plate, providing a very short low-inductance return for the Compton-generated I in the faceplate.

Noise suppression design has been predicated on a system design of 3 individual totally enclosed "screen" rooms, or sets: the exposure screen room, the instrumentation screen room, and the individual conduits. Driving Compton I induced on cables in the exposure room, and I from screen room resonating, are returned to the faceplate where they originated by grounding all cable shields with plates connected into boxes made part of the screen rooms. In this way, I induced on shields cannot carry through to the instrument room.

The building contains a small machine shop which has a lathe, drilling machine, metal-cutting band saw, and a limited array of tools. This facility can be made available for minor work. For larger, more sophisticated projects and emergencies, model shops with trained machinists can be made available in nearby TRW buildings.

Double-cassetted shield boxes still can be used in the VULCAN facility either by resorting to the empty conduits or, with more certainty of producing low levels, by grounding both braids at the screen room wall before the cable bundle passes into the conduits. Compton-generated I in the exposure screen room cause it to resonate at a relatively high Q. The major frequency component is associated with the long 28-ft dimension of the room. Cable pickup from this cause can be largely suppressed by using double-shielded or solid-shielded cabling in the exposure room.

Single-point grounding has proved best suited to work occurring in frequency regimes where one-half the wavelength is long with respect to cable runs. In frequencies with shorter wavelengths, grounding is best in whichever way a low inductance return is achieved. There is no provision for a separate earth ground for the system other than code connections for dc protection to an existing salt-pit ground. Attempts have not been made to insulate the room from earth.

Dosimetry. Dose rate is measured for each pulse by a solid-state radiation PIN diode sandwiched between an equilibrium layer of Si slices, so that the detector is reading true Si dose rate. The detector is positioned in a region as close to the x-ray beam axis as possible without being shadowed by experiments. A copy of the pulse waveform is available for the experimenter.

Dose information can be obtained in a variety of ways. The facility includes both EG&G Model TL-3 and Teledyne Model TLD 7300 readers for reading a variety of TLDS, both LiF and CaF_2. For high-level work, the laboratory has made standard the use of the small Teledyne disks, SD-CaF_2-0.4, which are made with CaF_2 dispersed in a Teflon matrix 6 mm in da. and 0.4-mm thick. The disks can be used bare for in-situ measurement or can be used with Al equilibrium shields optimized for the machine spectrum measurements. On the average, it takes about 2 min to read out and process each dosimeter disk. Up to 6 dosimeters can be supplied and read out in real time for customers. Additional numbers may be used under these reading-time constraints, usually at extra charge. Measured relative accuracy of the dosimeters appears to be 3% rms. Calibration and standardization has been performed with the use of in-house Cs-137 and Co-60 sources, and a Co-60 source at Northrop Corporation. A Model 2502 Farmer secondary standard manufactured by Nuclear Enterprises and calibrated at the NBS has been used for the basic standardization, backed by a Landsverk 10,000-R meter, also calibrated at the NBS.

3.9.3 Support Capabilities

The facility test area, including the exposure screen room, can be fully secured for sensitive work; vaults and file in the building are available for sensitive storage. An experiment laboratory can be made available for other work, which also can be fully secured.

The TRW staff can generally be retained under contract to perform an entire experimental program, including design assistance, experiment planning, execution, and analysis, or a mix of any of these items.

Pricing is as follows:

1.	VULCAN (includes all pulsers, film, dosimetry, and instrumentation)	$1,650 per shift
2.	Additional Services	
	a. FEBETRON 705	$675 per shift
	b. Latchup	Requires special quote.

Prices are subject to change without notice.

Time must be reserved for use by outside customers at least 1 month in advance to assure desired scheduling. Normal working hours at the facility are 8:30 a.m. to 5:30 p.m. Second-shift operations can be scheduled when required. In general, the machine will be available for use 5 days per week.

It is necessary to clean and wipe the field-emission diode approximately every 30 to 40 shots. Turnaround time for this operation is about 1 hr. The facility is generally manned from 6 a.m. to 9:30 p.m. for general maintenance. Users are advised to schedule setup and teardown within the hours of 6 to 8:30 a.m. and 5:30 to 9:30 p.m. so that the regular shift hours, for which a charge is incurred, are used for machine pulsing.

The facility is located in Building 84 of the TRW Systems Group, Redondo Beach. It can be reached from downtown Los Angeles or from the International Airport by driving south on the San Diego Freeway to the Rosecrans (West) offramp. Building 84 is located at 14520 Aviation Boulevard (Lawndale), 3 blocks west of the offramp. As an alternate route, one can drive east on Century Boulevard from the Airport to Aviation Boulevard, then turn right (south) and continue on Aviation to Rosecrans Boulevard. A half block beyond Rosecrans, turn left into the driveway of TRW Semiconductors, Inc. The building is located at the end of the driveway.

For more technical information, call or write:

P.P. Guilfoyle
TRW Systems Group
Building 84, Room 1002
One Space Park
Redondo Beach, CA 90278
Telephone: (213) 535-0056

The TWX number is 910-325-6611. The customer on-site telephone number is (213) 536-2231.

3.10 HERMES II AND REBA/REHYD ELECTRON-BEAM GENERATORS

HERMES II and REBA/REHYD are high-energy electron-beam generators operated by Sandia Laboratories, Albuquerque, New Mexico. HERMES II has been in operation since February 1969. REBA has been fully operational since November 1969. REHYD is a water-insulated, low-impedance transmission line which was installed on the REBA facility in 1975. The three machines are described separately in the following paragraphs.

3.10.1 HERMES II

The HERMES II is a high-energy, pulsed, field-emission electron-beam or bremsstrahlung x-ray source. It was designed and constructed by Sandia Laboratories to provide high-dose-rate radiation-effects studies and material-response studies of rapid energy deposition. The principal components of HERMES II are a Marx generator, a Blumlein transmission line, and an output tube. Stored low-V energy is converted to high-V energy by the Marx generator and then transferred to the Blumlein transmission line, which serves as a fast-discharge, pulse-forming, low-inductance energy source for the output tube.

The Marx generator consists of a bank of capacitors which are charged in parallel and discharged in series by means of spark-gap switches. The negative-V output of the Marx generator is placed on the coaxial Blumlein transmission line consisting of three concentric cylinders. The V pulse formed by the Blumlein is impressed across the tube diode which consists of an insulating and vacuum-holding structure, a field-emission cathode, and an anode.

The anode used for the electron-beam mode of operation is a thin low-Z target which allows passage of the electrons with minimal energy loss. For the x-ray mode of operation, the anode used is a thick high-Z target, selected for maximum efficiency in converting electron-beam energy into bremsstrahlung x-radiation. Performance characteristics of the HERMES II are as follows:

1.	Marx Generator	
	a. Charging V	70 kV
	b. Repetition rate	3 pulses/hr
	c. Energy stored (maximum 100 kV charge)	1.0 MJ
2.	Diode	
	a. Peak diode V	10 MJ
	b. Peak diode I	100 kA
	c. Total beam energy	75 kJ
3.	Electron-Beam Environment	
	a. Transported beam energy	40-60 kJ
	b. Peak beam fluence	500 cal/cm^2
	c. Pulse width (FWHM)	50 ns

4. X-Ray Environment

a.	Peak dose pulse (at anode)	5×10^4 rad(Si)
b.	Peak dose rate (at anode)	1×10^{12} rad(Si)/s
c.	Pulse width (FWHM)	50 ns
d.	Pinched beam mode dose/pulse (at anode)	4×10^5 rad(Si)
e.	Pinched beam mode dose rate (at anode)	8×10^{12} rad(Si)/s

Figure 3-139 is a reproduction of a Compton diode output signal obtained during a HERMES II operation. Because the shape is independent of position and V level, an arbitrary scale has been used on the ordinate. The PWHM is 50 ns. The estimated accuracy of this value is ±5 ns.

3.10.1.1 Repetition Rate and Pulse Reproducibility

Pulse repetition rate for the x-ray mode is 1 shot each 20 min, with minimal degradation in the mean dose output. For pulses spaced at 20 min, the standard deviation in dose per pulse is 15%.

Pulse delay and pulse jitter are highly sensitive to machine conditions. While these quantities are relatively stable over a series of pulses, the effect of modifications in configuration and maintenance efforts cannot be predicted. Representative values over 2 recent series of pulses are:

Series	Pulse Delay (μs)	Pulse Jitter (μs)
1	11.5	±2.5
2	42.0	±5.0

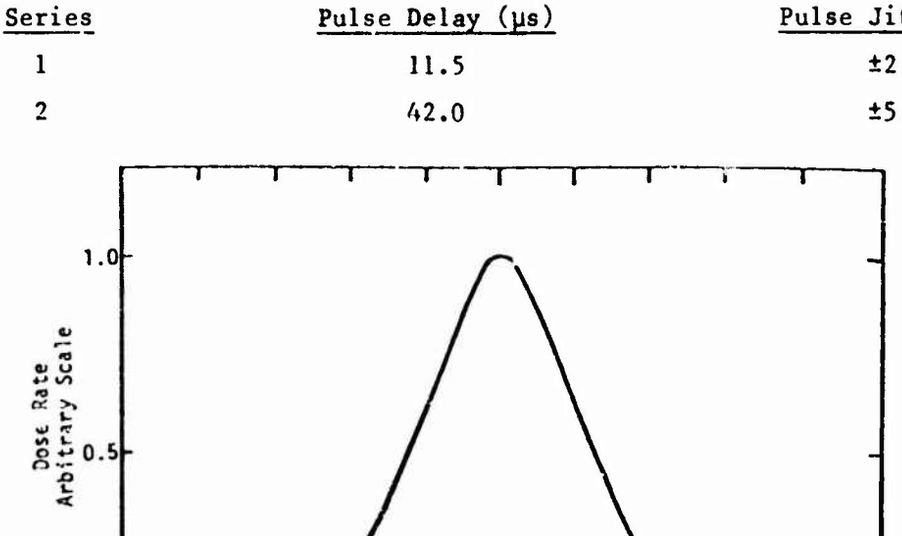

Figure 3-139. High-impedance diode x-ray pulse shape.

Series 1 is representative of the most frequent machine operating conditions. Pulse delay is measured from the occurrence of the Marx generator trigger signal to time of peak value of the anode-cathode gap I. Pulse jitter is given as the maximum observed variation from the mean in pulse delay.

RF interference measurements were made in the vicinity of the HERMES II experimenter's area. Peak electric fields of 3.1 kV/m are detected at the north screen room during a HERMES II firing. Proper use of available screen rooms, instrument vans, and shielding of the experiment and signal cables reduces the RF interference to an acceptable level. Shielding systems in use enable gathering of zero-time data that are of the order of 100 mV in magnitude.

The electron-beam energy fluence measurements are obtained by using a total-stopping graphite calorimeter. V and I waveforms are sampled by suitable monitors and displayed on oscilloscopes or on a Tektronix 7912 system. These latter two parameters are obtained on all HERMES II operations.

TLD-400 TLDs are used as the standard dosimeter. These are 0.317-cm by 0.317-cm chips of CaF_2 (Mn-activated) which will measure doses from 1 rad(Si) up to 6×10^5 rad(Si). Exposure levels of the dosimeters are determined by the Sandia Laboratories Diagnostic Laboratory. The Sandia Gamma Irradiation Facility, a Co-60 source, is used for calibration purposes.

Time-dependent x-ray measurements are made using Compton diodes, photodiodes, and PIN detectors.

3.10.1.2 Electron-Beam Mode Environment

Figure 3-140 illustrates the HERMES II differential energy spectrum, normalized to 1 electron. This information is obtained from time-synchronized V and I traces. Digitized values of the tube I and V are processed in a 3-parameter fitting program, taking proper account of tube inductance. Spectral results obtained by this method are used to calculate energy deposition profiles and photon spectra, which exhibit good agreement with measured data, and are estimated to be accurate to ±20%.

3.10.1.3 Total Beam Energy

The total beam energy produced by the high-impedance diode at normal operating parameters is approximately 75 kJ (18 kcal), but a significant fraction may be lost in focusing, depending on the experiment location. Transport efficiency and spatial distribution of the beam at the target are primarily dependent upon the drift chamber pressure and axial location of the experiment.

The total beam energy transported over a distane of 88.9 cm (35 in.) from the anode is plotted as a function of drift tube pressure in Figure 3-141. The scatter of data points about the fitted curve is relatively large. The variation of the beam transport efficiency as a function of axial position in the drift tube is illustrated in Figure 3-142. This series of measurements was made at 400

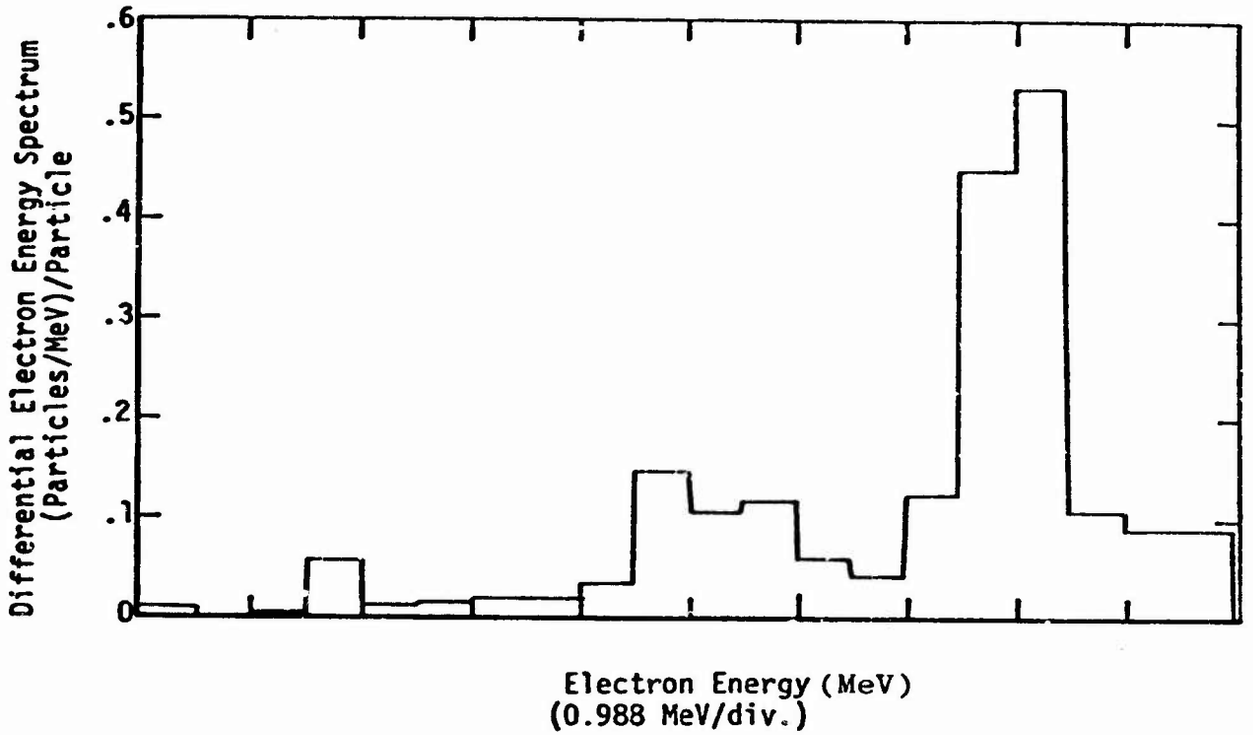

Figure 3-140. High-impedance diode electron energy spectrum.

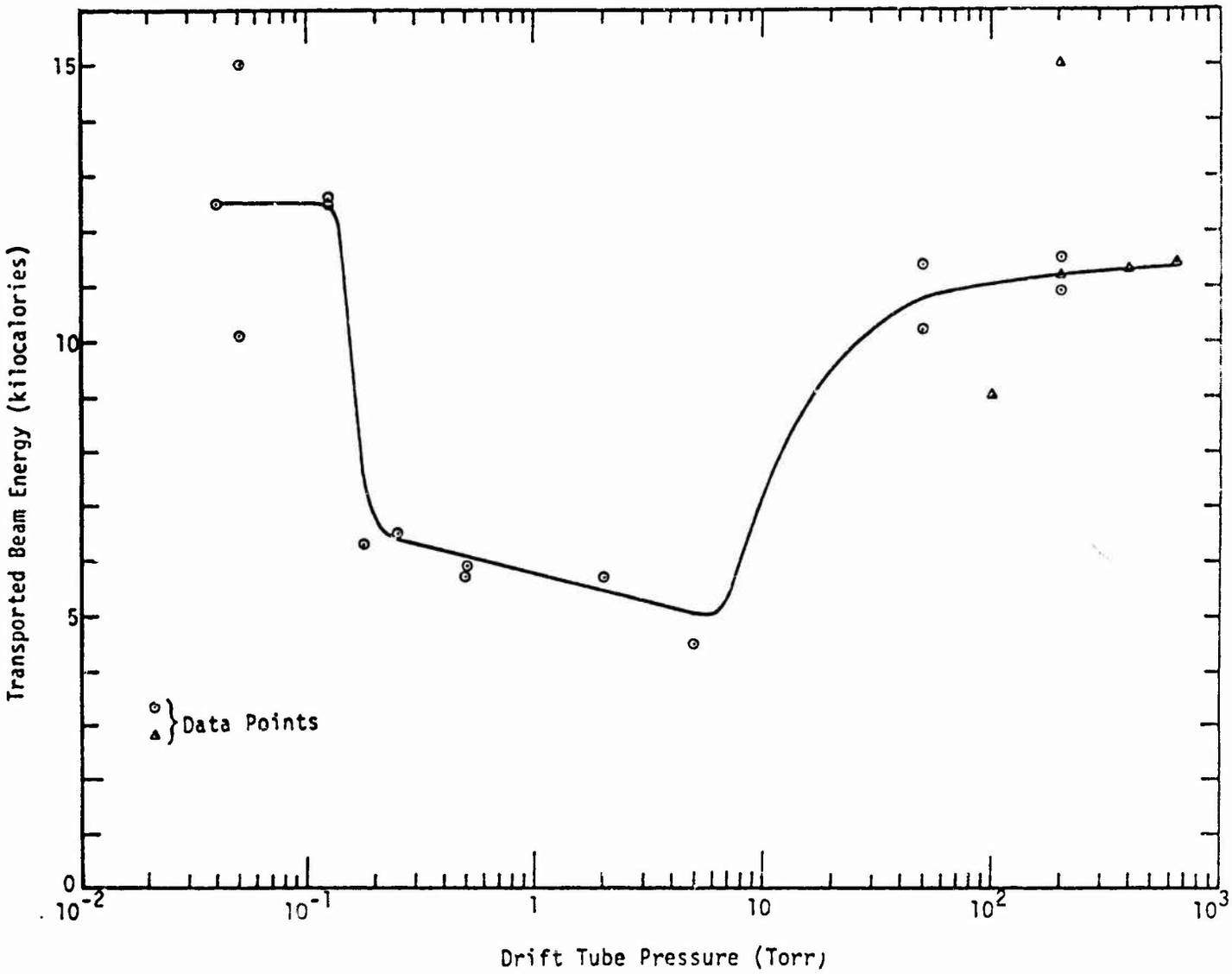

Figure 3-141. High-impedance diode electron-beam transport to 88.9 cm drift chamber position.

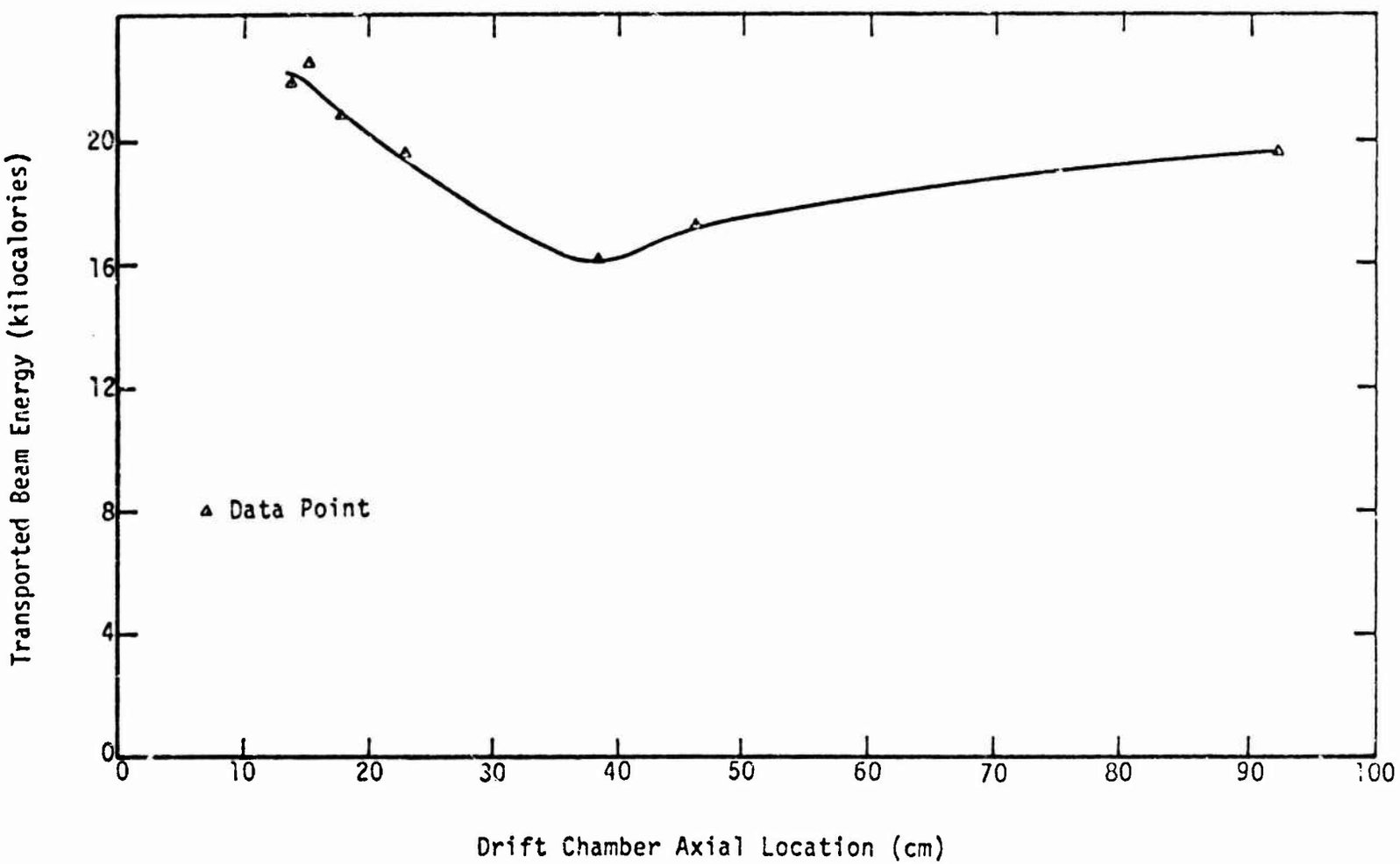

Figure 3-142. High-impedance diode electron-beam energy transport at 400-torr drift tube pressure.

torr in the drift chamber and is not necessarily representative of similar measurements at other background gas pressures.

Estimated accuracy of these data, obtained using a segmented, graphite total-stopping calorimeter, is ±20%. While the information presented is considered to be typical, significant variations are observed in nominally identical pulses which are separated by an extended period of machine operation and/or changes in the accelerator configuration. Note that an identical point on Figures 3-141 and 3-142, transported energy at 88.9 cm from the anode and background gas pressure of 400 torr, indicates results differing by approximately 40% for these 2 series. Over a single continuous series with identical conditions, however, the outputs are less scattered. Nevertheless, we stress the recommendation for routine measurements by each experimenter.

3.10.1.4 Beam Geometry

The spatial distribution of energy within the HERMES electron-beam is a sensitive function of diode and drift chamber conditions, and significant variations in the profiles may be observed from time to time. However, over a continuous series of identical pulses, the distribution is relatively stable. For these reasons, the information presented is only illustrative of expected profiles and their dependence upon system variables. If spatial distribution of the incident fluence is an important parameter of the experiment, it should be measured regularly during each series of nominally identical HERMES II shots.

Figure 3-143 is a typical set of beam profile measurements at various experiment locations in the drift chamber. It is important to note that profiles generally exhibit a drastic dependence upon pressure and should be determined for each test configuraton. Drift region pressure during these measurements was 400 torr. The data for Figure 3-143 were obtained with the segmented, graphite total-stopping calorimeter and have an estimated accuracy of ±20%.

3.10.1.5 Energy-Deposition Drift Chamber

Energy-deposition profiles for this HERMES electron beam have been measured using linear-array calorimeters. In addition, the spectrum calculated from I-V data can be used in an electron-photon transport code to compute the deposition profile. Figure 3-144 shows a comparison of measured data in Be using a linear-array calorimeter, with calculations at 45- and 60-degree angles of incidence. The measured curve was obtained at an incident fluence of 532 cal/cm^2; similar, but not identical, results are obtained at other fluences ranging between 66 cal/cm^2 and 488 cal/cm^2. The best agreement with experimental data is obtained at an angle of incidence between the 2 values presented.

3.10.1.6 Atmospheric Focusing Cone

An alternate drift chamber, the atmospheric focusing cone, is available for use in the high-impedance diode electron-beam mode. Both the cone and the 18.1-cm (7.125-in.) dia. cylinder are operated at atmospheric pressure. Therefore, the experiment is not subjected to a vacuum environment. However, control over the

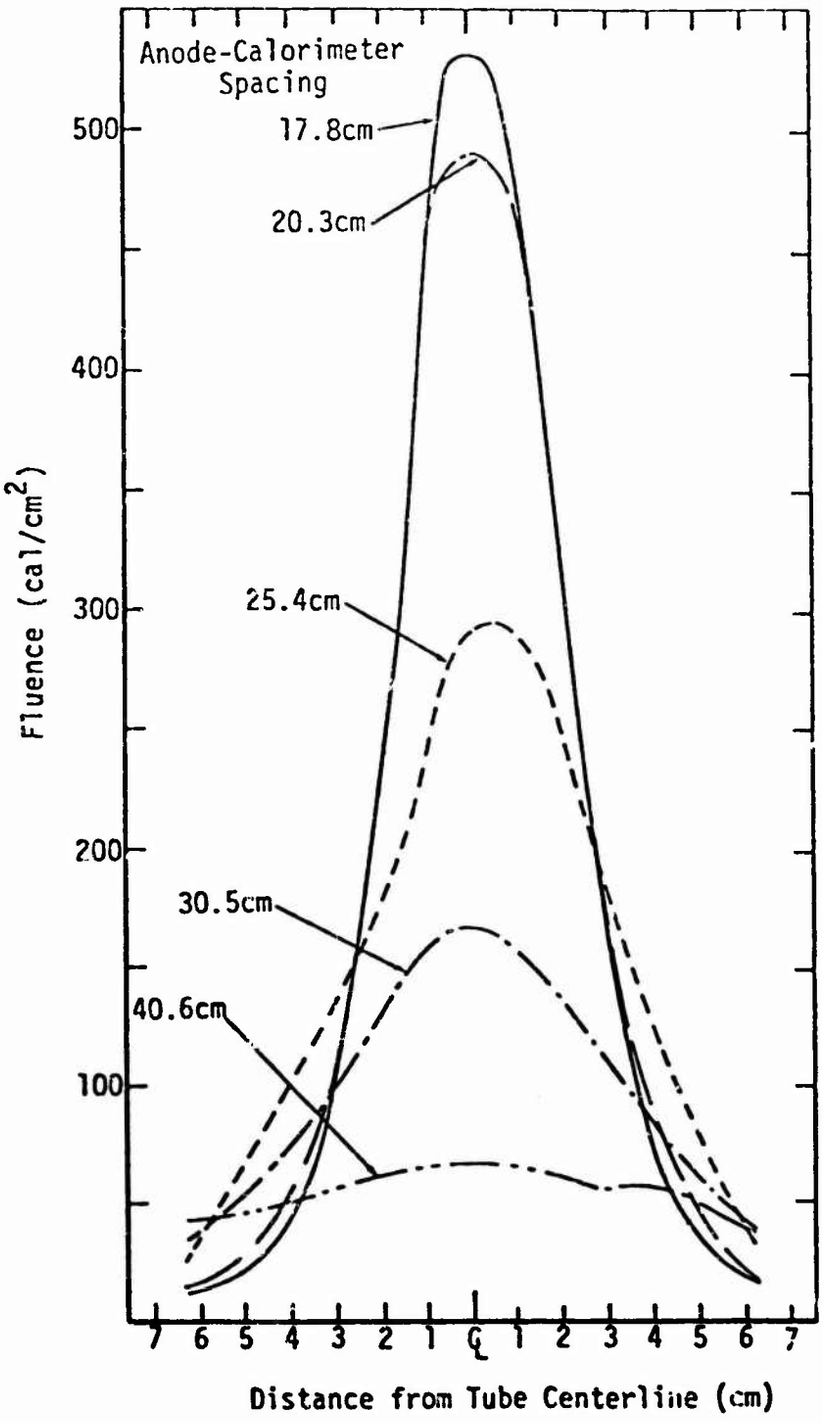

Figure 3-143. High-impedance diode electron-beam profiles at 400-torr drift tube pressure.

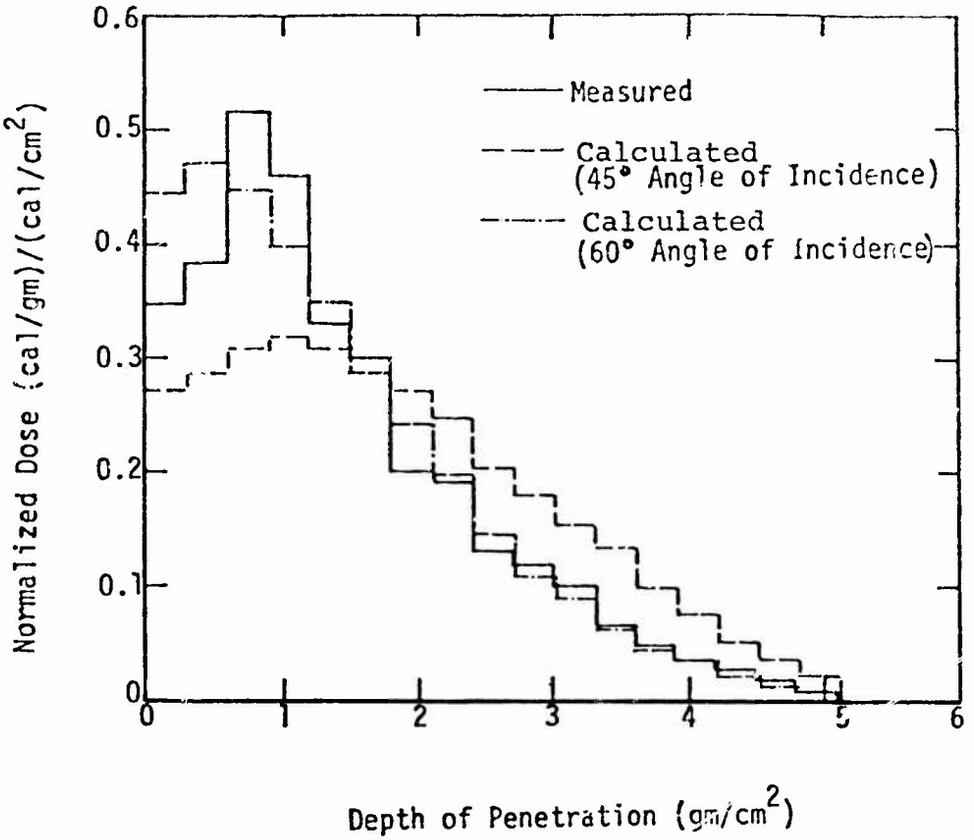

Figure 3-144. Dose depth profiles in Be.

exposure level and spatial distribution of the beam is limited to physical positioning of the sample.

Measurements of center line fluence as a function of calorimeter distance from the end of the focusing cone are presented in Figure 3-145. The data points are a composite of results obtained during several series of pulses using different calorimeters. Figure 3-146 illustrates radial fluence profiles at various distances into the cylinder. These plots were generated during a single continuous series.

3.10.1.7 Energy Deposition with Focusing Cone

Energy-deposition profiles for the HERMES II electron-beam using the focusing cone were determined using interferometer techniques. Figure 3-147 compares interferometer-measured and calculated dose-depth relationships at an effective angle of incidence of 30 degrees in quartz and tungsten carbide. The apparent discrepancy in effective angle of incidence between Figures 3-144 and 3-147 can be explained by noting that particle trajectories produced by neutral-gas focusing are complex, curved paths with strong dependence on position relative to the pinch and geometry of the drift chamber.

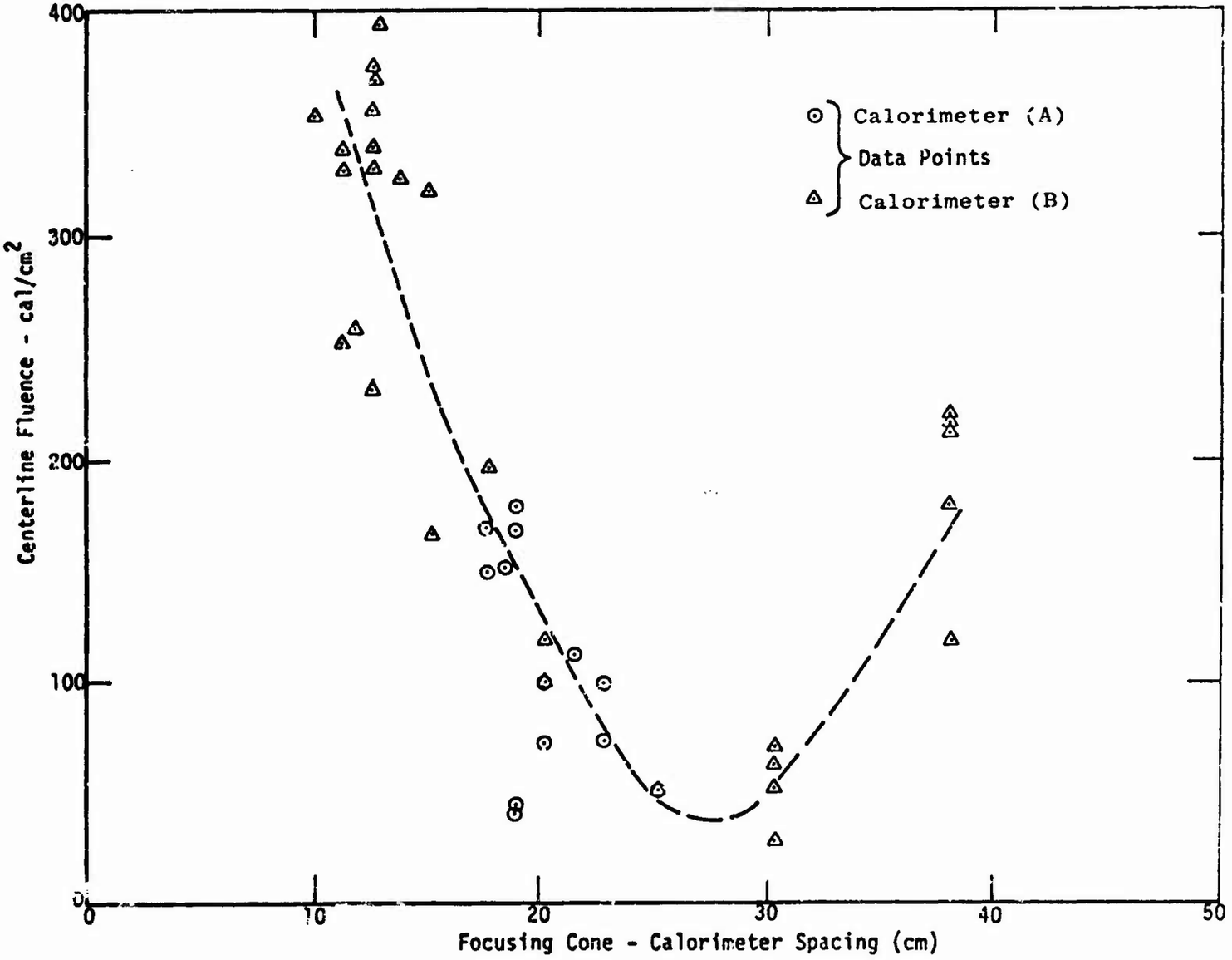

Figure 3-145. Center line fluence versus axial distance from the focusing cone.

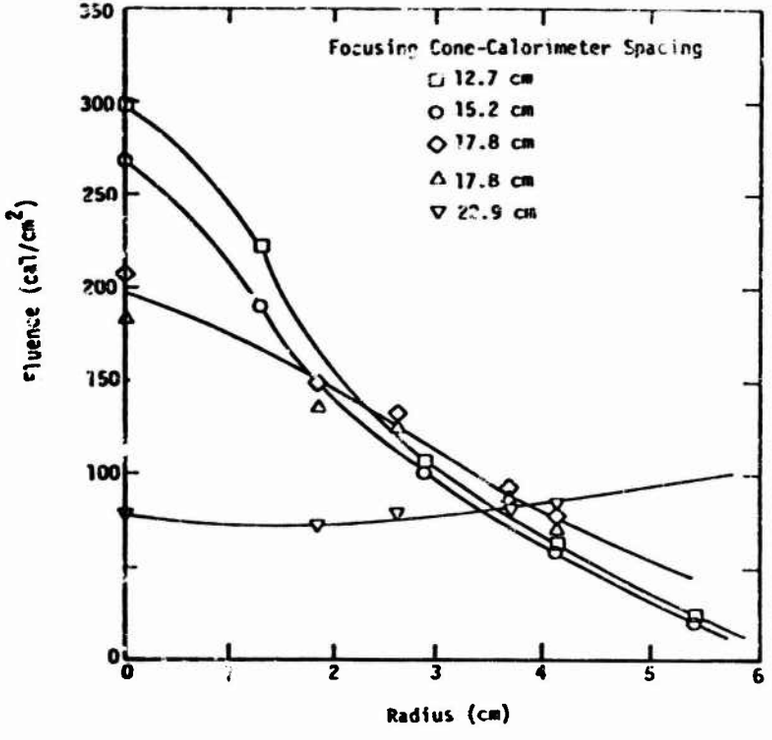

Figure 3-146. Fluence versus radial position.

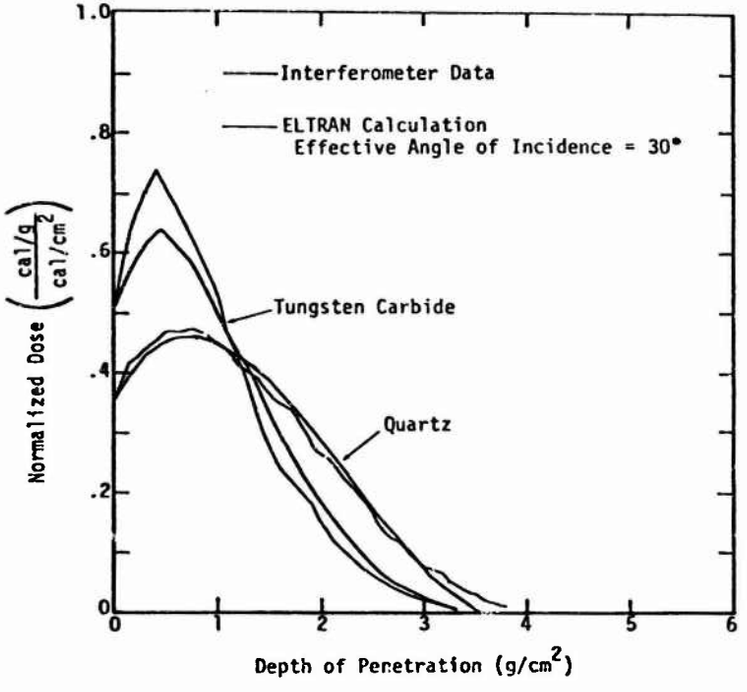

Figure 3-147. HERMES II high-impedance diode electron-beam depth-dose curves measured in the atmospheric focusing cone and calculated (incident fluence is approximately 80 cal/cm^2).

3.10.1.8 Environment Measurement Errors

The accuracy of the calorimeters used in HERMES II measurements is estimated at ±20%. Values from V and I output waveforms are accurate within about ±15% and ±10%, respectively. Reproducibility of both monitors is estimated to be within 5%.

3.10.1.9 X-Ray Mode Environment

Total Dose and Isodose Contours. The total dose per pulse and isodose contours in the exposure volume may be modified by altering numerous machine parameters, such as charge V, anode-cathode gap spacing and Blumlein oil (BOG) switch setting, but the desired outputs usually can be achieved by appropriate selection of the exposure location without altering the standard machine configuration.

The data presented in this section, taken at standard values for electrical and mechanical parameters of HERMES II, are as follows:

1. Maximum charge V — 70 kV
2. Anode-cathode gap — 28.5 cm
3. BOG spacing — 22.9 cm
4. Post-pulse-switch spacing — 9.4 cm.

This is the highest reliable level of machine operation at the present stage of development.

Figure 3-148 presents the total x-ray dose per pulse along the tube axis as a function of distance from the anode faceplate. Approximate $1/R^2$ dependence can be observed at distances in excess of 50 cm.

The exposure pattern of HERMES II has been shown to have good azimuthal symmetry. Transverse profiles of the total dose per pulse at several axial locations are illustrated in Figure 3-149. The experiment position at 7 cm from the anode, with a high and nearly uniform total dose over an area of 400 cm^2, is a frequently used location.

Figure 3-150 combines the on-axis and transverse dose mappings into a set of isodose contours for the HERMES II exposure volume. Relative doses in this figure are normalized to unity at the beam center line on the anode faceplate. The isodose-per-pulse contours for HERMES II have been established by dose measurements using Ag_3PO_4 and Co glass dosimeters and CaF_2 TLDs. The TLDs are calibrated in rad(Si), whereas the glasses have been calibrated in rads to the particular glass, using the Sandia Gamma Irradiation Facility Co-60 source. Results were interpreted by the Sandia Laboratories Dosimetry Laboratory. The accuracy and reproducibility of the particular dosimetric systems in use are estimated at ±15% or better, depending upon the detector redundance employed.

Output Waveform and Dose Rate. Dose rate as a function of time has been measured using photodiodes, Compton diodes, and PIN semiconductor detectors at various positions in the experimental volume. The majority of data lead to the

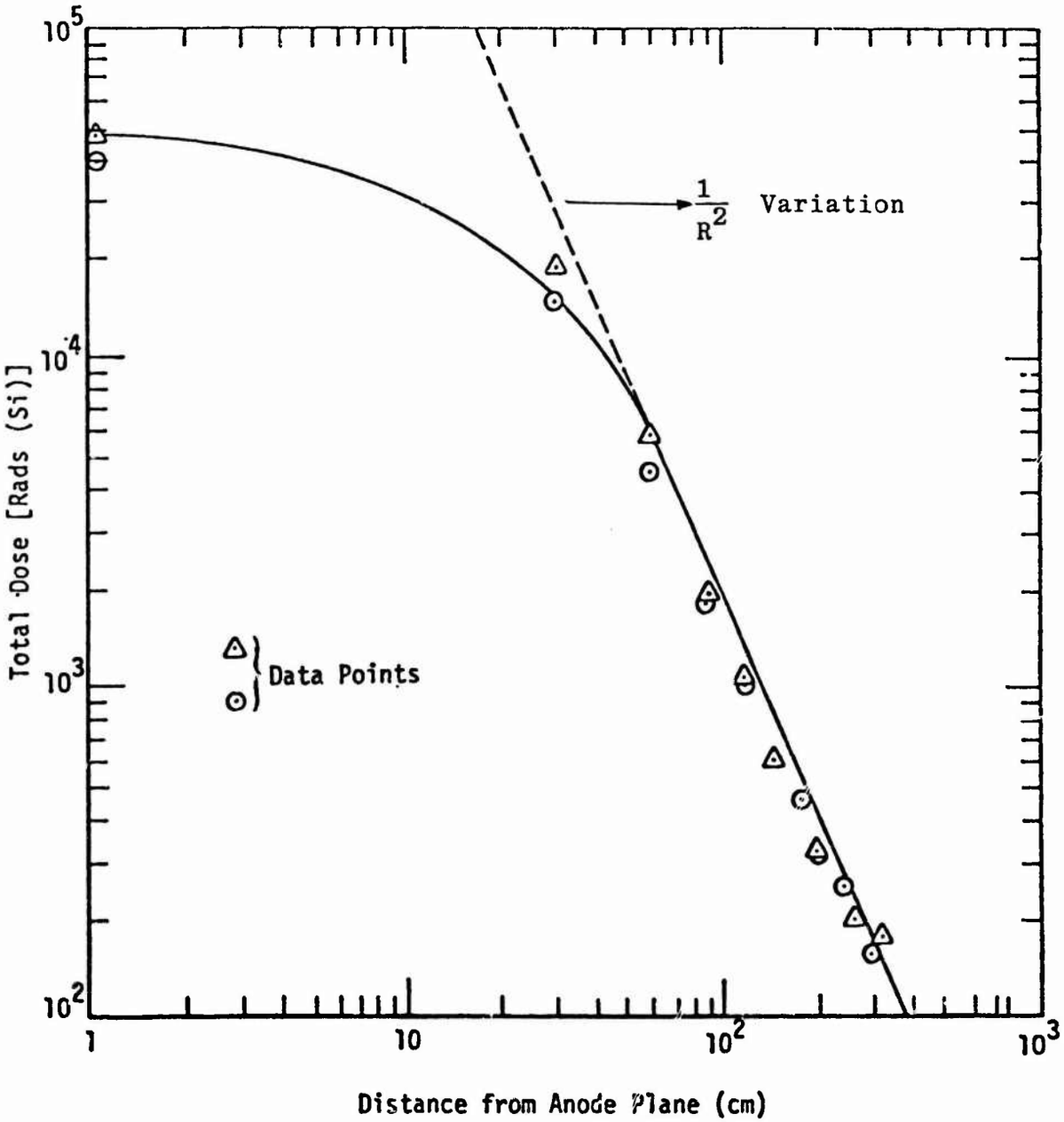

Figure 3-148. High impedance diode x-ray dose per pulse as a function of distance from tube surface.

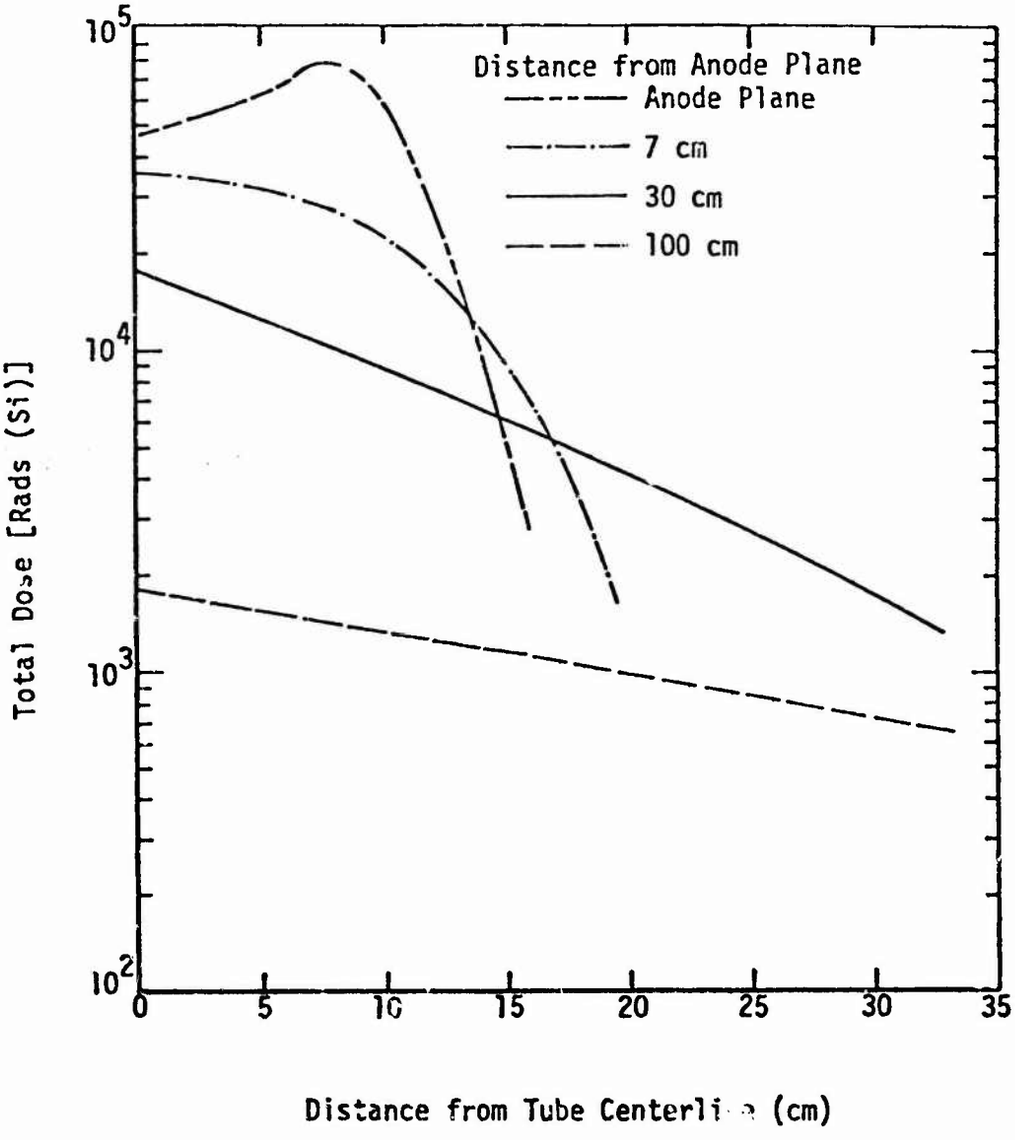

Figure 3-149. Transverse high-impedance diode bremsstrahlung dose profiles.

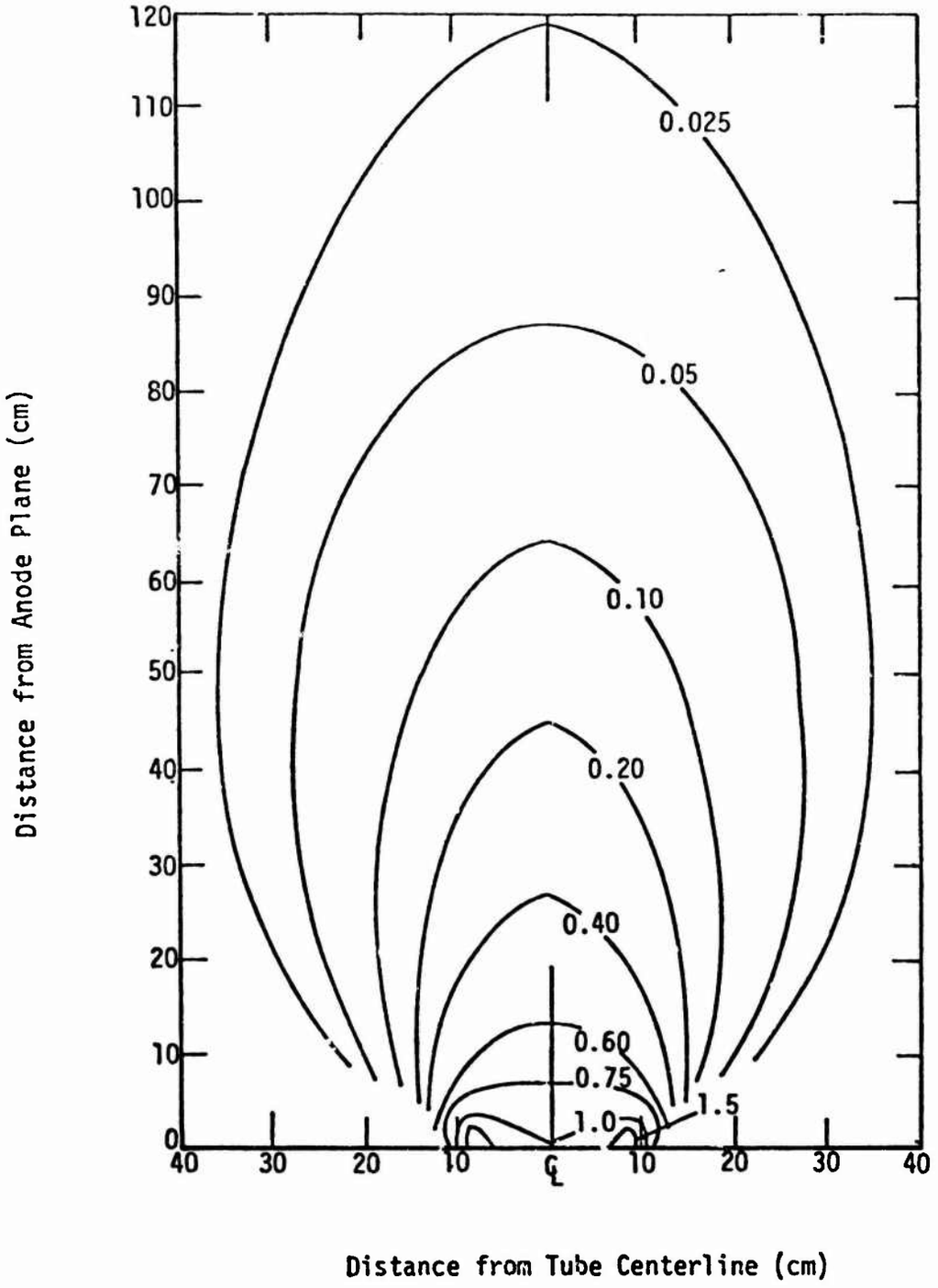

Figure 3-150. HERMES II high-impedance diode isodose curves.

conclusion that pulse shape is independent of position and dose. A reproduction of the Compton diode output signal is shown in Figure 3-139. Full pulse width at half-maximum rate is 50 ns ± 5 ns.

X-Ray Spectrum. A magnetic Compton spectrometer, designed to measure the γ-ray spectrum from intense pulsed sources in the presence of γ-rays, electrons and/or neutrons, has been used to characterize the HERMES II bremsstrahlung environment. The measured results at 2 values of charging V are shown as smooth curves in Figure 3-151. Shown also in the figure for comparison are the semi-empirical spectra, normalized to the γ-spectrometer results, obtained from the ETRAN-15 Monte Carlo code using an electron spectrum derived from tube I-V data and a 1-dimensional approximation for the Ta anode.

Pinched-Beam X-Ray Mode. The pinched-beam, or enhanced bremsstrahlung x-ray mode of HERMES II operation was developed to generate bremsstrahlung x-rays from a self-focused HERMES electron-beam rather than from the diffuse distribution at the anode of the high-impedance diode. In this way, higher dose and dose-rate capabilities could be achieved at the expense of total beam energy.

The pinched beam provides a maximum dose of 3×10^5 rad(Si) and a dose rate of 6×10^{12} rad(Si)/s. This represents an increase in dose by a factor of 5 over the peak capabilities of the high-impedance diode x-ray mode.

Total Dose. Total dose per pulse along the beam axis versus distance from the composite anode is presented in Figure 3-152. Approximate $1/R^2$ dependence can be observed at distances in excess of 20 cm.

Transverse profiles, generated by averaging 2 pulses with off-axis measurements in four directions, are illustrated in Figure 3-153.

Figure 3-154 combines the on-axis and transverse dose mappings into a set of isodose contours for the enhanced bremsstrahlung x-ray environment. Relative doses in this figure are normalized to unity at the beam center line on the anode plane. At distances exceeding 20 cm from the anode plane and within an angle of approximately 80 degrees, symmetric about the center line, the exposure pattern closely resembles that of a point source.

Data for these figures were obtained with CaF_2 TLDs, calibrated in rad(Si) on a Co-60 irradiation source. Estimated accuracy and reproducibility of these measurements is ±15%.

Dose rate as a function of time measured during a HERMES II pinched-beam x-ray mode operation, using a Compton diode detector, is similar to that of the standard x-ray mode shown in Figure 3-139.

Environment Measurement Errors. HERMES II x-ray dosimetry measurements are capable of an accuracy and reproducibility of within ±10%.

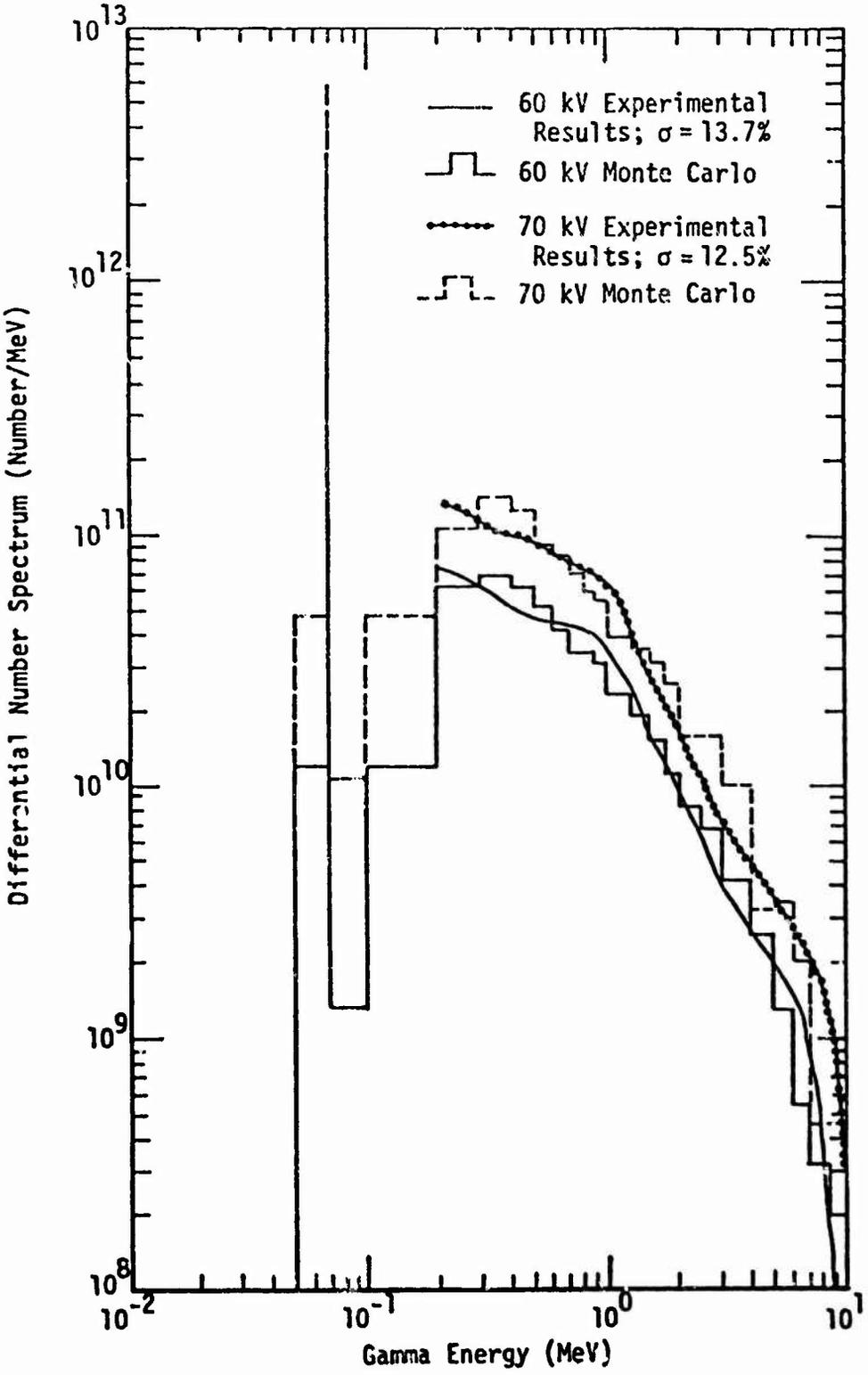

Figure 3-151. HERMES II high-impedance diode photon spectrum.

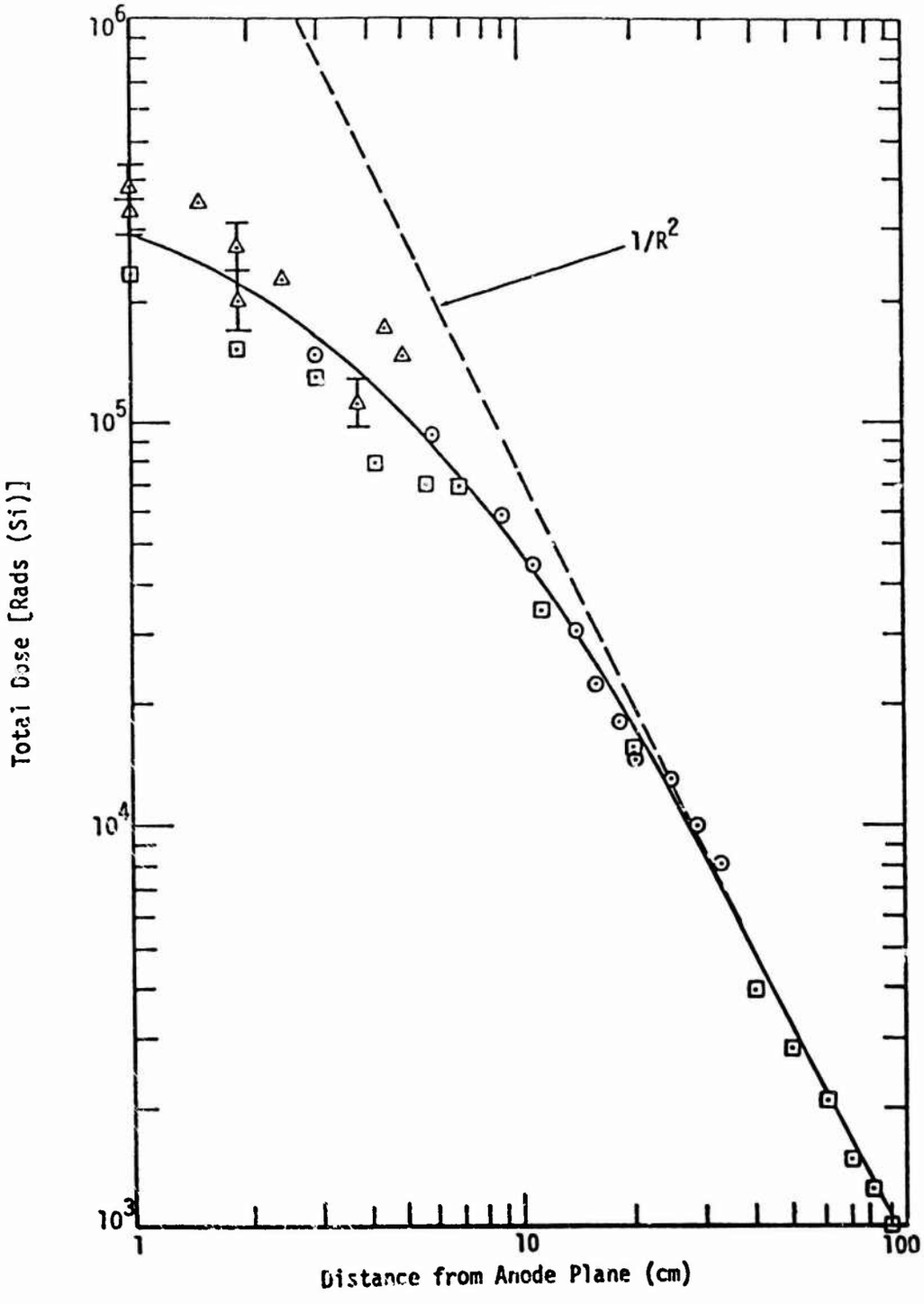

Figure 3-152. Pinched-beam mode x-ray dose per pulse as a function of distance from tube surface.

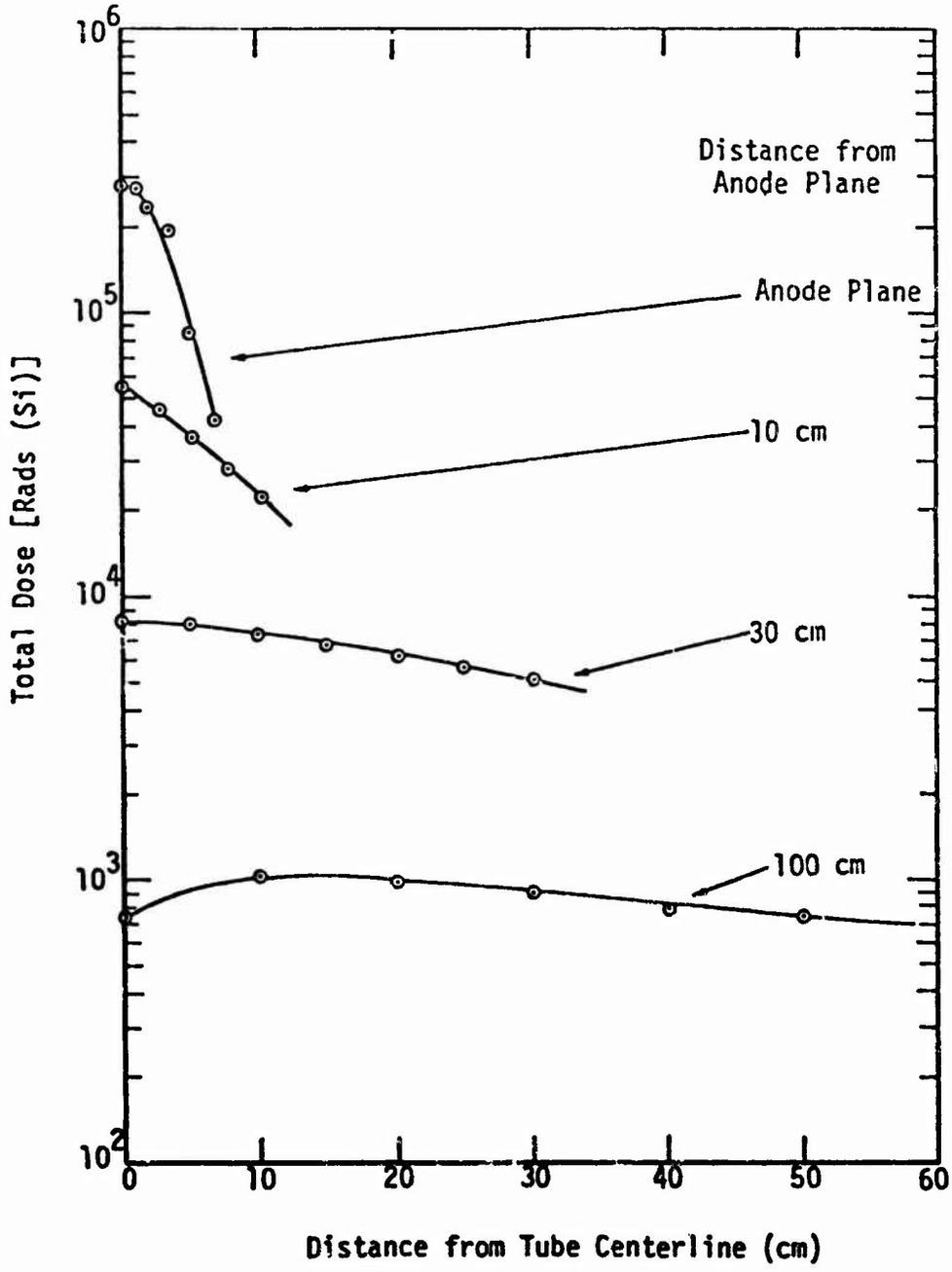

Figure 3-153. Transverse pinched beam bremsstrahlung dose profiles.

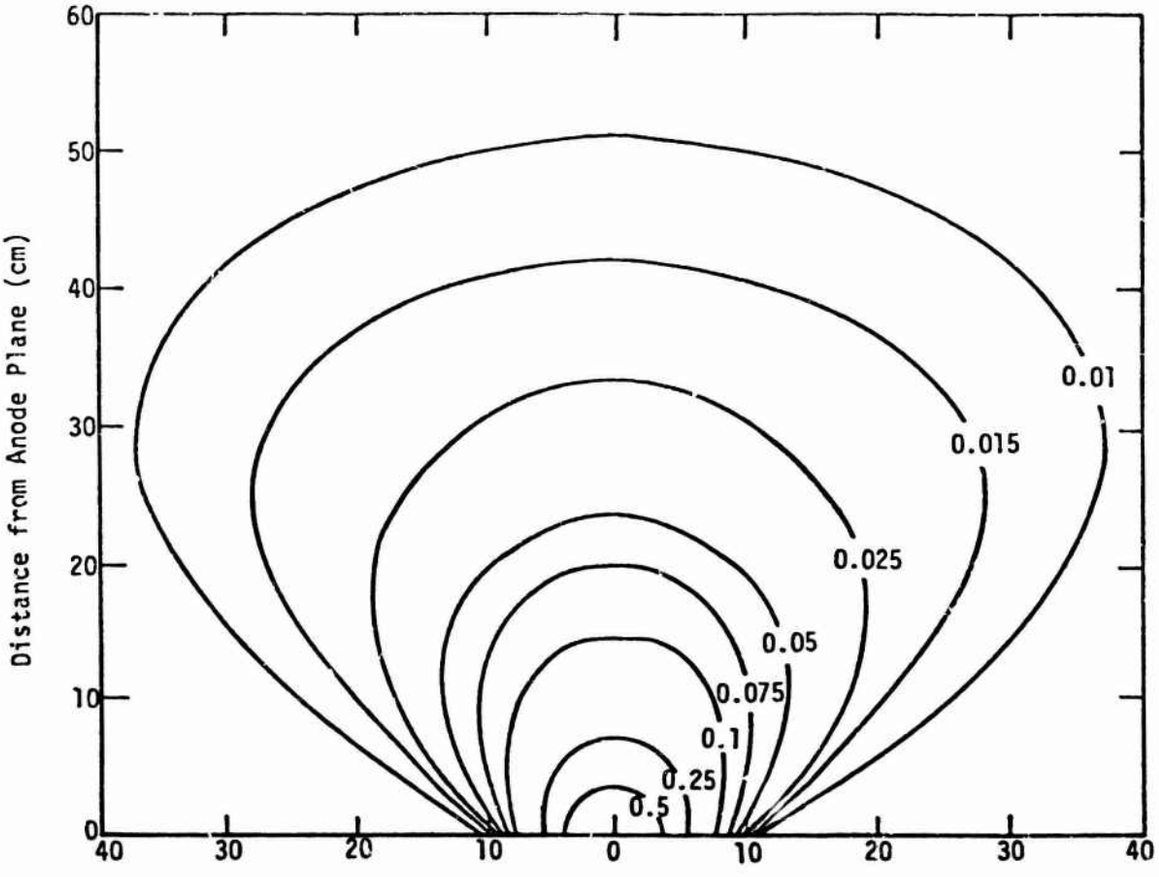

Figure 3-154. Enhanced bremsstrahlung mode isodose contours.

3.10.2 REBA

The REBA is a high-energy, pulsed, field-emission electron-beam or bremsstrahlung x-ray source. It was designed and constructed by Sandia Laboratories to provide an energy source of short duration for determining material responses to rapid surface and in-depth energy deposition. The principal components of REBA are a Marx generator, a Blumlein transmission line, and an output tube. Stored low-V energy is converted to high-V energy by the Marx generator and then transferred to the Blumlein transmission line, which serves as a fast-discharge, pulse-forming, low-inductance energy source for the output tube.

The Marx generator consists of a bank of capacitors which are charged in parallel and discharged in series by means of spark-gap switches. The negative-V output of the Marx generator is placed on the coaxial Blumlein transmission line which consists of 3 concentric cylinders. The V-pulse formed by the Blumlein is

impressed across the tube diode which consists of an insulating and vacuum-holding structure, a field-emission cathode, and an anode.

The anode used for the electron-beam mode of operation is a thin low-Z target which allows passage of the electrons with minimal energy loss. For the x-ray mode of operation, the anode used is a thick high-Z target, selected for maximum efficiency in converting electron-beam energy into bremsstrahlung x-radiation. Three electron-beam modes, high-impedance, low-impedance, and long pulse, each with its own unique set of environmental characteristics, are currently operational. In this section, the principal features of each environment are identified.

3.10.2.1 Performance Characteristics

The following is a list of REBA performance characteristics:

1. Marx Generator
   - a. Charging V — 70 kV
   - b. Repetition rate — 6 pulses/hr
   - c. Energy stored (maximum 100-kV charge) — 95 kJ
2. Diode
   - a. Peak diode V — 3.2 MV
   - b. Peak diode I — 40 kA
   - c. Total beam energy — 10 kJ
3. Electron-Beam Environment
   - a. Transported beam energy — 6.7 kJ
   - b. Peak beam fluence — 400 cal/cm^2
   - c. Pulse width (FWHM) — 70 ns
4. X-Ray Environment
   - a. Peak dose/pulse (at anode) — 1.8×10^4 rad(Si)
   - b. Peak dose rate (at anode) — 2.6×10^{12} rad(Si)/s
   - c. Pulse width (FWHM) — 70 ns.

3.10.2.2 Current Waveform and Distribution

Figure 3-155 presents the beam-power-versus-time waveforms, calculated from tube V and I measurements, and normalized to unit peak. The pulse width at half-power points is 60 ns and is estimated to have an accuracy of ±20%. This curve is considered to be representative of the waveform at the experiment location.

The beam geometry of REBA is highly dependent upon the pressure in the drift chamber. A compact Faraday-cup array has been used to measure the time development of the spatial distribution in a 10-in. (25.4-cm) dia. drift tube at air

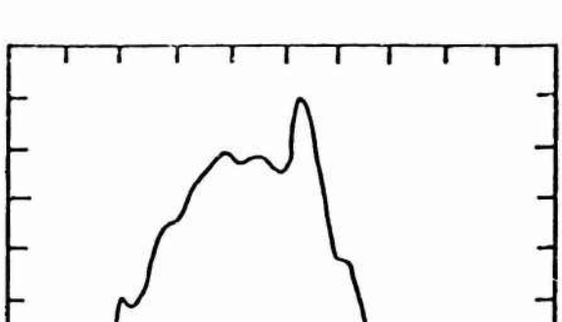

Figure 3-155. Beam power output waveform.

pressures of 22.5 torr, 3.9 torr, and 520, 320, 160, and 90 μm. Contour maps constructed from these data display the formation and decay of the pinch structure. Figure 3-156 shows profiles of constant I density (A/cm^2) during time of maximum pinching for a 3-MeV beam propagating in a drift tube filled with air at 22.5 torr. The primary I in the drift tube was ~40 kA and the net I was ~22.5 kA. The beam is essentially symmetric about the axis.

Figure 3-157 is a typical result of beam-profile measurements at the normal experiment location for several values of pressure, using a pressure cone (described later). Except for this variable pressure, machine configuration and operating conditions were held fixed at nominal values during the measurement. Exit cone pressure was maintained at ambient during this diagnostic experiment. Increasing rear cone pressure clearly depresses peak values of the incident fluence, approaching a nearly uniform distribution of 40 to 50 cal/cm^2 at atmospheric pressure.

The data for Figure 3-157 were obtained with the segmented graphite total-stopping calorimeter and have an estimated accuracy of ±15%. Total beam energy is the surface integral of the incident fluence profile.

3.10.2.3 Repetition Rate and Pulse Reproducibility

The Marx generator pulse repetition rate is nominally 6 pulses/hr, which must be shared between the REHYD machine and REBA. Operating experience has indicated the following standard deviations within a continuous series of nominally identical REBA high-impedance diode electron-beam pulses:

1.	Tube V	± 5%
2.	Tube I	± 5%
3.	Total beam energy	±10%
4.	Peak fluence	±20%

Pulse delay and pulse jitter are highly sensitive to machine conditions. While these quantities are relatively stable over a series of pulses, the effect of modifications in configuration cannot be predicted. During most of the operating history of REBA, the pulse delay has been 5 to 17 μs with a jitter of

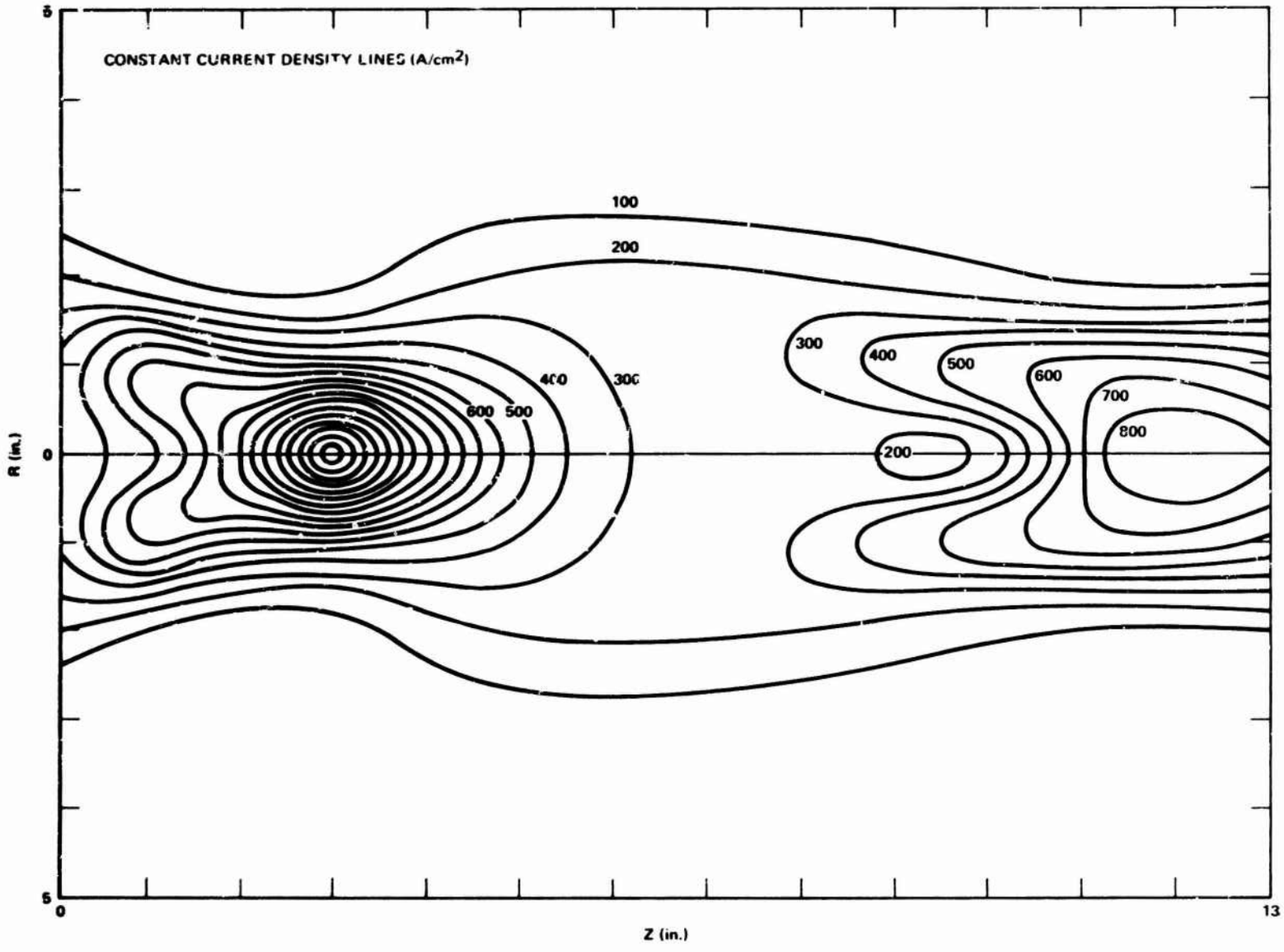

Figure 3-156. Contour map of REBA beam at 22.5-torr pressure.

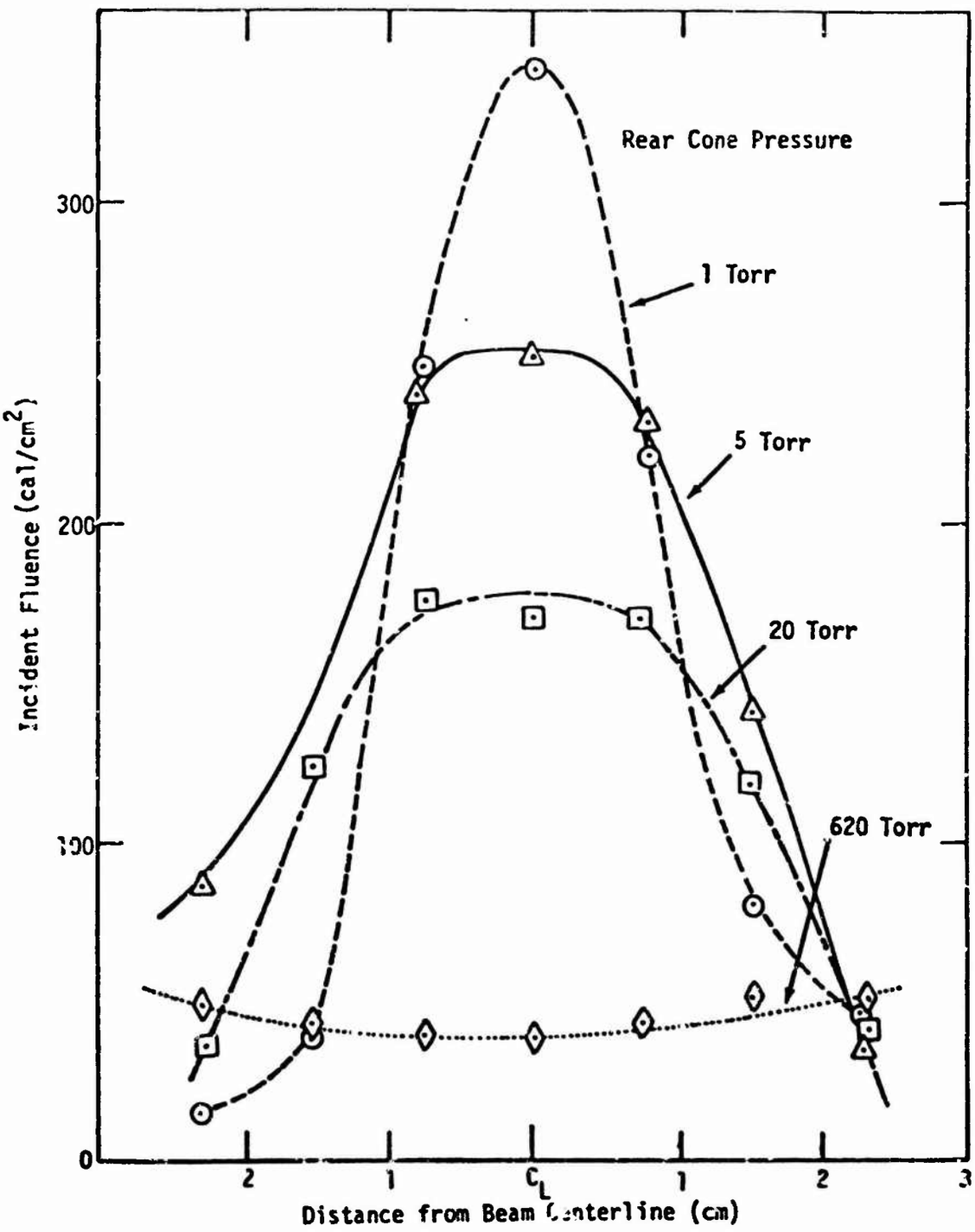

Figure 3-157. Beam profiles at experiment location.

±2 μs. Pulse delay times of up to 25 μs have been observed at times. Pulse delay is measured from the occurrence of the Marx generator trigger signal to time of peak value of the anode-cathode gap I. Pulse jitter is given as the maximum observed variation from the mean in pulse delay.

3.10.2.4 Electrical Noise

Peak electric fields of 4.6 kV/m were detected during a REBA firing. In addition, 6.6-kV/m fields were found during HERMES II operations and 5.7-kV/m fields caused by REHYD pulse.

RG/22 B/U- and RG/214-type cables are used for data acquisition. These cables are shielded with steel conduit to within 30 ft of REBA, and then are carried through flexible μm metal which carries the remainder of the cable to the experiment. This shielding system enables gathering zero-time data that is of the order of 100 mV in magnitude.

3.10.2.5 Diagnostic Techniques

Electron-beam energy-fluence measurements, including beam profile and characteristic deposition curves, are obtained using planar- and linear-array calorimeters, respectively. The outputs of these calorimeters are fed into the Sandia Data Acquisition and Display System (DADS) and reduced data are returned in the form of scope displays and teletype tabulations. V and I waveforms are sampled by monitor resistors and are also digitized through the use of the DADS facility. Other monitors, such as Rogowski coils and capacitative V monitors, have been used to determine machine output characteristics.

X-ray dose measurements are currently determined by CaF_2 (Mn-activated) TLDs. The Sandia Gamma Irradiation Facility Co-60 source is used for calibration.

3.10.2.6 Electron-Beam Mode Environment

High-Impedance Diode. The high-impedance diode is the original design configuration of the REBA facility and, operated in the electron-beam mode, constitutes the majority of machine experience.

The drift cone is divided by a thin film into 2 chambers in which gas pressure can be individually controlled. The typical exposure geometry has the sample located at the 16.6-cm^2 area near the pressure-cone exit. The environment at this location is virtually independent of pressure in the exit cone, which is, therefore, normally operated at 620 torr (ambient). Rear-cone pressure is adjusted to achieve the desired beam characteristics. The pressure cone is available at the facility. Sample chambers of special design must be provided by the experimenter.

The nominal operating characteristics for the high-impedance configuration are:

1.	Marx Generator	
	a. Charging V	70 kV
	b. Repetition rate	6 pulses/hr
2.	Diode	
	a. Peak diode V	3.2 MV
	b. Peak diode I	40 kA
	c. Total beam energy	10 kJ (2390 cal)
	d. Impedance	65 to 70 ohms
3.	Target Electron Beam Environment	
	a. Transported beam energy	1,600 cal
	b. Peak fluence	400 cal/cm^2
	c. Pulse width	70 ns

Most parameters of this configuration can be adjusted within certain limits, if necessary, but additional diagnostic time must be scheduled when nonstandard conditions are desired.

Optional rectangular and cylindrical drift chambers are also available for the high-impedance diode electron-beam mode.

Total Beam Energy. The total beam energy produced by the high-impedance diode at normal operating parameters is approximately 10 kJ (2,390 cal), but a significant fraction may be lost in focusing, depending on the experiment location. Transport efficiency and spatial distribution of the beam at the target are primarily dependent upon the rear-cone pressure and are virtually independent of gas pressure in the exit cone. All data shown were taken at atmospheric pressure in the exit cone.

At normal tube operating V and I, the total beam energy available at the drift cone exit is plotted as a function of rear cone pressure in Figure 3-158.

Figure 3-159 presents the variation of average fluence over a 2.3-cm^2 area on the beam center line with rear-chamber pressure. Again, the diode is operating at nominal conditions. These data were obtained using segmented graphite total-stopping calorimeters. Estimated accuracy of these measurements is ±15%.

Electron Energy Spectrum. Electron energy spectra information is generally obtained from time-synchronized V and I traces. At Sandia, digitized values of the tube I and V, plus the drift cone exit I, are processed in a 3-parameter fitting program, taking proper account of tube inductance. Spectral results obtained by this method are used to calculate energy-deposition profiles and photon spectra, which exhibit good agreement with measured data. The technique is estimated to be accurate to ±25% nominally.

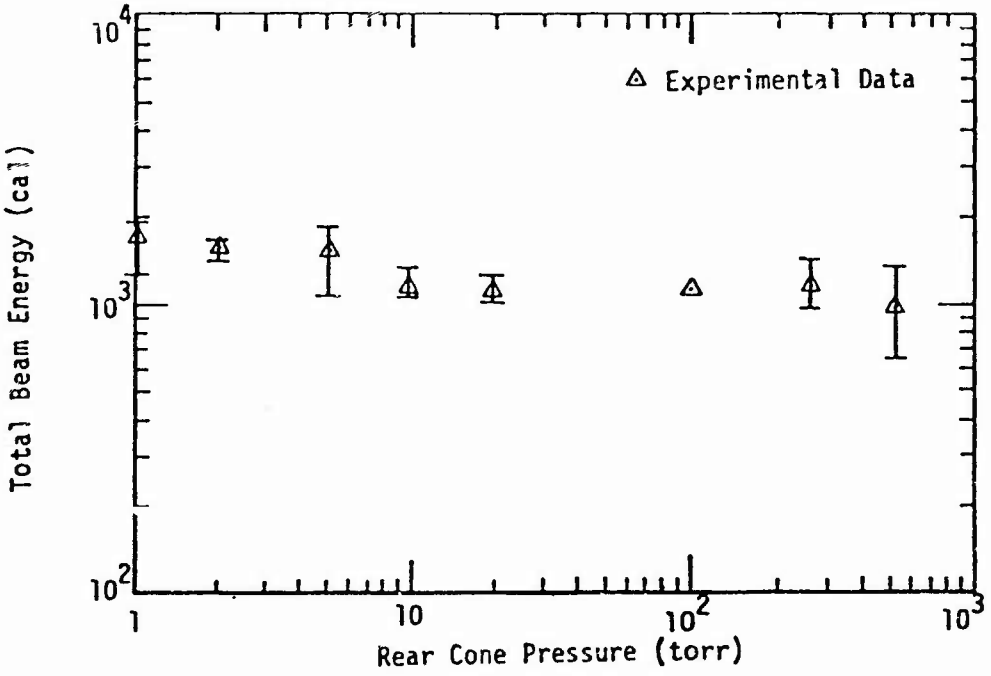

Figure 3-158. Total beam energy versus rear-cone pressure.

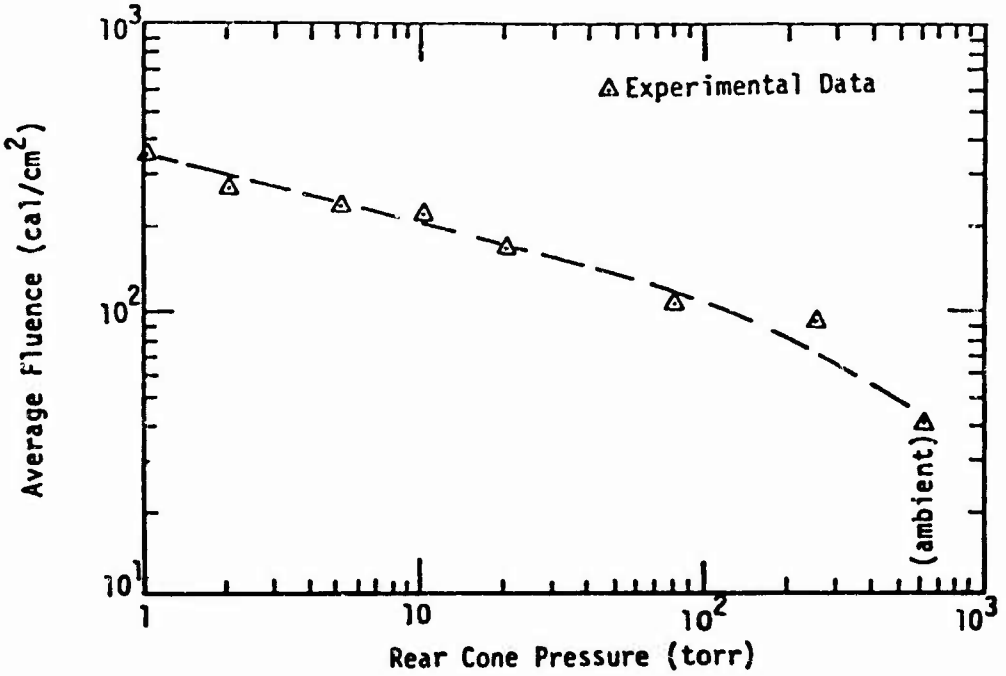

Figure 3-159. Average fluence near beam center line versus rear-cone pressure.

Figure 3-160 illustrates the REBA differential energy spectrum, normalized to 1 electron. The information was generated according to the technique briefly described above.

Energy Deposition. Energy-deposition profiles in REBA have been determined experimentally using linear-array calorimeters and a variety of other techniques. In addition, deposition profiles can be calculated from the I-V derived spectrum in conjunction with an electron transport code. Figures 3-161 and 3-162 compare measured deposition profiles, normalized to 1 cal/cm^2 in Fe and Mo, at nominal tube operating conditions, with code predictions for an average angle of incidence of 15 degrees. Another set of experimental data in C indicates the energy deposition is essentially independent of the incident-fluence level and, thus, independent of rear-cone pressure or position in the beam. The close agreement of experiment and theory tends to confirm the spectral prediction technique and to demonstrate the ability to calculate deposition profiles in other materials.

Low-Impedance Diode with Axial Magnetic Field. The low-impedance diode in REBA provides the capability for generating beam characteristics which maximize near-surface energy deposition in material samples. To accomplish this objective, tube V and electron energies below the initial design values, as well as increased diode I are required. These operating parameter changes are realized by inserting a low-impedance diode, which has a smaller overall length, larger cathode shank diameter, and close spacing between the cathode tip and anode.

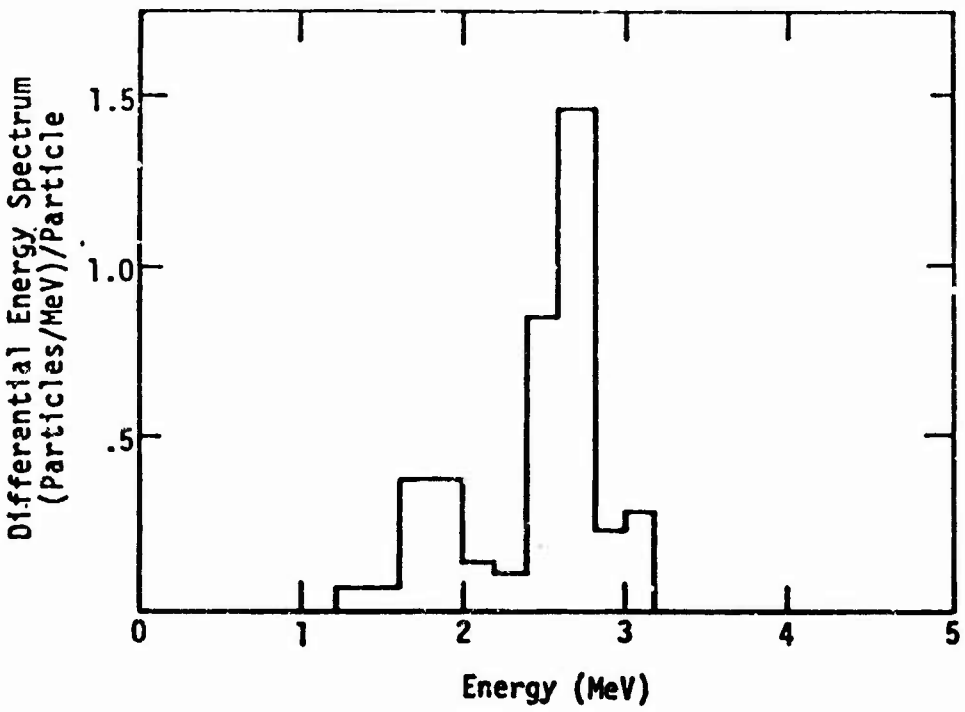

Figure 3-160. REBA electron energy spectrum.

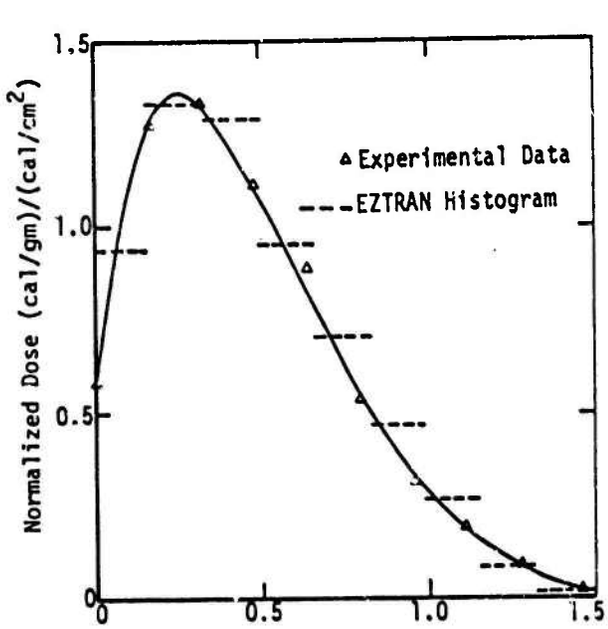

Figure 3-161. REBA energy deposition profile in Fe.

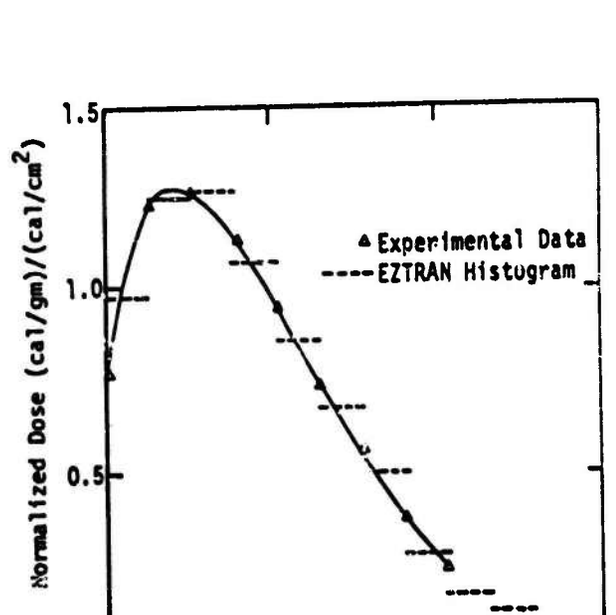

Figure 3-162. REBA energy deposition profile in Mo.

This configuration also allows external application of an axial magnetic (B_z) field in the anode-cathode region and drift tube to propagate the beam away from the tube face efficiently, to increase the fluence by magnetic compression, and to improve pulse reproducibility.

We must emphasize that the REBA facility does not provide the drift tube, the guide field solenoid of the magnetic compression coils. These components must be designed and fabricated by the experimenter to fulfill his requirements. The REBA staff will consult in the design to ensure mechanical compatibility with existing hardware and electrical compatibility with the capacitive energy bank for pulsing magnetic-field coils.

The principal variables of the low-impedance diode are the magnetic compression ratio, M, and the magnetic field strength at the anode, B_0. The nominal operating characteristics obtained with this low-impedance-diode/drift-region configuration are:

1.	Marx Generator	
	a. Charging V	70 kV
2.	Diode	
	a. Peak diode V	1 MV
	b. Peak diode I	100 kA
	c. Total beam energy	8 kJ (1,900 cal)
	d. Repetition rate	1 pulse/hr
3.	Target Electron-Beam Environment	
	a. Magnetic bottle ratio	1 to 5
	b. Transported beam energy	1,600 to 1,900 cal
	c. Peak fluence	>500 cal/cm^2
	d. Pulse width	70 ns

Low-Impedance Diode Output Waveform. Figure 3-163 presents beam power versus time waveforms calculated by using tube V and I traces. The peak output, normalized to unity in the figure, was 0.13 TW. The pulse width is approximately 55 ns between half-power points with the B_θ sensor and slightly narrower, 50 ns, using the Rogowski coil I measurement. Estimated accuracy of these determinations is ±10%.

Conditions of the pulse used in the illustrations of this section consisted of a 2.5-cm cathode tip with an anode-cathode spacing of 0.8 cm.

Low-Impedance Diode Electron Energy Spectrum. The REBA low-impedance diode electron energy spectrum is generally obtained from time-synchronized V and I traces. Digitized values of the tube V and I are processed, taking proper account of tube inductance. The differential energy spectrum of a sample low-impedance diode electron-beam pulsed operation, normalized to 1 electron, is illustrated in Figure 3-164.

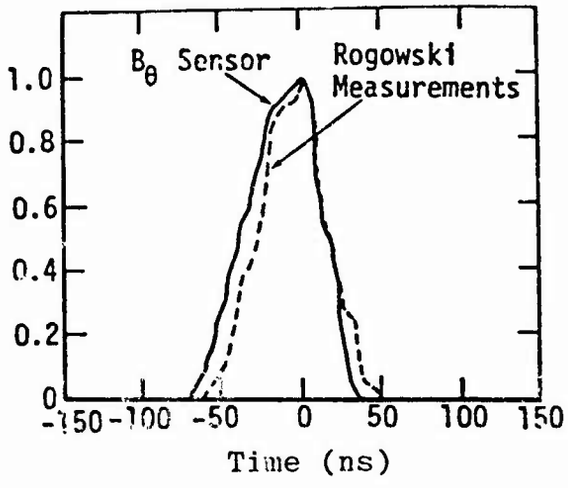

Figure 3-163. Low-impedance diode power output waveform.

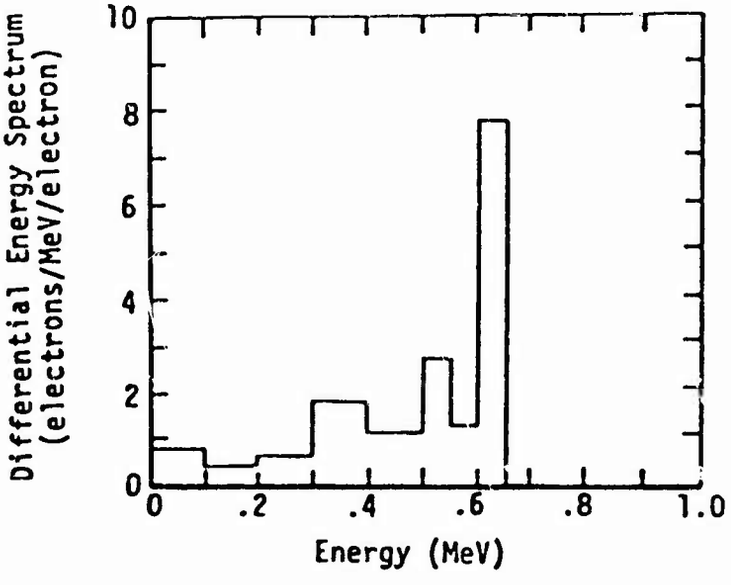

Figure 3-164. Low-impedance diode electron energy spectrum (with B_θ sensor).

Long-Pulse Electron-Beam Mode. Pulse forming for the long-pulse electron-beam mode of REBA is accomplished by eliminating intermediate energy storage in the Blumlein transmission line and impressing the Marx generator output V directly across the diode. Output-pulse V, therefore, approximately follows the slow-ramp-function increase, which is characteristic of the Marx generator and the tube impedance.

The drift chamber currently available for use is a cylindrical tube approximately 48 cm in length and 29.9 cm I.D. Beam propagation is aided by drift-tube evacuation and application of an axial magnetic field. The B-field strength is used as a primary control on fluence.

The Marx generator charging V for long-pulse-mode operation is nominally 90 kV. Peak diode V in the range of 1.5 to 2.2 MV are observed, with full width at half-maximum voltage of 0.5 to 0.8 μs. Peak currents are of the order of 20 kA, and the pulse width at half-maximum current is approximately 0.7 μs.

The system now operates with total beam energies of 6,000 to 10,000 cal delivered to a calorimeter located 40 cm from the anode. Energy conversion efficiencies of 35 to 50% of the Marx stored energy have been realized. The measured beam energy fluences range from 100 cal/cm^2 to approximately 400 cal/cm^2, depending primarily upon the strength of the external axial magnetic field and the cathode-emission area.

Experimenters interested in using the long-pulse mode should obtain the latest data from the REBA staff.

Environment Measurement Errors. The accuracy of calorimeters used in REBA measurements is estimated at ±20%. V waveforms from resistive/capacitive dividers are accurate to about ±15%. The I waveform measured by a B_θ sensor or Rogowski coil mounted in the anode chamber is accurate to about ±10%. Reproducibility of these monitors is estimated to be within 5%.

3.10.2.7 X-Ray Mode Environment

The REBA facility has pulsed bremsstrahlung output characteristics which are useful for many radiation effects experiments. There are currently 3 bremsstrahlung modes with sufficient history and adequate definition to be considered operational: (1) large area irradiation with the high-impedance diode, (2) long pulse, and (3) diode internal pinch. In this section, the dose and dose rate capabilities of these modes are summarized to enable a potential experimenter to determine the usefulness of REBA in his proposed application.

High-Impedance Diode Dose Maps and Beam Profiles. Figure 3-165 presents the total x-ray dose/pulse at measurement positions along the tube axis as a function of distance from the anode. Approximately $1/R^2$ dependence can be observed at distances in excess of 15 cm. Off-axis determinations of photon dose at 0, 25, 50, and 75 cm from the anode surface are depicted in Figure 3-166. It is observed that, at all distances shown, beam uniformity normal to the tube axis is reasonably good over an area of approximately 80 cm^2. Large-scale transverse profiles are shown in Figure 3-167. The measurements exhibited good azimuthal symmetry of the exposure pattern.

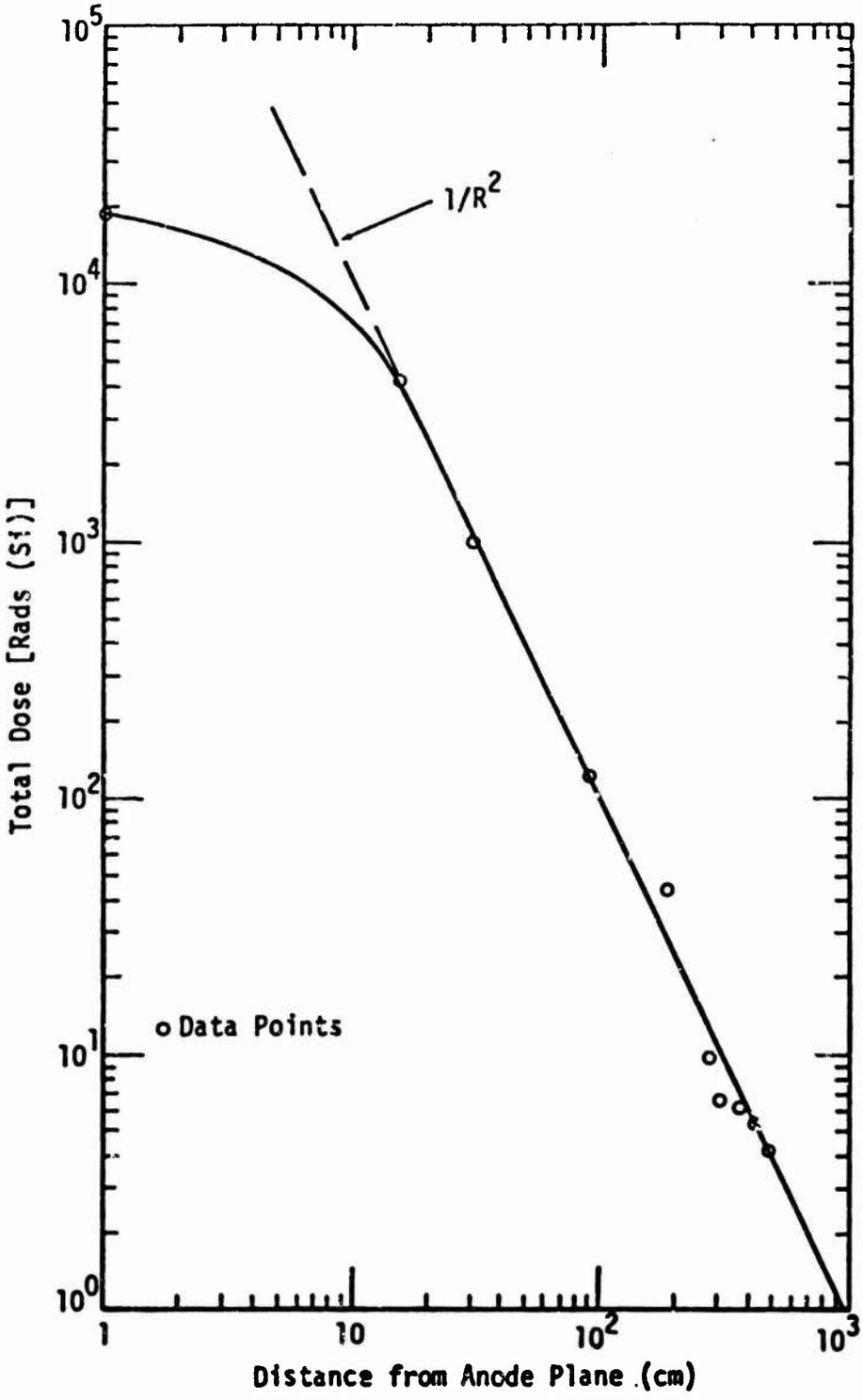

Figure 3-165. High-impedance diode dose/pulse as a function of distance from the tube surface.

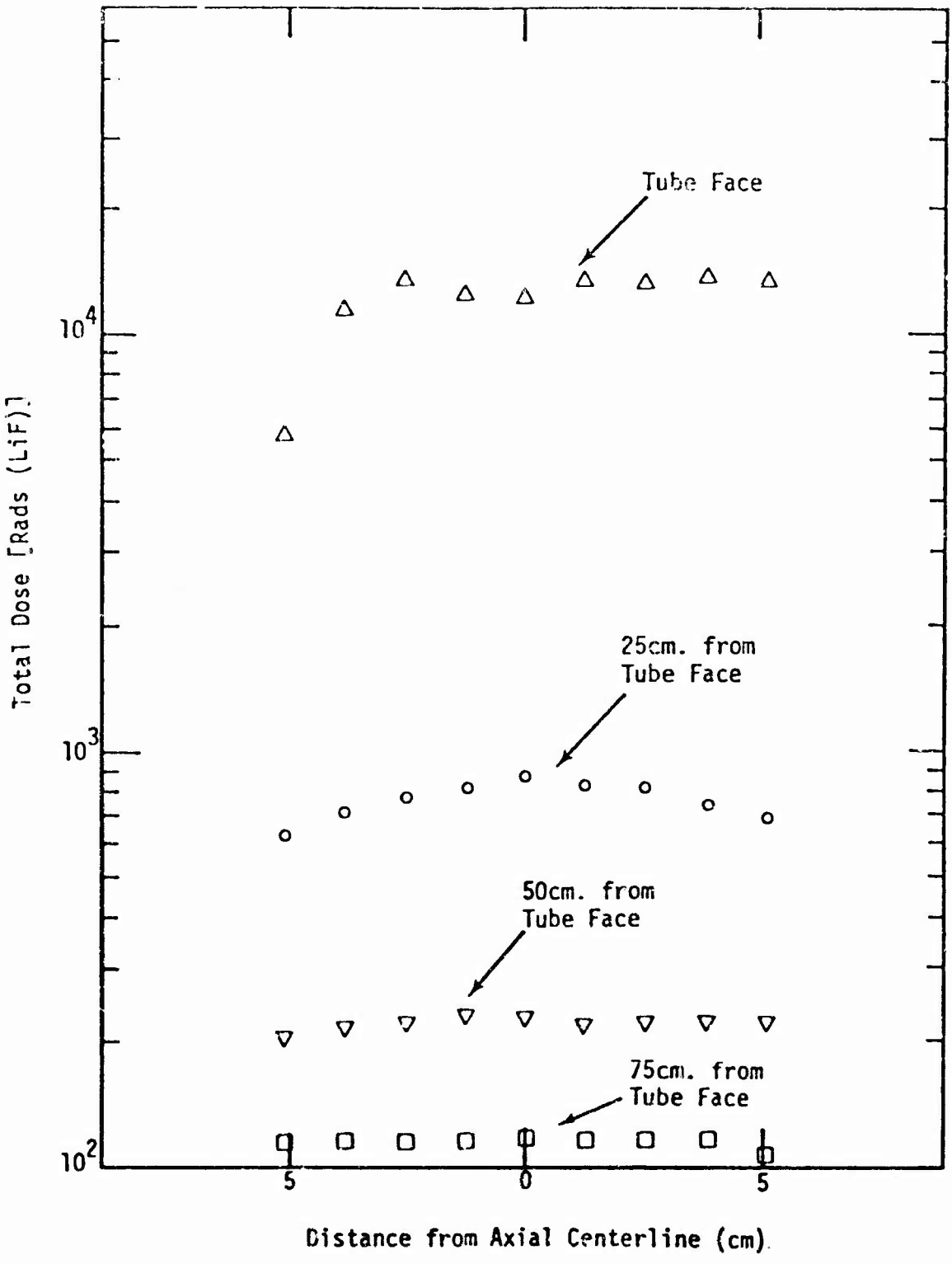

Figure 3-166. Photon beam profiles normal to diode axial center line.

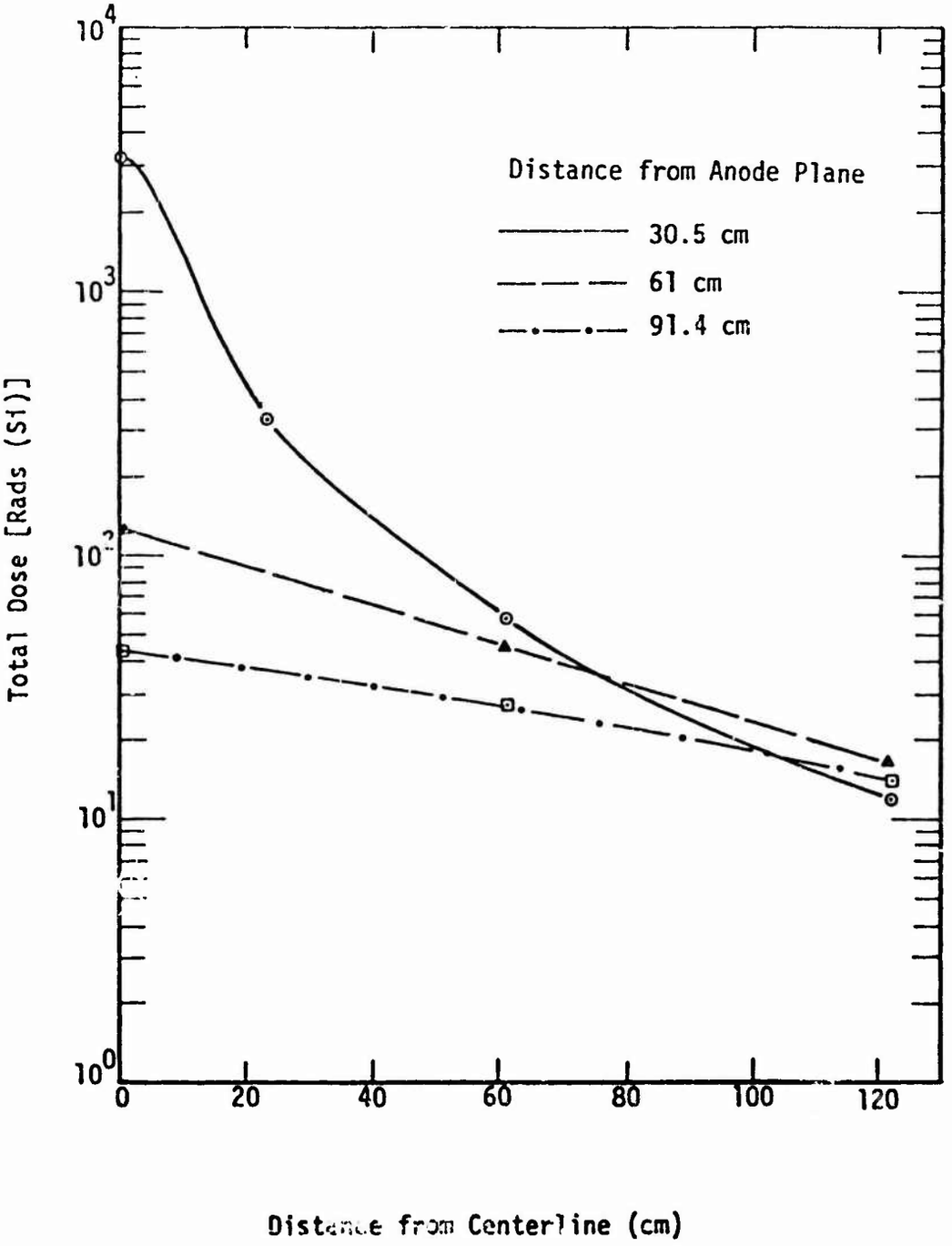

Figure 3-167. Photon beam large-scale profiles normal to the diode axial center line.

Output Waveform and Dose Rate. Photon-dose-rate measurements were obtained using a 25-μm thick PIN detector of area 25 mm^2, and were photographically recorded from the oscilloscope trace. The detector was located at a sufficient distance from the machine to assure linear response. No evidence exists to expect any substantial pulse shape difference as a function of position in the test cell. Figure 3-168 is a reproduction of the PIN-detector output signal obtained during a REBA operation, normalized to a peak dose rate of unity. Pulse width at half-maximum dose rate is approximately 50 ns.

X-Ray Spectrum. The photon energy spectrum of the high-impedance diode x-ray output has not been measured. However, a calculated spectrum is illustrated in Figure 3-169. A computation of a photon energy spectrum was performed using an electron energy spectrum, determined from digitized tube V and I waveforms. Electron transport and photon generation in the anode materials were simulated using the 1-dimensional Monte Carlo code.

Long-Pulse X-Ray Mode. Potential applications for a pulse width of the order of 1 μs, with a limited dose rate, could utilize the long-pulse x-ray mode of operation. The diode V and I waveforms of a long-pulse operation are illustrated in Figure 3-170. These have been combined acording to the computer program techniques, which correct for the tube inductive effects to determine the beam power plot shown in Figure 3-171. Note that the full pulse width at half-maximum beam power is approximately 440 ns.

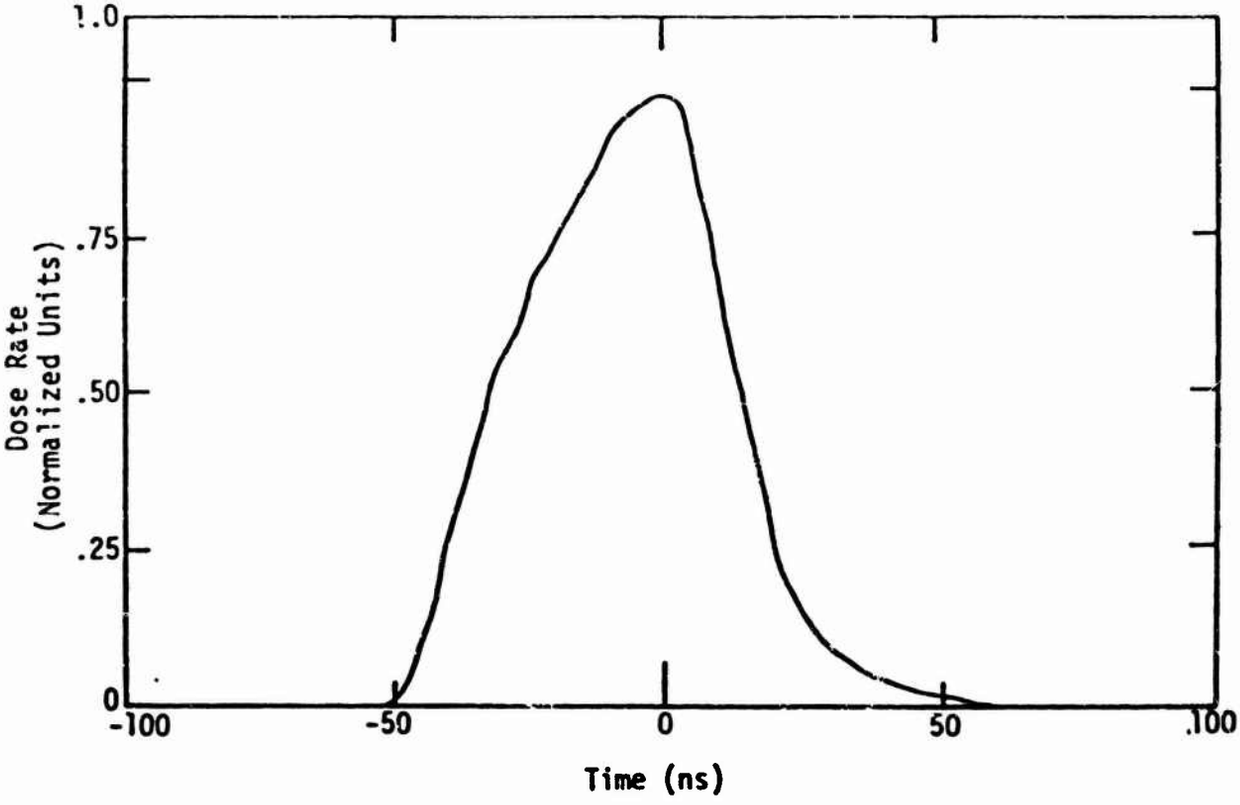

Figure 3-168. Photon dose rate versus time.

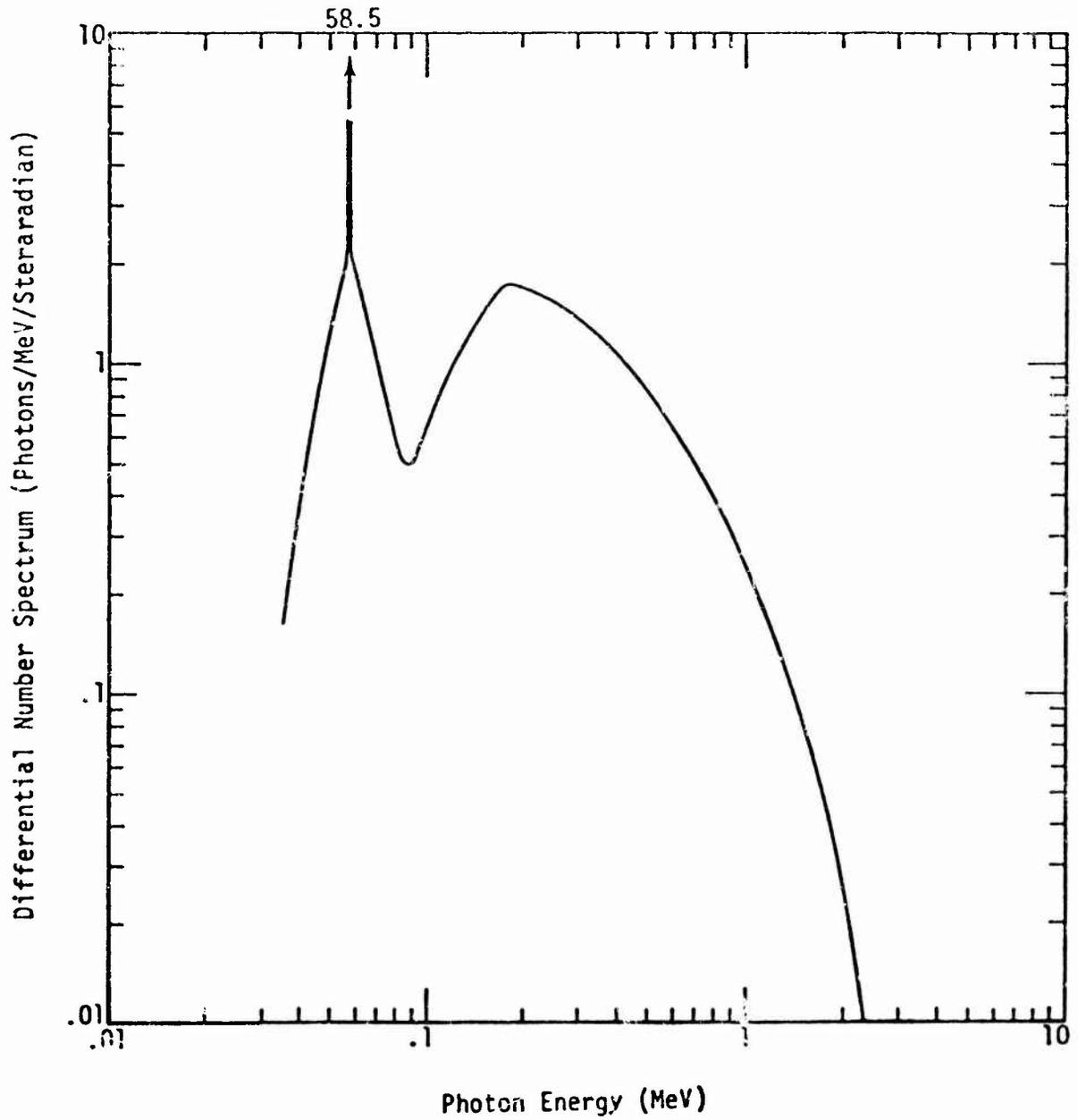

Figura 3-169. REBA high-impedance x-ray mode photon spectrum.

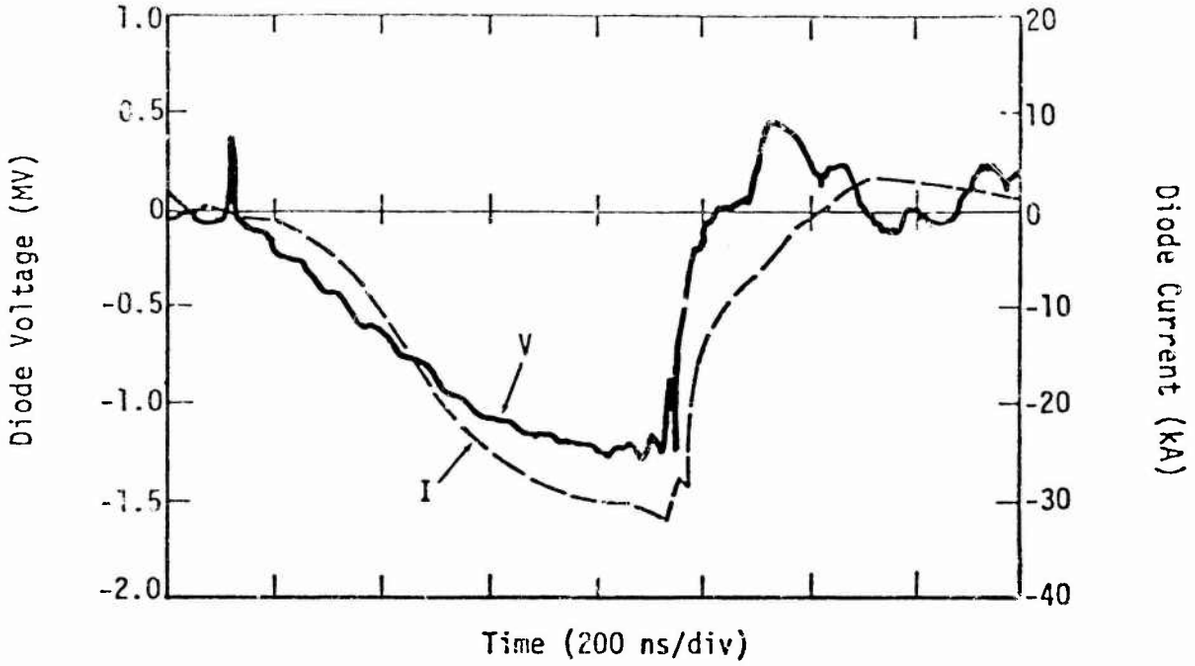

Figure 3-170. Long-pulse-diode V and I waveforms.

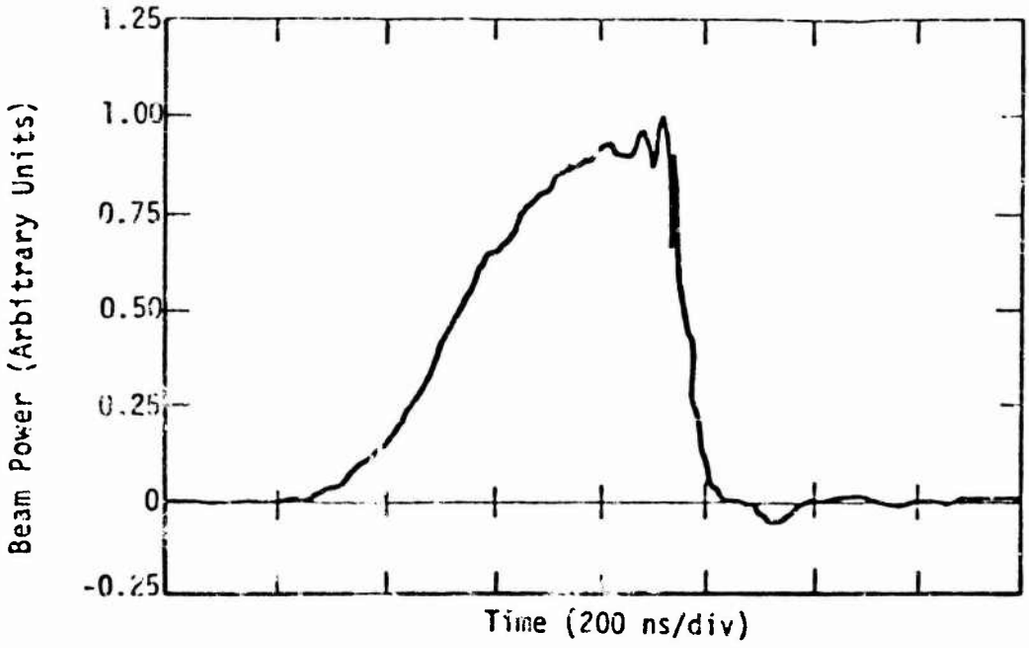

Figure 3-171. Long-pulse beam power waveform.

X-ray output measurements were taken at the anode plane and at locations 14.6 cm from the faceplate. Figure 3-172(a) is a PIN diode output signal from a monitor on the beam center line at the anode plane. The total dose obtained at this point was 2.5×10^4 rad(Si), corresponding to a peak dose rate of approximately 7.0×10^{10} rad(Si)/s. Figure 3-172(b) presents similar results for the exposure position on the beam axis, 14.6 cm from the anode. The total dose was 2.8×10^3 rad(Si). Several repetitions of the measurement have been taken at the second position, with results ranging from 1.3×10^3 to 2.8×10^3 rad(Si). Total dose, measured 5 cm off center line at the 14.6-cm location, indicates an integrated exposure which is approximately the same as that on-axis.

Experimenters interested in using the long pulse should consult the REBA staff for the current status.

Internal Pinched-Beam X-Ray Mode. The REBA internal pinched-beam x-ray mode is obtained by employing a bremsstrahlung converter within the low-impedance diode.

A summary of internal pinched-beam x-ray mode data is presented in Table 3-16. The converter, denoted as 0.5-in. tungsten carbide, is a total-stopping graphite plate in which a 1.27-cm dia. tungsten carbide disk is embedded. The 0.25-in. tungsten carbide target is similar, except that the tungsten carbide disk is only 0.64 cm in dia. The standard 0.051-cm Ta converter is the third target denoted in the summary. Reproductions of typical Compton diode output waveforms, normalized to unity peak, are illustrated for 2 of these converters in Figure 3-173.

Using the tungsten carbide/graphite converter in this mode will provide a nearly point source, and it has been used in radiography experiments. Total dose/pulse is of the same order as the high-impedance mode. However, because of the narrow pulse shape, of the order of 25 ns, peak dose rate is approximately 8×10^{11} rad/s. The spectrum will be softer than that of the high-impedance diode x-ray mode because of the lower V_{tube}.

With a Ta converter, the total dose in the internal pinched-beam mode is smaller than that available from the high-impedance diode, and dose rates are approximately the same. The photon spectrum for this arrangement is illustrated in Figure 3-174.

Environment Measurement Errors. Data shown in Figures 3-165 and 3-167 were taken with CaF_2 TLD-400 TLDs. The dosimeters are calibrated in rad(Si) using the Sandia Gamma Irradiation Facility, a Co-60 source. Reported measurements for Figure 3-166 were obtained with LiF TLDs, calibrated on the Co-60 source. Uncertainty in the absolute total dose is approximately ±10%.

Operating experience has indicated the following standard deviations within a continuous series of nominally identical REBA high-impedance diode x-ray pulses:

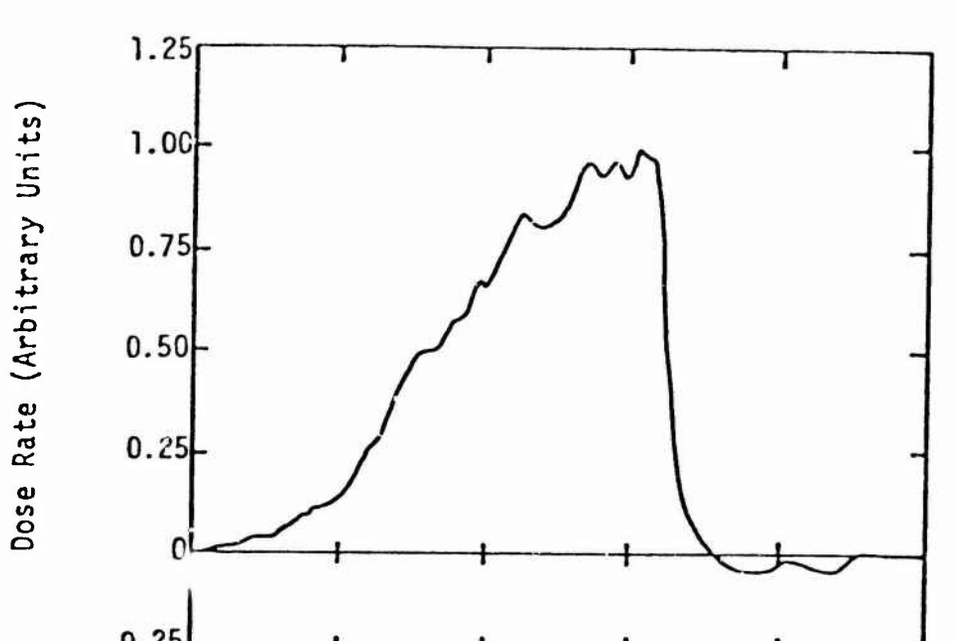

a) Anode Plane

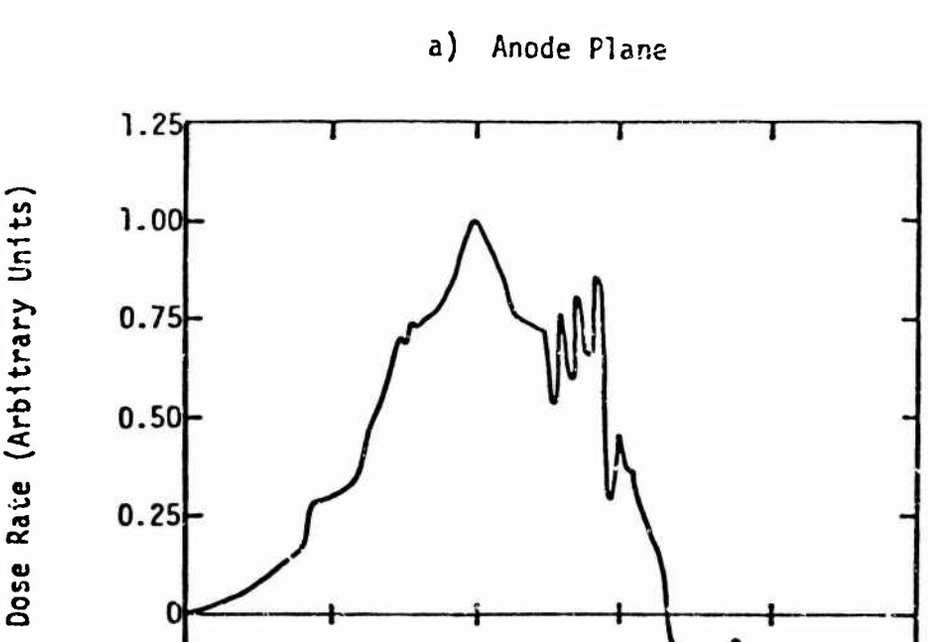

b) 14.6 cm from Anode Plane

Figure 3-172. Long-pulse photon dose rate versus time.

Table 3-16. Pinched-beam x-ray mode data synposis.

Shot	Converter	Anode Cathode Gap (cm)	V_{tube} (MV)	Compton Diode Data		
				Full Width Half Maximum (ns)	Time to Peak (ns)	Center Line Dose at Anode rad(Si)
7252	0.5" WC	1.27	1.83	34	104	1.55×10^4
7253	0.5" WC	1.27	1.94	18	100	1.47×10^4
7256	0.25" WC	1.27	1.73	34	96	1.60×10^4
7259	0.25" WC	1.27	[illegible]0	29	104	1.91×10^4
7260	0.25" WC	1.27	1.78	22	120	1.88×10^4
7261	Std. Ta	7.62	2.40	22	84	5.00×10^3
7262	Std. Ta	7.62	2.39	26	84	3.70×10^3
7263	Std. Ta	7.62	2.22	34	92	3.87×10^3
7264	Std. Ta	7.62	2.44	32	84	5.00×10^3
7265	Std. Ta	7.62	2.44	32	80	5.37×10^3
7266	Std. Ta	7.62	2.28	32	80	4.90×10^3
7267	Std. Ta	7.62	2.40	34	80	5.20×10^3
7361	0.25" WC	1.90	1.89	29	109	2.44×10^4

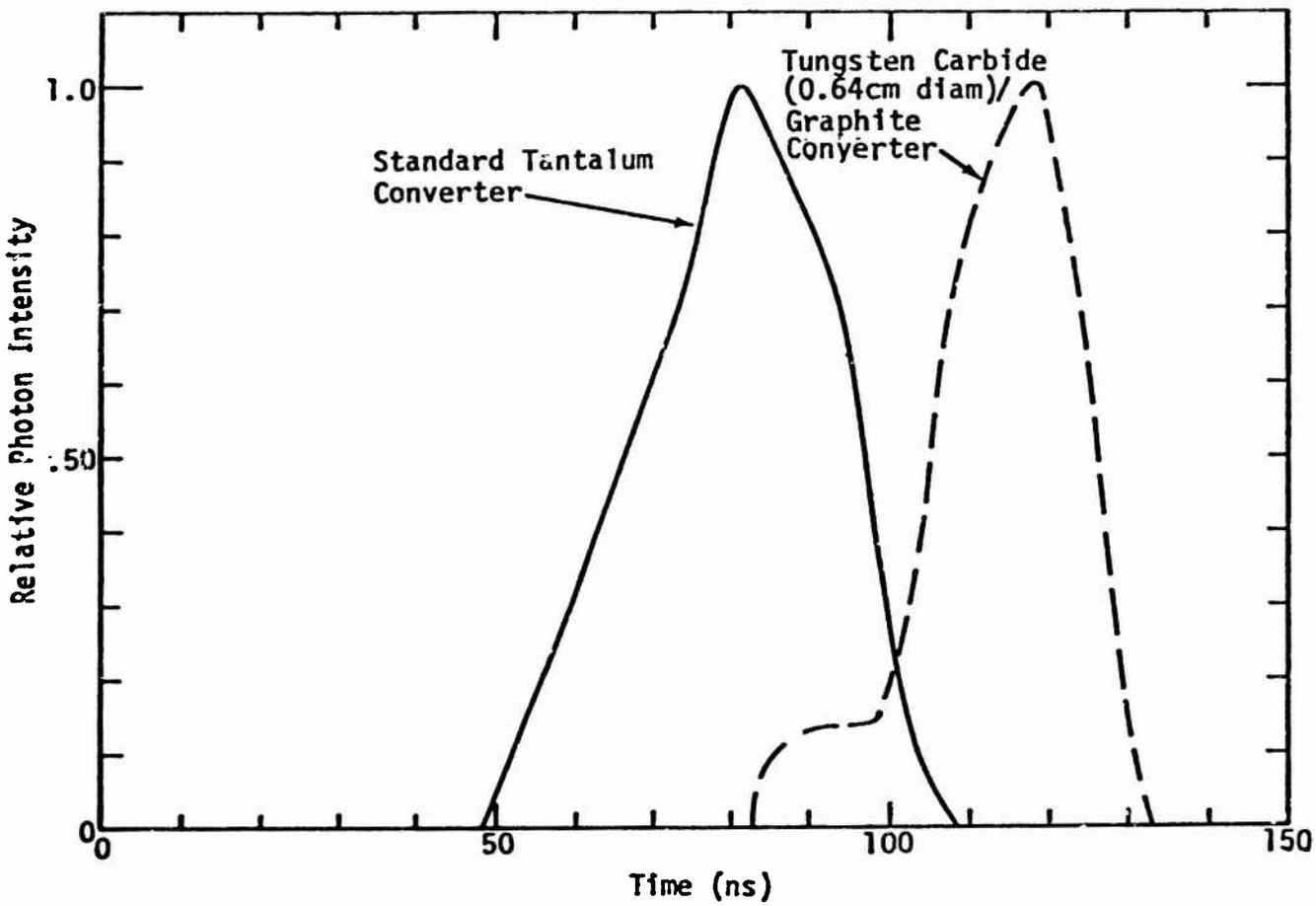

Figure 3-173. REBA photon output versus time (Compton diode monitor output normalized to unity peak).

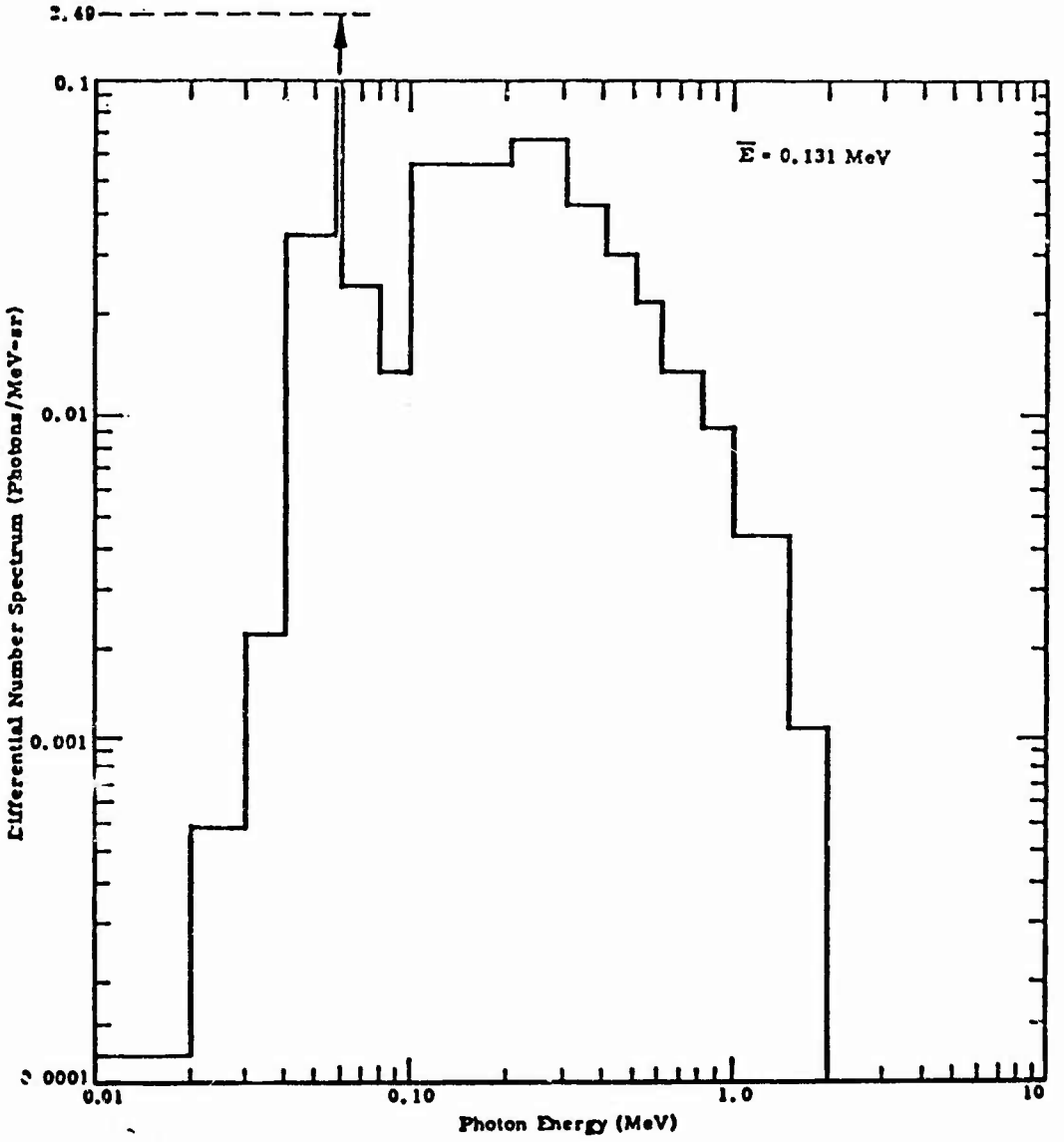

Figure 3-174. Internal pinched-beam x-ray mode photon energy spectrum (forward 30 degrees). (Anode-cathode gap spacing is 7.62 cm and the anode is a 0.051-cm Ta converter (0.051-cm Ta, 0.823-cm C, and 0.051-cm Al).)

1.	Tube V	± 5%
2.	Tube I	± 5%
3.	Total dose/pulse	±20%

There may be additional variance between 2 nominally identical series which are separated by changes of machine configuration, or an extended time interval.

3.10.3 REHYD

The north side of the REBA Facility was modified to accommodate a low-impedance water transmission line. For reference and operation identification, the modified line is known as REHYD. REHYD is a high-energy, pulsed, field-emission bremsstrahlung x-ray source which also can be operated as an electron-beam generator. It was designed and constructed by Sandia Laboratories to provide an energy source of short duration for x-ray exposure of weapon systems and components, and for determining material responses to rapid energy deposition. The principal components of REHYD are a Marx generator, a water-insulated transmission line, and an output tube. Stored low-V energy is converted to high-V energy by the Marx generator and then transferred to the transmission line, which serves as a fast-discharge, pulse-forming, low-inductance energy source for the output tube.

The Marx generator consists of a bank of capacitors which are charged in parallel and discharged in series by means of spark gap switches. The negative-V output of the Marx generator is placed on the coaxial transmission line consisting of an energy-storage section, a self-breakdown main switch, a prepulse switch, and a pulse-forming line. The V pulse formed by the transmission line is impressed across the tube diode which consists of an insulating and vacuum-holding structure, a field-emission cathode, and an anode.

For the electron-beam mode of operation, the anode used is a thin low-Z target which allows passage of electrons with minimal energy loss. External magnetic-beam compression is generally utilized to focus the extracted electron beam for maximum energy deposition into a specific test specimen. The anode converter assemblies used for the x-ray mode of operation are thick high-Z targets selected for maximum efficiency in converting electron-beam energy into bremsstrahlung x-radiation.

3.10.3.1 Performance Characteristics

Performance characteristics of REHYD are as follows:

1. Marx Generator

a.	Charging V	85 to 90 kV
b.	Repetition rate	1 pulse/2 hr
c.	Energy stored (maximum 100-kV charge)	95 kJ

2. Diode

a.	Peak diode V	1.3 MV
b.	Peak diode I	300 to 600 kA
c.	Total beam energy	36 kJ

3. Electron-Beam Environment

a.	Transported beam energy	20 to 25 kJ
b.	Peak beam power	0.4 TW
c.	Pulse width (FWHM)	80 ns

4. X-Ray Environment

a.	Peak dose/pulse	7 cal/gm in 1-mil Au
b.	Pulse width (FWHM)	80 ns

Output Waveform. Figure 3-175 is a reproduction of a PIN diode output signal obtained during a REHYD pulse. Because the shape is independent of position and V level, an arbitrary scale has been used on the ordinate. The REHYD diode-cathode configuration is usually adjusted to obtain maximum integrated area under the curve, which in turn produces maximum energy deposition. The FWHM dose rate is approximately 80 ns. Estimated accuracy of the value is ±5 ns.

Electrical Noise. RF interference measurements were made in the vicinity of the REHYD experimenter area. Peak electric fields of 5.7 kV/m are detected during a REHYD firing. However, proper use of available screen rooms and instrument vans, and shielding of the experiment and signal cables significantly reduce the RF interference to an acceptable level. Shielding systems enable gathering of zero-time data that are of the order of 100 mV in magnitude.

Diagnostic Techniques. The electron-beam energy fluence measurements are obtained by using total-stopping graphite calorimeters. One-mil gold discs in the vicinity of the target are used for x-ray measurements. V and I traces are sampled by B_θ or Rogowski coils and displayed on oscilloscopes. TLD-400 (CaF

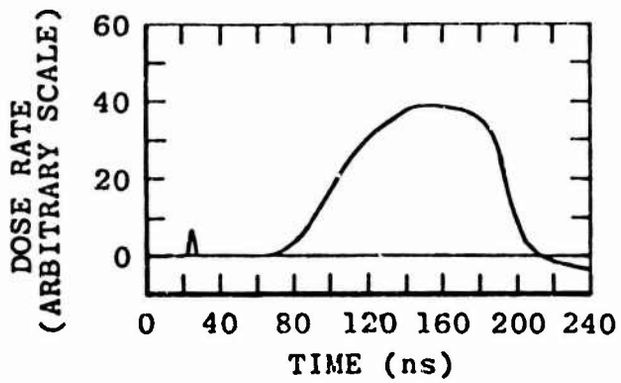

Figure 3-175. REHYD PIN diode pulse shape.

and LiF) TLDs are used for measurement of bremsstrahlung output. The Sandia Gamma Irradiation Facility, a Co-60 source, is used for calibration purposes. Time-dependent x-ray measurements are made by using PIN detectors.

3.10.3.2 Electron-Beam Mode Environment

Electron-Beam Energy Spectrum. Electron energy spectra are generally obtained from time-synchronized V and I data which are processed through a transient digitizer and computer system. A hard copy is produced for every shot. Figure 3-176 illustrates the REHYD differential energy spectrum drawn from Shot #2009.

Total Beam Energy. The total beam energy is derived from a plot of the integral of the generated power curve in W/s and by applying the proper conversion factor to obtain the energy in joules. Figure 3-177 represents a typical energy plot redrawn from a computer hard copy.

Repetition Rate and Reproducibility. Pulse repetition is 1 shot in 2 hr, because of diode cleaning and target replacement. The standard deviation in dose/pulse is 15%, with a maximum deviation of approximately 25% from the mean. Pulse delay and pulse jitter are nominally 6 μs and 100 ns, respectively. Pulse delay is measured from the occurrence of the Marx generator trigger signal to time of peak value of the anode-cathode gap I. Pulse jitter is given as the maximum variation from the mean in pulse delay.

Beam Geometry. The spatial distribution of energy within the REHYD is a function of the cathode-diode, drift chamber size, and configuration. Figure 3-177 was obtained using an exposure area of 9 cm^2. Other configurations are available with exposure areas ranging from 0.3 cm^2 to 35.8 cm^2. Calorimetric measurements are made prior to, and/or during, each shot.

Environment Measurement Errors. The accuracy of the calorimeter used in REHYD measurements is estimated at ±20%. Values from V and I output waveforms are accurate to ±7%. Reproducibility of both monitors is estimated to be within 5%.

3.10.3.3 X-Ray Mode Environment

X-Ray Converter Assemblies and Diode Configuration. Composite assemblies of high-Z materials, such as Ta, along with graphite and kevlar which serve as absorbers and debris catchers, are used to convert the electrons into bremsstrahlung x-radiation. Performance characteristics with a Mod II diode, drift chamber, B_z coil, and a 9-cm^2 exposure area are shown in Table 3-17. The magnetic compression ratio was 2:1.

Photon Energy Spectrum. Monte Carlo calculation techniques were used to generate the bremsstrahlung energy spectrum (Figure 3-178) using as input an electron energy spectrum determined from traces of diode I and V. For these calculations, the peak anode-cathode gap V was assumed to be 1.0 MV, and peak I was assumed to be 325 kA. As a low-resolution check on the spectral data, the ratio of dose (1-mil Au) to dose (LiF TLD-400) was calculated to be 15, which is in reasonably good agreement with the measured value of 13. Additional spectral

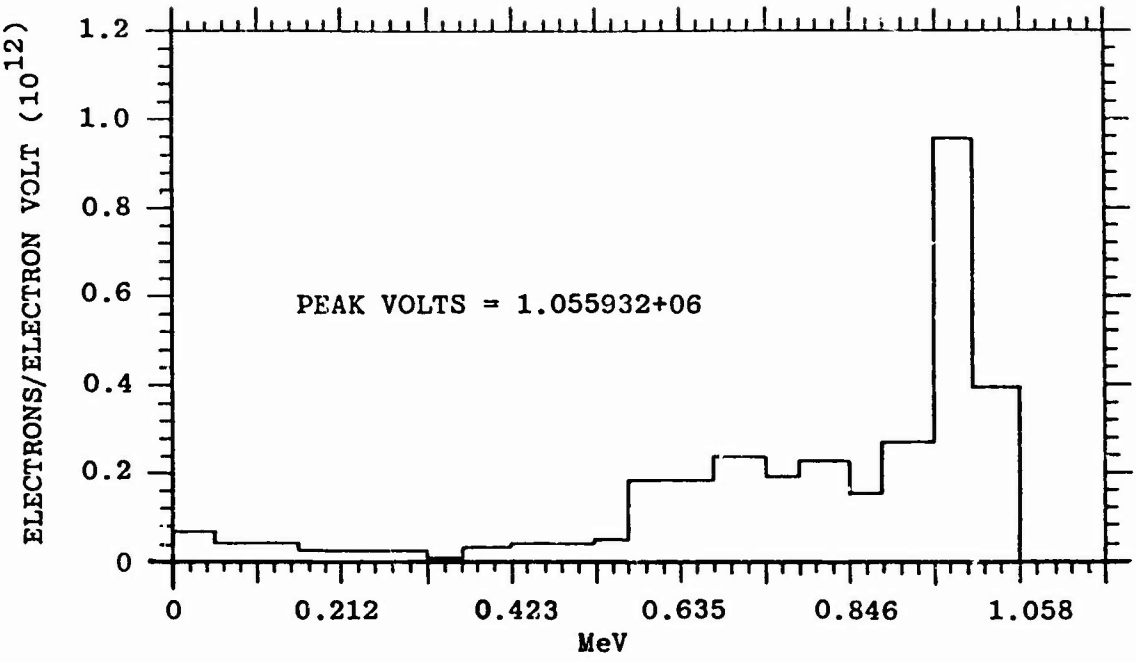

Figure 3-176. Electron-beam energy spectrum.

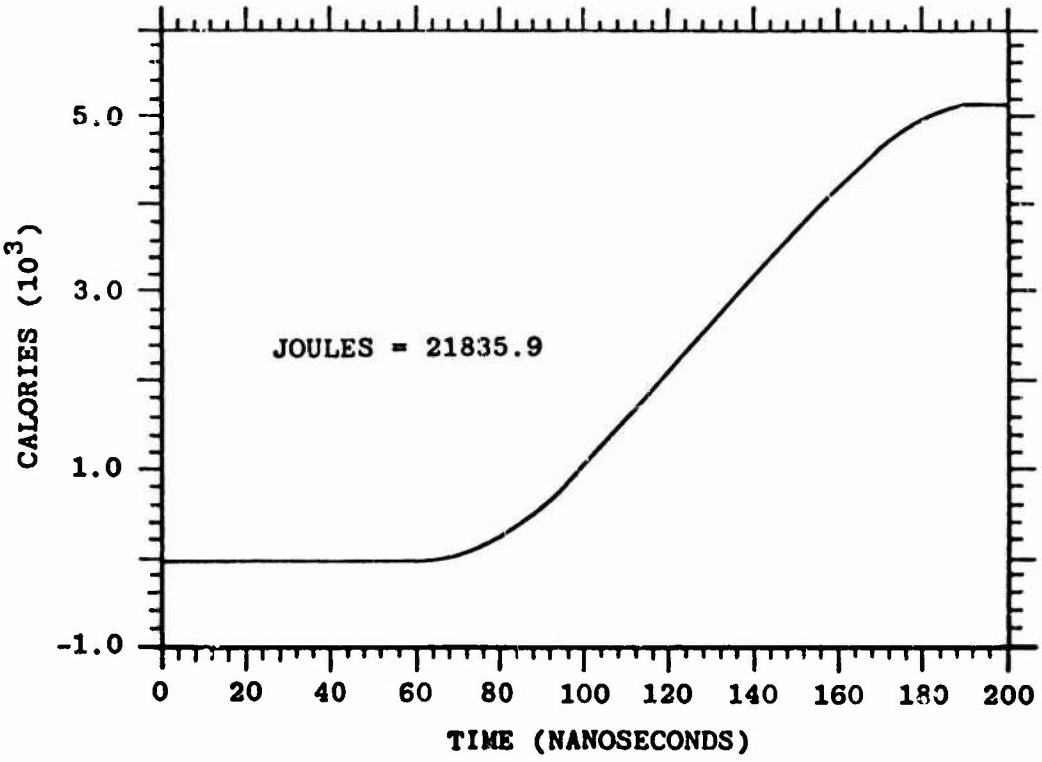

Figure 3-177. Total-beam energy.

Table 3-17. REHYD performance characteristics with MOD II diode configuration and advanced converter assembly.

Diode Design	V_{max} (MV)	I (MA)	Δt_p (ns)	E_B (kJ)	$Dose_{max}$ (cal/g)	Δt_{brem} (ns)	Exposure Area (cm^2)
Mod II	1.2	0.30	170	20-25	7	90	9

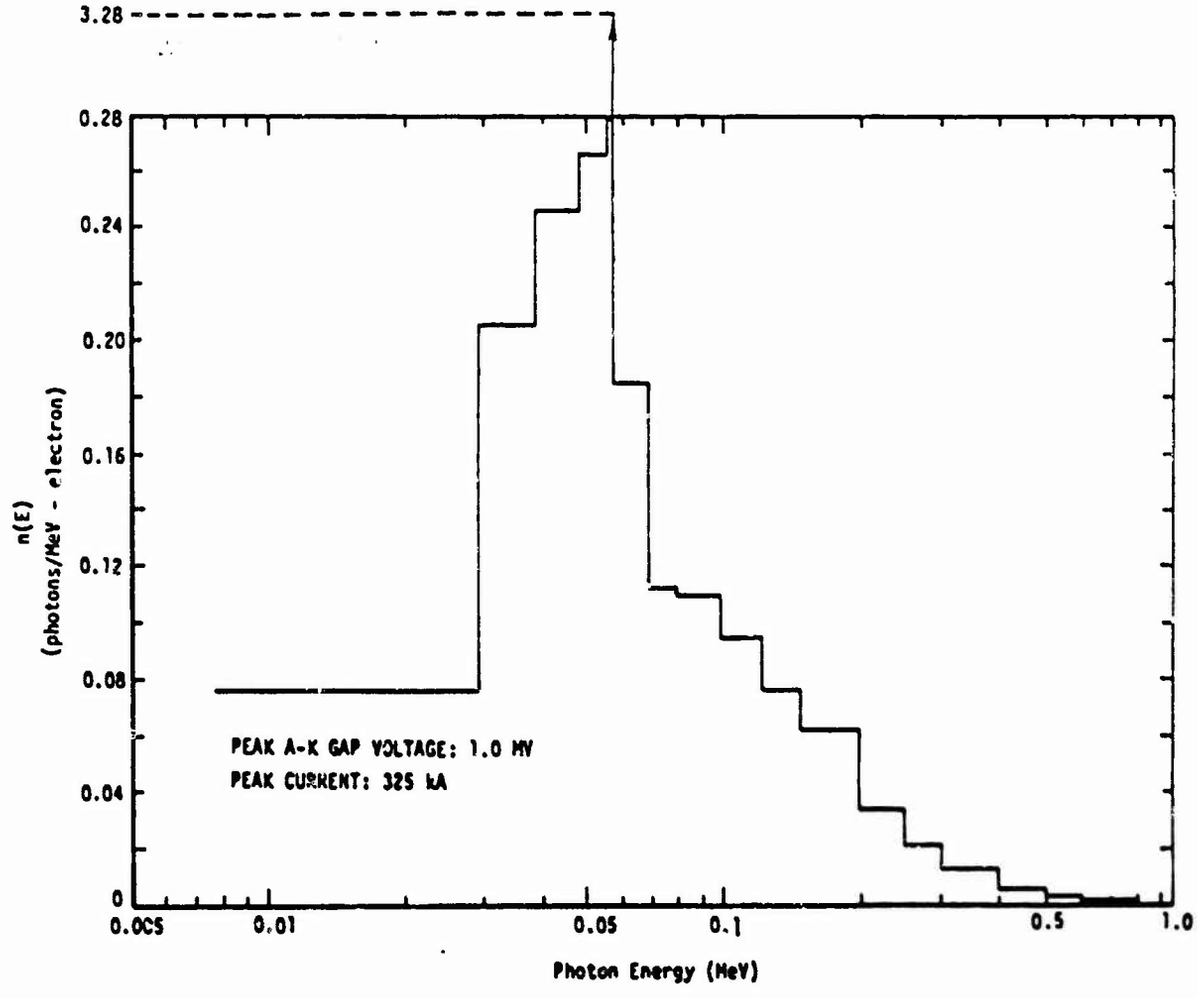

Figure 3-178. Calculated REHYD photon energy spectrum for Shot No. 282.

data were obtained with filter-fluorescence measurements, and comparisons of these measured spectra with theoretical results are shown in Figures 3-179 and 3-180.

Environment Measurement Errors. The accuracy and reproducibility of REHYD x-ray dosimetry measurements (1-mil Au) within an environment range of 0.25 to 10 cal are ±5%.

3.10.4 Experimental Facilities

3.10.4.1 Location

HERMES II, REBA, and REHYD occupy Building 6596 in Sandia Laboratories Technical Area V. A map of the area, which is located approximately 8 km (5 mi.) south of the main technical area, is given in Figure 3-181.

3.10.4.2 HERMES II Test Area

Figure 3-182 shows the physical layout and dimensions of that section of the building containing the HERMES facility. Also shown is an area south of the building where a user can place his own instrumentation vans. Entry into the facility is provided by the 3.88-m-wide by 6.1-m-high (12.75-ft by 20-ft) door into the test cell or by the 3.6-m-wide by 6.1-m-high (12-ft by 20-ft) roll-up door on the south side of the building. The screen room next to the shield wall is for the experimenter's use.

When HERMES is pulsed, no one is permitted beyond the sliding gate; users will normally remain in the experimenter's area, outlined by a dashed line in Figure 3-182.

3.10.4.3 HERMES II Test Cell

A detailed plan view of the HERMES test cell is shown in Figure 1-183. The drawing is to scale and indicates the area available for use by the experimenter. Particular items of which the experimenter should be aware include:

1. A metal grating platform 3 m by 7.9 m and 1.8 m above the floor (10 ft by 26 ft by 6 ft) occupies the entire floor area of the test cell. When the platform is in place, the beam center line is 1.66 m (5.45 ft) above the grating. The actual test volume measures approximately 6 m (20 ft) in width and 3 m (10 ft) in depth. The inset in Figure 1-183 is an elevation drawing showing this configuration.
2. An instrumentation cable boom, 3 m (10 ft) in length, is mounted on the south wall of the test cell at a height of 2.44 m (8 ft) above the platform. Attached to the boom are two extension arms, each 1.52 m (5 ft) in length. Both the boom and the arms can be swiveled to various positions. Extending from the instrumentation boom to the cross plates on the arms are solid RF shieldings (conduits)

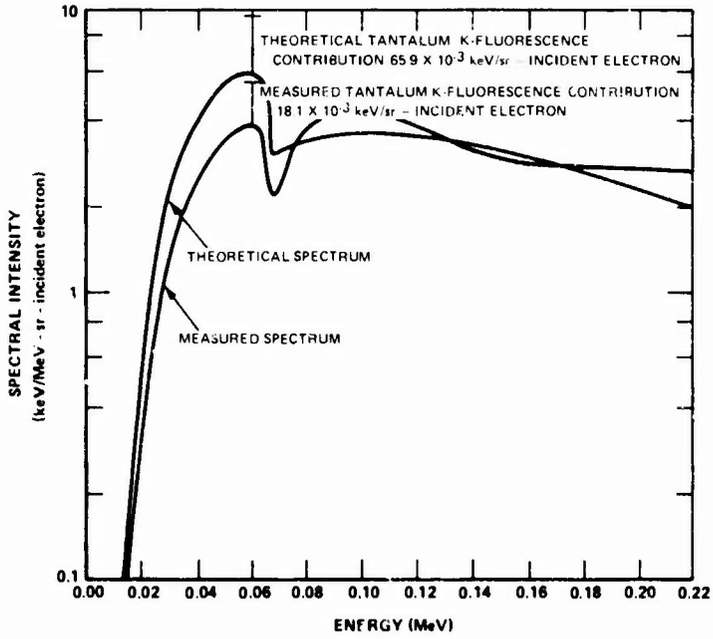

Figure 3-179. REHYD x-ray spectra along forward-directed normal to converter for energies less than 0.2 MeV (normalized to 1.0 keV/sr-electron).

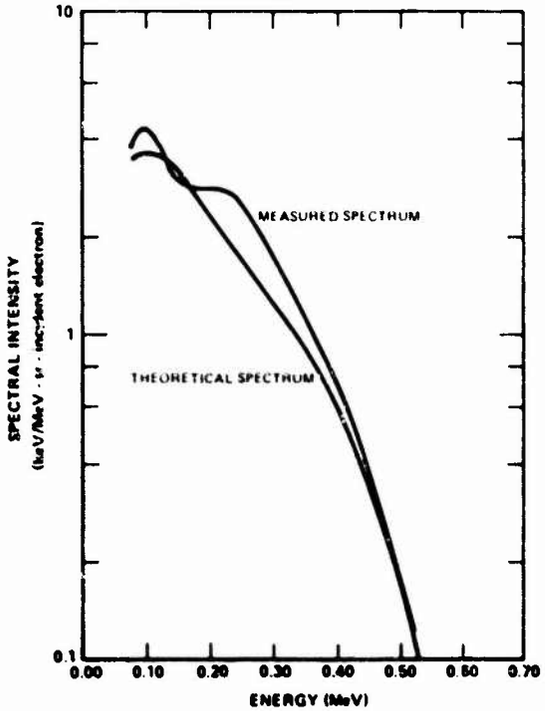

Figure 3-180. REHYD x-ray spectra along forward-directed normal to converter for energies greater than 0.1 MeV (normalized to 1.0 keV/sr-electron).

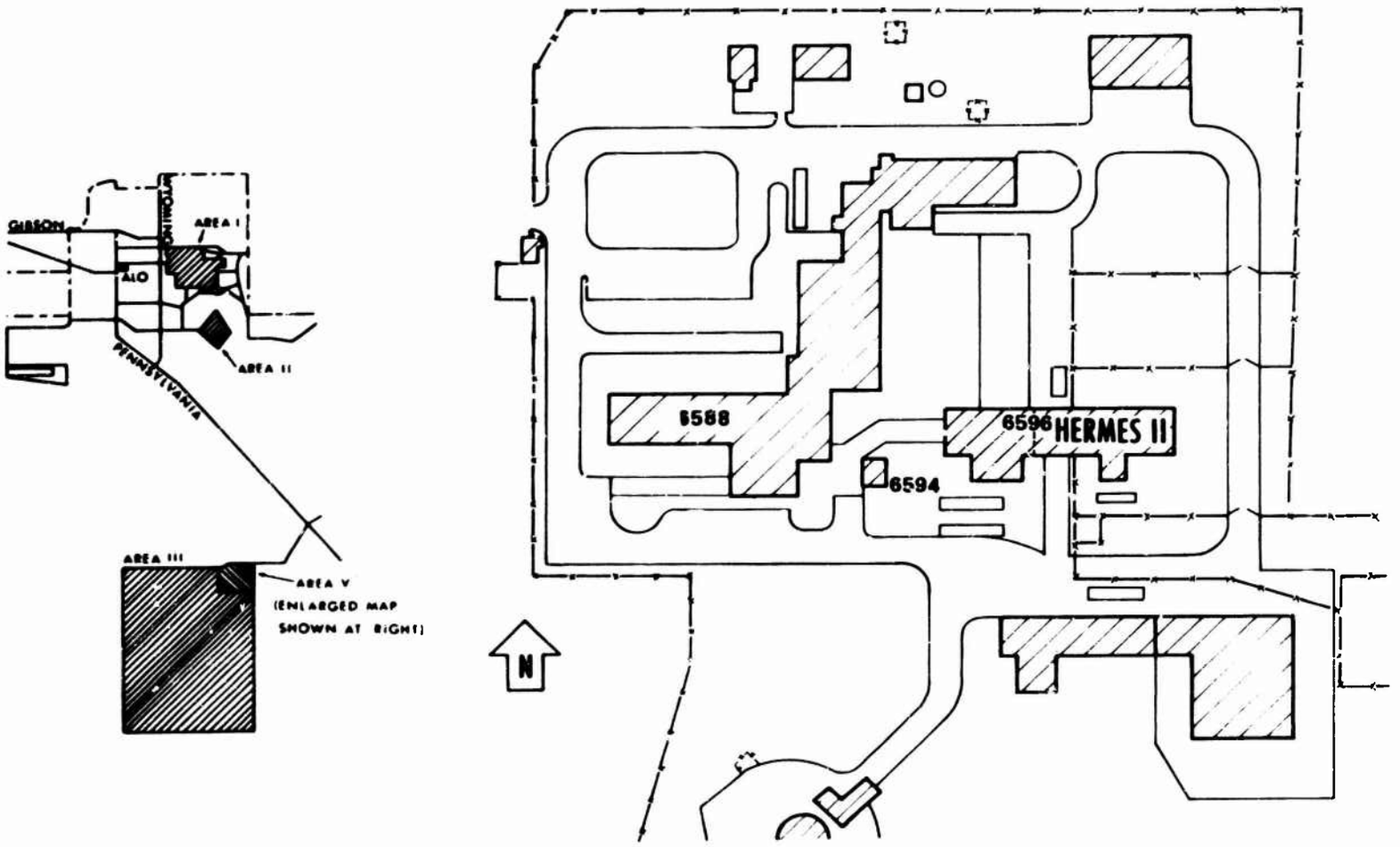

Figure 3-181. Map of Sandia Laboratories Technical Area V.

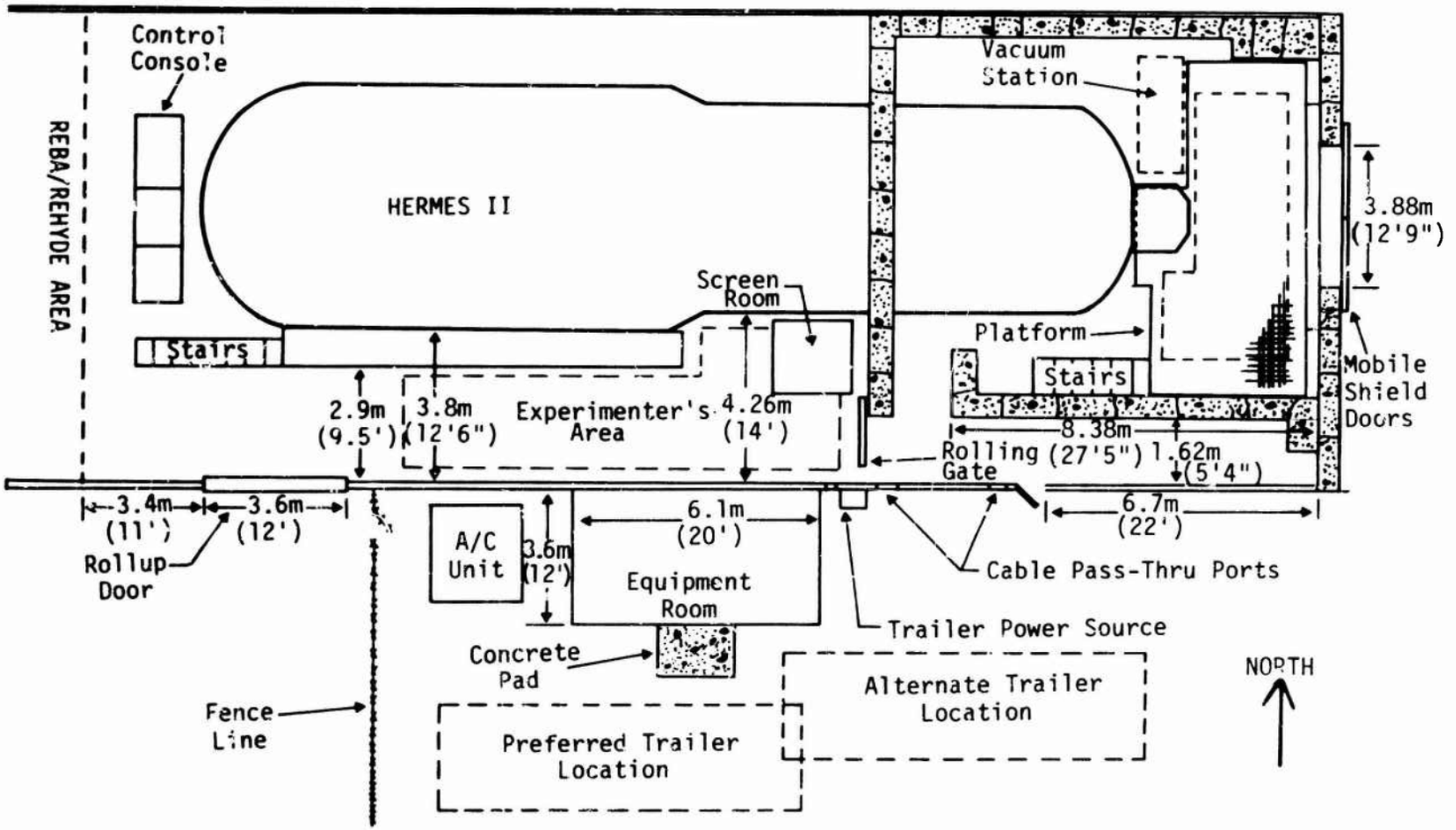

Figure 3-182. HERMES II facility area in Building 6596.

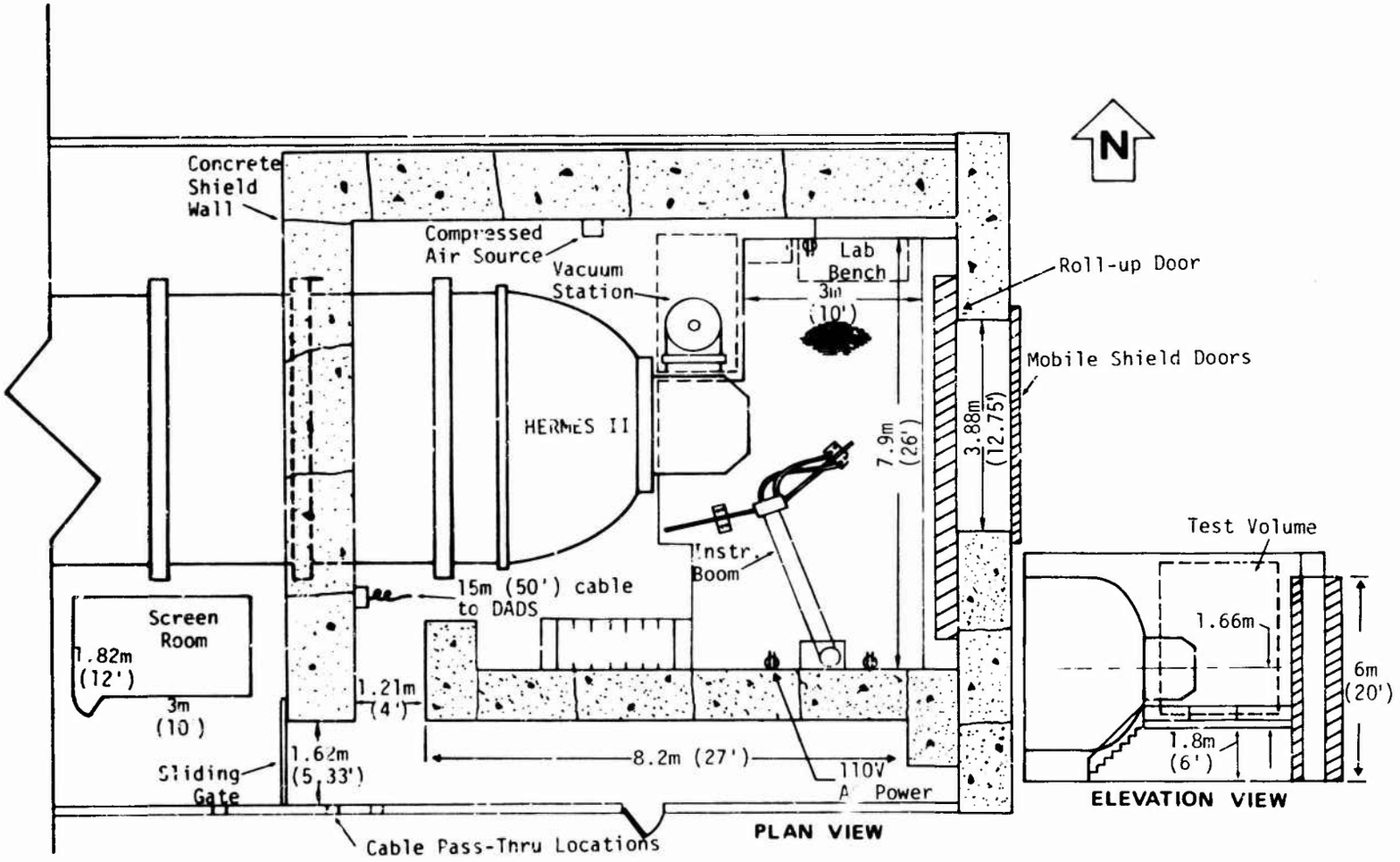

Figure 3-183. Detail plan view of HERMES II test cell and inset showing an elevation view.

which terminate in flexheads. These conduits shield coaxial cables that connect directly to the instrumentation vans outside the building.

3. There are 3 electrical power junction boxes in the test cell, as indicated in Figure 1-183. Each box has 4 outlets providing 110-V, 1-ϕ ac power.

An overhead crane with 1,800-kg (2-ton) capacity is available to lift large or heavy experimental equipment within the HERMES II test cell. The facility normally provides any other equipment necessary for handling heavy items.

A mobile hydraulic table, with dimensions of 1 m by 2 m, is provided for positioning experiments in the HERMES test cell. The table top can be adjusted in height and can lift a maximum of 1,800 kg (4,000 lb). Equipment tiedown points are provided by numerous recesses in the concrete shield wall of the test cell which exposes steel reinforcing bars.

3.10.4.4 REBA Test Area

Figure 3-184 shows the physical layout and dimensions of that section of the building containing the REBA facility. The REHYD accelerator and test cell is shown in dashed lines. The Marx generator located between the two transmission lines is used to charge both machines. The screen room located under the platform adjacent to the Marx generator is for the experimenter's use.

A roll-up door, 6.1 m (20 ft) high and 6.1 m (20 ft) wide, on the west side of the building, provides access to the REBA area.

3.10.4.5 REBA Test Cell

A detailed plan view of the REBA test cell is shown in Figure 3-185. The drawing is to scale, and indicates the area available for use by the experimenter. Particular items of which the experimenter should be aware include:

1. The vacuum station located under the anode chamber cannot be moved.

2. An instrumentation cable boom, 2.1 m (7 ft) in length, is attached to the north wall of the test cell at a height of 2.1 m (7 ft) above the floor. It is on a hinge, allowing it to be swiveled to various positions. Extending 1.5 (5 ft) beyond the end of the boom are lengths of mu-metal flex shielding hose. Each contains coaxial cables and terminates in a flexhead. The flexhead mates the experiment's cables to those going directly to the instrumentation vans.

3. Approximately 3 m (10 ft) of multiconductor shielded cables enter the test cell through a port in the floor next to the west wall. This cable connects the cell with the DADS, which is used to record calorimeter data.

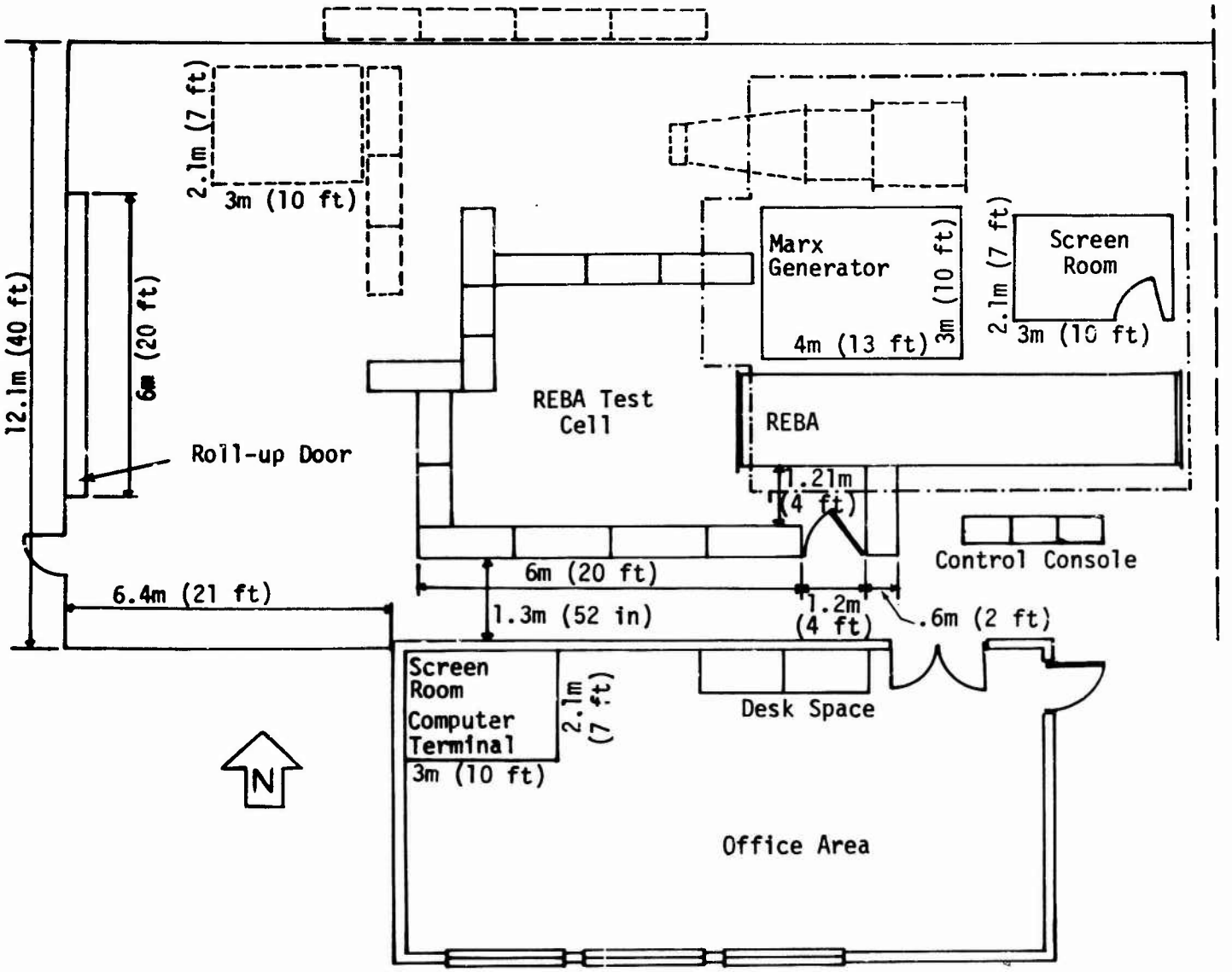

Figure 3-184. REBA facility area in Building 6596.

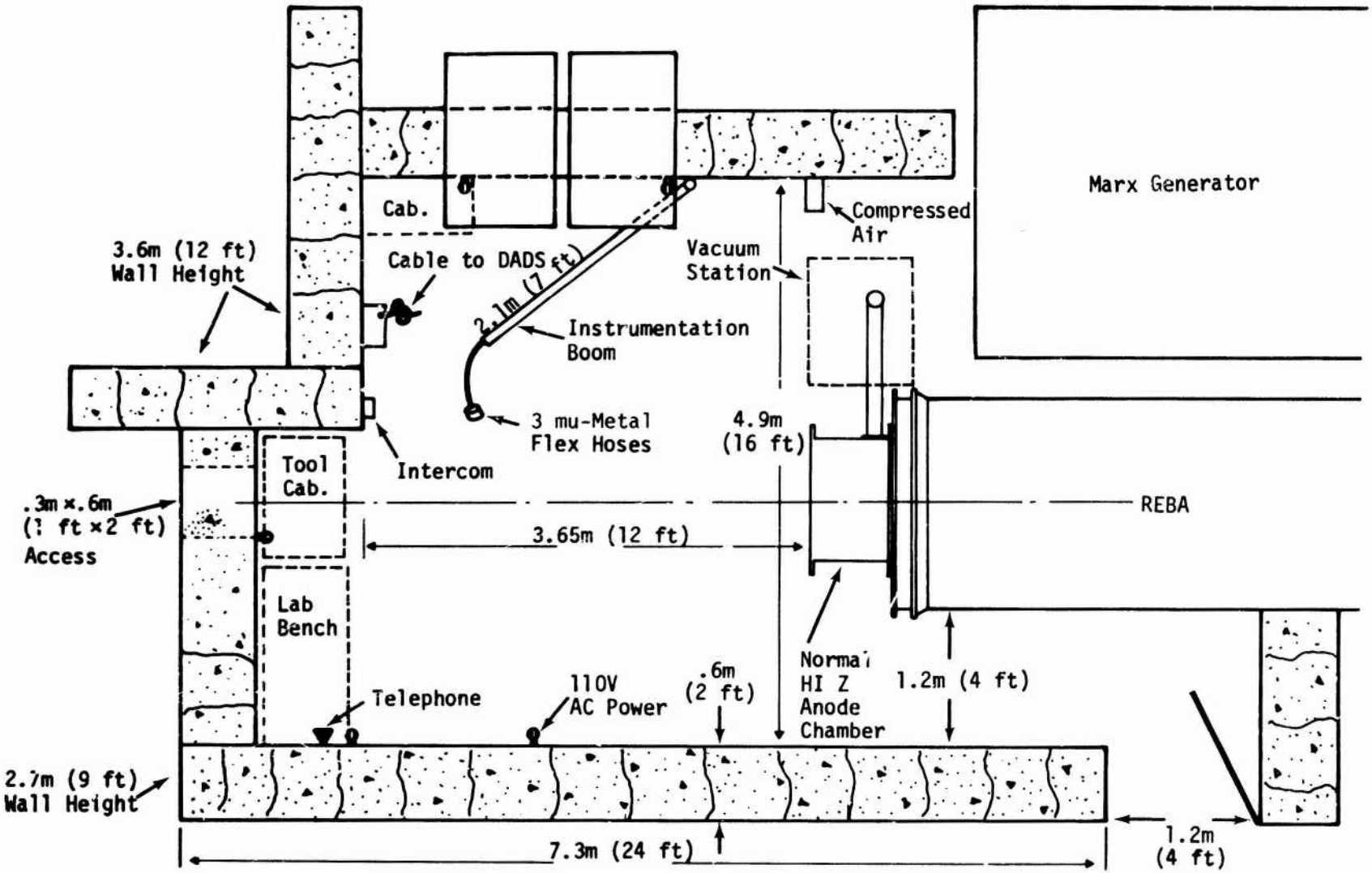

Figure 3-185. Detailed plan view of REBA test cell.

4. There are 5 electrical power junction boxes placed on the shield wall at various heights above the floor. Each box has 4 outlets providing 110-V, 1-ϕ ac power.

5. Power also can be supplied to the experiment through the RG 214/U cable from the instrumentation van. The power level supplied is limited to the V and I which can be safely transmitted over the coaxial cable.

6. Two 20-kV, 56-kJ capacitor banks are located on the cell wall; these can be operated in parallel.

7. A compressed-air extension hose is located on the wall near the vacuum station.

8. In the west wall of the cell is a rectangular port, approximately 0.3 m by 0.6 m (1 ft by 2 ft) in size. It is centered 1.66 m (65.5 in.) above the floor in the line of sight of the REBA beam. The port, which usually is filled by a concrete plug, provides visual access to an experiment during exposure.

9. An intercom system connects the test cell with the control console and the instrumentation van.

Access to the facility is through the roll-up door previously mentioned. For experimental equipment which is too large to fit through the test cell door, an overhead crane with 5,400-kg (6-ton) capacity is available to lift the apparatus into the test cell. The facility normally provides any other equipment necessary for handling heavy items.

There are several tables available for positioning an experiment in the REBA beam. Equipment tiedown points are provided by numerous recesses in the concrete shield wall of the test cell which exposes steel reinforcing bars.

3.10.4.6 REHYD Test Area

The physical layout of REHYD and building access area with respect to the REBA facility are shown in Figure 3-184.

3.10.4.7 REHYD Test Cell Area

A plan view of the REHYD test cell, which is located on the north side of the REBA facility, is illustrated in Figure 3-186.

The Marx generator, capacitor banks, control console, and an extended screen room are shared by both accelerators. In general, REHYD is equipped with similar utilities and power as described in the REBA test cell.

3.10.5 Instrumentation and Instrument Vans

3.10.5.1 Screen Rooms and Electronics

Walk-in screen rooms adjacent to the experimenter's areas are for use by the experimenter. Each has four 110-V, 1-ϕ ac power outlets in 4 junction boxes in

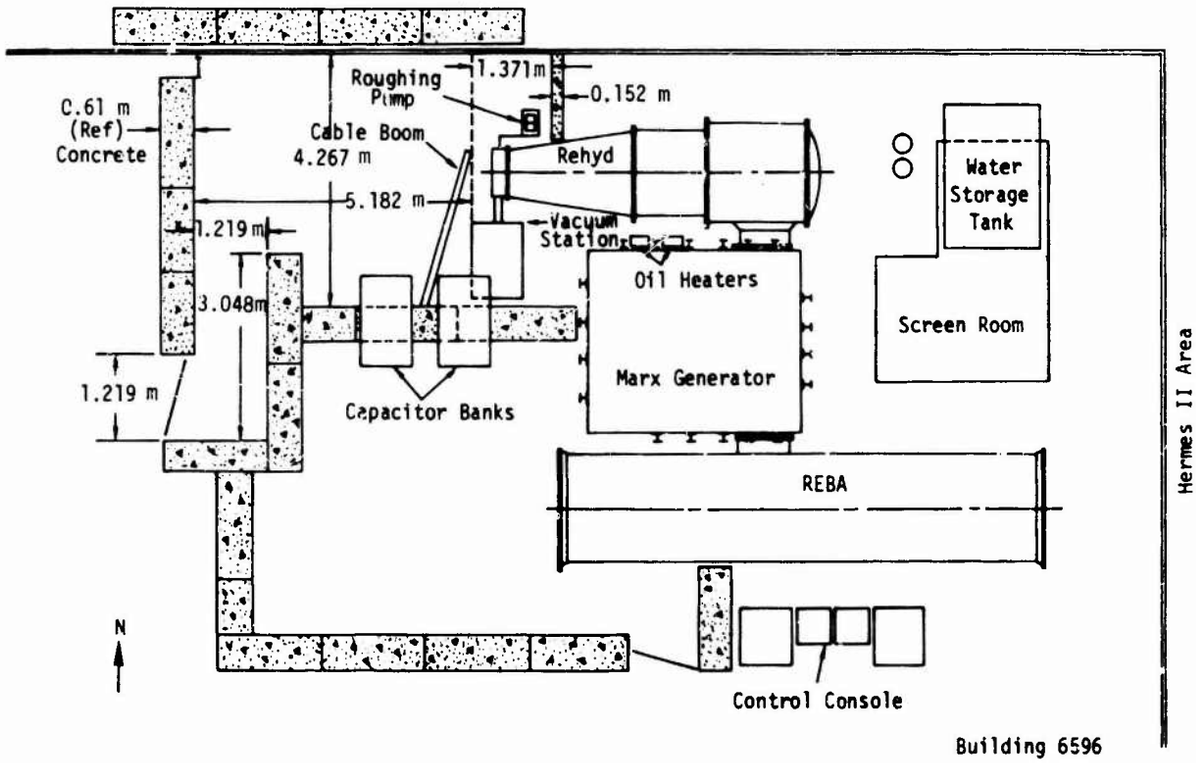

Figure 3-186. Layout of REHYD and north radiation cell.

the room. Electronic signals are passed between the screen room and the test cell by means of a wall panel containing 15 HN feedthrough bulkhead connectors. Also, the panel has 4 waveguides of 4 cm (1.5 in.), 5 cm (2 in.) and 10 cm (4 in.) dia. for passing cabling through the wall. Shielded cabling, which must be provided by the experimenter, should be at least 18.3 m (60 ft) long to reach from the screen room to the HERMES test cell and 9.15 m (30 ft) long for REBA and REHYD.

Specialized monitoring equipment for FXR experiments normally must be provided by the user. A limited number of oscilloscopes are presently available (for use in the screen rooms) as a part of the normal facility use charge. In addition, completely equipped Sandia Laboratories instrument vans are located adjacent to Building 6596 and are available to experimenters on a supplemental contractual basis. These are described in the following paragraph.

3.10.5.2 Instrumentation Vans

The HERMES, REBA, and REHYD facilities are supported by instrumentation vans from Sandia Laboratories Field Instrumentation Department (1120). Personnel from this department set up and collect data and are available to advise the experimenter on the use of the instrumentation and to offer suggestions for best utilization of this capability. Use of the instrument vans and consultation with the instrumentation group is recommended.

The vans are connnected to the HERMES test cells by RG/214 50-ohm coaxial cables, RG/22B cables, and twisted-pair shielded wires. The cables are protected by solid RF shielding (conduit) over all but the last 1.5 m (5 ft) in front of the accelerator, where triaxial cable is used instead. As an option, 5:1 cable equalizers (Hi-pass filters) can be placed in series with the coaxial cables to compensate for high-frequency signal loss.

The following is a current list of the instrumentation and systems available in the vans for experiment support:

1. Oscilloscopes*

Manufacturer	Model	Sensitivity		Bandwidth	Qty.
HP	183D	Horizontal:	1 ns/div to 50 ns/div	250 MHz	15
		Vertical:	0.01 V/div to 1 V/div		
Fairchild	757F	Horizontal:	50 ns/div to 2 s/div	100 MHz	17
		Vertical:	0.02 V/div to 40 V/div		

2. Signal Generators

Manufacturer	Model	Purpose	Qty.
Tektronix	RM 181	To provide time marks on oscilloscope traces	1
EH	127	Pulse output for general use	1
Rutherford	A12	Multiple delay (3 pulses) generator	1
EH	132A	General pulse and single delay use	1
LLL	LE9891-1M2	Pulse for triggering oscilloscopes	1
Wavetekk	144	General signal generator use	1
EECO	811	Time code generator	1
Tektronix	109	Fast risetime pulse for system checks	1
EG&G	SG-29-A	Fiducial generator for correlating data	1
TRW/STL	46	Delay generators	5

* These oscilloscopes are equipped with Beatty-Coleman rollback Polaroid cameras which can use 10,000 ASA Polaroid film.

3. Regulated Power Supplies

An assortment of dc power supplies is available to cover almost any V or I requirement the installed cables are rated to carry.

4. Meters and Testers

Manufacturer	Model	Purpose	Qty.
NANOFAST	536	Time-interval measurement	1
EG&G	LE1 3807-1	Direct reading cable length in ns	1
Ballantine	AC-DC	Precision V calibrator	1
HP	738BR	Precision V source	1
HP	3476A	Digital multimeter	1
HP	3400A	rms voltmeter	2
HP	5233L	Electronic counter	1

5. Recorder Data Graph

Manufacturer	Model	Sensitivity	Bandwidth	Qty.
CEC	1-133	1 mV or greater	5 khz max.	1 each (14 channel)

6. Multiplex Data Recording System

This system consists of all the V-controlled oscillators, filters, amplifiers, discriminators, and tape-recording equipment necessary to record and playback up to 48 channels of 20-kHz data. If a higher frequency option is desired, the system can be used to record up to 13 channels of 400-kHz data.

Experimenters planning to use the multiplex system should coordinate their plans with the instrumentation personnel at least 60 days in advance of the planned experiment date. This will allow signal-conditioning cards to be built and simulation equipment adapted for dry-run system checkout prior to experiment arrival.

7. Transient Digitizer System

This system consists of the following major items

a. 11 each, Tektronix R7912 Transient Digitizers capable of recording single-shot transients in the 500-MHz frequency range (and below)

b. 1 each, Digital Equipment Corporation PDP 11/10 computer (operating under Tektronix WDI-RT 11-02 software) with 32K core memory

c. 1 each, International Memory System (dual disk memory with up to 2.5-megaword storage capability).

The data from this system are hardcopy plots and/or digital data recorded on cassettes.

This system is presently being used with several electron-beam/FXR facilities in Area V. Time constraints prevent sophisticated new software from being incorporated on short notice (unless supplied by the experimenter). Experimenters who want to process their data with special software should make the arrangements at least 30 days prior to the scheduled test date.

Preliminary arrangements for instrumentation van services can be made through the Operations Supervisor in the Beam Source Applications Division. The instrumentation personnel in the Simulator Instrumentation Division (1126) also may be contacted at (505) 264-4447.

3.10.5.3 User-Provided Instrument Vans

An area on the south side of Building 6596 is available if the experimenter wishes to provide his own shielded instrumentation trailer at the HERMES II facility. Two Appleton AEO-10453 100-A, 220-V, 3-ϕ female power connectors are installed at the trailer location. Power cables should not be less than 9.1 m (30 ft) in length and should terminate with a compatible Appleton connector.

Monitor cables from this trailer location to the HERMES test cell should be at least 24.4 m (80 ft) in length.

3.10.6 Timing and Sequencing

Timing and sequencing circuits of the REBA/REHYD installations are relatively versatile and can be modified to meet the requirements of an experimenter if advance notice is provided.

If no magnetic field is to be applied, the fire signal, a 28-V fast-rising pulse into a 50-ohm load, is the first occurrence. If an external field is used, the start operation energizes the field coils and the fire signal is automatically sent when the field reaches proper strength, several ms later. The fire signal can be combined in an AND gate with an "experiment ready" signal, if desired. After a variable pulse delay of approximately 4 μs, the Marx generator begins to erect. Tube output occur approximately 1.2 μs later.

At occurrence of the fire signal, a 28-V fast-rising pulse, several μs in duration, is available for use by experimenters. The pulse delay from this leading edge is approximately 5.2 μs and jitter is of the order of several hundred ns.

A pickoff from the Marx generator V monitor also can be supplied to the experimenter. Pulse delay from this signal is approximately 1 μs, with jitter of ±30 ns.

For HERMES II, the Marx generator trigger signal is the reference time signal. This may be used to trigger an on-hand delay generator capable of delivering

up to 3 timing signals from 100 ns to 1 s after reference time. A photodiode or Compton-diode trigger signal from the HERMES II machine output also is available.

A pulse operation is normally initiated manually, but can be started by the experimenter's sequencing circuits, if necessary. This requires a fast-rising pulse in excess of 20 V magnitude with a duration of 5 to 7 μs to be delivered into a 50-ohm load. If this firing pulse, which triggers the Marx generator, is to be provided by a user's sequencing unit, it must be initiated within 10 s after a verbal command from the operator.

Other timing requirements must be arranged for by prior consultation. If the experimenter's procedures require a detailed time sequence, his sequencing usually can be made to initiate the trigger signal.

3.10.6.1 On-Line Computer Data Collection and Processing

The DADS has been programmed to reduce data of electron-beam energy fluence measurements. The system includes the EMR 6130 digital computer and a remote terminal in the screen room in the office area of Building 6596.

The DADS accepts the outputs of planar and linear array calorimeters. These data are then reduced using a library program in the computer. The reduced data, which are returned in the form of oscilloscope displays and teletype tabulations, include beam profiles and characteristic deposition curves.

The output of the calorimeter goes directly to the remote terminal of the DADS system through a previously mentioned multiconductor shielded cable. This cable extends into the test cell and is fitted with a 100-pin connector. Experimenters may use their own calorimeters, but must check with facility personnel to ensure compatibility with the system. The software on DADS assumes that a Chromel-Alumel Type K standard thermocouple is being used.

V and I waveforms are sampled by monitor resistors and are also digitized through the use of DADS. The user can also supply his own FORTRAN program and operate on the data in real time. Output is available as cathode ray tube (CRT) displays, or in printed form from the remote terminal in the screen room.

The DADS is available to all experimenters, including use of the remote terminal at the accelerator facility.

3.10.7 Support Staff

The operating staff of an accelerator, exclusive of instrumentation personnel, normally consists of 2 operators and a supervisor. These personnel will assist the experimenter in determining and establishing the correct experimental setup. This assistance includes positioning the equipment and setting up other necessary equipment, such as vacuum systems. Under normal circumstances, however, they do not provide monitoring or instrumentation services.

If experiments involve radioactive or toxic substances, a Sandia Laboratories health physicist is assigned the responsibility of regulating personnel exposures and ensuring that proper handling procedures are employed.

The Sandia technical staff is available for consulting services only on a limited basis.

3.10.8 Computational Facilities

There are two computer facilities in Building 6588 available to the experimenter for running FORTRAN programs.

In addition to supporting the DADS, the EMR 6130 computer performs standard processing and execution of programs. This enables the experimenter to operate on experimental data as they are processed and digitized by the DADS. There is also a remote terminal in Building 6588 which gives the user access to the CDC 6600 and CDC 7600 computers in Area I. The terminal includes a CRT display unit for accessing the computers, a card reader, a 136-character line printer, and an IBM 028 keypunch machine. Instructions for operating this equipment are provided at the terminal. For those who wish to submit their programs at the main computing center, a courier makes regular deliveries to Area I.

3.10.9 Experiment Preparation and Office Spaces

The test cells can be used for experiment preparation when they are not otherwise in use and when the machine is not undergoing maintenance. Other areas outside of the test cells also can be used, but only when they are not being utilized. As a rule, space is limited and the experimenter should, as much as possible, have his equipment ready when he arrives at the facility.

3.10.10 Dosimetry

The Sandia Laboratories Dosimetry Laboratory is available for use by all FXR experimenters. The laboratory uses the TLD-400 TLD as the standard dosimeter. It is a 0.317-cm by 0.317-cm by 0.089-cm (0.125-in. by 0.125-in. by 0.035-in.) chip of CaF_2 (Mn-activated) which will measure doses from 1 rad(Si) up to 6×10^5 rad(Si). Sandia Laboratories will provide and read a limited number of dosimeters for the experimenter. If the experimenter needs a significant number of dosimeters, he should make his requirements known to the Dosimetry Laboratory in Building 6594. It normally requires about 20 min to prepare and read a dosimeter series using a TLD reader. Because of this time constraint and because the laboratory supports several facilities, the experimenter should arrange a dosimeter reading schedule with the Dosimetry Laboratory personnel at (505) 264-7567.

3.10.11 Photographic Services

The experimenter should arrange to make use of the services of the Photographic and Reproduction Services Department (3170). Experimenters may also provide their own photographic equipment and material. Cameras and film are included with all Sandia oscilloscopes.

3.10.12 Shop Facilities

Light machine-shop facilities, such as a grinder-buffer and a drill press, are available at the REBA site. The facility staff will assist the experimenter with minor machining tasks. Additional questions should be addressed to the Facility Supervisor.

3.10.13 Scheduling and Contract Procedure

Experiments should be scheduled at least 6 months in advance and a test plan submitted at least 30 days prior to the scheduled test date. This may be done by contacting the Operations Supervisor in the Beam Source Applications Division (5232) at (505) 264-2676 or 264-3197. At the time of scheduling, the availability of required monitoring equipment should be determined, the environmental conditions required by the test should be discussed, and any arrangements regarding the services mentioned in this section should be concluded.

It is suggested that propsective users of the beam accelerators make a preliminary visit to the facilities to acquaint themselves with them and to gain first-hand information on the compatibility of experiment and machine.

The services of HERMES II, REBA, and REHYD are available to agencies of the DoE and the DoD, and to private corporations having DoE or DoD contracts. Such use must be justified on the basis that the selected facility provides a unique environment not available elsewhere, and that such use will not interfere with Sandia programs.

DoE and DoD agencies or contractors desiring to use the facilities are required to establish a contract with the Special Programs Division of the Albuquerque Operations Office of the DoE. The complete mailing address is:

Director, Special Programs Division
DoE
Albuquerque Operations Office
Albuquerque, NM 87115

This contract should be requested only after making full technical arrangements with Sandia Laboratories.

Preliminary arrangements, including technical information, schedule availability, and procedural requirements, are made directly with the Beam Source Applications Division (5232) of Sandia Laboratories. The complete mailing address is:

Operations Supervisor
Beam Source Applications Division (5232)
Sandia Laboratories
Post Office Box 5800
Albuquerque, NM 87115

Telephone contact may be made by calling (505) 264-2676 or 264-3197. Following this contact, negotiations with the DoE, Albuquerque Operations Office, should begin.

3.10.14 Cost Information

Preliminary cost information can be obtained from the Operations Supervisor. Final cost information is obtained from the Albuquerque Operations office of DoE.

3.10.15 Security and Visitor Control

A DoE Q clearance or DoD Secret clearance with Restricted Data certification is required to gain entry to the accelerator facility. Security arrangements should be completed at the earliest convenient time, but not less than 2 weeks before any preliminary visit or use of the accelerator.

Security arrangements must be made through Sandia Laboratories at the following address:

Visitor Access and Administration Section
Division 3433-1
Sandia Laboratories
P.O. Box 5800
Albuquerque, NM 87115
Telephone: (505) 264-4494.

3.10.16 Shipping Information

To avoid any delays in shipment, users are urged to ship materials at least 2 weeks in advance of the date they will be needed. Address shipments to:

Operations Supervisor
Beam Accelerator Facility Building 6596
Beam Source Applications Division (5232)
Sandia Laboratories
P.O. Box 5800
Albuquerque, NM 87115

3.11 NORTH CAROLINA STATE UNIVERSITY PULSERAD MODEL 940 ELECTRON-BEAM GENERATOR

The IBM Pulserad Model 940, donated to North Carolina State University (NCSU) by IBM Corporation, will be operational around 1980. The FXR facility consists of a Marx generator that pulse charges a Blumlein voltage doubler that in turn drives the accelerator tube. Nominal peak V delivered to the tube is 6.5 MV.

3.11.1 Test Parameters

The Pulserad Model 940 operating characteristics are:

1.	Tube V	6.5 MV
2.	Average electron energy	3.5 MeV
3.	Total beam energy/pulse	8.0 kJ
4.	Electron-beam I	80.0 kA
5.	Pulse width (FWHM)	40 ns
6.	X-ray dose/pulse at 1 m	200 R
7.	X-ray dose at tube face	25 kR
8.	Peak dose rate at 1 m	5.6×10^9 R/s
9.	Dose reproducibility	±6%
10.	Timing jitter	±100 ns

These data are not definitive and are meant only as a guide.

Total beam energy is dependent upon charging V, master switch gap setting, and cathode-anode configuration. It can be varied from 4 to 12 kJ. Beam geometry is a function of machine operation parameters, pressure in the drift chamber, and distance from the anode. An automatic pressure-controller allows the operator to preselect the beam shape, which is a cone of variable half-angle. Quantitative data are available for various operating conditions. Maximum repetition rate is 1 pulse every 3 min for a maximum of 40 pulses. Changes in experimental setup and data recording usually limit operation to 10 to 20 pulses/day.

Pulse repeatability is approximately ±6%. Pulse delay is approximately 3 μs without external delay, which is adjustable up to 10 ms. Timing jitter is ±100 ns.

Electrical noise is a function of distance from the machine and machine charging V. At IBM, an open coaxial cable in the shield box terminated in 50 ohms at the scope caused a noise signal of approximately 0.5 mV at 10^8 R/s and 20 mV at 10^{11} R/s.

3.11.1.1 Electron-Beam Mode Environment

No data are available except to verify total beam energy.

3.11.1.2 X-Ray Mode Environment

X-ray dose measurements are shown in Figures 3-187 through 3-191. Oscilloscope traces of a PIN diode pulse shape monitor are shown in Figure 3-192. Measured energy deposition profile in Al is shown in Figure 3-193.

Reproducibility of the dosimeter reader system is ±1% to identical exposures. The absolute error introduced by calibration with a Co-60 source is estimated to be ±15%.

3.11.2 Procedural Information

For cost and technical information contact:

North Carolina State University
Dr. Wesley O. Doggett
P.O. Box 5432
Raleigh, NC 27650
Telephone: (919) 737-2426

Shipments should be directed to the above address.

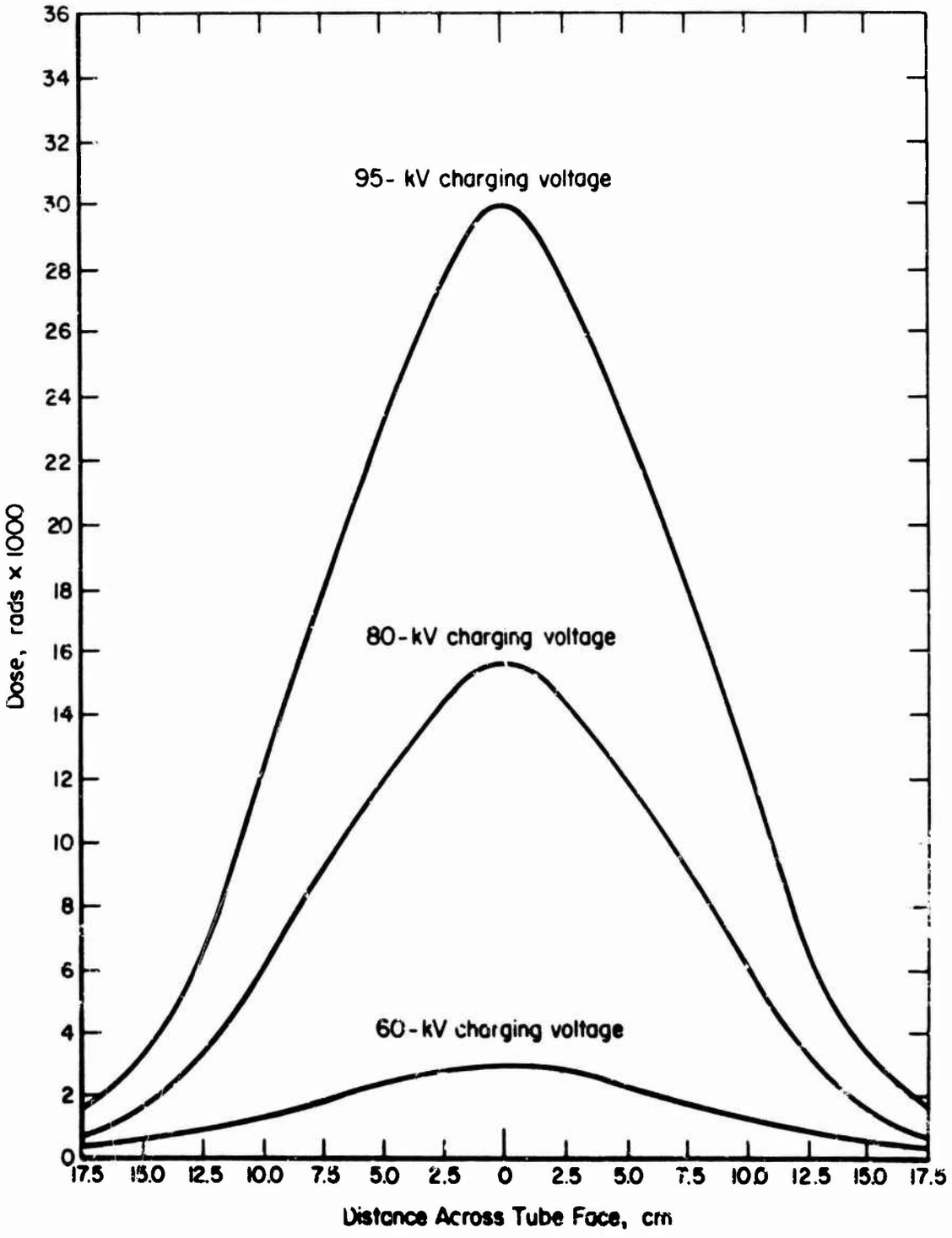

Figure 3-187. Faceplate dose distribution.

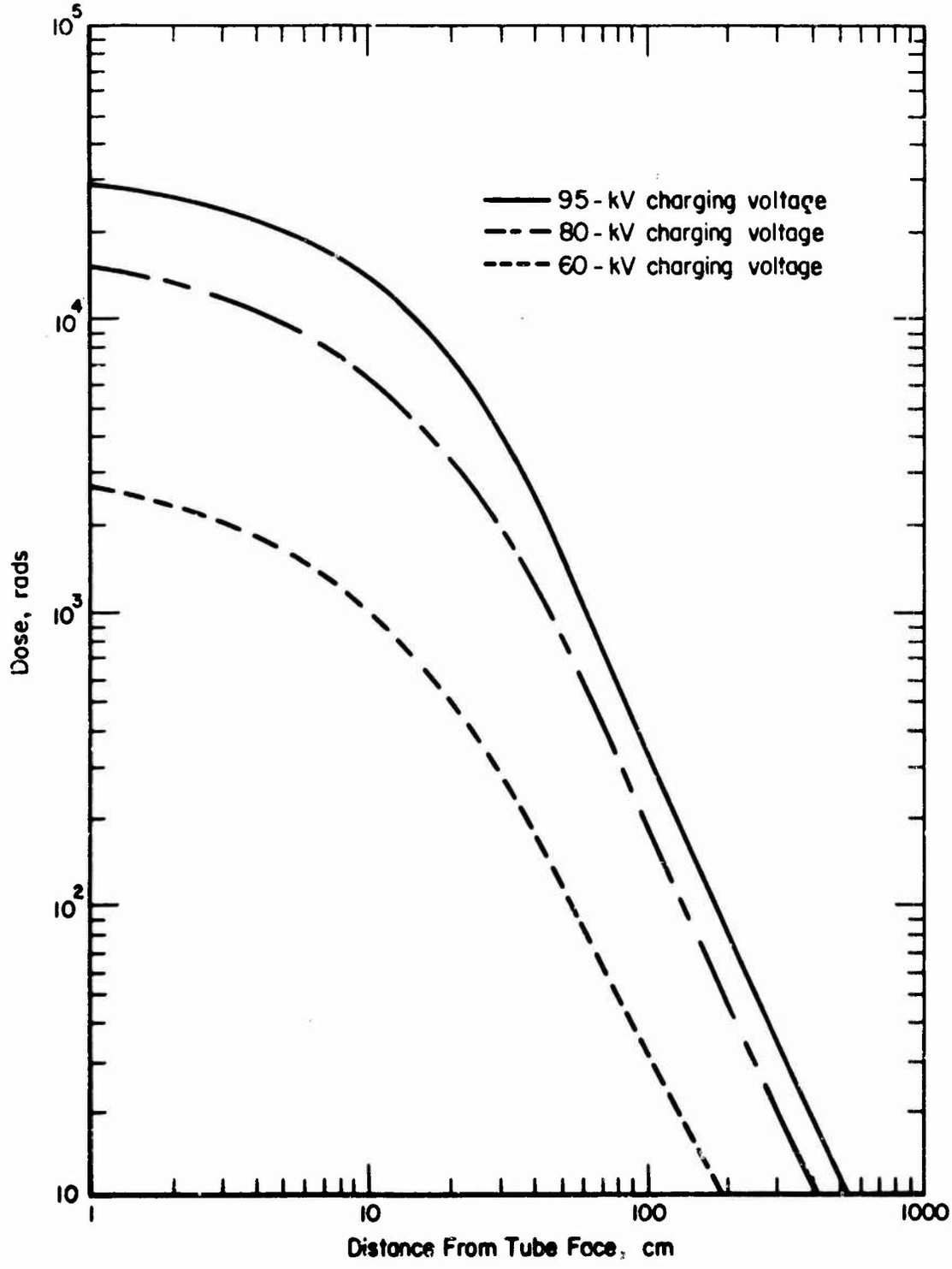

Figure 3-188. Dose levels on axis.

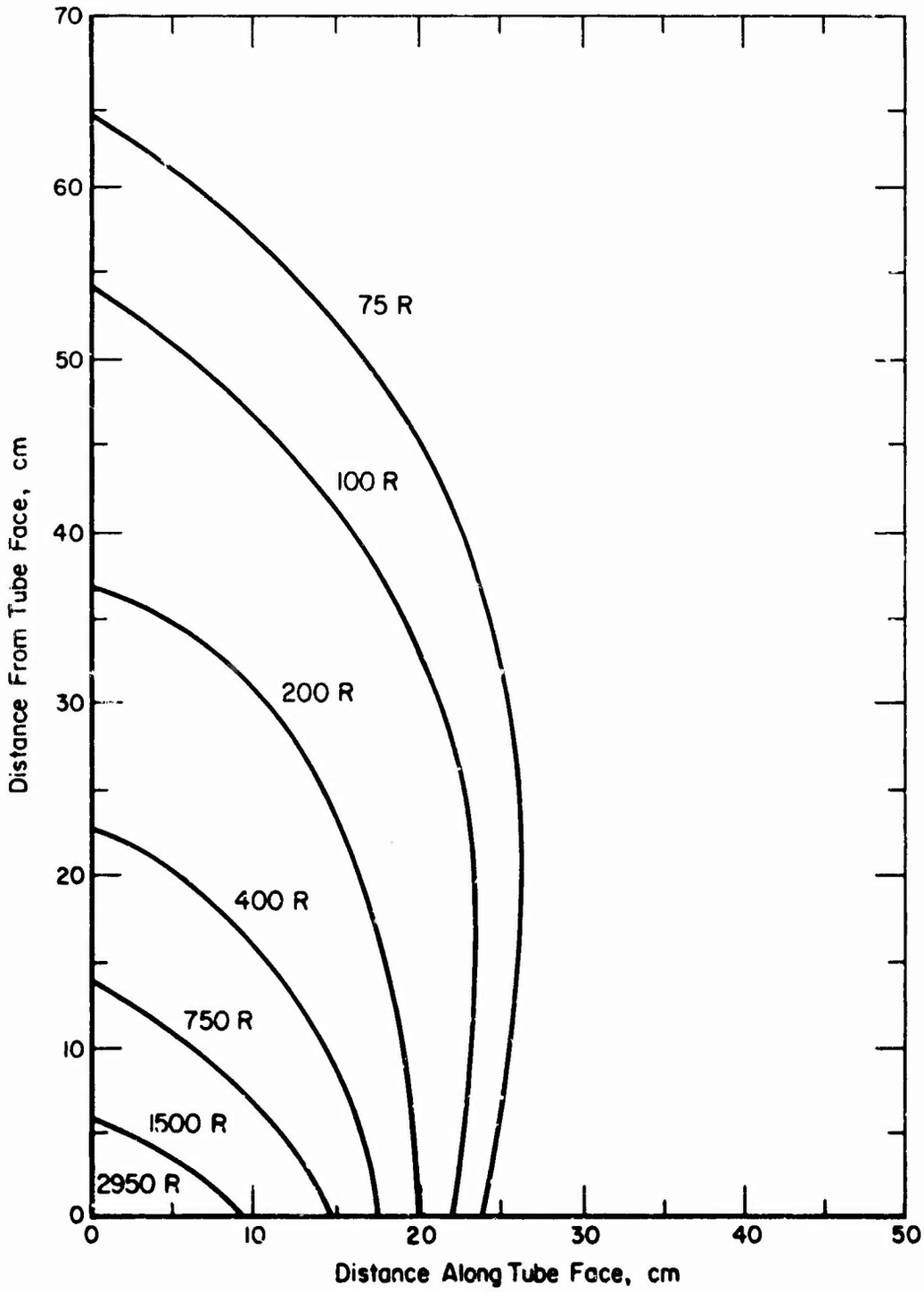

Figure 3-189. Isodose curves for 60-kV charging V.

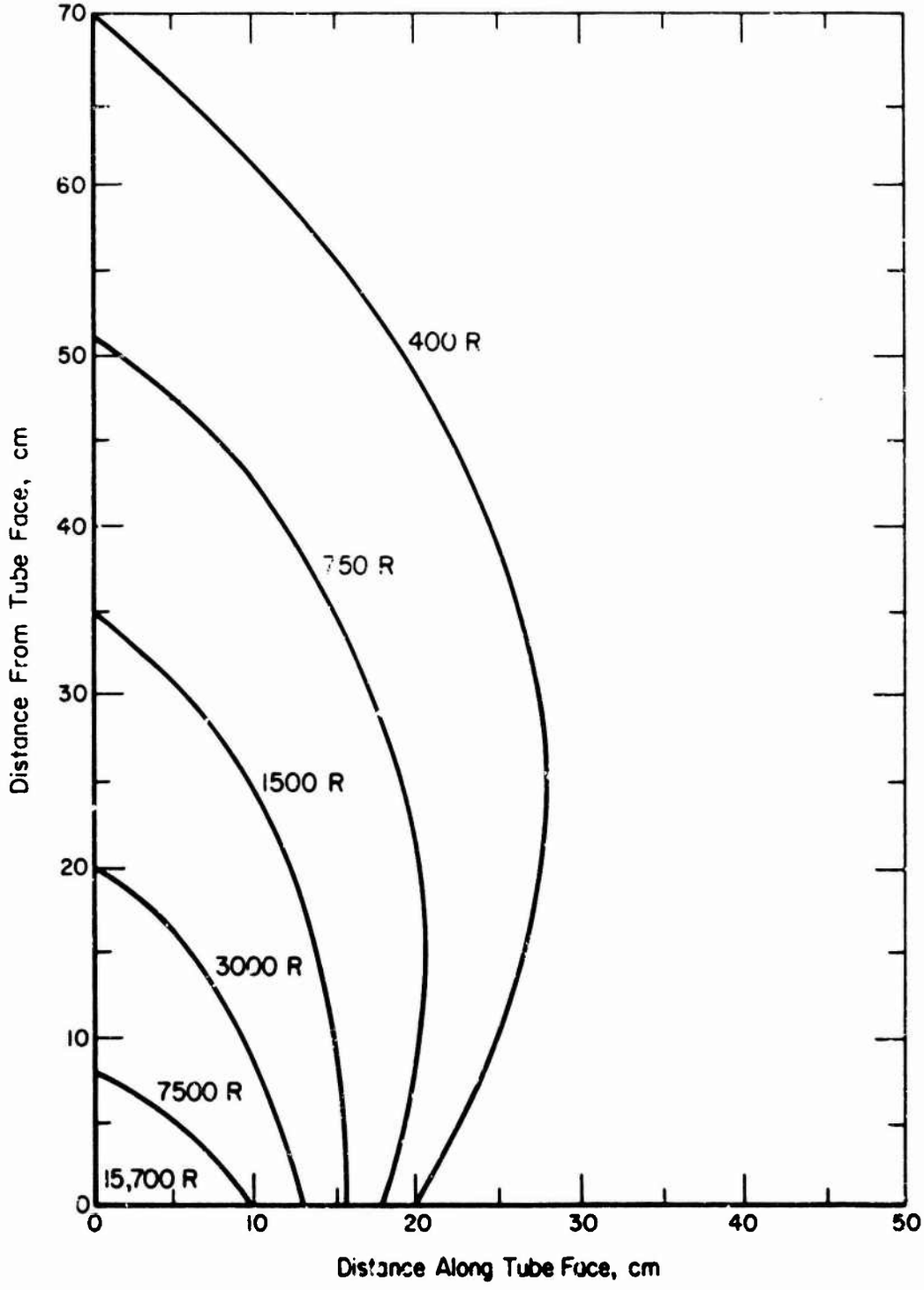

Figure 3-190. Isodose curves for 80-kV charging V.

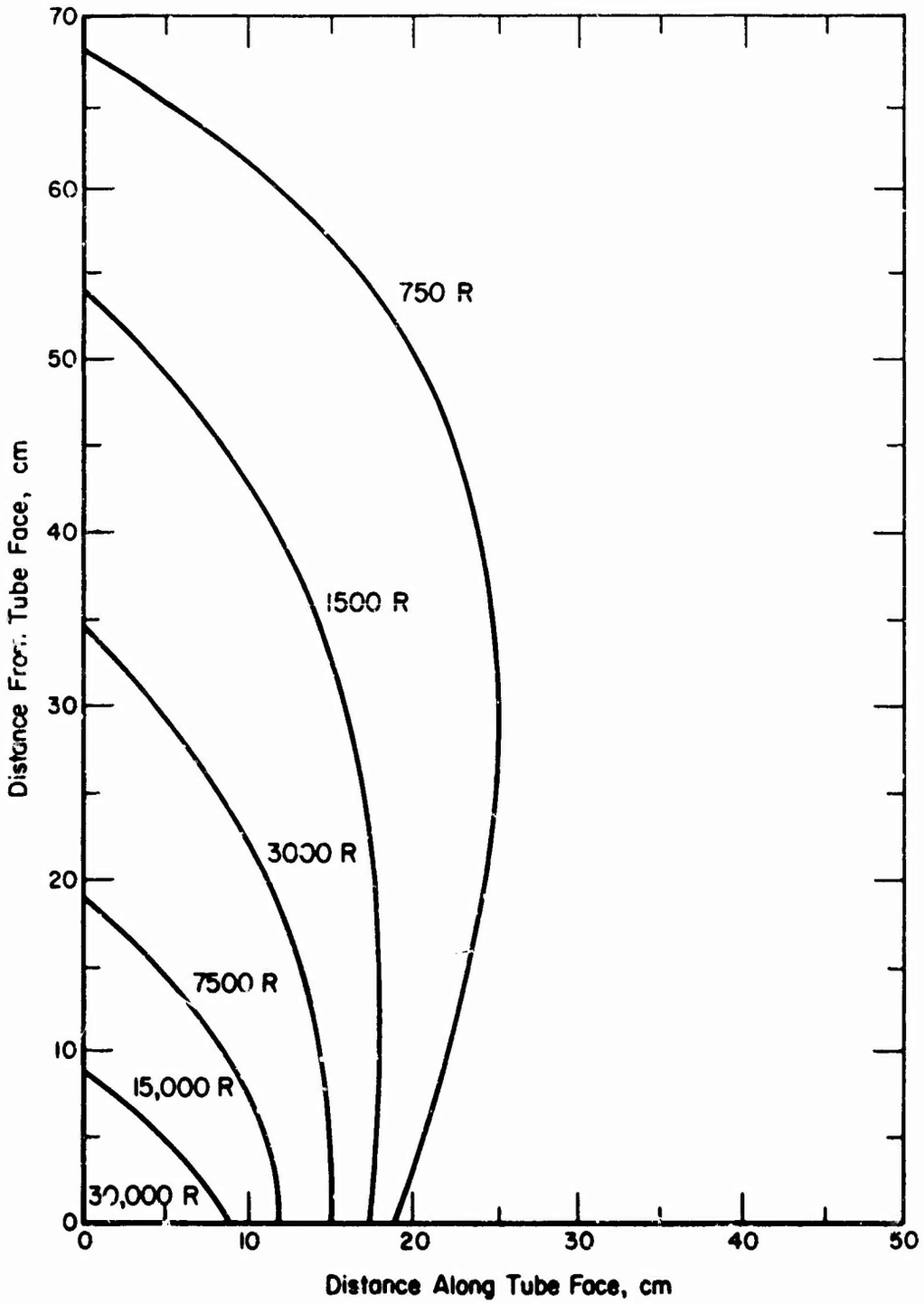

Figure 3-191. Isodose curves for 95-kV charging V.

Vertical - 3.6×10^8 R/s/cm
at 1 m from tube face

Horizontal-0.020 μs/cm

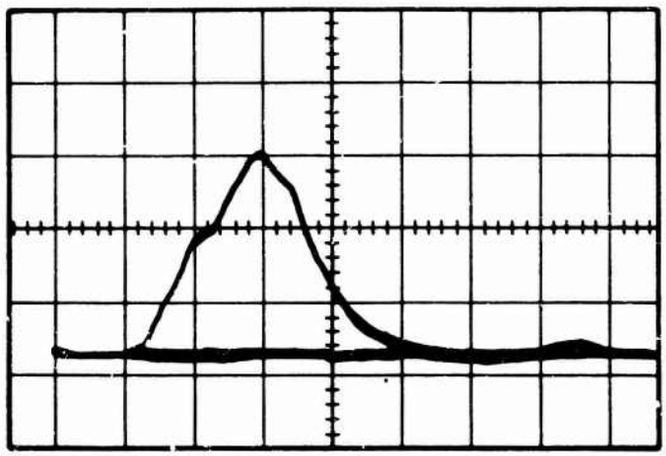

Vertical - 2.6×10^9 R/s/cm
at 1 m from tube face

Horizontal-0.020 μs/cm

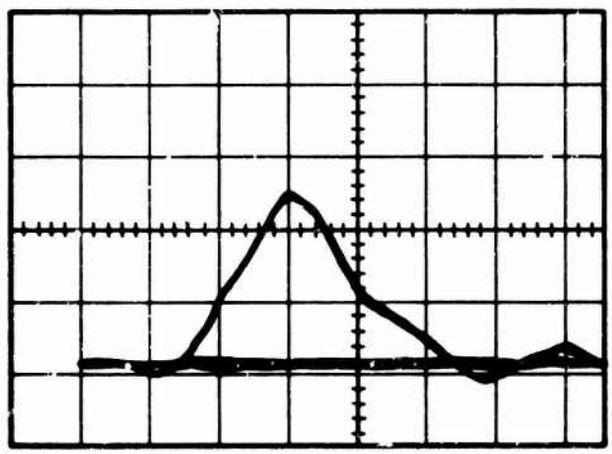

Vertical - 2.6×10^9 R/s/cm
at 1 m from tube face

Horizontal-0.020 μs/cm

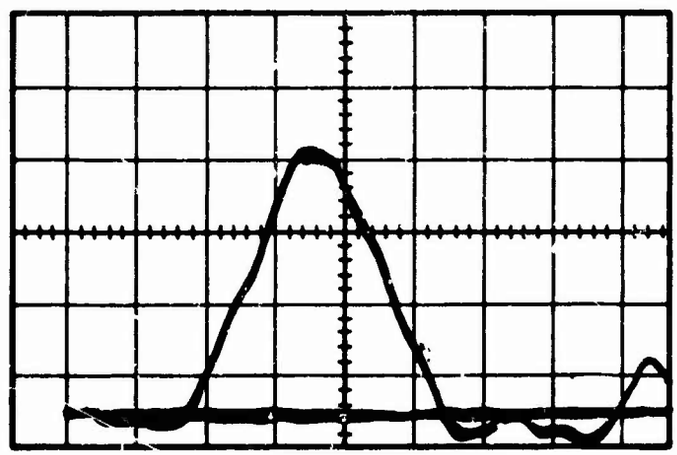

Figure 3-192. X-ray pulse shapes.

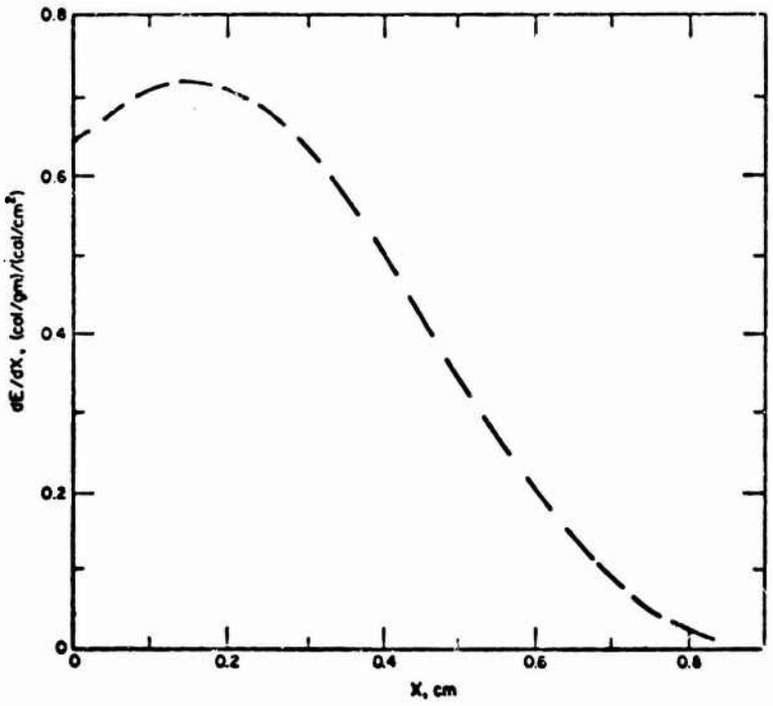

Figure 3-193. Measured energy deposition profile in Al.

3.12 HARRY DIAMOND LABORATORIES AURORA FACILITY

The AURORA facility was sponsored by the DNA to provide the DoD with the capability of measuring TREE in large weapon systems. DNA has the authority and overall responsibility for funding, scheduling, and providing certain technical direction, operational guidance, and planning functions for this facility. This includes assuring that the best interests of DoD are maintained throughout all testing accomplished at AURORA and that each test performed is technically sound.

AURORA is managed, operated, and maintained for DNA by the U.S. Army Harry Diamond Laboratories (HDL). HDL has the prime responsibility for providing technical direction and support to the facility user in the areas of simulator operation, test configuration, instrumentation, and dosimetry. In addition, HDL is responsible to U.S. Army Materiel Command (USAMC) for radiation safety and provides DNA with technical advice concerning operations and user test programs.

3.12.1 General Characteristics

The pulser receives energy from a conventional ±60-kV dc power supply, stores it, and delivers the energy in a short burst at high V. This is achieved by increasing the V in steps. The first such increase is in the Marx generator. This is an array of capacitors which are charged in parallel and then switched to a series configuration, thereby multiplying the V by the number of stages, n.

In the AURORA simulator, the Marx generator consists of 4 separate generators with a common output. Each generator contains 95 stages of 4 series-parallel-connected capacitors charged to a maximum of ±60 kV. With the maximum charge, the energy stored is 5.2 MJ and the output V is 11.5 MV.

The Marx generator charges, in parallel, 4 Blumlein pulse-forming networks. Each of these is a charge-in-parallel, discharge-in-series system which consists basically of 2 charged transmission lines, one of which is reversed in polarity by shorting the input end by means of a command-triggered switch. (In the AURORA simulator, the 2 lines are in 1 triaxial configuration.) This stage will produce twice the charge V into an open circuit and has an output impedance equal to the sum of the nominal impedance of the lines. It acts as a pulse-forming network in that it will deliver its full charge V to a matched load in a pulse whose length is determined by the electrical length of the Blumlein.

The pulse from the Blumlein is conducted to the field-emission diode on a coaxial structure through a graded tube which separates the vacuum coax region from the oil insulation of the Marx generator and Blumlein.

The AURORA simulator utilizes 4 Blumleins, 4 tubes, and 4 bremsstrahlung targets. The 4 targets are the sources of radiation that produce the specified radiation field. The vacuum coaxial transmission lines are bent through 45 degrees to bring the cathode-anode region near the machine center line and the targets are inclined 23 degrees from the machine center line. The targets are each 26 in. in dia. and form a square array with 2.5 ft between centers. At present, all 4 sections must be fired simultaneously. Means of "double pulsing" or firing only 1 of 2 sections are under consideration.

3.12.2 Physical Characteristics

The floor plan of the AURORA facility is shown in Figure 3-194. The loading dock has a self-adjusting platform to simplify moving equipment on or off trucks and opens into the staging area through an 8-ft^2 door opening. Equipment may be brought in directly from the loading dock and assembled in the staging area, which has a usable area of 29 ft by 34 ft. Duplex wall outlets provide 120-V, 1-ϕ power. The setup room, data room, test cell, and security vault all open directly off the staging area. The entrance into the test cell shield room is a door 8 ft, 10 in. wide by 8 ft, 6 in. high. A 6,000-lb capacity electric fork-lift is available for use in the test cell, staging area, and loading dock.

The setup room and user's office are the base of operations while testing at the AURORA facility. The laboratory area is 16 ft by 28 ft and is equipped with work benches and power (120 V, 1 ϕ and 208 V, 3 ϕ). The user must supply his own tools, instrumentation, etc. The dark room is available to the user by prior arrangement.

3.12.3 Test Cell and Data Room

The test cell extends 65 ft back from the radiation window and, from the beam center line, 18 ft toward the data room and 30 ft toward the outside wall. The beam center line is 70 in. from the floor. The floor-to-ceiling height is 15 ft and the limiting height is 13 ft, 8 in. to the air-conditioning ducts along the side of the room. As previously noted, the shield room door opening into the test cell is 8 ft, 10 in. wide by 8 ft, 6 in. high.

There is an inertial pad 6 ft by 9 ft just inside the radiation window which rests on its own foundation and is partially decoupled from the building.

Figure 3-195 shows the network of cable trenches which shield the cables from radiation. These trenches are inside the EM-shielded volume, and the smallest is 12 in. wide and 16 in. deep. They have 2-in. thick steel covers. The user must supply his own cable for reaching from the test cell to the data room. To get from anywhere on the machine center line to the user rack in the data room via the cable trenches, 100 ft of cabling is required. The facility supplies an 86-ft long Metex douple-zip tube of 5 and 6 in. dia., which is normally used with double-cassette shielding (supplied by the user). The outer zip is normally terminated at the test cell wall and the inner zip at the data room wall.

The cable bundle goes through one of the three 8-in. dia. conduits (dashed lines) that go from the cable trench to the data room beneath the raised computer-type floor. The cables then can be tied into the user rack or run directly to the high- or low-frequency patch panels.

A radiation pulse detector, referred to as the trigger monitor detector (TMD), is mounted between the test cell and data room walls; it provides a trigger to a trigger generator/fan-out system for oscilloscope triggering and fiducial marks.

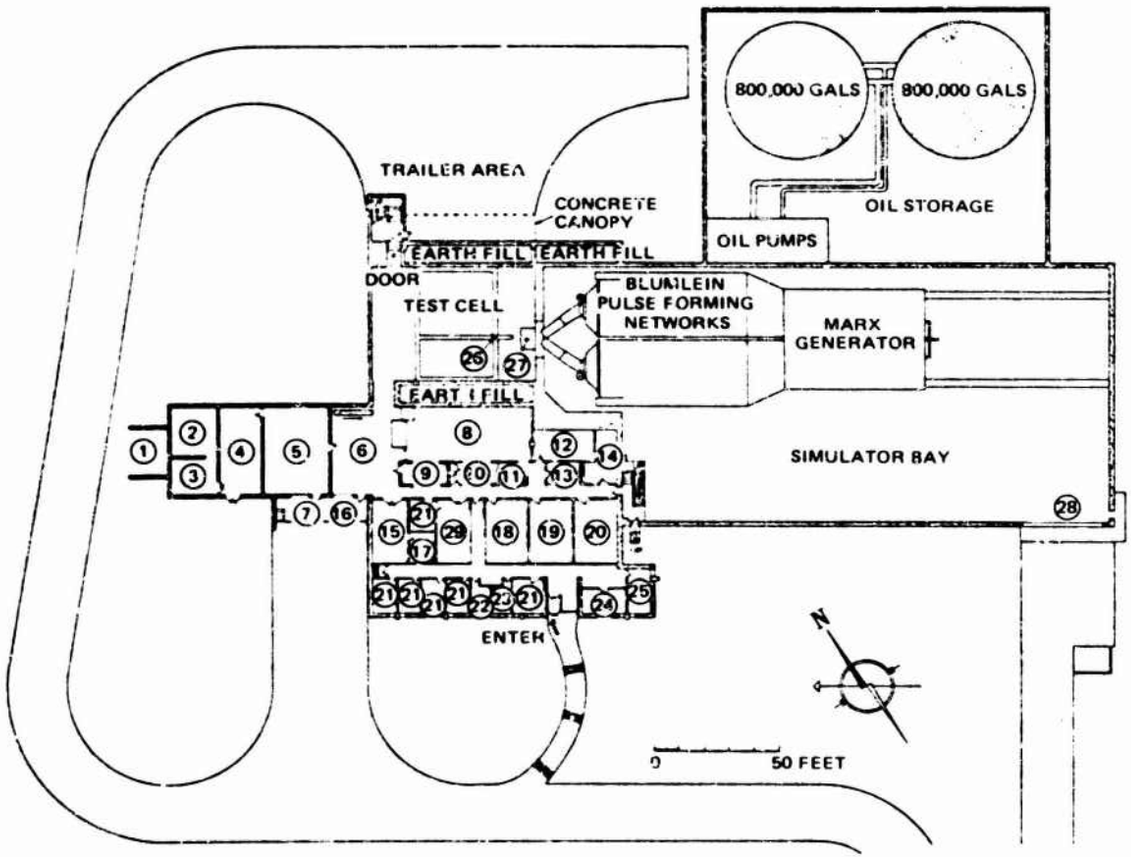

LEGEND

1. TRANSFORMERS
2. FOAM FIRE PROTECTION SYSTEM
3. POWER DISTRIBUTION & CONTROL
4. HEATING PLANT
5. AIR CONDITIONING EQUIPMENT
6. STAGING AREA
7. LOADING DOCK
8. DATA ROOM
9. SECURITY VAULT
10. STORAGE ROOM
11. DARK ROOM
12. CONTROL ROOM
13. OPERATIONS OFFICE
14. LOCKER ROOM
15. SET-UP ROOM
16. LOAD LEVELER
17. USER'S OFFICE
18. DOSIMETRY LAB
19. INSTRUMENTATION LAB
20. HIGH VOLTAGE LAB
21. STAFF OFFICES
22. REST ROOM (MEN)
23. REST ROOM (WOMEN)
24. DIRECTOR'S OFFICE
25. CONFERENCE ROOM
26. CABLE TRENCHES
27. INERTIAL PAD
28. ROLL UP DOOR
29. COMPUTATION & DRAFTING

Figure 3-194. AURORA facility floor plan.

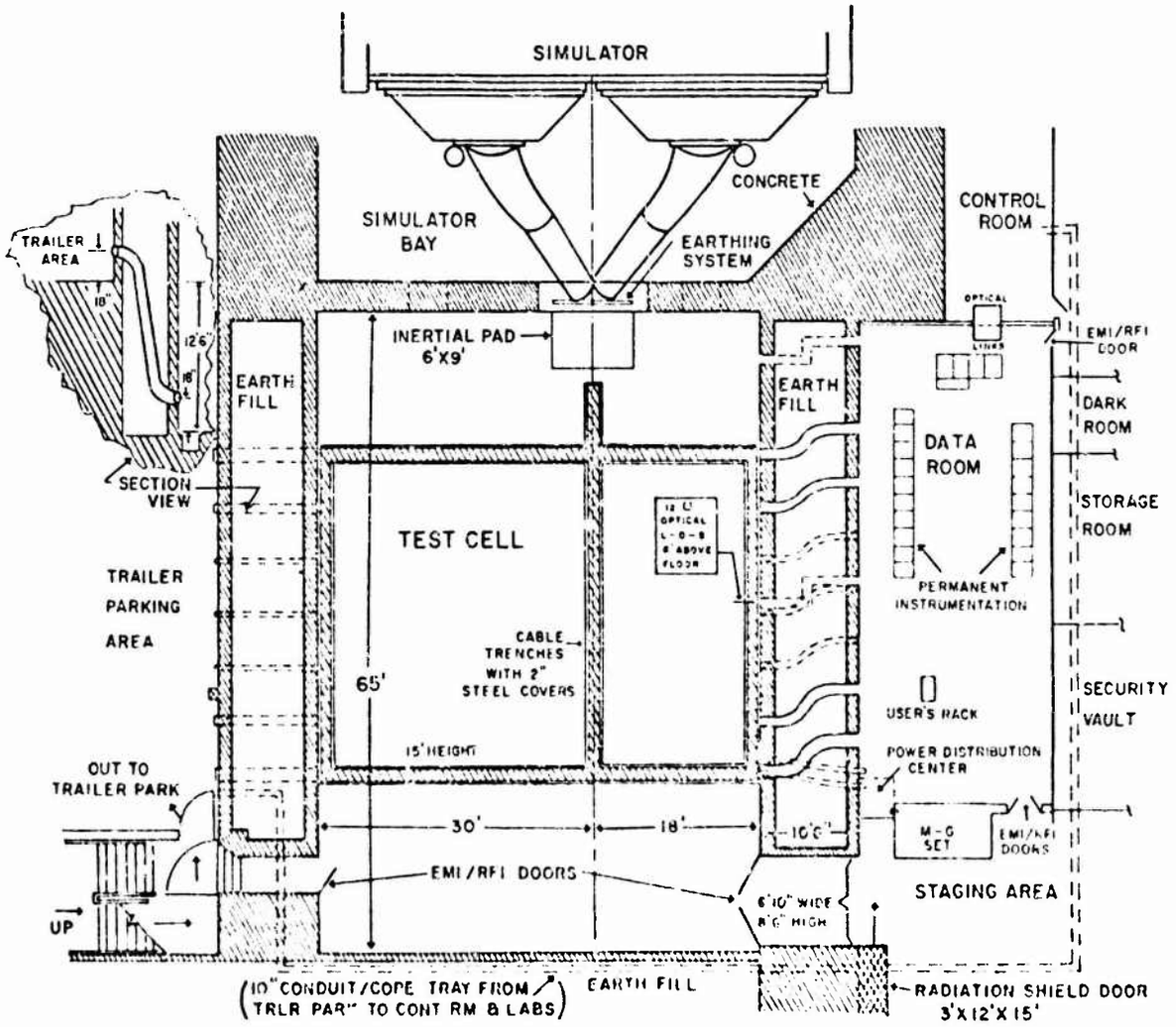

Figure 3-195. Test cell and data room.

Two 16-in. and two 12-in. dia. cable conduits from the test cell into the data room (18 in. above the data room floor) are also available to the user. Two offset square optical ports at the beam center line (6 ft above the test cell floor) with front surface mirrors installed are available, one 5 ft away from the beam entrance window and the other 30 ft from the window.

3.12.4 Data Room Layout

The data room is 21 by 49 ft, with approximately one-half the area used for permanently installed facility instrumentation which is controlled by the data room sequencing system. Most of this instrumentation is available to the experimenter. The remainder of the data room is available for user-supplied equipment which can be tied into the sequencing and run interlock system, if desired.

The permanent instrumentation section of the data room is shown in Figure 3-195. Along the wall nearest the control room is the data room control console which is operated by HDL personnel to meet the needs of the user. The Tektronix Type 519 oscilloscopes used to monitor the radiation pulse are also in this section, as are the "zero clock" and the time-interval meters. The remainder of the data room oscilloscopes are in the fast instrumentation section which is along the wall adjacent to the test cell. This location permits the shortest possible cable run from the radiation area. Also in this section are the high-frequency patch panel, the delay generators, and the trigger/marker fan-out system which provides pulses (initiated by the TMD) for scope triggers and fiducial markers. The remaining data room instrumentation is contained in the low-frequency section. It consists of 1 tape recorder, 2 oscillographs, the data scanner, signal conditioners, calibration equipment, and the low-frequency patch panel.

Also shown in Figure 3-195 is the user's rack, where access is provided to the facility instrumentation via the following cables:

To	Number of Cables	Type of Cable	Connector Type
High-frequency patch	38	RG213	GR
High-frequency patch	12	RG58	BNC
Low-frequency patch	8	RG58	BNC
Low-frequency patch	96	TSL	Trimm Type 357
Console	4	RG213	GR
Console	4	RG58	BNC

There are also 3 stations of the sequencer-controlled relays on a terminal strip on the user's rack.

A paved trailer area is available for instrumentation vans. The area is approximately 60 ft long along the test cell wall and is 12.5 ft above the test cell floor. It is reached by an extension of the facility entrance road. Power is available from a 75-kVA, 480-V, 3-ϕ, 3-wire, 100-A circuit breaker panel. There are also two independent, transformer-isolated, 75-kVA, 208-V, 3-ϕ, 4-wire power drops. Each drop is available at a separate 200-A fused disconnect switch. The fourth wire grounds are connected together and to local earth ground through a 2-pole single-throw switch which provides for complete isolation of trailer power systems. Cable conduits leading to the test cell are provided. Cabling to the control room can be provided and communications with the data room can be made through the optical links. There is a direct personnel access to the test cell from the trailer park through an 11-ton concrete door. The area has a station on the building intercom system, a speaker on the paging system, and provisions for a telephone extension.

3.12.5 Operating Characteristics

AURORA operating characteristics at 115-kV charge V are:

1. Peak Blumlein V — 11 MV
2. Blumlein source impedance — 22 Ω

3.	Field-emission diode impedance	35 Ω
4.	Peak electron-beam energy	10 MeV
5.	V pulse width (FWHM)	190 ns
6.	Bremsstrahlung pulse width (FWHM)	130 ns
7.	Charging system capacitance	703 μF
8.	Stored energy	4.7 MJ
9.	Total electron-beam energy/pulse	2.0 MJ
10.	Electron-beam I	1.2 MA
11.	Peak I density	--

The present working hours of the AURORA facility are 0800 to 1630 Monday through Friday. In 1 work-day the facility can deliver a maximum of 6 pulses, starting at 0915 and ceasing at 1545. Typically, however, the user turnaround time limits the operation to 4 shots/day. On the average, a full day must be devoted to maintenance after 8 shots at 110 kV or 16 shots at 90 kV.

Pulse delay is nominally 4.5 μs. This delay is defined as the time interval between the command pulse and the peak of the radiation pulse in the test cells. The timing precision (jitter) of the radiation pulse is better than ±50 ns from command.

The extent of automated operation is indicated in the listing of data room instrumentation. The intent is to automate routine operations to the fullest extent compatible with flexibility and, thereby, minimize human errors. Communication between the data and control rooms is by optical links to preserve RFI/EMI isolation. All automated operations are controlled by the countdown clock which counts seconds from -300 to +300. The clocks in the data room and the control room are synchronized. The simulator typically will be fired at clock zero with both automated and manual "holds," where necessary. The simulator can be triggered either automatically or manually from the data room or control room, by the user or the facility operator. The constraints are that the data room must issue a "data room ready" signal for charging to commence, and the control room must issue "fire ready" for the simulator to be fired by any of the options; that is, the control room must issue the permission signal for firing. It is desirable to fire the machine less than 30 s after charge is complete, the sooner the better. Charging the simulator requires about 2 min, for 110 kV charge V.

The sequencer is run by the one-count-per-second clock and will start and stop tapes, chart recorders, and the data scanner. It will open and close shutters, arm oscilloscopes, sweep base lines and rearm, and illuminate graticules. All of these operations are individually programmable so that they can be performed at any time within ±99 s of zero time in the countdown. There are 3 auxiliary switch stations on the sequencer that appear on a terminal strip at the user rack for controlling user equipment, if desired. The sequencer also offers the option to program an automated hold at any selected time until "fire ready" is received from the control room so that, for instance, tapes are not

started until it is reasonably certain that the countdown will proceed without further holds. Automatic holds also will be affected by any failures of the automated equipment such as tapes not up to speed at a specified time, a scope or camera not armed, etc. These problems can be corrected or the interlock bypassed by the data room operator at the discretion of the user.

Fast timing is accomplished by use of 2 discriminator trigger generators (GCSG-72) and fan-outs that can be triggered from any desired source, such as the trigger monitor detector. The outputs are used to trigger oscilloscopes, provide fiducial marks, stop the zero clock, and stop time-interval meters. Oscilloscopes can be triggered less than 160 ns after radiation begins, which precedes any signal, by at least 100 ns, that can get to the scopes from the test cell via normal cable routes. Programmed early triggers can be provided as required.

The simulator has a jitter of ±50 ns from command. If the user wishes to synchronize the machine firing with his experiment, he must supply the pulse. This pulse is normally injected in the data room at the user rack via a 50-ohm coax cable with a BNC panel connector. The pulse is routed through a specially built Lockout Trigger Generator (LTG) which prevents more than one trigger pulse from entering the simulator trigger system. The LTG (either 50-ohm or 1,000-ohm input) requires a positive-going pulse or waveform, with at least 5 V amplitude, and an effective risetime within the range of 10 ns to 1 μs. Pulse trains, continuous waveforms, or a V step are acceptable, within the above criteria, providing the user realizes that the simulator will be triggered on the first positive excursion of his trigger signal.

The degree of automation described exists mainly to minimize errors. In this vein, dry runs can be made where a pulse with preset delay substitutes for the simulator delay and output pulse.

The test cell and data room shown in Figure 3-195 are electromagnetically shielded with cable conduits between them. These 2 rooms can be electrically isolated from each other or connected together via the cable conduits. There is a low-impedance grounding system (counterpoise) accessible at the radiation window which can be used to ground the test cell shield room, the simulator, or both. The combination of these groundings and room interconnections that gives the lowest noise environment for a given test will be used. The enclosures are designed to produce 120-db attenuation from 1 kHz to 1 GHz. Noise-free power from a motor-generator set is supplied to the test cell and data room. The power allotments for user equipment are:

	480 V, 3 ϕ, 3 wire	208 V, 3 ϕ, 4 wire	120 V, 1 ϕ, 3 wire
Data Room	33 kVA (40 A/ϕ)	15 kVA (40 A/ϕ)	45 kVA (125 A/ϕ)
Test Cell	25 kVA (30 A/ϕ)	15 kVA (40 A/ϕ)	22 kVA (60 A/ϕ)

Presently, the test cell shield is tied to the counterpoise and the test cell and data room are not connected. Using this arrangement, the EM noise from the simulator is in the submillivolt level inside the shielded enclosure. The dominant EMI is due to the 1,000 A of Compton I flowing from the test cell wall.

Noise measurements using a double cassette and double-zip tube, as described in ¶3.12.3, yielded varying results, depending on the dose level and orientation of the cable end. In general, the noise after the first 200 ns is a few tens of mV.

The noise pulse occurring during radiation is several hundred mV at highest dose levels. Noise measurements with a dummy package are worthwhile if noise is expected to be a problem. The noise pulse during radiation resembles the radiation pulse in shape, as does the Compton I which has been measured with a B loop.

The bremsstrahlung from the AURORA simulator is directed into the test cell through the EMI shield. The test cell is described in ¶3.12.3.

3.12.6 Dose Maps

Figures 3-196 through 3-198 show the isodose contours in the test cell normalized to 1×10^3 rad(Si) at the maximum level. These numbers should be multiplied by 45 to obtain the dose for each isodose contour. The radiation level is varied by moving the test package in the test cell. The radiation dose also can be lowered by about a factor of 4 by using a lower charging V.

Figure 3-196 is a plan view of the entire test cell showing gross isodose contours determined in a horizontal plane 70 in. above the floor (i.e., coinciding with the machine axis). Major features of the test cell, such as cable trenches and 1-m grid intersection marks on the floor, are included for ease in locating a given position.

A 1-m dia., 1-m long cylinder containing the hot spot has been mapped in detail (shown in Figure 3-196 by the dotted lines). Figures 3-197 and 3-198 show intersections of the 3-dimensional isodose contours with 0- and 45-degree R-Z planes and the Z = 0- and 25-cm planes, respectively.

3.12.7 X-Ray Mode

The pulse width at the one-half maximum is generally about 125 to 130 ns. The rise and fall times of the pulse are typically 60 ns. The dose rate ($\dot{D}$) has been calculated for many shots and is given by

$$\frac{\text{Total dose}}{\text{FWHM} \times 1.09} = \dot{D} \quad .$$

At the present level of operation, approximately 3×10^{11} rad(Si)/s can be obtained uniformly over an 8-in. dia. sphere.

3.12.8 X-Ray Spectrum

The x-ray spectrum has not been measured. The calculated spectrum is shown in Figure 3-199. This spectrum was calculated using the best available beam parameters and the electron-photon Monte Carlo transport code, TIGER.

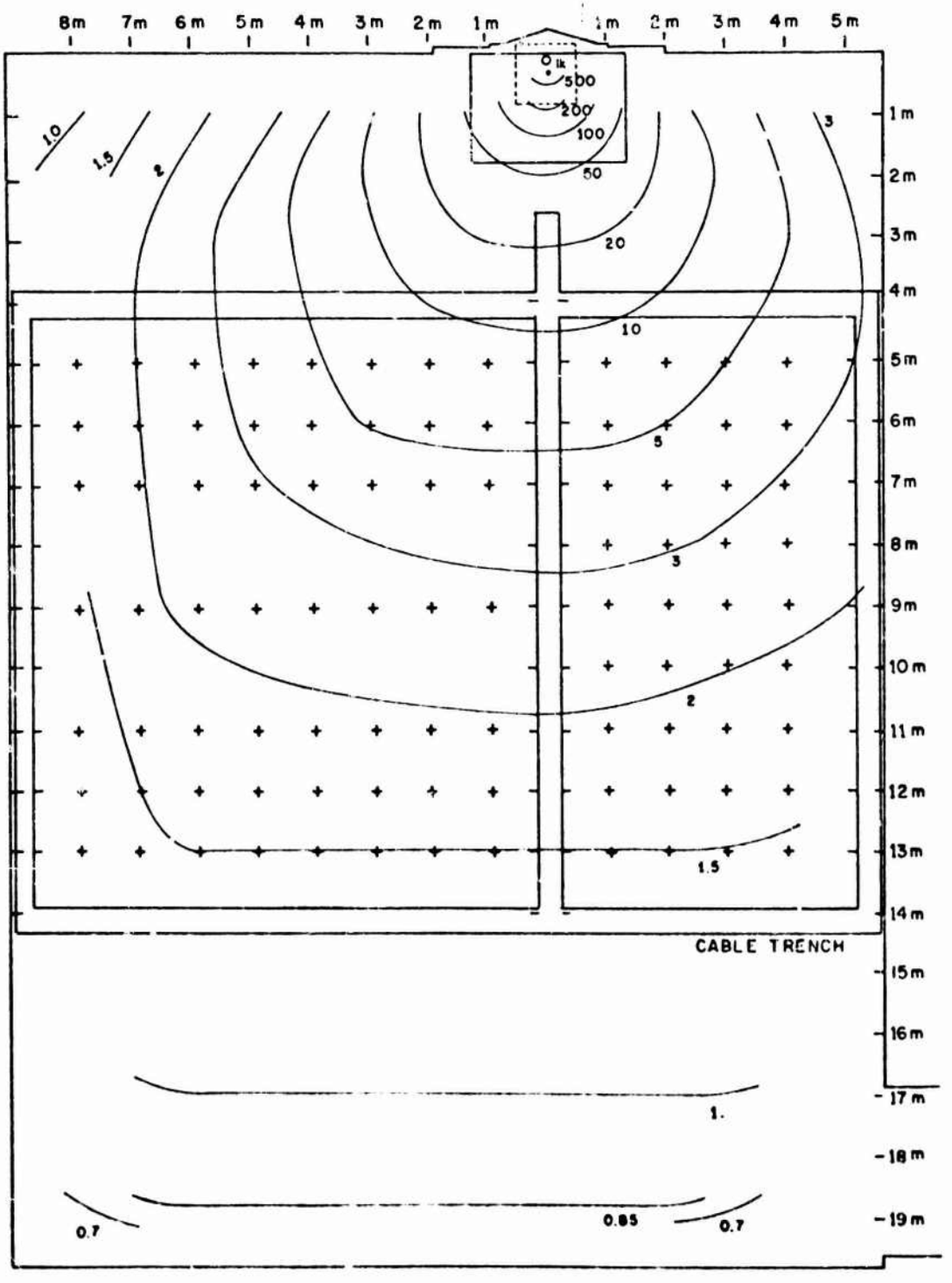

Multiply all Values by 45 to Determine Doses in Rad (Si).

Figure 3-196. Isodose contours in the test cell.

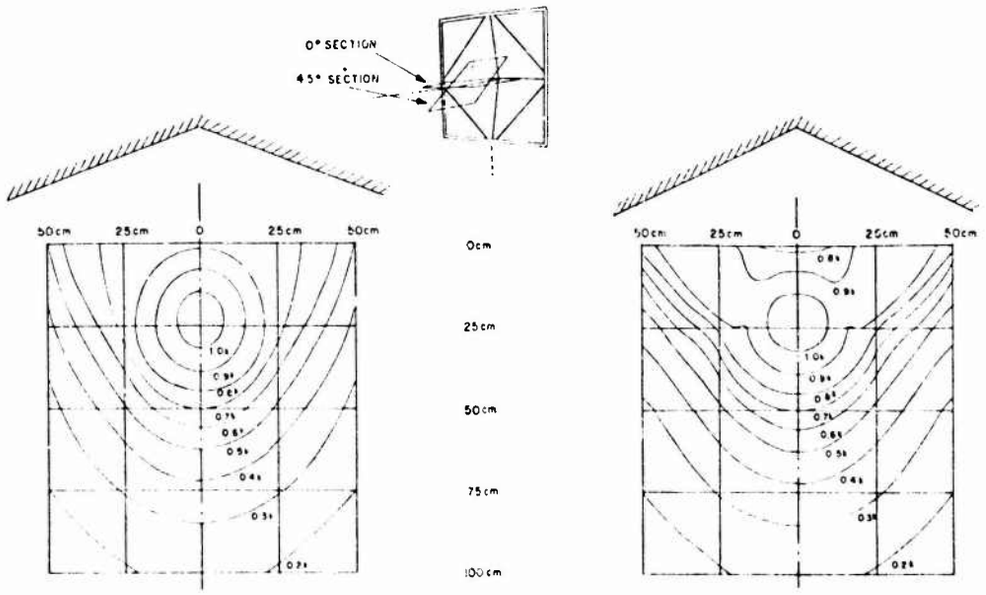

a. 0° Section

b. 450° Section

Multiply all Values by 45 to Determine Dose in Rad (Si)

Figure 3-197. Detailed isodose contours in 0- and 45-degree R-Z planes.

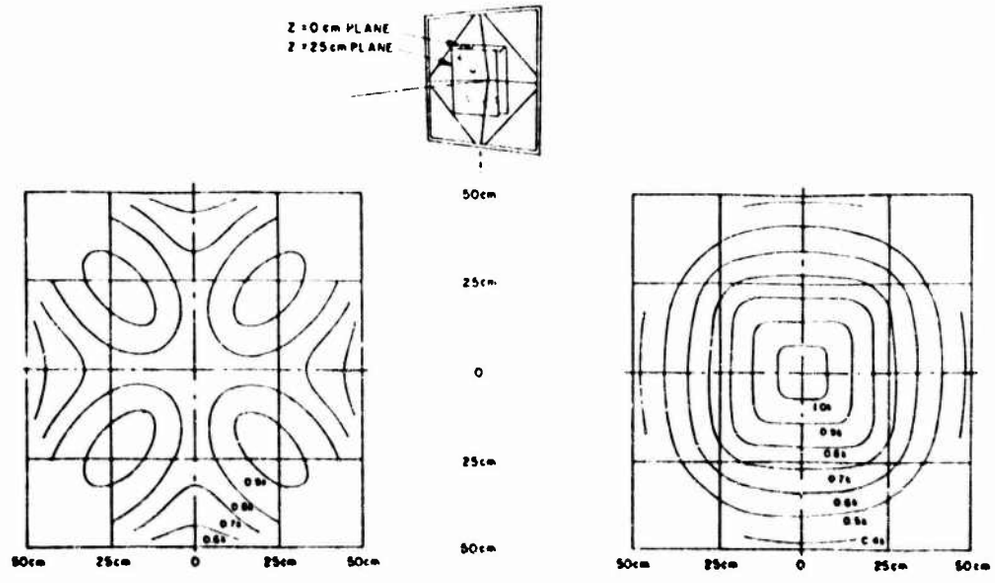

c. Z = 0 cm Plane

d. Z = 25 cm Plane

Multiply all Values by 45 to Determine Dose in Rad (Si)

Figure 3-198. Detailed isodose contours in Z = 0- and 25-cm planes.

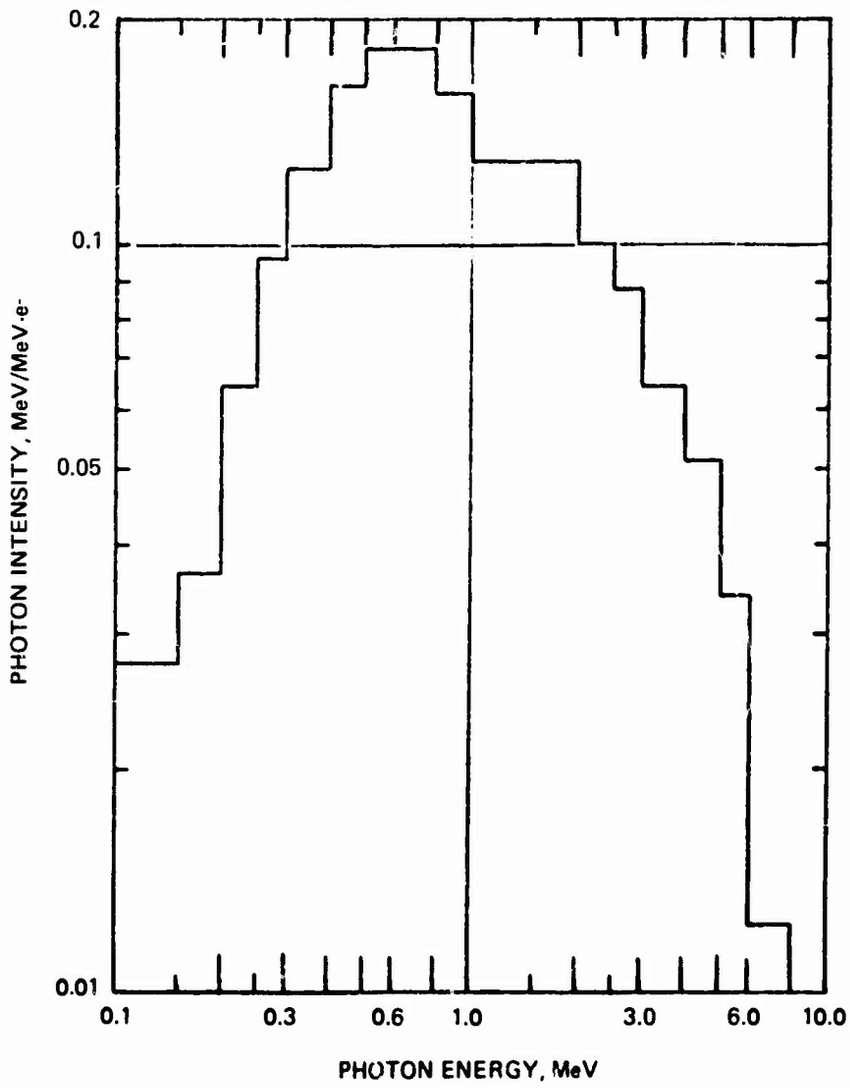

Figure 3-199. AURORA bremsstrahlung spectrum.

3.12.9 Electron Mode

The AURORA facility has the ability to irradiate objects directly with the electron beam. The beam is brought out of the anode-cathode region through a Ti foil into a drift chamber where experiments can be mounted. The electron beam is also used to produce high-intensity bremsstrahlung from a tungsten carbide target placed in the beam pinch. This technique produces 250 krad(Si) over a 1-in. spot.

The beam parameters for 90-kV charging voltage are:

1. Electron energy (V-beam) 8 MeV
2. Beam I (I-beam) 240 kA
3. Beam energy (E-beam) 325 kJ

4.	Pulse width	200-ns FWHM
5.	Max. energy fluence	E/A 500 cal/cm^2

The energy deposition profile shows an extrapolated range in Al of 4 gm/cm^2 and a maximum dose at a depth of 1 gm/cm^2 of 0.5 (cal/gm)/(cal/cm^2). Details of the energy deposition, fluence maps, and experimental hardware will be supplied upon request.

3.12.10 Support Capabilities

The following facility instrumentation is available to the user.

3.12.10.1 Oscilloscopes

All oscilloscopes are of the type needed for high writing rates, i.e., P-11 phosphors and f/1.3 lenses. Single-sweep arming/confirm camera shutter/confirm, baseline sweep, and graticule are automated. The types and quantity available are 12 Tektronix R556 with 12-1A1 and 24-1A5 plug-in units and 4 Tektronix Type R7903 with the following:

Time Units		Plug-in Amplifiers	
Number	Type	Number	Type
1	7B92	2	7A19
4	7B70	2	7A19-001
1	7B71	4	7A16
		4	7A13
		2	7A21N

3.12.10.2 Tape Recorders

The tape units have automated start-stop, automated speed confirm, servo speed control, IRIG A time code with 1-ms resolution, and search capability to 1-ms record time resolution. The tape units are:

1. One Sangamo 4784 with 30 channels of RF record/reproduce, a bandpass of dc-80 kHz (at 120 ips), tape speeds of 1-7/8 to 120 ips, ±250-mV full-scale differential input with line-to-line input impedance of 50 kohms.
2. One Ticor II (Mincom), with a capability of 12 channels of direct record/reproduce, a band pass of 1.5 MHz at 120 ips, tape speeds of 7-1/2 to 120 ips, 0.25-V full-scale, single-ended input impedance about 10 kohms. (Note: Ticor II is presently removed but could be reconnected if required by the user.)

3.12.10.3 Oscillographs

Two Honeywell 1912 Visicorders with a variety of galvanometers are available. They have time code and automated start-stop. Available are 30-dc amplifiers, 8 gage control bridge amplifiers, and 8 thermocouple control units (copper-constantan).

3.12.10.4 Data Scanner

The scanner is a Type 6401-2 Vidar 100-channel scanner, with high-speed printer, 20 channels/s maximum scan rate and 3-wire input for twisted-shielded pair, and automated start-stop. Thermocouple compensation is available. At the present, 90 channels of mV readout (1 μV resolution), 10 channels of chrome-alumel compensated readout, and 10 channels of iron-constantan readout are available. It is planned to connect the output to a minicomputer and increase the scan rate to 50 channels/s.

3.12.10.5 Timing Instrumentation

Available are: (1) one Eldorado 650 Digital Delay Generator, 1 ns to 1 s, by 1-ns increments, (2) two Systron-Donner 110B delay and pulse generators with 180-ns to 50-ms delay, 0.05% jitter, rise time of 4 ns to 500 μs, and pulse width of 10 ns to 5 ms, (3) one Systron-Donner 8150 time code generator with 1-ms resolution and display, which codes tapes to 1-ms resolution and oscillographs and data scanner to 1-s resolution (the time code generator remote unit gives the time of the shot to 1-ms resolution), (4) two Eldorado Time Interval Meters, 10-ns resolution, 100-ns to 1-s time interval, and (5) one Eldorado 796 Time Interval Meter with 1-ns resolution, 1-s maximum time interval.

3.12.10.6 Dosimetry

HDL will supply passive dosimetry of the thermoluminescent type. All of the normally used phosphors can be made available (LiF, CaF_2, $Li_2B_4O_7$, and $CaSO_4$) in both powder and teflon matrix form. HDL will assist the experimenter in specifying the dosimetry for this experiment.

The dosimeter system commonly used is CaF_2 in a teflon matrix. These dosimeters are supplied in the center of a 9/16-in. dia. and 1/2-in. length Al cylinder for electron balance when used on the exterior of a test package. They also can be used bare inside a test package, or they can be supplied in a TO-5 transistor can. Ta-balanced dosimeters are also available. The facility can read out 20 of these dosimeters per hr. The user can select which dosimeters he wants read out immediately after the shot. The facility will apply the proper correction for fading.

A prompt radiation detector on or near the simulator center line is part of the dosimetry available. After each shot, users are typically provided with a typed data sheet which includes the shot parameters, a graph of the dose rate versus time, and the dose and dose rate at the peak of the bremsstrahlung pulse for each dosimeter used.

3.12.10.7 Security Provisions

The building has all necessary security features, including controlled access. There are safes for documents and an 8- by 19-ft vault for classified hardware up through a level of Secret. All HDL personnel have at least a Secret clearance. All visitors to the facility should send their clearance to Harry Diamond Laboratories, Attention: Security Office, DELHD-ASE, 2800 Powder Mill Road, Adelphi, Maryland 20783.

3.12.11 Procedural Information

Inquiries should be directed to;

Harry Diamond Laboratories
2800 Powder Mill Rd.
Adelphi, MD 20783
Attn: Mr. Paul Caldwell, DELHD-RBI
AURORA Facility
Telephone: (202) 394-2290

The user will submit to DNA a General Program Plan 8 months prior to the desired test date. Further details on this requirement may be obtained from the contacts just listed. An exception to the 8-month requirement may be made in urgent cases; however, no assurance regarding the facility availability and support can be given.

Cost information can be obtained from

Director
Defense Nuclear Agency
Attn: RAEV (AURORA Project Officer)
Telephone: (202) 325-7026, 7088
A/V 221-7026, 7088

The shipping address is:

Harry Diamond Laboratories
AURORA Facility
2800 Powder Mill Road
Adelphi, MD 20783
Attn: Stewart E. Graybill

3.13 HONEYWELL FX-25 ELECTRON-BEAM GENERATOR

The IPC FX-25 FXR machine operates with a maximum charging V of 4 MV, with nominal charging V of 3.3 MV, yielding an electron-beam energy of 2.4 MeV in the high-impedance mode or 900 keV in the low-impedance mode. Figure 3-200 shows the facility layout.

Electron-beam experiments may be performed by setting them up in the drift tube. This tube is partially evacuated under normal conditions, but it may be operated at ambient pressure if desired. The inside dimensions of the drift tube are 6 in. in dia. and 22 in. in length.

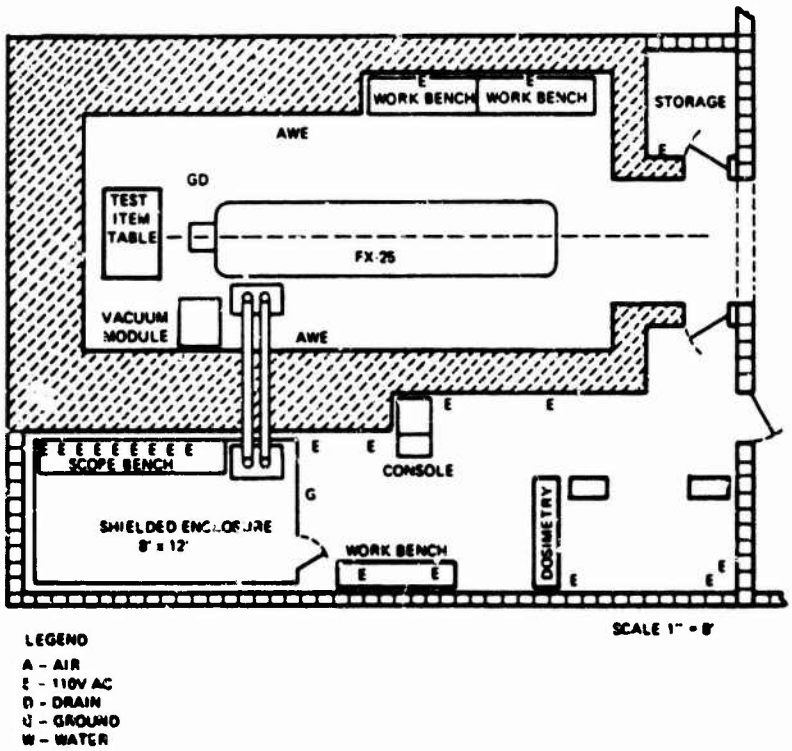

Figure 3-200. FXR facility layout.

3.13.1 Test Parameters

Sections 3.14 and 3.15 contain data on FX-25s at other locations.

The geometry of the electron-beam within the drift tube is strongly dependent upon the pressure of the tube. Energy flux measurements are made for each test position to be used. Data which may be used for selecting a preliminary exposure position are available for various pressure levels and at several points in the drift tube.

Operating charcteristics of the FX-25 are:

1.	Charging V	3.3 (4.0 max.) MV
2.	Maximum electron-beam energy	2.5 MV at 3.3 MV charging V
3.	Tube I (typical)	25,000 A
4.	Total energy/pulse	1,200 J
5.	Maximum electron flux	100/cal/cm^2
6.	Minimum electron flux	0.5 cal/cm^2
7.	X-ray dose (22 ± 5 ns, FWHM)	
	a. Total dose at surface of tube	2,500 rad(Si)
	b. Dose rate at surface of tube	1.25×10^{11} rad(Si)/s
	c. Total dose at 30 cm from tube	34 rad(Si)
	d. Dose rate at 30 cm from tube	1.7×10^{9} rad(Si)/s
8.	X-ray dose (high-intensity mode)	20 ns, FWHM
	a. Total dose at surface of tube	26,000-38,000 rad(Si)
	b. Dose rate at surface of tube	1.9×10^{12} rad(Si)/s
9.	Pulse repetition rate	1.2 m

These data are not definitive and are meant only to be used as a guide.

The maximum pulse repetition rate is 1.2 m/pulse in the bremsstrahlung mode. The limit for electron-beam testing is usually 1 pulse/10-m interval, due to the requirement of changing samples and stabilizing pressure within the drift tube. The nominal pulse delay is 700 ns between the fire command to the trigger light source and onset of radiation at the target. The jitter associated with this delay is within ±12 ns for any 10 successive shots.

The shielded enclosure, steel duct system, and test cassette provide complete protection from RF noise problems during x-ray testing of discrete components, circuits, or electronic systems. The shielded enclosure has been certified as exceeding requirements of MIL-STD-285. All power within the shielded enclosure is filtered. No unfiltered circuits of any type enter the enclosure, except those data cables which are protected by the steel duct system.

No electronic devices have been tested as active units while undergoing exposure to the electron-beam environment.

3.13.2 Diagnostic Techniques

Diagnostic techniques in the electron-beam mode include:

1. Graphite and Al total-stopping calorimeters
2. Thin-film dosimeters for beam profile and intensity
3. Deposition profiles (thin films interleaved between metal foils)

4. Return I shunt

5. Capacitive V monitor (cathode V)

Diagnostic techniques in the x-ray mode include:

1. Photodiode - scintillation radiation detector (waveform)

2. PIN photodiode - radiation detector (waveform)

3. Return I shunt

4. Capacitive V monitor

5. Dose maps and point dosimetry with TLD ribbon (chip)

6. Dose depth profiles with TLD-loaded arrays.

3.13.2.1 Electron-Beam Mode Environment

The electron-beam flux deposited at any point within the drift tube is strongly dependent upon the pressure in the tube. The experimenter may select any flux level within the range of 0.5 to 100 cal/cm^2. The flux distribution is symmetrical about the longitudinal axis at any point along the axis; therefore, it would be well for the test configuration to incorporate axial symmetry regarding position of sample holders on the test assembly. There is no evidence of the beam wandering within the drift tube.

Figure 3-201 shows the waveform of electron-beam V and I outputs.

Current
14.1 kA/cm
20 ns/cm
3/8 inch cathode

Voltage
3.03 MV/cm
20 ns/cm
3/8 inch cathode

Figure 3-201. Oscilloscope traces of electron-beam output waveform, V and I.

The electron-beam spectra shown in Figures 3-202 and 3-203 were generated at 3.3-MV charging V with 3/8-in. and 2-in. cathodes, respectively. Spectra are somewhat dependent on cathode-to-target spacing and cathode tip configuration; therefore, the standard operating procedure in the facility is to charge each shot to 3.3 MV and maintain a 3.5-cm cathode-to-target gap. The 3/8-in. cathode is tapered at 45 degrees, with point slightly blunted. The 2-in. cathode is terminated in a flat carbon plate with "waffle-grid" pattern machined into the face.

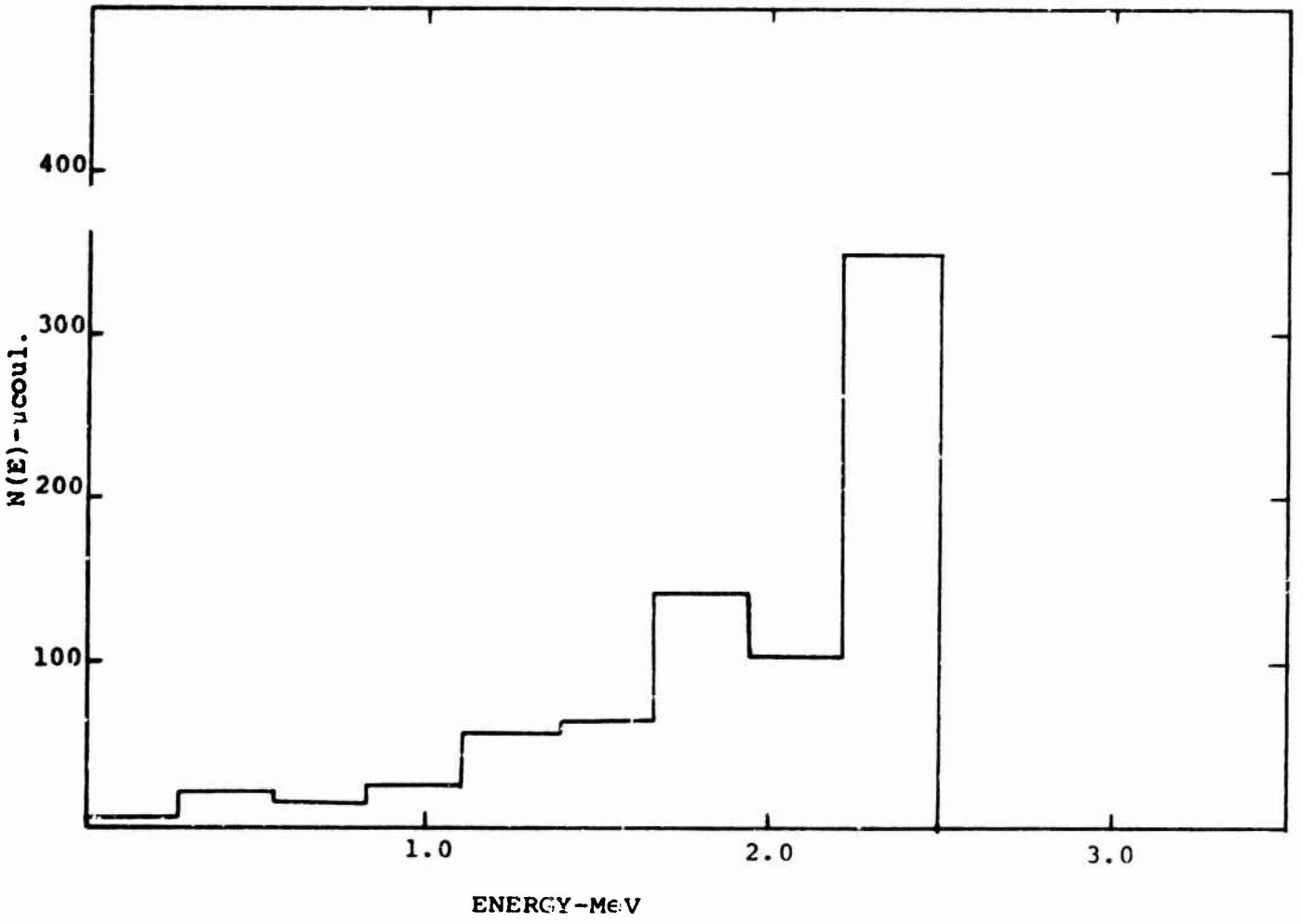

Figure 3-202. Electron beam spectrum with 3/8-in. cathode at 3.3 MV charging V.

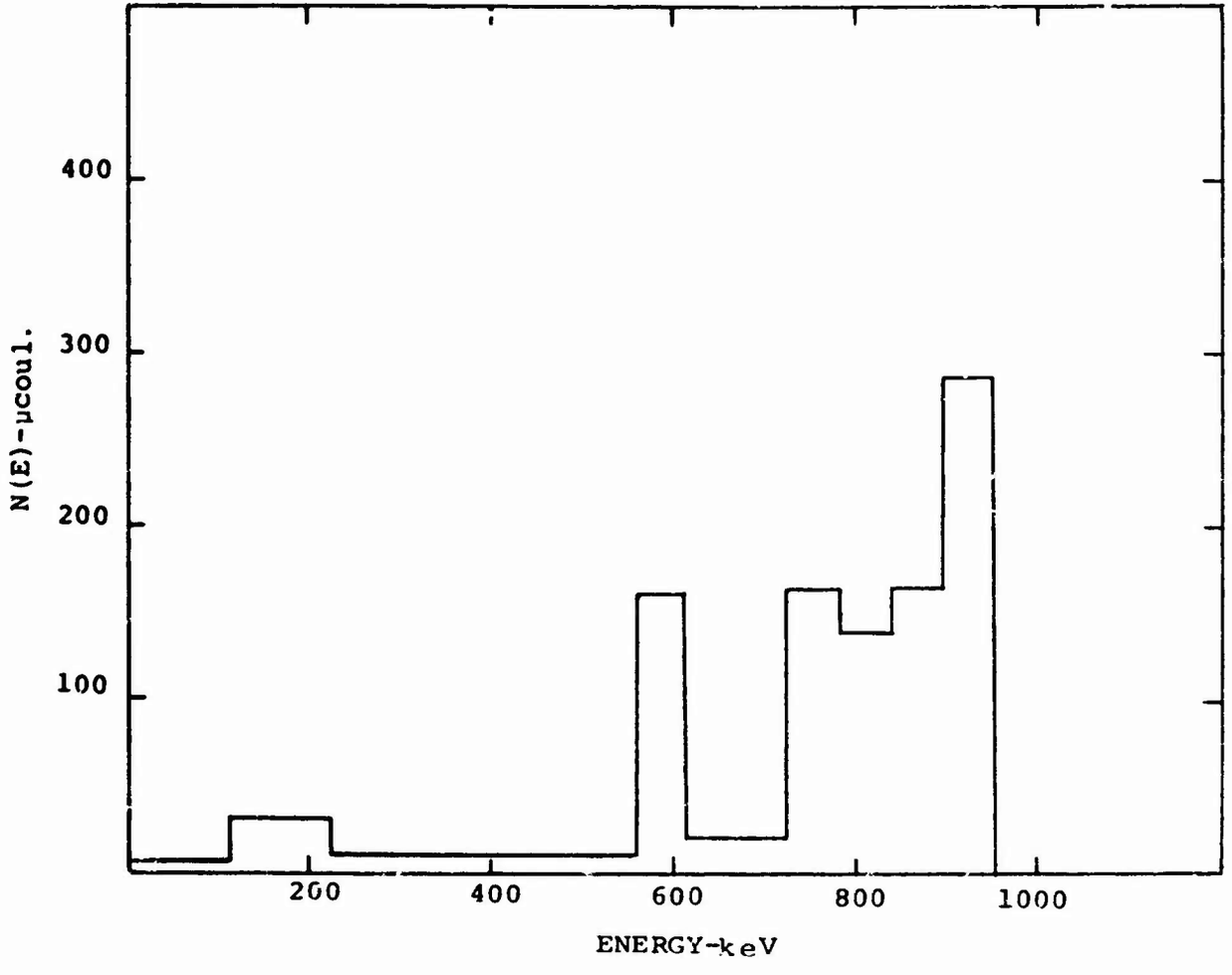

Figure 3-203. Electrom beam spectrum with 2-in. cathode at 3.3 MV charging V.

Figures 3-204 and 3-205 show the energy dose-depth profiles for the 3/8-in. and 2-in. cathodes, respectively. These plots show the relative dose versus depth in the materials (Al and Fe) indicated and are based on measurements with stacked foils and cellophane dosimeters.

3.13.2.2 X-Ray Mode Environment

The x-ray environment for 3.3-MV charging V, 3/8-in. cathode, and 3.5-cm cathode-to-target gap is shown in the center line maps and the spatial distribution maps of Figures 3-206 through 3-208. Center line data are presented for two conditions: (1) collimated by a 4-in. thick Pb shield with 2.5-in. port, (2) no collimation or other shielding in the field. The spatial distribution maps were determined with no collimation present. All data were obtained by means of TLD-100 thermoluminescent ribbon dosimeters (LiF). Accuracy of the TLD system is ±15% overall and measurements can be reproduced within ±5%.

The bremsstrahlung output pulse waveform is shown in Figure 3-209. The pulse width (FWHM) is 20 ns ± 5 ns. It was measured by a detector consisting of ITT FW114 photodiode with pilot-B scintillator. Charging V was 3.3 MV, with 3/8-in. cathode and 3.5-cm cathode-target spacing.

The x-ray spectrum for operation with the 3/8-in. cathode and 3.3-MV charging V has been computed and is shown in Figure 3-210.

3.13.3 Support Capabilities

Data recovery instrumentation available for use in the facility includes the following:

1. Instrumentation
   a. 1 Tektronix 7844 oscilloscope
   b. 2 Tektronix 7904 oscilloscopes
   c. 4 Tektronix 7704 oscilloscopes
   d. 2 Tektronix 556 oscilloscopes
   e. 2 Tektronix 519 oscilloscopes
   f. 1 Tektronix 475 oscilloscope
   g. 2 Datapulse 110B pulsers
   h. 1 Datapulse 101 pulser
   i. 1 Hewlett-Packard 215A pulser
   j. 6 Kepco PCX-40 power supplies
   k. 1 John Fluke 8300A digital voltmeter
   l. 1 CTC 1086 dual-level calibrator
   m. 1 Tektronix 576 curve tracer
   n. 1 Tektronix FG502 function generator

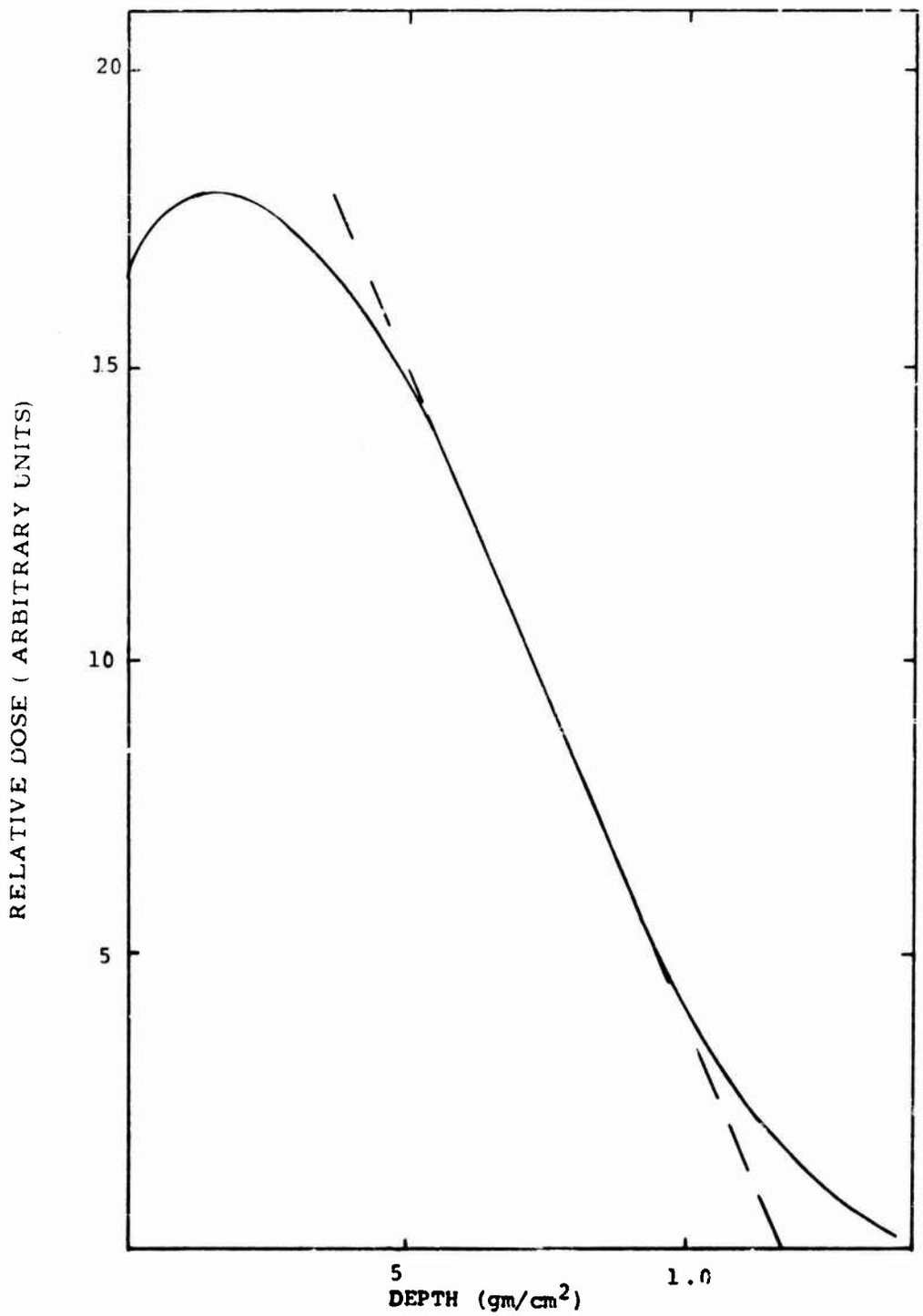

Figure 3-204. Depth dose with 3/8 in. cathode at 3.3 MV for stack of Al foils.

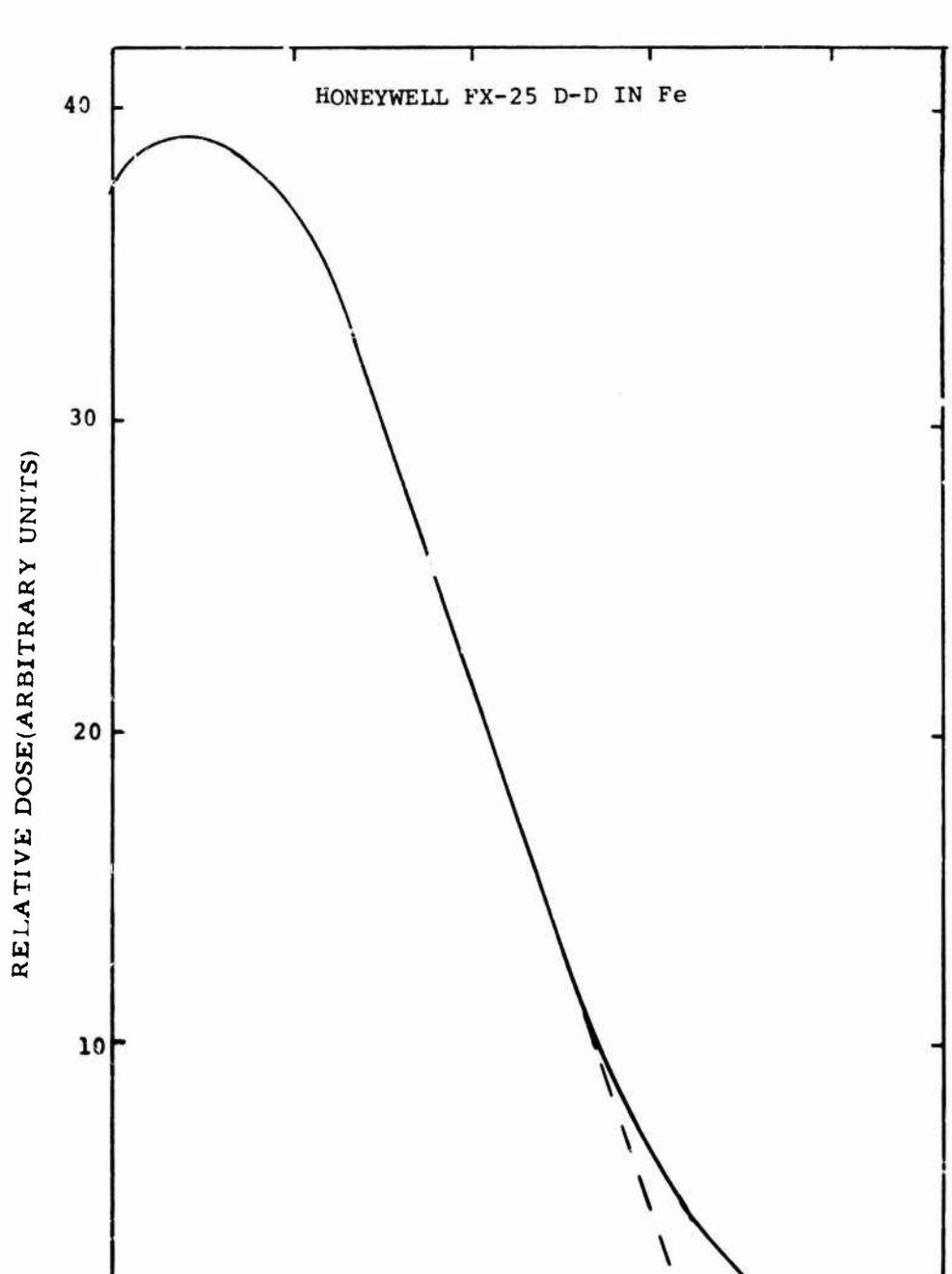

Figure 3-205. Depth dose with 2-in. cathode at 3.3 MV for stack of Fe foils.

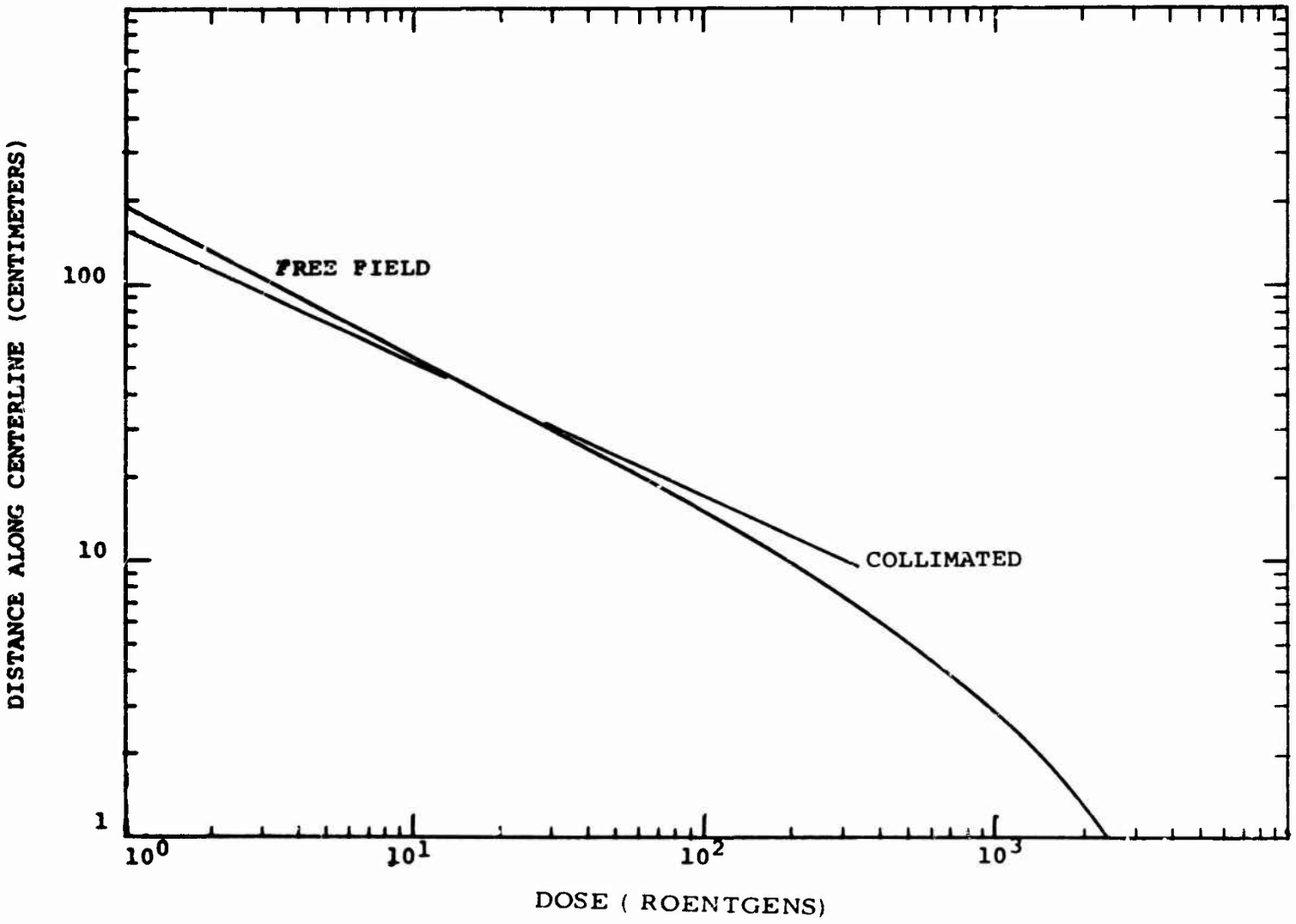

Figure 3-206. Total dose versus distance along centerline.

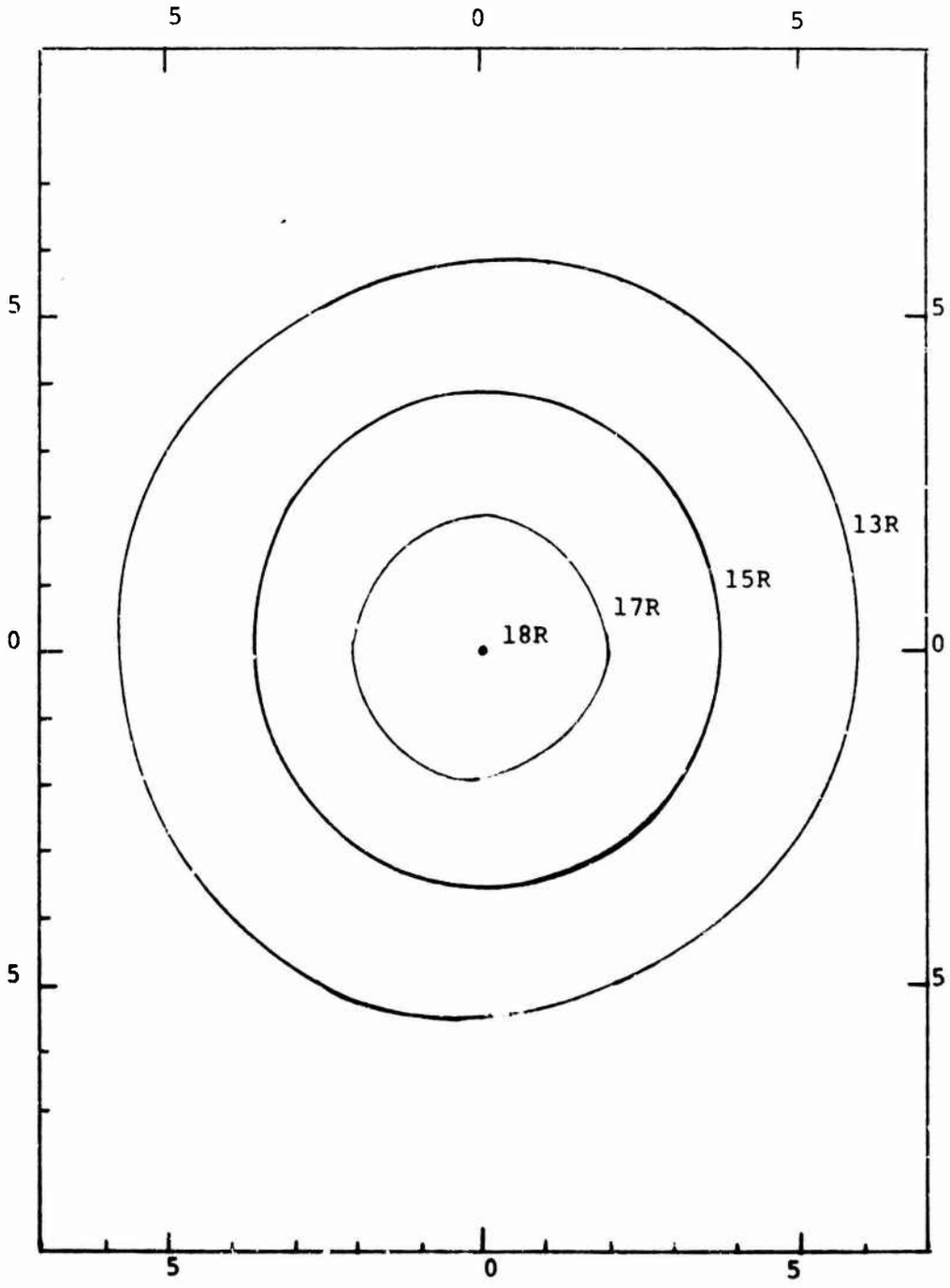

Figure 3-207. Radial dose distribution at 40 cm distance (collimated) (dimensions in cm).

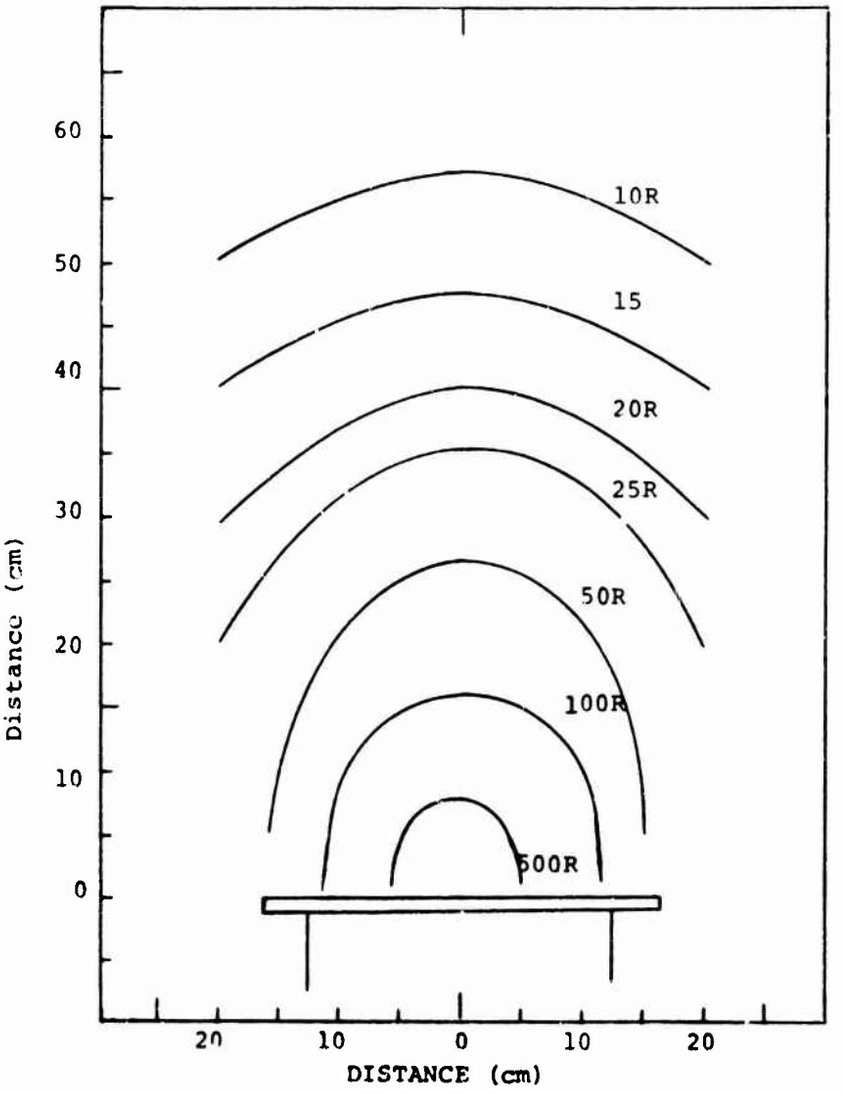

Figure 3-208. Dose distribution, horizontal plane.

Figure 3-209. Bremsstrahlung output pulses.

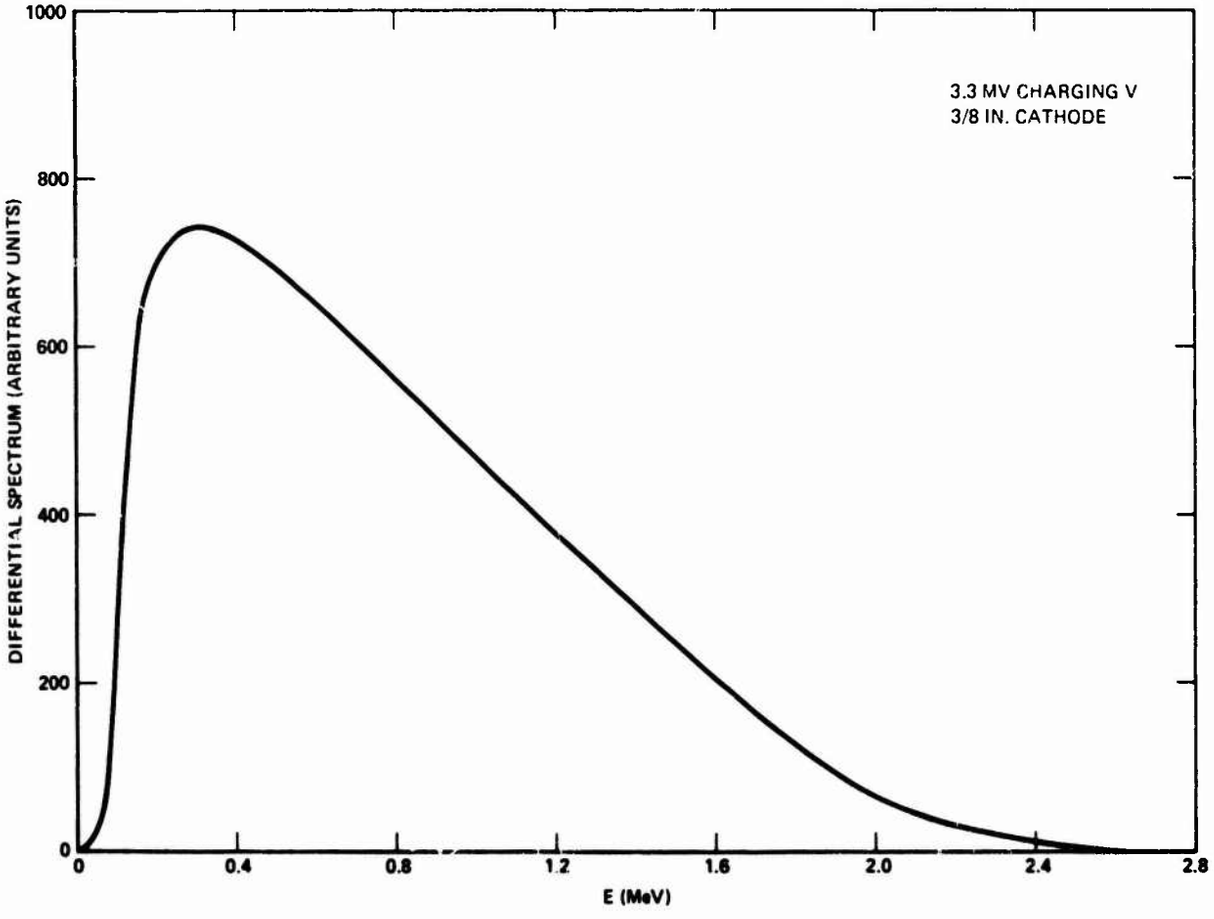

Figure 3-210. Honeywell FX-25 computed spectrum.

o. 1 Tektronix TG501 tire mark generator

p. 1 Tektronix SG504 sine wave generator

q. 1 Tektronix DC505 universal counter-timer

r. Other specialized power supplies, counters, voltmeters, and test instrumentation on hand

2. Power: 120-Vac, 3-ϕ, 1-ϕ, filtered power in shielded enclosures; 220-Vac, 3-ϕ and 120-Vac, 1-ϕ available in the machine room.

3. Cables: 20 each Trompeter triaxial TRC-50-2 cables and twinax TWC-78-2 cables installed in steel conduit extending between the shielded enclosure and the junction box in the machine room. Flexible steel conduit extends from the junction box to the test cassette.

Other specific instrumentation can be made available by prior arrangement.

A variety of timing signals are available. The 2 basic signals are the machine fire command pulse and the trigger pulse generated by a PIN diode at radiation emission. Three pulse generators and a console delay system may be used in conjunction with each other to delay radiation emission, pretrigger oscilloscopes, synchronize circuit functions, or combine these actions.

One 8- by 12-ft Rayproof Series 81 shielded enclosure is available in the instrumentation room. The enclosure exceeds MIL-STD-285 attenuation requirements for electric and magnetic fields. Filtered power consists of three 120-Vac, 1-ϕ, 50-A circuits. Plans include expansion of this room to 8 ft by 20 ft, and the addition of another 8- by 12-ft room.

The x-ray dosimetry system consists of Harshaw 2000 TLD readout instruments, LiF TLD-100 chips, and 2 types of CaF_2 TLD chips. The chips are calibrated in a known field, using the calibrated Co-60 source in conjunction with a Victoreen Condenser R-meter. The R-meter has been calibrated by the NBS. The Harshaw 2000 TLD readout system is recalibrated and maintained by Harshaw on a semiannual basis.

Electron-beam dosimetry consists of a 16-channel total-stopping C calorimeter and a single-channel Al calorimeter. Thin-film dosimetry is also on hand, with an American Instruments microphotometer for readout. Special dosimetry problems should be discussed with the facility staff.

Arrangements may be made for use of the Honeywell Computer System, consisting of Honeywell 6080, CDC 6600, and Honeywell 2000 computers. A complete manufacturing facility is available. This shop system is capable of constructing test electronics or fixtures ranging from simple model shop operations to complex systems. Adequate preparation space is available for the experimenter to set up, check out, and repair test electronics. Space for administration, data reduction, and conference is also available.

The facility maintains Tektronix cameras using Polaroid film for each of the oscilloscopes in the shilded enclosure. Camera backs for both flatpack and roll film are available. A Polaroid copying camera is also available. Honeywell maintains a photographic laboratory with complete still-photography and printing facilities. The Standard Test Cassette accepts test boards with 41-pin ELCO 7022 connectors. The board size limits are 5 in. wide, 4 in. high, and 1 in. deep. The depth could be increased if needed. The capability of building larger cassettes exists at the facility.

The Circuit and Piece Part Data Acquisition System consists of 6 line drivers, 2 current transformers, 2 ac input-output lines of 50 ohms, and 8 dc power lines. The specifications on these are as follows:

1. Line Drivers
    a. Bandwidth: dc to 100 MHz
    b. Input impedance: 10^{10} ohms
    c. V gain: 0.5
    d. V swing: 36 V; i.e., ±18V, 0 to +36, 0 to -36

2. Current Transformers

   a. Bandwidth: 10 kHz to 100 MHz

   b. Insertion impedance: 0.04 ohms

   c. Peak current: 100 A

Standard test boards are available for photocurrent measurements on diodes, zeners, transistors, and FETs. Also available are test boards for characterization of many digital and linear devices.

Electron-beam experiments are performed in a drift tube with a 6 in. I.D. and a 22-in. length.

Administrative and technical inquiries should be directed to:

Honeywell, Inc.
13350 U.S. Highway 19
St. Petersburg, FL 33733
Attn: Mr. Graff
Telephone: (813) 531-4611, Ext. 2669

Lead time of 1 month is required to schedule use of the facility. Information may be obtained directly from Honeywell. Costs and charges associated with use of the facility may be obtained directly from Honeywell.

The shipping address is:

Honeywell, Inc.
Honeywell Warehouses
13733 W. Rena Drive
Largo, FL 33540
Attn: J. Griessel (Plt E-1)

3.14 RAYTHEON RADIATION FACILITY, EQUIPMENT DEVELOPMENT LABORATORY

Raytheon maintains a radiation facility in Sudbury, Massachusetts, to provide nuclear effects simulation capabilities to the Survivability/Vulnerability (S/V) group. The facility is also available to outside experimenters on a service rental basis. Figure 3-211 is a layout of the facility, which contains FXR machines, a radioactive materials handling room, and a well characterized dosimetry system. The S/V section has an NRC (formerly AEC) by-product materials license which is required for neutron damage studies.

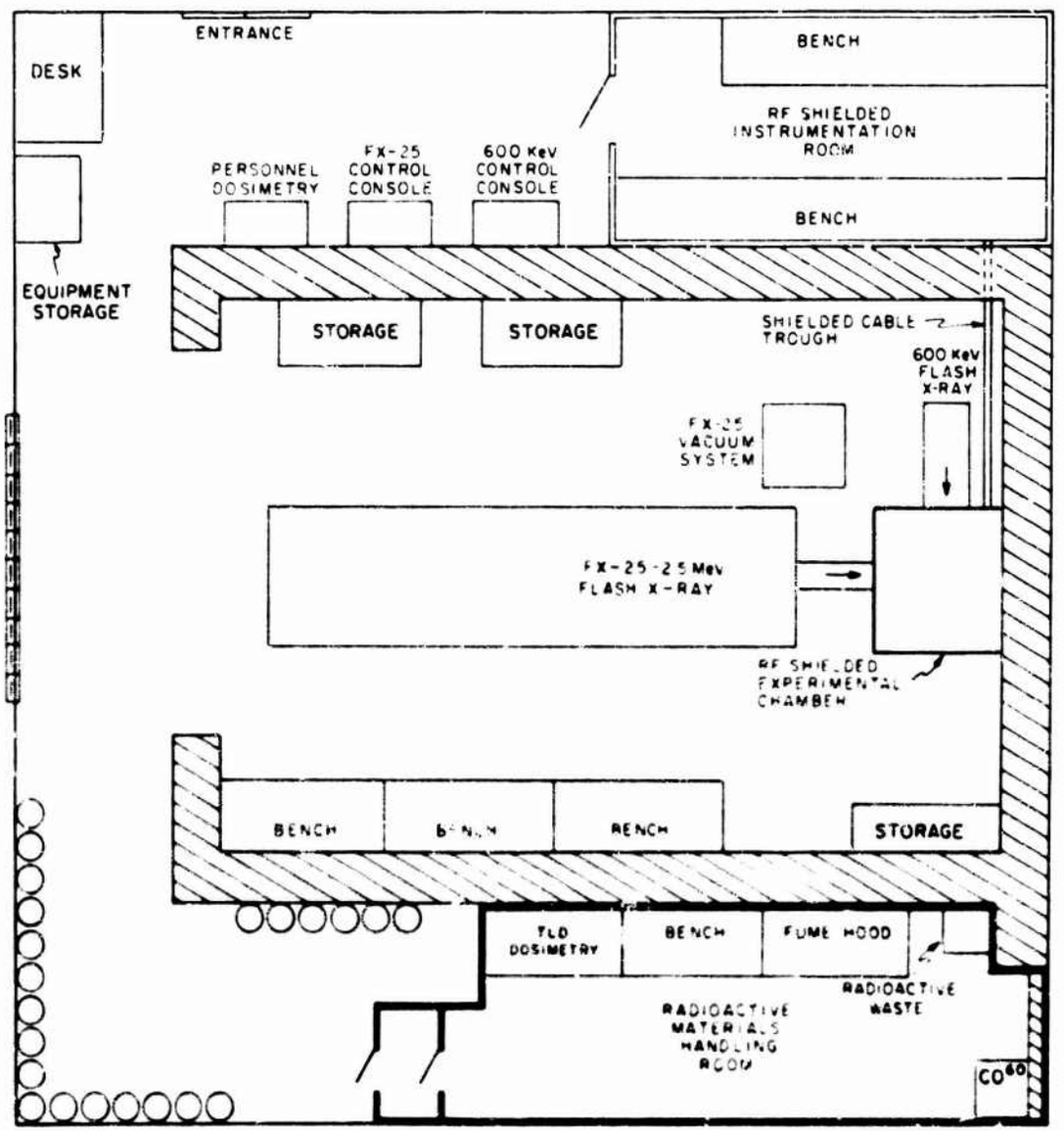

Figure 3-211. Raytheon Radiation Laboratory.

3.14.1 Operating Characteristics

The two FXR machines provide complementary capability in that they are of different emission energies and pulse widths.

3.14.1.1 Field Emission Corporation Model 730/2650

The Field Emission FXR is used primarily for testing piece parts and small circuit modules in low-dose-rate transient γ environments:

1.	Charging V (E_o)	600 kV
2.	Output I	1,500 A
3.	Pulse width (effective)	90 ns
4.	Peak dose rate	10^6 to 2×10^8 rad(Si)/s
5.	Total dose	18 rad(Si) max
6.	Effective photon energy	135 keV

3.14.1.2 Ion Physics FX-25

Sections 3.13 and 3.15 contain data on FX-25s at other locations.

Higher doses and dose rates are produced with the IPC FX-25 FXR machine than with the 730. The FX-25 can be used in either the γ or electron-beam mode. Conversion between radiation modes can be made in less than 1 hr. The specifications of the FX-25 FXR system are as follows:

1.	Normal terminal charging V (E_o)	3.5 MV
2.	Maximum electron-beam energy ($@E_o$ = 3.5 MV)	2.8 MeV (normal mode)
3.	Tube I (typical)	20,000 A
4.	Pulse width (effective)	20 ns
5.	Total energy/pulse	1,200 J
6.	Electron flux at 5 cm (pinch mode)	500 J/cm^2
7.	Maximum electron fluence	120 cal/cm^2
8.	Maximum γ dose (per shot):	
	a. Total dose at tube surface	3,000 rad(Si)
	b. Total dose at 30 cm from anode	90 rad(Si)
9.	γ dose rate:	
	a. Unattenuated	2×10^8 to 1.5×10^{11} rad(Si)/s
	b. Attenuated	2×10^8 to less than 5×10^4 rad(Si)/s

c. Pinch mode	1×10^{11} to 1×10^{12} rad(Si)/s
10. Repetition rate	1/min, max.
11. Pulse delay	Nominally 500 ns
12. Timing jitter	±15 ns
13. Machine pulse control	Experimenter has option of command firing by providing a trigger or manual pulsing by operator.

3.14.1.3 Electrical Noise

The facility contains two walk-in shielded enclosures. One is used as the experiment exposure chamber and the other for test instrumentation. The interconnecting power and data lines pass through a 20-ft metal conduit connecting both rooms electrically. Circuits for transient γ test can be set up inside a Mu metal box located in the exposure chamber. This allows the doubled-shielded test configuration recommended in the "Preferred TREE Procedures." Electrical noise can be held to a few mV or less when low-impedance (50-ohm) driving circuits are used.

3.14.2 Electron-Beam Mode

In the electron-beam mode, energy fluences up to 120 cal/cm^2 are available by use of the magnetic self-focusing phenomenon peculiar to high-density relativistic electron beams. Surface doses on the order of 5×10^{11} rad(Si) are attainable with a total deposition time of 50 ns (20-ns FWHM). This energy deposition rate makes the FX-25 an ideal energy source for thermomechanical damage studies and material (high strain rate) response investigations. Figure 3-212 shows the relative electron-energy distribution available with the standard 3/8-in. dia. cathode.

The FX-25 may also be modified for use as a source of lower energy electrons suitable for surface deposition and shock propagation studies. A special low-impedance cathode is used. The shank geometry employs a 2-in. dia. cathode with a graphite emitter, and is adjustable to allow the accurate gap settings necessary for the low-impedance electron-beam operation (see Figure 3-213). Conversion to this mode of operation requires no more time than other intermode conversions.

V and I time profiles at the cathode of the FX-25 can be monitored with the diagnostic collar on a shot-to-shot basis. This information is used with an in-house computer code (FX SPEC) to give electron-energy spectrum information as shown in Figures 3-212 and 3-213.

3.14.3. X-Ray Mode

The FX-25 uses a Ta anode to obtain bremsstrahlung conversion. The resultant photon spectrum has a maximum energy of 2.8 MeV with the peak effective energy of

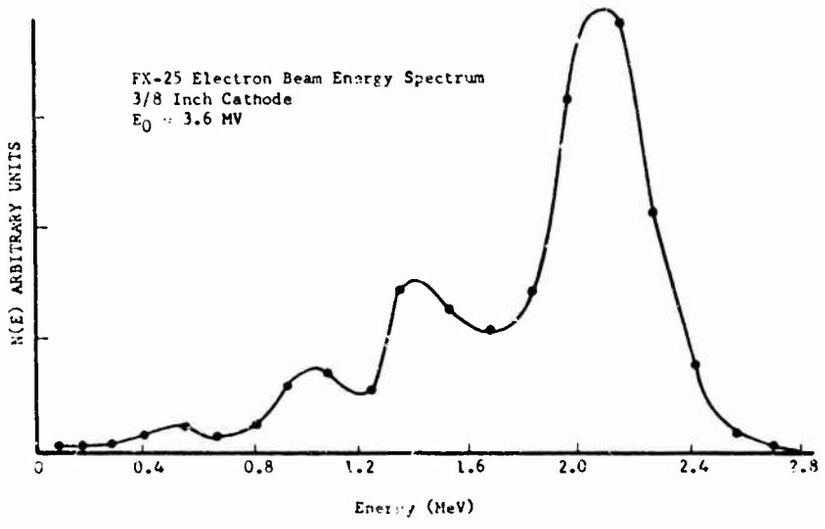

Figure 3-212. Pulsed electron-beam energy spectrum (normal mode).

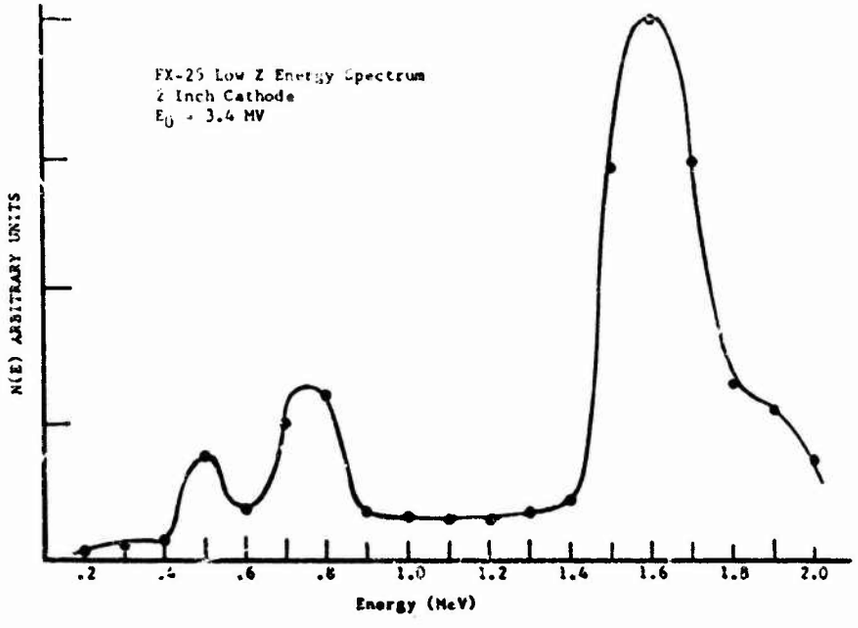

Figure 3-213. Pulsed electron-beam energy spectrum (low-Z mode).

the distribution being approximately 1.2 MeV. Peak dose rates of 1.5×10^{11} rad(Si)/s and reproducibilities of better than 5% are realized.

The FX-25 also may be operated in the pinch mode to increase the machine output by a factor of 10 for irradiation of small-area piece parts.

The FX-25 produces a radiation field pattern which is well suited for testing large components or circuit modules. The spatial distribution of the radiation from the machine is illustrated by Figure 3-214, which shows the isodose contours. A typical radiation intensity-versus-time profile, measured with a PIN diode detector, is shown in Figure 3-215.

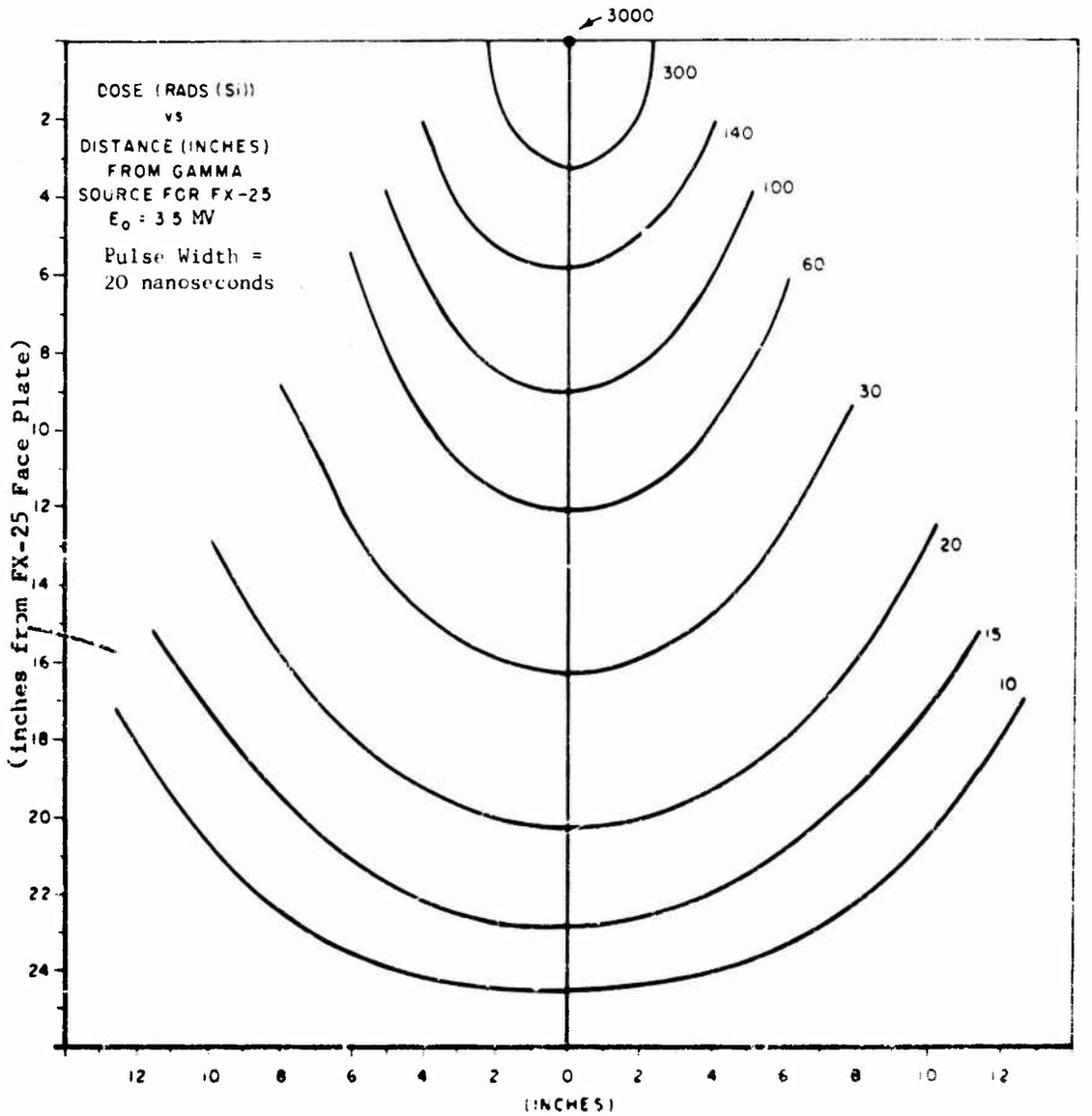

Figure 3-214. Dose spatial distribution for FX-25.

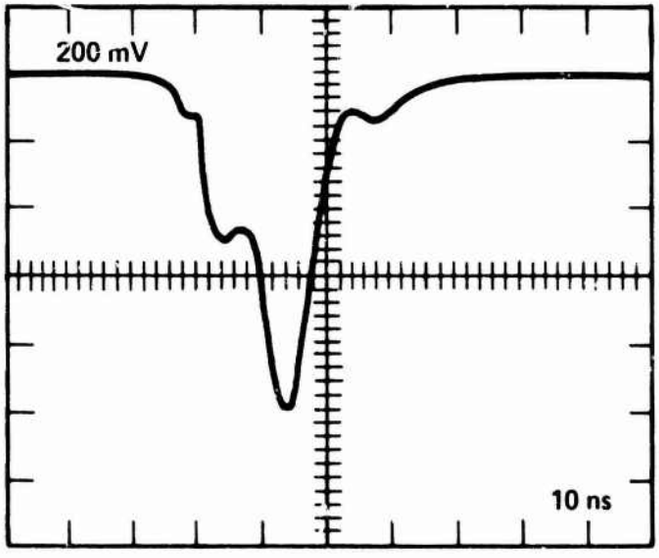

Figure 3-215. Radiation pulse profile, FX-25 (T = 10 ns/div).

3.14.4 Support Capabilities

Facility personnel provide machine operation, dosimetry support, and electronic test circuit and fixturing design or consultation. Operation of data recovery instrumentation is also available upon request.

Camera-equipped dual-beam oscilloscopes are used to record experimental data. Fast oscilloscope traces of radiation pulse shape and experiment responses are recorded using high-speed film and oscilloscope options for writing speed enhancement. Equipment such as pulse generators and power supplies are normally available to the experimenter. Special equipment such as counters, function generators, etc. can be made available by prior arrangement.

Triggering signals referenced to the machine pulse command signal are readily available. To eliminate a common transient test problem, RF noise, both machines are arranged to fire into a walk-in RF-shielded enclosure. A second shielded room also has been installed in the laboratory to house electronic test equipment. This shield room is fully instrumented to support transient γ and electron-beam tests. A 1-dimensional positioning platform with remote readout is used to control the distance of a sample from either FXR. The platform has a travel range of 37 in. and positions to an accuracy of a few hundredths of an inch. P-11 phosphor CRTs, 10,000 speed film, and other writing speed enhancement techniques are used in recording oscilloscope data. A full range of photographic laboratory services can be made available by prior arrangement.

The Reliability Analysis Laboratory (RAL) occupies 3,000 ft^2 and has the following special facilities:

1. Complete microsection facility
2. Metallurgical microscopes
3. Optical interferometer for thin-film measurements
4. Microphotographic equipment
5. Special electrical test equipment for testing microelectronics circuitry
6. Air-abrasive and high-speed cutting tools for module analysis
7. X-ray equipment
8. Low-high temperature probes for analyzing in-circuit device performance
9. Microprobing station for electrically contacting individual components within an IC.

Automatic semiconductor testers with magnetic-tape data storage are available for obtaining statistical data on parameter variances. Also available is an IR microscope for sensing temperatures of a device without physical contact. In addition, the following equipment is available for identification of unknown materials and characterization of various organic substances such as encapsulants, adhesives, and conformal coatings:

1. 2,500- to 40,000-nm Infrared Dual Beam Grating Spectrophotometer
2. 190- to 3,000-nm Dual Beam Grating Spectrophotometer
3. Thin-Layer Chromatograph
4. High-Pressure Liquid Chromatograph
5. Thermogravimetric Analysis (TGA).

A Cambridge Stereoscan Scanning Electron Microscope (S-4) with an energy dispersive x-ray analysis system to determine elemental content of the material under observation, is adjacent to the RAL. This instrument features spatial resolution down to 125 Å with a wide range of continuously variable magnifications from 20X to 100,000X. The microscope's primary function is to support reliability and failure analysis studies in areas such as metallurgical sciences, thin-film and microelectronic technology. Complete and thorough analyses are made possible by virtue of the instrument's versatile specimen imaging modes.

3.14.5 Dosimetry

Chromel-alumel thermocouples welded to very thin Ti disks are used to measure the incident radiation dose for samples in the FX-25 electron beam. The sensor discs are placed directly in front of the test samples during exposure. Temperature rise in the sensor is recorded on an oscilloscope trace photograph which is convertible directly to energy deposition in the calorimeter. This is related to deposition in the sample by means of a Monte Carlo electron transport computer code (ELTRAN). A total-stopping C calorimeter is also available for measuring the

incident electron fluence. This instrument is generally used for beam-mapping studies and is not considered an active dosimeter.

CaF_2 and LiF ribbon TLDs are used for ionizing radiation measurements. Their small size makes them a good approximation to the idealized point dosimeter. Useful dose range extends from 0.01R to 6×10^4R. The dosimeters can be reused after being subjected to the proper thermal annealing cycle. Dose-rate independence is exhibited to above 2×10^{11}R/s. Their electron response is generally equivalent to their γ response. Readout is accomplished on a Harshaw TLD Readout System (Model 2000).

An organic scintillator (Pilot B), coupled to a high-I biplanar photodiode (ITT FW114) detector, is available for monitoring the high-intensity, short-duration pulse from the FX-25. The diode signal can be used to trigger electronic testing support equipment such as an oscilloscope.

Reverse-biased PIN diodes are used to provide an accurate time profile of the radiation pulse of either FXR machine. The diodes provide output I which is a linear function of dose-rate with the PIN junction operating fully depleted. Bias levels of 250 and 1,000 V are used to maintain the necessary depleted condition. Diodes of 3 complementary sensitivities are presently used:

1. Quantrad 100-250-BG 2.2×10^{-7} A/rad(Si)/s
2. Quantrad 004-250-BG 8.9×10^{-9} A/rad(Si)/s
3. Unitrode UM 7202 B 6.6×10^{-10} A/rad(Si)/s

The detector output signal is calibrated with TLDs to establish a signal V versus radiation-dose relationship.

A 1.2-Ci Co-60 (receipt date 3/16/72) source is located in the Radioactive Materials Handling Room. The source will accept samples of cylindrical shapes of up to 2 in. dia. It is calibrated at regular intervals with an NBS-certified Ionization Chamber R-Meter, and is used as a calibration source for dosimeters such as thermoluminescent materials and personnel monitors.

3.14.6 Computational Facilities

Raytheon has in house and available to the S/V section two major computing facilities plus several smaller facilities. A Univac 1108 and CDC 6700 are operational at the Raytheon Bedford Laboratories with remote service available at Sudbury. In addition, the Sudbury remote terminal services an outside CDC 6700, Univac 1108, and IBM 360.

All of the major software programs presently being used in the industry are available at Raytheon:

1. **DAFFER II: a photon deposition program which includes the effects of fluorescence and scattering in both the forward and reverse direction**

2. ELTRAN: A Monte Carlo code which computes electron transport of a single or multienergetic electron spectrum incident upon a target consisting of up to 20 different material slabs

3. WONDY: A 1-dimensional shock propagation code which solves the finite difference analogs to the Lagrangian equations of motion

4. PUFF V-EP: A hydrodynamic code used to predict the characteristics of 1-dimensional shock pulses associated with the absorption of photons by materials, or with the impacts of flyer plates on the surface of materials.

There are 3 transient analysis programs currently being used by the S/V section to predict circuit and system response and to provide correlation between laboratory test results and predicted responses. These programs are CIRCUS, SCEPTRE, and TRAC. All 3 programs perform essentially the same task of analyzing the response of an electronic circuit to an arbitrary forcing function with the additional capability of determining the operation of the circuit in an ionizing radiation environment. Each program has its own peculiarities, and for any particular analysis one of the programs is generally more desirable than the others.

3.14.7 Procedural Information

For further information contact:

Raytheon Equipment Development Laboratory
528 Boston Post Road
Sudbury, MA 01776
Attn: H.L. Flescher or R.N. Diette
Telephone: (617) 443-9521, Ext. 2531 or 2319

A lead time of 1 month is desired (and often required) for scheduling.

Cost and charges for facility rental are subject to fluctuation. Request for facility rental and cost information should be directed to the attention of R.N. Diette and inquiries related to analysis or study programs to the attention of H.L. Flescher.

Shipments should be directed to:

Raytheon Equipment Development Laboratory
528 Boston Post Road
Sudbury, MA 01776
Location 1K5

3.14.8 Applicability and Availability

The Raytheon FXR facility provides transient radiation environment simulation applicable to TREE experiments. The facility is available to experimenters on a noninterference basis with Raytheon internal programs. The S/V group maintains a technically oriented professional staff for support and consultation.

The laboratory is located on Route 20 in Sudbury, Massachusetts, and is within an hour's drive from Boston, with overnight accommodations close by.

3.15 GENERAL ELECTRIC FX-25 ELECTRON-BEAM GENERATOR

The General Electric (GE) Radiation Effects Laboratory, Valley Forge, includes an IPC FX-25 FXR machine, equipments for electron and bremsstrahlung operation, and dosimetry and data recovery instrumentation. Figure 3-216 is a layout of the FX-25 laboratory facility.

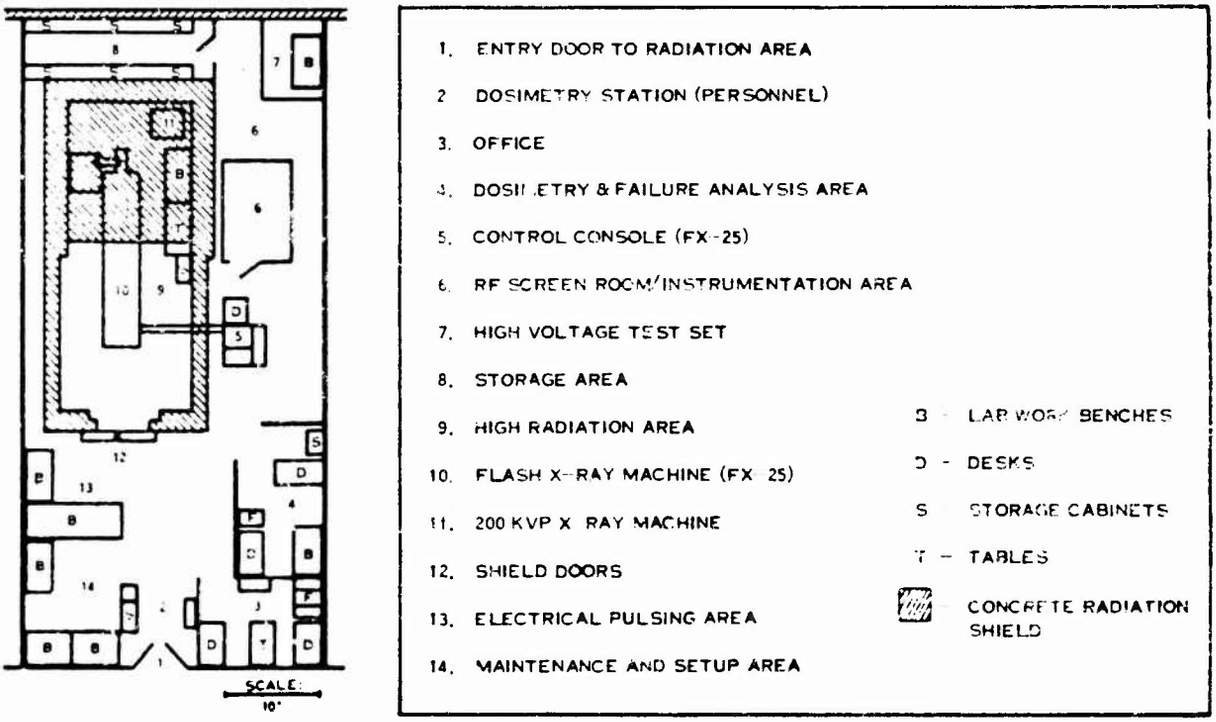

Figure 3-216. GE FX-25 laboratory layout.

3.15.1 Operating Characteristics

Maximum electron energy is 2.4 MeV. Equipments and procedures are available for electronics and materials single-dose exposures of 1 krad to 20 Mrad. Bremsstrahlung exposures of up to 3,500 rad(Si) are obtained on small samples. Nominal operating characteristics of the FX-25 are as follows:

1. Charging V	3.6 (4.0 max.) MV
2. Maximum electron-beam energy	2.5 MV at 3.3 MV charging V
3. Tube I (typical)	20,000 A
4. Total energy/pulse	1,200 J
5. Maximum electron flux	100/cal/cm^2
6. Minimum electron flux	0.4 krad(Si)

7. X-ray dose (22 ± 5 ns, FWHM)

a.	Total dose at surface of tube	3,200 rad(Si)
b.	Dose rate at surface of tube	1.25×10^{11} rad(Si)/s
c.	Total dose at 30 cm from tube	40 rad(Si)
d.	Dose rate at 30 cm from tube	2×10^{9} rad(Si)/s
8.	Pulse repetition rate	2 min
9.	Trigger jitter	5 ns
10.	Firing V	2.4 to 4.0 MV

These data are not definitive and are meant only to be used as a guide.

Sections 3.13 and 3.14 contain data on FX-25s at other locations.

3.15.2 Electron-Beam Mode

A 6-in. dia. drift tube with controllable vacuum is used for beam shaping, beam transport, and experiment mounting. The beam is annular at the FET transmission anode, pinches to the geometric center line at 5 cm, and then diverges at high vacuum. Under controlled vacuum conditions, the optimum beam transport conditions give the longitudinal fluence map shown in Figure 3-217. Figure 3-218 shows beam dia. for various peak fluence requirements. Aperturing and scattering foils may be used to further tailor the beam. Figure 3-219 presents the electron-mode pulse shape. The electron-beam spectrum has been measured using a 180-degree fixed-field magnetic spectrometer. Data are shown in Figure 3-220. Figure 3-221 presents one set of measured depth-dose data. Calculated depth-dose plots for various operating conditions are also available for Al and other materials.

Pulse reproducibility and predictability are within the limits of dosimetry techniques under high vacuum conditions. When drift-tube vacuum and gas mix are controlled to tailor the dose, their repeatability affects the electron fluence. Diagnostics are used to monitor each pulse. Shot-to-shot jitter is better than 5 ns.

A summary of the FX-25 electron-beam diagnostics available for electron exposures is as follows:

1.	Calorimeters	
	a. 16-chip C array	
	b. Depth-dose foil array	
	c. Al disk/thermocouples	
2.	Current	Rogowski coil
3.	Pulse shape	Scintillator photodiode

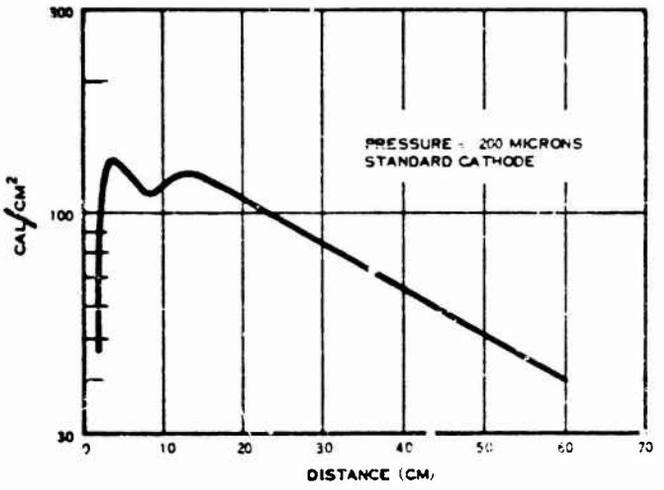

Figure 3-217. FX-25 electron-beam map (longitudinal).

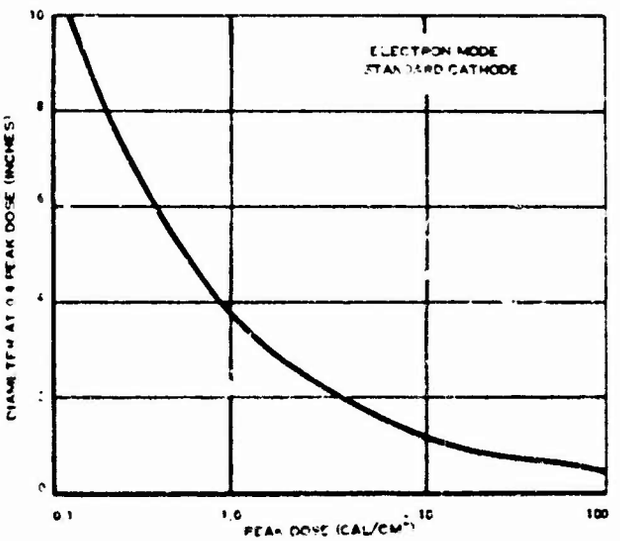

Beam Diameter Versus Peak Dose

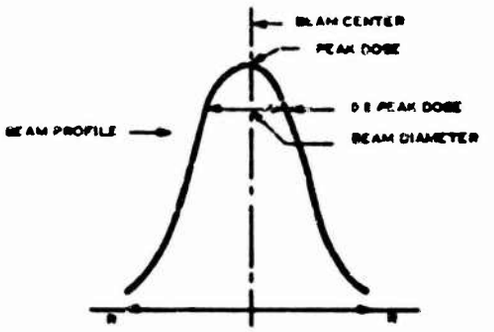

Figure 3-218. Typical beam profile.

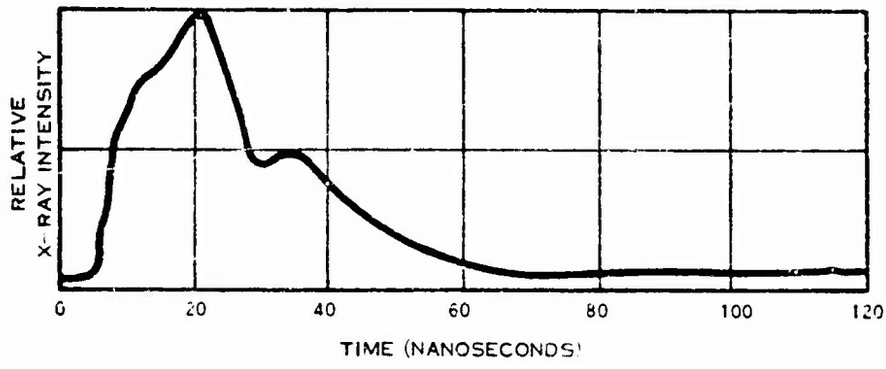

Figure 3-219. Pulse shape, electron-beam mode.

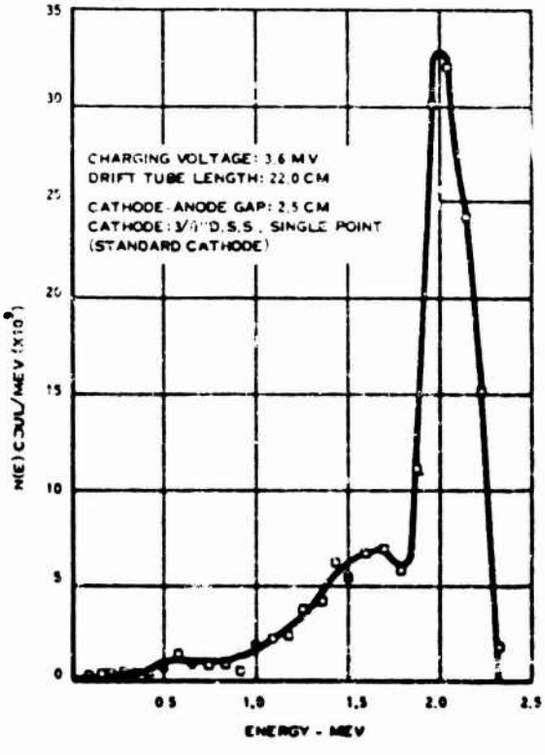

Figure 3-220. Electron energy spectrum of GE FX-25 unit.

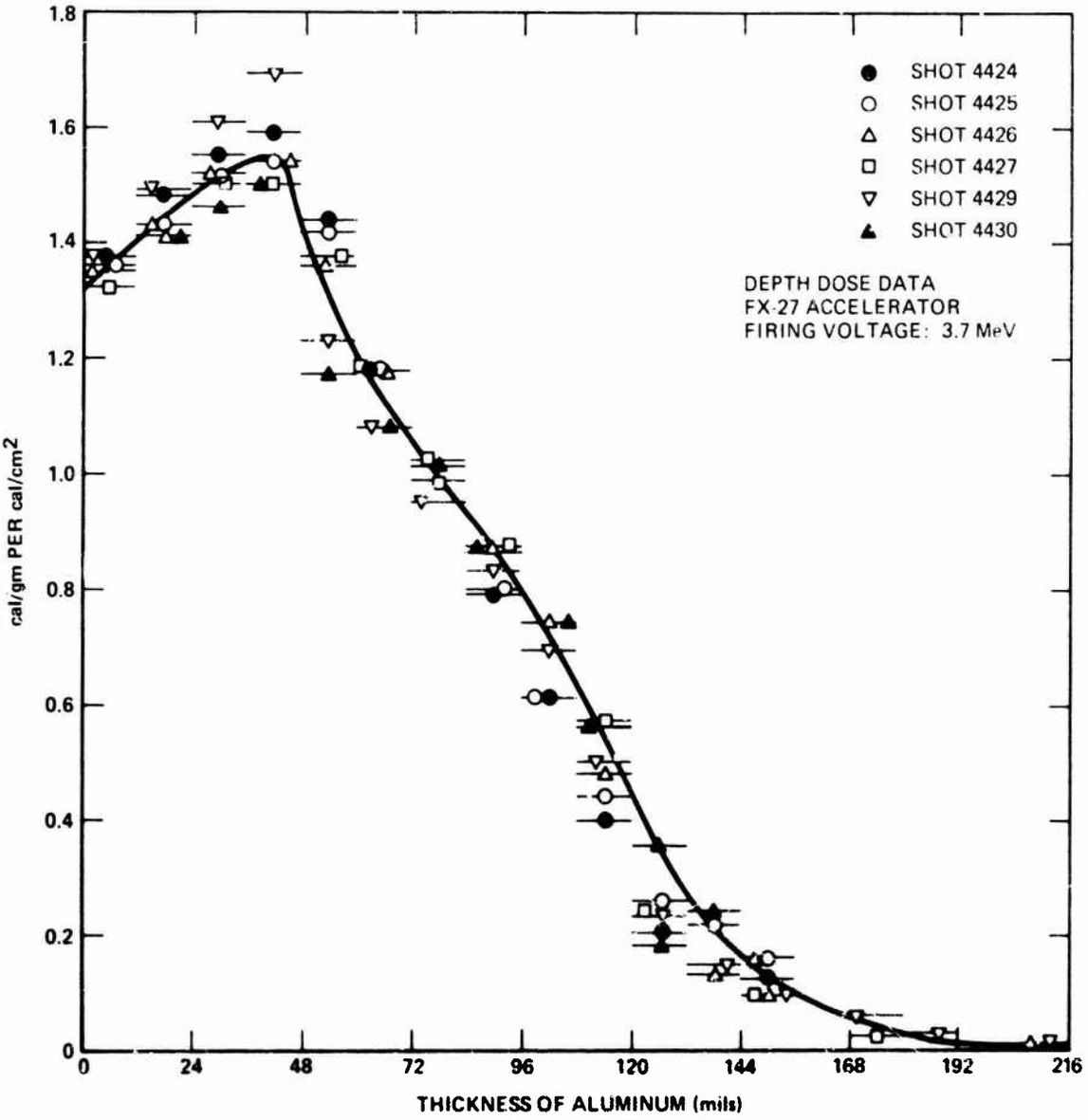

Figure 3-221. Measured depth-dose data.

4. Dosimetry
   a. Powder, rod, disk TLDs
   b. Radiation sensitive paper
   c. Blue cellophane.

The FX-25 is inherently a quiet machine. To minimize noise and sample effects, a Faraday cage is used for complete experiment containment. This cage surrounds the exposure volume and utilizes triaxial cables to an RF screen room.

3.15.3 X-Ray Mode

The x-ray dose for a 3.6-MV charging voltage, 3/8-in. cathode, 15-mil Ta anode, and ac gap of 2.8 cm is shown in Figure 3-222. Dose detail is available for other operating conditions.

The x-ray pulse waveform shown in Figure 3-223 is for a 3.6-MV firing V. These data were obtained with a pilot-B scintillator/ITT FW114 photodiode combination detector and a Tektronix 519 oscilloscope. IPC calculations for a 3.6-MV charging V are presented in Figure 3-224.

The FX-25 is consistent in its output as to pulse shape, intensity, and shot-to-shot jitter. Dose repeatability is better than TLD measurement precision, although slightly dependent upon different operator's charging rates.

3.15.4. Support Capabilities

The Radiation Effects Laboratory will support tests with minimal to full service, as required by the user, both in test planning and test conduct. Staff will operate the FX-25 and dosimetry, and is available for assistance in other areas of testing, as required.

A 7-ft by 10-ft Lundgren double-shilded screen room is available, with cabling to the exposure area. Considerable electronics are available for use by prior arrangement. In the transient data recovery area, this includes single- and dual-beam oscilloscopes of 33- to 1,000-MHz bandwidth capability and cameras. Also, 2 Tektronix digitizer data channels are available. General test equipment available includes current probes, voltmeters, power supplies, pulse generators, and discrete device testers. Specialized equipment includes remote-controlled sample positioners, line drivers, lead shielding, and RF-shielded sample boxes.

The principal dosimetry method used is TLD with an Isotopes Model 7100B reader, and a wide range of dosimeter shapes and phosphors. Calibration is done on site utilizing Co-60 sources.

A combined effects chamber is available for pulsed electron-beam and x-ray exposures. This chamber has in-situ optical measurement capability, rotating multiple sample holder, fast pump down (10^{-7} torr attainable vacuum), hot and cold temperature control, and electrical feedthroughs.

Shop facilities, setup areas, and data reduction/conference areas can be provided upon request.

3.15.5 Procedural Information

Administrative and technical inquiries for facility rental or contracted testing should be directed to:

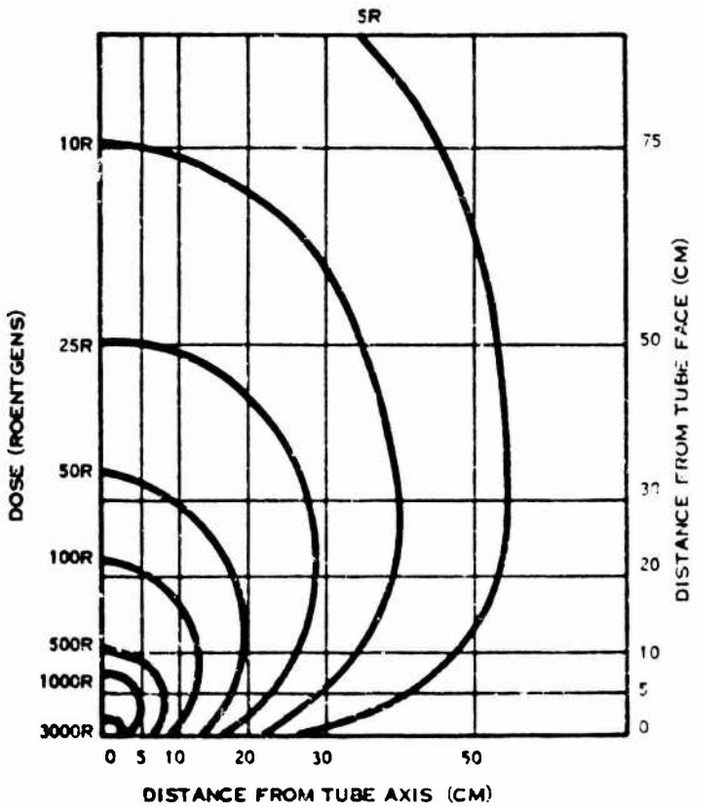

Figure 3-222. FX-25 x-ray dose map.

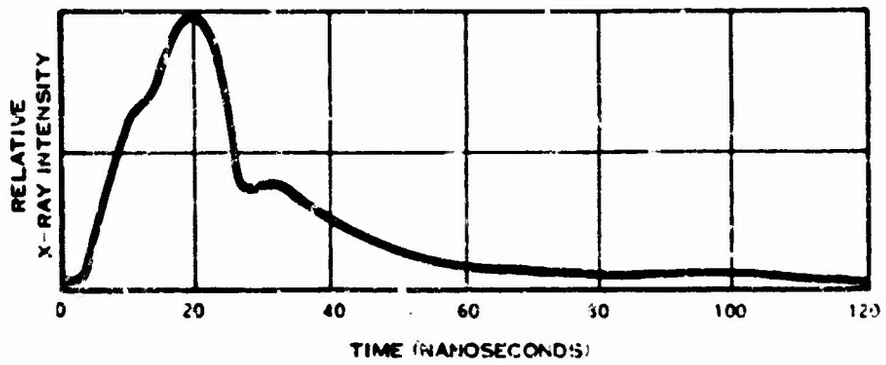

Figure 3-223. Pulse shape, x-ray mode.

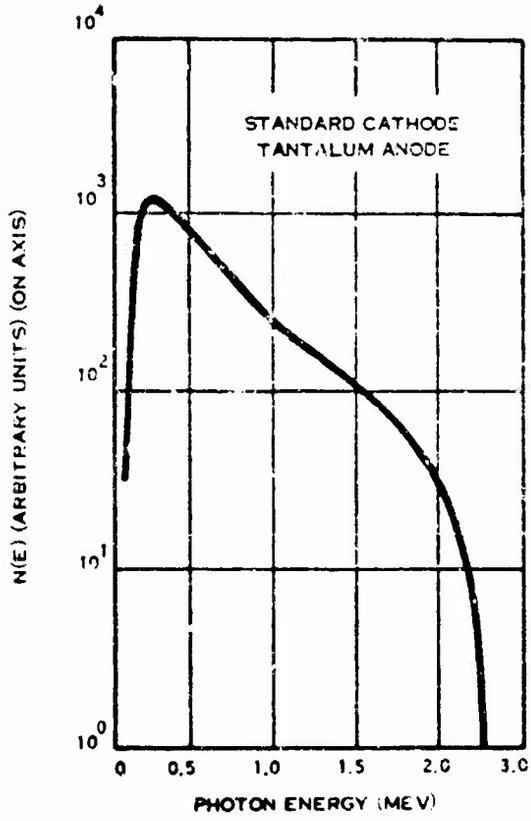

Figure 3-224. FX-25 bremsstrahlung spectrum.

Space Division
General Electric Company
P.O. Box 8555
Philadelphia, PA 19101
Attn: J.C. Peden
Telephone: (215) 962-2000

Cost and charges for facility use may be obtained from Mr. Gene Tyrell, Technology Marketing Manager, at the above address. His telephone number is (215) 962-2787. Shipments should be directed to:

Space Division
General Electric Company
CCF8 Building
Third Avenue
King of Prussia, PA 19406

3.16 ROME AIR DEVELOPMENT CENTER FXR FACILITY

3.16.1 Electron-Beam Mode

The Rome Air Development Center (RADC) FXR facility generates, in the electron-beam mode, 200 A at 2.0 MeV through a 1-cm^2 exit window for 20 ns. Total beam energy is 800 J. Repetition rate is 1 shot per 4 min. Maximum dose rate at window is 4×10^{13} rad(Si)/s. Dosimetry used is TLD and PIN diodes calibrated versus TLDs. TLD standard deviation is 5% and accuracy is ±15%.

3.16.2 X-Ray Mode

Dose at target is 3,000 rad(Si). Dose at 30 cm is 50 rad(Si). The $1/r^2$ relation holds into about 10 cm. Beam size at target is approximately 2.5 in. (FWHM). Divergence is approximately 29 degrees (FWHM from beam center line). Maximum dose rate is 1.5×10^{11} rad(Si)/s at the target and 1.5×10^{8} rad(Si)/s at 30 cm.

3.16.3 Support Capabilities

An FXR operator and dosimetrician are available for test support.

Minimum cable length is 50 ft.

Two to four oscilloscope channels are available.

3.16.4 Procedural Information

For further information regarding use of the RADC FXR facility, contact:

RADC/ESR, Stop 30 (Bldg. 1126)
Hanscom AFB, MA 01731
Attn: Lester F. Lowe
Telephone: (617) 861-3445

3.17 CASINO

3.17.1 Operating Characteristics

The DNA CASINO facility is currently being changed and upgraded at the Naval Ordnance Laboratory (NOL), White Oak, Maryland. It is an FXR facility designed to generate pulses of electrons which may be used directly for materials research or converted to bremsstrahlung radiation. An outline of the CASINO simulator is shown in Figure 3-225. Basically, CASINO is 4 machines operating in synchronization to produce 4 electron pulses. These electron pulses are magnetically guided into a common converter box where part of their energy is converted into bremsstrahlung photons. Each of the 4 CASINO modules consists of 4 major parts: 1) one-half of a Marx tank, (2) a water-dielectric pulse-forming line, (3) a field-emission diode, and (4) a transport system for guiding the electrons to the converter. Each of the 2 Marx tanks serves 2 water pulse-forming lines, and is capable of generating V up to 4 MV. After the pulse is shaped in the water pulse-forming lines, the energy is delivered to the diode. From there, the 1-MV, 1-MA electron beam is delivered to the beam guidance system which drifts the electron beam to the converter box. The converter box is rectangular in shape and is irradiated at each end with 2 electron beams. The resulting bremsstrahlung radiation is emitted from the top and bottom of the converter box, where the test object(s) is located. In the electron mode, the converter is removed and the present design calls for the 4 beams to be magnetically turned upward. The electron-beam FWHM pulse width is about 60 ns. Figure 3-226 shows the CASINO photodiode output (Reference 1).

The extensive amounts of transient information required to properly operate and extract experimental data from the CASINO simulator made the use of conventional oscilloscopes and cameras impractical as the prime instrumentation system. Taking advantage of recent milestone advances in transient analog-to-digital (A/D) conversion, in particular the Tektronix 7912 transient digitizer, and the

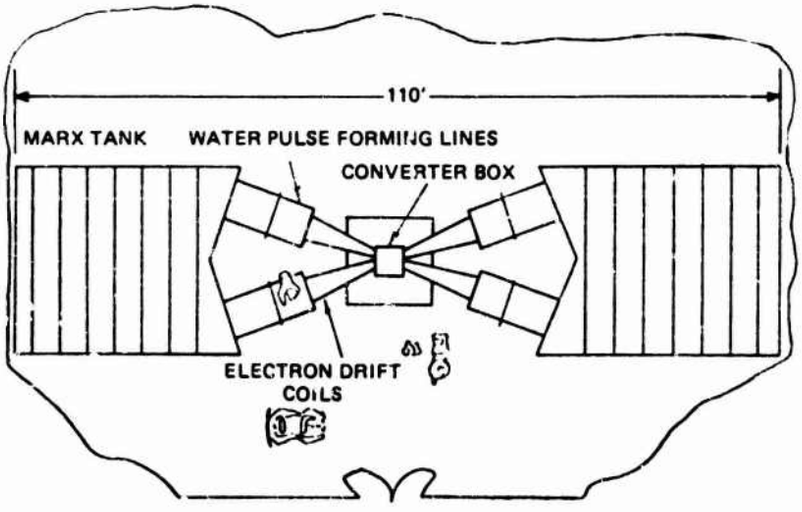

Figure 3-225. Outline of CASINO simulator.

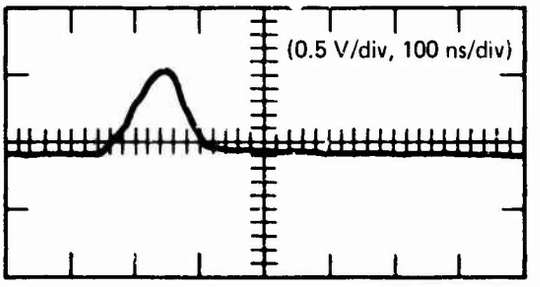

Figure 3-226. Typical CASINO photodiode output time history.

versatility and power of the modern minicomputer, a completely computerized instrumentation system has been designed, built, and programmed for the CASINO facility. The system not only gathers and processes data needed to operate and assess the performance of the simulator but it also provides numerous channels for the experimenter's use covering a frequency range from 0 to 500 MHz. A simple programming method allows the experimenter to do limited processing on his data or to store it on tape for processing at a later time. The CASINO data system is basically a computer, computer peripherals, and 3 types of A/D converters. There are 2 Digital Equipment Corporation (DEC) PDP 11/40 computers, 1 for the facility or machine data system, and 1 for the user system. The two systems together comprise the CASINO instrumentation system and share software and peripherals. However, the system has been organized to allow the user's system to be operated in a more limited capacity independent of the facility system. Sophisticated software, dealing with the acquisition and analysis of single transient software, completes the essential features of this relatively unique instrumentation system.

3.17.2 Supporting Facilities

An abbreviated main floor plan of the CASINO facility is shown in Figure 3-227. This figure highlights those features that are of particular interest to the prospective user.

3.17.2.1 Exposure Cell

The radiation exposure cell measures 19 ft wide by 36 ft long and has a ceiling height of 20 ft. Although much of this space is required by the water lines, vacuum pumps, coils, and supporting structures, the user should find more than adequate usable space above and below the converter and in the floor area, shown shaded. Beneath the converter, at floor level, there is a 5-ft by 6-ft seismic block for mounting fixtures and experiments which are sensitive to movement, or which must be held fixed at some particular coordinates. The roof of the test cell and the outside wall are removable if the need arises to place objects which cannot fit through the test cell door. The cell area is completely air-conditioned and is equipped with an adequate supply of ac power outlets. The cell forms an RF shield as well as a radiation shield; the RF enclosure is primarily to minimize the RF noise escaping from the room. Six 6-in. conduits run from the

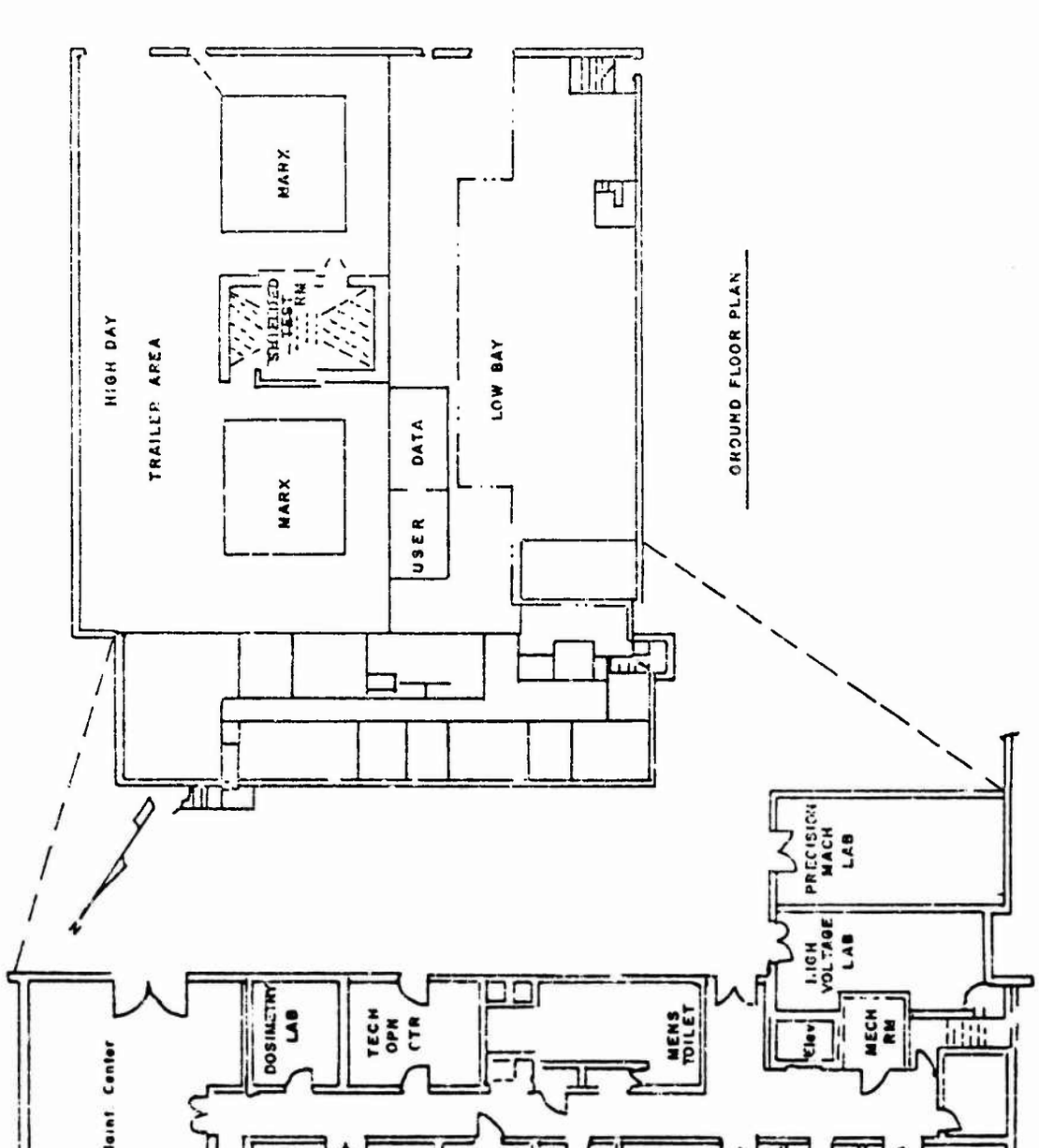

Figure 3-227. CASING facility.

vicinity of the target to a point adjacent to the user instrumentation enclosure and another 2 conduits terminate in the trailer area. These conduits are dedicated to cable runs for user experiments. Two large trenches are also available for routing cables into the exposure cell.

3.17.2.2 User Data (Instrumentation) Room

The user instrumentation room is located adjacent to the exposure cell and may be occupied during testing. The room is an all-steel, all-welded RF enclosure which has a shielding effectiveness of at least 120 db for electric fields from 1 kHz to 100 MHz, and plane wave fields from 400 MHz to 10 GHz. Attenuation to magnetic fields ranges from 70 db at 1 kHz to about 14 db at 60 Hz. The user data room is partitioned into 2 sections; the smaller section measures 20 ft by 15 ft, and the larger section is 25 ft by 15 ft. The smaller section is committed to the digital instrumentation system; the larger is generally available to the user for his own instruments and those analog channels furnished by the facility. The user data room is powered by a motor generator (MG) set which is primarily used to smooth power-line variations. The room is dc- and RF-isolated from both the MG and house power. RF line filters are on every power line entering the enclosure. The room may be completely isolated from ground by 0.5 Mohm or connected to its own grounding system. Air-conditioning is forced under the computer-type flooring to help cool equipment racks.

3.17.2.3 Trailer Area

CASINO can conveniently accommodate 2 Nevada Test Site (NTS) type 50-ft by 10-ft trailers adjacent to the exposure vault. Commercial power of 50 kW is available for each trailer and 150-kW diesel-generated power is available as well. The trailer area also has provisions for air-conditioning, heat exhaust, and cable conduits into the test cell.

3.17.2.4 Miscellaneous Facilities

In the office laboratory area of the facility there are 2 user laboratories which measure approximately 20 ft by 14 ft and a supporting 10-ft by 14-ft office for each. These areas have easy access to the main floor and can serve as assembly areas for fairly large experiments. A 12-ft by 14-ft vault is also available for lock-up of classified hardware. A small darkroom and a microcircuits laboratory equipped with 2 clean benches also may be used by facility users. A 20-ton bridge crane spans the high bay area to service the machine, blockhouse, and experimenter's needs.

3.17.3. Procedural Information

For further information, direct inquiries to:

D.L. Kenyon
Naval Surface Weapon Center
Bldg. 132
White Oak, Silver Spring, MD 20910
Telephone: (301) 395-1878

3.17.4 Reference

1. Chivington, E.P, D.M. Clement, C.E. Wuller, and P.J. Madle, "Investigations of Nonlinearities and Multiple Exposure Anomalies of Shielded Cables at CASINO," TRW Defense and Space Systems Group, Redondo Beach, California, *IEEE Transactions on Nuclear Science*, Vol. NS-25, No. 3, June 1978.

3.18 GAMBLE

3.18.1 Operating Characteristics

The Gamble II Pulse Generator is currently being changed and upgraded. It is designed to deliver 60 kJ of electrical energy into a 0.6-ohm load with 20 nH of series inductance within a time interval of 50 ns. The peak V across the 0.6-ohm load is 1 MV. The generator (with an addition to the tapered transformer) may have a capability of delivering up to 200 kJ into a zero-inductance 0.25-ohm load in 50 ns, again with a peak V of 1 MV. The latter possibility will depend on the V breakdown data concerning water, remaining applicable up to 10-MV levels; holding of breakdown up to 8 MV by the polyurethane diaphragm and Marx generator; and the development of command-triggered switches operating at 8 to 10 MV. All of these are possible and expected.

The generator consists of the following major components operating in the manner indicated: (1) a Marx generator charges a water-dielectric coaxial intermediate storage capacitor in 1.2 μs; (2) the intermediate capacitor transfers its charge through an overvoltaged water switch to the pulse-forming line in 180 ns; (3) the pulse-forming line launches a 50-ns I pulse through a second overvoltaged water switch into the high-impedance input of a water-dielectric tapered coaxial-line transformer; (4) the transformer propagates the 50-ns pulse and delivers it at a lower impedance to the beam tube; (5) the beam tube accelerates electrons across the anode-cathode gap and permits conversion of a part of the electron energy into bremsstrahlung radiation, which is transmitted through a window to the test area.

3.18.2 Procedural Information

For further information, direct inquiries to:

Mr. Vitkovitsky or Mr. John D. Shipman
Naval Research Laboratories
Plasma Research Laboratories (Code 6700.1)
Washington, D.C. 20375
Telephone: (202) 767-2610

SECTION 4

LINEAR ACCELERATORS

4.1 INTRODUCTION

An electron LINAC produces a well defined beam of electrons. For irradiation studies, the electron beam can be used directly or can be converted to bremsstrahlung x-rays or neutron/γ radiation. LINACs are widely used as a pulsed radiation source in TREE studies because of their variable pulse length, intensity, and particle energy.

Some characteristics common to all LINACs and important to TREE studies are:

1. Peak I is achieved at energies near the center of the energy range, and it approaches zero at the upper limit
2. Minimum beam dia. (affecting peak dose rates and maximum sample size) are in the range of 0.5 to 2 cm at the beam exit window
3. A minimum nonzero operational-beam energy exists
4. Through the use of the direct-electron beam, dose rates above 10^{11} rad/s can be obtained
5. At many facilities, the pulse width and dose rate may be independently varied over a wide range without changing sample position or test configuration
6. Single or multiple pulses are normally available upon command
7. Short rise- and fall-time pulses are normal operational characteristics
8. Pulse width is in the range of 0.01 to 20 μs
9. The bremsstrahlung dose rate obtained will be at least a factor of 100 less than the direct-electron dose rate.

The major disadvantage in using a LINAC is the restriction imposed on sample size when the electron beam is used directly. Other significant disadvantages are associated with the obtainable dose rates and pulse width range.

Figure 4-1 is a copy of the form sent to the individual organizations with LINAC facilities requesting information for this handbook.

I. Electron Mode, Environment

A. Dose as a function of distance and position (mapping)

B. Dose rate versus distance and position (mapping)

C. Output waveform versus time for various beam characteristics

D. Beam geometry (area, divergence, dia. at window, etc.)

E. Electron-energy spectrum versus time and position for various beam characteristics (e.g., as function of voltage and pulse width)

F. Repetition rate, duty cycle, and pulse reproducibility/predictability

G. Limits on pulse width as functions of repetition rate and total energy

H. Conditions for maximum power operation (beam energy, pulse width, repetition rate, peak current)

I. Diagnostic techniques used in environment measurements

J. Discussion of errors in environment measurements

K. Electrical noise (experimental configuration dependent)

II. Bremsstrahlung Mode, Environment

A. Target material and filters

B. Dose mapping

C. Dose-rate mapping

D. Output waveform versus time for various beam characteristics

E. Photon-energy spectrum versus time and position for various beam characteristics

F. Repetition rate, duty cycle, and pulse reproducibility/predictability

G. Limits on pulse width as functions of repetition rate and total energy

H. Conditions for maximum power operation (beam energy, pulse width, repetition rate, peak current)

I. Diagnostic techniques used in environment measurements

J. Discussion of errors in environment measurements

K. Electrical noise (experimental-configuration dependent)

III. Support Capabilities

A. Professional and nonprofessional technical support staff

B. Screen room

C. General electronics available; power, cabling, and minimum cabling requirements

Figure 4-1. Data requested from organizations with LINAC facilities.

D. Timing signals

E. Dosimetry available (active and/or passive)

F. Calculational capabilities

G. Shop support

H. Experiment preparation laboratories available

I. Target-room description (beam-port arrangements, etc.)

J. Photographic equipment and materials.

IV. Procedural Information

A. Contact (technical and nontechnical)

B. Scheduling

C. Cost information if available and/or releasable

D. Shipping address

Figure 4-1. (continued).

4.2 IRT CORPORATION LINAC

4.2.1 Characteristics

The IRT Electron-Linear-Accelerator Laboratory has 2 L-band LINACs. The first LINAC has 1 accelerating section and operates in the energy range of 1 to 25 MeV. Pulse width can be varied from 10 ns to 8 μs. At maximum efficiency, beam energy is 12.5 MeV and peak beam I is 1 A. Peak beam I is 10A for pulse widths less than 100 ns. For pulse widths greater than 100 ns, peak I of 1 A may be obtained.

The second LINAC has 2 accelerating sections and operates in the energy range of 4 to 50 MeV. At maximum efficiency, beam energy is 25 MeV and peak beam I is 750 mA. Pulse width can be varied from 10 ns to 6 μs.

4.2.2 Test Parameters

Operating characteristics of the 1-section LINAC are as follows:

1. Microwave frequency	1,300 MHz
2. Number of accelerating sections	1
3. Energy range	1 to 25 MeV
4. Beam energy at maximum efficiency	12.5 MeV
5. Peak beam I at maximum efficiency	1.0 A
6. Rated average power	
a. At 5 MeV	1.8 kW
b. At 10 MeV	6.5 kW
c. At 12.5 MeV	10 kW
d. At 15 MeV	9.7 kW
e. At 20 MeV	6.5 kW
7. Maximum peak beam I	
a. For pulses of 0.1 μs and longer	1.0 A
b. For pulses of 100 ns and less	10 A
8. Beam pulse width	0.01 to 8 μs
9. Pulse repetition rates/s	
a. At 8.0 μs	Single pulse
b. At 4.5 μs	Single pulse to 180
c. At 2.5 μs	Single pulse to 360
d. At 0.5 μs and shorter	Single pulse to 720
10. Energy spectrum, $\Delta E/E$ (FWHM)	~3%

Operating characteristics of the 2-section LINAC are as follows:

1. Microwave frequency	1,300 MHz
2. Number of accelerating sections	2
3. Energy range	4 to 50 MeV
4. Beam energy at maximum efficiency	25 MeV
5. Peak beam I at maximum efficiency	750 mA
6. Rated average power	
a. At 10 MeV	2 kW
b. At 20 MeV	12 kW
c. At 30 MeV	12 kW
d. At 40 MeV	9 kW
7. Maximum peak beam I (cell pulse widths)	750 mA
8. Beam pulse width	0.01 to 6 μs
9. Pulse repetition rates/s	
a. At 6 μs	Single pulse to 180
b. At 2.5 μs	Single pulse to 360
c. At 0.5 μs and shorter	Single pulse to 720
10. Energy spectrum, ΔE/E (FWHM)	~3%

The electron-beam loading factor is 12.5 MeV/A. Pulse shape is generally rectangular, with distortion related to experimental port and beam energy resolution. Single pulses can be delivered at any pulse width within the nominal pulse-width range. Beam-spot dia. is typically in the range of 0.2 to 1.0 cm. The shape of the spot can be made round or elliptical through the use of quadrupole focusing lenses. Extra large spot sizes can be produced by scattering from a foil.

Environment output characteristic data are given in Table 4-1. Beam mappings of typical experiment configurations are shown in Figures 4-2 through 4-5.

Electron, x-ray, and neutron dosimetry measurements are made using standard Co glass, fission foils, ionization chambers, TLD, and calorimetric dosimetry techniques.

Typically, RF electrical noise of a few mV may be expected approximately 1.5 to 2 μs prior to the radiation pulse.

4.2.3 Support Capabilities

The IRT staff associated with the LINAC facility consists of nuclear physicists, chemists, and engineers competent in all phases of TREE experimentation. IRT can provide guidance in the preparation of experimental programs, or can

Table 4-1. Environment output characteristics.

Mode	LINAC Configuration Values	
	One-Section	Two-Section
Electron-Beam Mode		
Dose at 1 ft, rad(air)/pulse	$>10^6$	$\sim 10^6$
Dose rate at 1 ft, rad(air)/s	$\sim 10^{12}$	$\sim 10^{11}$
X-ray Mode		
Dose at 1 ft, rad(air)/pulse	200	100
Dose rate at 1 ft, rad(air)/s	$\sim 10^8$	$\sim 10^9$
Neutron Mode		
Yield, n/pulse	$\sim 5 \times 10^9$	10^{11}
Maximum yield rate, n/s	$\sim 5 \times 10^{15}$	10^{17}
Sustained yield rate, n/s	$\sim 5 \times 10^{10}$	10^{13}
Energy resolution $\Delta E/E$ (full width)	2%	2%

Notes:

1. Data are not definitive and are meant to be used only as a guide.
2. Spectral data typically are for photo-fission spectra.

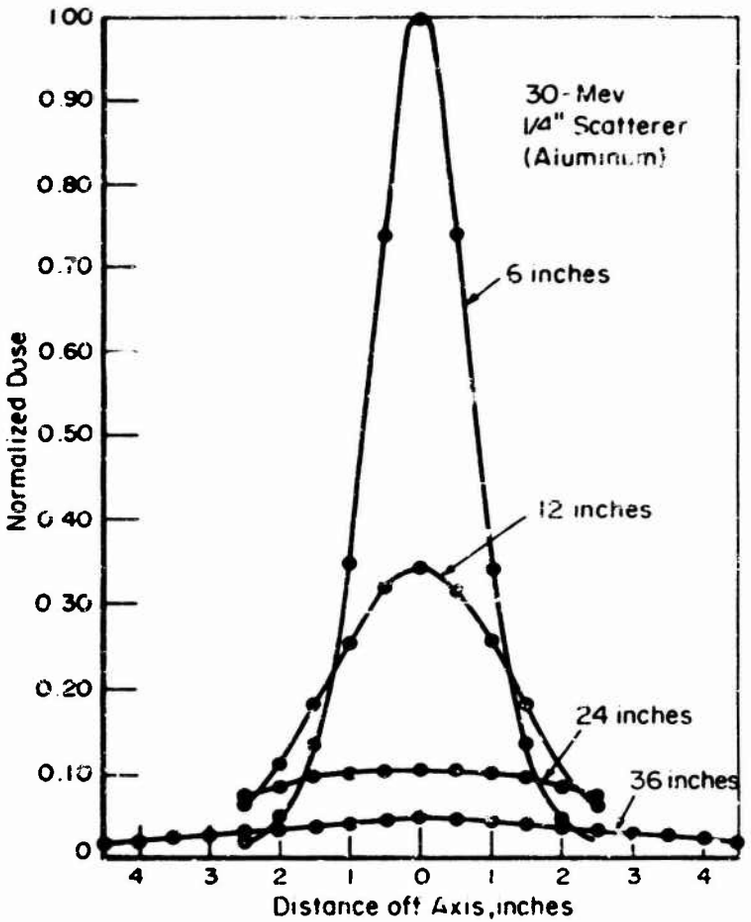

Figure 4-2. Beam mapping with 1/4-in. Al scatterer and 30-MeV electrons.

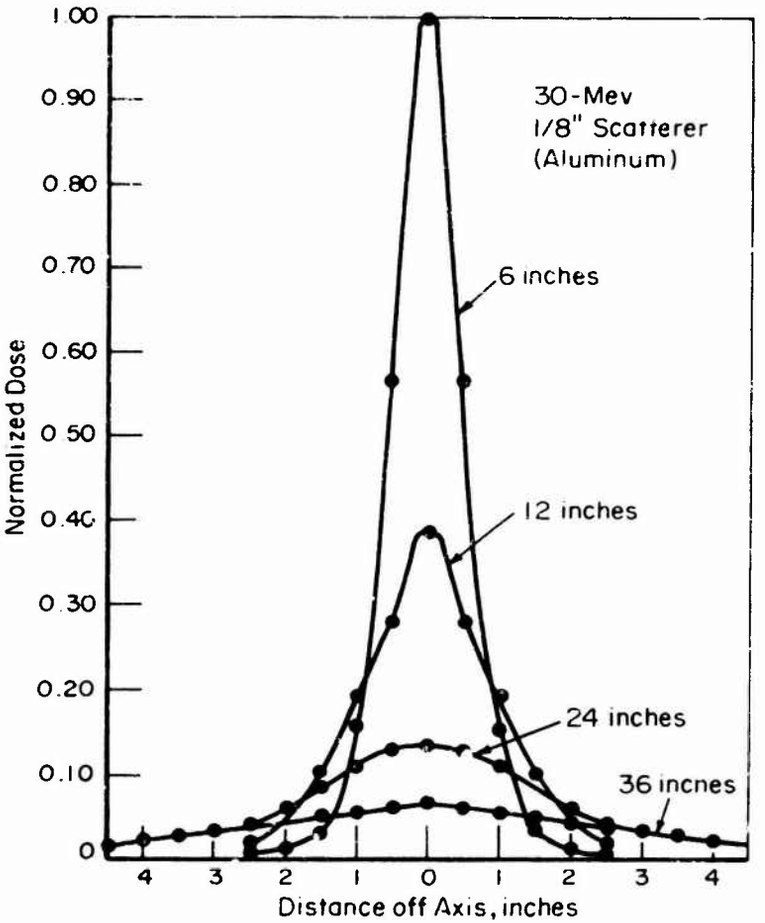

Figure 4-3. Beam mapping with 1/8 in. Al scatterer and 30-MeV electrons.

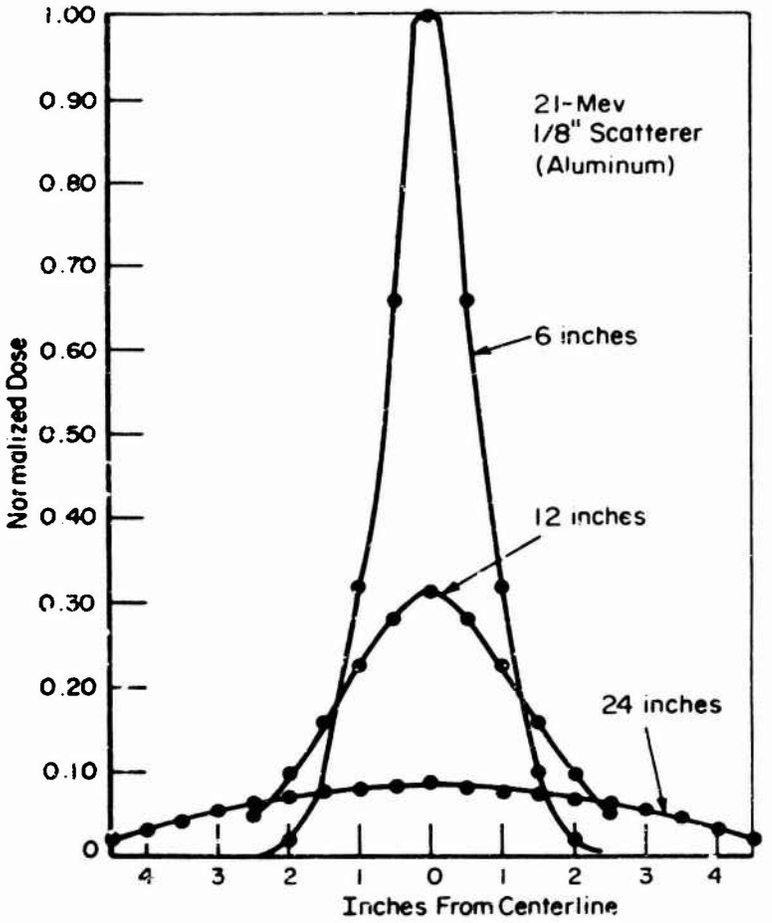

Figure 4-4. Beam mapping using 1/8-in. Al scatterer and 21-MeV electrons.

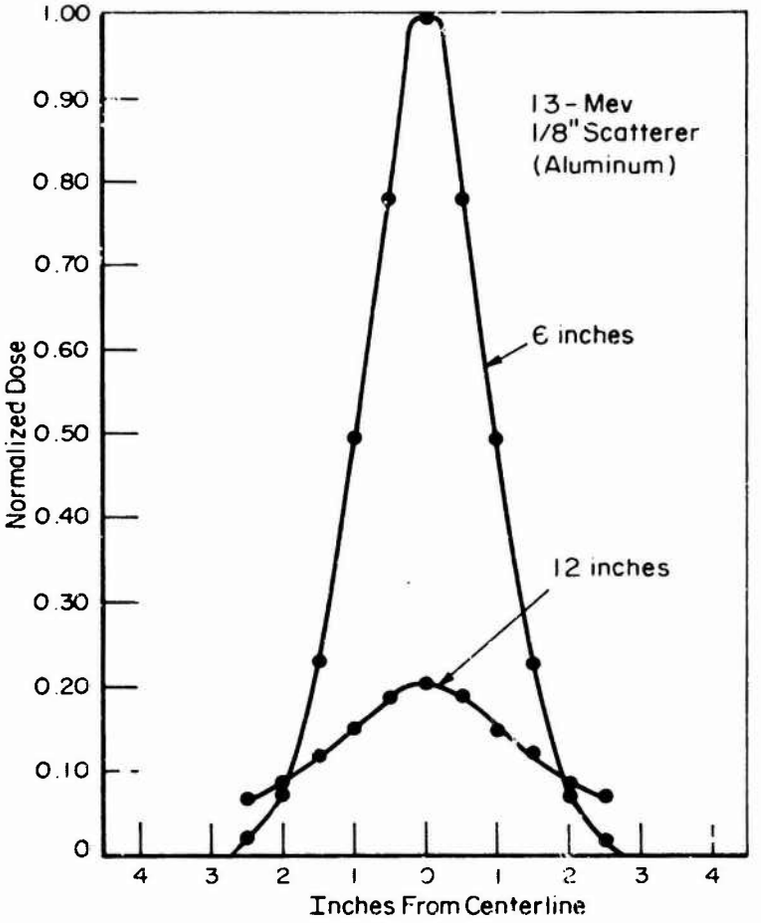

Figure 4-5. Beam mapping using 1/8-in. Al scatterer and 13-MeV electrons.

handle programs in their entirety. The operational staff will operate the accelerators and provide engineering and technician support and assistance to the experimenter, as appropriate.

Some electronic equipment, light machine shop tools, a variety of operating timing signals, limited on-site office space, and experiment preparation laboratories are available. Arrangements may be made to use the IRT Corporation photographic laboratory. Film for Polaroid scope cameras is readily available. A screen room is not available and, generally, is not required even for recording low-level signals.

IRT does not routinely include dosimetry services. Available by special arrangement are Co glass, cinemoid film, standard TLD, S pellets, and calorimetric dosimetry. IRT can provide technical assistance in making dosimetry measurements.

The LINAC beam can be extracted at 15 different target positions distributed among 6 independent irradiation cells. This arrangement permits beam usage by a large number of researchers. Programs are conducted with due consideration given to the incompatibilities between experiments. Neutron experiments, which generally result in target and room activation, are confined to 1 of 2 separate cells. A high resolution port is provided for low-background work.

A significant feature of the facility is that personnel may occupy certain areas while radiation experiments are being conducted in other areas. This permits set up of elaborate experiments without the need to shut down the facility. Tables and associated test equipment are provided, but specialized equipment must either be provided by the experimenter or fabricated at the facility.

4.2.4 Procedural Information

Inquiries related to the use of the LINAC facility or its cost should be directed to:

IRT Corporation
P.O. Box 80817
San Diego, CA 92138
Attn: D.E. Willis (714) 453-1693 or
J.W. Harrity (714) 565-7171

Shipments should be addressed to:

IRT Corporation
10955 John Jay Hopkins Drive
San Diego, CA 92121
Attn: J.W. Harrity or D.E. Willis

4.2.5 Applicability and Availability

The IRT LINACs are applicable to, and readily available for, TREE experimentation. The accelerators are operated and maintained on a 24-hr basis with

experimental research utilizing approximately 2,000 hr during a calendar year. The facility is located north of San Diego, California.

4.2.6 Reference

1. Adcock, D.R., et al., "The General Atomic Electron Linear Accelerators," Gulf General Atomic Report, May 22, 1967.

4.3 NRL LINAC

4.3.1 Characteristics

The NRL LINAC is a 3-section, S-band accelerator which operates in the energy range of 5 to 65 MeV. At maximum efficiency, the beam energy is 42 MeV and the peak beam I is 0.5 A. Pulse width can be varied from 0.03 to 1.4 μs. Operating characteristics of the NRL LINAC are as follows:

1.	Microwave frequency	2,858 MHz
2.	Number of accelerating sections	3
3.	Energy range	5 to 65 MeV
4.	Maximum efficiency operation	
	a. Beam energy	42 MeV
	b. Peak beam I	0.5 A
	c. Rated average power	8 kW
5.	Beam pulse width (FWHM)	0.03 to 1.4 μs
6.	Pulse repetition rates/s	5, 15, 30, 60, 180, 360
7.	Average beam I	
	a. Port 1	250 μA
	b. Port 2	100 μA (maximum)
	c. Port 3	100 μA
	d. Port 4	100 μA
8.	Energy spread, ΔE/E	0.4 to 10%
9.	Transient mode operation	
	a. Beam energy (average)	30 MeV
	b. Peak beam I	2 A
	c. Beam pulse width (FWHM)	50 ns

An improvement program is now under way that will increase the I in the transient mode to 6 A in late 1978. The energy spread (item 8) is sensitive to beam energy and I.

4.3.2 Test Parameters

Electron-beam loading characteristics are given in Figure 4-6. Energies below 5 MeV are nearly impossible to obtain, and at 5 to 7 MeV unanalyzed beam I are limited to 100 to 200 MA peak. Because the energy spread of the raw beam may be as large as 15 to 20% (FWHM), deflection and collimation of the beam reduces the available I.

The pulse shape for longer pulses (0.5 to 1.4 μs) in beam 1 are approximately rectangular. As the pulse length is reduced, the shape is more triangular.

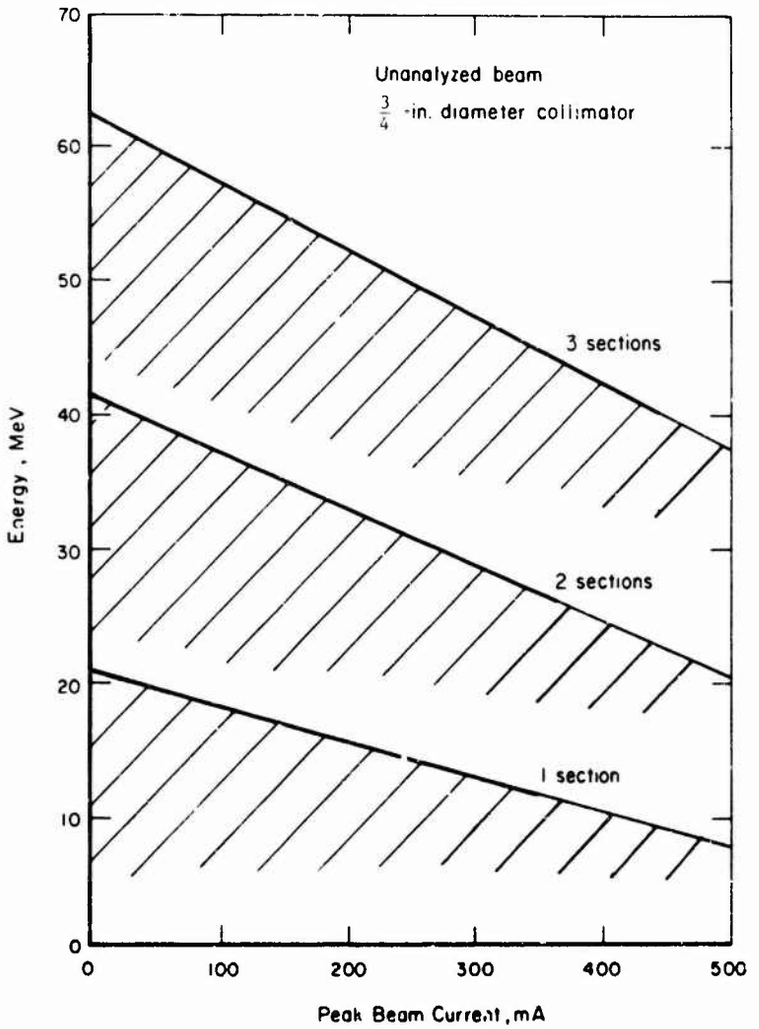

Figure 4-6. Beam loading characteristics.

Pulses appearing in beams 3 and 4 are somewhat less regular in shape due to the energy-time relationship within the duration of the pulse. Best rise time achieved on short pulses is 14 ns, although this could be improved with sufficient demand. On single pulse exposures, pulse amplitude predictability of ±5% is typical, with dark I background radiation less than 0.5% for a single 4×10^4 rad(Si) pulse.

Environment characteristics of the NRL LINAC are as follows:

1.	Electrons	
	a. Peak I (50-ns pulse)	2 A
	b. Peak I (1.4-μs pulse)	0.5 A
2.	X-rays (10 cm from converter plate)	1×10^3 rad(Si)/pulse
3.	Neutrons	1×10^6 1-MeV equivalent (neutron/cm^2)/pulse

The value of item 3 was measured 11.5 cm from the center of the target and behind a 4-in. Pb γ-ray shield.

4.3.3 Electron-Beam Geometry and Energy Spread

Beam-spot dia. is typically in the range of 0.2 to 1.0 cm. The shape of the spot can be made round or elliptical through the use of quadrupole focusing lenses. Extra large spot sizes can be produced by scattering from a foil. Beam energy width, $\Delta E/E$ (FWHM), of the raw beam is 10% at 38 MeV and 1.0% at 56 MeV for the equilibrium mode. The energy width of deflected beams is adjustable by means of slits in the magnetic analysis system. The transient mode featuring high peak I of short duration would exhibit a FWHM of 20 to 30%.

A compact target of water-cooled Ta plates is available for neutron irradiations. To emphasize fast neutrons, a minimum of water is used. Three to 4 in. of Pb is employed to reduce γ contamination. Preliminary spectral measurements indicate a broad peak at about 1 MeV, with a differential flux of about 7×10^{12} neutrons/cm^2/coulomb of LINAC beam at a point 90 degrees to the beam direction, 11 cm from the center of the target. Gamma contamination at this point is about 4×10^4 rad(Si) per coulomb of LINAC beam. A coulomb of 42-MeV electrons is collected in about 6 hr (see Reference 4).

Electron-beam I measurements are made in 2 ways. One of these consists of an I transformer through which the electron beam passes just before emerging from the water-cooled exit window. The second involves Faraday cup techniques, employed after the beam has emerged through the window. Both give results having errors less than ±5% (see Reference 5). Absorbed dose measurements are made using TLDs and reverse-biased Si diodes. These are calibrated against an absolute Si calorimeter (Reference 6) or a Co-60 source.

Neutron intensity measurements are available using S disks that give neutrons/cm^2 for energies above 3 MeV. Neutron spectrum information is also available. Dose measurements for neutrons are made using Li^6 and Li^7 enriched TLDs (Li^6F_2, Li^7F_2).

For the dose measurements involving use of the reverse-biased Si diode, digital readout is available, which gives total integrated dose for each pulse.

The electrical noise within the LINAC laboratory space can be separated into noise synchronous or not synchronous with LINAC radiation pulse. Each of these categories can be subdivided into radiated noise and conducted noise. The most significant source for nonsynchronous noise is that associated with the Si controlled rectifiers (SCRs) used in the waveguide cooling system for the LINAC. The conducted component appears as several "gliches" of about 4-V amplitude and 50-μs duration appearing on the 115-Vac service lines.

The typical radiated component is such that a signal having a maximum amplitude of 3 mV peak-to-peak and a characteristic frequency of 4 kHz lasting for 5 ms is induced in a 60-ft length of semi-flexible, 1/2-in.-dia. coax cable with the cable terminated at its input end with 50 ohms. The predominant source of noise synchronous with the LINAC radiation pulse is that associated with the

klystron modulators. The conducted component appears on the 115-Vac service lines with a maximum amplitude of 5 V peak-to-peak, with an average frequency of about 1.5 MHz and lasting for 20 μs.

The radiated component (measured within Room 101) will induce a signal in an inductive loop 5 in. in dia. and terminated in 50 ohms, having a maximum amplitude of 15 mV with a frequency of 14 MHz and lasting for 10 μs.

By various means, periodic improvements in all of these noise levels have been made and will continue to be made.

4.3.4 Support Capabilities

The primary function of the NRL LINAC is to investigate those problems involving the interaction of high-energy radiation with matter in which the Navy has an inherent interest. Groups with similar problems are welcome to use the facility and usually can be accommodated in a manner convenient to all concerned.

The services of a complete operational and technical support staff are available. The staff includes dosimetry and instrumentation technicians, as well as accelerator operators and professional supervisors. The LINAC professional staff is oriented primarily toward applied nuclear physics research. In addition, many other workers at NRL are involved in TREE activities. A member of the NRL professional staff serves as coordinator of the TREE interests.

Electronic equipment includes an assortment of modular plug-in components normally found in a nuclear physics laboratory and several dual-beam oscilloscopes (Tektronix models 7044, 551, and 555). It is recommended that anyone contemplating use of this facility check to see if specific electronic equipment required is available.

A variety of timing and trigger signals are available to the experimenter. The prime signal is a 5-V trigger pulse either synchronous with, or preceding, the LINAC pulse. This trigger pulse has a rise time of 0.2 μs and a pulse width (FWHM) of 2 μs. The timing pulse system is improved by the installation of standard logic circuits. A preset scaler is included in the LINAC auxiliary circuitry that permits the selection of the number of pulses to be used for the irradiation. This number can be preset for anything from a single pulse to 999,999.

A screen room is not available.

Dosimetry is available for all radiations produced at the NRL LINAC. Table 4-2 indicates the several kinds of dosimetry used.

Computational facilities are available. These include electronic desk calculators, an on-line computer for experimentalists (Varian 6201), and a time-sharing terminal, all in the same building as the LINAC. Located a short distance (0.1 mi) from LINAC is the research computation facility of NRL. Limited shop facilities are located in the NRL LINAC building. Various other shops within NRL may be used by special arrangement.

Table 4-2. Types of dosimetry used.

Radiation or Particle	Dosimetry Method
Electrons	CaF_2 (TLDs) Reverse-biased diode[a]
X-rays	CaF_2 (TLDs) Reverse-biased diode[a] Si calorimeter
Neutrons	Li^7F_2 (TLDs) Li^6F_2 (TLDs)
[a]Digital readout available with reverse-biased diode.	

Experiment preparation areas and office space are limited. Photographic equipment is not readily available at the NRL LINAC Laboratory. Photographic services of NRL can be provided for by special arrangement.

A floor plan of the NRL LINAC Laboratory is shown in Figure 4-7. The LINAC beam can be extracted at 5 different beam ports. Experiment floor space is at a premium. If the user requires more than 6 to 8 ft in length along the beam axis, a special setup may be required. The main unanalyzed electron beam is extracted at Ports 1 and 2. Bremsstrahlung is generally produced at Port 3. Lower intensity or selected energy electron beams are available at the remaining ports. A rapid transfer system for the insertion and retrieval of samples for activation exposure has its termination in beam 4 (10 cm in front of a water-cooled bremsstrahlung target containing 20 foils of 10-mil Ta). An x-ray intensity of about 10^7 rad/min is available here for routine activation experiments.

Closed-circuit television is available for checking the beam spot position and shape or for observing experiment apparatus. If the user requires frequent changes to apparatus inside the experimental area, consideration should be given to providing remote control of such apparatus.

4.3.5 Procedural Information

Inquiries related to the use of the NRL LINAC or costs and charges for its use should be directed to:

Dr. Bruce J. Faraday or
Mr. Robert M. Farr
Code 6620
Naval Research Laboratory
Washington, D.C. 20375
Telephone: (202) 767-3116 or 767-3938

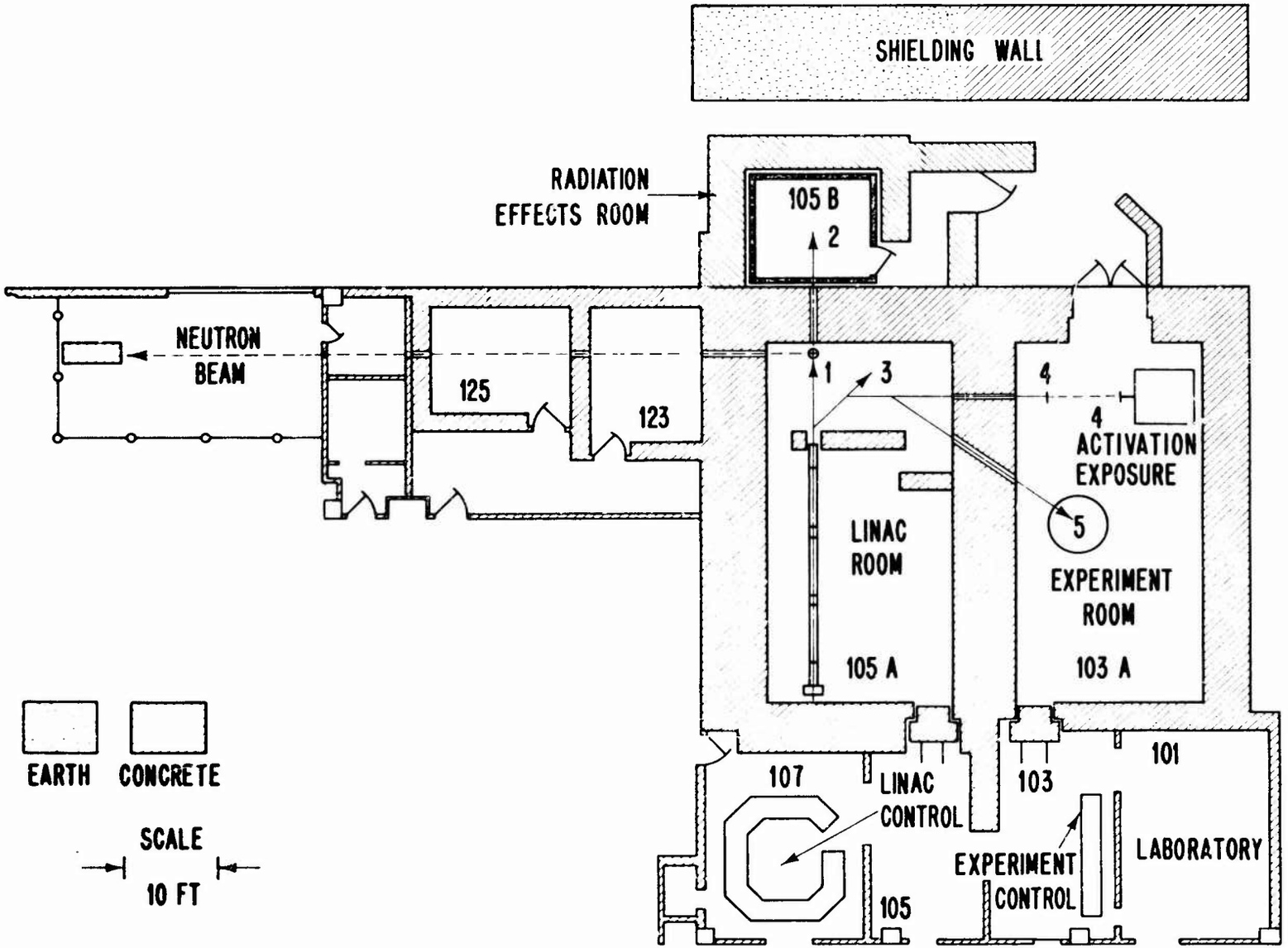

Figure 4-7. LINAC laboratory floor plan.

Shipments should be addressed to:

U.S. Naval Research Laboratory LINAC
Building 75
4555 Overlook Avenue, S.W.
Washington, D.C. 20375

4.3.6 Applicability and Availability

NRL maintains an active interest in TREE technology, and the LINAC is available and amenable to TREE experiments. The staff is actively working on pertinent radiation problems and is willing to provide facility support to TREE experimenters. In response to increased interest in TREE research, NRL encourages inquiries from outsiders about use of its facility. The laboratory is located just south of Washington, D.C.

4.3.7 References

1. "USNRL LINAC: Characteristics and Safety Procedures," unpublished report available from NRL, June 1966, revised March 1969.

2. "Report of LINAC Operation," issued semiannually as an NRL Memorandum Report.

3. Godlove, T.F., et al., "The NRL 55 MeV Electron Linear Accelerator," Report of NRL Progress, January 1964.

4. Cohen, L. and J. Ritter, "Measurement of Linac-Produced Neutron Spectrum," Report of NRL Progress, December 1974.

5. Murray, K. and C. Guenzer, "An Absolute Measurement of Dose Rate from Energetic Electron Beams," accepted for publication, RSI, 1978.

6. Murray, K., "An Absolute Silicon-Dose Calorimeter," Nuc. Inst. & Meth. 107, 109-113, 1973.

4.4 BREL LINAC

4.4.1 Characteristics

The Boeing Radiation Effects Laboratory (BREL) LINAC is a 3-section, S-band accelerator which operates in the energy range of 3 to 33 MeV. By utilizing only 2 accelerating sections, operations can be conducted in the energy range of 1 to 17 MeV. At maximum efficiency in the 33-MeV configuration, beam energy is 16.5 MeV and peak beam I is 0.7 A. Pulse width can be smoothly varied from 0.04 to 6 μs. For the 17-MeV configuration, the corresponding values are 8.5 MeV, 1.6 A, and 0.03 to 6 μs.

4.4.2 Test Parameters

Operating characteristics of the BREL LINAC for the 17- and 33-MeV operating configurations are given in Table 4-3. Beam-loading characteristics are given in Figure 4-8. Characteristic pulse shapes, as obtained from Tektronix 519 oscilloscope traces, are given in Figure 4-9. Repetition rates are given in Table 4-3. Single pulses can be delivered for any pulse width within the normal pulse-width range. Pulse reproducibility and predictability data are available upon request. Duty cycle is 0.1%.

4.4.3 Electron-Beam Geometry and Energy Spread

Electron-beam geometry and energy spread for the BREL LINAC are as follows:

1.	Beam divergence	≤1 milliradian
2.	Beam-spot dia.	0.1 to 2 cm
3.	Beam energy width, ΔE (FWHM) (Pulse width >0.25 μs for 1 to 17 MeV) (Pulse width >0.50 μs for 3 to 33 MeV)	0.3 MeV

The shape of the spot can be made round or elliptical through the use of quadrupole focusing lenses. Extra large spot sizes can be produced by scattering from a foil.

Environment output characteristic data as obtained are given in Table 4-4 and Figures 4-10 through 4-14.

TLD dosimetry is used for field maps and routine experimental dosimetry. Boeing's TLD system is calibrated with a 3,000-Ci in air Co source. The system accuracy is estimated at ±15%. A guide to the general spectral distributions to be expected is shown in Figure 4-15. These spectra were calculated using ETRAN, a Monte Carlo computer program designed to compute the transport of electrons and photons through extended media. The spectra shown for 10, 20, and 30 MeV are not the "on-axis" spectra, but rather the "integrated overall angles" spectra. Limited angular spectral data exist; however, because of the long computer run times involved, it is suggested that the data shown in Figure 4-15 be used as a guide. If more precise spectral data are needed, an ETRAN calculation can be performed for the specific experimental geometry involved.

Table 4-3. BREL LINAC operating characteristics.

Parameter	LINAC Configuration	
	17 MeV	33 MeV
Microwave Frequency	2,856 MHz	2,856 MHz
Number of Accelerating Sections	2	3
Energy Range	1 to 17 MeV	3 to 33 MeV
Electron Energy at Maximum Power	8.5 MeV	16.5 MeV
Rated Average Power	4 kW at 1 MeV 10 kW at 4 MeV 14.5 kW at 8.5 MeV 10 kW at 13 MeV 4 kW at 16 MeV	4 kW at 3 MeV 10 kW at 10 MeV 12 kW at 16.5 MeV 10 kW at 23 MeV 4 kW at 30 MeV
Maximum Efficiency Operation		
Beam Energy	8.5 MeV	16.5 MeV
Peak Beam I	1.6 A	0.7 A
Rated Average Power	14.5 kW	12 kW
Beam Pulse Width (FWHM)	0.03 to 6 μs	0.05 to 6 μs
Pulse Repetition Rates/s		
At 6-μs Pulse Length	1, 7.5, 15, 30, 60, 120	
At 1-μs Pulse Length	Continuously variable to 550	
Maximum Deliverable Peak I[a]		
Pulse Width (FWHM) > 0.25 μs	1.2 A	--
Pulse Width (FWHM) 0.03 to 0.05 μs	2.5 A	--
Pulse Width (FWHM) > 0.5 μs	--	1.2 A
Pulse Width (FWHM) 0.05 μs	--	2.5 A

[a]Analyzed beam delivered to output window ~30 ft from end of last accelerating section.

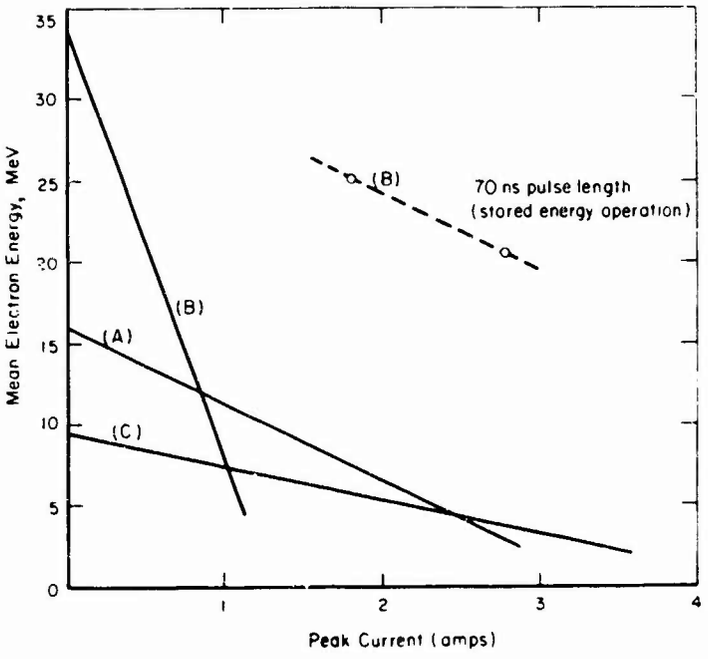

Figure 4-8. BREL LINAC beam loading characteristics.

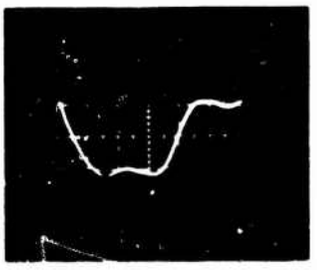

Horizontal Scale: 10 ns/div.
Vertical Scale: 1 A/div.

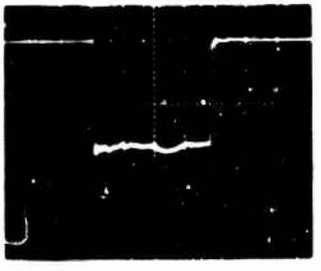

Horizontal Scale: 1 μs/div.
Vertical Scale: 200 mA/div.

Figure 4-9. BREL LINAC electron-beam pulse shapes.

Table 4-4. BREL LINAC environment characteristics.[a]

Parameter	LINAC Configuration	
	10 MeV	25 MeV
Electron Beam Mode		
Dose Rate at Exit Window	$>10^{11}$ rad(Si)/s•A	b
Dose Rate at 30 cm	3×10^{9} rad(Si)/s•A	b
X-Ray Mode (W target and 1/8-in. Al filter)		
Dose Rate at 30 cm	6×10^{6} rad(Si)/s•A	8×10^{7} rad(Si)/s•A
Neutron Mode (depleted U-238 target)[c]		
Yield Rate (n/s)	b	7×10^{12} n/s
Yield/pulse	b	$\sim 6 \times 10^{10}$ n/pulse
n/γ Ratio (n/cm^2•rad(air))		
No Shield	b	1.4×10^{6} n/cm^2•rad(Si)
4-in. Pb Shield	b	6.7×10^{8} n/cm^2•rad(Si)

Notes:

[a]Data are not definitive and are meant only to be used as a guide.

[b]Data not obtained.

[c]For neutron energy spectrum, see Figures 4-15 and 4-16.

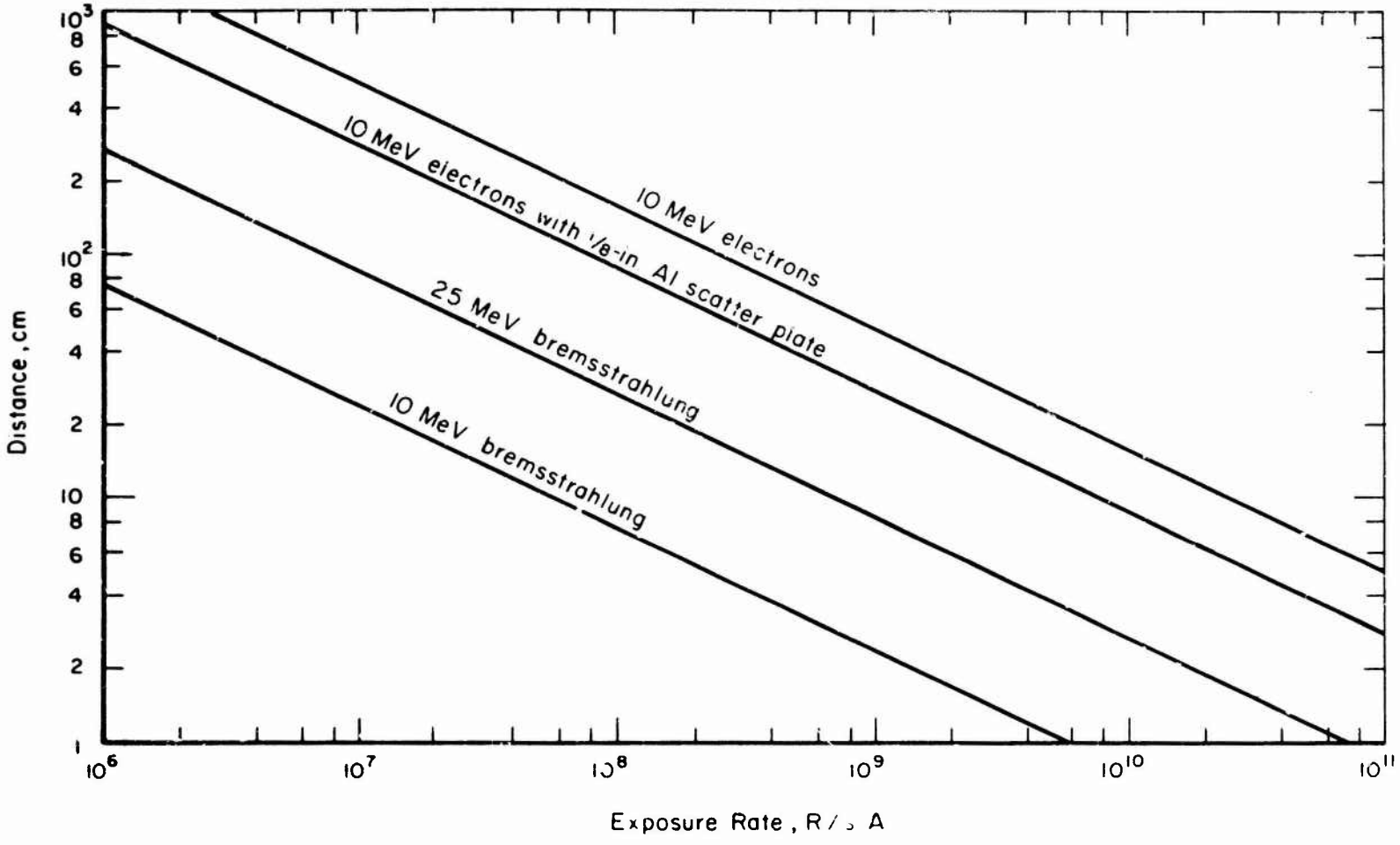

Figure 4-10. Theoretical electron and bremsstrahlung exposure rates as a function of distance from beam port.

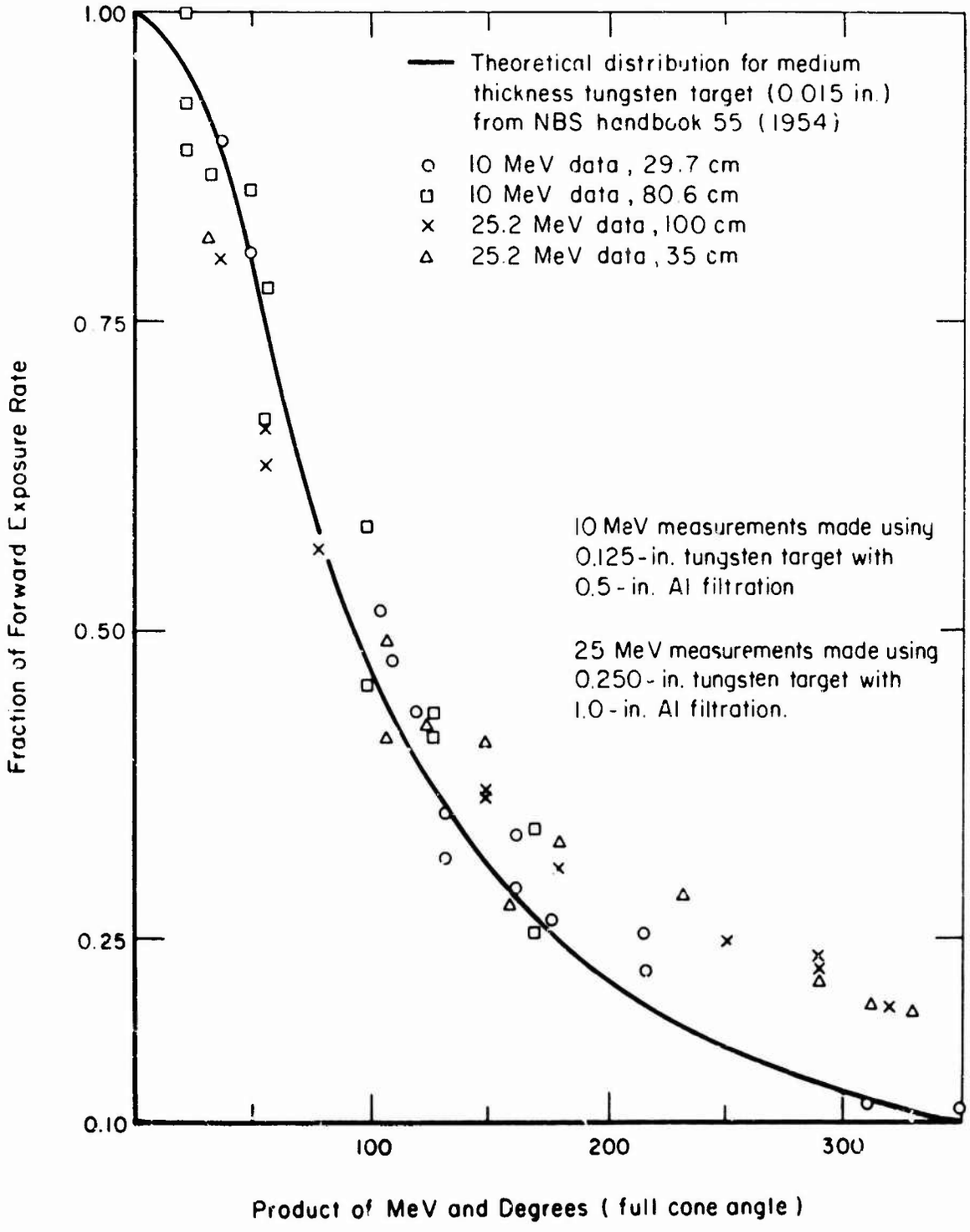

Figure 4-11. Thick target bremsstrahlung energy-angle distribution.

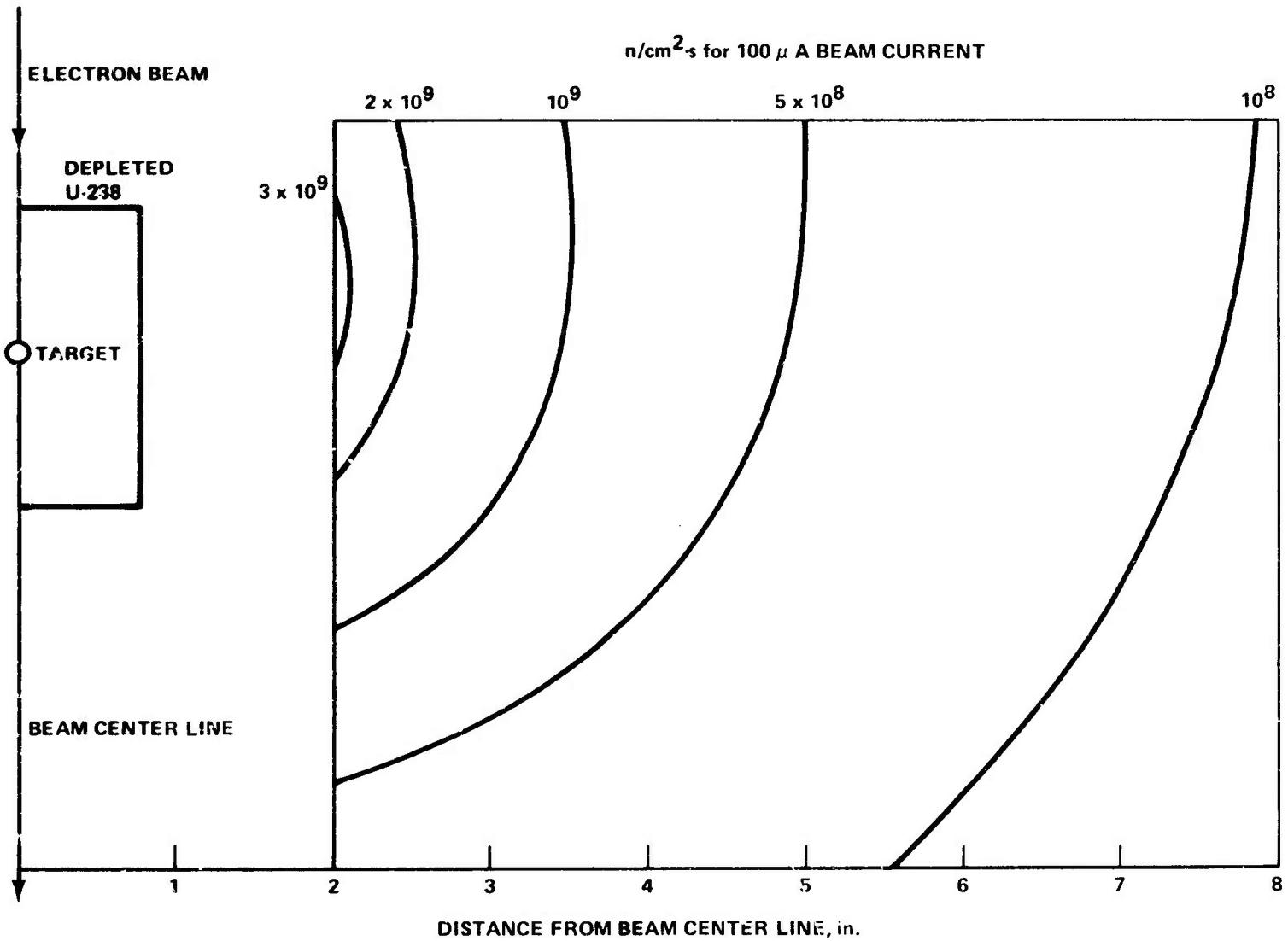

Figure 4-12. Fast neutron (E > 3 MeV) flux density in permanent-damage test fixture.

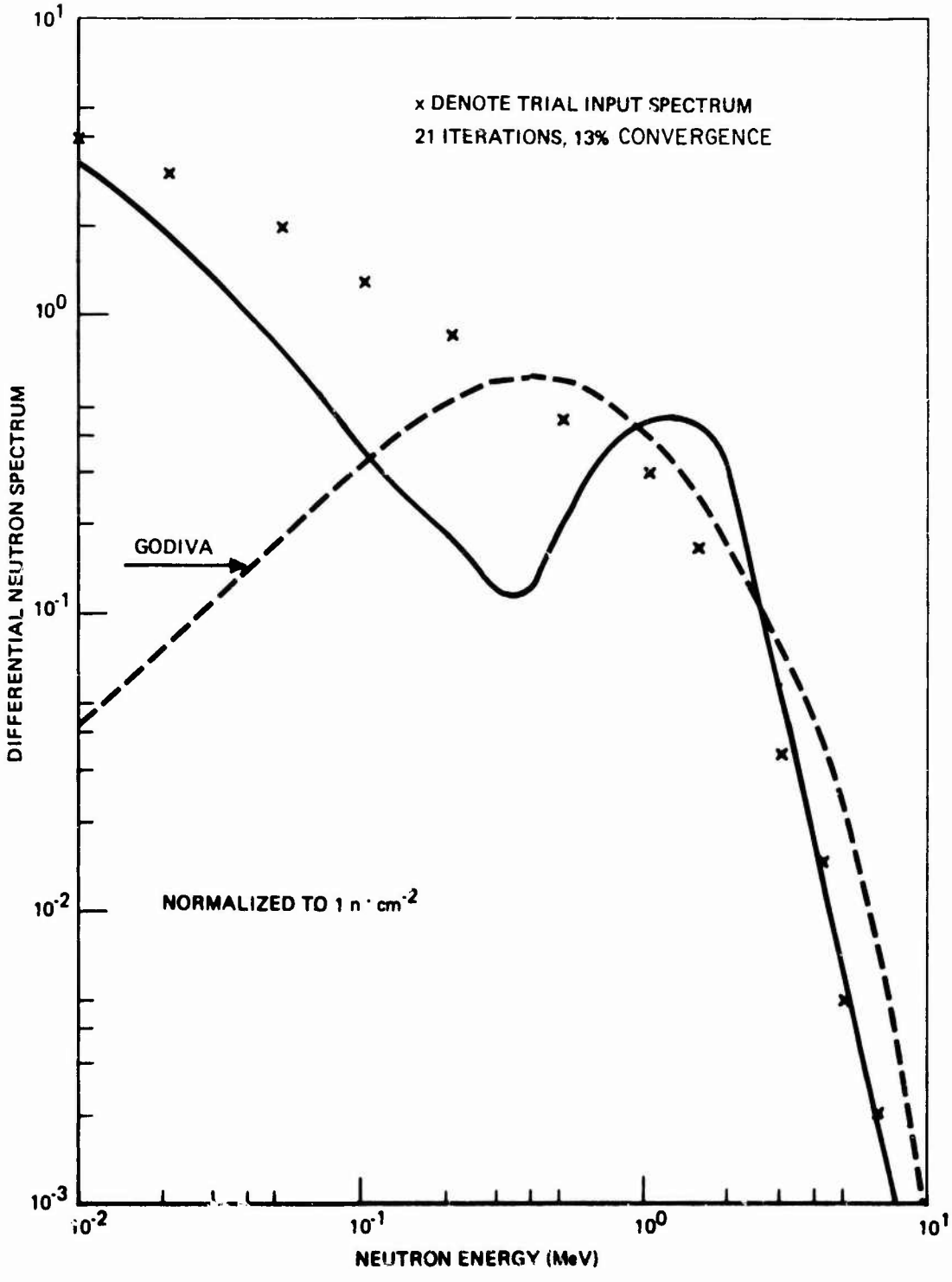

Figure 4-13. Differential neutron spectrum.

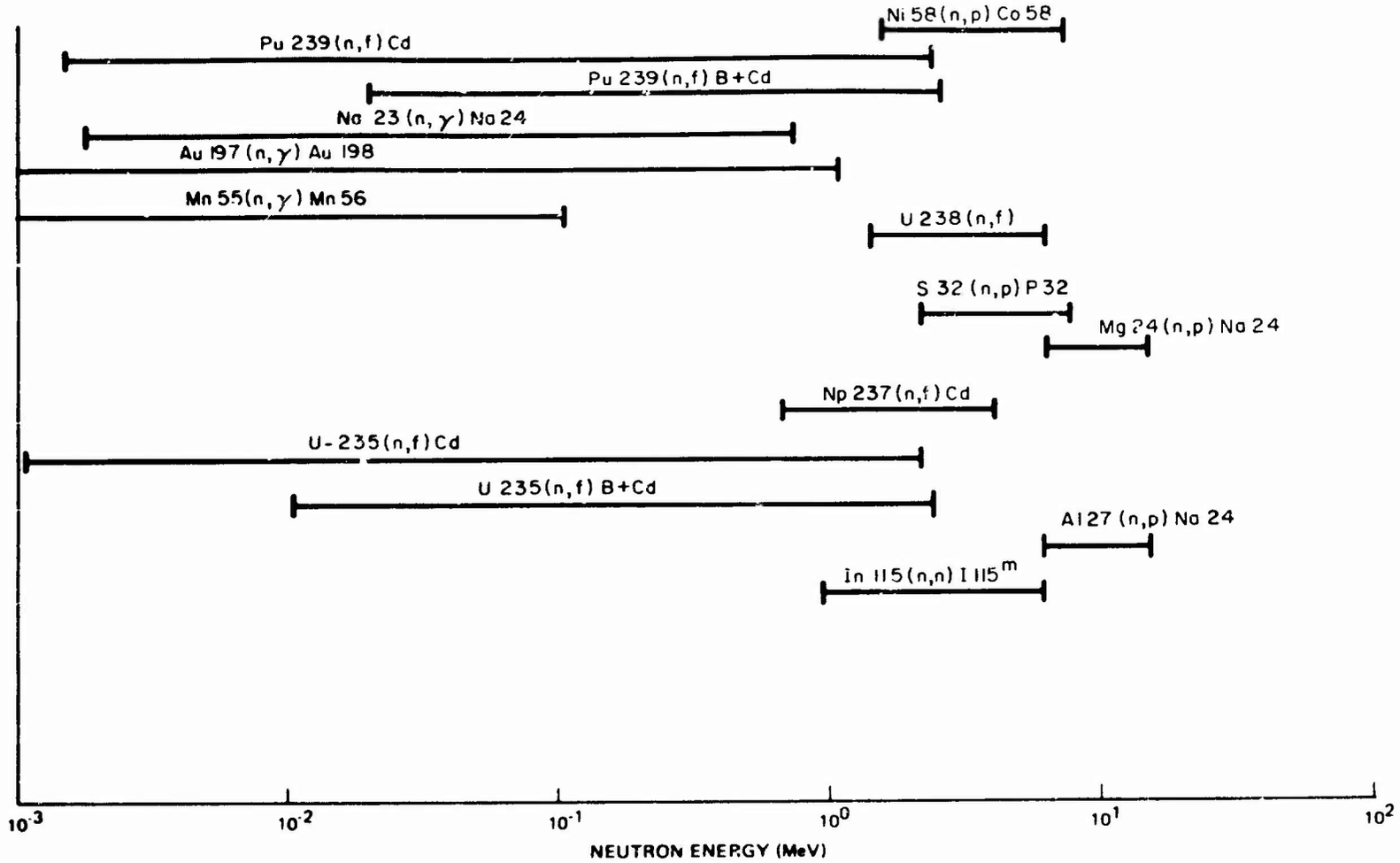

Figure 4-14. Energy range for reactions used to obtain neutron spectrum (only 5% of the foil's total response lies above, and 5% below the energy indicated).

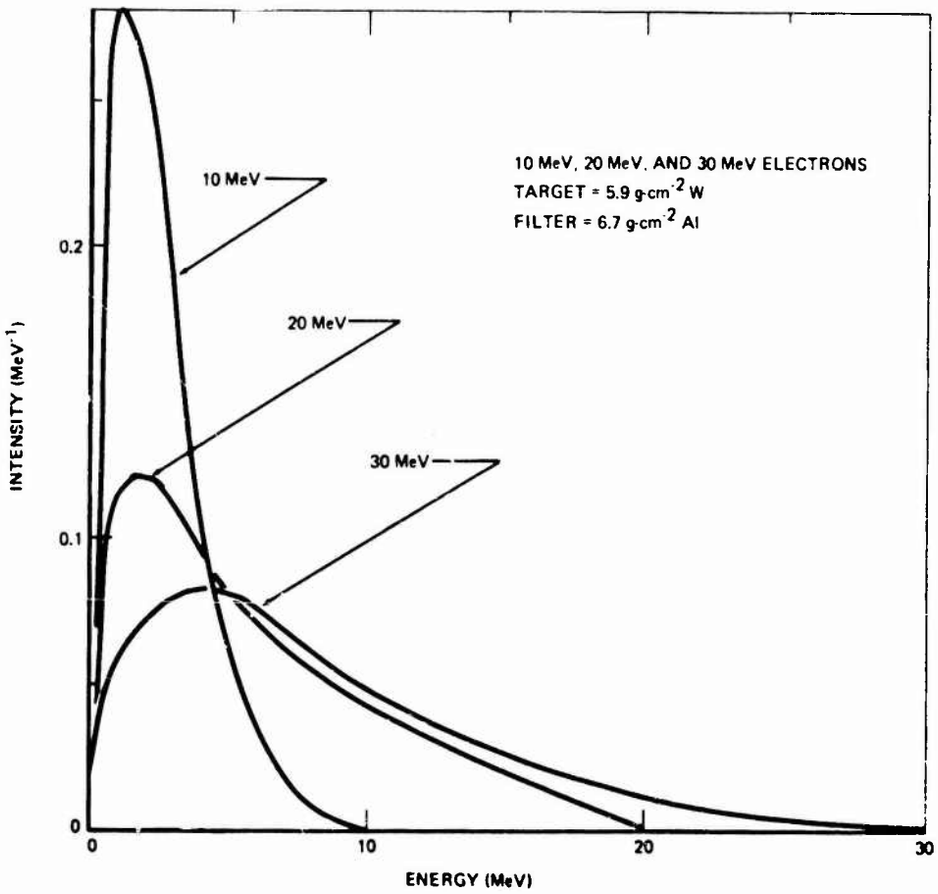

Figure 4-15. BREL LINAC bremsstrahlung.

The neutron fluence map of the permanent-damage test fixture (Figure 4-12) was made with S pellets, which when properly calibrated provide a measure of the fluence of neutrons with energy >3 MeV. The data are commonly corrected to indicate the fluence of neutrons with E > 0.010 keV by applying an experimentally measured Pu/S ratio of 25. This ratio, while higher than the ratio for a prompt critical reactor (~8), is consistent with the experimentally measured differential neutron spectrum described below.

The neutron spectrum was measured in the rotating irradiation test facility by exposing and counting 18 different fission and activation foils. The measured activities were used as an input, with a trial input spectrum, into an iterative computerized spectrum unfolding code, SAND-II. After 21 iterations, the program converged to a solution to within 13%, i.e., the rms deviation of measured activities to calculated activities for the spectrum shown was 13%. Figure 4-13 also shows the trial input spectrum and compares the photoneutron spectrum to a prompt critical reactor, in this case Godiva.

Well shielded signal cables are used to eliminate ground-loop and spurious noises. Quantitative electrical noise data are available upon request.

4.4.4 Support Capabilities

BREL will provide support to experiments as required. Complete or partial experimental programs can be carried out by BREL alone or any degree of help can be supplied. The services of a complete operational and technical support staff are available on either a full-time or consulting basis. This staff includes dosimetry and instrumentation technicians, as well as machine operators. The professional staff of the Radiation Physics Group, which numbers more than 30 engineers and physicists, is exclusively engaged in radiation effects and environmental simulation programs. The staff is competent in TREE activities.

Electronic equipment available for experimental use includes dual-beam 500-MHz oscilloscopes, pulsers, and power supplies. General-purpose test equipment is available from the Boeing test equipment stores. Test equipment requirements should be coordinated with BREL at least 2 weeks in advance of testing.

Signal and power cables are provided. Instrument power includes 12 Vac, 220 Vac, and 440 Vac. Triggering signals responding to machine command signals are readily available. An arrangement of fixed delays makes possible a wide range of trigger timing signals. No screen room is associated specifically with the BREL LINAC. Signal conduit connecting the test area with the data acquisition and read-out room contain cables of the triaxial and low-noise type. Care is taken to eliminate ground-loop and other spurious noise sources.

The BREL staff will conduct or lend assistance in dosimetry measurements. Bremsstrahlung and electron-beam dosimetry and beam mapping are generally done with LiF TLDs. BREL maintains a complete dosimetry laboratory for specialized problems. The experimenter has the option of performing his own dosimetry, if desired. Arrangements can be made for use of the Boeing computer center. There are complete machine shop facilities capable of constructing experiment apparatus.

A 20- x 30-ft bay adjoining the FXR instrumentation room is available for experimenter use and there is additional floor space in the LINAC area. Office space and conference room facilities are limited. BREL maintains a complete photographic laboratory with a full complement of equipment. Oscilloscope cameras and film and two 4 x 5 view cameras with complete accessories are readily available.

Experiments are conducted at the beam ports to which the beam is directed by a series of deflecting magnets. Ample floor space and spacious test areas are associated with the beam-port positions. Test stands and other support equipment are provided.

4.4.5 Procedural Information

Technical inquiries should be directed to:

The Boeing Aerospace Company
Research and Engineering Division
P.O. Box 3999
Seattle, WA 98124

Attention: Boeing Radiation Effects Laboratory
E.M. Costello
Mail Stop 2R-00
Telephone: (206) 655-2954

Administrative inquiries should be directed to:

The Boeing Aerospace Company
Research and Engineering Division
P.O. Box 3999
Seattle, WA 98124
Attention: H.M. Kilborn
Organization 21143
Mail Stop 8C-26
Telephone: (206) 773-3449

Scheduling is arranged on an individual basis through the BREL technical contact. It is expected that only nominal lead times will be required.

Costs and charges associated with use of the BREL LINAC facility may be obtained directly from the BREL administrative contact.

The shipping address is:

Boeing Radiation Effects Laboratory
1420 South Trenton Street
Building 15-10
Seattle, WA 98108

4.4.6 Reference

1. "Boeing Radiation Effects Laboratory," descriptive brochure, available from BREL.

4.5 NWEB LINAC

4.5.1 Characteristics

The LINAC of the Nuclear Weapon Effects Branch (NWEB), Army Missile Test and Evaluation, is a 2-section, S-band accelerator which operates in the energy range of 2 to 48 MeV. Pulse width can be varied from 0.01 to 10 μs.

4.5.2 Test Parameters

As with all LINACs, the electron I available over the entire energy range is not constant, being a maximum near the center of the range and approaching zero at the upper limit. The maximum also varies with pulse width. The pulse is essentially square with typical LINAC characteristics. The klystron pulse width is constant at 12 μs. Beam pulse width is determined by the electron-injection pulse. For pulses in the ns range, the pulse approaches a triangular shape (see Figures 4-16 and 4-17).

Repetition rate is 10, 20, 30, 60, or 120 pulses/s. Single pulses can be delivered for any pulse width within the normal pulse-width range. Duty ratio is a maximum of 0.12%.

Electron-beam loading characteristics are given in Figure 4-18. Beam dia. at the exit port is approximately 2 mm and increases with distance from the port. Extra large spot sizes can be produced by scattering from a plate. A qualitative estimate of the beam geometry can be obtained by examining the radial dependence of electron dose rate as given in Figure 4-19. Typical energy spread can be seen in Figures 4-21 and 4-22. Curves of electron and x-ray exposure rate as a function of distance from the beam window-bremsstrahlung target are given in Figures 4-19 and 4-20. These data were obtained from photodiode measurements with the LINAC operating at an energy of 26 MeV and a beam I of 500 mA. The exposure measurements were made in 1966 and agree well with theoretical calculations.

Measurements have been made of the electron-beam energy spectrum using a magnetic spectrometer. Results for 2 different operating energies are given in Figures 4-21 and 4-22.

Normal operating procedure for the LINAC is to adjust the machine to deliver the desired dose at a given test position as determined from dosimetry measurements. The experiment is then conducted at that machine adjustment. Dosimetry measurements are made with TLD techniques. Beam-locating and survey measurements are made using CaF chips, and a calibrated diode is extensively used, in conjunction with the Waveform Processing System. It is expected that normal dosimetry errors are associated with the measurements.

A screen room can be utilized, and care is taken to ensure proper shielding of test signal cables.

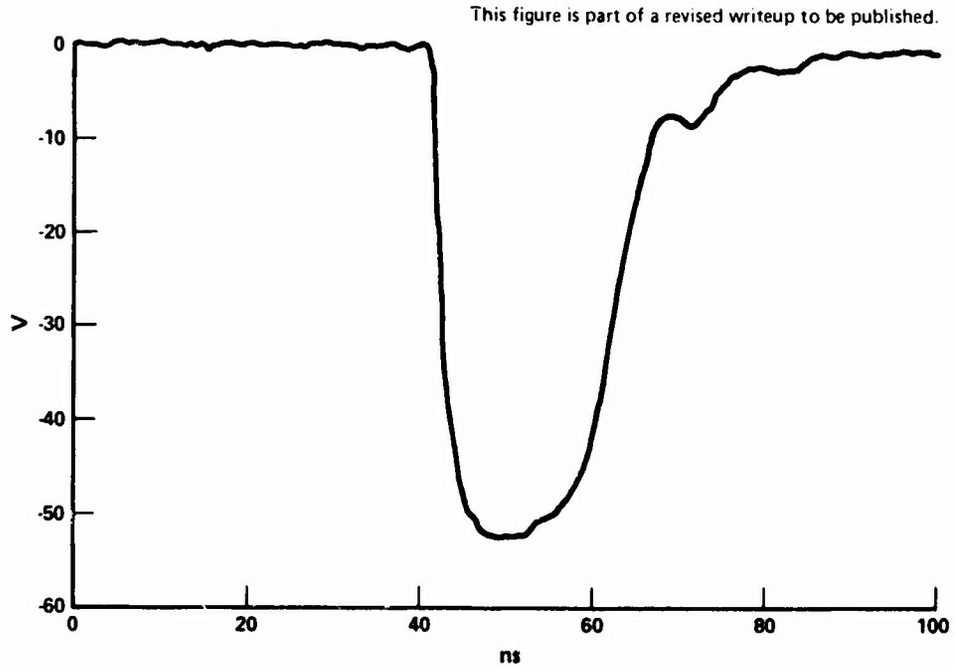

Figure 4-16. NWEB LINAC pulse shape.

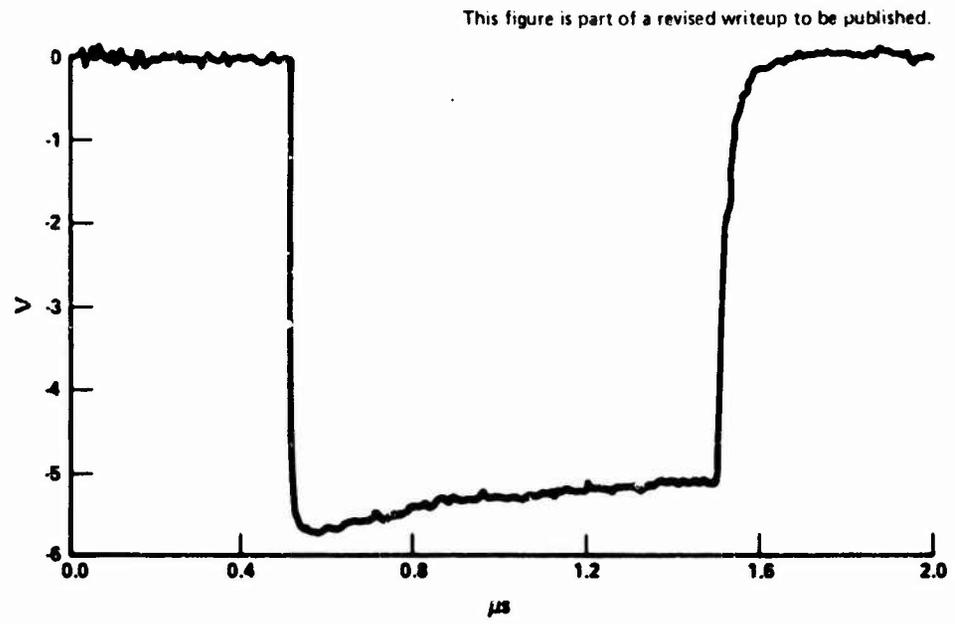

Figure 4-17. NWEB LINAC pulse shape.

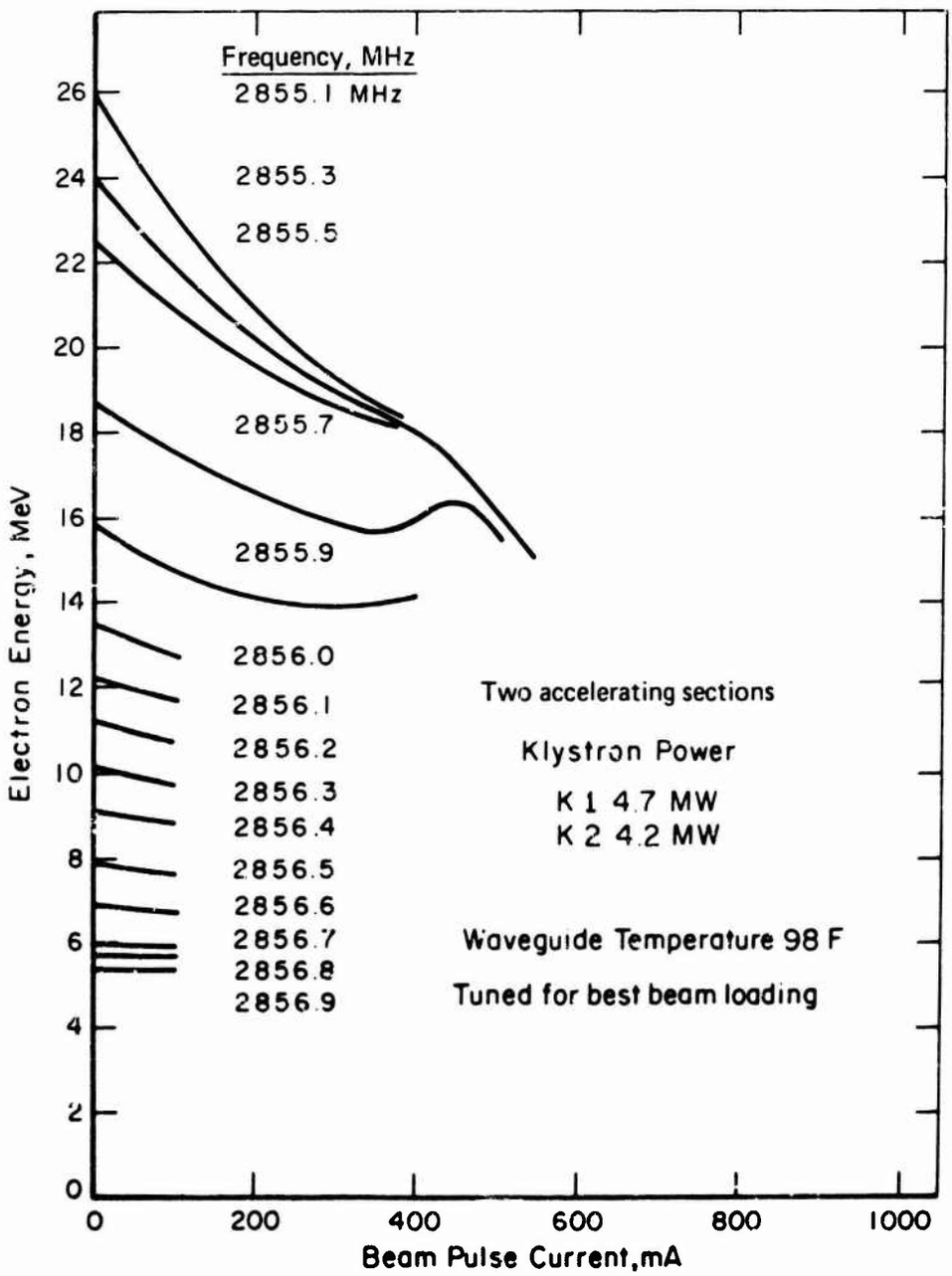

Figure 4-18. Beam loading characteristics.

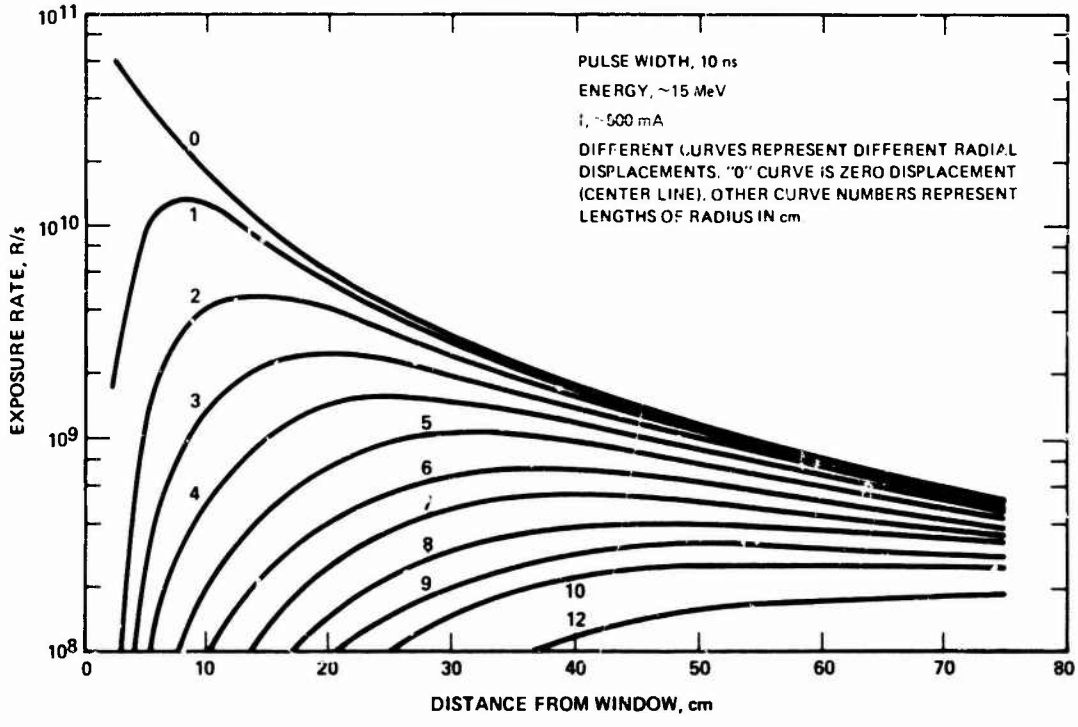

Figure 4-19. Exposure rate for electrons.

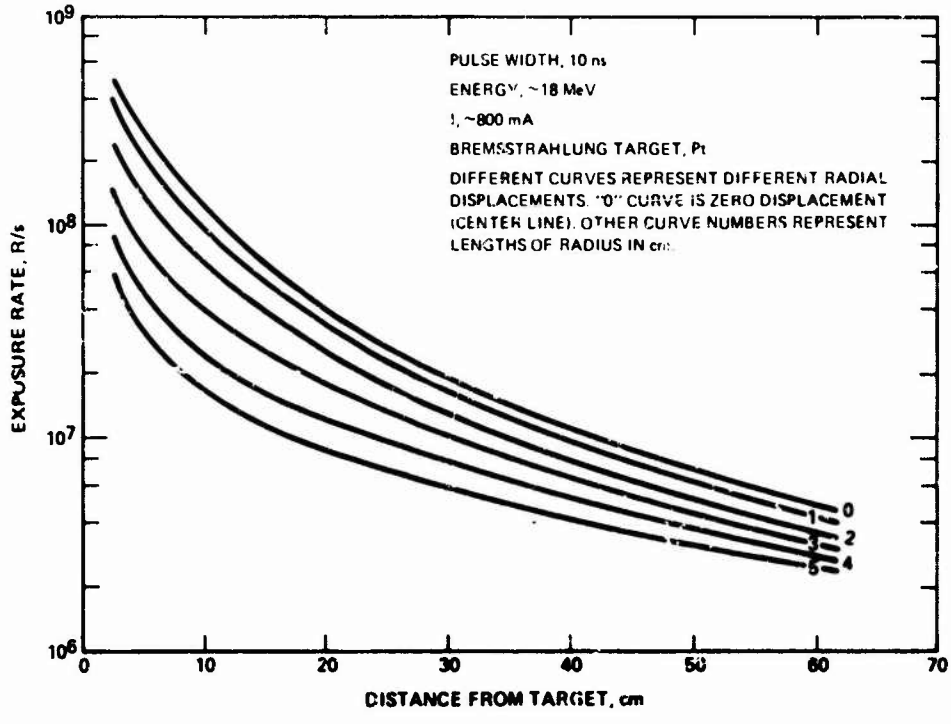

Figure 4-20. Exposure rate for x-rays.

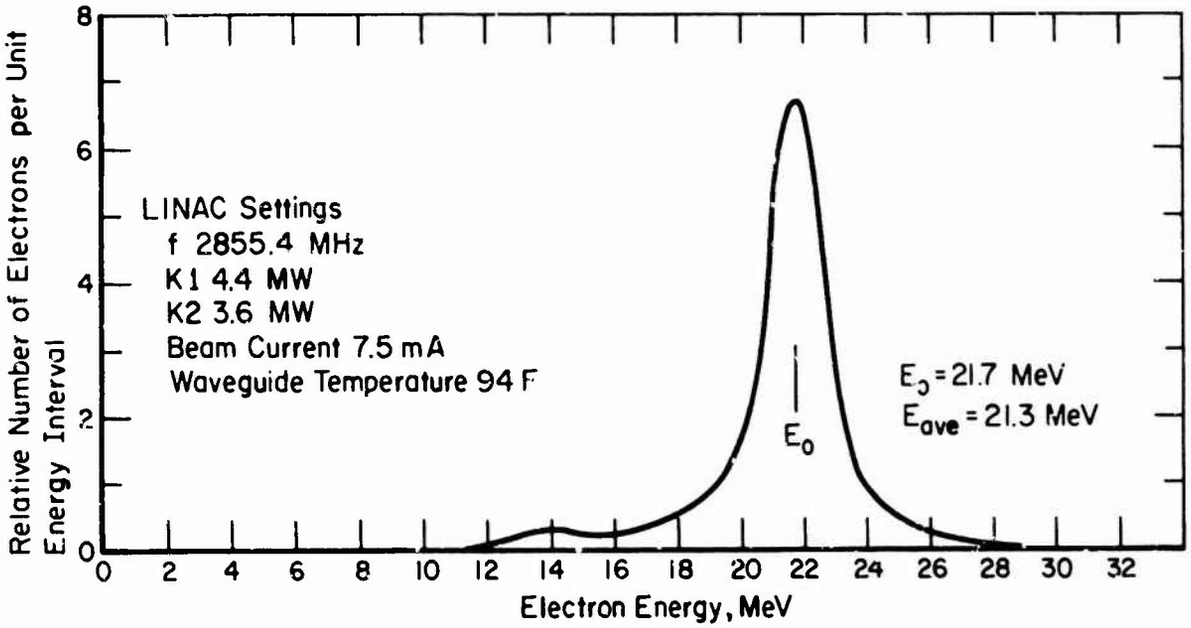

Figure 4-21. Electron energy spectrum (21.7-MeV peak, values good to ±3% of peak value).

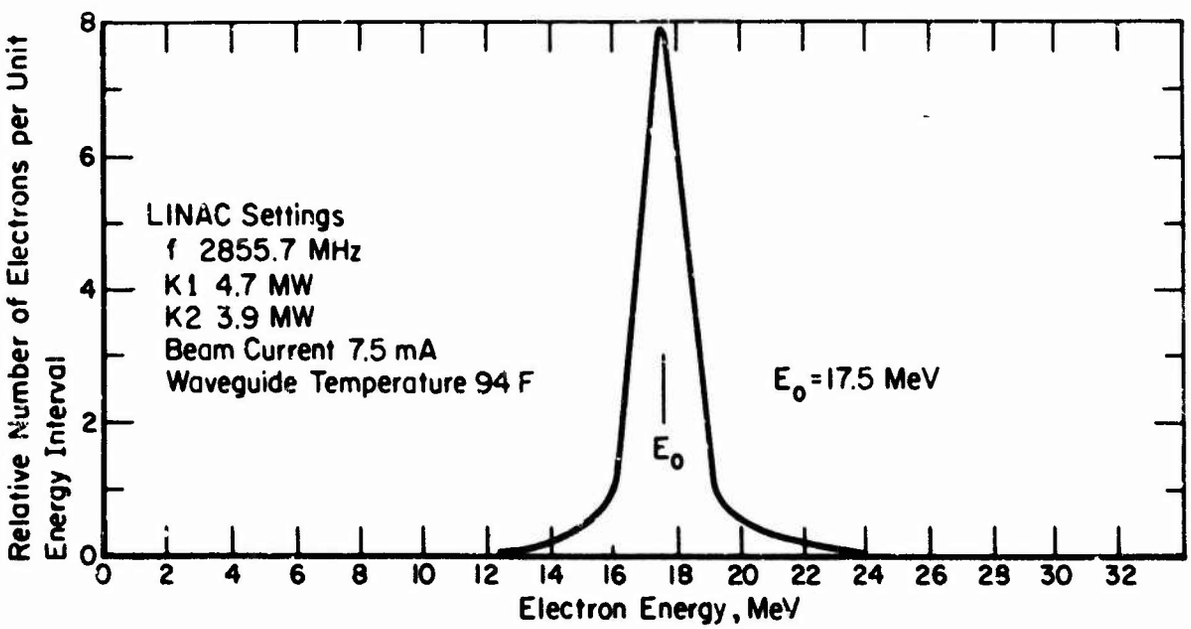

Figure 4-22. Electron energy spectrum (17.5-MeV peak, values good to ±3% of peak value).

4.5.3 Support Capabilities

The prime mission of the facility is to support experimenters and, when available, to provide necessary personnel and equipment for full operational and working assistance. Facility personnel operate the LINAC. The limited professional staff, enhanced by scientific and engineering personnel from university and college faculties, is available in support of all experimental programs.

Instrumentation trailers equipped for monitoring and recording experimental data are available on a contract basis. There are adequate facilities and space for the experimenter to utilize his own instrumentation trailers. Electronic equipment and support components maintained for use by experimenters are as follows:

Item	Quantity
FR600 Ampex magnetic tape recording and reproducing 14-channel system (8 channels, 300 ∿ to 500 kc of direct recording; 14 channels, dc to 40 kc of FM recording; 1-7/8 to 120 in./s tape speeds)	1
FR600 Ampex magnetic tape recording and reproducing 7-channel system (7 channels, 300 ∿ to 1 Mc, direct recording only; 15 to 120 in./s tape speeds)	1
CP100 Ampex magnetic tape recording and reproducing 14-channel system (14 channels, 300 ∿ to 250 kc of direct recording; 28 channels, dc to 20 kc of FM recording; 1-7/8 to 60 in./s tape speeds)	2
1612 Visicorder oscillograph (36 channels, 120 to 5 kc; 1/10 to 160 in./s tape speeds)	1
1508 Visicorder oscillograph (24 channels, 1 to 5 kc; 1/10 to 80 in./s tape speeds)	2
Brush oscillograph (8 channels. dc to 120 ∿)	2
VR1500 Ampex video recorder	1
555 Tektronix oscilloscope - L, D, 1A1, 1A2, CA, W, Z Plug-ins	14
321 Tektronix portable oscilloscope	3
564 Tektronix storage oscilloscope	1
450 Dumont oscilloscope cameras	12
C19 Tektronix oscilloscope camera	1
200 AB Hewlett Packard audio oscillator	3
500 Fairchild semiconductor multi-parameter tester	1
4000 Fairchild semiconductor multi-parameter tester	
600 Fairchild semiconductor multi-parameter tester	
Kepco KS-36-30M power supply	2

Item (continued)	Quantity (continued)
HP 721 power supply	
HP 723A power supply	
24-ft instrumentation van, flat bed, with racks	2
180 Tektronix time-mark generator	2
181 Tektronix portable time-mark generator	2
1217B General Radio pulse generator	1
HP 214 pulse generator	2
B7 Rutherford Electronics pulse generator	5
Hewlett Packard 202A function generator	1
226B Computer Measurements Corporation counter timer	4
Beckman 6146 Eput and timer counter	2
523 C. R. Hewlett Packard counter timer	2
127 Tektronix differential preamplifier (2 channels)	5
TS312-FSM-1 Hewlett Packard audio oscillator	1
Tektronix 575 curve tracer, with type 175 high-current adapter	2
Tektronix 576 curve tracer	1
196A Hewlett Packard oscilloscope camera	4

Dosimetry and health-physics services and support are available. The equipment and instrumentation of the dosimetry laboratory are:

Item	Quantity
400-channel pulse-height analyzer, portable	1
4000 channel analyzer computer based system	5
γ-spectroscopy system using a 3-in. x 3-in. NaI scintillation crystal	1
Li drifted germanium (GE(Li)) detectors	5
Automatic sample-changing, β-counting system	1
Automatic data printout system	1
2-pi gas-flow counting system	1
LiF TLD system	1
CaF_2 TLD system	3
Calibration sources	Various

A Waveform Processing System (WPS) is used in conjunction with the LINAC. It is capable of acquiring and analyzing up to 10 waveforms simultaneously, using Tektronix R7912 transient digitizers. The data from these digitizers are fed into a PDP 11/35 computer, which has a 128K word memory. Additional storage for memory and data is provided by a dual floppy disk. The system is operated through an R4010 terminal using SPS basic software. A digital-processing oscilloscope is also attached to the system. All data analysis can be done within seconds of the pulse. Data can be stored on disk, or printed on a hard copy, available approximately 1 min after the pulse.

Light machine shop facilities are available at the site. Adequate experiment preparation laboratories, personnel offices, security storage, radioactive storage, radiation chemistry laboratories, and conference rooms are available at the site. Professional photographic support is available at the facility. Authorization for photographic support must be obtained from the Missile-Range Administration.

The NWEB LINAC beam is directed into a rectangular test cell approximately 6-m wide, 8-m long, and 6-m high. A table for supporting test samples and equipment is located in front of the beam port. The table can be moved longitudinally vertically and horizontally either from inside the test cell or remotely from the control console. Signal cables from the test cell are strung through under-floor conduits to a screened instrument room. Access to the test cell is through roll-back shielding doors.

4.5.4 Procedural Information

The LINAC is operated by the NWEB of the Army Missile Test and Evaluation command. Technical and administrative inquiries should be addressed to:

Commander
Attention: STEWS-TE-AN (L.L. Flores)
White Sands Missile Range
NM 88002

The telephone contact is Mr. L.L. Flores, (915) 678-1161/1163.

A nominal lead time is required for scheduling. However, in advance of a firm scheduling commitment, an experiment test plan must be submitted and approved.

Costs and charges associated with use of the NWEB LINAC and facility can be obtained directly from the technical coordinator. Shipments should be directed to:

Transportation Officer
White Sands Missile Range
NM 88002
Attention: Nuclear Effects Directorate

Classified mailings and shipping addresses should be arranged for, through proper channels, on an as-needed basis.

4.5.5 Applicability and Availability

The NWEB LINAC is one component of a laboratory whose specific mission is to provide facilities for use by U.S. Government agencies or their contractors to conduct experiments that require nuclear irradiation. The accelerator is readily available and amenable to TREE experiments. The laboratory has the capability for carrying out, on a project basis, complete or partial experimental programs. A full operating staff is permanently assigned to the facility, although the professional staff is not extensive.

The NWEB LINAC is located within the confines of the WSMR. Operations may involve considerable commuting distance between available overnight accommodations and the site. Arrangements for daily transportation are to be made by the experimenter. If the LINAC must be used during other than normal working hours, such arrangements must be made in advance.

4.5.6 References

1. "Characteristics of Nuclear Effects Branch Radiation Facility and Operational Procedures," Memorandum, Army Missile Test and Evaluation Directorate, March 1966.

2. "Experimenter's Guide for the Nuclear Weapon Effects Laboratory," White Sands Missile Range, New Mexico, September 1973.

4.6 EG&G LINAC

4.6.1 Characteristics

The LINAC at EG&G's Santa Barbara Division is a 2-section, L-band machine capable of accelerating electron beams in the energy region of from 1 to 30 MeV. Beam I ranges from 0.5 to 30 A, pulse widths from 50 ps to 4.5 μs, and the repetition rate up to 360 pps.

The LINAC is equipped with 2 identical beam transport systems, each of which contains 2 bending magnets and 1 quadrupole magnet. One system is located after the first accelerating section and permits beams with energies between 1 and 9 MeV to be brought out to either of 2 experimental ports. The other system is located after the second, or high-energy accelerating section (8 to 30 MeV), and has experimental ports at 0, 45, and 90 degrees. The 90-degree port in each system is achromatic.

The neutron time-of-flight apparatus includes a single evacuated flight path located at 90 degrees with respect to the electron-beam direction when it is directed into the 90-degree port. The flight path length can be varied from 12 to 30 m to allow flexibility in maximizing the data acquisition rate versus energy resolution.

The most unique feature of the LINAC is its capability to produce the 50-ps beam pulse, thus providing an extremely versatile tool for diagnosing radiation-induced, short-lived phenomena.

4.6.2 Test Parameters

Typical LINAC operating characteristics are as follows:

1. Minimum electron energy	1 MeV
2. Nominal electron energy	16 to 18 MeV
3. Maximum electron energy	30 MeV
4. Peak electron beam I at nominal energy	
a. Pulse length (4.5 μs)	0.50 A maximum
b. Pulse length (1.0 μs)	0.70 A maximum
c. Pulse length (100 ns)	2.0 A maximum
d. Pulse length (10 ns)	2.0 A maximum
e. Pulse length (50 ps)	30 A maximum
5. Pulse length variation	50 ps to 4.5 μs
6. Pulse repetition rate variation	Single to 360 pps
7. External pulsing capability	Single to 360 pps
8. Pulse-height flatness	Within ±5%
9. Beam dia. for 90% I	1 cm

10. Energy spread at 0.1-μs pulse length	50% in 10%; 90% in 37%
11. Stability	Within ±2.5%
12. Gun I	5 A maximum
13. Gun V	150 kV maximum
14. Average beam I	485 μA maximum
15. Average beam power	7.8 kW maximum
16. Peak dose rate (at nominal beam energy)	
a. Electron	1.9×10^{20} e/s
b. γ	6×10^{6} R/s/A at 1 m

Figures 4-23 through 4-28 show typical beam characteristics.

4.6.3 Support Capabilities

The LINAC is housed in a 6,000-ft^2 building containing 4 major areas: (1) a control and data recording room, (2) an irradiation area, (3) an RF source room, and (4) a neutron time-of-flight facility. Figure 4-29 shows the LINAC facility floor plan.

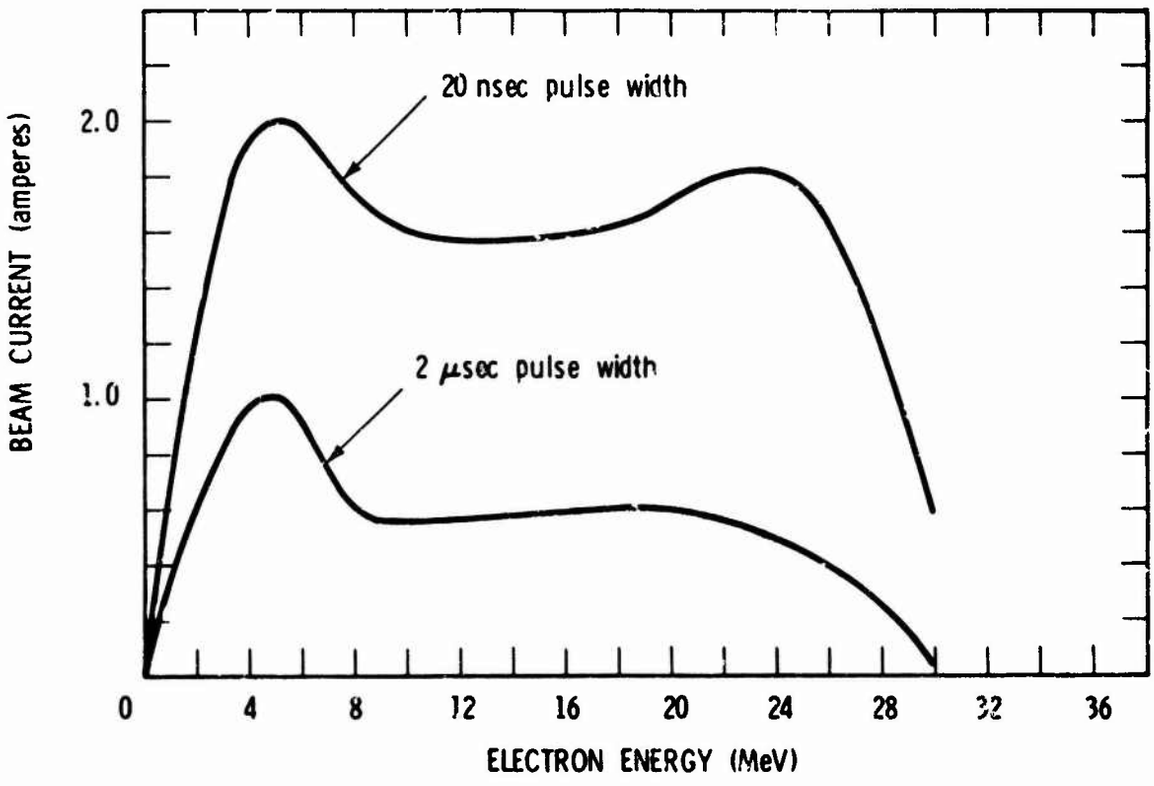

Figure 4-23. Maximum accelerated beam I.

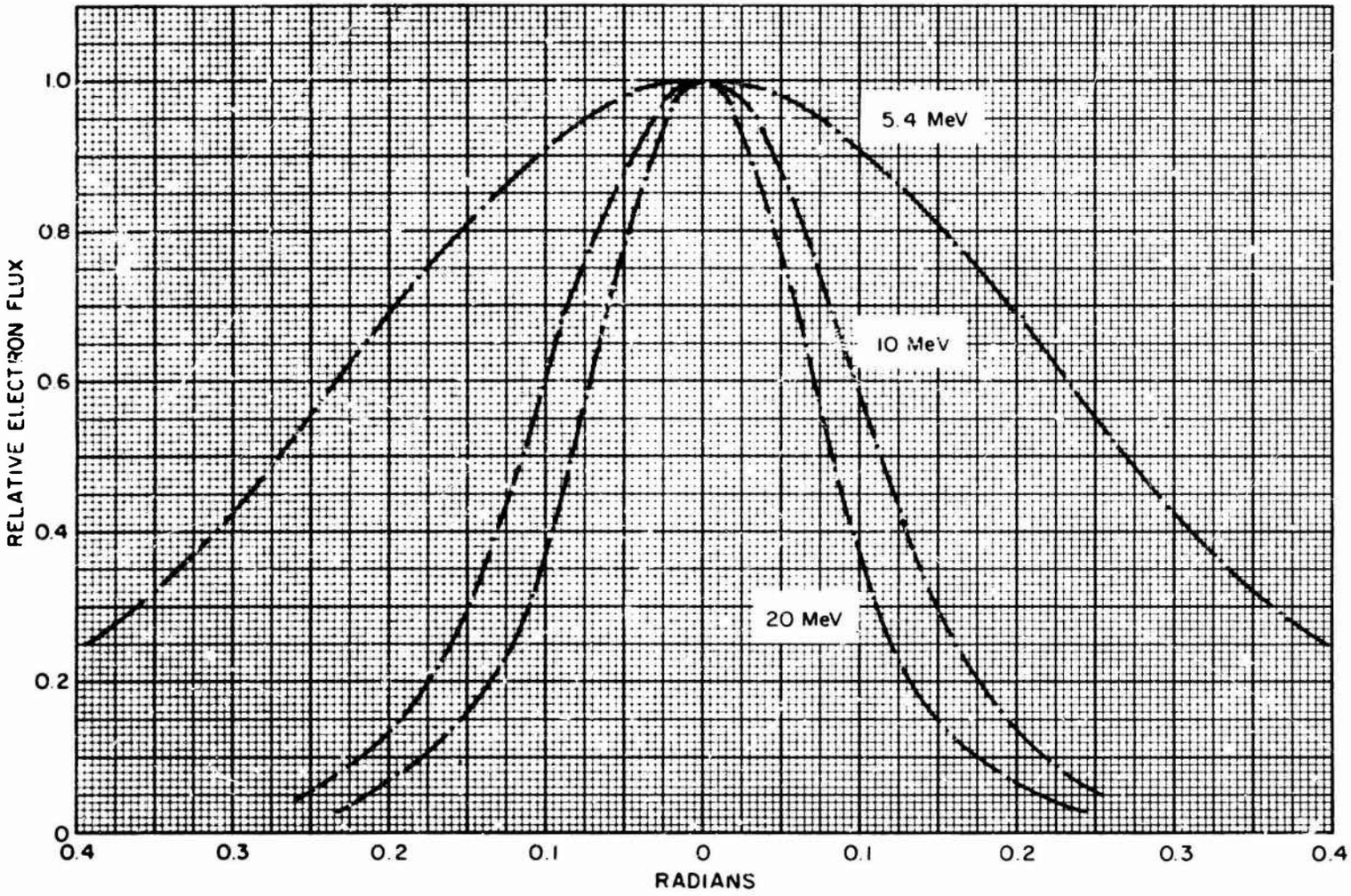

Figure 4-24. Effect of electron energy on beam divergence, standard window, 100 cm, zero port.

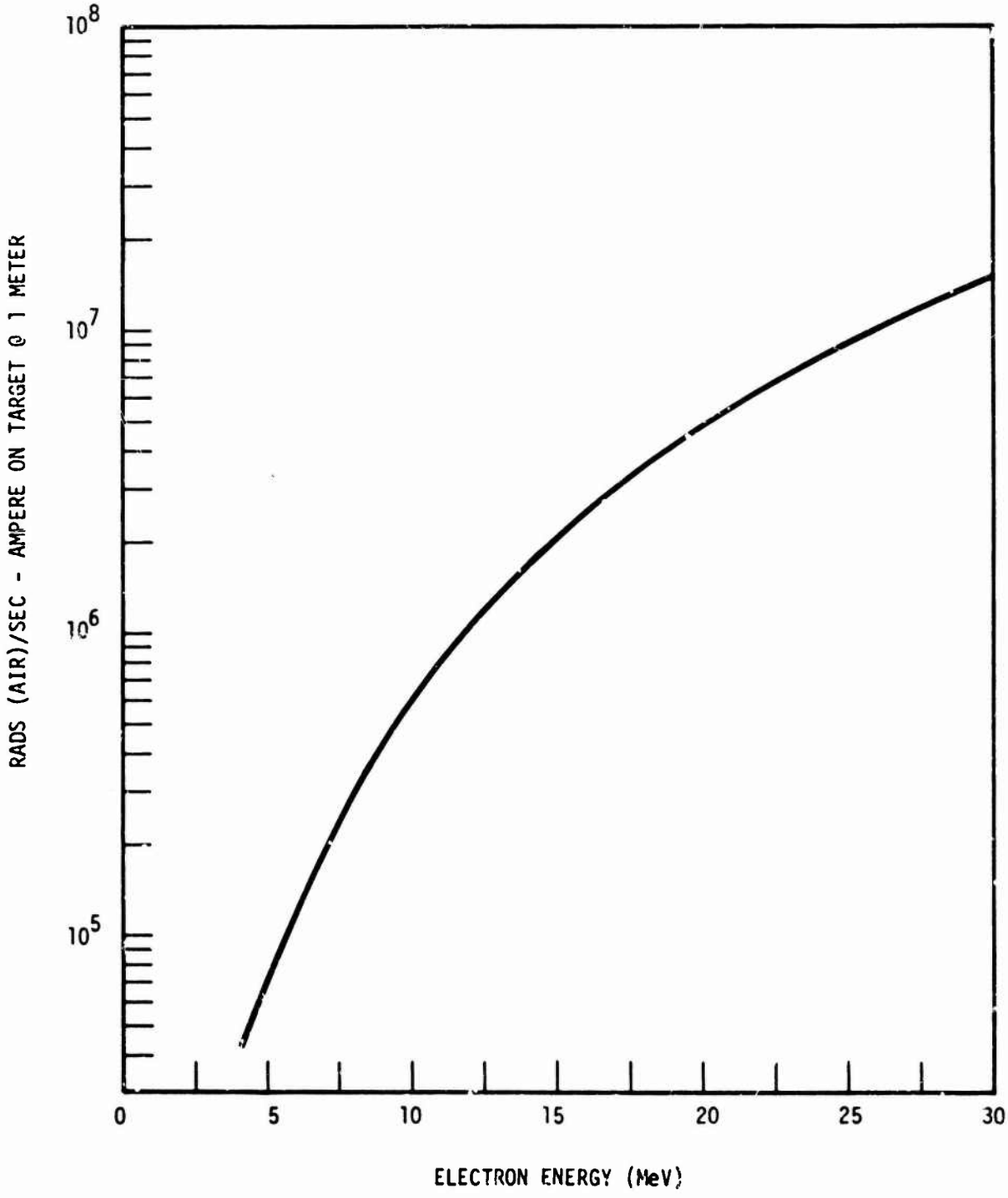

Figure 4-25. Axial bremsstrahlung intensity from 0.15 radiation length Au-W target filtered by 1.125 in. of Al.

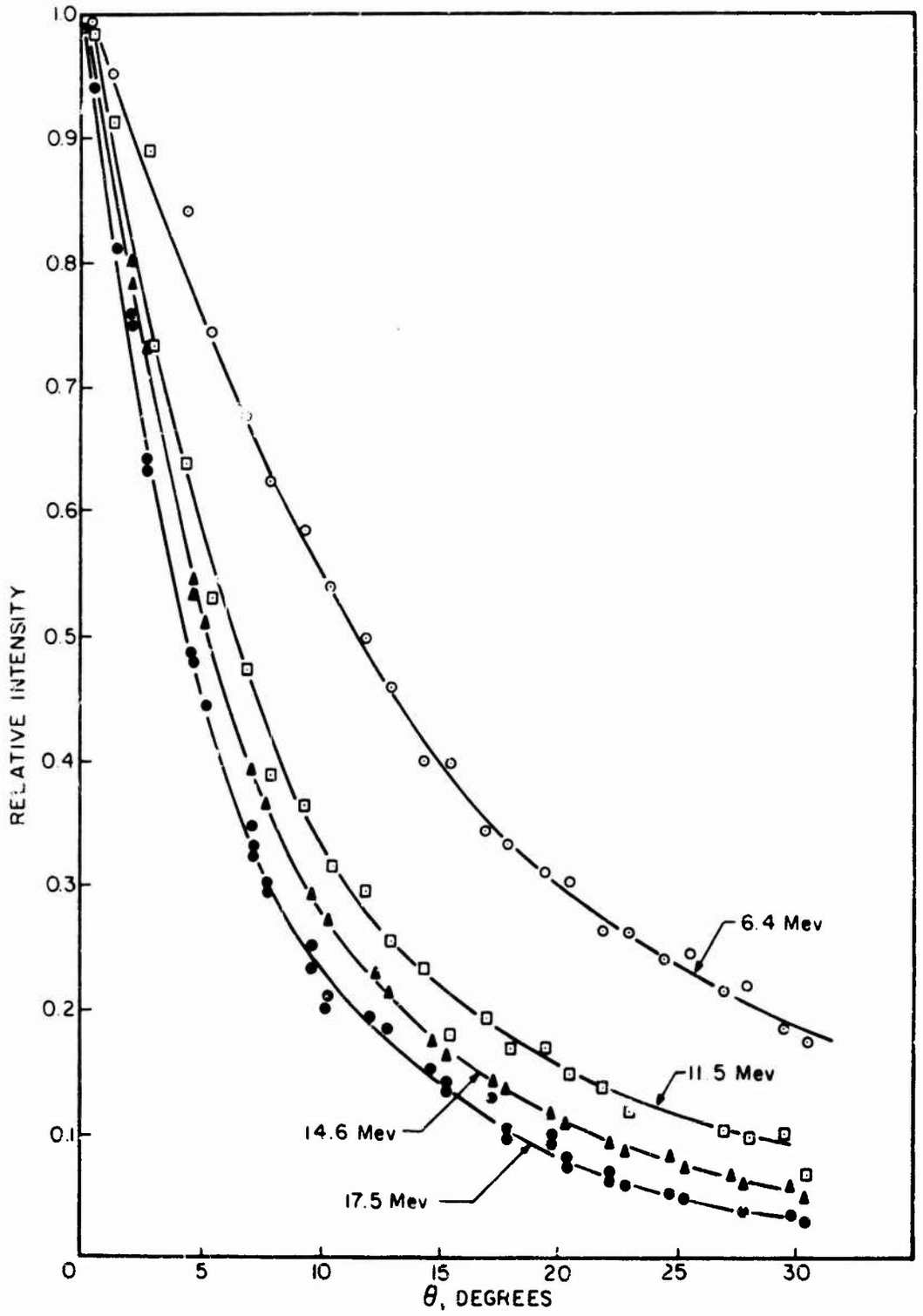

Figure 4-26. Bremsstrahlung angular distribution for 0.15 radiation length Au-W target with 1.125-in. Al filter.

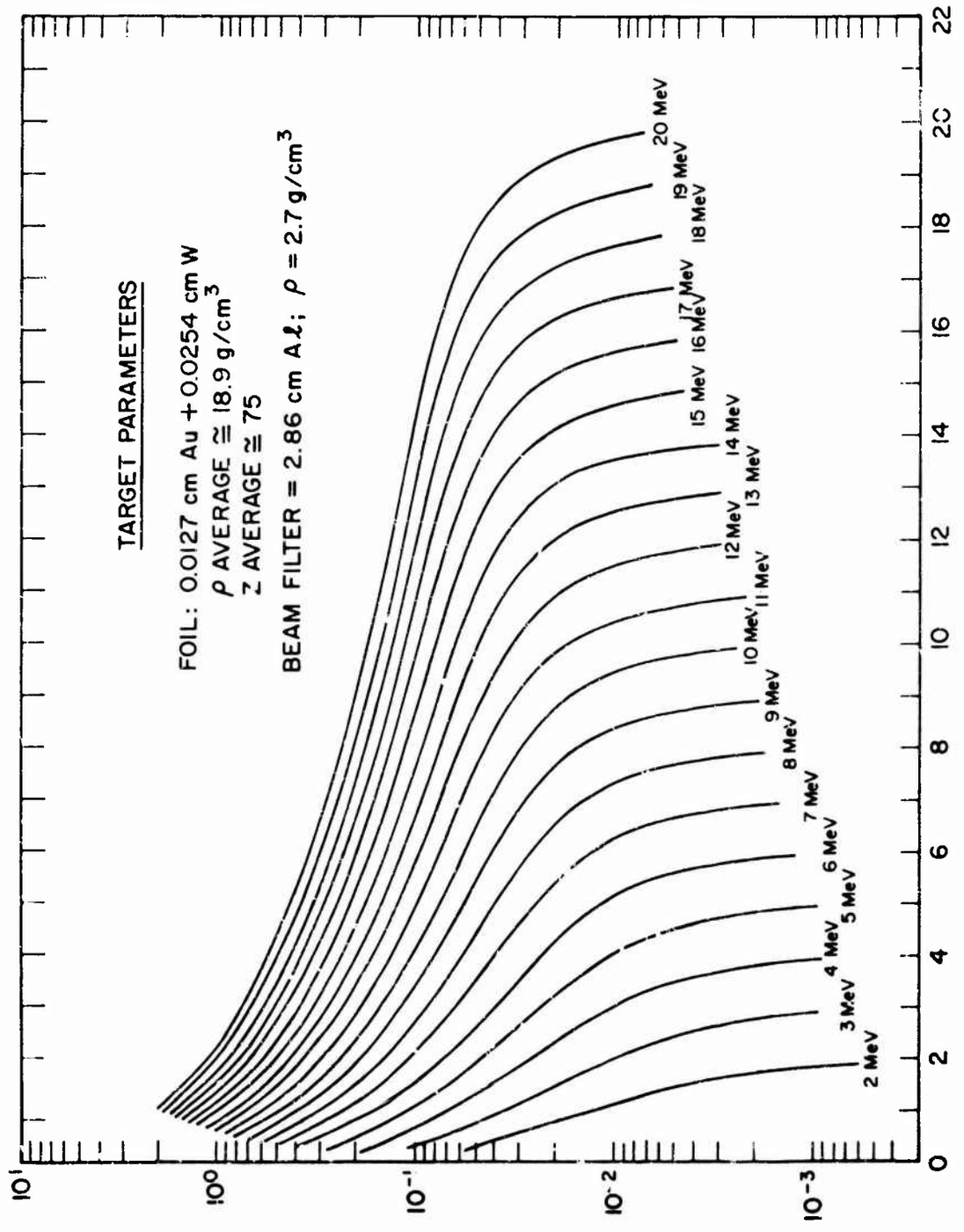

Figure 4-27. Calculated bremsstrahlung spectra for LINAC target.

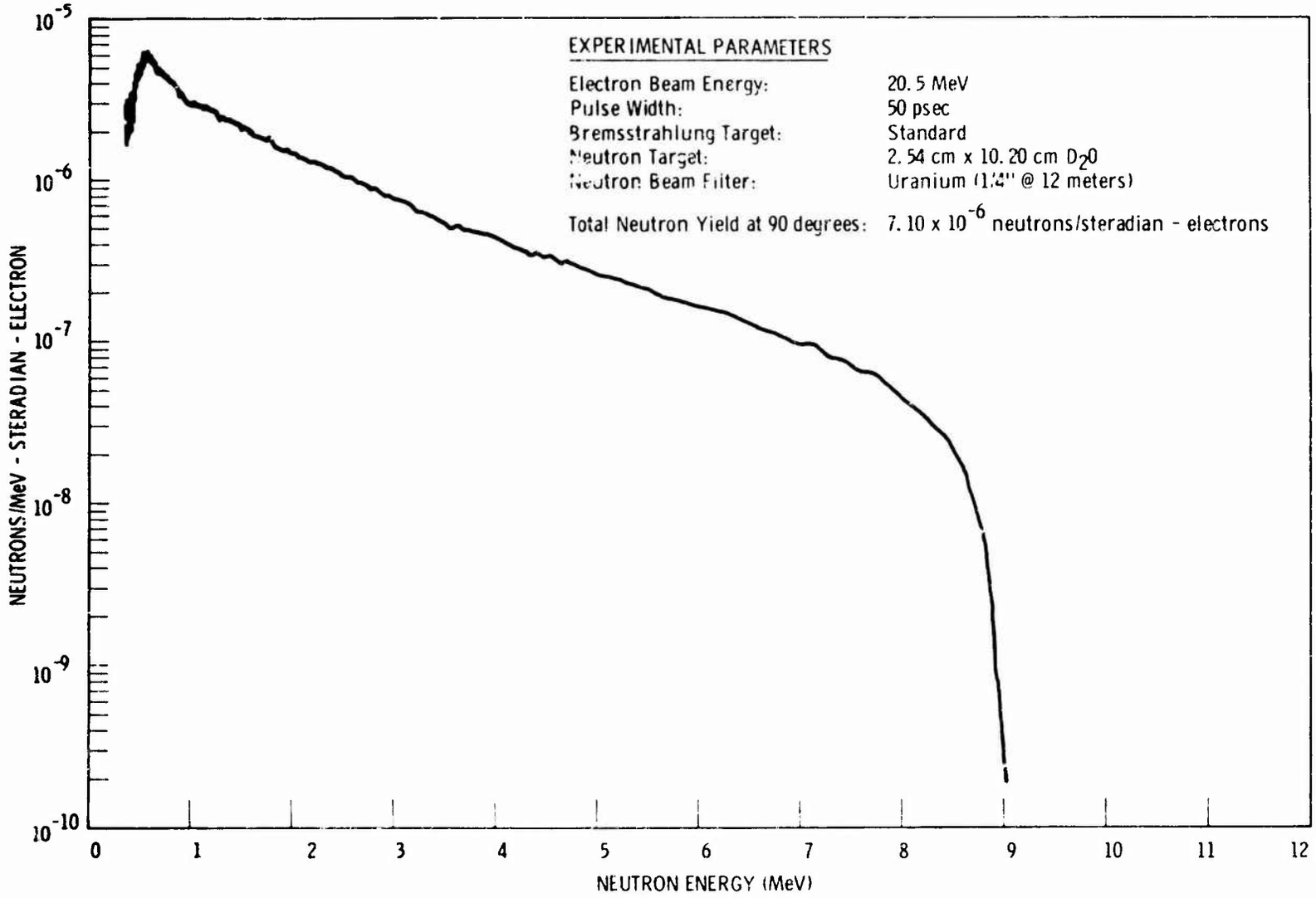

Figure 4-28. Neutron energy spectra produced by 20.5-MeV bremsstrahlung incident on D_2O target.

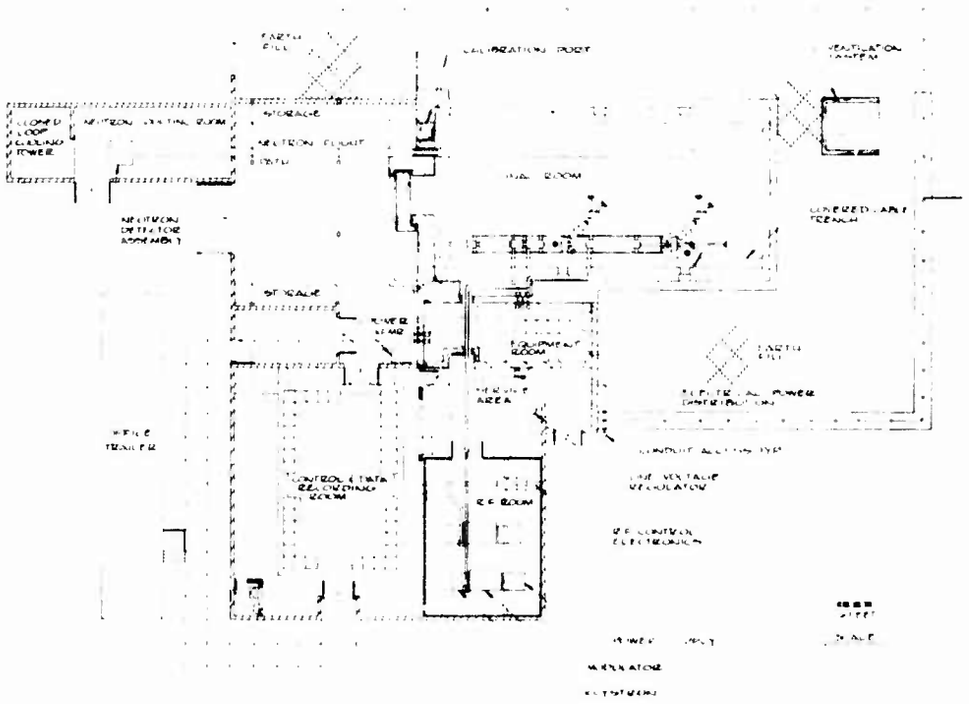

Figure 4-29. LINAC facility floor plan.

The control and data recording room contains centralized equipment for monitoring and control of all facility operations, including various electronic circuits of the RF power supply, the accelerator, and the associated vacuum and cooling systems. Closed-circuit TV provides visual monitoring of the experimental area, and a radiation monitoring and protection system is an integral part of the facility.

In addition to the equipment for machine control and operation, numerous items of equipment are available for use by the experimenter. These include pulse-height analyzers, scalers, I integrators, power supplies, oscilloscopes, electromagnets, numerous modules of nuclear counting equipment, etc.

Approximately 15 ft of clear space is available around each experimental port for use by the experimenter. A large Faraday cup and a 1% slit assembly is provided for beam energy measurements. A bridge crane is available for handling heavy items.

Available to those using the LINAC is the Santa Barbara Division scientific staff whose members are experienced in the fields of accelerator design and operation, neutron time-of-flight measurement, nuclear spectroscopy, radiation chemistry, radiobiology, dosimetry, radiation detector research and development, and instrumentation design.

The neutron counting room provides sufficient space for a variety of detector types and configurations. A detector made up of a 2-in.-dia. by 2.5-in.-long NE-213 fluor coupled to a 56 AVP photomultiplier is provided for fast-neutron

detection. Time-to-pulse-height converters and associated equipment are also available. This apparatus, coupled with the 50-ps LINAC beam, provides a unique tool for high-resolution neutron time-of-flight measurements. This capability is directly applicable to the measurement of neutron scattering cross sections and to the study of complex shields such as those used for reactors in space applications.

4.6.4 Procedural Information

Experimenters interested in using the facility should allow approximately 6 weeks for scheduling and processing of applications. Additional technical information, schedules, and applications for DoE approval are available by contacting:

EG&G, Inc.
130 Robin Hill Road
Goleta, CA 93017
Telephone: (805) 968-0456

4.6.5 Applicability and Availability

The LINAC, located at EG&G's laboratories in Santa Barbara, California, is available for public use on research programs sponsored by the U.S. Government. All applications for facility use require DoE approval. Experimental time on the machine is scheduled on a non-interference basis with DoE Nevada Operations Office programs.

4.7 AFRRI LINAC FACILITY

4.7.1 Characteristics

The AFRRI LINAC is a Varian Model V-7725 electron LINAC installed in the late 1960's. It is a medium-energy, high-I, traveling-wave accelerator which operates in the S-band at an RF frequency of 2,856 MHz. Two modes of operation are available: (1) Mode 'A', a moderate-energy (13 to 20 MeV) mode using 4 short accelerating sections, and (2) Mode 'B', a high-energy (20 to 45 MeV) mode in which 2 additional long sections are utilized. Important operational parameters for these 2 modes are listed in Table 4-5.

Conversion of the electron beam to photons is accomplished via Ta bremsstrahlung converters. Typically 11.8 g/cm^2 Ta thickness is used in an air-cooled configuration for low-energy operation, and in a water-cooled configuration for high-energy operation.

4.7.2 Support Capabilities

The exposure room (22 x 30 ft) has a single-beam entry port. Some cabling is provided from the exposure room to the investigator's readout room; additional cabling can be installed by the user. Timing signals can be provided upon request.

Support activities, such as dosimetry and health physics, are available with prior scheduling and coordination. The dosimetry normally furnished utilizes ionization chambers and TLDs.

4.7.3 Test Parameters

AFRRI LINAC specifications are listed in Table 4-5.

4.7.4 Procedural Information

More information can be obtained by contacting Head, Accelerator Branch (telephone 202/295-1096), or Chief Engineering Technician (202/295-1288). Typically, 1 to 2 months of lead time is needed to schedule an experiment. The cost for LINAC use is $155.00/hr, which includes dosimetry. Normal working hours are 0700 to 1600, but these may be extended by prior arrangement.

Address all correspondence to:

AFRRI
Building 42, NNMC
Bethesda, MD 20014
Attention: Accelerator Branch

Table 4-5. AFFRI LINAC specifications.

Parameter		Value	
		Mode 'A'	Mode 'B'
	Energy Range	13 to 20 MeV	20 to 45 MeV
	Maximum Beam Energy at 1 A Peak I	13 MeV	--
	Maximum Beam Energy at 0.75 A Peak I	--	30 MeV
	Beam Pulse Length (continuously variable)	0.01 to 5 μs	0.01 to 5 μs
	Maximum Pulse Repetition Rate	120/s	120/s
	Maximum Duty Factor	0.0006	0.0006
Bremsstrahlung	Maximum Average Forward Exposure Rate at 1 m	6×10^2 R/s	1.8×10^3 R/s
Bremsstrahlung	Peak Instantaneous Exposure Rate at 1 m	1×10^6 R/s	3×10^6 R/s
Bremsstrahlung	Maximum Exposure/pulse at 1 m (5-μs pulse)	5 R	15 R
	Peak Instantaneous Number (neutrons)	--	8×10^{15} n/s
electrons ($1\ cm^2$ beam in H_2O)	Maximum Average Dose Rate	1.2×10^8 rad/s	9×10^7 rad/s
electrons ($1\ cm^2$ beam in H_2O)	Peak Instantaneous Dose Rate	2×10^{11} rad/s	1.5×10^{11} rad/s
electrons ($1\ cm^2$ beam in H_2O)	Maximum Dose/pulse	1×10^6 rad	7.5×10^5 rad

4.8 ROME AIR DEVELOPMENT CENTER LINAC

4.8.1 Test Parameters

Test parameters of the Rome Air Development Center (RADC) LINAC in the electron mode are as follows (with d = distance from window in cm, x = distance off beam center line in cm):

1. Dose $\simeq \frac{1.3 \times 10^{12}}{d^2} e^{-14(x/d)^{1.5}} \frac{\text{rad(Si)}}{\text{ampere-s}}$ $(d > 15)$

2. Dose rate $\simeq \frac{1.3 \times 10^{12}}{d^2} e^{-14(x/d)^{1.5}} \frac{\text{rad/s}}{\text{ampere}}$ $(d > 15)$

3. Beam dia. at window $\simeq$ 1 cm

4. Beam divergence (half-dose line) $\simeq \pm 7.5$ degrees from beam center line

5. Repetition rate = single pulse to 180 pulses/s (maximum duty cycle = 10^{-3})

6. Pulse widths: 10, 20, 50, 100, 500 ns; 1, 2, and 4.3 μs

7. Maximum peak power: 10 MeV, 100-ns pulse at 2 A

8. Dosimetry:

   a. TLD, CaF_2: Mn-teflon disks - standard deviation = 5%, accuracy = ±15%

   b. Faraday cup, I accuracy = ±3%

   c. Calorimetry, accuracy = ±3%.

Test parameters in the bremsstrahlung mode are:

1. Tungsten or Al targets

2. Maximum dose rate $\simeq 5 \times 10^6$ rad(Si)/s at 10 MeV, 2 A, and 100-ns pulse width

3. Repetition rate = 180 pulses/s (maximum duty cycle = 10^{-3})

4. Dosimetry

   a. TLD, CaF_2: Mn-teflon disks - standard deviation = 5%, accuracy = ±15%

   b. Calorimetry, accuracy = ±3%

   c. PIN diodes (calibrated versus TLDs which in turn were calibrated versus standardized Co-60 source).

4.8.2 Support Capabilities

Support capabilities include:

1. LINAC operator and dosimetrician.
2. Patch panels in control and target areas. Also, direct cabling capability (minimum length, 65 ft), and 6 to 10 oscilloscope channels.
3. Two-port output, straight through and 30 degrees. Target room dimensions are 12 x 12 x 42 ft.

4.8.3 Procedural Information

For further information, contact:

RADC/ESR Stop 30 (Bldg. 1127)
Hanscom AFB, MA 01731
Attention: Lester F. Lowe
Telephone: (617) 861-3445

4.9 OGDEN AIR LOGISTICS COMMAND LINAC

4.9.1 Characteristics

The Ogden Air Logistics Command (ALC) LINAC facility is located at the Little Mountain Test Annex (LMTA) of Hill Air Force Base. The LINAC is a 2-section, L-band accelerator operating in the energy range from 10 to 25 MeV. At maximum efficiency, the beam energy is 17 MeV and peak beam I is 0.5 A. Pulse widths can be varied from 40 ns to 6 μs.

4.9.2 Test Parameters

Operating characteristics of the LMTA LINAC are as follows:

1.	Microwave frequency	1,305 MHz
2.	Number of accelerating sections	2
3.	Beam energy range	10 to 25 MeV
4.	Beam energy at maximum efficiency	17 MeV
5.	Peak beam I at maximum efficiency	500 mA
6.	Rated average power	1 kW
7.	Maximum peak beam I	500 mA
8.	Beam pulse width	0.04 to 6 μs
9.	Pulse repetition rate/s (all pulse widths)	Single pulse, 0.5, 1, 2, 5, 10, and 20

Electron-beam loading characteristics are shown in Figure 4-30. The pulse shape is basically rectangular for longer pulses (see Figure 4-31), and as the pulse length is reduced the shape becomes more triangular (Figure 4-32). Rise and fall times of the pulse are typically 15 ns. Single pulse control is available near the data recording console for use by the customer. In addition, an external sync input (+10 V at 1 μs) is available for single pulse and all repetition rates up to 20 pps. Figure 4-33 shows typical pulse reproducibility and predictability (10 pulses (at 1 pps) superimposed).

Beam divergence (with 0.25-in. Al diffuser) is ~5 degrees, and beam-spot dia. is 0.2 to 2.0 cm. The shape of the spot can be made round or elliptical by using focusing lenses. Larger spot sizes may be produced by scattering with an Al diffuser.

The LMTA LINAC electron beam can be used directly as a radiation source, or converted to x-rays by means of a bremsstrahlung target (Ta). As of this writing, no photo-fission target is available.

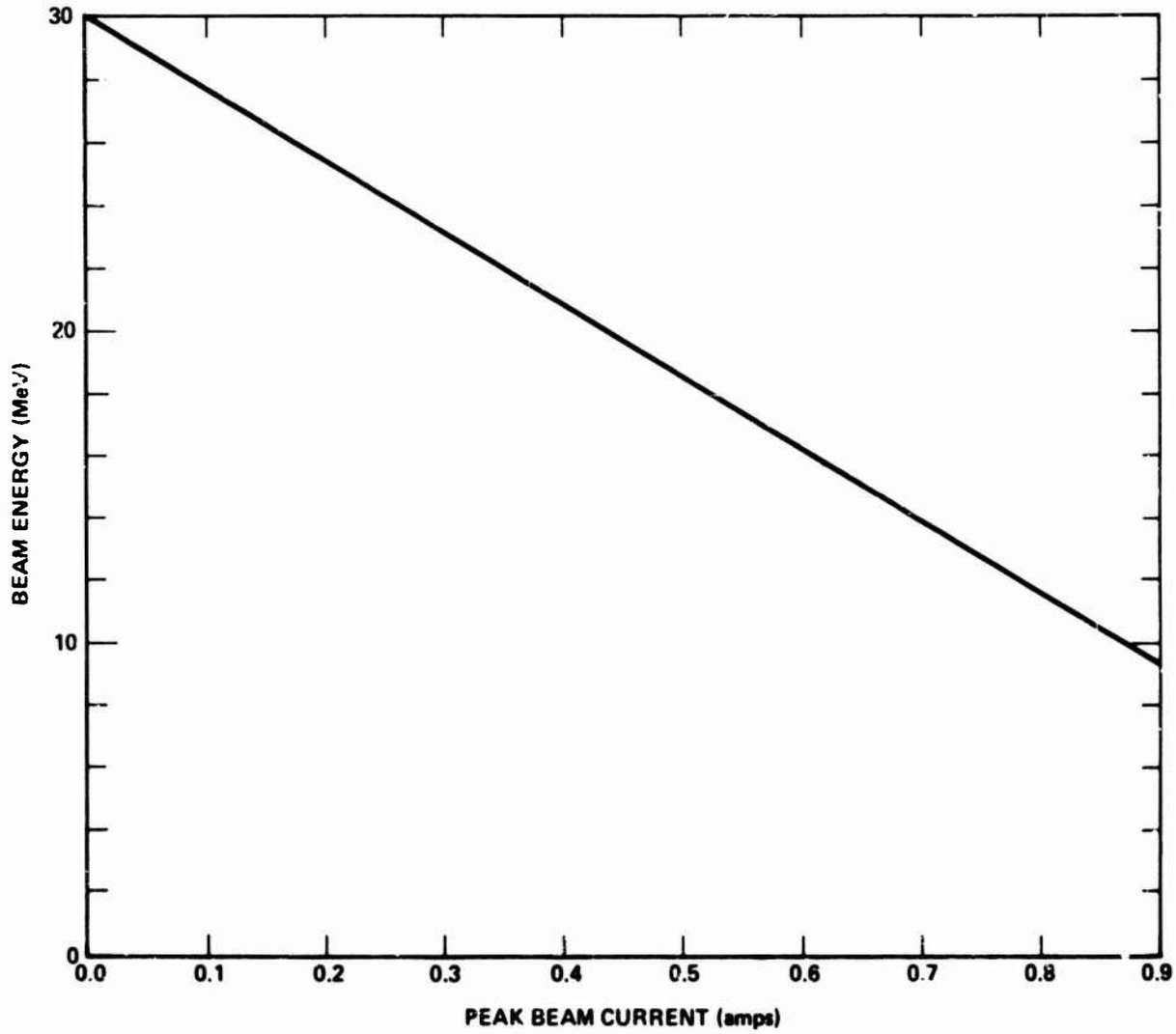

Figure 4-30. Beam loading characteristics.

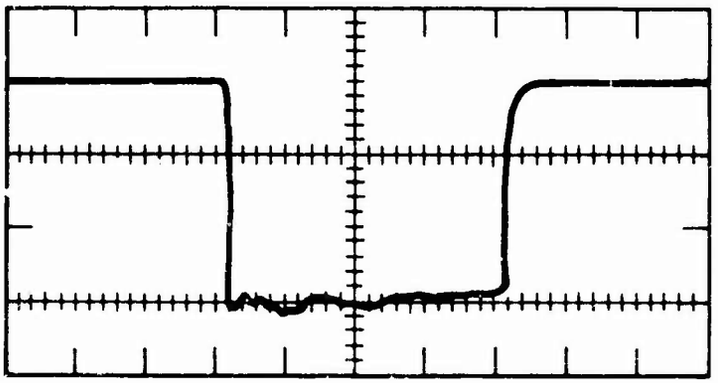

(Redrawn from scope picture)

Figure 4-31. Radiation pulse waveform.

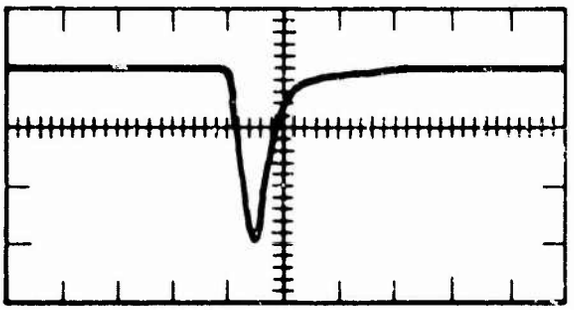

(Redrawn from scope picture)

Figure 4-32. Radiation pulse waveform (short pulse).

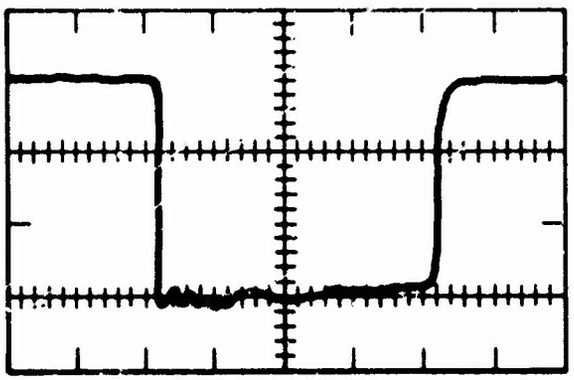

(Redrawn from scope picture)

Figure 4-33. Radiation pulse waveform (10 pulses).

Environment output characteristic data are as follows:

1. Electron-beam mode
   a. Dose rate at exit window — $>2 \times 10^{10}$ rad(Si)/s
2. X-ray mode
   a. Bremsstrahlung converter (0.040-in. Ta with 2-in. Al) — $\sim 5 \times 10^{8}$ rad(Si)/s
3. Neutron mode — No data available

Data presented above are not definitive and are meant only to be used as a guide.

4.9.3 Support Equipment

Measurements of radiation can be made in several ways. The LMTA LINAC facility has PIN diodes, TLDs, Secondary Emission Monitor (SEM), Si calorimeter, and thermistor calorimeter. PIN diodes furnish active dosimetry and can be used again and again. It is recommended that the customer provide his own PIN diodes and calibrate them at the LMTA LINAC facility. LMTA LINAC facility PIN diodes have been calibrated using TLDs and have an error of less than ±20%.

TLDs are either CaF_2 or $CaSO_4$. Both have been calibrated against a CS-137 source (traceable to NBS) at Hill AFB. Accuracy is ±5%. Secondary Emission Monitors (SEMs) are active dosimetry (qualitative only). The secondary emission on a foil in a vacuum is measured. Si calorimetry is active dosimetry, read out on a chart recorder. Accuracy is ±10%. Thermistor calorimetry is active dosimetry, read out on a chart recorder also. Accuracy is ±15%.

Electrical noise occurs starting approximately 3 μs prior to the radiation pulse and lasting for ~6 μs. The frequency of this noise is ~4 kHz. Signals as low as 1 mV can be recorded (see Figure 4-33) using proper noise canceling techniques.

4.9.4 Support Capabilities

All support capabilities are available to the customer at no additional fee. The staff of the LMTA LINAC consists of physicists, engineers, technicians, and operators who are available to assist and/or consult with the customer.

Two racks of data recording equipment and the items listed in Table 4-6 are available to the customer at no additional charge. Inquiries for specific equipment should be made 4 weeks in advance. The customer is required to furnish all film; however, Polaroid cameras are available with either roll or flatpack backs.

Signal, power, and control cables are provided as shown in Table 4-7. These cables are in 4-in. metal conduits with 1 conduit dedicated to the customer for his own special cabling (special cabling is customer-furnished). Sync timing signals are available at the data recording racks. These signals may be delayed from 0 to 30 μs. No screen room is used with the LMTA LINAC. Care has been taken to eliminate ground loop and spurious noise sources.

Table 4-6. Electronic equipment.

Item	Model	Manufacturer	Quantity
Oscilloscopes	R7844	Tektronix	2
Plug-Ins	7A16A	Tektronix	4
Plug-Ins	7A19	Tektronix	2
Plug-Ins	7A24	Tektronix	1
Plug-Ins	7A26	Tektronix	5
Plug-Ins	7B92A	Tektronix	4
Plug-Ins	7M13	Tektronix	3
Oscilloscope	183D	H.P.	2
Plug-Ins	1830A	H.P.	2
Plug-Ins	1840A	H.P.	2
Oscilloscope	R556	Tektronix	1
Plug-Ins	Type L	Tektronix	2
Plug-Ins	Type CA	Tektronix	2
Camera (Polaroid)	C52	Tektronix	5
Camera (Polaroid	C32	Tektronix	2
Pulse Generator	110B	Systron-Donner	2
Pulse Generator	214A	H.P.	1
Pulse Generator	101	Data Pulse	1
Function Generator	3312A	H.P.	1
Generator/Sweeper	8601A	H.P.	1
Universal Bridge	4260A	H.P.	1
Power Supplies	6200B	H.P.	8
Power Supplies	6205B	H.P.	4
Power Supplies	6256B	H.P.	1
Power Supplies	6274B	H.P.	1
Current Source	6177C	H.P.	1
Current Probe	6042	Tektronix	1
Current Probe	CT2	Tektronix	10
Vector Voltmeter	8405A	H.P.	1
Digital Voltmeter	4800	Dana Labs	1
Digital Multimeter	3465A	H.P.	2
VOM	269-3	Simpson	2
Sampling Voltmeter	3406A	H.P.	1
Measuring System (Counter)	5300B	H.P.	1
Curve Tracer	576	Tektronix	1
Digital IC Tester	480/B	Alma	1
Linear Circuit Tester	1730	Gen Rad	1
Transistor/Diode Test Set	2610 ABGR/SCR/Z	Mastec	1

Table 4-7. Instrument cabling.

Type of Cable	Length (ft)	Type of Connector	Quantity
RG-58A/U	125	BNC Female	30 each
RG-214A/U	125	Type N Female	10 each
TRC50-2 (TRIAX)	125	TRIAX	10 each
#16 Twist w/shield	125	Banana Jack Female	15 pair
#16 Multi-Conductor	125	Banana Jack Female	20 each

Table 4-8 shows the dosimetry available at the LMTA LINAC. TLDs and PIN diodes are the most popular. The staff will conduct or assist the customer in dosimetry measurements, or the customer may opt to perform his own dosimetry.

Table 4-8. Dosimetry available at LMTA.

Radiation	Dosimetry Method
Direct Electrons	SEM
	CaF_2 (TLDs) High Dose
	$CaSO_4$ (TLDs) Low Dose
	PIN Diodes
	Si Calorimetry
	Thermistors
X-rays	CaF_2 (TLDs) High Dose
	$CaSO_4$ (TLDs) Low Dose
	PIN Diodes
	Si Calorimetry
	Thermistors

Under supervision, an HP Model 9831A programmable calculator (basic language) with a Model 9866B printer and a Model 9862A plotter are available. Storage for customer programs is not available.

Machine shop capabilities are limited to a band saw, drill press, sander, welder, break and shear (small), and hand tools.

An electronics buildup laboratory is available to the customer. This laboratory contains benches, stools, hand tools, etc. An office has been set aside for the customer for use as a data reduction, conference, and lounge room.

No provisions for photographic services have been made as of this writing. However, with prior notice, arrangements can be made for the customer to take his own photographs.

The test area where specimens are irradiated is ~15 ft^2. A remote-controlled table is available for use on the center port of the LMTA LINAC. This table can be controlled on 3 axes remotely with 12 preset positions in the lateral axis.

A closed-circuit TV monitors the test cell and an intercom provides communications to the control room area.

4.9.5 Procedural Information

Technical inquiries should be directed to:

TRW DSSG, Inc.
P.O. Box 368
Clearfield, UT 84015
Attention: G.G. Spehar
Telephone: (801) 773-1340

Administrative inquiries should be directed to:

Chief, Hardness Program Manager
Ogde ALC/MMETH
Hill Air Force Base, UT 84406
Telephone: (801) 777-5651

Scheduling is arranged on an individual, first-come-first-served basis as long as it does not interfere with OO-ALC scheduled testing. A nominal lead time is required since a test plan must be submitted and approved prior to customer use of the LINAC.

Cost for use of the LMTA LINAC is on a "machine tieup" basis. Costs and charges may be obtained from the administrative contact above.

The shipping address is:

Little Mountain Test Annex
12,000 West 12th Street
Ogden, UT 84404
Attention: LINAC Facility

Care should be exercised that 12,000, not 1,200, West 12th is on the address since 1,200 West is the regional IRS facility. U.S. Postal Service is not available at LMTA. The customer is responsible for contacting shipping agents on outgoing shipments.

4.9.6 Applicability and Availability

The LMTA LINAC facility was designed specifically as a TREE LINAC and is usually readily available to the customer. A descriptive brochure (see Reference 1)

and a TREE LINAC Test/Users Guidebook (see Reference 2) are available upon request.

The LMTA LINAC facility is 12 miles west of Ogden, Utah, within easy commuting distance of overnight accommodations.

4.9.7 References

1. "TREE LINAC Facility," descriptive brochure of LMTA LINAC Facility.

2. "TREE LINAC Test/Users Guidebook," pamphlet outlining customers' responsibilities, etc. for using the LMTA LINAC Facility.

4.10 LASL PHERMEX

4.10.1 Characteristics

PHERMEX is a high-I, high-energy, standing wave electron accelerator that provides very intense but short bursts of γ rays. It consists of 3 right circular cylindrical accelerator cavities. Each cavity is excited at 50 Mc/s. The mode and frequency define a cavity dia. of 4.6 m. The cavity length and minimum useful electric field strength were fixed at 2.6 m and 4×10^6 V/m. An unloaded Q of 1.3×10^5 is consistent with these values for each of the Cu-lined cavities. The fields are 6×10^6 V/m in the first upstream cavity, 5×10^6 V/m in the second, and 4×10^6 V/m in the third. The corresponding stored energies are 1,600, 1,200, and 300 J, respectively, with a peak electron energy of about 26 MeV.

4.10.2 Test Parameters

PHERMEX may be characterized by the following parameters:

1.	Beam energy	27 MeV
2.	Beam I at target	30 A
3.	Pulse length	0.2 μs (or 0.1 μs)
4.	Radiation output (at 1 m)	30 R (or 10 R)
5.	Radiation source dia.	3 mm

This operating level was attained in the spring of 1966.

Detailed data on beam divergence may be found in Reference 1.

The mailing address is:

Los Alamos Scientific Laboratory
P.O. Box 1663
Los Alamos, NM 87544

4.10.3 Reference

1. Venable, Douglas, et al., "PHERMEX, a Pulsed High-energy Radiographic Machine Emitting X-rays," LA-3241 TID, Los Alamos Scientific Laboratory, May 15, 1967.

4.11 RENSSELEAR POLYTECHNIC INSTITUTE (RPI) LINAC

4.11.1 Characteristics

The RPI LINAC, in the Department of Nuclear Engineering, operates at 45 to 80 MeV, with pulse widths from 7 ns to 4.5 μs. The I varies from 0.67 A to over 5 A.

4.11.2 Test Parameters

Typical operating conditions are given in Table 4-9. Electron-beam specifications are as follows:

1.	Electron energy	
	a. Maximum	Over 80 MeV
	b. Minimum	Below 20 MeV
2.	Maximum electron-beam power	
	a. During narrow pulse	400 MW
	b. Average	Over 50 kW
3.	Maximum electron-beam I	
	a. During narrow pulse	Over 5 A
	b. Average	Over 1.1 mA
4.	Electron pulse width	Variable from 7 ns to 4.5 μs
5.	Repetition rate	Variable from single pulses to 720 pps at pulse lengths below 1 μs; to 300 pps for pulse length greater than 1 μs.
6.	Electron-beam properties	Over 80% of beam contained in a 2-cm-dia. circle.* Full angle divergence of 10^{-3} rad.

Figure 4-34 shows beam intensity versus distance from the target.

4.11.3 Procedural Information

For further information, contact:

R. C. Block, Director
Gerttner LINAC Laboratory
NES BLDG
Tibbits Avenue
Rensselear Polytechnic Institute
Department of Nuclear Engineering
Troy, NY 12181

---

*Can be focused to less than 0.5-cm-dia. circle.

Table 4-9. RPI LINAC typical operating conditions.

Parameter	RF Pulse			
		Short[b]		
	Long[a] (Maximum Average Power)	Maximum Peak Power	Maximum Average Power	Maximum Average Power with Model 12 Pulser
Electron Energy	45 MeV	Over 80 MeV	60 MeV	70 MeV
Electron-Beam I				
During Pulse	Over 0.8 A	Over 5 A	0.67 A	1.8 A
Average	Over 1,100 μA	50 μA at 500 pps 72 μA at 720 pps	340 μA at 500 pps 490 μA at 720 pps	140 μA at 500 pps 200 μA at 720 pps
Electron Pulse Width	4.5 μs	20 ns	1 μs	170 ns
Electron-Beam Power				
During Pulse	36 MW	400 MW	40 MW	120 MW
Average	Over 50 kW	4.0 kW at 500 pps 5.8 kW at 720 pps	20 kW at 500 pps 29 kW at 720 pps	10 kW at 500 pps 14 kW at 720 pps
Neutron Production	6.5×10^{11} neutrons/pulse	3.2×10^{10} neutrons/pulse	1.6×10^{11} neutrons/pulse	8.4×10^{10} neutrons/pulse
Neutron Production Rate				
During Pulse	1.4×10^{17} neutrons/s	1.6×10^{18} neutrons/s	1.6×10^{17} neutrons/s	5.0×10^{17} neutrons/s
Average	2.0×10^{14} neutrons/s at 300 pps	1.6×10^{13} neutrons/s at 500 pps 2.3×10^{13} neutrons/s at 720 pps	8×10^{13} neutrons/s at 500 pps 1.2×10^{14} neutrons/s at 720 pps	4.2×10^{13} neutrons/s at 500 pps 6.0×10^{13} neutrons/s at 720 pps
X-Ray Production[c]	210 rad/pulse	32 rad/pulse	90 rad/pulse	63 rad/pulse
X-Ray Production Rate[c]				
During Pulse	4.7×10^{7} rad/s	1.6×10^{9} rad/s	9.0×10^{4} rad/s	3.8×10^{8} rad/s
Average	6.4×10^{4} rad/s	1.6×10^{4} rad/s at 500 pps 2.3×10^{4} rad/s at 720 pps	4.5×10^{4} rad/s at 500 pps 6.5×10^{4} rad/s at 720 pps	3.1×10^{4} rad/s at 500 pps 4.5×10^{4} rad/s at 720 pps

Notes:
[a] 6.5-μs wide RF pulse-forming network.
[b] 2.5-μs wide RF pulse-forming network.
[c] At 1 m in front of the x-ray target.

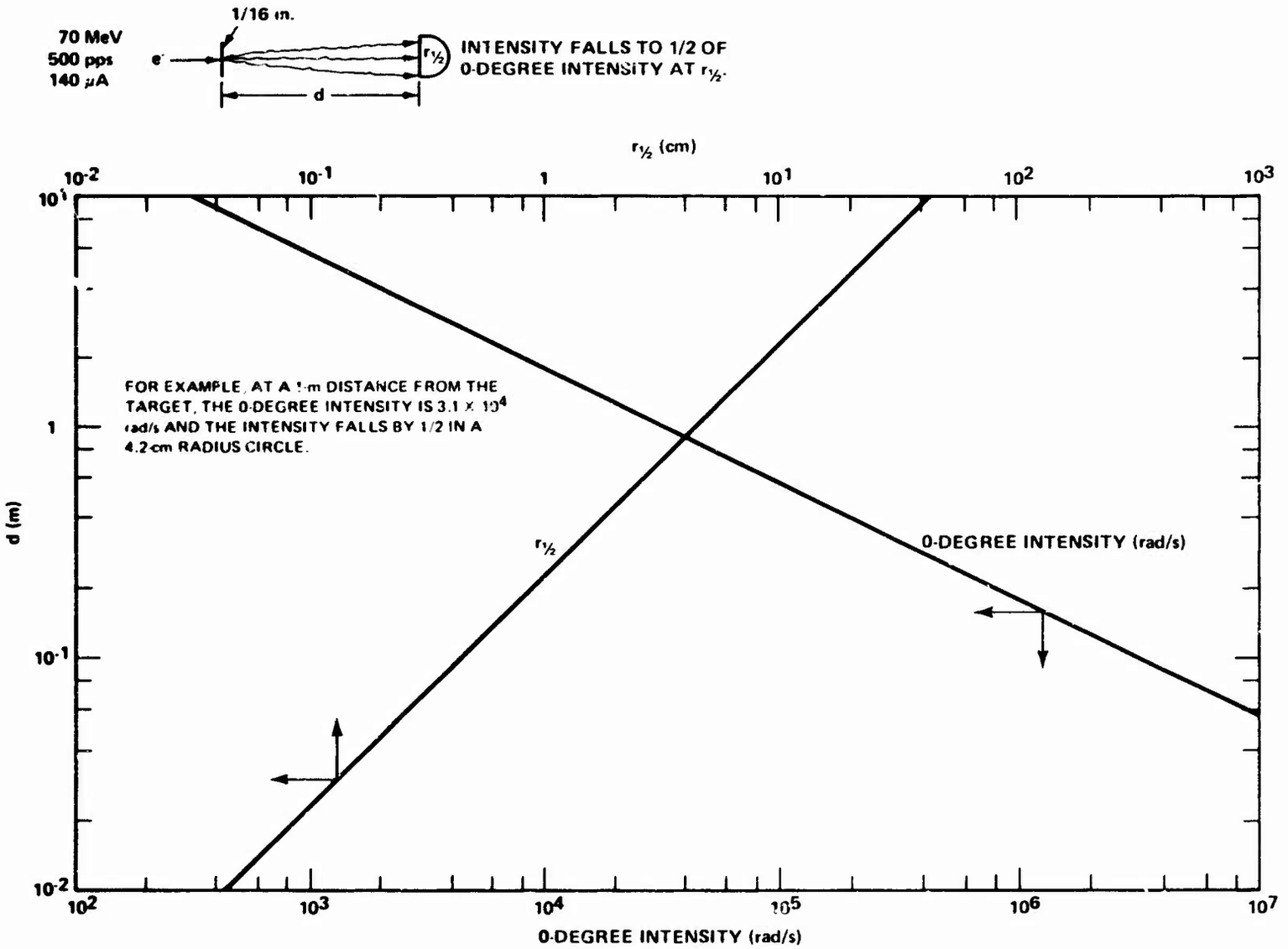

Figure 4-34. Intensity versus distance from target.

APPENDIX A

LIST OF ABBREVIATIONS

A	ampere
ac	alternating current
AFWL	Air Force Weapons Laboratory
ALC	Air Logistics Command
APRF	Army Pulse Radiation Facility
cal	calorie
Ci	Curie
cm	centimeter
CRT	cathode ray tube
DADS	data acquisition and display system
DAS	data acquisition system
db	decibel
dc	direct current
dia.	diameter
DNA	Defense Nuclear Agency
DoD	Department of Defense
DoE	Department of Energy
eV	electron volts
FBR	fast burn reactor
ft	feet
FXR	flash x-ray
FWHM	full width half maximum
g	gram
G	gauss
HE	high explosive
HEPA	high-efficiency particulate air
HP	Hewlett Packard
hr	hour
I	current
IC	integrated circuit
I.D.	inner diameter
in.	inch
IPC	Ion Physics Corporation
kg	kilogram
kV	kilovolt
kW	kilowatt
l	length
LINAC	linear accelerator
LLL	Lawrence Livermore Laboratory
LSI	large-scale integration
m	meter
MeV	million electron volts
min	minutes
mrad	millirad
Mrad	megarad
ms	millisecond
MSI	medium-scale integration
MV	megavolt
MW	megawatt
n	neutron
NBS	National Bureau of Standards
nm	nanometer
ns	nanosecond
NWEB	Nuclear Weapon Effects Branch
O.D.	outer diameter
PI	Physics International
pps	pulse per second
ps	picosecond
PVC	polyvinyl chloride
PWHM	pulse width half maximum
R	roentgen
RF	radio frequency
rms	root mean square
s	second
SNG	steady-state neutron generator

TA	technical area
TLD	thermoluminescent dosimetry
TREE	transient radiation effects on electronics
TW	terawatt
V	voltage, volt
VSWR	voltage standing wave ratio
W	watt
WPS	Waveform Processing System
WSMR	White Sands Missile Range
wt	weight
w/o	weight-percent
γ	gamma
ϕ	phase
μf	microfarad
μs	microsecond

DISTRIBUTION LIST

DEPARTMENT OF DEFENSE

Assistant Secretary of Defense
Program Analysis & Evaluation
ATTN: M. Doffredo

Assistant to the Secretary of Defense
Atomic Energy
ATTN: Executive Assistant

Command and Control Technical Center
ATTN: C-362, G. Adkins

Defense Advanced Rsch. Proj. Agency
ATTN: J. Fraser

Defense Electronic Supply Center
ATTN: DESC-ECS, D. Hill
ATTN: DESC-ECS, J. Counsil
ATTN: DESC-EQM, R. Grillmeier
ATTN: DESC-ECT, J. Niles
ATTN: DESC-ECT, D. Droege
ATTN: DESC-ECS, J. Dennis
ATTN: DESC-ESA
ATTN: DESC-CEP, D. More

Defense Logistics Agency
ATTN: DLA-SE
ATTN: DLA-QEL, J. Slattery

Defense Material Specifications & Standard Office
ATTN: L. Fox

Defense Nuclear Agency
ATTN: RAEV, M. Kemp
ATTN: DDST
ATTN: RAEV, A. Kubo
ATTN: RAEV, W. Mohr
4 cy ATTN: TITL

Defense Technical Information Center
12 cy ATTN: DD

Field Command
Defense Nuclear Agency
ATTN: FCPR

Field Command
Defense Nuclear Agency
Livermore Division
ATTN: FCPRL

National Security Agency
ATTN: T. Brown
ATTN: G. Daily
ATTN: P. Deboy

NATO School (SHAPE)
ATTN: U.S. Documents Officer

Undersecretary of Defense for Rsch. & Engrg.
ATTN: Strategic & Space Systems (OS)

Armed Forces Radiobiology Rsch. Inst.
ATTN: R. Schaffer

DEPARTMENT OF THE ARMY

Aberdeen Proving Ground
Department of the Army
ATTN: S. Harrison
ATTN: STEAP-MT-R, A. Kazi

BMD Advanced Technology Center
Department of the Army
ATTN: ATC-T
ATTN: ATC-O, F. Hoke

BMD Systems Command
Department of the Army
ATTN: BMDSC-HW, R. Dekalb

Research, Development and Acq.
Department of the Army
ATTN: Advisor for RDA Analysis, M. Gale

Harry Diamond Laboratories
Department of the Army
ATTN: DELHD-N-P
ATTN: DELHD-N-P, F. Balicki
ATTN: DELHD-N-RBC, J. McGarrity
ATTN: DELHD-N-RBH, J. Halpin
ATTN: DELHD-N-RBH
ATTN: DELHD-N-RBH, H. Eisen
ATTN: DELHD-N-RBI, P.Caldwell
ATTN: J. Silverstein

U.S. Army Armament Research & Development Cmd.
ATTN: DRDAR-LCA-PD

U.S. Army Communications R&D Command
ATTN: D. Huewe

U.S. Army Material & Mechanics Rsch. Ctr.
ATTN: DRXMR-H, J. Hofmann

U.S. Army Missile Command
3 cy ATTN: RSIC

U.S. Army Nuclear & Chemical Agency
ATTN: Library

White Sands Missile Range
Department of the Army
ATTN: STEWS-TE-AN, M. Squires
ATTN: STEWS-TE-AN, T. Leura
2 cy ATTN: L. Flores

DEPARTMENT OF THE NAVY

Naval Air Systems Command
ATTN: AIR 350F

Naval Electronic Systems Command
ATTN: Code 5045.11, C. Suman

Naval Ocean Systems Center
ATTN: Code 4471

DEPARTMENT OF THE NAVY (Continued)

Naval Postgraduate School
ATTN: Code 0142
ATTN: Code 1424

Naval Research Laboratory
ATTN: Code 5216, H. Hughes
ATTN: Code 6600, J. McElinney
ATTN: Code 6601, E. Wolicki
ATTN: Code 6701, J. Brown
ATTN: Code 5210, J. Davey
ATTN: Code 6627, C. Guenzer
ATTN: Code 6650, A. Namenson
ATTN: Code 6620, B. Faraday
ATTN: Code 5210, J. Killiany

Naval Sea Systems Command
ATTN: SEA-06J, R. Lane

Naval Ship Engineering Center
ATTN: Code 6174D2

Naval Surface Weapons Center
ATTN: Code F30
ATTN: Code F31

Naval Weapons Center
ATTN: Code 233

Naval Weapons Evaluation Facility
ATTN: Code AT-6

Naval Weapons Support Center
ATTN: Code 7024, T. Ellis
ATTN: Code 70242, J. Munarin
ATTN: Code 7024, J. Ramsey

Office of Naval Research
ATTN: Code 427, L. Cooper
ATTN: Code 220, D. Lewis

Office of the Chief of Naval Operations
ATTN: OP-985F

Strategic Systems Project Office
Department of the Navy
ATTN: NSP-2015
ATTN: NSP-230, D. Gold
ATTN: NSP-2701, J. Pitsenberger
ATTN: NSP-27331, P. Spector

DEPARTMENT OF THE AIR FORCE

Air Force Aero-Propulsion Laboratory
ATTN: POD, P. Stover

Air Force Avionics Laboratory
ATTN: TEA, R. Conklin
ATTN: DHE

Air Force Geophysics Laboratory
ATTN: SULL, S-29
ATTN: SULL

Air Force Institute of Technology
ATTN: ENP, J. Bridgeman

DEPARTMENT OF THE AIR FORCE (Continued)

Air Force Materials Laboratory
ATTN: LTE
ATTN: LPO, R. Hickmott

Air Force Systems Command
ATTN: DLW
ATTN: XRLA, R. Stead
ATTN: DLCA
ATTN: DLCAM, T. Seale

Air Force Technical Applications Center
ATTN: TAE

Air Force Weapons Laboratory
Air Force Systems Command
ATTN: ELP, G. Chapman
ATTN: ELP, J. Mullis
ATTN: ELP, R. Maier
ATTN: ELP, M. Knoll
ATTN: ELT, J. Ferry
3 cy ATTN: SUL

Air Logistics Command
ATTN: MMEDD
ATTN: MMETH
ATTN: OO-ALC/MM, R. Blackburn

Ballistic Missile Office
Air Force Systems Command
ATTN: MNNG
ATTN: MNNL
ATTN: MNNH, J. Tucker

Foreign Technology Division
Air Force Systems Command
ATTN: TQTD, B. Ballard
ATTN: PDJV

Headquarters Space Division
Air Force Systems Command
ATTN: C. Kelly

Headquarters Space Division
Air Force Systems Command
ATTN: AQT, W. Blakney
ATTN: AQM

Headquarters Space Division
Air Force Systems Command
ATTN: DYS

Headquarters Space Division
Air Force Systems Command
ATTN: SZJ, R. Davis

Rome Air Development Center
Air Force Systems Command
ATTN: RBRP, C. Lane
ATTN: RBRM, J. Brauer

Strategic Air Command
Department of the Air Force
ATTN: XPFS, M. Carra

DEPARTMENT OF THE AIR FORCE (Continued)

Rome Air Development Center
Air Force Systems Command
ATTN: ESE, A. Kahan
ATTN: ETS, R. Dolan
ATTN: ESR, W. Shedd
ATTN: ESER, R. Buchanan
ATTN: ESR, P. Vail
ATTN: ESR, L. Lowe

DEPARTMENT OF ENERGY

Department of Energy
Albuquerque Operations Office
ATTN: Document Control for WSSB

DEPARTMENT OF ENERGY CONTRACTORS

Lawrence Livermore Laboratory
ATTN: Document Control for Technical Information Dept.
ATTN: Document Control for P. Walker

Los Alamos Scientific Laboratory
ATTN: Document Control for J. Freed

Sandia Laboratories
ATTN: Document Control for J. Barnum
ATTN: Document Control for F. Coppage
ATTN: Document Control for J. Hood
ATTN: Document Control for R. Gregory
ATTN: Document Control for W. Dawes
ATTN: Document Control for Mr. Choate

Lawrence Livermore Laboratory
ATTN: L. Peterson

OTHER GOVERNMENT AGENCIES

Central Intelligence Agency
ATTN: OSI/RD
ATTN: OSI/MTD, A. Padgett

Department of Commerce
National Bureau of Standards
ATTN: Security Officer for J. Mayo-Wells
ATTN: Security Officer for J. French
ATTN: Security Officer for K. Galloway
ATTN: Security Officer for J. Humphreys
ATTN: Security Officer for S. Chappell
ATTN: Security Officer for R. Scace
ATTN: Security Officer for W. Bullis

NASA
Goddard Space Flight Center
ATTN: J. Adolphsen
ATTN: V. Danchenko

NASA
George C. Marshall Space Flight Center
ATTN: M. Nowakowski
ATTN: EG02
ATTN: L. Hanifer
ATTN: H. Yearwood

NASA
ATTN: J. Murphy

OTHER GOVERNMENT AGENCIES (Continued)

NASA
Lewis Research Center
ATTN: M. Baddour

NASA
Ames Research Center
ATTN: G. DeYoung

DEPARTMENT OF DEFENSE CONTRACTORS

Advanced Research & Applications Corp.
ATTN: R. Armistead
ATTN: L. Palcuti

Aerojet Electro-Systems Co.
ATTN: T. Hanscome

Aerospace Corp.
ATTN: W. Willis
ATTN: S. Bower
ATTN: D. Fresh

Aerospace Industries Assoc. of America, Inc.
ATTN: S. Siegel

Advanced Microdevices, Inc.
ATTN: J. Schlageter

Battelle Memorial Institute
ATTN: R. Thatcher

BDM Corp.
ATTN: D. Alexander
ATTN: R. Pease
ATTN: D. Wunch

Bendix Corp.
ATTN: E. Meeder

Boeing Co.
ATTN: D. Egelkrout

Boeing Co.
ATTN. W. Rumpza
ATTN: A. Johnston
ATTN: I. Arimura
ATTN: C. Rosenberg
ATTN: E. Costello

Burr-Brown Research Corp.
ATTN: H. Smith

University of California
ATTN: TRIGA III, Berkeley Research Center

California Institute of Technology
ATTN: A. Shumka
ATTN: A. Stanley
ATTN: W. Price

Cincinnati Electronics Corp.
ATTN: L. Hammond
ATTN: C. Stump

Control Data Corp.
ATTN: J. Meehan

DEPARTMENT OF DEFENSE CONTRACTORS (Continued)

Charles Stark Draper Lab., Inc.
ATTN: R. Bedingfield
ATTN: A. Schutz
ATTN: P. Greiff
ATTN: R. Ledger
ATTN: C. Lai

University of California at Irvine
ATTN: G. Miller

University of Denver
ATTN: Security Officer for F. Venditti

E-Systems, Inc.
ATTN: K. Reis

EG&G, Inc.
ATTN: L. Hocker

Electronic Industries Assn.
ATTN: J. Hessman

EMM Corp.
ATTN: F. Krch

Exp. & Math Physics Consultants
ATTN: T. Jordan

Ford Aerospace & Communications Corp.
ATTN: Technical Information Services
ATTN: J. Davison

Ford Aerospace & Communications Corp.
ATTN: D. Cadle

Franklin Institute
ATTN: R. Thompson

Garrett Corp.
ATTN: R. Weir

General Dynamics Corp.
ATTN: W. Hansen
ATTN: N. Cohn

General Dynamics Corp.
ATTN: R. Fields
ATTN: O. Wood

General Electric Co.
ATTN: J. Andrews
ATTN: J. Peden
ATTN: R. Casey

General Electric Co.
ATTN: J. Palchefsky, Jr.
ATTN: Technical Library
ATTN: W. Patterson
ATTN: R. Benedict
ATTN: R. Casey

General Electric Co.
ATTN: J. Reidl

General Electric Co.
ATTN: R. Hellen

DEPARTMENT OF DEFENSE CONTRACTORS (Continued)

General Electric Co.
ATTN: D. Cole
ATTN: J. Gibson

General Electric Co.
ATTN: D. Pepin

General Electric Company-TEMPO
ATTN: DASIAC
ATTN: M. Espig
ATTN: J. Rosenfeld

General Electric Company-TEMPO
ATTN: DASIAC

General Research Corp.
ATTN: Technical Information Office
ATTN: R. Hill

George C. Messenger
Consulting Engineer
ATTN: G. Messenger

Georgia Institute of Technology
ATTN: R. Curry

Georgia Institute of Technology
ATTN: Res. & Sec. Coord. for H. Denny

Goodyear Aerospace Corp.
ATTN: Security Control Station

Grumman Aerospace Corp.
ATTN: J. Rogers

GTE Sylvania, Inc.
ATTN: L. Blaisdell
ATTN: C. Thornhill
ATTN: L. Paupies

GTE Sylvania, Inc.
ATTN: J. Waldron
ATTN: P. Fredrickson
ATTN: H. Ullman
ATTN: H & V Group

Harris Corp.
ATTN: C. Anderson
ATTN: J. Cornell
ATTN: T. Sanders

Honeywell, Inc.
ATTN: R. Gumm

Honeywell, Inc.
ATTN: C. Cerulli

Honeywell, Inc.
ATTN: Technical Library

Honeywell, Inc.
ATTN: K. Gaspard

Honeywell, Inc.
ATTN: J. Griessel

DEPARTMENT OF DEFENSE CONTRACTORS (Continued)

Hughes Aircraft Co.
ATTN: R. McGowan
ATTN: J. Singletary

Hughes Aircraft Co.
ATTN: D. Shumake
ATTN: E. Smith
ATTN: W. Scott

IBM Corp.
ATTN: H. Mathers
ATTN: T. Martin
ATTN: F. Tietse

IIT Research Institute
ATTN: I. Mindel

Institute for Defense Analyses
ATTN: Technical Information Services

Intel Corp.
ATTN: M. Jordan

International Business Machine Corp.
ATTN: J. Ziegler

International Tel. & Telegraph Corp,
ATTN: Dept. 608
ATTN: A. Richardson

Intersil Inc.
ATTN: D. MacDonald

IRT Corp.
ATTN: J. Harrity

JAYCOR
ATTN: L. Scott
ATTN: T. Flanagan
ATTN: P. Stahl

Johns Hopkins University
ATTN: P. Partridge

Kaman Sciences Corp.
ATTN: J. Lubell
ATTN: M. Bell
ATTN: D. Bryce

Litton Systems, Inc.
ATTN: G. Maddox
ATTN: J. Retzler

Lockheed Missiles & Space Co., Inc.
ATTN: E. Smith
ATTN: C. Thompson
ATTN: H. Phillips
ATTN: P. Bene
ATTN: M. Smith
ATTN: E. Hessee

Lockheed Missiles and Space Co., Inc.
ATTN: J. Smith
ATTN: J. Crowley
ATTN: J. Riley

DEPARTMENT OF DEFENSE CONTRACTORS (Continued)

ION Physics Corp.
ATTN: R. Evans

Ktech Corp.
ATTN: D. Keller

Kansas State University
ATTN: L. Peterson

M.I.T. Lincoln Lab.
ATTN: P. McKenzie

Magnavox Govt. & Indus. Electronics Co.
ATTN: W. Richeson

Martin Marietta Corp.
ATTN: H. Cates
ATTN: R. Gaynor
ATTN: W. Janocko
ATTN: W. Brockett

Martin Marietta Corp.
ATTN: E. Carter

Maxwell Labs., Inc
ATTN: J. Rauch

McDonnell Douglas Corp.
ATTN: M. Stitch
ATTN: D. Dohm
ATTN: Library

McDonnell Douglas Corp.
ATTN: J. Holmgrem
ATTN: D. Fitzgerald

McDonnell Douglas Corp.
ATTN: Technical Library

Mission Research Corp.
ATTN: C. Longmire

Mission Research Corp.-San Diego
ATTN: R. Berger
ATTN: V. Van Lint
ATTN: J. Azarewicz
ATTN: J. Raymond

Mission Research Corp.
ATTN: R. Pease

Mitre Corp.
ATTN: M. Fitzgerald

Motorola, Inc.
ATTN: A. Christensen

Motorola, Inc.
ATTN: L. Clark

National Academy of Sciences
National Materials Advisory Board
ATTN: R. Shane

DEPARTMENT OF DEFENSE CONTRACTORS (Continued)

State University of New York at Buffalo
ATTN: P. Orlosky

National Semiconductor Corp.
ATTN: A. London
ATTN: R. Wang

University of New Mexico
ATTN: H. Southward

North Carolina State University
ATTN: W. Doggett

Northrop Corp.
ATTN: P. Eisenberg
ATTN: T. Jackson
ATTN: J. Sreur

Northrup Corp.
ATTN: D. Strobel
ATTN: P. Gardner
ATTN: L. Apodaca
ATTN: R. Turner

Physics International Co.
ATTN: J. Shea
ATTN: Division 6000
ATTN: J. Huntington
ATTN: Facilities Manager

Pennsylvania State University
ATTN: Breazeale Nuclear Reactor Facility

R & D Associates
ATTN: R. Poll
ATTN: S. Rogers
ATTN: C. MacDonald

Rand Corp.
ATTN: C. Crain

Raytheon Co.
ATTN: J. Ciccio

Raytheon Co.
ATTN: H. Fleischer
ATTN: A. Van Doren

RCA Corp.
ATTN: G. Brucker
ATTN: V. Mancino

RCA Corp.
ATTN: D. O'Connor
ATTN: Office N103

RCA Corp.
ATTN: R. Killion

RCA Corp.
ATTN: J. Saultz
ATTN: E. Van Keuren

RCA Corp.
ATTN: W. Allen

DEPARTMENT OF DEFENSE CONTRACTORS (Continued)

Rensselaer Polytechnic Institute
ATTN: R. Gutmann
ATTN: R. Block

Research Triangle Institute
ATTN: Sec. Office for M. Simons, Jr.

Rockwell International Corp.
ATTN: T. Oki
ATTN: J. Bell
ATTN: V. Strahan
ATTN: G. Messenger
ATTN: V. De Martino

Rockwell International Corp.
ATTN: D. Stevens

Rockwell International Corp.
ATTN: TIC, BA08
ATTN: T. Yates

Sanders Associates, Inc.
ATTN: L. Brodeur

Science Applications, Inc.
ATTN: V. Ophan
ATTN: V. Verbinski
ATTN: J. Naber
ATTN: D. Long

Science Applications, Inc.
ATTN: W. Chadsey

Science Applications, Inc.
ATTN: D. Stribling

Singer Co.
ATTN: J. Brinkman

Singer Co.
ATTN: R. Spiegel

Sperry Rand Corp.
ATTN: Engineering Laboratory

Sperry Rand Corp.
ATTN: R. Viola
ATTN: C. Craig
ATTN: P. Maraffino
ATTN: F. Scaravaglione

Sperry Rand Corp.
ATTN: D. Schow

Sperry Univac
ATTN: J. Inda

Spire Corp.
ATTN: R. Little

SRI International
ATTN: P. Dolan
ATTN: A. Whitson
ATTN: B. Gasten

Teledyne Ryan Aeronautical
ATTN: J. Rawlings

DEPARTMENT OF DEFENSE CONTRACTORS (Continued)

Texas Instruments, Inc.
ATTN: R. Stehlin
ATTN: A. Peletier
ATTN: F. Poblenz

TRW Defense & Space Sys. Group
ATTN: A. Witteles
ATTN: R. Kingsland
ATTN: A. Pavelko
ATTN: P. Guilfoyle
ATTN: H. Holloway
ATTN: O. Adams

TRW Defense & Space Sys. Group
ATTN: F. Fay
ATTN: R. Kitter
ATTN: M. Gorman

TRW Systems and Energy
ATTN: D. Millward
ATTN: B. Gililland
ATTN: D. Smith

DEPARTMENT OF DEFENSE CONTRACTORS (Continued)

Vought Corp.
ATTN: R. Tomme
ATTN: Library
ATTN: Technical Data Center

University of Texas
ATTN: E. Draper

University of Wisconsin
ATTN: TRIGA Nuclear Reactor Facility

Washington State University
ATTN: W. Wilson

Westinghouse Electric Co.
ATTN: L. McPherson

Westinghouse Electric Corp.
ATTN: D. Crichi
ATTN: H. Kalapaca

Westinghouse Electric Corp.
ATTN: J. Hicks

ERRATA SHEET

for

DNA 2432H dated 1 January 1979

TREE SIMULATION FACILITIES - Second Edition

Attached are three summary tables. Please insert these tables in the back of the report.

80 € 19 023

TREE SIMULATION FACILITIES GUIDE

(INSERT FOR DNA 2432H)

Compiled by
M. A. Espig

February 6, 1980

TREE SIMULATION FACILITIES GUIDE

The three tables in this guide (to be inserted in the TREE Simulation Facilities Handbook) summarize the principal data presented in the revised Handbook (DNA 2432H), January 1979 edition. The tables are:

Pulse Reactors

Flash X-ray Machines

Linear Accelerators

All of the data has been furnished by the facility personnel. The numbers presented in the tables are mostly maximum values, except as noted otherwise. The user is cautioned not to attempt correlation of the data for any of the machines since the measurement conditions are not the same for all columns. Also, no precise correlations should be attempted between different machines.

PULSE REACTOR SIMULATOR SUMMARY TABLE

FACILITY	PEAK PULSE POWER LEVEL, MW	MAX FLUENCE n/cm^2 (E>10 keV)	PEAK PULSE FLUX $n/cm^2/s$ (E>10 keV)	MAX GAMMA DOSE, rads (Si)/pulse	PEAK PULSE GAMMA RATE, rads (Si)/s	n/γ RATIO, $n/cm^2/\gamma$ rad	PULSE WIDTH RANGE, μsec (FWHM)	REPETITION RATE
1. Sandia Pulse Reactor (SPR-III) (Kirtland AFB, NM 87115)	118,000	6×10^{14}	8×10^{18}	1.7×10^{5}	2.22×10^{9}	3.6×10^{9}	76 - 237	2 bursts/hr
2. Army Pulse Reactor Facility (APRF) (Aberdeen Proving Ground, MD 21005)	6,800 150,000	6×10^{14}		3.9×10^{5}	2.4×10^{9}	4.5×10^{9}	45 - 1,000	105 min
3. Army Fast Burst Reactor Facility (FBR) (White Sands Missile Range, NM 88002)	65,000	7×10^{13}		2×10^{4}	1×10^{8}		50	1 burst/ 75 min
4. White Sands Missile Range Steady State Neutron Generator (SNG) (NM 88002)			7×10^{9}				$1 - 10^{4}$	$10 - 10^{5}$ (pulses/sec)
5. Sandia Pulse Reactor (SPR-II) (Kirtland AFB, NM 87115)	89,000	1×10^{15}		1.5×10^{5}		6.6×10^{9}	40 - 150	1 burst/ 2 hr
6. Lawrence Livermore, Super Kukla Prompt Burst Reactor (Mercury, NV 89023)	160,000 - 400,000	2×10^{15}	5×10^{18}	2.7×10^{5}	7×10^{8}	7.4×10^{9}	400 - 2,000	1 burst/ day
7. Northrop Reactor Facility (Triga Mark F) (Hawthorne, CA 90250)	1,800	6.5×10^{14}	1.9×10^{13}	4.3×10^{5}	1.6×10^{4}	1.4×10^{10}	10,000	
8. Pennsylvania State University Breazeale Nuclear Reactor (Triga Mark III) (University Park, PA 16802)	2,000	2.2×10^{14}	2.5×10^{13}	2×10^{6}R	9.6×10^{4}		15,000	4 bursts/hr
9. General Atomic Triga Reactor Facility (Triga Mark I)	1,100	9.7×10^{14}	5.4×10^{16}	3.0×10^{6}	6.1×10^{7}	3.8×10^{8}	16,000	10 bursts/ hr
(Advanced Triga Prototype) (San Diego, CA 92138)	6,700	9.5×10^{14}	1.4×10^{17}	2.8×10^{6}	4.2×10^{8}	4×10^{8}	6,300	10 bursts/ hr
10. Sandia Laboratories Annular Core Pulse Reactor (ACPR) (Kirtland AFB, NM 87115)	29,500	3.7×10^{15}		3.3×10^{6}			65,000	15 bursts/ hr
11. State University of New York at Buffalo Reactor (New York 14214)	2,000		3.15×10^{10}		2×10^{7}R/hr		15,000	3 bursts/hr
12. AFRRI Reactor Facility (Triga Mark F) (Bethesda, MD 20014)	1,800						10,000	1.3 bursts/ hr
13. University of Wisconsin Triga Nuclear Reactor Facility (Madison, WI 53706)	12,200						15,000	4 pulses/ hr
14. U.C. Irvine Dept. of Chemistry Triga Reactor (Irvine, CA 92717)	1,000						11 000	6 pulses/ hr
15. Washington State University Reactor (Pullman, WA 99164)	2,000							
16. U.C. Triga Mark III (Berkeley, CA 94720)	1,350						12,000	6 bursts/ hr
17. Kansas State University Triga Mark III (Manhattan, KS 66506)	250		10^{16} (E>0.2eV)		2.5×10^{7}			4 bursts/ hr
18. University of Texas at Austin Triga Mark I (Austin, TX)								

PULSE REACTOR SIMULATOR SUMMARY TABLE

AK PULSE WER LEVEL, MW	MAX FLUENCE n/cm^2 (E>10 keV)	PEAK PULSE FLUX $n/cm^2/s$ (E>10 keV)	MAX GAMMA DOSE, rads (Si)/pulse	PEAK PULSE GAMMA RATE, rads (Si)/s	n/γ RATIO, $n/cm^2/\gamma$ rad	PULSE WIDTH RANGE, μsec (FWHM)	REPETITION RATE	PULSE REPRODUCIBILITY	WORKING VOLUME IN
18,000	6×10^{14}	8×10^{18}	1.7×10^{5}	2.22×10^{9}	3.6×10^{9}	76 - 237	2 bursts/hr		7 dia x 20 high
6,800 150,000	6×10^{14}		3.9×10^{5}	2.4×10^{9}	4.5×10^{9}	45 - 1,000	105 min	±2%	4.2 dia x 7.8 high
65,000	7×10^{13}		2×10^{4}	1×10^{8}		50	1 burst/ 75 min	±5%	50 x 50 x 20 ft chamber
		7×10^{9}				$1 - 10^{4}$	$10 - 10^{5}$ (pulses/sec)		
89,000	1×10^{15}		1.5×10^{5}		6.6×10^{9}	40 - 150	1 burst/ 2 hr		1.5 dia x 8 high
160,000 - 400,000	2×10^{15}	5×10^{18}	2.7×10^{5}	7×10^{8}	7.4×10^{9}	400 - 2,000	1 burst/ day		18 dia x 30 high
,800	6.5×10^{14}	1.9×10^{13}	4.3×10^{5}	1.6×10^{4}	1.4×10^{10}	10,000			8 x 8 x 10 ft chamber
2,000	2.2×10^{14}	2.5×10^{13}	2×10^{6}R	9.6×10^{4}		15,000	4 bursts/hr	±10%	6.5 dia x 36 high
100	9.7×10^{14}	5.4×10^{16}	3.0×10^{6}	6.1×10^{7}	3.8×10^{8}	16,000	10 bursts/ hr	±5%	1.25 dia x 24 high
700	9.5×10^{14}	1.4×10^{17}	2.8×10^{6}	4.2×10^{8}	4×10^{8}	6,300	10 bursts/ hr	±5%	1.25 dia x 6 high
9,500	3.7×10^{15}		3.3×10^{6}			65,000	15 bursts/ hr	±5%	9 dia x 46 high
2,000		3.15×10^{10}		2×10^{7}R/hr		15,000	2 bursts/hr		6 dia x 100 long
800						10,000	1.3 bursts/ hr	±2%	
2,200						15,000	4 pulses/ hr		
000						11,000	6 pulses/ hr		
000									
350						12,000	6 bursts/ hr		
50		10^{16} (E>0.2eV)		2.5×10^{7}			4 bursts/ hr	±3%	

FLASH X-RAY SIMULATOR TABLE

	FACILITY	TOTAL BEAM ENERGY PER PULSE, joules	PEAK ELECTRON BEAM CURRENT, amps	AVERAGE PARTICLE ELECTRON ENERGY, MeV	PEAK ELECTRON ENERGY FLUENCE PER PULSE, cal/cm^2	MAX. X-RAY INTENSITY/ PULSE, rad (Si)	MAX. X-RAY DOSE RATE, rad (Si)/s	PULSE WIDTH RANGE, ns		PULSE REPETITION RATE	PULSE REPRODUCIBILITY
								ELECTRON MODE	X-RAY MODE		
1	Febetron 705 Electron Beam System, Northrop, Kaman Sciences, Lockheed Palo Alto, EG&G	400	5,000	1.4	25	7,000 R		20 - 50	20	10/s	± 5%
2	Febetron 706 Electron Beam System, Lockheed, EG&G, Triangle Institute, Westinghouse	12	7,000	0.5	2	100	4×10^{10} R/s	3	3	1/min	± 3%
3	ION Physics Corp., FX 35 Electron Beam Generator Burlington, MA 01803	1,650		0.4 - 2.5	220	2,000		35	20		± 5%
4	Boeing FX 75 Electron Beam Generator, Seattle, WA 98124	9,000	60,000	3.5	400	1.8×10^4	3×10^{11} R/s	29	29	1/2 min	± 10%
5	Harry Diamond Labs FX-45 Electron Beam Generator Adelphi, MD 28783	2,500	23,000	2.4	75	88		25	25	1/7 min	± 4
6	Physics International Pulserads San Leandro, CA 94577										
	225W	10,000	200,000	0.1 - 0.7	250	30,000 R		65	65		
	738	6,000		0.2 - 0.8				50	50		
	1150	40,000		1.4 - 4.2	100	50,000R	10^{12}	60	60	1/3 min	
	OWL II	110,000	1×10^6	0.3 - 1.0	520			110			
	PITHON II	Classified									
7	Maxwell Labs San Diego, CA 92123										
	BLACKJACK 3	30,000	550,000	0.7	>1,000			30 - 60	60	1/45 min	
	BLACKJACK 3 Prime	30,000		1.0				30 - 65	60		
8	TRW Redondo Beach, CA 90278										
	Vulcan FXR	>15,000	100,000	4.0	> 150	60,000	10^{12}	48	45	1/5 min	
	705 Febetron	400	5,000	2.0	140	7,000		20	20	1/min	
9	Sandia Labs Albuquerque, NM 87115										
	Hermes II	75,000	100,000	9 - 11	500	4×10^5	8×10^{12}	50	50	3 hr	± 15%
	REBA	10,000	40,000		400	1.8×10^4	2.6×10^{12}	70	70	6 hr	± 10%
	REHYD	36,000	600,000			7 cal/gm (Au)		80	80	1/2 hr	± 15%
10	North Carolina State University Pulserad Model 940 Electron Beam Generator Raleigh, NC 27650	8,000	80,000	3.5		25,000 R	5.6×10^9 R/s	40	40	1/3 min	± 6%
11	Harry Diamond Lab Aurora Facility Adelphi, MO 20783	2×10^6 (4 beams)	1.2×10^5	8	500	1×10^6	3×10^{11}	190	125	4/day	
12	Honeywell FX 25 Electron Beam Generator Largo, FL 33540	1,200	25,000	2.4	100	38,000	1.9×10^{12}	20	20	6/hr	
13	Raytheon Radiation Facility Sudbury, MA 01776										
	730/2650		1,500	2.0		18	2×10^8	90	90		
	FX 25	1,200	20,000		120	3,000	1.0×10^{12}	20	20	1/min	
14	General Electric, FX-25 Philadelphia, PA 19101	1,200	20,000	2.0	1.0	3,000	1.25×10^{11}	22	22	1/2 min	
15	Rome Air Development Hanscom AFB, MA 01731	800	200	2.0		3,000	1.5×10^{11}	20	20	1/4 min	
16.	Casino Naval Surface Weapons Center, Silver Springs, MO 20910	Classified									
17.	Gamble II Naval Research Lab Washington, DC 20375	Classified									

LINEAR ACCELERATOR SIMULATOR TABLE

	FACILITY	ENERGY RANGE, MeV	MAXIMUM PEAK BEAM CURRENT, amps	ELECTRON DOSE, rad (Si)	ELECTRON DOSE RATE, rad (Si)/s	X-RAY DOSE, rad (Si)	X-RAY DOSE RATE, rad (Si)/s	NEUTRON YIELD, n/pulse	MAX NEUTRON YIELD RATE, n/s	PULSE WIDTH RANGE, μsec	PULSE REPETITION RATE PULSES
1.	IRT Corporation LINAC (San Diego, CA 92138)	1 - 25	10	10^6	10^{12}	200	10^8	5×10^9	5×10^{15}	0.01 - 8	10 - 720
2.	NRL LINAC (Washington, DC 20375)	5 - 65	2	4×10^4		1,000		1×10^8		0.03 - 1.4	5 - 360
3.	BREL LINAC (Seattle, WA 98124)	3 - 33	2.5		$>10^{11}$		6×10^6	6×10^{10}	7×10^{12}	0.04 - 6	1 - 550
4.	NWEB LINAC (White Sands Missile Range, NM 88002)	2 - 48			6×10^{10}		5×10^8			0.01 - 10	10 - 120
5.	EG&G LINAC (Goleta, CA 93017)	1 - 30	30		1.5×10^7		1.8×10^8			5×10^{-5} -4.5	1 - 360
6.	AFFRI LINAC (Bethesda, MD 20014)	13 - 45		10^6	2×10^{11}	15				0.01 - 5	1 - 120
7.	Rome Air Development Center LINAC (Hanscom AFB, MA 01731)	10	2				5×10^8			0.01 - 4.3	1 - 180
8.	Ogden Air Logistics Command LINAC (Hill AFB, VT 84406)	10 - 25	0.5		2×10^{10}		5×10^8			0.04 - 6	1 - 20
9.	LASL PHERMEX (Los Alamos, NM 87544)	27	30							0.2	
10.	RPI LINAC (Troy, NY 12181)	>80	>5			210	1.6×10^9	3.2×10^{10}	1.6×10^{18}	0.007 - 4.5	1 - 720